Dressing heart smart: an e-textile based garment for home-based ECG monitoring

By

Meseret Nigatie Teferra

Thesis

Submitted to Flinders University

for the degree of

Doctor of Philosophy (Biomedical Engineering)

College of Science and Engineering

May 2021

This page is left blank intentionally

Abstract

Cardiovascular disease (CVD) continues to be the leading cause of death and the primary reason for hospitalization worldwide. As a result, the medical system is enormously affected considering the unprecedented increment of life expectancy over previous decades. The investment in hospital infrastructure and the burden on health care facilities required to support the rapidly increasing number of patients can be minimized if centre-based cardiac rehabilitation is conducted outside of the hospital premises. Electronic-textile (e-textile)-based cardiac monitoring offers a viable option to allow cardiac rehabilitation programs to be conducted outside of the hospital.

This Ph.D. thesis presents the design, construction, and testing of a diagnostic level e-textile-based electrocardiogram (ECG) smart vest. The main findings are I) In an attempt to identify the knowledge gap and map the available evidence on e-textile based cardiac monitoring, a systematic scoping review was conducted based on a prior protocol. The systematic review concluded that the use of a 12-lead, personalized, home-based cardiac rehabilitation monitor containing fully textile-integrated electronics with diagnostic capability is yet to be reported. Therefore, there is potential for future research in this area. Additionally, motion artefact continues to be a challenge. II) A miniature ECG hardware suitable for wearable application and extended ambulatory monitoring was realized. III) A versatile, smart ECG vest that is easy to use and could be worn for seamless ambulatory monitoring was successfully implemented. The desired compression pressure applied by the smart garment for a stable-skin electrode interface was experimentally estimated. IV) The optimal electrode placement regarding the EASI

configuration was studied. In this regard, placing the 'A' and 'I' electrodes on the left and right anterior axillary point respectively and the 'E' electrode slightly lower than the lower sternum (xiphoid process) showed higher signal quality compared to the standard EASI electrode placement during sideways movement, sitting / standing from a chair and climbing stars. V) The method of connecting the textile electrodes to the smart ECG vest was examined, and it was determined that there was no significant signal quality difference between the ECG collected from the removable electrodes and the ECG from the embedded textile electrodes. However, removable textile electrodes could be swapped without affecting the integrity of the smart ECG vest while increasing its flexibility. VI) A pilot study was conducted to compare the performance of the textile-based ECG against the traditional Holter monitor. The results showed that there was no significant difference between the ECG from the textile-based electrodes in the smart vest and the reference ambulatory monitor.

The standard ambulatory monitor utilizes sticky wet-gel electrodes where the ECG quality deteriorates over time due to the drying of the gel-interface. Moreover, the ECG lead wires reduced the comfort of the users. On the other hand, the proposed textile-based ECG monitor has embedded wires and textile electrodes. The smart ECG vest is easy to use and could be worn without the need for assistance to put on/off for seamless ambulatory monitoring. The intuitive design significantly reduced the time need to train the users. Therefore, the proposed textile-based EASI 12-lead equivalent ECG monitor could be a viable option for long-term real-time monitoring of cardiac activities, and a clinical trial is recommended based on a population with a known cardiac disease to validate and produce clinically significant results.

Table of Contents

List of Figures

List of Tables

List of Abbreviations

AFE ………………………………………………………………………… Analog front-end

ApEn …………………………………………………………………… Approximate entropy

AR ……………………………………………………………………………... Autoregressive

basSQI ………………………………………………… Baseline power signal quality index

BPM / bpm ………………………………………………………………. Beats Per Minute

bSQI …………………………………………………… Beat detection signal quality index

CR …………………………………………………………………… Cardiac Rehabilitation

CVD …………………….. Cardiovascular Disease

ECG ……..……………………………………………………………... Electrocardiogram

EEG …………………………………………………………………… Electroencephalogram

EMD ………………………………………………………….... Empirical mode decomposition

EMG ……………………………………………………………………… Electromyogram

E-textile ………………………………………………………………… Electronic textile

FEA ……………………………………………………………………… Front End Amplifier

FFT…………………………………………………………………… Fast Fourier transform

FSR …………………………………………………………………… Force-sensing Resistor

GPRS …………………………………………………………… General Packet Radio Service

GPS ……………………………………………………………… Global Positioning System

GUI …………………………………………………………………… Graphic User Interface

HBCR ………………………………………………… Home-based cardiac rehabilitation

HR ………………….. Heart Rate

HRV …………………... Heart Rate Variability

IIR ………………………………………………………………... Infinite Impulse Response

IMF ………………………………………………………………... Intrinsic mode function

MagIC ………………………………………………… Maglietta Interattiva Computerizzata

PC ………………………………………………………………………… Personal Computer

PCB …………………………………………………………………… Printed Circuit Board

PDA ……………………………………………………………… Personal Digital Assistant

PRD …………………………………………….. Percentage Root Mean Square Differences

PSD …………………………………………………………………… Power Spectral Density

pSQI ……………………………………………………………… Power signal quality index

QRS ………………………. The most visible component of a typical ECG and is composed of Q, R, and S waves of the ECG tracing

QT………………………… The interval between the start of the Q wave to the end of the T wave on a typical ECG tracing

QTc……………………………………………………………………… Corrected QT interval

SNR …………………….. Signal to Noise Ratio

SPI ………………………………………………………………… Serial Peripheral Interface

SPS / sps ………………………………………………………………… Samples Per Second

SSR …………………………………………………………………………… Signal to Signal Ratio

USB …………………………………………………………………………… Universal Serial Bus

VR ………………………………………………………………………………………… Virtual Reality

Declaration

I confirm that this thesis does not contain any material without acknowledgment any work previously summited for an award in any higher institution; and to the best of my knowledge and belief, does not incorporate any material previously published or written by another person except where due reference is made.

Signature: *Meseret Nigatie Teferra*

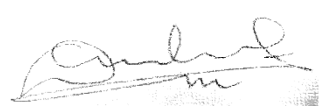

December 24, 2020

Acknowledgments

My most profound acknowledgment goes to the Almighty GOD. "The LORD is my light and my salvation, whom shall I fear? The LORD is the stronghold of my life, of whom shall I be afraid? When the wicked advance against me to devour me, it is my enemies and my foes who will stumble and fall. Though an army besieges me, my heart will not fear; though a war breaks out against me, even then I will be confident." Psalm 27: 1-3.

I would like to gratefully extend my sincere thanks to all the people who gave generously of their time. I especially thank my supervisors Professor Karen J. Reynolds, Prof. Robyn Clark, and Dr. David Hobbs, for your patience, motivation, enthusiasm, and the immense guidance you gave me through every stage of the research. My sincere thanks also go to staff members of the electrical and mechanical workshop, Mr. Craig Peacock, for his valuable comments and technical support throughout the design and development of the ECG hardware and Dr. Michael Liedlgruber for his assistance in writing the MATLAB scripting during the data analysis. All staff members of AAIT and CINOP Global, especially Mr. René Lenssen, I thank you very much for your caring and continuous support. My friends and families, I thank you very much for you have been with me throughout my journey.

In addition, I want to thank the Tom Simpson Trust Fund and the National Heart Foundation of Australia for supporting the research and the Medical Device Research Institute for kindly granting me access to laboratories and tool kits for the test work of each stage and construction of the ECG hardware and the smart ECG vest prototype. And finally, Enu and Lilu, your flawless love and caring is my strength; thank you very much for being there.

This page is left blank intentionally

Chapter 1. Introduction

Chronic diseases are "diseases that cannot (fully) be cured given the current state of medical science" (Rijken and Dekker, 1998, p. 143) with the potential of irreversible and long-lasting effect (Rijken and Dekker, 1998, p. 143, Australian Institute of Health and Welfare, 2015). Clinical rehabilitation for chronic diseases or post-operative conditions is usually performed based on training with particular protocols designed for each patient and conducted under the supervision of professionals. During the rehabilitation process for heart conditions, Holter monitors are used to provide feedback about cardiac activities. However, the traditional Holter monitor can be inconvenient for the patient due to the electrocardiogram (ECG) lead wires and sticky electrodes. Moreover, the ECG electrodes have a relatively short shelf life and can only be used once. The gel-interface dries over time and the signal quality deteriorates in long-term ambulatory application (Marozas et al., 2011). This thesis focuses on an alternative to the traditional Holter monitor - a textile-based ECG monitor.

1.1. Background review

The heart, blood vessels and circulating blood constitute the cardiovascular system that provides nutrients to organs of the body and excretes cell metabolism by-products (Bullock et al., 2001, p. 99, Klabunde, 2012, p. 24). In addition to metabolites, blood also carries hormones and enzymes, which regulate the functions of cells (Batzel et al., 2007, p. 1). Though the lymphatic system is external to the blood circulation circuit, it also falls under the cardiovascular system for its exchange functionality of essential fluid and proteins from the interstitial space into the circulation system (Swartz, 2001, Klabunde, 2012, p. 2, Zimmermann, 2016).

Cardiovascular disease (CVD) "is a collective term used to denote diseases of the heart and blood vessels" (Australian Institute of Health and Welfare Australian Institute of Health and Welfare, 2011a, Sankaran, 2012, p. 361, The Department of Health, 2016). CVD is the number one cause of death worldwide, exceeding the mortality rate of cancer (Sankaran, 2012, Australian Institute of Health and Welfare, 2016). CVD was responsible for 29% of all deaths worldwide in 2001 (Lilly and Braunwald, 2012). Each year the number of CVD-induced deaths increases, with the worldwide annual death due to CVD predicted to be 32% of all deaths in 2020 and 33% of all deaths in 2030 (Lilly and Braunwald, 2012).

Disorders that fall under CVD include heart diseases, cerebrovascular disease (stroke) and peripheral vascular diseases (Mackay and Mensah, 2004, pp. 18 - 19, Loue and Sajatovic, 2012, p. 362). Stroke and coronary heart disease are the two most common types of CVDs. For example, 85% of CVDs in 2016 were due to stroke and coronary heart disease (Naghavi et al., 2017).

The World Health Organisation defines cardiac rehabilitation (CR) as:

> the coordinated sum of activities required to influence the underlying cause of cardiovascular disease favourably, as well as to provide the best possible physical, mental and social conditions, so that the patients may, by their own efforts, preserve or resume optimal functioning in their community and through improved

health behaviour, slow or reverse the progression of the disease (Woodruffe et al., 2015, p. 2).

A CR program involves physicians and allied health professionals who provide secondary prevention for patients who are recovering from cardiac (Kraus and Keteyian, 2007, p. 1, Woodruffe et al., 2015). Kraus and Keteyian (2007) define secondary prevention as "an intervention or treatment that reduces the risk of recurrence, progression, or mortality in a person known to have a cardiovascular disease" (Kraus and Keteyian, 2007, p. 142).

Varieties of CR modes and approaches are used worldwide (Perk et al., 2007). However, many of the models nowadays are somehow standardized and comprised of baseline patient assessment, nutritional counselling, physical activity counselling, exercise training, risk factor management, and psychosocial interventions (Perk et al., 2007, Bennett, 2012, p. 6, American Association of Cardiovascular Pulmonary Rehabilitation, 2013).

1.1.1. Home-based cardiac rehabilitation: an alternative approach for the traditional cardiac rehabilitation

Home-based cardiac rehabilitation (HBCR), as an alternative approach to the traditional centre-based CR, is conducted in "the home or other non-clinical settings such as community centres, health clubs, and parks" (Thomas et al., 2019, p. e70). There is increasing evidence that supports the viability of HBCR (Jolly et al., 2007, Arena et al., 2012, Anderson et al., 2017, Dunn et al., 2017, Rohrbach et al., 2017). An HBCR program, assisted by advances in electronic and internet technologies, offers a viable option (Sarela et al., 2009, pp. 1 - 2) to clinic-based CR as the HBCR can be tailored to match the patient’s lifestyle (Jolly et al., 2009). Home-based rehabilitation modalities developed so far fall into one of three categories: mobile-based, virtual reality fused wearable sensor CR platforms, and other technologies.

Smartphone-based cardiac rehabilitation modalities

There are a growing number of chronic disease management programs that make use of the inherent properties of a mobile phone. Attributes like communication platforms, computing power, user-friendly interfaces, storage capacity, and small size for portability contribute to the flourishing applications of telecom technology in the health care system (Ahtinen et al., 2009, p. 1, Sarela et al., 2009, p. 2). Many mobile applications are being developed to follow-up and manage personal well-being.

One such tool is the Wellness Diary (Ahtinen et al., 2009). This is a mobile-based electronic journal covering weight, exercise steps, diet, stress level, sleep duration and quality, tobacco use, and alcohol consumption. Patients choose the parameters and mark the diary accordingly. Another tool, Mobile Coach, is a mobile application designed to manage physical activities. It generates an activity schedule and provides recommendations based on the initial exercise period and intensity parameters selected by the patient. The third type of mobile application is based on relaxation or meditation-type approaches. For example, mobile application SelfRelax has been used to lessen users' stress levels through coordinated practices that involve scheduled periodical physical manoeuvring backed by entertaining background sounds and other techniques (Ahtinen et al., 2009, pp. 2 - 3).

Ahtinen et al. (2009) conducted a study based on 119 (35 male and 84 female) volunteers using the Wellness Diary, Mobile Coach and SelfRelax. The applications were installed on two mobile phones (Nokia 5500 and Nokia E50) for the experiment. The authors reported that the three mobile applications were found to be valuable, easy to use and accepted by the participants, although participants felt a diminished interest in the Wellness Diary as time went by due to the repetitive nature of the activities.

Särelä et al. (2009) developed another mobile-based HBCR platform, Care Assessment Platform (CAP), aimed at cardiac outpatients. This HBCR program is composed of specialized tools (Wellness Diary Connected and Step Counter) and covers six weeks of risk factor management integrated with educational topics on CVD, with telemonitoring chosen as the means of intervention. Using the Wellness Diary Connected platform, mentors could provide follow-up notes and undertake weekly consultations with patients remotely. With built-in web-access, patients could access resources, set-up further rehabilitation goals and read the descriptive personal feedback regarding their progress. Step Counter counts the patient's stride during movement using an embedded accelerometer in the phone and provides immediate feedback. However, no evidence was reported regarding the clinical effectiveness of the platform to mitigate cardiac risk factors even though the authors mentioned a Randomized Controlled Trial (RCT) to be conducted to validate their system.

Iancu-Constantin et al. (2015) proposed a service-oriented, architecture-based CR software that would allow real-time interactive communication between the patient and a remotely located physician. According to the paper, the CR program would have two stages. The first stage would consist of a week-long stay hospital where the patient would be given user-level training on a smartphone loaded with CR services software. When discharged, the patient would be able to use the installed application throughout the second stage of the HBCR process, which would last about three months. Nothing has since been reported about the clinical effectiveness or outcomes from the proposed system.

In a similar scenario, Jaworek and Augustyniak (2011), proposed mobile technology to realize a cardiac telerehabilitation application based on heart rate variability (HRV) and motion analysis. A remote supervisory server will control a wireless ECG acquisition module though it is unclear how this will be implemented. A Global Positioning System (GPS) sensor already available in the mobile device will calculate the location and speed of the user. Architecturally, the system will be composed of five modules: the data exchange module, the QRS (a combination of the Q, R and S waves of a typical ECG tracing) detection module (for HRV analysis), a GPS algorithm for motion analysis, a personalized training program, and an alarm module. The proposed application is under development and nothing was reported about its clinical relevance.

Virtual reality fused wearable sensor cardiac rehabilitation platforms

Schultheis and Rizzo (2001, p. 298) define virtual reality (VR) as an artificial environment where users interact with a computer and complex data to mimic real-life activities

(Schultheis and Rizzo, 2001). Burdea et al. (1996) define VR as "a high-end user-computer interface that involves real-time simulation and interactions through multiple sensorial channels of vision, auditory, tactile, smell, and taste" (Burdea et al., 1996, p. 6).

Apart from the slight differences in definitions, scholars agree that VR is a three-dimensional, real-time, interactive simulation such that human immersion in a computer-generated artificial environment is manifested (Schultheis and Rizzo, 2001, Burdea and Coiffet, 2003, Mihelj et al., 2014).

There are four fundamental attributes of a virtual reality (VR) system. The first component is a computer-generated virtual environment, which hosts distinctive three-dimensional objects, environment topology, and intermediaries, as well as user interface elements. The second crucial element of VR is a virtual presence that could be either physical, achieved through synthesized stimuli, or mental whereby the user assumes the virtual environment is real and responds to it. Automatically perceiving the whereabouts and other pertinent data from the real world, VR is also expected to provide appropriate sensory feedback (visual, audio, or haptic) for users. Finally, responding to users' actions (interactivity) is the fourth element, which upgrades the performance of VR to near real-life situations (Mihelj et al., 2014, pp. 1 - 12).

In March 1992, the first international conference on VR entitled "*Interfaces for Real and Virtual Worlds*" was held in France. Later the same year, medical doctors, as well as engineers, met in San Diego to discuss and draft the potential use of VR in the field of health care systems, marking a new era for VR - augmented medical practices. A little over a year later, the Institute of Electrical and Electronics Engineers held its first VR conference in Seattle, and henceforth VR became one of the Institute's mainstream areas (Burdea and Coiffet, 2003).

Nowadays, scholars are striving to extend the concept of VR-based gaming technologies, cloud computing, the internet of things and wearable sensors for health care applications (Sotiriadis et al., 2016, p. 416).

Using the concept of computational intelligence, Pirovano et al. (2012) proposed a self-adaptive computer game for CR. It is different from other gaming protocols in that the current game is continuously remodelled and updated based on the patient's ongoing performance using an Intelligent Game Engine for Rehabilitation. Lu et al. (2012) devised a personalized CR system called CARLOS, based on the principle of motion sensing. Currently, it is under a service trial with pilot verification. In terms of architecture, the CARLOS system is composed of wearable wireless sensor networks for real-time vital signal measurement and motion-sensing technologies that drive the user-friendly virtual gaming platform.

One of the systems benefitting from the concept of VR based gaming is HeartHealth, an e-health program that delivers a convenient exercise-based CR package through gaming. The platform has two front-end interfaces: a physiotherapeutic 3D gaming interface and an Android application. The main interface, the 3D gaming environment, captures the patient's movement via a Microsoft Kinect V2 sensor and wearable wireless inertial measurement units and stores the results in the cloud system. Then the Motion Evaluation Specific Enabler, embedded in the gaming architecture, analyses the ongoing motion by comparison with a pre-recorded reference. It then provides instant feedback to the patient and updates the patient's performance in the online personal diary. Hence, both the medical personnel and the patient can track the rehabilitation journey and assess progress. The Android-based interface, on the other hand, serves as a portable medium for medical experts to follow up with their patients (Chatzitofis et al., 2015).

Soares et al. (2013), cited in Vieira et al. (2017), developed another Kinect-based VR game for CR called RehabPlay. The Unity3D gaming engine receives motion-related inputs from the user through the Kinect sensors and generates a simulated virtual exercise environment. The monitoring software package then coordinates and records the entire activity. The software also analyses and generates feedback. A minimum of six months is needed to achieve a result.

Other home-based cardiac rehabilitation technologies

There is a handful of technologies applied to HBCR that differ from the groups above. One such system is MULTI-FIT. It is one of the home-based programs that provide a platform for programs designed for the management of cardiovascular risk factors and associated conditions. An example is a computer-based nutritional counselling program (Sarela et al., 2009, p. 2).

Available in the United Kingdom, the heart manual is a collection of individualized self-help tools organized in a six-week-long program. It bolsters the patient's overall awareness of the CVD, provides systematic strategies for combating cardiac episodes, and hence helps to manage associated risk factors. The program can be paper-based or digital, and is designed for patients who suffer from myocardial infarction and/or revascularization (Deighana et al., c2017, p. 1).

To sum up, exercise therapy based on the concept of motion analysis is the characteristic feature shared by many HBCR systems discussed above. Real-time ECG monitoring was not the focus of these systems and in many was not included.

1.1.2. Wearable and electronic textile technologies

The success of a CR model relies on the availability of technologies that promote quick recovery and assist in resuming the usual routines and activities of daily living (American Association of Cardiovascular Pulmonary Rehabilitation, 2013). Wearable technologies and electronic textiles are becoming an attractive opportunity and will be discussed in the following section.

1.1.2.1. Wearable technologies

Wearable electronics are defined as devices that are able to generate, transmit, modulate and detect electrons, and that can be worn comfortably to serve a specific purpose (Tao, 2005, p. 1). Tao (2001) suggested one of the general architectures used as a building block of good wearable electronics. The configuration Tao recommends incorporates input and output interfaces to collect and display information, communication modules to transmit and receive information, data, and energy management technologies as well as integrated circuits.

Sensors are integrated with wearable electronics and either attached or often embedded into the wearable interface. They are used to collect a variety of physiological stimuli and respond accordingly (Tao, 2005, pp. 2 - 3). Many physiological conditions, for instance, temperature, HR, respiration rate, blood pressure, or gait analysis can be monitored with the aid of wearable sensors (Mukhopadhyay, 2015, pp. 3 - 8). An example that illustrates the application of wearable sensors is given in Figure 1.1. In this figure, a wireless wearable garment that monitors different vital-signs (ECG, Electromyogram (EMG), oxygen saturation) and activity levels can be implemented based on the idea of embedded electronics and circuit wiring in the clothing.

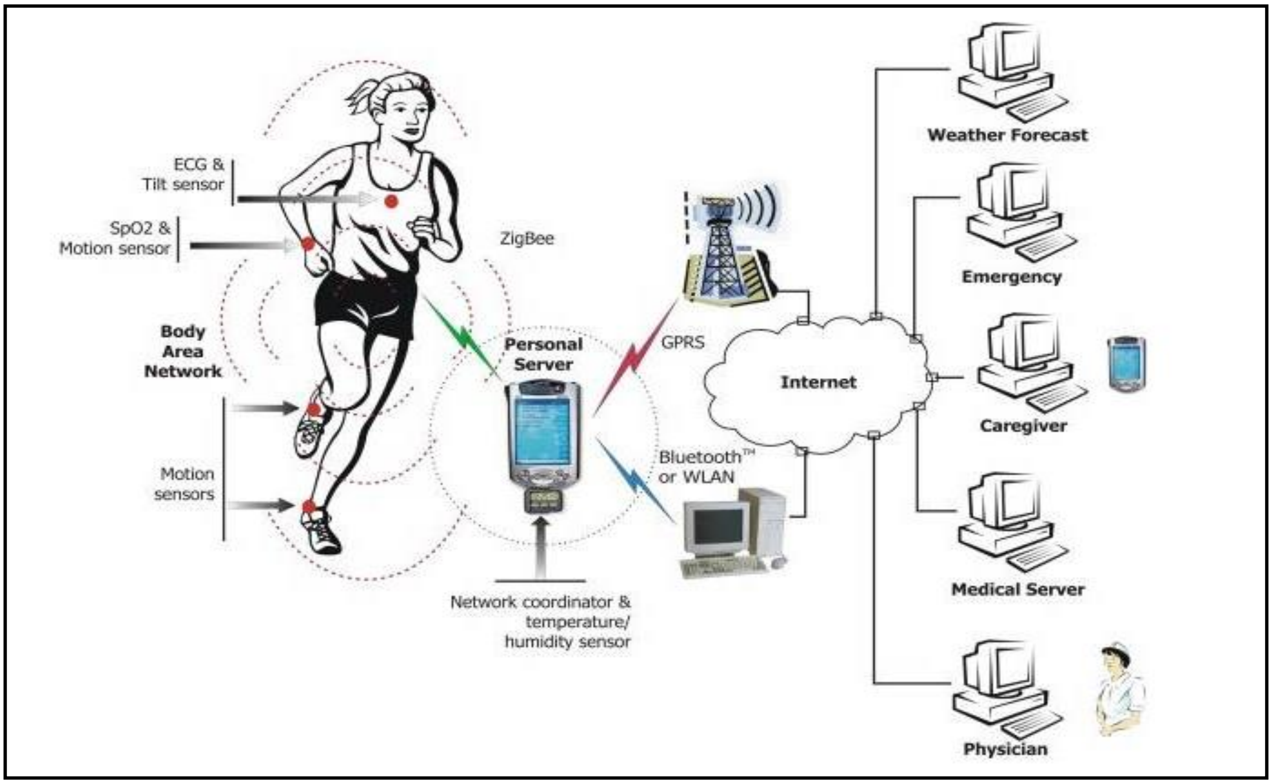

Figure 1.1: Ambulatory monitoring based on wearable sensors *(source: http://wikid.io.tudelft.nl/WikID/index.php/Wearable_Health_Monitoring_Systems;* cited 2019 April 22*).*

In developed countries, people have longer life expectancies than in less well-developed countries. However, with longer life expectancy comes increased risk of multiple chronic and usually complex health conditions. In this regard, wearable systems find a highly useful application to monitor those chronic and debilitating health care problems either in the hospitals or remotely (Shyamal Patel et al., 2012, pp. 1 - 3), as depicted in Figure 1.2. Looking at the general architecture (Figure 1.2), the telemonitoring system could be implemented from the wearable body sensor network to collect various physiological signals and transfer the data wirelessly to the remote workstation. The wireless feature of the wearable telemonitor increases the user's comfort and activity level.

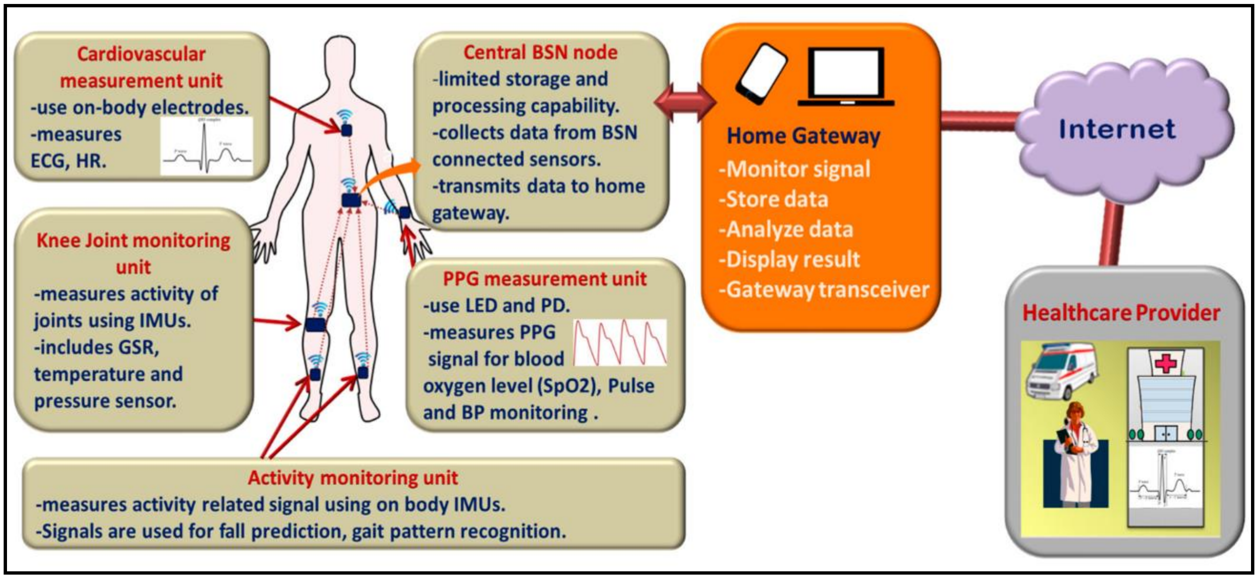

Figure 1.2: Telemonitoring based on wearable sensors (Source: Majumder et al. (2017), Figure 1, also available at: https://www.mdpi.com/1424-8220/17/1/130).

In the field of medicine, particularly in cardiology, a variety of wearable devices has been developed to monitor the cardiac activities of patients while they are engaging in their day-to-day life. The advantages of wearable devices include the diagnosis of mild, infrequent and undetectable cardiac episodes like atrial fibrillation as well as fatal abnormal arrhythmias (Yan and Kowey, 2011, pp. 90 - 91). Below are brief reviews of some of the commercially available wearable technologies for cardiac monitoring: Holter monitor, ambulatory blood pressure monitor, minimally invasive implantable loop recorder, and in-hospital telemetry system.

The Holter monitor

Perhaps the most common wearable electronics used in the field of cardiology is the Holter ECG monitor (Figure 1.3). Holter monitoring is a mobile ECG monitor used to record cardiac activities over an extended period without affecting the daily living of the patient (Rodríguez et al., 2010, p. 521, Wojnarowski et al., 2011, p. 137). From their first inception in the year 1963 (Zareba, 2013, p. 125), Holter monitors have been used for long-term ECG monitoring for patients with an active lifestyle but with slight cardiac disorders (Chaudhuri et al., 2009, p. 6). The assumption is patients have frequent cardiac abnormalities that take place within 24 or 48 hours.

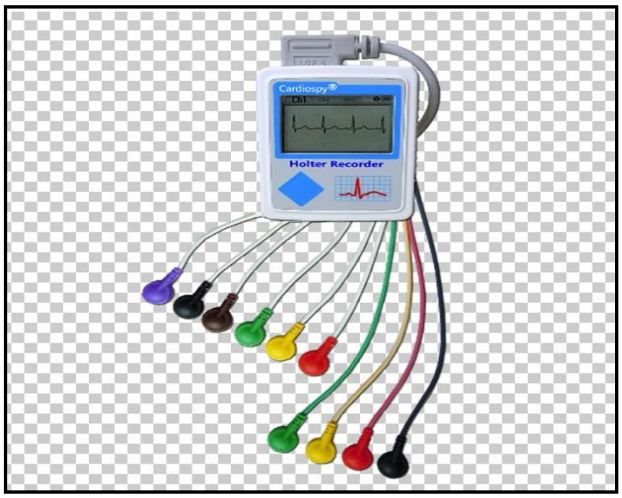

Figure 1.3: Holter monitor (*Source:* https://imgbin.com/png/xjpZzMQx/Holter-monitor-electrocardiography-medicine-cardiology-monitoring-png; cited 2019 March 2).

Even though the Holter system is useful, it also presents some challenges. The first problem related to the Holter recording system is noise from motion artefact (Chaudhuri et al., 2009, pp. 5 - 9). Discomfort from the electrodes and lead cables for multi-day recording is another challenge (Rosero et al., 2013, pp. 144 - 148). Finally, if the symptoms of the patient are infrequent and do not occur within the anticipated 24 or 48 hours, there is a chance of missing an arrhythmia (Yan and Kowey, 2011, p. 91, Shanmugam and Liew, 2012, p. 115).

Implantable loop recorder

Challenges arising from the Holter monitoring, and the need for more extended cardiac monitoring, led to another innovation called the implantable loop recorder or insertable cardiac monitor. This implantable loop recorder "is a subcutaneous ECG monitoring device used for diagnosis in patients with any recurrent unexplained cardiac episodes of the heart" (Min, 2011, p. 113). With an extended recording option exceeding one year, the insertable loop recorder enables physicians to determine the presence of symptoms and correlates the symptoms with the respective heart rhythms (Min, 2011, p. 113).

Insertable loop recorders are assumed to be the best way to monitor syncope. However, the single lead recording may result in data loss if the acquired ECG is corrupted due to noise artefact, and the need for a surgical procedure for implantation also is an issue for some patients (Yan and Kowey, 2011, p. 92).

Ambulatory blood pressure monitor

One of the determinants of a healthy cardiovascular system is blood pressure (Stanner, 2005, p. 13). Initially suggested by Nikolai S. Korotkoff in the year 1905, pressure measurement is usually performed using auscultatory methods. Historically, this has been done manually using a sphygmomanometer and stethoscope. However, more recently a number of semi-automated or fully automated measurement devices have become available (Meyer-Sabellek et al., 1990). First developed in 1962 (McGrath, 2002, p. 588), the ambulatory blood pressure monitor is a portable wearable system that measures blood pressure based on pre-determined regular intervals, without hampering the patient's daily-living (Pickering et al., 2006, Australian Family Physician, 2011, p. 877). Prognosis of ailments due to hypertension is possible from careful investigation of a pressure profile recorded using ambulatory blood pressure monitors worn by a patient located remotely from the hospital environment (Weber and Drayer, 1984).

Existing ambulatory blood pressure monitors use any of the three techniques to determine the pressure. The first method, auscultation, uses a blood flow profile to identify the start and end of the Kortokoff sound collected via microphone to determine the upper and lower pressures while the cuff is inflating and deflating. It tends to underestimate systolic pressure (McGrath, 2002). In the cuff oscillometer technique, on the other hand, the systolic and diastolic pressures are derived from the pressure swing of the cuff using different algorithms. Rarely, overestimation of systolic pressure happens due to transmitted cuff oscillation pressure (McGrath, 2002). The third method is based on the volumetric oscillation of a finger under the cuff. The diastolic pressure corresponds to the beginning of the finger volume oscillation, while systolic pressure is determined at the point where the fluctuation of finger volume is maximum (McGrath, 2002, p. 589).

In terms of functionality, the ambulatory blood pressure monitor gives a better prediction than individual manual blood pressure measurements (McGrath, 2002).

In-hospital telemetry system

In-hospital telemetry systems are used in coronary intensive care units of health care facilities (Turakhia et al., 2012, p. 1665). Funk and co-workers cited in Yan and Kowey (2011) argued that patients of fatal arrhythmias could be saved if they are closely monitored and provided with immediate medication (Yan and Kowey, 2011, p. 96). In terms of wireless protocols, telemetry systems operate based on the principle of frequency modulation. Most of them utilize a standard television channel with a modulation frequency in the range of 0.3 kHz to 3 kHz. At the same time, some companies such as Hewlett Packard have chosen the mobile communication band with a carrier frequency of 450 MHz (Andes 1983, p. 196).

Unlike the Holter monitor, the in-hospital telemetry system offers real-time cardiac monitoring. Telemetry systems are mainly reliable and are an effective way of in-hospital monitoring, with built-in alarm and recording capability. The simplest telemetry transmitter comes with three-electrodes. However, most telemetry monitors are of five electrodes configuration (Yan and Kowey, 2011). Further information regarding electrode configurations will be discussed in Chapter 3, section, section 4.4.2.

1.1.2.2. Electronic-textile technologies

Electronic textiles, also known as e-textiles, are defined as "fabrics that have electronics and interconnections woven into them" (Wagner et al., 2002, Jones et al., 2003, Mark Jones et al., 2003, Stoppa and Chiolerio, 2014, p. 11957, Dias, 2015).

Researchers from various disciplines strive to maximize the usability of e-textiles for multiple applications. In the field of medicine, electronic garments could be the perfect choice for continuous, non-invasive telemonitoring of an individual's physiological conditions where wearable monitoring is a mandatory requirement (Angelidis, 2010b).

In the field of cardiology, researchers have developed e-textile based sensors that can monitor the cardiac activities of patients while they are engaging in their day-to-day life. These e-textile ECG electrodes produce signals of acceptable quality (Fleury et al., 2015) and are resistant to repeated washing in aqueous solutions without losing their properties (Bourdon et al., 2005, Coosemans et al., 2006). So far, both contact (resistive) and noncontact (capacitive) based ECG transduction from e-textile sensors have been proposed. A concise summary is given below.

Contact (resistive) based ECG transduction

Paradiso et al. (2005) reported a wearable physiological monitor from piezoresistive yarns and metal-based fabric sensors which aimed to measure respiration, ECG, and temperature. The system consisted of a wireless portable patient unit (known as WEALTHY) and a remote server for data visualization and analysis. The test results of the system revealed increased level of noise (no quantitative data was reported) for increased physical activity, and hence, the HR was the only value able to be computed from the collected signal during physical activity.

Jourand et al. (2010) employed the concept of e-textiles to develop a robust Sudden Infant Death Syndrome monitor. In the proposed design, the sensors were integrated into a tight elastic garment to acquire heart rhythm (from three textile electrodes) and breathing (accelerometer). The wireless transceiver module (Nordic nRF24L01) delivered the data to a remote processing computer running MATLAB. The prototype measured breathing volume with an R^2 value of 0.85 compared to a look-up table of reference values from a spirometer test.

Bouwstra et al. (2011) reported a smart Jacket ECG monitor for prematurely born babies in the Neonatal Intensive Care Unit. The authors used a TMSI Refa8 amplifier and ASA-lab 4.7.3 software (from ANT, Enschede, the Netherlands) to collect the ECG signal. ECG from textile electrodes and wet ECG electrodes were compared where the ECG from the gel-based electrodes showed higher signal strength and lower sensitivity to motion artefact (no quantitative data was reported). Moreover, a video signal and 3D acceleration (3D-ACM) sensor were employed to investigate body movement affecting ECG quality. A strong correlation was observed between the acquired ECG, accelerogram data, and body movement (no quantitative data was reported).

In a related study, Cho et al. (2011) used textile electrodes embedded into a garment to measure vital signs. As the electrodes were not fixed on a particular position on the body, a slight motion caused the electrodes to drift to a different location. Hence, the signal was highly prone to motion artefact. The focus of the research was to develop clothing that produced the least amount of electrode displacement to optimise ECG signal quality, especially under dynamic conditions. The authors suggested three ECG sensors placed three centimetres away from the reference electrode and each other, forming an equilateral triangle configuration. Four types of modularized garments were used: ‘chest-belt-type,’ ‘cross-type,’ ‘X-type,’ and ‘Curved-X-type’ and two male subjects participated in the experiment. Of the four prototypes, the 'cross-type' garment, consisting of three electrodes placed 3cm apart from each other and between leads V3 and V4 electrodes in the standard 12 ECG configuration, produced a lower motion artefact (cross-type: SNR = 28.8063dB; Chest-belt-type: SNR = 24.44dB; Curved-X-type: SNR = 21.47dB; X-type: SNR = 19.65dB).

Varadan et al. (2011) implemented an e-bra for heart monitoring using two gold nanowire electrodes woven into a standard bra. Attached to the bra was an e-Nanoflex module used to acquire ECG data and transmit the signal to a mobile phone for display. The e-bra was designed as a single-lead ECG monitor based on a modified two electrodes placement. Vehkaoja et al. (2011) also described a wireless wearable ECG monitor for night-time heart detection where three textile electrodes were implanted in a measurement T-shirt. The authors reported 99.8% ECG R-peak recognition and a positive contribution to signal quality by sweating.

An unobtrusive night-time ECG monitor based on eight silver-coated polyamide yarn electrodes embroidered into a bed sheet was reported by Peltokangas et al. (2012). Wires were woven between the bedsheet and the mattress to connect the ECG sensors and ECG hardware. A Universal Serial Bus (USB) was used for buffering data from the ECG monitor to the processing computer. Data were analysed offline using MATLAB software. Using Zhengzhou's R-peak detection method, an average 94.9% heartbeat detection rate based on ECG signals collected from healthy men over 29 nights (213.8 hours of data) was reported.

Pereira et al. (2013) implemented a wearable vital sign measurement shirt based on ADS1198 multichannel, 16-bit delta-sigma analogue to digital converter from Texas Instruments and three textile sensors. The ADS1198 was connected to the NI USB-8451 board from National Instruments via a serial peripheral interface (SPI) and through USB to a processing computer. LabVIEW installed on a computer was employed to configure, acquire, and process bio-signals from the ADS1198. Compared to the dry textile electrodes, ECG from wet textile electrodes produced higher signal quality (no quantitative data was reported).

Lim and Kim (2014) presented a wearable healthcare system based on three textile electrodes integrated into the chest area of the clothing to replace the ECG from the standard limb leads. The ECG hardware was equipped with a bandpass filter (0.5Hz – 50Hz) frequency range as well as an adaptive impulse correlation filter. As the ECG was acquired from modified bipolar electrodes which are different from the standard ECG and Mason-Likar (Papouchado et al., 1987) lead placements, the authors conducted a correlation study. The ECG acquired from their system showed a high correlation (Pearson Correlation, R = 0.95) with the ECG acquired at the precordial V3 lead position of the standard 12-lead ECG.

Morrison et al. (2014) integrated 12 textile electrodes based on Mason-Likar electrode placement and power-efficient wireless HR monitoring into a garment. The Mason-Likar electrode placement is a modified version of the standard 12-lead ECG where the extremity electrodes (RA, LA, RL and LL) in the standard 12-lead ECG are moved to the trunk to mitigate excessive motion artefact during stress ECG (Clifford et al., 2006). The authors reported that the shirt acquired and wirelessly transmitted an encrypted 12-lead ECG up to 10m from the user and consumed 984μW power. When the control unit was configured to acquire a single lead ECG, the power consumption was reduced to 95μW.

Takahashi et al. (2015) proposed a home-based single lead e-textile cardiac monitor for infants. Three textile ECG sensors were placed on the palm side of the participant's wrist using a modified bipolar electrode placement. The test results showed 96% accuracy of R-wave detection and 1% RR interval error for resting and minor movement.

Wang et al. (2015) combined the concept of e-textile and wireless sensor networks to develop an ECG monitor comprised of a smart garment, sensor node containing ECG hardware and a Bluetooth module, gateway server (android tablet), and a health cloud. Though the number of electrodes used was not explicitly mentioned, the garment-integrated sensors were arranged to pick a signal of lead-II equivalent from a standard lead configuration. The authors reported 37 dB signal to noise ratio (SNR) based on KL-79106 ECG simulator and 99.5% average QRS detection sensitivity and positive prediction using data from the MIT database.

Boehm et al. (2016) developed a multichannel Holter monitor from textile electrodes embedded in a T-shirt. The prototype was tested on three scenarios (lying down, sitting, and walking). The RR intervals were extracted and compared with the results of a reference Holter monitor where a low mean relative error of 0.96% was obtained.

Noncontact (Capacitive) ECG acquisition

Ueno et al. (2007) studied the application of capacitively coupled textile electrodes for ECG acquisition. Two square textile sensors were secured to a mattress aligning to the right and left scapulae of the subject when lying in the supine position. A reference electrode was positioned at the lower right back region. A bedsheet was used as the dielectric material for the capacitive sensors to acquire ECG from the dorsal area of the body. The authors examined the effect of electrode contact area on signal quality by applying different size electrodes (10, 40, and 70cm^2). ECG acquired from the 70cm^2 showed a higher gain across the entire ECG bandwidth (0.01Hz - 500 Hz) where ECG from the 10cm^2 textile electrodes showed distorted QRS complex (no quantitative data was reported). Clothing of thickness 395µm, 463µm, and 1020µm was used to study the effect of clothing thickness on capacitive coupling, where increasing thickness resulted in higher signal quality. Compared to a reference ECG, the ECGs from their system showed higher noise level (no quantitative data was reported).

Fuhrhop et al. (2009) proposed a multi-layered capacitive textile electrode with an inbuilt amplifier and impedance matching circuits and a large reference electrode (an area of 250cm^2) to acquire ECG. The authors reported that the ECG collected from capacitive-coupled electrodes while the subject was casually walking and sitting on a chair showed increased noise compared to the ECG acquired from the contact-based textile electrodes.

Chamadiya et al. (2013) exploited the concept of capacitive coupling to implement a contactless textile ECG monitor for a non-intensive care unit setup. As the ECG signal acquired through capacitive coupling is noisy, a robust signal conditioning circuit comprised of pre-and post-amplifiers, and an analog signal processing differential filter was employed. They tested the system in different setups (on a stretcher, hospital bed, and wheelchair), and concluded that capacitively coupled electrodes could be a potential option for long term ECG monitoring.

Atallah et al. (2014) used an array of eight capacitively coupled textile electrodes embedded in the middle of a mattress guarded by a reference electrode to monitor babies in the neonatal intensive care unit. The special electrode placement guaranteed a minimum of two textile sensors aligned with the baby's body. According to the report, experimental conditions affected the HRV, where neonates in the prone position showed better ECG readings. Moreover, automatic channel selection produced a better result compared to the manual counterpart, and motion artefact and poor electrode-body contact affected ECG quality.

Cai et al. (2017) reported a flexible printed circuit board-based single-lead ECG module, from three textile electrodes embedded in a garment together with a smartphone display. A spongy gap filler backed the circular electrodes to a convex structure. Testing the prototype in different conditions (standing, sitting, lying in the supine position, and walking at 5 km/h), the authors concluded that the proposed capacitive ECG monitor could produce acceptable ECG tracing.

Instead of a rigid electrode, Li et al. (2017) used a conductive textile woven with stainless steel of 0.1mm diameter as a capacitive electrode. As the surface of the textile electrode was flexible, coupling capacitance varied continuously, which in turn affected the stability of the data acquisition system. Li's suggested solution was to use a three-dimensional woven composite conductive textile electrode. The proposed textile electrode exhibited high delamination and impact resistance, super damage tolerance, and high density that enabled the textile electrode to retain its shape and produce a stable coupling capacitance. The predicted coupling capacitance was proportional to the quality of the ECG data acquired. Practically, the signal received from the electrodes was in the order of mV but affected by interference noise.

Sun et al. (2017) suggested an e-textile H-shirt for exercise ECG monitoring and lactate measurement. Most of the research done on textile electrodes to acquire ECG is prone to an unstable skin-electrode interface, and hence, motion artefact is the major issue, especially during exercise. To alleviate this problem, the authors proposed a textile ECG electrode integrated into a highly elastic shirt, which ensures better skin-electrode contact.

The common theme reported across the studies was motion artefact. As the textile electrodes were not attached to the skin firmly, electrode movement relative to the skin was observed. The most reported ECG configuration was single-lead ECG. However, 12-lead ECG is the gold standard and in the case of noisy ECGs, the availability of redundant leads increase the dynamic range in the acquired signal. In this regard, the problems summarised above will be addressed in the thesis.

The studies detailed in section 1.1.2.2 were either at their experimental stage or were evaluated based on either simulated data, data from the MIT-BIH Arrhythmia Database, healthy volunteers, or a combination. For the purpose of this thesis, which is focused on CR, a systematic scoping review of the literature on electronic-textile ECG monitoring of cardiac patients was conducted and will be presented in Chapter 2.

1.2. Context

Summarized below are the underlying concepts which informed the need for Ph.D. research.

The need for long-term cardiac monitoring

Scholars pointed out that CVD is the number one non-communicable disease causing death worldwide with an estimated life loss of 17.92 million people in the year 2015 (Roth et al., 2017a, p. 10). Each year this number keeps growing, with the estimated worldwide annual death toll from CVD predicted to be 23.6 million by 2030 (Loue and Sajatovic, 2012, p. 362). Cardiac disease and stroke constituted more than 85% of the CVD incidents (Laidler, 1994, Fawcus, 2000, Roth et al., 2017a, Roth et al., 2018, Zipes et al., 2019).

Based on the Australian Institute of Health and Welfare (2016) data, CVD continues to be the leading lethal chronic disease in Australia. Deaths due to CVD even exceed deaths due to cancer (Australian Institute of Health and Welfare, 2016). For example, CVD accounted for 34% of total deaths in 2008 compared with 29% from cancer (Australian Institute of Health and Welfare, 2011b). A report from the National Heart Foundation of Australia (National Heart Foundation of Australia, n.d.) showed that in 2017, around 43,500 people died due to CVD. CVD affects one person in six in Australia and kills one individual every 12 minutes. From all CVD incidents, coronary heart disease is the leading disorder, with 18,590 (12% of all deaths) in 2017 alone. Coronary heart disease continues to claim one life every 28 minutes (National Heart Foundation of Australia, n.d.).

In Australia, there were more than half a million hospitalizations due to CVD as a primary cause in 2016/17 (National Heart Foundation of Australia, n.d.). As a result, the burden on health care providers is tremendous considering the unprecedented increment of life expectancy over the last decades. Beyond Australia, cardiovascular traumas have an enormous effect on the global economy, and on lower and middle-income countries in particular (Roth et al., 2018).

According to Jahrsdoerfer et al. (2005), the majority of the cardiac ischaemic events (70% - 90%) detected on the ECG tracing are clinically silent. Decker et al. (2003) recommended 12-lead continuous ECG monitoring to record the onset of infrequent acute coronary syndrome events. Moreover, a study published in 2019, long-term ambulatory ECG monitoring plays a vital role in detecting the onset of ventricular dysrhythmias and atrial fibrillation. Ventricular dysrhythmias are the prominent factors indicating heart failure, stroke, and cardiac death. Therefore, there is an increased demand for long-term cardiac monitoring (2019a).

Cardiac rehabilitation at home: a viable option for the centre-based program

So far, two CR contexts are reported: home-based and in the hospital. Different scholars studied the possibilities of HBCR as a potential replacement for the standard centre-based approach.

Dalal et al. (2010) compared both the home-based and centre-based CR of patients mainly after myocardial infarction or revascularization. The authors reported that there was no noticeable difference between both methods and concluded they could be used interchangeably (Dalal et al., 2010).

In a randomized controlled trial comprised of 525 patients (myocardial infarction or coronary revascularization), Jolly et al. (2009) revealed that there was no significant difference between the home-based monitoring and the control group (hospital setup) (Jolly et al., 2009).

In a related study, Oerkild et al. (2012) conducted a randomized clinical trial (n = 40 patients; age = 65 - 92 years) and reported an increased exercise capacity (six minute-walk test) of the cardiac patients in a home-based setup (increased distance from baseline = 33.5m, p=0.02) compared to the in-hospital CR program (increased distance = 10.1m, p=0.5) (Oerkild et al., 2012).

The main hindering factors that affect centre-based CR include the distance from the service centres and hence, transportation issues, strict rehabilitation schedules compared to the participant's job and / or community obligations, and no insurance to cover the CR costs (Jones et al., 2007, Bakhshayeh et al., 2019).

On the other hand, HBCR showed better adherence and lower dropout rates to the centre-based rehabilitation program (mean number of sessions/week, home-based = 3.2 ± 1.0; centre-based = 2.7 ±1.3) over six months (Carlson et al., 2000). In a similar study, Arthur et al. (2002) compared home-based and hospital-based cardiac rehabilitation of patients after Coronary Artery Bypass Grafting. Using the RAND SF-36 survey tool, the home-group reported higher social support (home-group = 36.0 ± 4.9; hospital-group = 34.6 ± 6.4; p = 0.05) and superior improvement in 'health-related' quality of life (home-group = 51.2 ± 6.4; hospital-group = 48.6 ±7.1; p = 0.004). Therefore, it is reasonable to assume that CR in the home could be an alternative solution to mitigate the growing demand for CR and continuous follow-up. In this regard, this research was focused to design, develop, implement, and test a 12-lead diagnostic quality textile-based ECG that could be used to monitor cardiac patients at home.

In this research we are targeting high-risk patients who have limited access to specialist care such as rural and remote patients with chronic cardiac conditions such as heart failure (CHF). These populations can benefit most from CR with significant improvements in exercise capacity, quality of life and reduction in hospitalisations. Despite its reported benefits, only a small number of patients with CHF attend CR due to poor adherence, and improper exercise may even lead to adverse events. Remote ECG monitoring system has the potential to overcome these obstacles. Cardiac telerehabilitation using monitoring devices and remote communication with patients is now increasingly used for long-term management of cardiovascular diseases outside the hospital environment. Providing objective feedback data and allowing patients to track their own progress can improve patients' self-management skills and thereby improve their adherence. Home based monitoring is convenient, can reduce anxiety, and improve the quality of life and prognosis of patients at lower medical costs compared with conventional CR without monitoring.

E-Textiles based technologies as an alternative solution for the growing demand for healthcare

Population aging in developed countries increases the demand for available health care. At the same time, the prevalence of CVD is also higher in this group (Mukhopadhyay, 2015). These demographic changes are placing increasing pressures on the medical system, where CVD is the primary reason for hospitalization, especially for older people

(National Heart Foundation of Australia, n.d.). Electronic-textile (e-textile) based cardiac monitoring offers a viable option (Jolly et al., 2009, Sarela et al., 2009) where the long-term ambulatory monitoring can be conducted outside of the hospital premises.

The future of wearable and electronic textiles: financial implication

During the last two decades, wearable technology research and industries showed unprecedented growth (Tong, 2018), where the global market value by 2025 is forecasted to be $62.82 billion (2019c). A 2019 report on the commerce of smart textiles predicted that the e-textile technology market was $878.9 million in 2018 and would grow at a compound annual growth rate of 30.4% to $5.55 Billion by 2025 (2019b).

1.3. Thesis Outline

The thesis is composed of seven chapters and 11 appendices.

Chapter 1 is an introduction that covers the background and the context of the thesis examining the cardiovascular system and technologies applied to CR. A systematic scoping review on electronic textile-based ECG monitoring of cardiac patients is detailed in Chapter 2. Chapter 3 presents the research design and outlined methodologies.

The design, analysis and implementation of the hardware, software, smart ECG vest, and textile electrodes of the proposed textile-based ECG monitor are presented in Chapter 1. Chapter 1 also addresses the specification and component selection, progressing through detailed design and analysis followed by simulation and prototyping.

Following the successful construction of the textile-based ECG monitor, module-level testing and evaluation were performed. The module-level testing and analysis were conducted according to the experimental protocols outlined in Chapter 5, sections 5.3.1.2, 5.3.2.2, and 5.4.1.2 and the results are presented in Chapter 5, sections 5.3.1.3, 5.3.2.3, and 5.4.1.3. Furthermore, the compression pressure applied by the vest for a readable ECG tracing was experimentally estimated and the results are presented in Chapter 5, section 5.4.2.5.

Chapter 6 is dedicated to system-level testing and evaluation. The first stage of the testing studied the influence of electrodes' characteristics on signal quality (section 6.4). The effect of smart ECG vest design, electrode placement and the textile electrode to the smart ECG vest attachment on the acquired ECG was examined (section 6.5). Moreover, it compares the ECG signal collected from textile electrodes and the commercial wet-gel electrodes using the proposed textile-based ECG monitor (section 6.6). In the second stage of testing (section 6.7), the performance of the proposed ECG monitor was compared against the traditional reference Holter monitor using measurable signal quality matrices.

In Chapter 7, the limitations and recommendations are presented following the thesis summary and contributions to the textile-based ECG monitoring. Finally, it concludes that *the proposed textile-based EASI 12-lead equivalent ECG monitor could be a viable option for long-term real-time monitoring of cardiac activities, and a clinical trial is recommended based on a population with a known cardiac disease to validate and produce clinically significant results*.

This page is left blank intentionally

Chapter 2. Electronic-textile electrocardiogram monitoring in cardiac patients: a scoping review

2.1. Introduction

CVDs are disorders of the heart and blood vessels and include coronary heart disease, cerebrovascular disease, and rheumatic heart disease, among other conditions. Four out of five CVD deaths are due to heart attacks and strokes. Individuals at risk of CVD may demonstrate raised blood pressure, glucose levels and lipid levels, as well as overweight and obesity. These can all be easily measured in primary care facilities. Identifying those persons at the highest risk of CVDs and ensuring they receive appropriate treatment can prevent premature deaths. Access to essential medicines and basic health technologies in all primary healthcare facilities is essential to ensure that those in need receive treatment and counselling (Lorimer and Hillis, 1985, Mackay and Mensah, 2004, Caplan and Sumner, 2006, Sankaran, 2012).

CVD is the number one cause of death globally, accounting for more people annually than any other non-communicable disease (Naghavi et al., 2017, Roth et al., 2018). An estimated 17.92 million people died of CVD in 2015 (Roth et al., 2017b). The global death toll dropped slightly to 17.6 million in 2016 (Naghavi et al., 2017) and rose again to 17.8 million in 2017 (Roth et al., 2018). Within CVD related deaths, 85% result from a heart attack and stroke. Over three-quarters of CVD deaths take place in low- and middle-income countries (Naghavi et al., 2017, Roth et al., 2018).

Clinical practices of CR are based on evidence-based medicine (National Heart Foundation of Australia, 2012, Amsterdam et al., 2014, Woodruffe et al., 2015, Chew et al., 2016). In general, CR strives to reduce cardiac-related morbidity and mortality and to maximize the physical function of patients so that they can perform activities of daily living (Schwaab, 2010, Woodruffe et al., 2015). A contemporary CR program involves physicians and allied health professionals working together to deliver an extensive program that can reduce the risk of further cardiac episodes. Structured exercise programs are among the core constituents of a CR program, which are prescribed based on two important factors: specificity of the training, and progressive overload. Varieties of CVDs affect the cardiovascular organs differently and the concept of specificity plays an essential role in assessing and develop an individualized exercise package appropriate to the patient. The second concept of progressive overload refers to the three adjustable parameters (intensity, duration and frequency) of the performed exercise. These parameters should be fine-tuned to deliver enough stimulus to the desired organ that then triggers a visible result (Kraus and Keteyian, 2007). Intensity dictates HR and ratings of perceived exertion that are of clinical importance for CR. For a normal person, the HR and peak oxygen consumption show a linear relation (Kraus and Keteyian, 2007). Hence, the target in CR is to develop an effective physical activity plan that results in a comparable response and targeted HR (Kraus and Keteyian, 2007).

The ECG refers to the electrical activity of the heart. It is a function of the potential difference between two electrodes placed on the body (John Bullock et al., 2001, Arthur

C. Guyton and Hall, 2006, Rogers, 2011, Eric P. Widmaier et al., 2014). ECG is essential to evaluate and predict life-threatening ventricular arrhythmia and is one of the critical components monitored across the delivery of prescribed exercise programs in cardiac patients (Keteyian et al., 1995, Meissimilly et al., 2009, Kim et al., 2012, Price et al., 2016). Graded exercise test (clinically known as stress ECG test), for instance, is one of the common exercise packages performed in controlled hospital premises. It finds application in the diagnosis of ischemia, the prognosis of cardiac events and the assessment of functional capacity. The results of the stress ECG test are used as a baseline for the prescription of exercise therapy in CR programs. Graded exercise testing in coronary heart disease patients provides an estimation of ST-segment depression, HR, blood pressure and overall exercise performance (Kraus and Keteyian, 2007).

CVD has also been reported to be the primary reason for hospitalization, especially for the elderly (National Heart Foundation of Australia, n.d.). Indeed, healthcare providers are already struggling to cope with demand, and there is increasing pressure to promote home-based healthcare services. For patients with cardiac disease, e-textile based rehabilitation programs may offer a viable option, particularly if the CR and / or monitoring can take place in the community and outside of major hospitals, reducing the burden on an already struggling healthcare system (Jolly et al., 2009, Sarela et al., 2009).

2.1.1. The rationale for the scoping review

To scope the current research on e-textile use for cardiac monitoring, a preliminary initial search in PubMed and IEEE Xplore was conducted followed by the analysis of text words contained in the title and abstract, and of the index terms used to describe the articles.

We identified several peer-reviewed studies on e-textile based ECG monitoring of cardiac patients (Di Rienzo et al., 2005, Coosemans et al., 2006, Di Rienzo et al., 2010, Di Rienzo et al., 2013, Balsam et al., 2018, Di Rienzo et al., 2006a). Additionally, the authors identified one scoping review (Fleury et al., 2015) focused on the usability of e-textile technology across a broad range of clinical rehabilitation, but was not specific to cardiac applications. Therefore, this scoping review explored the research literature on the use of e-textiles for ECG monitoring (resting, signal-averaged, ambulatory or exercise) of cardiac patients in a healthcare setting, community or home setting.

2.1.2. Review questions

The research questions for this scoping review were:

1. What is known from the existing literature about utilizing e-textile ECG to monitor cardiac patients?
2. What are the basic physiological parameters that can be measured using e-textile based ECG monitoring of cardiac patients?
3. When considering e-textile based ECG monitoring of cardiac patients:
    a. How many and what type of sensors are required for precise detection of the respective parameters?
    b. How are the issues of data storage, connectivity and power requirements addressed?
    c. How are signal quality and stability managed for extended ambulatory activities?

2.2. Methods

This scoping review was conducted strictly following the JBI methodology for scoping reviews (Aromataris and Munn, 2017). This review was conducted following a priori protocol (Teferra et al., 2019a).

2.2.1. Inclusion criteria

2.2.1.1. Participants

In this scoping review, only research studies that included patients who qualified for CR programs or continuous ambulatory monitoring were considered. Studies with patients who experienced one or more of the following cardiac events were considered for inclusion: i) heart failure, ii) cardiomyopathy conditions, iii) medically managed acute myocardial infarction (MI), either STEMI (ST-elevation myocardial infarction) or non-STEMI, which includes or excludes post-MI revascularization, iv) medically managed coronary artery disease (CAD) (e.g., stable angina), v) revascularization procedures, including percutaneous coronary interventions and/or coronary artery bypass graft surgery, vi) post insertion of the implantable defibrillator and permanent pacemaker, vii) repair and replacement of valve device(s), viii) device implant for ventricular assist, and ix) heart transplant.

2.2.1.2. Concept

The key concepts that were addressed were resting, signal-averaged, ambulatory or exercise ECG monitoring based on e-textile technologies or e-textile based CR. Studies were not considered if they focused only on specific aspects of the e-textile ECG monitor rather than a complete ECG monitor. For example, studies were excluded if they solely focused on the e-textile electrodes / active electrode design, software algorithms, Graphic User Interface (GUI) design, web socket or application program development, optimal electrode placement, wireless sensor topology / body area network / healthcare network. In addition, due to time constraints and lack of budget for translation, only studies written in English were considered.

2.2.1.3. Context

The context for this scoping review was the globally published and unpublished research literature on e-textile use for cardiac patients as an in-hospital patient or outpatient and its use for home-based exercise or long-term ambulatory monitoring.

2.2.1.4. Types of studies

This scoping review considered both experimental and quasi-experimental study designs, including randomized controlled trials, non-randomized controlled trials, before and after studies, and interrupted time-series studies. In addition, analytical observational studies, including prospective and retrospective cohort studies, case-control studies, and analytical cross-sectional studies, were considered for inclusion. This review also considered systematic reviews, descriptive observational study designs, including case series, individual case reports and descriptive cross-sectional studies for inclusion.

The number of research studies conducted on e-textile technologies has increased in the last two decades. Additionally, e-textile based ECG technologies did not exist before 2000 (Teferra et al., 2019a). Therefore, studies published in English and published from January 2000 to March 2018 were considered for inclusion in this review.

2.2.2. Search strategy

The search strategy aimed to find both published and unpublished studies. A three-step search strategy was used. An initial limited search of PubMed and IEEE Xplore was undertaken, followed by an analysis of the text words contained in the title and abstract and the index terms used to describe the articles. A second search using all identified keywords and index terms was undertaken from August 2017 to March 2018 across the following databases and registered trials: Ovid Medical Literature Analysis and Retrieval System Online (Medline), PubMed Central (PMC), Institute of Electrical and Electronics Engineers (IEEE Xplore), Cumulative Index to Nursing and Allied Health Literature (CINAHL), Cochrane Database of Systematic Reviews, Web of Science, Scopus, Expanded Academic ASAP, ProQuest, ProQuest Dissertations & Theses Global, SPORTDiscus, ENGINE – Australian Engineering Database (Informit) and Google Scholar; Cochrane Central Register of Controlled Trials, ClinicalTrials.gov, Australian New Zealand Clinical Trials Registry (ANZCTR) and Clinical Trials Connect (CTC). The search for unpublished studies and gray literature included reference lists, book chapters, and theses as well as conference studies. Finally, the reference lists of all reports and articles selected for critical appraisal were searched for additional studies. The full search strategy is provided in Appendix A.

2.2.3. Study selection

Following the search, all identified citations were loaded into Endnote V8.2 (Clarivate Analytics, PA, USA) with duplicates removed. Titles and abstracts were screened by two independent reviewers (MT and JR) for assessment against the inclusion criteria for the review. The full text of potentially eligible studies was retrieved and assessed in detail against the inclusion criteria by two independent reviewers (MT and JR). The details of studies that met the inclusion criteria were imported into the Joanna Briggs Institute's System for the Unified Management, Assessment and Review of Information. Full-text studies that did not meet the inclusion criteria were excluded and reasons for their exclusion are provided in Appendix B and Appendix C. Any disagreements that arose between the reviewers were resolved through discussion or with a third reviewer (CK).

2.2.4. Data extraction

Data were extracted from studies included in the review by two independent reviewers (MT and JR), using a modified data extraction tool attached in Appendix D and Appendix E. The data extracted included specific author details, year, and country, aims, purpose or objectives of the study, sample size and type of participants, electronic-textile integration, physiological parameters monitored, number of leads, ECG acquired, application platform, and context and key findings related to the scoping review questions. Any disagreements that arose between the reviewers were resolved through discussion or with a third reviewer. Authors of studies were contacted to request missing or additional data if required.

2.3. Results

2.3.1. Characteristics of included studies

Addressing the objectives proposed in the scoping review protocol, common themes across the included articles were analysed. The first author (MT) charted the critical features of e-textile based ECG monitoring using the data extraction tool (Appendix D) by reading each article. The co-authors later verified the results. Aligned with the Population, Concept and Context (PCC) mnemonics, three thematic frameworks for analysis and discussion were proposed:

- Population:
    - Adult cardiac patients and paediatric/neonates
- Concepts:
    - Features of the ECG monitors
    - Level of electronic integration
    - Quality control
    - Physiological parameters monitored.
    - Sensor specifications
    - Data storage, connectivity, and power requirements
    - Signal quality and stability
    - Context: inpatient and outpatient services

These themes were selected based on the review questions and literature analysis. The narrative summary presented in section 2.3.3 was based on these thematic frameworks.

2.3.2. Study inclusion

The search conducted on September 6, 2017 identified 1965 citations and 24 grey literature articles, of which 995 duplicates were removed. An additional 787 titles did not meet the eligibility criteria. Abstracts of 207 publications were reviewed for further eligibility, of which 168 studies were excluded with justification (Appendix B). Moreover, 38 study authors were contacted to request missing or additional data as required, with 16 responding within eight weeks. The remaining 22 studies were excluded (Appendix C). Therefore, the final data set comprised of 17 studies. Two of the studies (Bourdon et al., 2005, Di Rienzo et al., 2005) were published in 2005, three studies (Coli et al., 2006, Coosemans et al., 2006, Di Rienzo et al., 2006a) in 2006 and the remaining 12 studies after January 2010. Fourteen of the studies were from Europe (Spain (n=5), Italy (n=4), Belgium, France, Germany, Poland, and Portugal (n=1; each)). The remaining three studies were from Asia (Taiwan (n=1), Thailand (n=1) and India (n=1)). The search results are summarized in the PRISMA flow diagram (Figure 2.1).

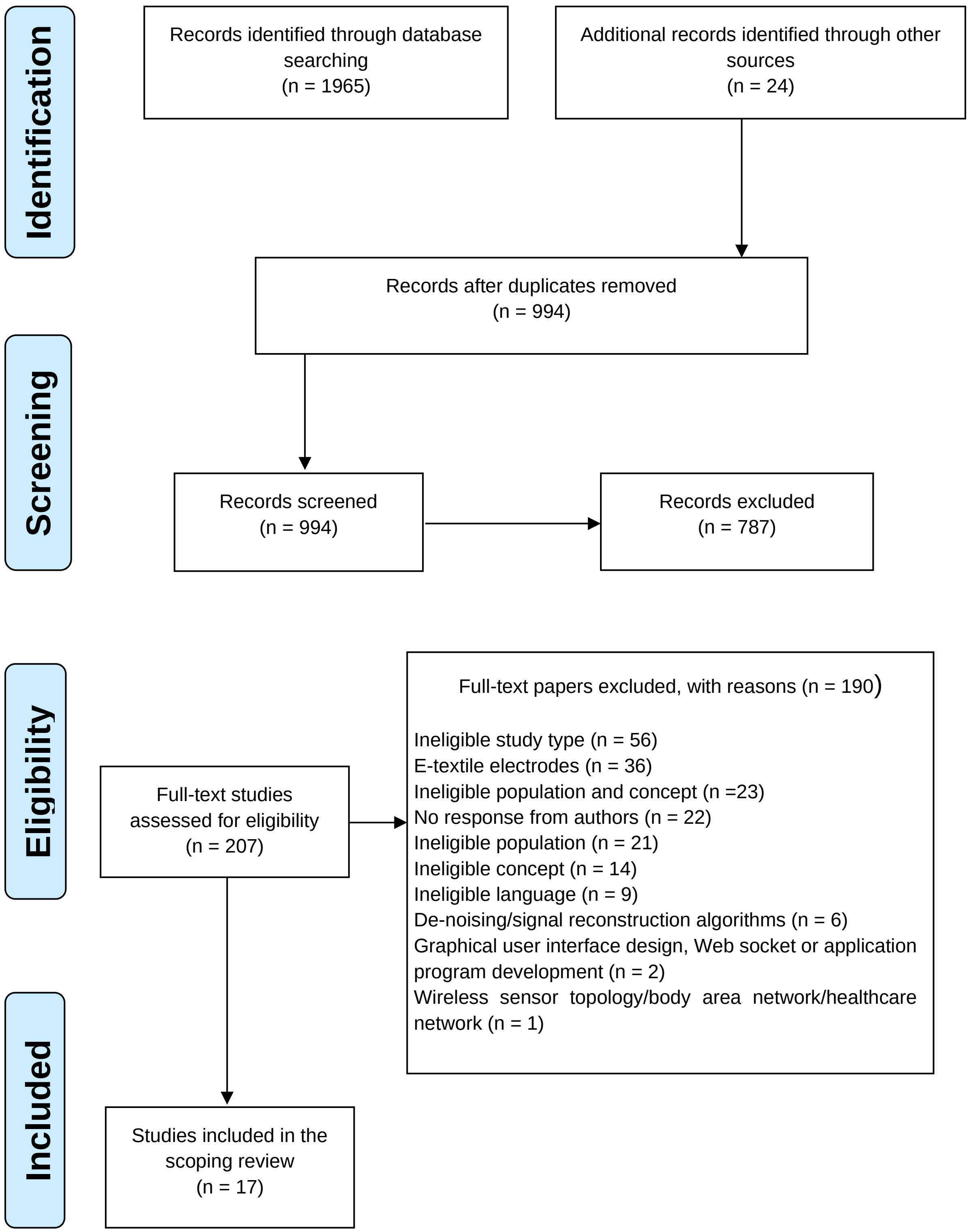

Figure 2.1: PRISMA flow diagram: search results, study selection, and inclusion of the scoping review

2.3.3. Narrative summary of the review findings

Resting ECG was the most common form of ECG acquired (n=10) (Bourdon et al., 2005, Di Rienzo et al., 2005, Coli et al., 2006, Coosemans et al., 2006, Di Rienzo et al., 2013, Olmos et al., 2014, Hsiao et al., 2015, Yu et al., 2017, Balsam et al., 2018, Di Rienzo et al., 2006a) followed by exercise ECG (n=6) (Di Rienzo et al., 2005, Coli et al., 2006, Perez De Isla et al., 2011, Di Rienzo et al., 2013, Romagnoli et al., 2014, Di Rienzo et al., 2006a) and ambulatory ECG (n=5) (Bourdon et al., 2005, Di Rienzo et al., 2013, Yu et al., 2017, Balsam et al., 2018, Di Rienzo et al., 2006a). Table 2.1 shows the number of e-textile based ECG monitoring of cardiac patients. A detailed summary outlining the study characteristics and technical specifications of the garments presented is reported in Appendix D and Appendix E, respectively.

Table 2.1: Summary of e-textile based cardiac monitoring.

S. No.	ECG acquired	No. of studies (n=17)
1.	Resting ECG (Bourdon et al., 2005, Di Rienzo et al., 2005, Coli et al., 2006, Coosemans et al., 2006, Di Rienzo et al., 2013, Olmos et al., 2014, Hsiao et al., 2015, Yu et al., 2017, Balsam et al., 2018, Di Rienzo et al., 2006a)	10
2.	Exercise ECG (Di Rienzo et al., 2005, Coli et al., 2006, Perez De Isla et al., 2011, Di Rienzo et al., 2013, Romagnoli et al., 2014, Di Rienzo et al., 2006a)	6
3.	Ambulatory ECG (Bourdon et al., 2005, Di Rienzo et al., 2013, Yu et al., 2017, Balsam et al., 2018, Di Rienzo et al., 2006a)	5
4.	Not mentioned (unknown) (Di Rienzo et al., 2010, Lopez et al., 2010, Kakria et al., 2015, Trindade et al., 2016, Pandian and Srinivasa, 2016)	5

Note: *Some studies use multiple types of ECG monitoring*

2.3.3.1. Number of participants and target population

Of the 17 studies reviewed, 16 studies reported a sample size of two or more cardiac patients ((n=220) (Balsam et al., 2018), (n=40) (Di Rienzo et al., 2013, Kakria et al., 2015), (n=31)(Perez De Isla et al., 2011, Olmos et al., 2014, Romagnoli et al., 2014, Hsiao et al., 2015, Di Rienzo et al., 2006a), (n=15) (Di Rienzo et al., 2005, Coli et al., 2006), (n=8) (Trindade et al., 2016), (n=5) (Bourdon et al., 2005, Lopez et al., 2010, Yu et al., 2017), (n=3) (Di Rienzo et al., 2010) and (n=2)(Coosemans et al., 2006)). For the remaining study (Pandian and Srinivasa, 2016), the sample size was not clearly stated.

Fifteen studies (88%) focused on adult populations. On the other hand, critically ill premature infants, as well as full born neonates, require continuous physiological monitoring. However, only Coosemans et al. (2006) examined neonates where the prototype was tested on two infants aged 12 and 21 weeks. Additionally, Balsam et al. (2018) investigated both adults and neonates and discussed the challenges of using the Nuubo ECG monitor in the paediatric population.

2.3.3.2. Concepts

Features of the ECG monitors

Recent advancements in the field of e-textiles have led to the integration of ECG monitors into various garments sensing multiple physiological parameters. Concerning established garments, the Maglietta Interattiva Computerizzata (MagIC) system was the most studied system (n=4) (Di Rienzo et al., 2005, Di Rienzo et al., 2010, Di Rienzo et al., 2013, Di Rienzo et al., 2006a), closely followed by the Nubbo ECG monitor (commercially developed ECG by Nuubo, a European company developing health technology, located in Spain; n=3) (Perez De Isla et al., 2011, Olmos et al., 2014, Balsam et al., 2018) and the WEALTHY system (Wearable Health Care System project by the European Commission from 2002-2005; n=2) (Bourdon et al., 2005, Coli et al., 2006).

The most commonly reported ECG monitor characteristics included frequency response, power requirement, wireless communication, data storage and application platform. The majority of the studies (n=11) (Bourdon et al., 2005, Di Rienzo et al., 2005, Coli et al., 2006, Di Rienzo et al., 2010, Di Rienzo et al., 2013, Romagnoli et al., 2014, Hsiao et al., 2015, Kakria et al., 2015, Yu et al., 2017, Balsam et al., 2018, Di Rienzo et al., 2006a) did not specifically report the frequency response. Eight (47%) (Coosemans et al., 2006, Di Rienzo et al., 2010, Lopez et al., 2010, Di Rienzo et al., 2013, Trindade et al., 2016, Yu et al., 2017, Balsam et al., 2018, Pandian and Srinivasa, 2016) studies provided information about the power requirement of the e-textile based ECG monitor, where low power consumption was the most common feature.

Regarding wireless communication, Bluetooth was the most popular choice, with 41.2% (n=7) (Perez De Isla et al., 2011, Di Rienzo et al., 2013, Olmos et al., 2014, Hsiao et al., 2015, Trindade et al., 2016, Balsam et al., 2018, Di Rienzo et al., 2006a) followed by general packet radio service (GPRS) (n=2) (Bourdon et al., 2005, Coli et al., 2006) and combined wireless communication (based on WIFI / 3G/ GPRS and Bluetooth; n=2) (Di Rienzo et al., 2010, Kakria et al., 2015). Four studies (Di Rienzo et al., 2005, Coosemans et al., 2006, Romagnoli et al., 2014, Yu et al., 2017) did not mention the wireless communication protocol applied to their system.

Kakria et al. (2015) and Trindade et al. (2016) both addressed the issue of data privacy and security during the time of wireless transmission. Approximately half of the included studies (Di Rienzo et al., 2010, Perez De Isla et al., 2011, Di Rienzo et al., 2013, Olmos et al., 2014, Romagnoli et al., 2014, Kakria et al., 2015, Yu et al., 2017, Balsam et al., 2018) reported the use of a memory card to store the acquired ECG signal locally or as intermediate storage. Additionally, a personal computer (PC) was used to acquire, visualize and store ECG data in five e-textile ECG monitors (Di Rienzo et al., 2005, Coli et al., 2006, Lopez et al., 2010, Di Rienzo et al., 2006a, Pandian and Srinivasa, 2016). The platform is a way of presenting the data for the user, with computer-based applications the most popular platform (n=10) (Bourdon et al., 2005, Coli et al., 2006, Di Rienzo et al., 2010, Perez De Isla et al., 2011, Di Rienzo et al., 2013, Olmos et al., 2014, Hsiao et al., 2015, Balsam et al., 2018, Pandian and Srinivasa, 2016). Trindade et al. (2016) reported the only study using a mobile-based wireless ECG, while three studies (Di Rienzo et al., 2005, Kakria et al., 2015, Di Rienzo et al., 2006a) described a dual-modality (both computer and personal digital assistant (PDA) / mobile-based) application platform. It is unclear how the data were presented to the user in the remaining three studies (Coosemans et al., 2006, Romagnoli et al., 2014, Yu et al., 2017).

One of the cornerstones for the design and implementation of a wearable technology that significantly affects the acceptance and performance of the system is unobtrusiveness and comfort to the wearer. Comfort and proper adherence to the wearable systems were mentioned in more than 82% (n=14) of the studies. However, only five groups of researchers conducted qualitative (Di Rienzo et al., 2010, Di Rienzo et al., 2013) or quantitative (Bourdon et al., 2005, Coli et al., 2006, Hsiao et al., 2015) studies on the level of comfort. Collecting feedback from participants regarding the level of comfort, 27 out of 30 (Di Rienzo et al., 2010) and 38 out of 40 (Di Rienzo et al., 2013) participants responded that the MagIC was comfortable. On the other hand, Coli et al. (2006) conducted an ad-hoc comfort scale (1 worst, 5 best) interview and reported a comfort level of 3.93 ± 0.80 while Hsiao et al. (2015) reported a comfort level of 4.2/5.0.

Level of electronic integration to the garment

Electronic integration into the textile clothing was one specific concept investigated by this scoping review. In all studies, the textile electrodes were embedded in the garment. However, advanced development was evident in three studies (Coosemans et al., 2006, Trindade et al., 2016, Pandian and Srinivasa, 2016) where off-the-shelf components or custom-made electronic boards were attached to a fabric substrate.

Quality control

Eight (47%) of the studies (Bourdon et al., 2005, Di Rienzo et al., 2005, Coli et al., 2006, Perez De Isla et al., 2011, Di Rienzo et al., 2013, Romagnoli et al., 2014, Kakria et al., 2015, Di Rienzo et al., 2006a) reported the use of a reference ECG monitor. Various studies used Wilcoxon matched pairs test, blind visual inspection, and Bland-Altman plots for data validation and check-up protocols (Di Rienzo et al., 2005, Coli et al., 2006, Di Rienzo et al., 2013, Di Rienzo et al., 2006a).

Bourdon et al. (2005) and Coli et al. (2006) reported that ECG quality was not different between the WEALTHY system and the traditional ECG monitor, while physical activity affected the signal quality in both systems. Conversely, Di Rienzo et al. (2013) specifically mentioned the MagIC textile-based wearable system as having superior quality in terms of motion artefact during physical exercise compared to the reference ECG. Perez De Isla et al. (2011) concluded that Nuubo's ECG monitor is more comfortable than conventional exercise ECG stress tests, while able to obtain similar results to the conventional exercise ECG stress tests.

Physiological parameters measured using e-textile based ECG

As expected in a review of textile-based ECG monitors, the primary physiological signal monitored was contact-based (resistive) ECG (n=17). The normal ECG morphology is composed of the P-Wave, QRS complex, T-wave and U-wave, including the PR, QT, ST and QRS intervals. In cardiology, ECG signal analysis is one of the standard methods for the diagnosis and identification of cardiac arrhythmia. The morphological parameters of diagnosis from ECG include QRS complex duration, RR interval, PR interval, QT interval, ST segment, and the R-wave amplitude. HRV analysis is a technique used to study variations in RR intervals and is useful to provide information on how the autonomic nervous system regulates cardiac activities (Romagnoli et al., 2014). Signal to noise ratio (SNR - the ratio of the strength of the ECG signal carrying information to undesired interference) indicates acquired ECG signal quality (Chakraborty and Das, 2012). Referring to the ECG features, beat-to-beat RR interval (where R is a point corresponding to the peak of the QRS complex of the ECG wave; and HRV (n= 8) (Bourdon et al., 2005, Di Rienzo et al., 2005, Di Rienzo et al., 2013, Romagnoli et al., 2014, Hsiao et al., 2015, Kakria et al., 2015, Di Rienzo et al., 2006a, Pandian and Srinivasa, 2016) followed by a signal to noise ratio (n=2) (Trindade et al., 2016, Yu et al., 2017) were the reported ECG parameters. Di Rienzo et al. (2013) specifically studied the morphology of the ECG waveforms. Almost 65% (n=11) (Bourdon et al., 2005, Coosemans et al., 2006, Di Rienzo et al., 2010, Lopez et al., 2010, Di Rienzo et al., 2013, Olmos et al., 2014, Romagnoli et al., 2014, Trindade et al., 2016, Yu et al., 2017, Balsam et al., 2018, Pandian and Srinivasa, 2016) of the studies reported the capacity of the e-textile ECG monitor to detect ECG abnormalities. Respiration was the second most explored parameter (n=6) (Bourdon et al., 2005, Di Rienzo et al., 2005, Coli et al., 2006, Di Rienzo et al., 2010, Di Rienzo et al., 2013, Di Rienzo et al., 2006a), followed by temperature (n=3) (Lopez et al., 2010, Kakria et al., 2015, Pandian and Srinivasa, 2016).

Sensor specifications

In regards to the number of ECG leads, eight (Di Rienzo et al., 2005, Di Rienzo et al., 2010, Lopez et al., 2010, Perez De Isla et al., 2011, Di Rienzo et al., 2013, Olmos et al., 2014, Hsiao et al., 2015, Di Rienzo et al., 2006a) of the included studies reported the use of two ECG electrodes followed by five (n=3),(Bourdon et al., 2005, Coli et al., 2006, Trindade et al., 2016) four (n=2)(Romagnoli et al., 2014, Balsam et al., 2018) and three (n=2)(Coosemans et al., 2006, Pandian and Srinivasa, 2016) electrodes. More than half of the included studies (59%, n=10)(Di Rienzo et al., 2005, Coosemans et al., 2006, Di Rienzo et al., 2010, Lopez et al., 2010, Perez De Isla et al., 2011, Di Rienzo et al., 2013, Olmos et al., 2014, Hsiao et al., 2015, Di Rienzo et al., 2006a, Pandian and Srinivasa, 2016) reported the use of the single-lead configuration, while only Yu et al. (2017) described a 12-lead ECG acquisition T-shirt. The 12-lead ECG is the baseline measurement and of the highest clinical relevance. The 12-lead ECG monitor has three independent and nine redundant leads. The availability of redundant leads is essential, especially for e-textile based cardiac monitoring, where motion artefact is a common problem reported across all studies. Additionally, accurate diagnosis of cardiac abnormalities often requires examination of multiple ECG leads (Drew et al., 1999). Hence, the signal acquired from 12-lead ECG has superior reliability and is less prone to data loss due to noise compared to the more common single lead configuration. One shortcoming of single lead ECG mentioned in (Di Rienzo et al., 2013) was that no reliable information regarding ST segment in ischemic patients could be obtained. In another study, Klootwijk et al. (1997) compared 3-lead ECG and the 12-lead ECG for long-term ambulatory monitoring of ischemia. The authors reported that the 12-lead ECG was superior (12-lead: 515 transient ischemia, in 88 patients (77%) vs. 3-lead: 311 transient ischemia, 71 patients (62%); $p<0.0001$). Moreover, Clifford and Oefinger (2006) argued that hence the human torso exhibits an 'anisotropic and nonstationary dielectric property', an accurate clinical description of electrical activity of the heart requires 12-lead ECG.

Across the included studies, a variety of textile sensors were used. Balsam et al. (2018), Perez De Isla et al. (2011) and Olmos et al. (2014) used biomedical e-textile BlendFix sensors to acquire ECG. Woven electrodes (Di Rienzo et al., 2005, Di Rienzo et al., 2006a) or knitted electrodes (Di Rienzo et al., 2010, Di Rienzo et al., 2013) made of conductive fibres were embedded in the MagIC ECG vest. The WEALTHY system has knitted smart textile sensors made up of stainless steel and viscose textile yarn (Bourdon et al., 2005, Coli et al., 2006). Coosemans et al. (2006) knitted textile electrodes on the elastic belt while Hsiao et al. (2015) used textile sensors composed of 80% polyester and 20% elastic fibres. Pandian and Srinivasa (2016) integrated commercially available MedTex 130 textile electrodes, while Trindade et al. (2016) used tubular knit fabrics. Yu et al. (2017), on the other hand, sewed ten Medtex P180 conductive fabrics on a commercially available men's fitness T-shirt from Nike Legend, Nike, Beaverton, Oregon, USA. The type of textile sensors used in the remaining studies was not clearly stated (Lopez et al., 2010, Romagnoli et al., 2014, Kakria et al., 2015).

Managing data storage, connectivity and power requirements for e-textile ECG monitoring

Data storage is one of the fundamental requirements to record ECG signals where the ECG data will be displayed in real-time or stored locally, transmitted to a remote nurse station and analysed later. In regards to the data storage, 11 of the included studies (65%) (Di Rienzo et al., 2005, Di Rienzo et al., 2010, Perez De Isla et al., 2011, Di Rienzo et al., 2013, Olmos et al., 2014, Romagnoli et al., 2014, Kakria et al., 2015, Trindade et al., 2016, Yu et al., 2017, Balsam et al., 2018, Di Rienzo et al., 2006a) presented integrated memory within the textile ECG monitor to save the data locally. In the rest of the studies, either the acquired ECG data was transmitted to a PC (Coli et al., 2006, Lopez et al., 2010, Pandian and Srinivasa, 2016) or nothing is mentioned (Bourdon et al., 2005, Coosemans et al., 2006, Hsiao et al., 2015).

In smart yarn applications, it is customary to collect different signals from several sensors, and hence connectivity of components is vital. To produce a workable electronic garment, engineers strive to develop permanent interconnection mechanisms that ensure high manufacturing yield and operational reliability. However, none of the included papers clearly stated the connectivity scheme used in the respective e-textile systems.

Additionally, the realization of a workable e-textile healthcare system hinges on power supply management and longer battery life. Power supply capacity directly affects the usefulness of the system, and power supply is, in general, a critical issue for e-textile applications. In the area of remote monitoring, for example, scholars are conducting intensive research to design and develop lightweight, flexible and longer battery life. In this regard, Coosemans et al. (2006) proposed a power option through an inductive link at 132 kHz, meaning that on-board batteries are not required. Di Rienzo et al. (2010) reported a system (MagIC) powered from a rechargeable lithium-ion battery with an initial lifetime of 60 hours per charge, which was upgraded to 72 hours in 2013 (Di Rienzo et al., 2013).

Signal quality and stability for extended ambulatory activities

One common problem reported across a majority of the included studies was noise from motion artefact. As the textile electrodes are not firmly attached to the skin, the slightest motion of the wearer changes the electrodes' site of attachment to the skin. The movement of textile electrodes, in turn, alters the electrical characteristics of the skin-electrode interface, producing motion artefact in the ECG signal. Hence, motion artefact increases with higher activity levels of the patient. To mitigate motion artefact, both hardware and software-based solutions have been suggested. One of the possible solutions proposed (Coosemans et al., 2006), was a modified analog front-end (AFE) circuit based on a high Common Mode Rejection Ratio (CMRR) AFE circuit in Driven Right Leg configuration. Another possible option for noise removal used in Yu et al. (2017) was a motion-artefact detection algorithm.

In addition to the improper fit of the clothing to the body, incorrect placement of the textile electrodes contributes to the motion artefact, where minor motion by the wearer leads to shifting of the electrodes. In this regard, it is essential to research the best position of the textile electrodes for optimal performance and quality signal transduction. Three studies (Bourdon et al., 2005, Di Rienzo et al., 2013, Trindade et al., 2016) reported the positive effect of sweating on signal quality, and this would be affected by electrode placement.

2.3.3.3. Context

Based on the protocol, the inclusion criteria captured both in-hospital and outpatient e-textile based cardiac services. Eleven studies (65%) (Bourdon et al., 2005, Di Rienzo et al., 2005, Coli et al., 2006, Coosemans et al., 2006, Lopez et al., 2010, Perez De Isla et al., 2011, Di Rienzo et al., 2013, Olmos et al., 2014, Hsiao et al., 2015, Trindade et al., 2016, Di Rienzo et al., 2006a) conducted their research within hospital premises while three studies (18%) (Di Rienzo et al., 2010, Yu et al., 2017, Balsam et al., 2018) reported outpatient services. The remaining three studies (18%) (Romagnoli et al., 2014, Kakria et al., 2015, Pandian and Srinivasa, 2016) did not provide clear contextual information.

2.4. Discussion

This study presents a scoping review of current research relating to e-textile based monitoring of cardiac patients. The outlined objectives and review questions were used to guide the analysis of current research. From 207 studies that were eligible for full text-review, only 8% (n=17) were included in the final study. Consistent with previous literature, our review only identified three e-textile based ECG monitors demonstrating electronic integration beyond the textile electrodes, mostly in the form of wiring and custom-made printed circuit board. Although progress has been made, research into e-textiles has not yet reached its ultimate objective of fully integrating electronic components into garments (Fleury et al., 2015).

In terms of the study population, most research has been done on adult populations even though continuous cardiac monitoring is recommended in children with life-threatening cardiac conditions like congenital heart block or to reduce the risk of sudden infant death syndrome where the infants are prone to an elevated risk of cardiac arrest (Coosemans et al., 2006).

Regardless of the usable attributes like communication platforms, computing power, user-friendly interfaces, storage capacity and smaller size for portability (Sarela et al., 2009), the majority of the ECG monitors used computer-based application platforms (n = 10) as opposed to mobile-based platforms (n = 3). The number of ECG sensors applied varies from two to 10 textile electrodes, while single lead ECG was the common configuration (n = 10). In addition to ECG, respiration and temperature were the two most sensed phenomena. Regarding the data storage, only 11 of the included studies presented intermediate data storage. However, no intermediate data storage means loss of data where there is no connection between the host computer and the textile ECG. That is a major drawback, especially for ambulatory ECG monitoring of intermittent cardiac abnormalities. Eight papers addressed the issue of power requirement, while Bluetooth was the top wireless communication protocol that was used by seven of the studies. Most importantly, the common problem reported across all included papers was noise from motion artefact.

Concerning the context, HBCR is effective in reducing mortality and cardiac events (Dalal et al., 2010). As a result, medical professionals often prescribe home-based rehabilitation treatments that greatly reduce in-hospital stays and allow patients to engage in a self-monitoring rehabilitation program (Chatzitofis et al., 2015). However, only three studies reported outpatient cardiac services.

2.4.1. Implications for research

E-textile based ECG monitoring is a multidisciplinary research area that demands collaboration among professionals to alleviate the increased pressure on healthcare providers and to address the rising demand for CR outside the hospital premises. In this regard, the key findings identified from the scoping review that can inform future research are summarized in Table 2.2.

Table 2.2: Key findings from the scoping review of e-textile based ECG monitoring of cardiac patients.

Gaps in the research literature
There is very little reported use of clinical/diagnostic quality 12-lead ECG using fully integrated textile sensors.
Although there is significant research documenting the following issues, more research is required to establish a consensus on feasible solutions: • Motion artefact reduction techniques • Optimal electrode placement • The issue of connectivity and power requirement
Textile-based ECG research has focused on adult populations, and monitoring of neonates is under-investigated
Few solutions exist for home-based / outpatient monitoring of cardiac patients

2.4.2. Strengths, limitations, and challenges

E-textile based cardiac monitoring is a cross-disciplinary field. As a strong point, the conduct of this scoping review integrates experts from Engineering (MT, KR, DH, AF), Health Science and Nursing (RC, CK, JR), and Library Science (PN) to examine a broad range of literature and develop the conceptual boundaries for e-textile based monitoring of cardiac patients in the hospital, in the community or at home. Additionally, the author conducted a comprehensive database search within the relevant date limit and mapped the key findings in each study (Appendix D and Appendix E).

In the scoping review, only studies written in English have been considered, with nine studies excluded due to language. Therefore, relevant information may have been excluded.

Screening papers based on abstracts was a significant challenge. From 994 articles that qualified for abstract screening, around 21% (n=207) of the studies either did not provide the necessary information within their abstract or did not have abstract. As a result, 207 papers were considered for full-text review, of which only 17 studies met the eligibility criteria. If the studies had been written with a clear structure, for example, following the CONSORT guideline (CONSORT transparent reporting of trials, n.d.), the majority of the studies, which were considered for full-text review, could have been excluded during the abstract screening stage.

2.5. Conclusions

With the expected increase in life expectancy and a higher rate of CVD incidence, healthcare providers will experience a higher burden of CVD-related events in the future. To alleviate this problem, progress has been made in recent years towards the concept of e-textile based monitoring and CR at home. Here, a systematic scoping review has been conducted on cardiac monitoring based on the advancement of electronic and circuit wiring into the clothing. The current study summarizes the existing literature related to e-textile based ECG monitoring of cardiac patients. To the best of our knowledge, a 12-lead personalized HBCR monitor using fully textile-integrated electronics and circuit wiring with diagnostic capability has yet to be reported. The primary technical issue reported across all studies was noise from motion artefact. In conclusion, though the recent advancements in signal quality and noise reduction are promising, there is potential for future research in home-based monitoring and diverse populations.

[1] This chapter is a non-final version of an article published in final form in (Teferra, MN, Ramos, JS, Kourbelis, C, Newman, P, Fleury, A, Hobbs, D, Reynolds, KJ & Clark, RA 2019, 'Electronic textile-based electrocardiogram monitoring in cardiac patients: a scoping review', JBI Database of Systematic Reviews and Implementation Reports, vol. 17, no. 10, pp. 1958-1998. https://doi.org/10.11124/JBISRIR-2017-003989) and slightly modified.

This page is left blank intentionally

Chapter 3. Research Design

3.1. Introduction

This chapter presents the problem definition, research methods used to design, implement, and test a 12-lead diagnostic quality ECG monitor from textile and circuit wiring embedded into a garment. Following a brief background, the chapter defines the aims and objectives of the thesis. It also elaborates on the research methods and finally draws a concise conclusion.

3.2. Problem definition

Cardiac monitoring is part of the CR program. Based on the results of the systematic scoping review (presented in Chapter 2), there was no 12-lead home-based ambulatory ECG monitor from textile integration and circuit wiring was reported. Moreover, noise from motion artefact and muscle tremor is one of the challenges, while discomfort from wrapping electrodes is another problem that opens the door for further studies.

On the other hand, current CR programs focus on self-care and risk factor reduction to prevent rehospitalisation for secondary events. Within this context, there is an increased demand for long-term ECG home monitoring as ventricular dysrhythmias and palpitations of indistinct cause and syncope or pre-syncope due to arrhythmia continue to be a major reason for cardiac death (McLellan and Mohamed, 2011, Mathes and Halhuber, 2012, Rosero et al., 2013). Therefore, the research aimed to design, develop, and evaluate a wearable e-textile based platform to expand ECG monitoring capability in post-discharge home rehabilitation of cardiac patients.

3.2.1. Research aims

The aims of this Ph.D. thesis were:

1. To design and implement a diagnostic level 12-lead equivalent textile-based ECG monitor prototype based on the EASI electrode configuration to bridge a gap in current practice:
    a. To design and implement a miniature ECG hardware optimized for wearable application.
    b. To design and implement a versatile ECG vest from textile electrodes and circuit wiring.
    c. To design and implement a Java-based desktop platform (ECG viewer) used to display the real-time ECG and save the data for later processing.
2. To test and evaluate the performance of the individual modules (the hardware, the ECG vest and electrodes, and the ECG viewer).
3. To test and evaluate the proposed textile-based ECG monitor prototype through various empirical tests and based on the standard Holter monitor.

3.2.2. Research questions

Based on the research aims, the following research questions were developed.

1. What is known from the existing literature about utilizing e-textile ECG to monitor cardiac patients?

2. What are the design parameters required to realize a 12-lead diagnostic ECG monitor from textile electrodes? What are the building blocks of a textile-based 12-lead ECG monitor?
3. How is the output of the ECG affected for known applied inputs? Is the ECG hardware capable of handling the necessary input-output required for extended ambulatory (home-based) monitoring?
4. How does washing affect the smart ECG vest and the textile electrodes?
5. What are the minimum and maximum compression pressures applied by the smart ECG vest for a stable skin-electrode interface?
6. Is ECG quality affected based on the area and the thickness of the textile electrodes?
7. Does the smart vest design contribute to ECG quality? How close and where on the body should the e-textile sensors be placed for optimal performance? Do the methods used to connect the textile electrodes to the smart vest affect signal quality?
8. Does sweating improve ECG quality? Do the textile electrodes result in an acceptable ECG tracing compared to the commercial wet-gel electrodes?
9. Is there a significant difference in performance between the proposed textile-based ECG monitor and the traditional Holter monitor if ECG is acquired during different body movements and activities of daily living?

Figure 3.1 summarizes the thesis chapters and where in the chapters the questions are addressed.

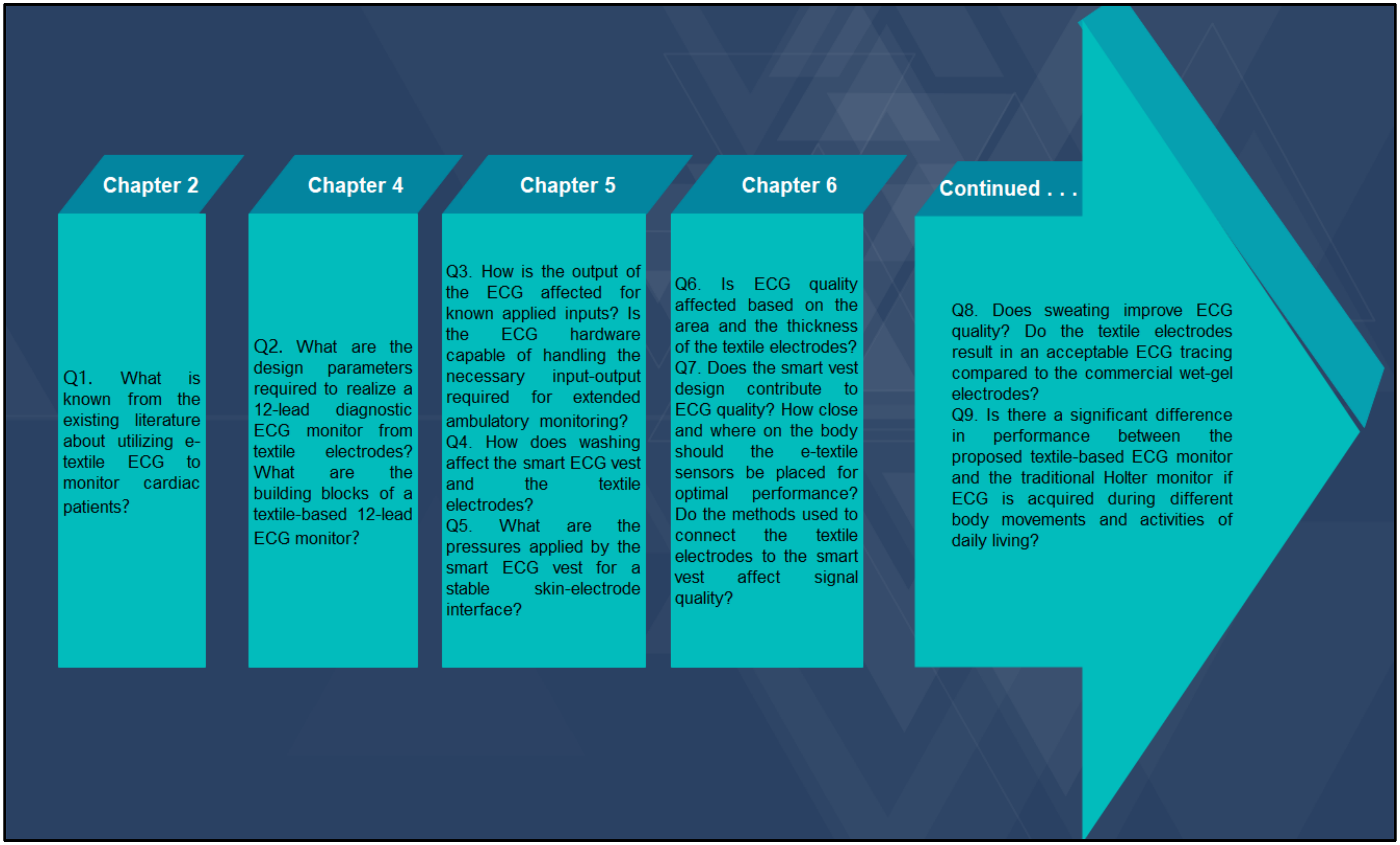

Figure 3.1: Thesis questions and the chapter section where the respective questions are addressed

3.3. System design and development: textile-based EASI 12-lead equivalent ECG monitor

The cone-shaped human heart is a muscular organ that is slightly bigger than a clenched fist and with an intrinsic timely coordinated contraction capability (Bullock et al., 2001, p. 99, Rogers, 2011, p. 24).

In composition, the heart contains three types of muscles. The atrial and ventricular muscles account for 99% of the myocardium, while the remaining 1% constitutes specialized excitatory and conductive muscles. These excitatory and conductive muscles initiate heartbeat and propagate action potential throughout the myocardium. The myocardium is an aggregate of many striated muscle cells of the myofibril. During depolarization, the actin slides over the myosin. Each cardiac muscle cell electrically connects one another in series and parallel fashion via a low resistance conduction pathway called an intercalated disk (Bullock et al., 2001, p. 99, Guyton and Hall, 2006, pp. 103 - 104, Widmaier et al., 2014, p .369).

Functionally, the heart operates as two electrically insulated syncytia, ventricular and atrial. The sinoatrial node is located next to the adjunction of the superior vena cava and the right atrium. It is an independent self-excitatory and the primary peacemaker of the myocardium. The discharging rate of the sinoatrial nodes governs the intrinsic HR. Generally, ionic current from the sinoatrial node travels down to the atria and the atrioventricular node via inter-nodal pathways. Then it propagates to the walls of the ventricles through the conduction network called the bundle of His and Purkinje fibres (Bullock et al., 2001, pp. 99 - 105, Hall, 2010, Widmaier et al., 2014, pp. 370 - 374).

The Dutch physiologist Willem Einthoven initially developed the systematic recording methods for the electrical activities of the heart, and he named the tracing ECG. A normal ECG, as shown in Figure 3.2, consists of P-wave (atrial depolarization), QRS-complex (ventricular depolarization), and T-wave (ventricular repolarization). It generally provides information related to the conduction as well as the performance of the heart (Bullock et al., 2001, p. 107, Guyton and Hall, 2006, pp. 123 - 125, Rogers, 2011, pp. 210 - 211, Widmaier et al., 2014, p. 374).

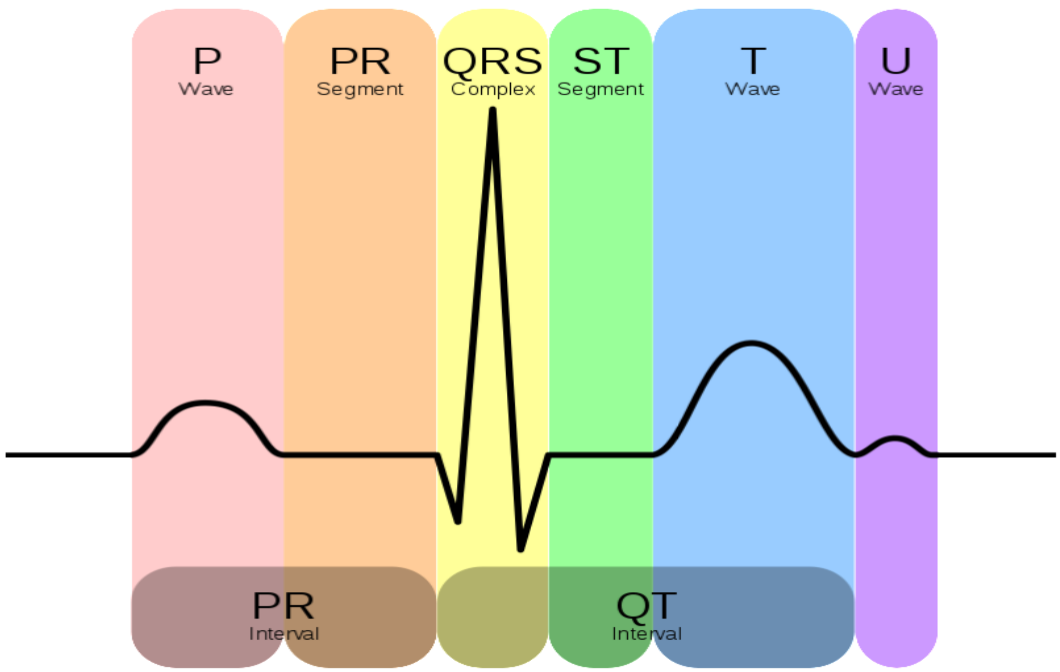

Figure 3.2: Normal ECG (*Source: https://en.wikipedia.org/wiki/Electrocardiography*; cited 2019 August 28)

An electrocardiograph is a machine that records the ECG tracing (Bullock et al., 2001, p. 107, Hall, 2010, Rogers, 2011, pp. 210 - 211, Widmaier et al., 2014, p. 374). The following section presents the research methodologies used to design, develop, and implement a wearable textile-based electrocardiograph.

3.3.1. Specific objectives

The specific objectives were:

1. To analyse, design and implement a 12-lead diagnostic level smart ECG "vest" prototype using textile sensors and circuit wiring.
2. To examine each building block within the e-textile ECG monitor to identify the challenges.

3.3.2. Research questions

1. What are the design parameters required to realize a 12-lead diagnostic ECG monitor from textile electrodes?
2. What are the building blocks of a textile-based 12-lead ECG monitor?

3.3.3. Methods

From the initial ideation stage, it was determined that the proposed system would have three primary modules: ECG hardware, the smart ECG vest including the electrodes, and the real-time ECG viewer. The smart e-textile clothing would collect 12-lead ECG from the user, and it relays to a remote workstation via a wireless serial interface. The ECG viewer loaded onto the remote workstation would be capable of real-time ECG display, providing immediate feedback, and would store the data for further processing. The data collected would be used to determine the actual health status of the person and monitor their rehabilitation progress over time. Figure 3.3 below depicts the proposed textile-based ECG monitor prototype.

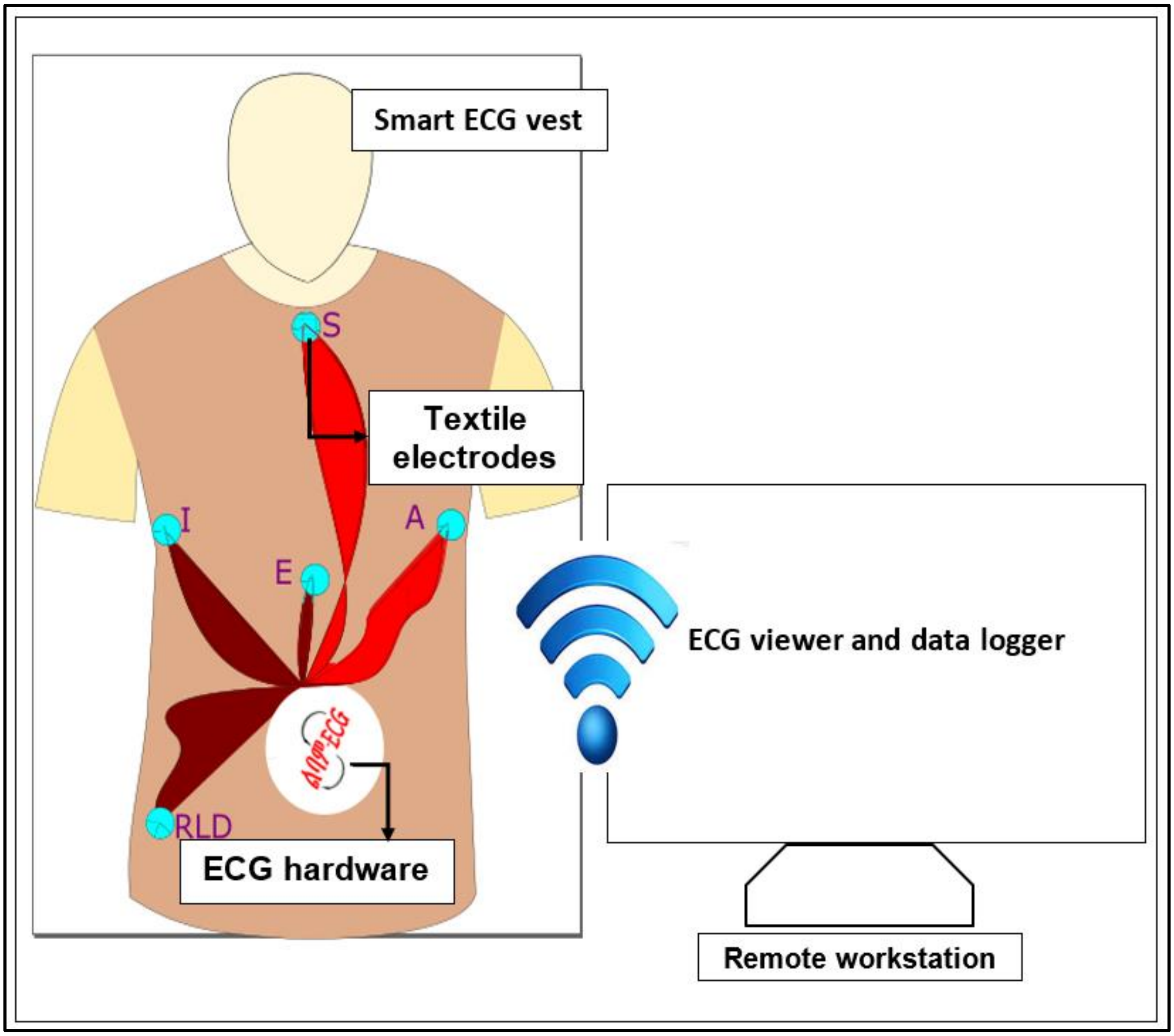

Figure 3.3: General system architecture (the ECG vest, textile electrodes, ECG hardware and the ECG viewer) of the proposed textile-based ECG monitor

The methods used to realize the respective modules of a diagnostic level 12 lead textile-based ECG system are summarized below.

3.3.3.1. ECG hardware

Functional blocks of the ECG hardware

1. **Front-end amplifier module:** As the ECG signal is small in amplitude and low in frequency, the signal is susceptible to noise. A well-designed front-end modifier module amplifies and de-noises the incoming ECG signal. A state-of-the-art bio-potential amplifier offers a higher common-mode rejection ratio as high as 120dB (Masters 2001).
2. **Central processing and transmitter modules:** These modules are the heart of the ECG monitor. After processing the incoming ECG signal (primary denoising in the digital domain, down-sampling, and packet formation), the central processing module transmits the data to the central station via the wireless module for real-time monitoring and diagnosis.
3. **Power supply module:** Supplies power for electronic components

Figure 3.4 depicts the functional block diagram of the suggested ECG hardware. At the centre of the functional block are the microcontroller and the ECG integrated circuit. The microcontroller is programmed through the micro-USB port. The Lithium battery powers the ECG hardware. The Bluetooth module buffers the real-time ECG to the host PC.

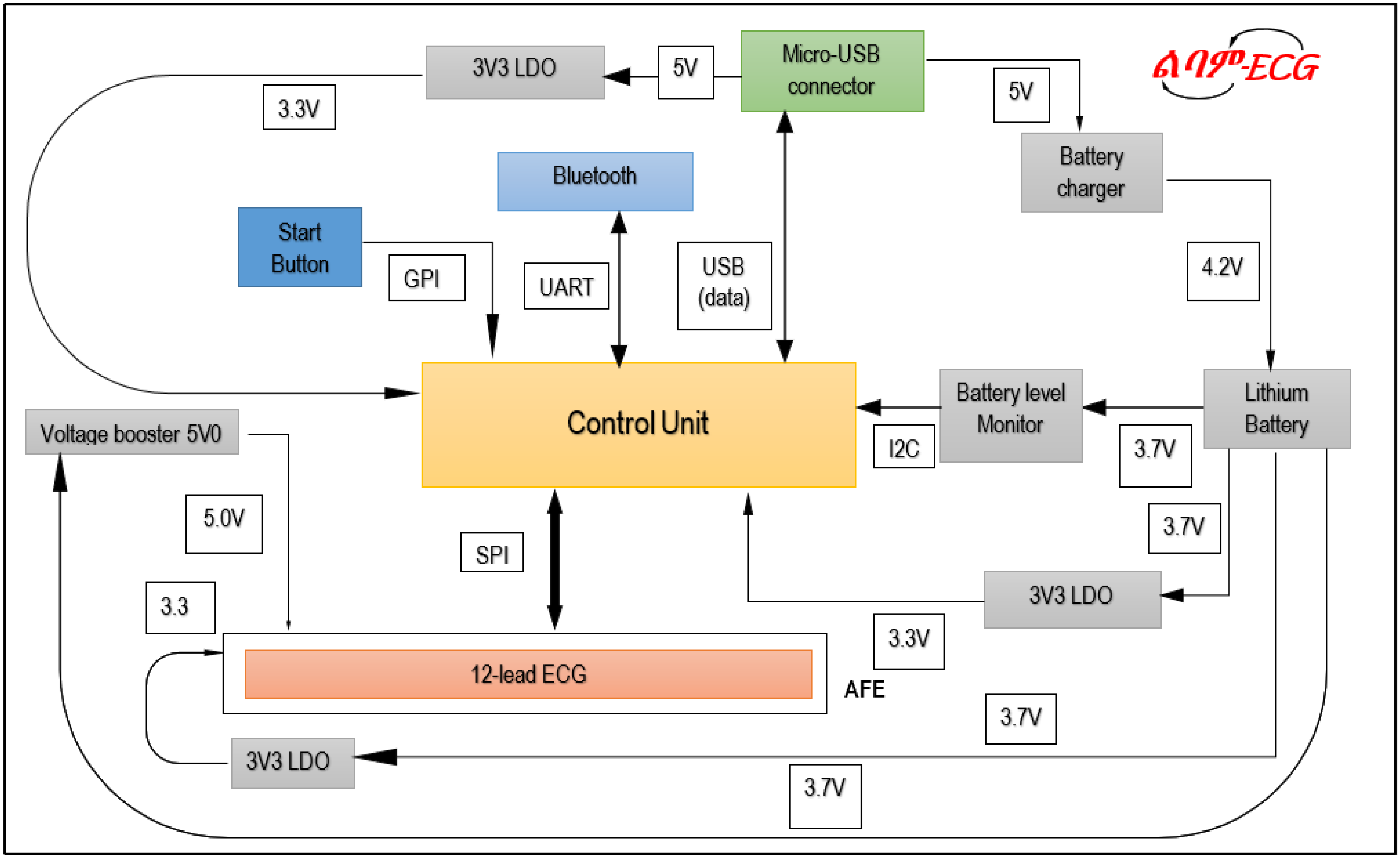

Figure 3.4: Functional block diagram of the suggested ECG hardware

Design and simulation of the ECG hardware

Having identified the basic building blocks of the ECG hardware, the next step was to design and model the respective functional blocks. PROTEL (Altium DXP designer) was used to design the ECG hardware because of its extensive library and user documentation (Altium Limited, n.d.). Additionally, an Altium designer is widely used at Flinders University, College of Engineering and Science, and hence support from the Engineering Services team was available if required.

Component selection for optimal ECG hardware development

A careful and full-scale component search was conducted on the following databases from September 2017 to August 2018: Arrow Electronics Australia Pty Ltd. (https://www.arrow.com/), Aztronics (http://shop.aztronics.com.au/), Digi-Key Electronics (https://www.digikey.com/), element14 Australia (https://au.element14.com/), Mouser Electronics Australia (https://au.mouser.com/), RS Components Australia (https://au.rs-online.com/web/) and X-ON (https://www.x-on.com.au/). Additionally, the following databases were searched to purchase off the shelf prototyping components: Adafruit (https://www.adafruit.com/), Core Electronics (https://core-electronics.com.au/), DFRobot (https://www.dfrobot.com/), eBay (https://www.ebay.com.au/), Little Bird Electronics (https://www.littlebird.com.au/), Pakronics (https://www.pakronics.com.au/), SparkFun Electronics (https://www.sparkfun.com/) and Electronics Direct (https://www.auselectronicsdirect.com.au/).

ECG hardware

The design and implementation of the ECG hardware involved specific requirements. The first issue to address was the safety of the developed ECG hardware to the user as it had parts connected to the patient. Therefore, it is was essential to ensure that the maximum allowable surge current from the power supply did not exceed the safe threshold, 10µA RMS at 50/60Hz (Laks et al., 1996).

ECG hardware measures the electrical activities of the heart which is low in amplitude and susceptible to noise (Watts and Shoat, 1987). One form of such noise source is the common-mode electrical signal picked up by the analogue front end (AFE) circuitry from the surrounding environment. As a common-mode signal does not contribute to the information contained within the ECG and distorts the signal of interest (ECG), a well-designed AFE has a higher common-mode rejection ratio (Webster, 2009, Dai et al., 2016). The ECG signal spans from 0.05Hz to 150Hz (Watts and Shoat, 1987, Kligfield et al., 2007). Therefore, filters implemented within the AFE circuitry of ECG hardware should meet the bandwidth requirements. Electromagnetic compatibility is another important aspect that needed to be considered to minimize radiation-induced disturbances in the acquired ECG (Montrose, 1996, Silberberg, 2001, Buchwald, 2017).

The above criteria were taken into account during the component analysis, schematic capture, PCB layers selection, PCB layout optimization and routing for the prototyping of the small-scale ECG hardware. Once the PCB was checked against design rules, the bill of materials was generated, and the PCB was printed at PCBWay (one of the leading PCB manufacturing companies in China). The bill of materials was used to buy the required components. Finally, the ECG hardware was assembled and tested in the design studio at Flinders University, Tonsley.

Firmware development for the ECG hardware

Firmware is software that controls and coordinates activities of an electronic device with options of easy modification and adaptability. In this regard, the control program of the proposed ECG monitor was written in C/C++ on the Atmel studio 7.0 and Arduino integrated development environment (IDE) 1.8.12. Integrated into the firmware were digital filters to denoise the acquired ECG in real-time.

3.3.3.2. ECG Vest and the textile sensors development

The ECG vest and textile electrodes were critical components for the successful implementation of the research. In this regard, the design and construction of the smart ECG vest involved identifying optimal electrode placement compared to the standard 12-lead ECG configuration, careful selection of a feasible ECG vest design from the possible alternatives suggested during the ideation stage, selection of suitable ECG acquisition methods, and appropriate textile fabrics. The ECG vest and textile sensors were modelled on the Autodesk Inventor software and produced in the Medical Device Research Institute (MDRI) laboratory at Flinders University, at Tonsley using a BERNINA 315 PE sewing machine.

3.3.3.3. The Realtime ECG viewer and data logger

The Realtime ECG viewer was standalone Java-based software used to display the real-time ECG and save the information for later analysis.

3.4. Conclusion

This chapter has presented the aim and objectives of the research, the research questions, the proposed methods to achieve the desired objectives, and highlighted the system design approaches used to implement a 12-lead textile-based ECG monitor.

This page is left blank intentionally

Chapter 4. Design and construction of the e-textile based EASI 12-lead equivalent ECG monitor

4.1. Introduction

This chapter details the design and construction of an e-textile based 12-lead ECG monitor starting from system design considerations, progressing through design and implementation of the textile-based ECG monitor prototype: ECG hardware, smart ECG vest and textile electrodes, and ECG viewer and data logger.

4.2. General design considerations

To successfully implement EASI 12-lead equivalent diagnostic quality ECG from the e-textile electrodes, miniature ECG hardware for real-time ECG monitoring, e-textile electrodes for bio-signal transduction, and a wearable ECG vest with embedded textile electrodes and wiring are fundamental (Schneegass and Amft, 2017, Shi et al., 2020).

4.2.1. Specific objectives

The objective was to design and implement a diagnostic level 12-lead equivalent textile-based ECG monitor prototype based on the EASI electrode configuration to bridge a gap in current practice. Specifically:

a. To design and implement a miniature ECG hardware optimized for wearable application.

b. To design and implement a versatile ECG vest from textile electrodes and circuit wiring.

c. To design and implement a Java-based desktop platform (ECG viewer) used to display the real-time ECG and save the data for later processing.

4.2.2. Research questions

1. What are the design parameters required to realize a 12-lead diagnostic ECG monitor from textile electrodes?
2. What are the building blocks of a textile-based 12-lead ECG monitor?

4.3. Design parameters

The proposed e-textile ECG monitor has three modules:

- The ECG hardware,
- The ECG vest and textile electrodes,
- Real-time ECG viewer and data logger

The design specification of the different modules is summarized below.

4.3.1. Specifications

Table 4.1 presents the design specifications for the proposed wearable ECG monitor.

Table 4.1: ECG hardware, e-textile based ECG vest and real-time ECG viewer design specifications.

ECG hardware		
No.	**Design requirement**	**Remark**
1.	Capable of collecting 12-lead ECG	Yes
2.	Real-time ECG monitoring option	Yes
3.	Recording Mode	Auto
4.	Heart Rate (HR) range	40 - 200 bpm
5.	Internal noise (Webster, 2009)	≤ 30μVp-p
6.	Frequency characteristics (Watts and Shoat, 1987, Kligfield et al., 2007, Webster, 2009)	0.05 -150 Hz
7.	Sampling frequency	>2BW
8.	Could be used as personalized home-based ECG monitor / Holter monitor and or in-hospital telemetry system:	Yes
9.	Capable of wireless data transmission	Yes
10.	Voltage supply (DC)	3.3V, 5V
E-textile based ECG vest		
No.	**Design requirement**	**Remark**
11.	Smart clothing containing embedded electronics and e-textile electrodes	Yes
12.	Minimal skin irritation	Yes
13.	Comfortable to wear	Yes
14.	size	unisex and adjustable
Real-time ECG viewer and data logger		
No.	**Design requirement**	**Remark**
15.	Intuitive data entry to identify patients	Yes
16.	Displayed information	Demographic information, lead label, HR
17.	Reference lead	Yes
18.	Option to change the reference ECG leads	Yes
19.	Save data for later processing	Yes

4.4. The ECG hardware

4.4.1. Specific objective

The specific objective of the study was to design and implement a miniature ECG hardware optimized for wearable applications.

4.4.2. Justification for the EASI lead system (EASI configuration)

One of the wearable electronics used in the field of cardiology is ambulatory ECG. From their first inception in the year 1963 (Zareba, 2013), Holter monitors have been used as a long-term ECG monitor for patients. The target population is those who have an active lifestyle but with slight cardiac disorders and infrequent cardiac abnormalities (Subhasis Chaudhuri et al., 2009). The 12-lead ECG monitor has superior diagnostics capability for cardiac abnormalities, however, the standard 10 electrodes Holter monitor is complex in construction and uncomfortable for the wearer. Additionally, one of the constraints for remote ECG monitoring is the bandwidth limitations of wireless technology (Dawson et al., 2009). Hence, one of the challenges in the design and implementation of an ambulatory ECG monitor is to reduce the number of leads while, at the same time, realizing a 12-lead ECG.

Nelwan (2005) summarized several reasons that hinder the recording of the standard 12-lead ECG, including excessive noise artefact due to the skin-electrode interface and unavailability of a particular ECG lead due to injury or surgery (Nelwan, 2005). Hence, it was decided to use a reduced set of ECG leads to generate the complete 12-lead ECG using a transformation matrix.

Referring to Geselowitz's dipole principle, the electrical activity of the heart could be fully explained from two independent leads (any of two of lead I, II, III) and one precordial ECG lead (preferably V2) (Malmivuo and Plonsey, 1995). In this regard, Drew et al. (2002) proposed ECG leads I, II, V1, and V5. Scherer et al. (1990) used leads I, II, and V2, while Wei et al. (2004) suggested ECG leads I, II, and two precordial ECG leads (V1, V6). Figure 4.1 illustrates the Mason-Likar 12-lead electrode placement from which one lead to 12-lead ECG configurations can be obtained.

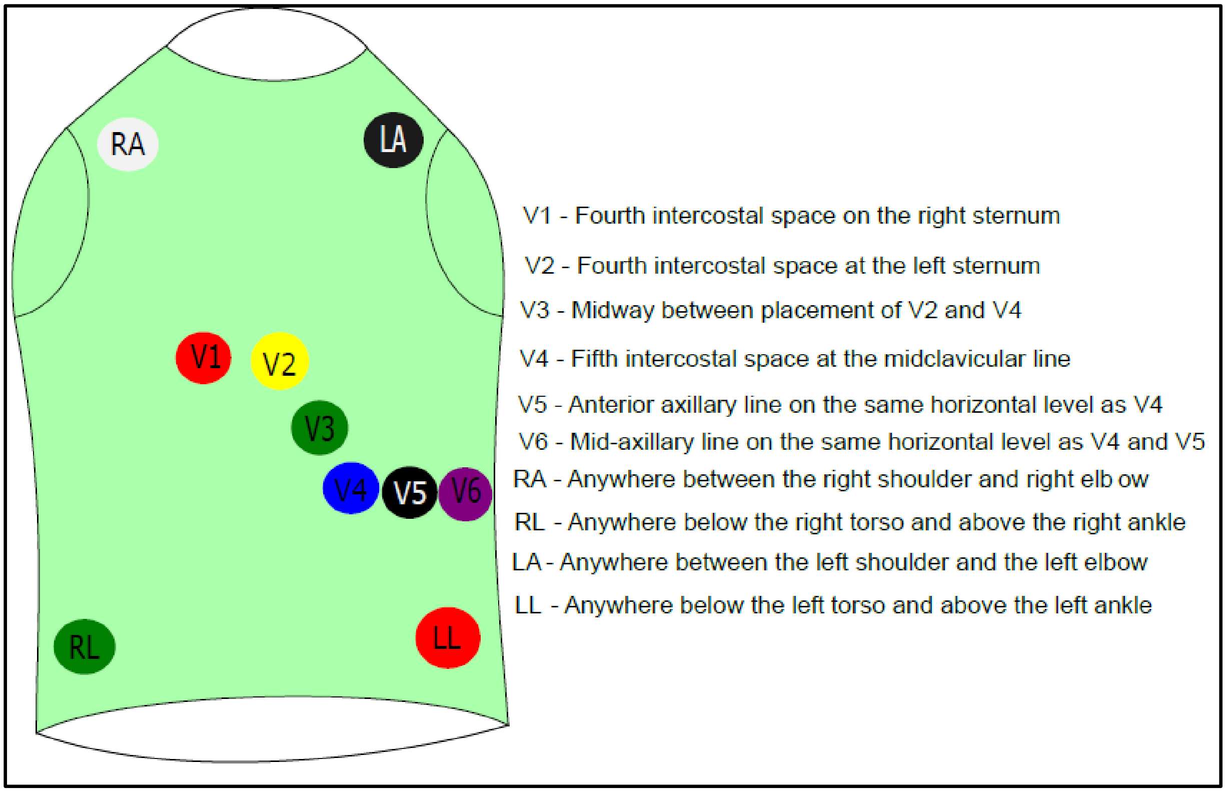

Figure 4.1: The Mason-Likar 12-lead ECG: chest (precordial) and limb (extremity) ECG sensor placement

Using the concept of Burger and van Milaan's lead system (Burger and Van Milaan, 1943), Dower et al. (1988) suggested the EASI lead system (EASI configuration). The authors showed that it is possible to drive 12-lead ECGs from a 5-electrode (E-A-S-I) lead system. EASI lead system uses easily accessible anatomical positions for electrode placement (Figure 4.2) that reduce the production cost, decrease the time needed to train the health and medical staff, and improve signal quality, comfort, and convenience for the user. Moreover, the EASI lead system allows the derivation of more clinically relevant (right-sided, posterior, orthogonal vectorcardiogram) ECG leads.

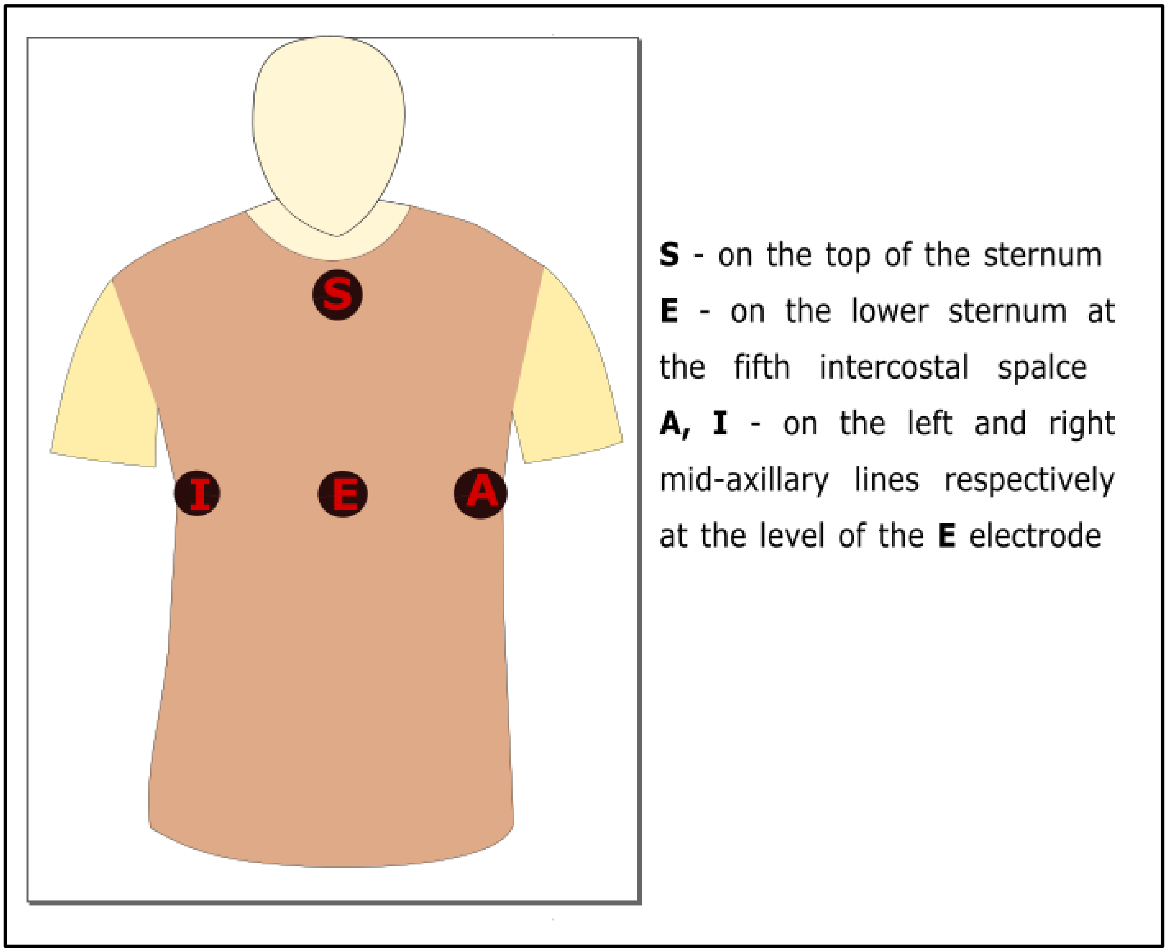

Figure 4.2: The EASI lead system ECG electrode placement.

Various studies have been conducted to validate the clinical relevance of the EASI lead system. Klein et al. (1997) studied the correlation between the standard 12-lead ECG and the 12-lead equivalent ECG from the EASI lead system based on 50 patients in the coronary care unit. The authors reported the EASI lead system has 89% myocardial infarction detection rate, 94% sensitivity, 93% specificity of the Q-wave in myocardial infarction detection and concluded that the EASI lead system could be adapted for diagnosis.

Drew et al. (1999) conducted a study of 540 patients to examine the possibilities of the EASI lead system for the diagnosis of multiple cardiac episodes. The authors reported a good agreement in detecting different cardiac abnormalities (cardiac rhythm = 100%; chamber enlargement-hypertrophy = 84%-99%; right bundle branch block = 95%; left bundle branch block = 97%; left anterior fascicular block = 97%; right anterior fascicular block = 99%; acute infarction = 100%, angioplasty induced ischemia and transient ischemia = 95% and 89%, respectively) between the EASI 12-lead equivalent and the standard 12-lead ECG.

Pahlm et al. (2003) compared the conventional 12-lead ECGs and those derived from EASI leads in children. The results revealed that there was an overall good agreement between the standard ECGs and the EASI 12-lead equivalent ECGs across different age groups. Moreover, conventional 12-lead ECG electrode placement could be difficult due to the smaller physical size of the infant's body, and hence the EASI electrode configuration offered advantages.

Feldman et al. (2005) compared the EASI lead system to the Mason-Likar 12-lead ECG in pre-hospital setting (emergency medical services) based on 200 patients with chest pain. The authors reported that there was no significant quality difference between the EASI 12-lead equivalent ECG and ECG from the Mason-Likar 12-lead ECG (detection of rhythm / conduction abnormalities: 96% agreement and ST-segment criteria for diagnosis of acute myocardial infarction = 94% agreement). Participants rated the EASI ECG electrodes as easy to use and more convenient than the conventional ECG, especially in women.

Moreover, Wehr et al. (2006) reported identical diagnosis results of acute coronary syndrome in a study conducted on 177 patients. In a similar study, Welinder et al. (2006) examined ECGs from EASI configuration and a reference standard 12 lead ECG from 221 children. The ECGs were interpreted by two experienced paediatric cardiologists. The authors reported that the variation in ECG quality between the EASI 12-lead equivalent ECGs and the ECGs collected from the reference standard ECG was within intrareader variability. Therefore, the authors concluded that the EASI lead system could be a potential alternative for the standard ECG in children.

Martínez et al. (2007) compared the QT-intervals from the EASI 12-lead equivalent ECGs to QT-intervals from the standard 12-lead ECGs. In the study 200 patients were considered. The multi-lead Pearson correlation coefficient between QT measurements from the two systems was 0.98. The QT-interval differences were less than 2ms except for leads V3 (mean difference = 2.7ms) and V5 (mean difference = -3.5ms) where the T-wave morphology was the major contributor to the observed variability. The authors concluded that the EASI lead system could be used for reliable QT monitoring given the multi-lead delineation approach.

Lancia et al. (2008) compared the standard 12-lead ECG and the 12-lead equivalent ECG from the EASI lead system in the Coronary Care Unit. Thirteen patients with acute myocardial ischemia and a history of myocardial infarction were considered where 97 pairs of ECGs were collected. The authors studied QRS amplitude, QT interval duration and 'J' point level. The QRS amplitudes were statistically different however, there was no clinically significant difference in the recorded QT-interval durations and 96.30% of the ECG leads examined resulted in a ‘J’ position difference less than 1 mm.

In another study, Welinder (2009) reported a high level of agreement between the standard 12-lead ECG and the EASI 12-lead equivalent in children.

Loreto et al. (2016) conducted an observational study on the accuracy of the EASI 12-lead equivalent ECG to monitor ST-segment and J-point by the nurses in the Coronary Care Units. Around 85% of the cumulative distributions of the absolute difference of the ST segment and the 'J' point were below 0.51mm, with the highest absolute difference observed in the lead V2 (ST-segment: mean = 0.69; SD = 0.65; J-point: mean = 0.49; SD = 0.56) and the lowest in lead-I (ST-segment: mean = 0.28; SD = 0.43; J-point: mean = 0.19; SD = 0.37). The authors concluded that the differences are not clinically relevant and therefore, the EASI lead system could be used for continuous monitoring of the ST-segment and the J-point.

Lancia et al. (2018) conducted observational comparative study to examine the accuracy of the EASI 12-lead equivalent ECG to monitor patients with Acute Coronary Syndrome (ACS) and Heart Failure (HF). ECGs were collected from 253 patients (men = 61.3%, average age = 71.3 ± 8.2 years and, HF = 19.4%) using the standard 12-lead ECG and the EASI system. The authors reported that there was no clinically significant difference between the systems regarding PR-intervals, QT-intervals and J-point values. However, the EASI 12-lead equivalent ECGs showed statistically significant difference QRS durations compared to the standard 12-lead ECGs (ACS, mean = 6.60ms; HF, mean = 4.15ms; p = 0.000).

Though not clinically significant, the ECGs collected from the EASI lead system showed a shift in the direction of the electrical axis in the frontal plane. This is a common problem of modified ECG electrode placement including the Mason-Likar 12-lead ECG (Klein et al., 1997, Welinder et al., 2006, Martínez et al., 2007).

In summary, the EASI lead system reduces the production and running costs as fewer ECG electrodes are used. It also reduces the time taken to train health and medical staff. Moreover, the EASI configuration improves signal quality, comfort and convenience for the user and less interference with clinical procedures. Therefore, it was decided to design the ECG monitor in this research based on the EASI configuration.

4.4.3. Selection of a bio-potential amplifier and analog front end development

Electrodes constitute the initial stage of bio-potential sensing. The performance of the sensors influences the overall accuracy of the signal acquisition chain. Hence, electrode design and implementation are critical. Moreover, the flicker noise (pink noise) of the amplifier is significant, especially at low frequency. As a result, the biopotential amplifier should be chosen carefully (Sazonov and Neuman, 2014).

Though possible to implement the ECG front-end amplifier from discrete components, low power analog integrated circuits are found to be effective as they have a smaller form factor and better system integration. In this regard, the ADS1298 low power, 8-Channel, 24-Bit AFE Bio-potential amplifier from Texas Instruments was chosen for the initial prototype development and later replaced by ADS1294 (Texas Instruments Incorporated, 2015), the same integrated circuit with four channels instead of eight.

4.4.3.1. The ADS1298 / ADS1294 ECG module

The ADS1298, or ADS1294 ECG module is a multichannel 24-bit delta-sigma analogue to digital converter with an embedded programmable gain amplifier (PGA), internal reference and onboard clock, built-in Right Leg Drive Amplifier, leadoff detection, Wilson central terminal (WCT), and test signals as well as a flexible sampling rate up to 32 Kilo samples per second (SPS) (Texas Instruments, 2015).

4.4.3.2. Passive analog filters and patient protection circuit

Analog filters

Hi-pass and low pass filters are used to eliminate the half-cell potential, to reduce preamplifier offset and reduce overall noise. Active Bessel filters exhibit a smooth transfer function (Franco, 2015, Schuler, 2019). However, one of the design factors for the wearable ECG monitor is lower power consumption (Teferra et al., 2019b). Therefore, a second-order passive RC-network is preferred (Figure 4.3) to reduce power consumption and circuit complexity.

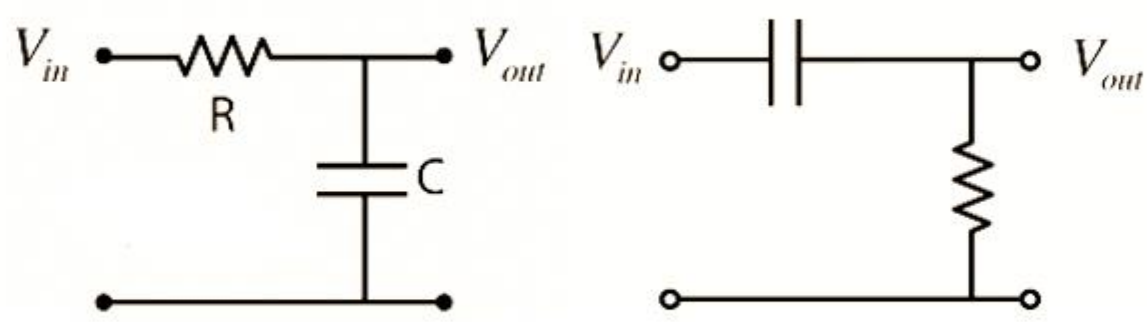

Figure 4.3: Low pass (left) and high pass (right) RC filter.

Based on the design criteria, the ECG signal frequency spans from 0.5Hz – 150Hz. In the hardware design, appropriate R and C values were selected to satisfy the low pass cutoff frequency (f_{LC}) of 150Hz and high pass cutoff frequency (f_{HC}) of 0.05Hz.

Patient protection circuit

Safety is a prime concern in biomedical design and applications to protect the patient and / or the operator from electric hazards should there be a fault. For instance, an ECG monitor has applied parts, and hence the maximum allowable current that flows through the ECG electrodes to the patient connected is 10 µA root mean square (RMS) (Laks et al., 1996).

In the proposed ECG hardware, a number of precautions were taken to protect the user. The ADS129X AFE ECG chip has a low leakage current (around 0.16nA, at $4.8V_i$, PGA = 1) (Texas Instruments Incorporated, 2015). A current limiting resistor (R = 22.1KΩ) combined with back-to-back connected diodes (1N4148WS from VISHAY; 500nA leakage current at 100ºC junction temperature and 20V reverse voltage) were used in the design (Figure 4.4).

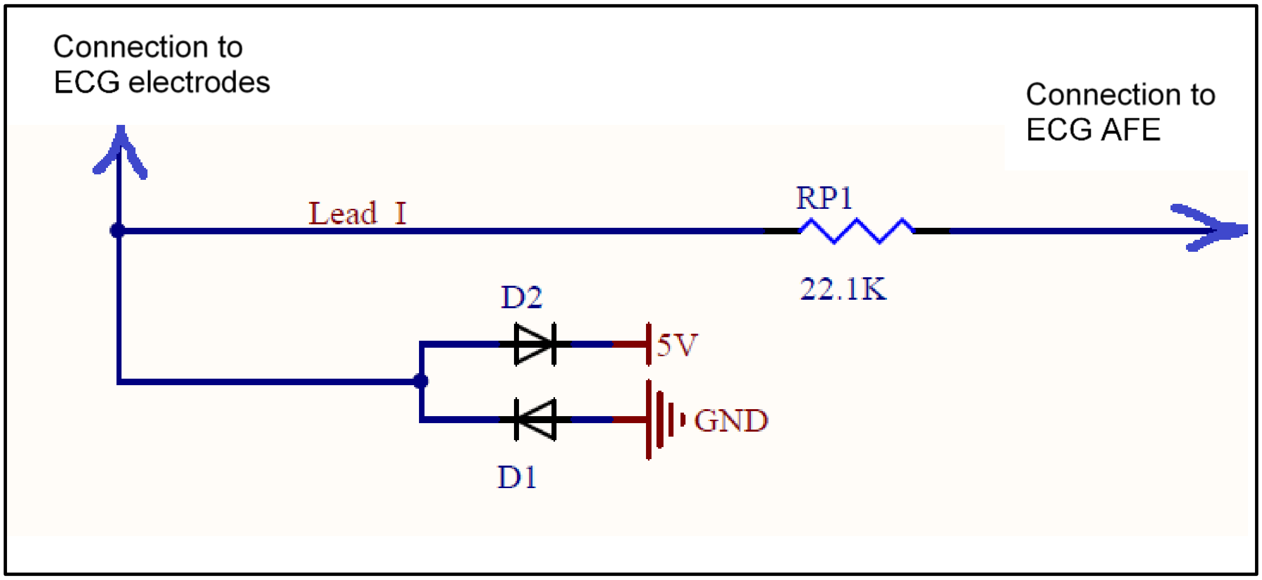

Figure 4.4: Snapshot of the patient protection circuit

Moreover, successful commercialisation of the proposed ECG hardware requires to satisfy the regulatory approvals and compliance with medical device standards conformity assessment against the medical device electrical safety standards (IEC60601) (Young, 2019) and quality management standards ISO13485 (Abuhav, 2018).

4.4.4. The central controller

Arduino and Teensy ecosystems offer a viable prototyping option. For the initial prototyping, Arduino Uno (Arduino, n.d.-b) and Arduino Mega 2560 (Arduino, n.d.-a) were used. The final prototype was based on Teensy 4.0 (PJRC, n.d.) for its smaller form factor and higher processing speed compared to the Arduino Uno and Mega 2560 (Table 4.2).

Table 4.2: Basic features of selected development boards

Basic features	Arduino Uno	Arduino Mega 2560	Teensy 4.0
Form factor			
Dimension (length(mm) x width(mm))	68.6 × 53.3	101.6 × 53.3	36.8 x 18.0
Weight (g)	25	37	2.8
Speed			
Processor	ATmega328P	ATmega2560	ARM Cortex-M7
CPU Speed	16 MHz	16 MHz	600 MHz
EEPROM [kB]	1	4	-
SRAM [kB]	2	8	1024
Flash [kB]	32	256	2048
Others			
Operating Voltage (V)	5	5	3.3
Digital input out pins	14	54	40
Analogue input outputs	6	16	14
Number of serial ports (UART)	1	4	7
Number of SPI ports	1	1	3
USB	1	1	2
Programming IDE	Free	Free	Free

4.4.5. Powering the ECG hardware

The ADS1298 requires 3.3V digital and 5V analogue supplies. Therefore, the Li-Po battery - Lithium-Ion Battery - 2000mAh from SparkFun Electronics (SparkFun Electronics, n.d.) combined with a Power Boost 1000 Charger - Rechargeable 5V Li-Po USB Boost, 1A - 1000C from Adafruit (Adafruit, n.d.) was selected to power the ECG hardware. A voltage regulator from Texas Instruments (Texas Instruments Incorporated, n.d.-b) was used to reduce the 5V supply to 3.3V.

4.4.6. Wireless ECG signal transmission

The HC-06 Bluetooth module, which operates at 2.4GHz industrial, scientific, and medical (ISM) band, a maximum baud rate of 2.1Mbs and based on Gauss frequency Shift Keying modulation (c2017) was integrated into the hardware module to buffer the ECG signal wirelessly to the remote receiver.

4.4.7. Printed circuit board (PCB) production and assembly

Once the component selection was completed, the ECG hardware schematics were captured on the Altium schematics editor (Figure 4.5). The next step was to transfer the hardware schematics to the PCB layout editor. The PCB layout was optimized for higher performance, better signal integrity, and compliance with electromagnetic compatibility standards. Then the Gerber file was sent to the PCB manufacturing company (PCBWay, n.d.) to print the PCB board. Finally, the prototype ECG hardware was assembled and tested in the design studio at Flinders University, Tonsley.

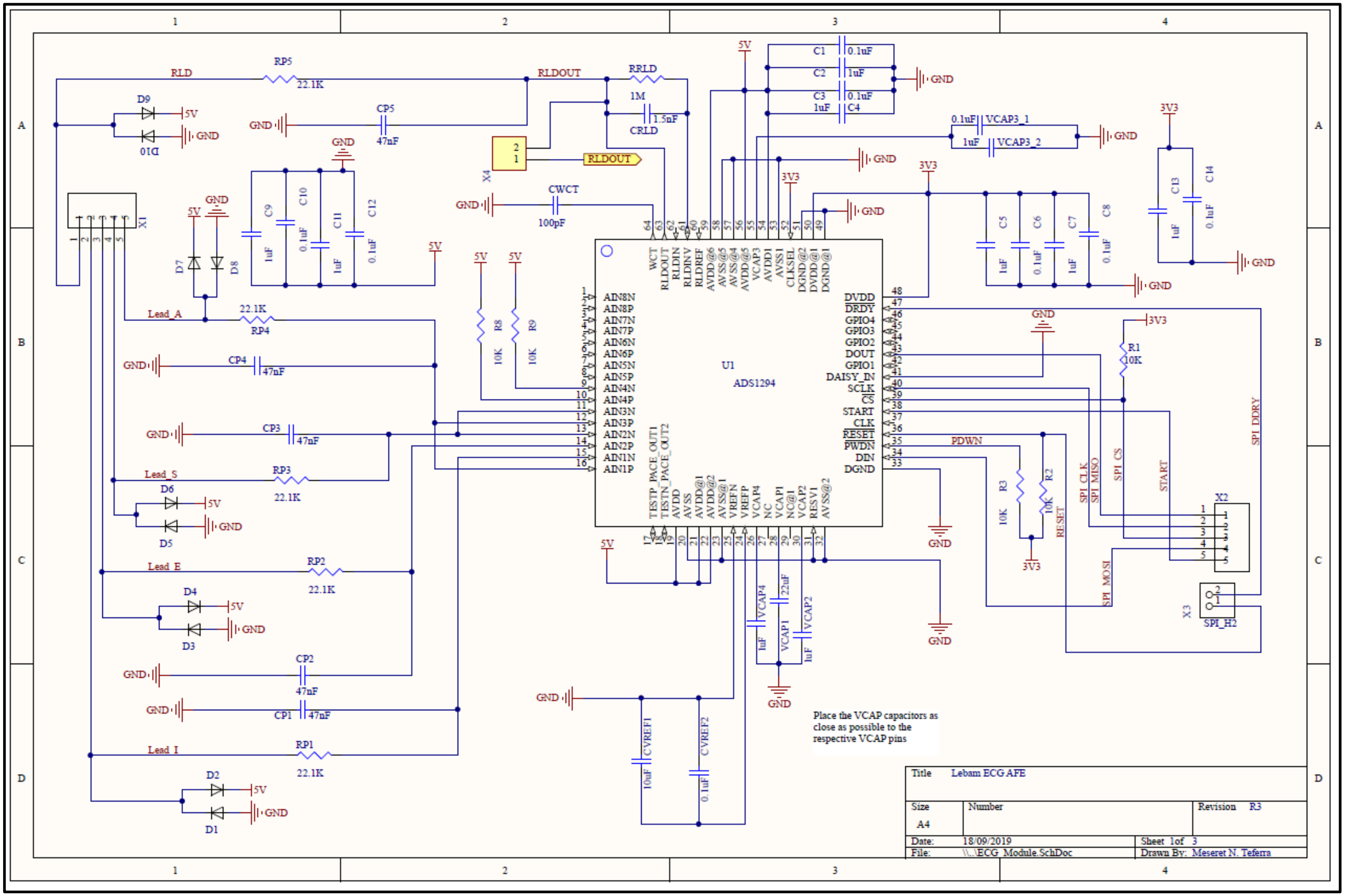

Figure 4.5: Partial view of the ECG AFE schematics

4.4.8. Programming the ECG hardware

Communication between the ADS1298 AFE and the microcontroller is via an SPI. The SPI has four digital signals: chip select (CS – active low), serial clock (SCLK), data in (DIN - Master out, slave in - MOSI) and data out (DOUT - Master in, slave out - MISO). The ADS1298 control registers are programmed via DIN pin, while data could be read from the chip through DOUT. Additionally, the ADS1298 data ready (DRDY – active low) pin signals the availability of data at the DOUT pin.

4.4.8.1. Interfacing the ADS1298 and the microcontroller: programming the serial peripheral interface

Based on the application information in the ADS1298 user manual (Texas Instruments, 2015, p. 58), the time required for successful SPI communication is given by the following formula.

$$t_{\mathrm{sck}} < \frac{t_{\mathrm{DR}} - 4 * t_{\mathrm{clk}}}{N_{BITS} * N_{CHANNELS} + 24} \qquad [4.1]$$

Where: t_{SCLK} *- the serial clock requirement for successful SPI communication;*

t_{DR} *- sampling time;* N_{BITS} *- number of bits and* $N_{CHANNELS}$ *- number of channels*

t_{clk} *- operating clock speed of the ADS1298 = 1/2.048MHz*

Considering the worst-case scenario where all the eight channels will be used to acquire ECG at 2Ksps, the minimum serial clock was calculated.

$$t_{sck} < \frac{\frac{1}{2000}s - 4*\frac{1}{2.048*10^{6}}s}{24*8+24} = \frac{0.0005s - 1.953125*10^{-6}}{216} = 2.3058*10^{-6}$$

$$t_{sck} < 2.3058\mu s$$

giving an SPI clock frequency (reciprocal of t_{sck}) of 433.7kHz.

Therefore, a clock frequency of 440KHz and above was necessary to enable SPI communication between the ADS129x and the microcontroller. Referring to the measurement datasheet (Texas Instruments Incorporated, n.d.-a), the ADS129x requires four clock cycles to execute a one-byte command.

$$t_{SDECODE} = 4*t_{SCK}$$

$$For\ 2.048\text{MHz clock}$$

$$t_{SDECODE} = 4*\frac{1}{2.048*10^{6}\,Hz} = 1.96\mu s/byte$$

Moreover, an opcode (a unique set of instructions used to program the ADS129x registers) is executed at the falling edge of the eighth serial clock cycle (t_{sck}). The time required to transfer one byte of an opcode without delay should be higher than $t_{SDECODE}$ and can be calculated as follows:

$$t > t_{SDECODE}$$

$$For\ t_{SDECODE} = 1.96\mu s$$
$$t = 8 * t_{sck} > 1.96\mu s$$
$$\rightarrow 8 * t_{sck} > 1.96\mu s \rightarrow \quad t_{sck} > \frac{1.96\mu s}{8}$$
$$t_{sck} > 0.245\mu s$$

$$f_{sck} = \frac{1}{t_{sck}} < \frac{1}{0.245\mu s} < 4.08MHz$$

The upper limit of the serial clock frequency is 4MHz. Therefore, the recommended SPI clock frequency is in the range of 0.44MHz to 4MHz.

Once the timing requirement of the serial port was calculated, the SPI modes of operation were studied. There are four SPI communication modes based on clock polarity and clock phase (Dhaker, 2018). The ADS1298 communicates with the master controller in *SPI MODE1* and *MSBFIRST*.

Atmel studio 7.0, combined with Arduino Studio 1.8.12, was used to write the ECG firmware using the Arduino Uno, or Mega 2560, or teensy 3.6, and finally on teensy 4.0 development board. The programming trial was commenced on the 15th of October 2018 by setting up the ADS1298 configurations registers (***CONFIG1, CONFIG2*** and ***CONFIG3***, and ***GPIO***) to test the successful paring of the ADS129X and the development board.

4.4.8.2. Writing the firmware

Once the SPI communication was secured, the initial firmware was written based on an algorithm depicted in Figure 4.6. Three groups of C/C++ functions were created: setup and configuration; Data retrieval and pre-processing; and Real-time digital filters.

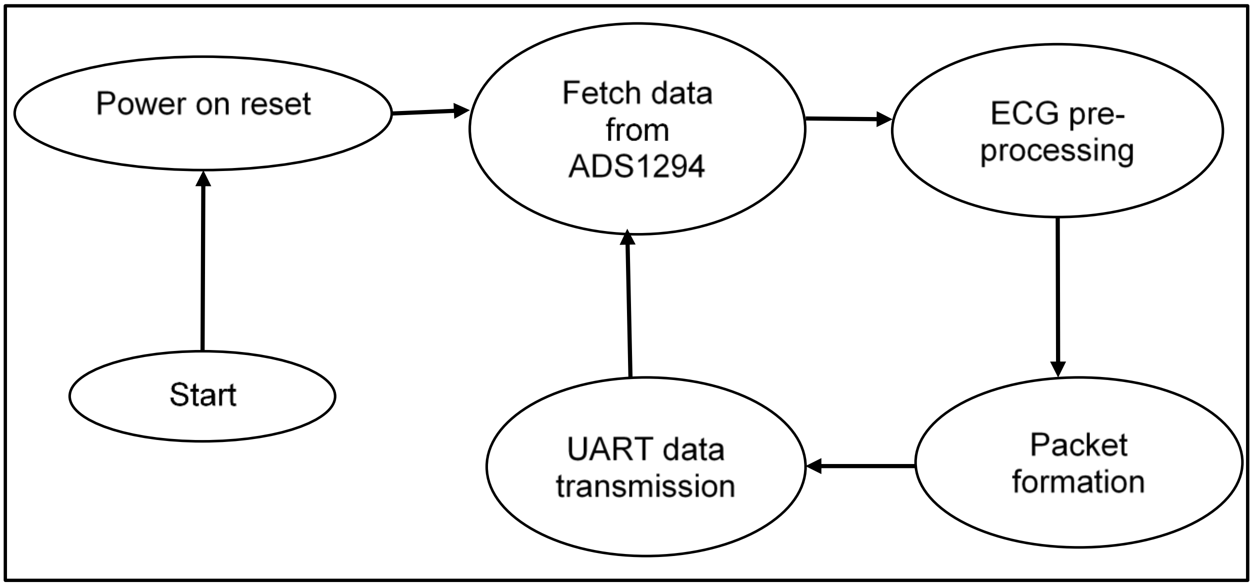

Figure 4.6: A simplified finite-state diagram of the ECG firmware sequencing

Setup and configuration functions

This group defines and initializes all input-output pins of the microcontroller. The functions initialize the serial ports, set up the ADS129x configurations registers, and handle the ADS129x power-on reset routines.

Data retrieval and pre-processing

Functions defined under this group are responsible for accessing the ECG data from the ADS129x through the SPI interface. The incoming data is structured into three base-ECG leads (V_{AI}, V_{AS}, V_{ES}), the noise removed (using a real-time digital filter), transmission packet created and sent over Bluetooth to the host PC.

Real-time digital filters

Real-time anti-hum (50Hz) filter

A digital anti-hum filter was designed and is presented in Appendix F. The coefficients of the filter were compared against MATLAB R2017a generated coefficients of a fourth-order Butterworth notch filter to minimize quantization error. Figure 4.7 presents the direct form-II transpose realization, and Figure 4.8 shows the magnitude and frequency response of the designed Butterworth Infinite Impulse Response (IIR) filter.

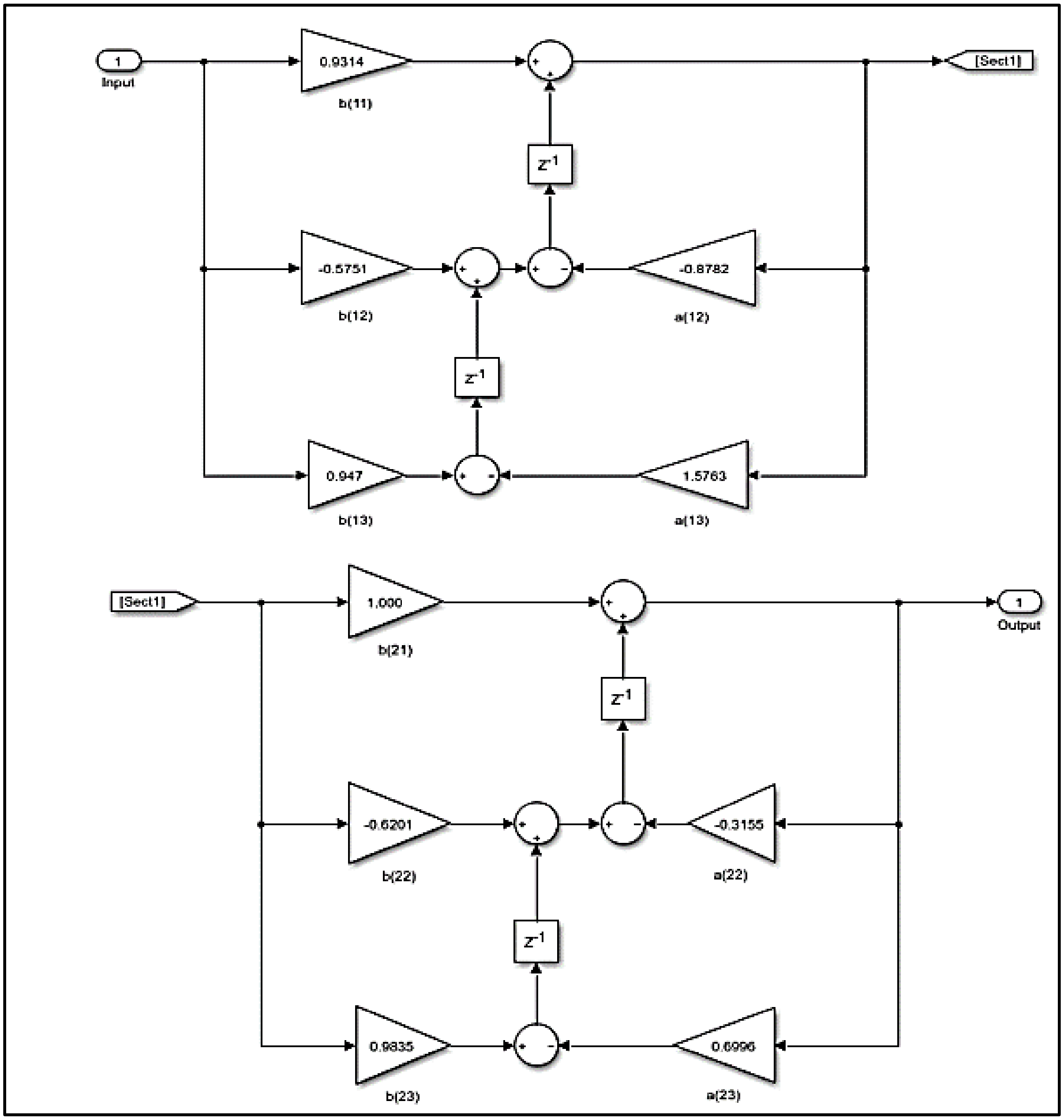

Figure 4.7: Direct from-II transpose second-order sections

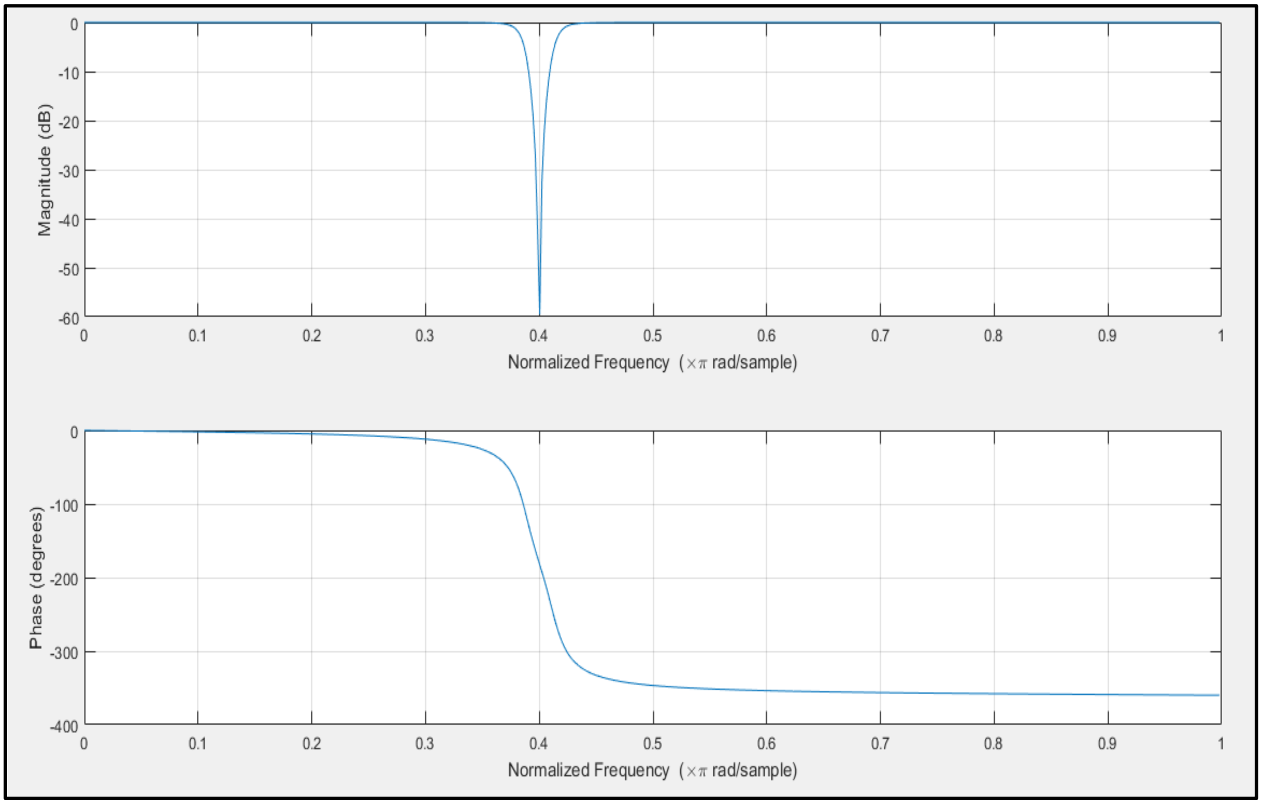

Figure 4.8: Magnitude and phase response of the realized IIR 50-Hz anti-hum filter (the 50Hz is normalized by the Nyquist frequency).

Real-time baseline wanders noise removal

In an effort to remove baseline wander and respiration noise from the acquired ECG signal, fourth-order high pass (F_C = 0.5Hz) and a smoothing low pass (F_C = 150Hz), Butterworth filters were implemented. The coefficients of the respective filters were generated using MATLAB IIR filter design, and C/C++ implementation was based on cascade direct from-II. Figure 4.9 shows the magnitude and phase responses of the low pass high pass filter, respectively.

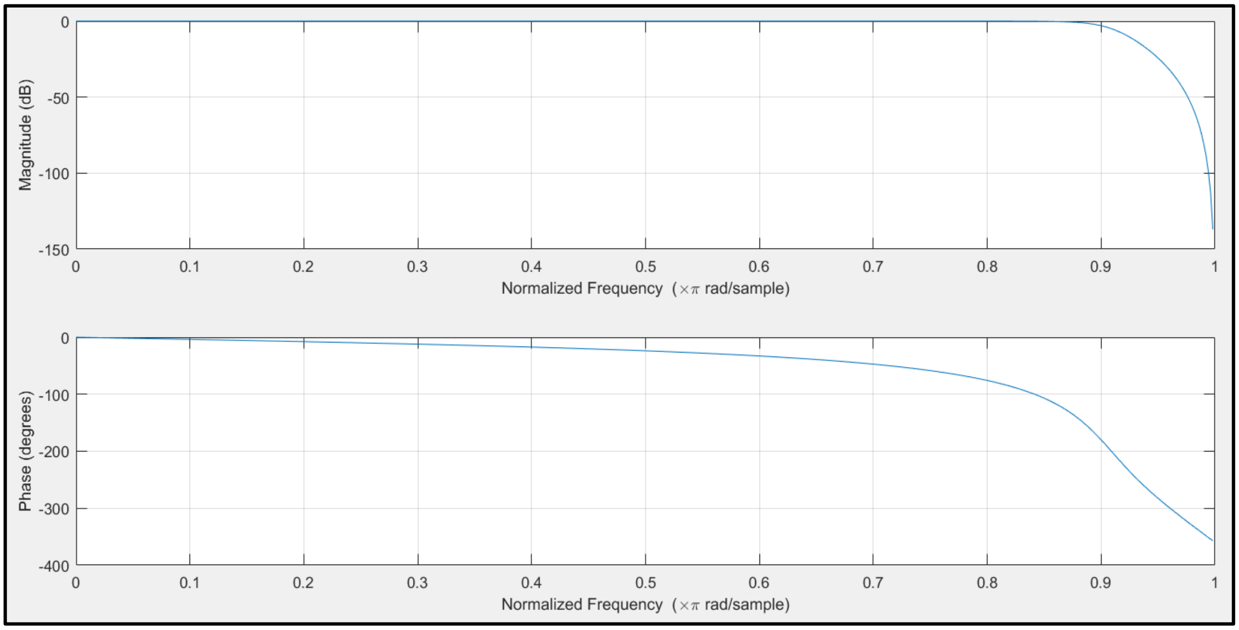

a) Low pass filter

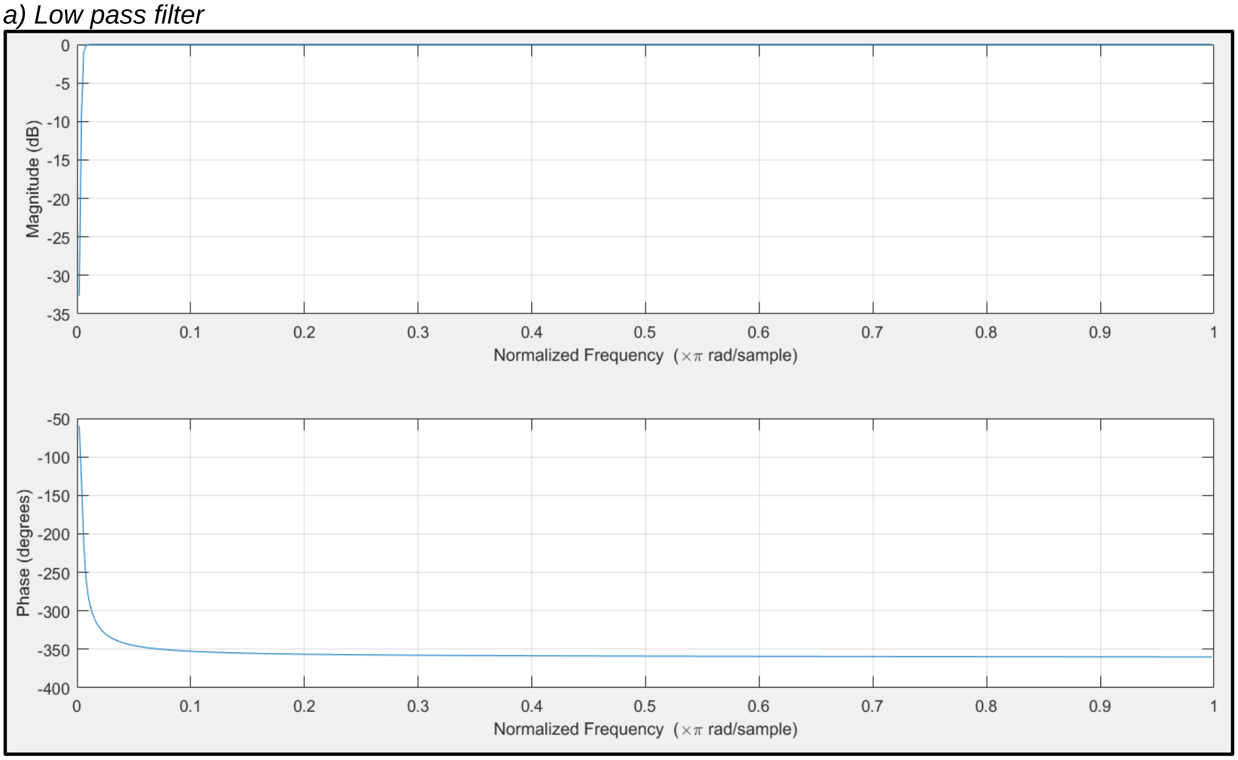

b) High-pass filter

Figure 4.9: Magnitude and phase response of the real-time IIR filters (the cut-off frequencies are normalised by the Nyquist frequency).

A C/C++ based real-time IIR notch filter was implemented based on Falco's DSPFilters (Falco, 2012). The stability of the IIR filter is dependent on the location of the poles of the transfer function. IIR filters are stable if poles are contained within the unit circle in the Z-domain. Quantization (round-off) errors affect the location of poles and zeros of the designed filter, where a slight error in coefficients may induce a more significant frequency deviation (Milivojevic, 2009). Moreover, the implementation of the digital filters with integer coefficients showed superior results compared to the floating-point coefficients (Lynn, 1971, Iliev et al., 2008). In this regard, 16bits binary scaling was used to augment computation efficiency and reduce round-off errors.

On the other hand, downscaling the 24bits ECG signal to 16bits due to hardware limitations, resulting in reduced quality in the acquired ECG signal. Hence, a 32 bits ARM-based microcontroller was used as opposed to an 8-bit AVR microcontroller.

Smoothing Kalman filter

Kalman filters are intensively used in real-time applications in general (Meinhold and Singpurwalla, 1983, Harvey, 1990, Crassidis, 2017, Kim and Bang, 2018) and ECG applications in particular (Sameni et al., 2005, Meau et al., 2006, Mneimneh et al., 2006, Sameni et al., 2006, Li et al., 2008, Sayadi and Shamsollahi, 2008, Moradi et al., 2014, Oster et al., 2015). In the proposed ECG monitor, a single variable Kalman filter was implemented based on the algorithm given in Figure 4.10, to smooth the noisy ECG.

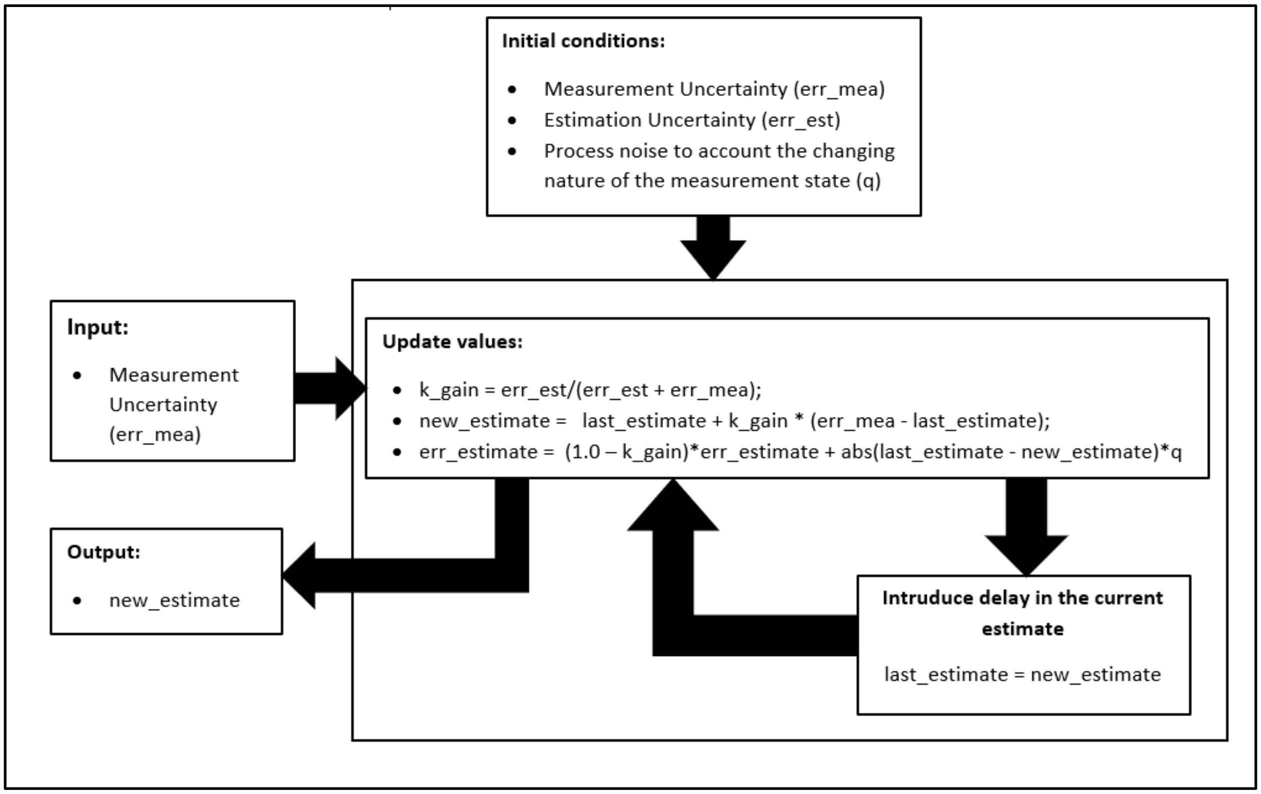

Figure 4.10: One dimensional (single variable) Kalman filter implementation algorithm

To summarize, the final firmware includes real-time IIR high pass / low pass filters and a smoothing Kalman filter.

4.4.9. ECG hardware prototype

4.4.9.1. Standard 12-lead ECG

Versatile hardware with multiple configurations based on ADS1298 AFE and capable of acquiring ECG from e-textile electrodes was designed and assembled (Figure 4.11). The hardware can be configured to acquire the standard 12-lead ECG or ECG from the EASI unipolar, or bipolar electrode configurations (5 electrodes).

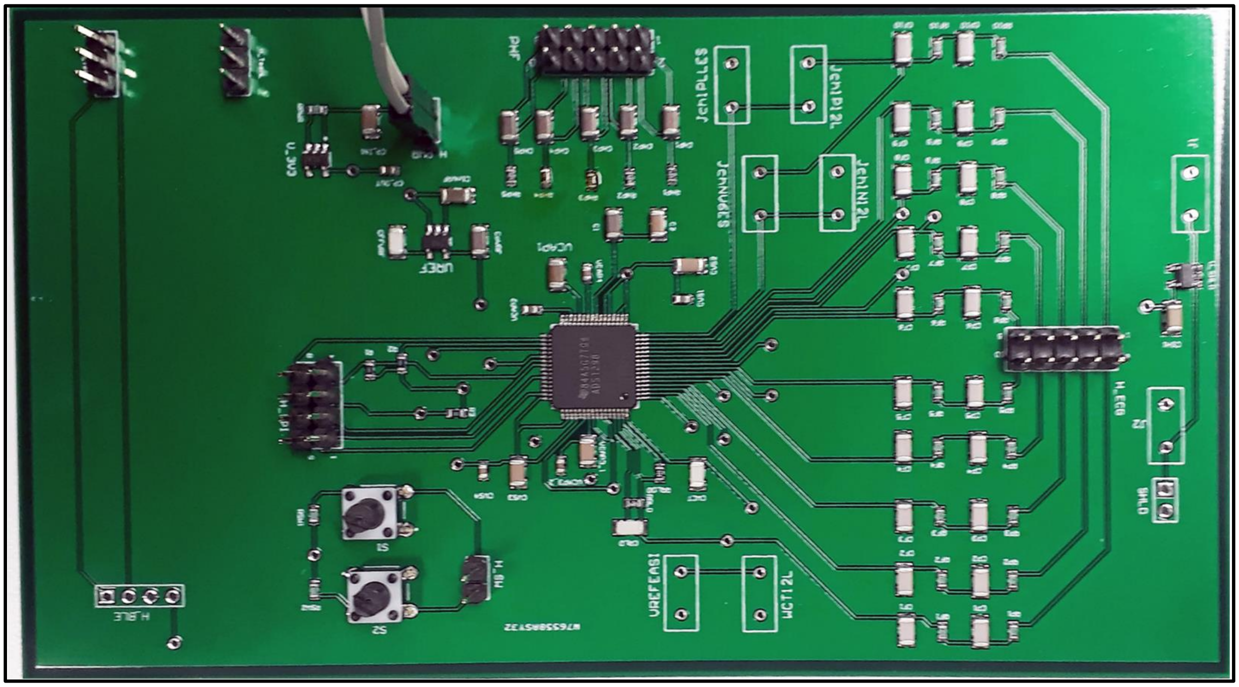

Figure 4.11: Twelve lead ECG prototyping hardware

4.4.9.2. EASI 12-lead equivalent ECG

As the EASI configuration was chosen to implement the final prototype, the ADS1298 was replaced with ADS1294 in the final ECG hardware to reduce power consumption, component density, and noise. The developed PCB had four layers and was divided into four sections: input and patient protection circuit, ECG - analogue front end (AFE), digital signal processing (DSP), and power circuit. Figure 4.12 illustrates the prototyping ECG hardware.

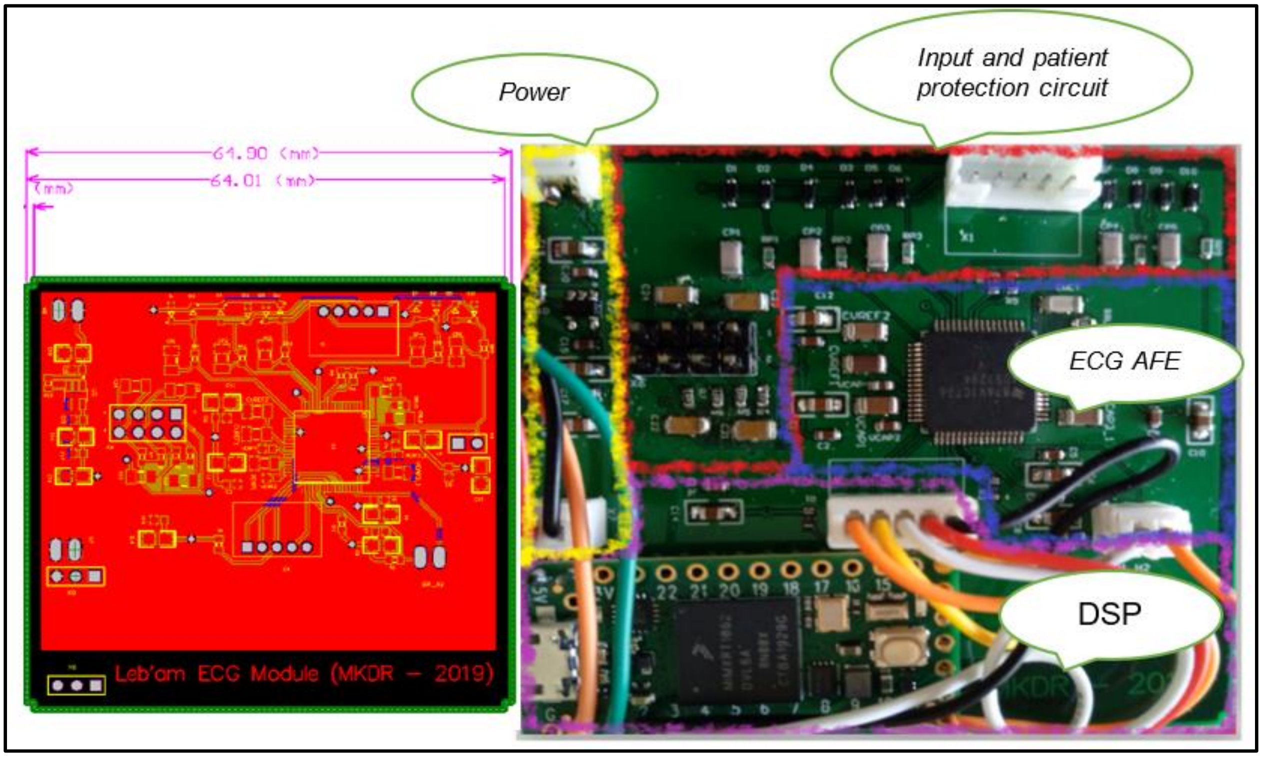

Figure 4.12: Prototyping ECG hardware PCB: 3D view (left) and the ECG hardware after assembly (right)

In summary, the final prototype of the ECG hardware is stand-alone that runs from a 5V DC power supply and is enclosed in a small box. There are three ports; a JST XH 5 pin, a 2.0 mm pitch female adapter to connect to the smart ECG vest, an off-on sliding power switch, and a micro-USB to charge the battery.

4.4.10. Enclosure box

An enclosure box (Figure 4.13) was designed using Autodesk Inventor 2018 and 3D printed in the design studio at Flinders University, Tonsley.

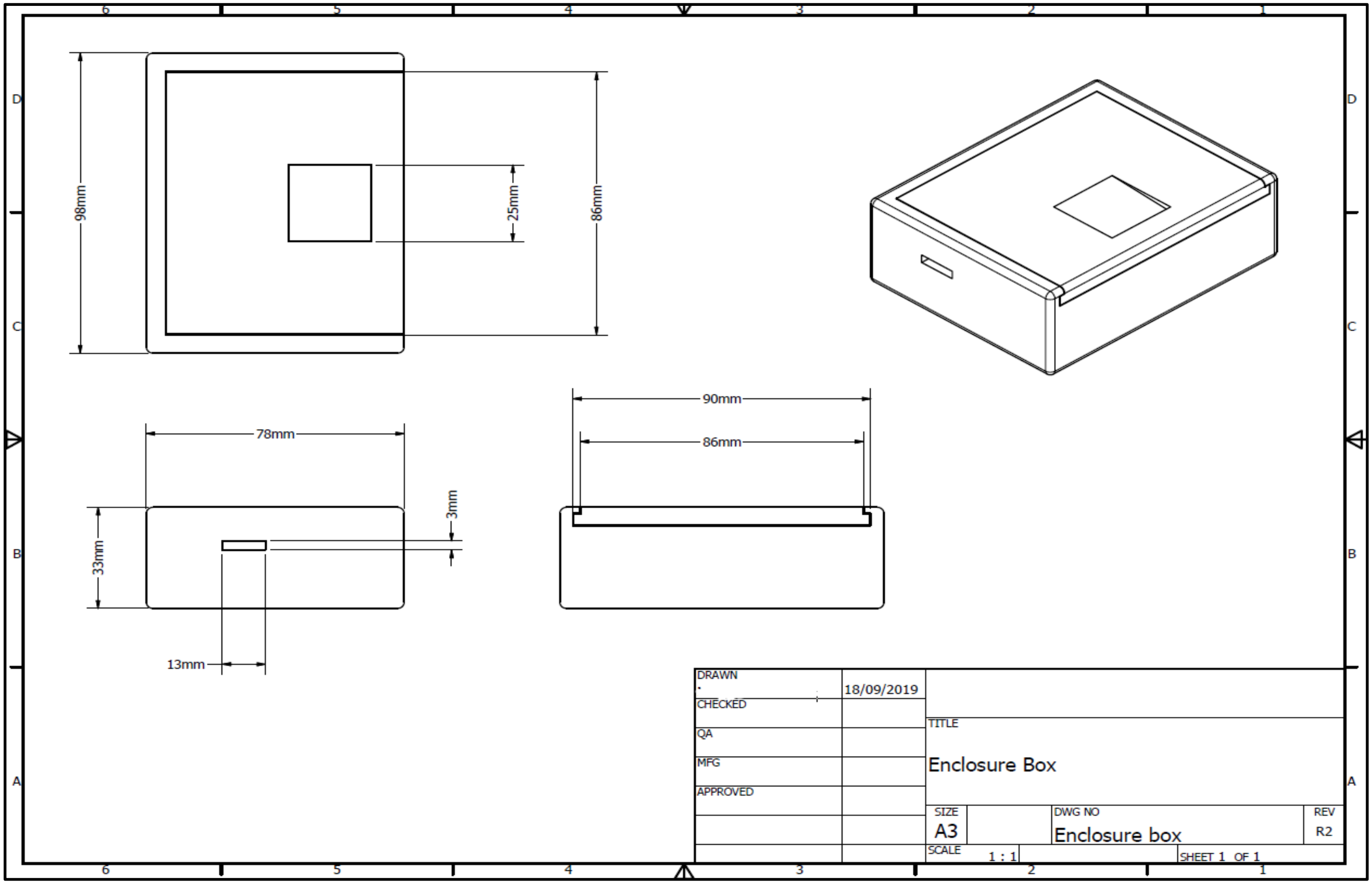

Figure 4.13: Enclosure box

4.5. Smart ECG Vest and the textile sensors

4.5.1. Specific objective

The specific objective of the study was to design and implement a versatile ECG vest from textile electrodes and circuit wiring.

4.5.2. The smart ECG vest

Once the hardware design and assembly were completed, the next task was to design and implement the ECG vest. The necessary features included a good fit between the textile electrodes and the patient's skin for quality ECG signal transduction, easy to wear, and comfortable for long term ECG monitoring. Additionally, the ECG vest required attachment points for the textile electrodes and the ECG hardware.

Therefore, the first issue to be addressed was the proper fit between the patient and the sensors. One of the options was to use a tight muscle fit T-shirt. The T-shirts proposed during the ideation stage are depicted in Figure 4.14. The major difference between these was the position of the zipper.

Figure 4.14: Sketches of the suggested tight-muscle fit T-shirt alternatives

Even though each of the illustrated tight-muscle fit T-shirts was produced, none of them granted a steady skin-electrode interface and required a lot more effort to put on, which would make it problematic for use by older people. As a result, a new design incorporating a hook-and-loop (Velcro-type) fastener (Figure 4.15) was developed (Figure 4.16).

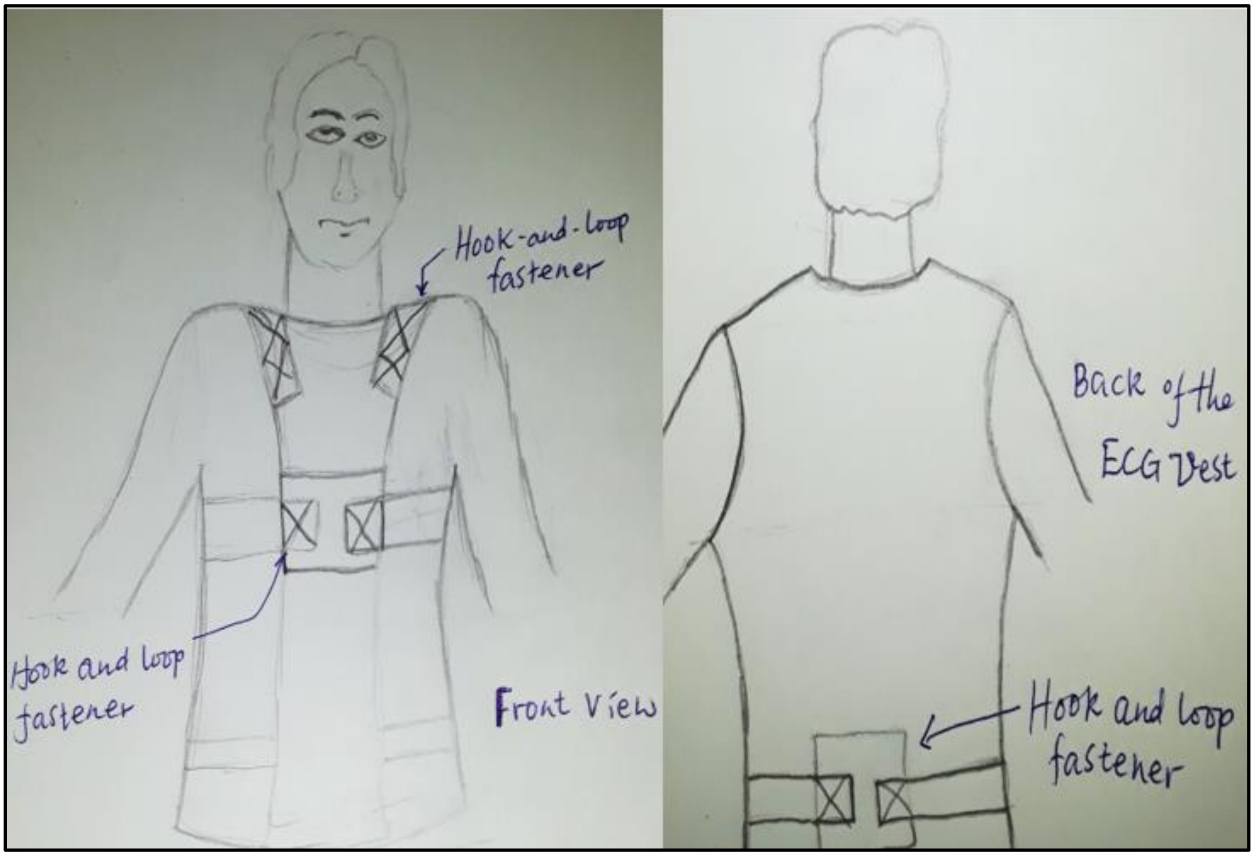

Figure 4.15: Sketches of the prototyping ECG vest with hook-and-loop fastener

Figure 4.16: The first ECG vest (left – proposed model; middle – anterior view and right – posterior view)

The Velcro fasteners on the left and right side of the neck run from the shoulder down towards the chest. The Velcro along the chest line loops around the back of the wearer and comes back to the chest. The combination of these Velcro fasteners hold the four electrodes (E, A, S, and I) firmly in place. The Velcro along the belly button secures the reference electrode and contributes to the overall stability of the textrodes.

The width of the hook-and-loop fastener for the '***A'*** and '***I'*** electrodes was selected so that it would not be too broad or too narrow. If the width of the loop is too broad, the slightest movement would generate excessive motion artefact and hence mask the ECG signal. If the width of the loop was too narrow, it would reduce the active electrode skin contact area, and hence the signal quality. Additionally, the smaller width loop would dig into the user's skin, which would reduce the wearer’s comfort. Therefore, a hook-and-loop width of 8cm (Figure 4.17) was selected considering the size of the e-textile electrodes (40mm^2, 60mm^2, and 70mm^2).

Figure 4.17 and Figure 4.18 depict the detailed design of the smart Vest.

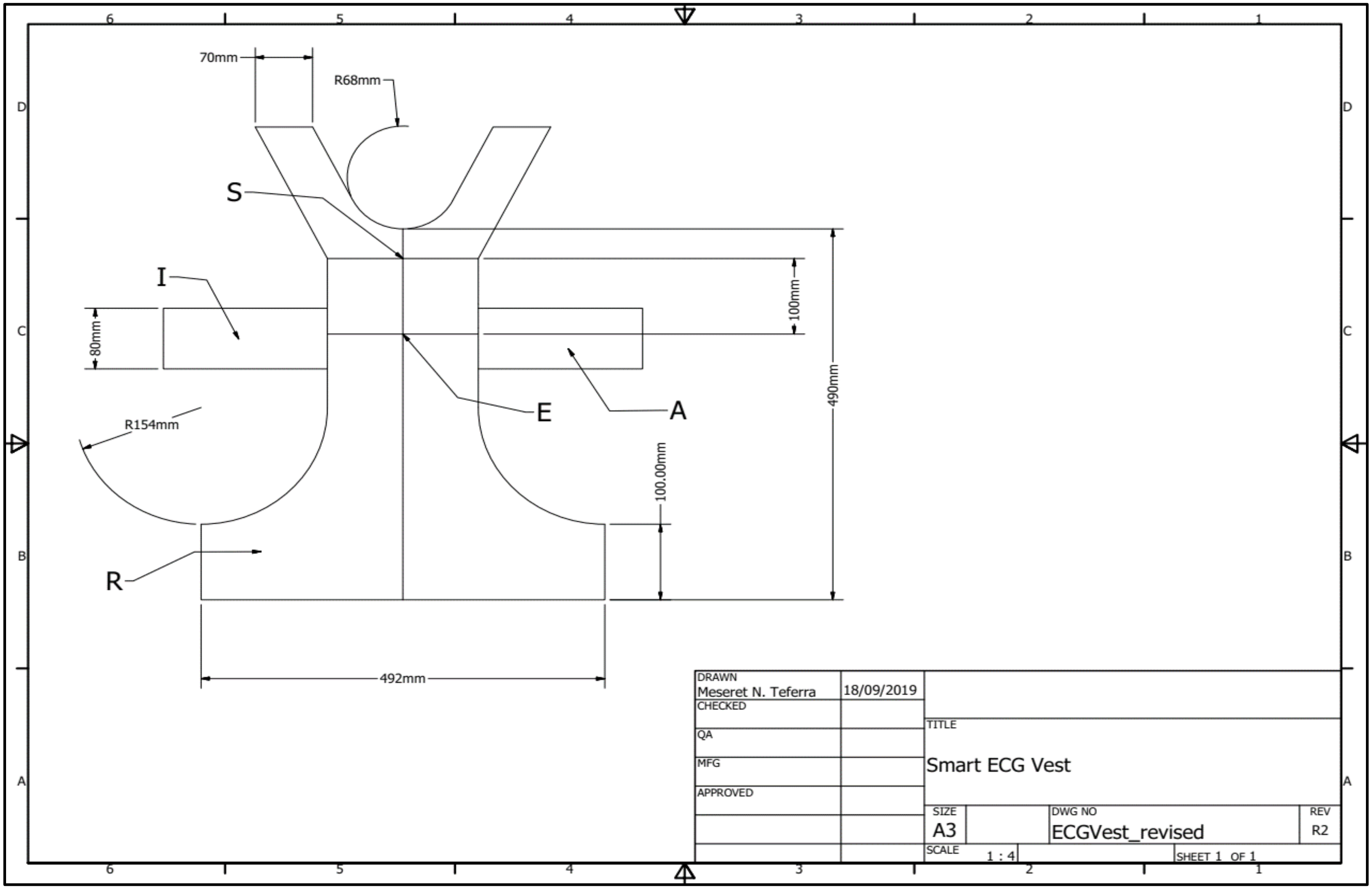

Figure 4.17: Anterior component of the smart ECG vest

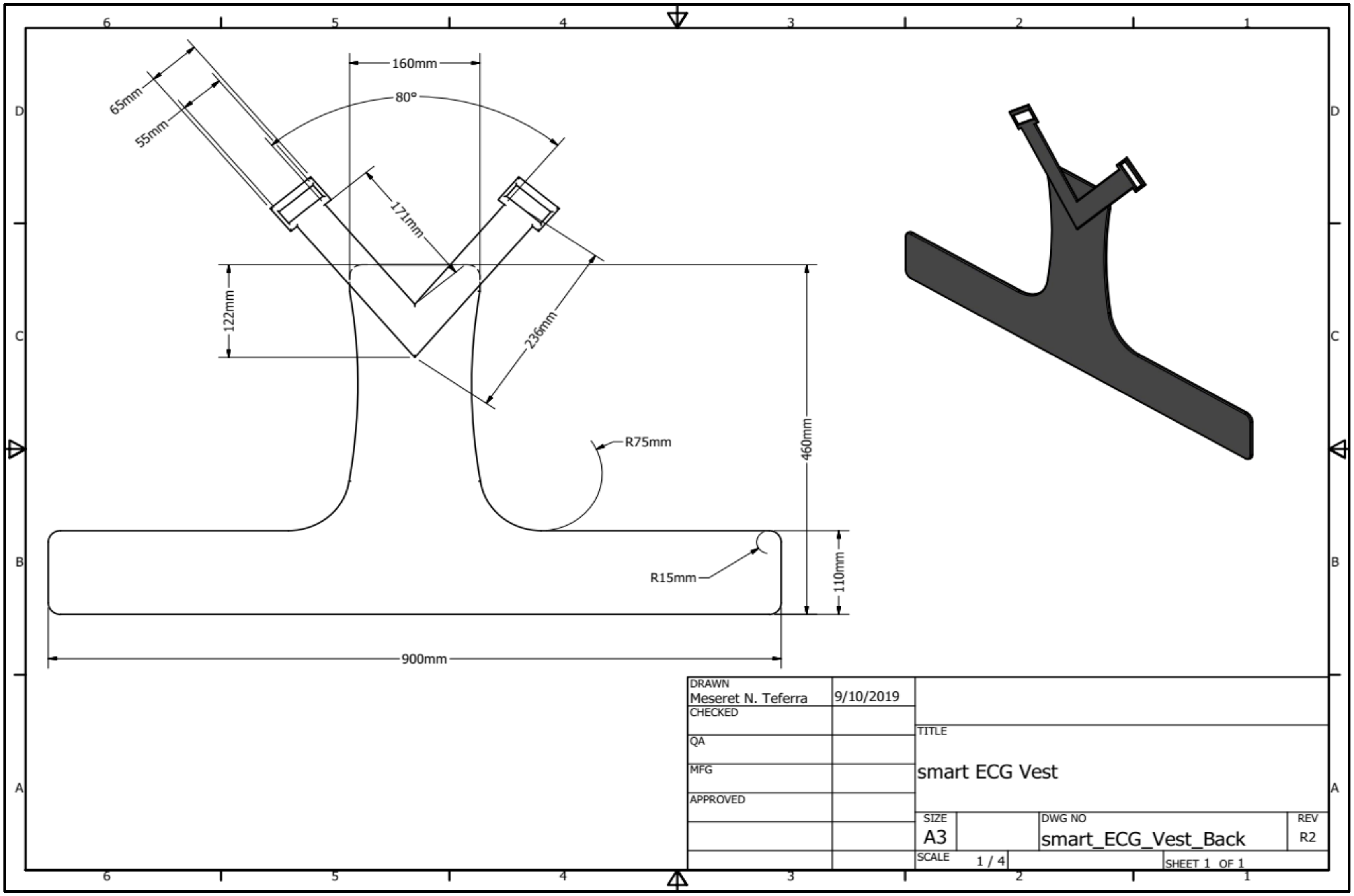

Figure 4.18: Posterior component of the smart ECG vest

4.5.2.1. Embedded wiring into the smart ECG Vest

The success of a smart yarn application relies on the proper connection between the sensors and the central controller. To date, both fixed connections (thermal joining, mechanical fastening, and adhesives), and removable connections (including hook and loop, snap fasteners, plug connectors, magnetic contacts, and conductive zippers) have been suggested in the literature (Mehmann et al., 2017). In this design, snap fasteners were chosen to increase the usability of the ECG vest, allowing commercially available wet or dry electrodes to be used instead of the textile electrodes if required.

Two options were considered for the connection of the textile electrodes to the ECG hardware: smart fabrics and wires. The former are easy to integrate into the clothing. However, they require proper insulation and it can be challenging to establish a firm interface between the fabric and the hardware connectors. Additionally, repeated washing degrades the conductivity of the clothing. The latter option, wires, are insulated, have fixed resistance value, and are easy to solder and secure to the connectors.

On the other hand, wires are relatively challenging to weave into the garment. Moreover, the soldering points become brittle and could break easily during washing. Despite these downsides, in the proposed design, five wires were integrated into the ECG vest. On one end, the wires were securely connected to a 12mm snap fastener. On the other side, a JST XH 5 pin, 2.0 mm pitch male adapter was used. The vest is made up of Mid Blue cotton and polyester bed sheet from K-mart (Kmart Australia, n.d.) and a white Lycra/Spandex four Way Stretch fabric from eBay (eBay Inc., n.d.). Figure 4.19 presents the ECG vest prototype.

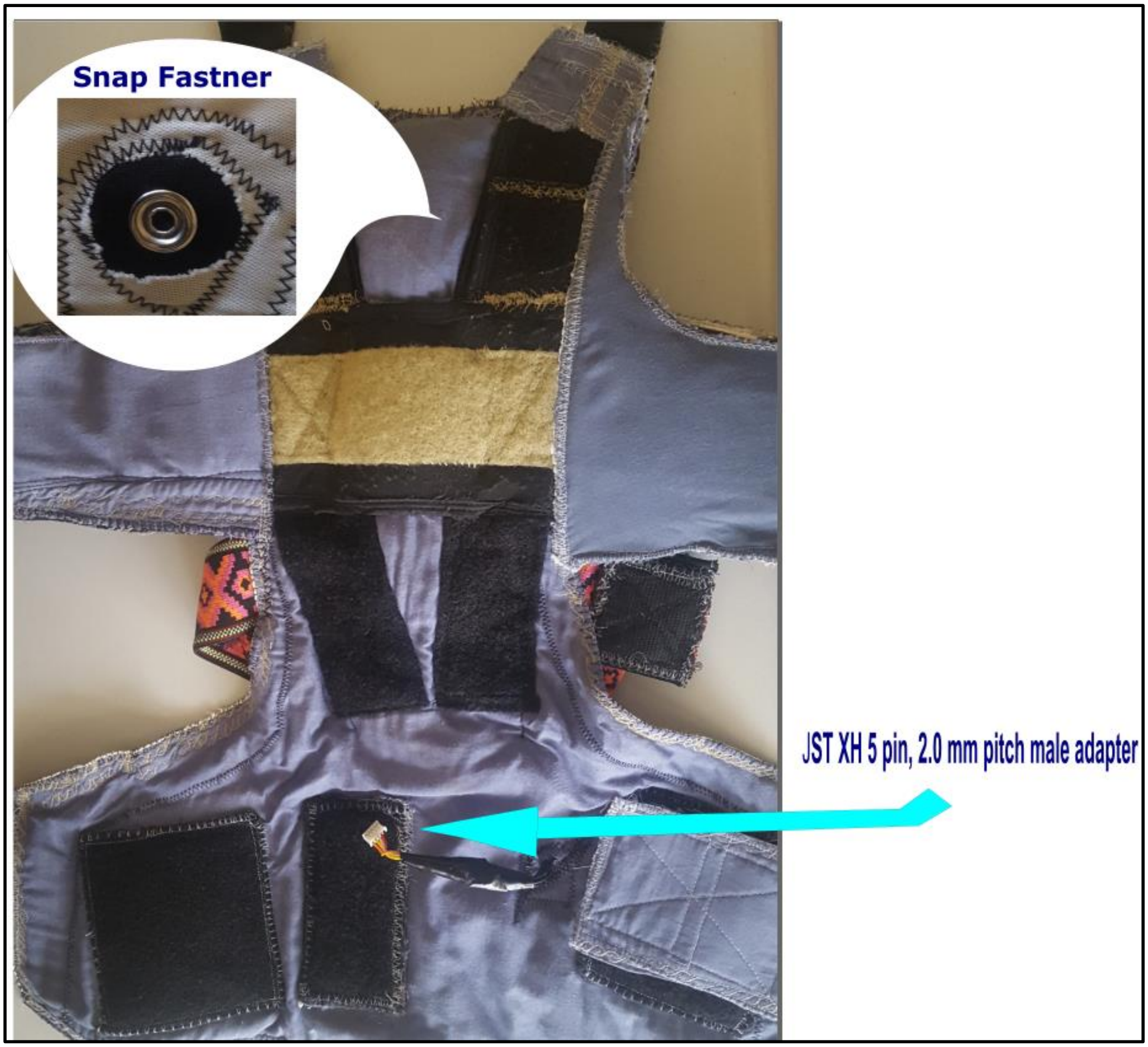

Figure 4.19: ECG vest prototype with embedded wires, JST XH 5 pin, 2.0mm pitch male adapter and 12 mm snap fastener.

4.5.2.2. Production of the smart ECG vest

A BERNINA - 315 PE sewing machine (BERNINA Australia, n.d.) was used to make the smart ECG prototype vests.

Two final prototypes of the ECG vest were made based on the models shown in Figure 4.17 and Figure 4.18. The first smart ECG vest (sECGVest1, Figure 4.20, left) consisted of both the posterior and the anterior components of the proposed model. The other smart ECG vest (sECGVest2, Figure 4.20, right) was based on the anterior segment alone with a slight modification allowing rapid prototyping and intuitive use.

Figure 4.20: The proposed smart ECG vests; sECGVest1(left) and sECGVes2 (right)

4.5.3. The textile electrodes

Nowadays, a variety of sensors are used to detect ECG, although silver/silver chloride (Ag/AgCl) electrodes, coupled with a conductive gel or saline adhesive electrolyte, are the most common. However, the wet electrolyte tends to dry over time, and hence signal quality deteriorates. In this regard, e-textile based ECG sensors could offer an alternative solution, especially for long-term cardiac monitoring (Meziane et al., 2015, van Langenhove, 2015, Tsukada et al., 2019).

So far, both passive (Paradiso et al., 2005, Coosemans et al., 2006, Jourand et al., 2010, Bouwstra et al., 2011, Varadan et al., 2011, Peltokangas et al., 2012, Carvalho et al., 2014, Yu et al., 2017) and active (Ueno et al., 2007, Fuhrhop et al., 2009, Xiang Chen et al., 2012, Chamadiya et al., 2013) textile sensors are proposed for long term ECG acquisition. Active textile electrodes require the integration of active components, which in turn draws power for proper operation. However, one of the primary requirements for wearable applications is low power consumption (Zheng et al., 2010). In this regard, passive textile ECG electrodes were chosen to reduce circuit complexity and power requirement of the e-textile based ECG monitor.

4.5.3.1. Making of the textile electrodes

The ECG sensors were implemented from three types of commercially available smart fabrics - Woven Conductive Fabric (silver-plated nylon), Knit Conductive Fabric (Silver), and Knit Jersey Conductive Fabric (63% cotton, 35% silver yarn and 2% spandex) from

Adafruit. The textile electrodes have different sizes of contact surface areas and the smallest was chosen as 40mm^2 based on a previous study by Marozas et al. (2011).

The textile electrodes were modelled on Autodesk Inventor 2018 (Figure 4.21). The model was printed on paper and used to cut the conductive fabrics to the size of the proposed textile electrodes (40mm^2, 60mm^{2,} and 70mm^2). Then, a 12mm male snap fastener was secured at the centre of the textile fabric using the Birch Snap Fastener Pliers (Spotlight Pty Ltd, 2020). Once the snap fastener was secured, a 3mm thick black PVC Foam (Bunnings, n.d.) was inserted between the smart fabrics. Finally, the BERNINA - 315 PE sewing machine was used to produce the electrodes in the MDRI laboratory at Flinders University, Tonsley.

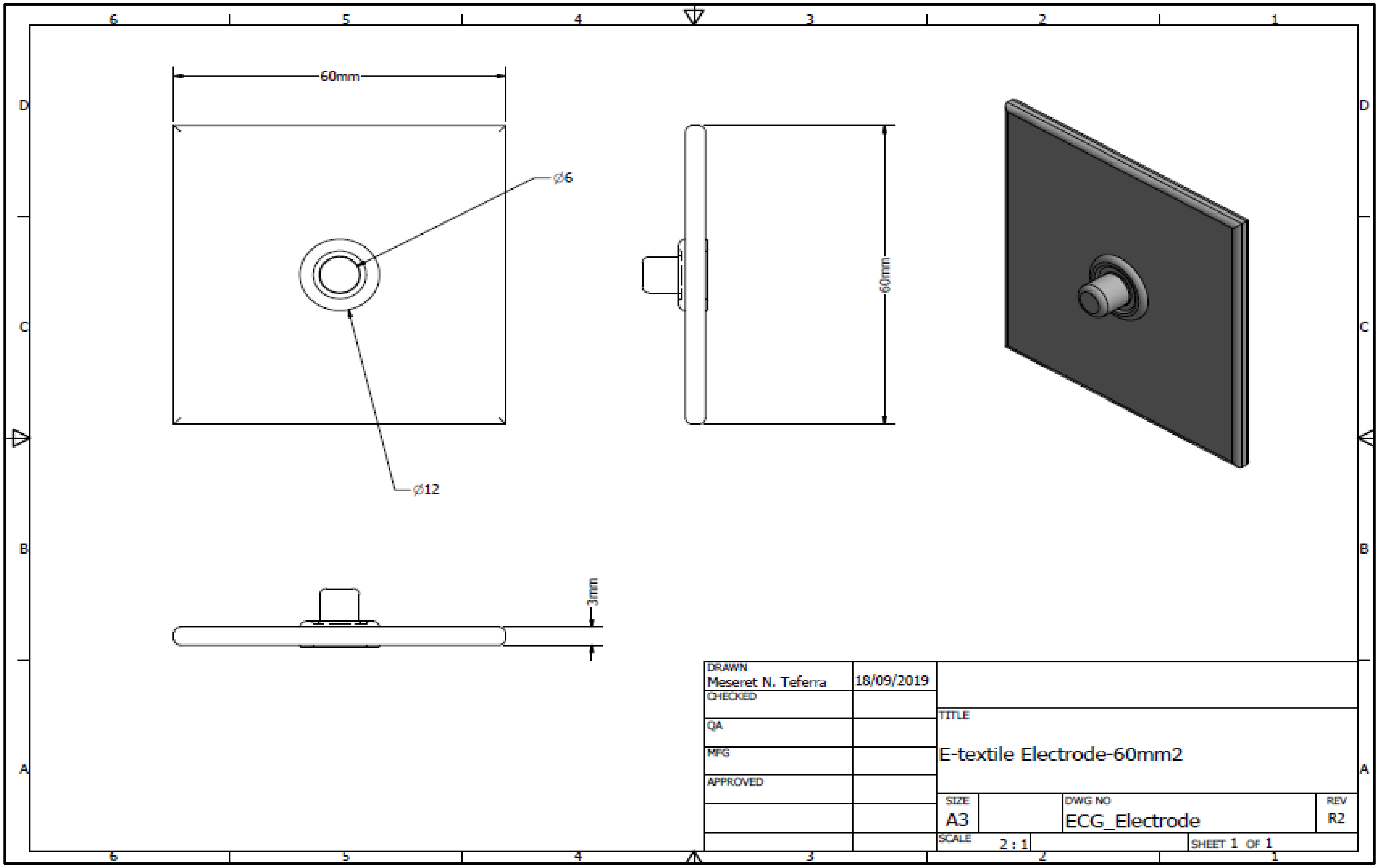

Figure 4.21: The e-textile ECG sensor (*Size: 60mm²*)

4.6. ECG viewer and data logger

The next step was to develop a platform where the real-time ECG will be displayed and saved for further analysis. The software is based on the telemetry viewer v0.5 by Farahbod (2018). The ECG viewer is based on OpenGL. It is GPU accelerated and optimized for real time application.

4.6.1. Specific objective

The specific objective of the study was to design and implement a Java-based desktop platform (ECG viewer) used to display the real-time ECG and save the data for later processing.

4.6.2. Software architecture

The general architecture of the Lebam ECG viewer is shown in Figure 4.22. The software incorporates user-friendly windows (Figure 4.23). The secured login page is the first window that pops up, followed by the parent window. The user has an option to fill the details of the patient and save the data ahead of ECG acquisition. The default value of the scaling factor (gain) is 2X; however, it is possible to change the gain according to the amplitude of the received ECG tracings. Before the start of the ECG exam, it is necessary to establish a proper serial connection (via Bluetooth) between the ECG hardware and the host PC. Clicking the START button on the bottom right corner of the parent window initiates the required wireless communication. On the ECG viewer, a real-time 12 led ECG is the default configuration. However, there is a three and five lead option.

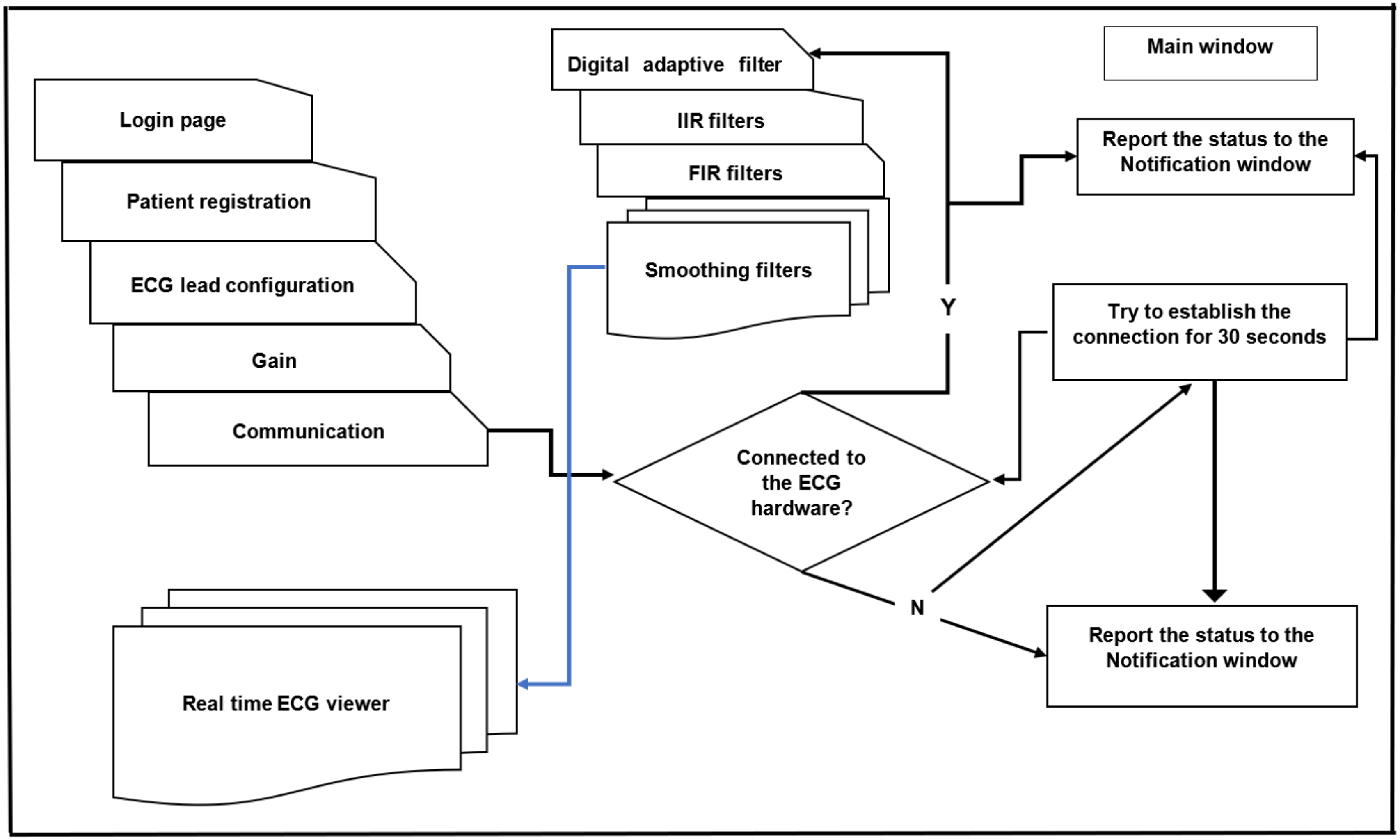

Figure 4.22: Lebam software architecture

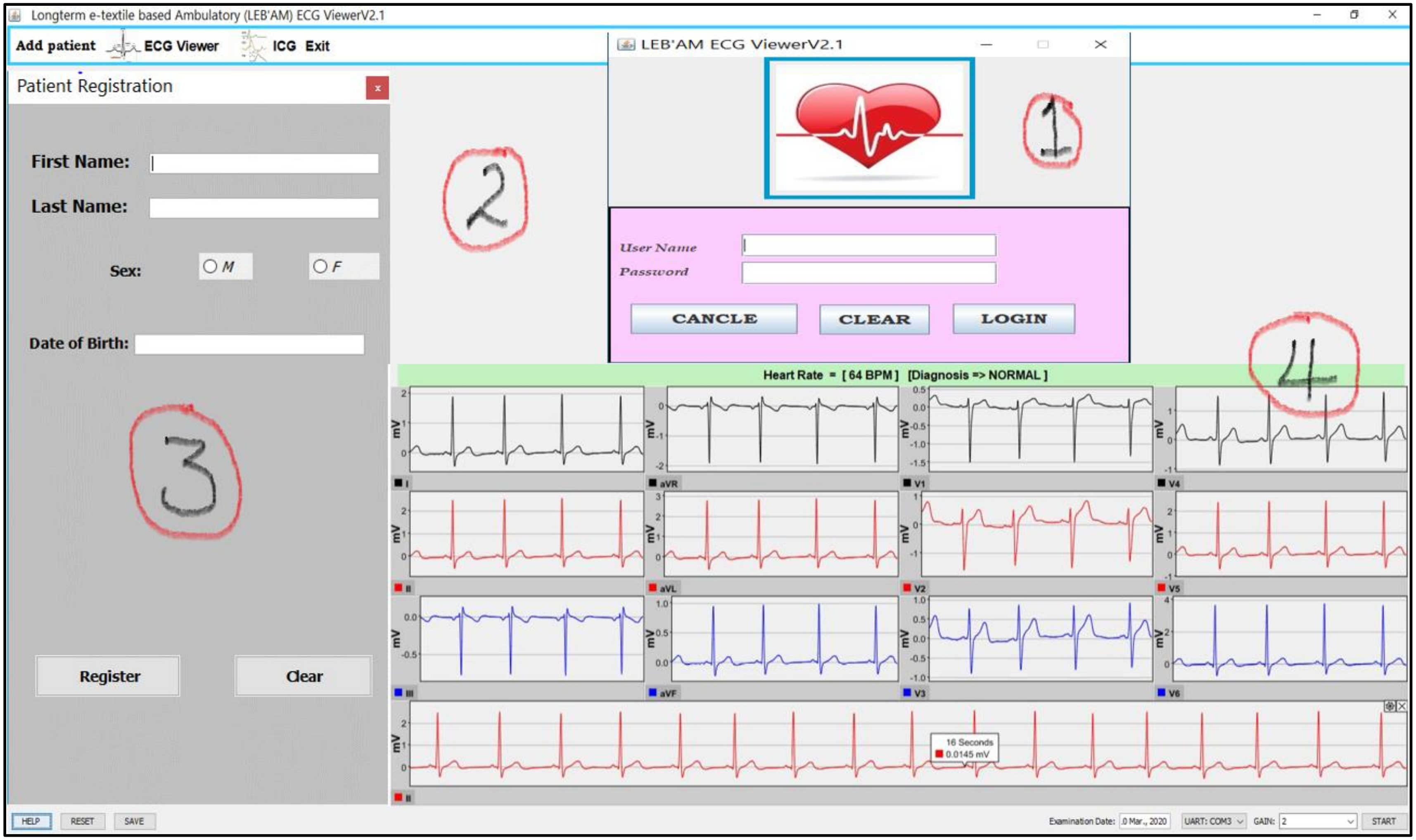

Figure 4.23: ECG viewer user-friendly GUIs: secured log-in page (1); parent window (2); patient registration (3) and real-time ECG display (4)

4.6.3. Java-based real-time digital filters

The underlying digital adaptive filter bank is comprised of IIR (Butterworth filters) and smoothing filters (moving average, Savitzky Golay, and Kalman filter) that are optimized for real-time application.

For the same filter order, IIR filters exhibit higher selectivity and attenuation than the FIR counterpart. Among the IIR filters, Butterworth filters have a maximum flat response in the passband (Singh et al., 2010, National Instruments, 2015). Therefore, Butterworth IIR filters were chosen. The Java-based real-time IIR filters are open-source application programming interfaces (API) and are adopted from Porr (2019). On the other hand, the moving average filter is a Java implementation of previous studies (Chen and Chen, 2003, Hu et al., 2011). The formula used to implement the Java-based moving average filter is given in equation 4.2 (Hu et al., 2011).

$$y[n] = \frac{1}{2\mathrm{N}+1}\sum_{m=-N}^{N} x[n+m]$$

Where x[n], y[n] = the input data and output data respectively [4.2]

2N+1 = filter length

The application of the Savitzky Golay filter for ECG denoising is well documented (Hargittai, 2005, Awal et al., 2011, Kaur and Singh, 2011, AlMahamdy and Riley, 2014). The real-time Java-based Savitzky Golay filter is a polynomial Finite Impulse Response filter where the coefficients were generated using a built-in MATLAB function for a given order and widow length (The MathWorks Inc., n.d.). Finally, the single variable Kalman filter was implemented based on the algorithm given in Figure 4.10. Figure 4.24, depicts the Java-based real-time ECG denoising sequencing.

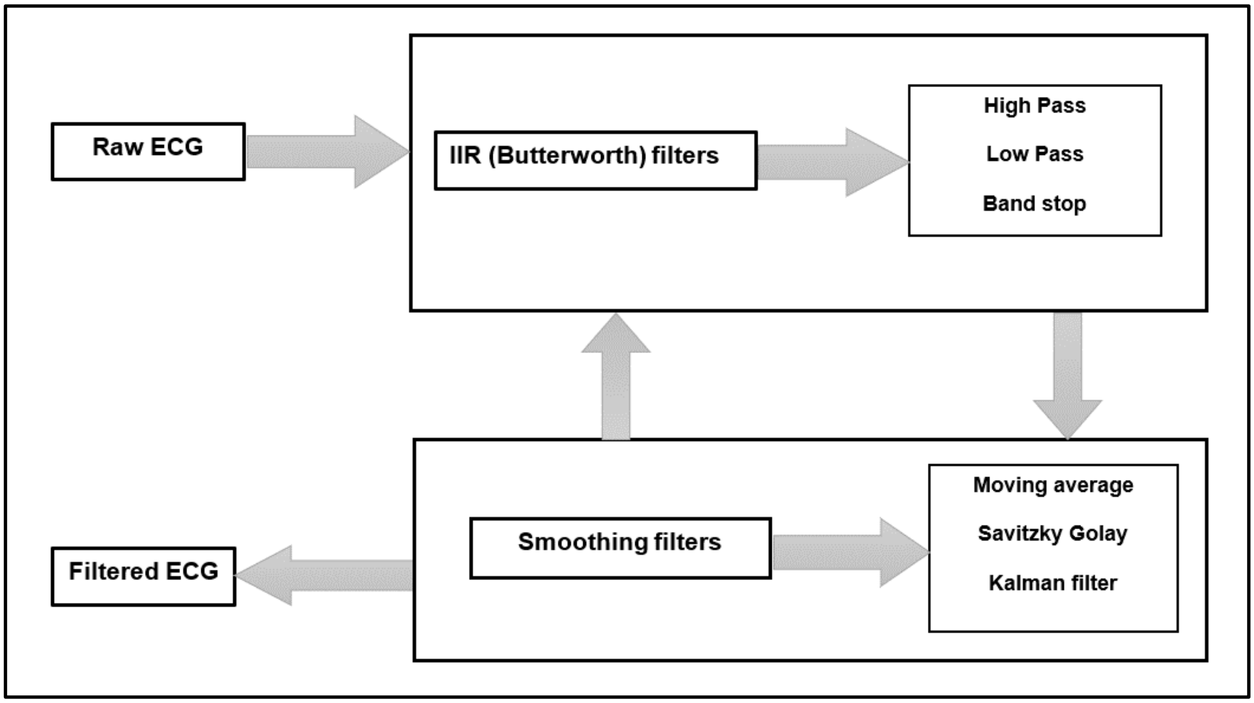

Figure 4.24: Flow chart illustrating the real-time ECG denoising.

4.7. The textile-based ECG monitor prototype

The textile-based ECG monitor consists of the smart ECG vest, textile electrodes, and the ECG hardware. The proposed ECG monitor measures ECG using textile sensors and wiring embedded in a garment. The general architecture of the complete system is illustrated in Figure 4.25. This can be compared with Figure 4.26, which shows the typical 12-lead ECG displayed on the real-time ECG viewer.

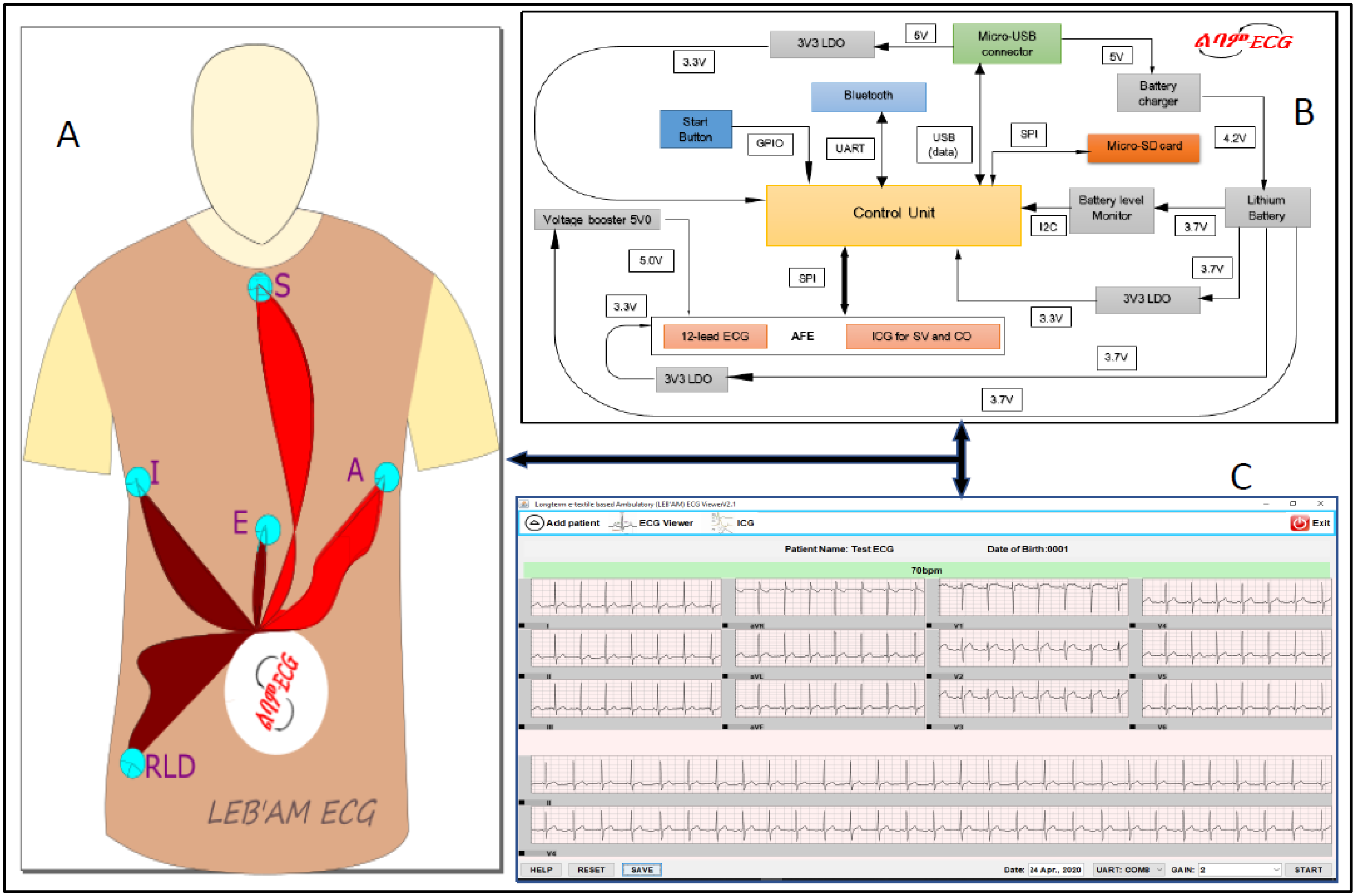

Figure 4.25: The e-textile based ECG monitor system architecture (***A** – smart Vest and embedded wiring;* ***B** – ECG hardware;* ***C** – ECG viewer and data logger*)

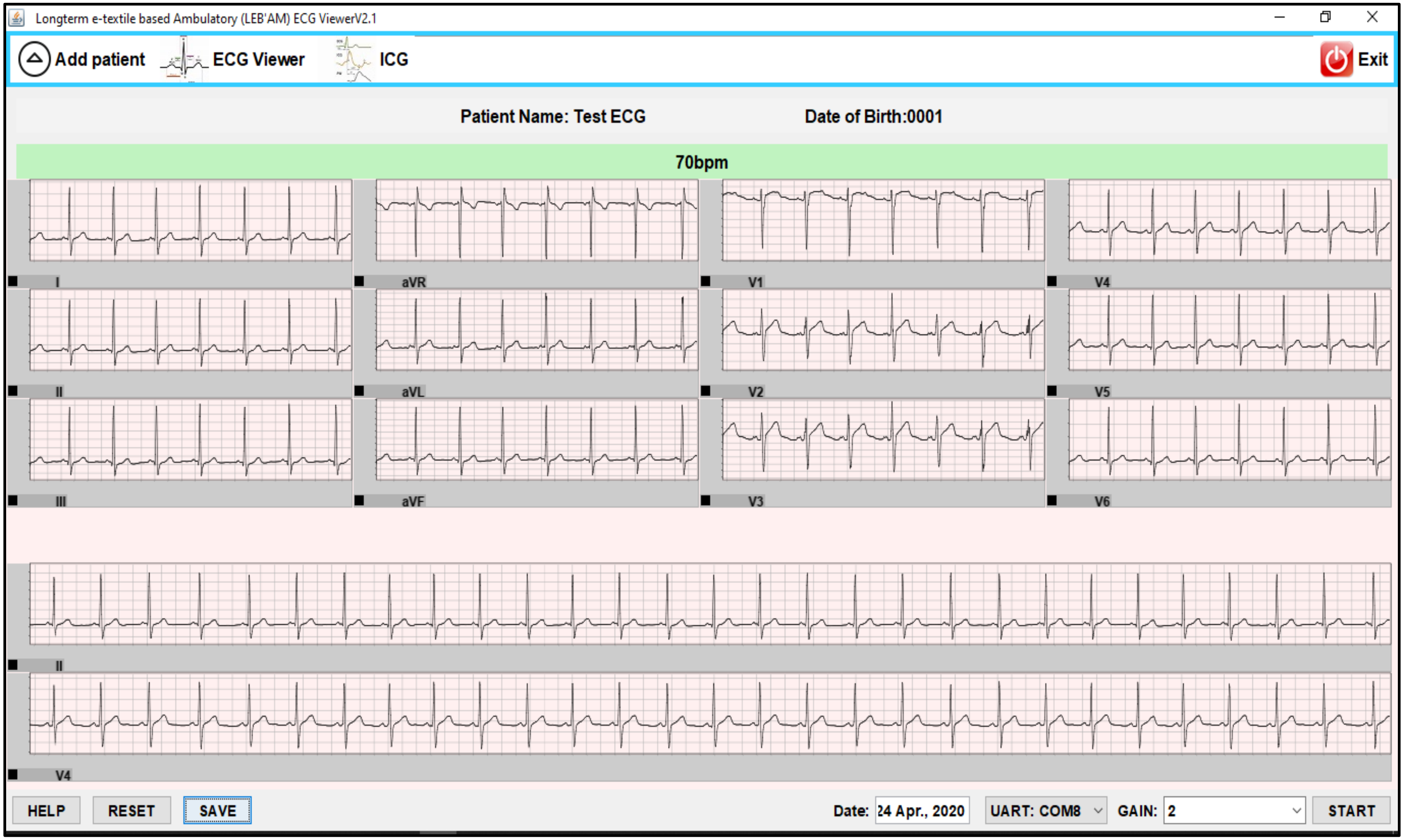

Figure 4.26: A snapshot of a 12-lead real-time ECG.

4.8. Conclusion

Twelve-lead ECG monitors are the gold standard for clinical diagnostics of cardiac abnormalities. However, for ambulatory monitoring, the standard ten electrode Holter monitor is complex in construction and can be uncomfortable for the wearer. This chapter presented the design and development of the e-textile 12-lead equivalent ECG monitor based on the EASI electrode configuration designed for telemonitoring of cardiac patients.

This page is left blank intentionally

Chapter 5. Electronic textile-based ECG monitor: module-level test and evaluation

5.1. Introduction

This chapter presents modular testing and assessment of the EASI 12-lead equivalent ECG monitor based on textile sensors and embedded wiring. The first set of tests (described in sections 5.3 and 5.4.1) was designed for testing and evaluation of the ECG hardware, the ECG viewer and data logger, and the smart ECG vest and textile electrodes. The second study (in section 5.4.2) presents the experimental determination of the compression pressure applied by the smart ECG vest for the successful transduction of ECG from the textile electrodes.

5.2. Specific objectives

The specific objectives were:

1. To evaluate the accuracy and reliability of the e-textile based EASI 12-lead equivalent ECG prototype electronics hardware module:
   a) To study the response of the ECG hardware to known inputs such as ADS129X specific built-in test signals and test signal from the ProSim 3.0 Vital sign simulator (Section 5.3.1)

b) To examine the ability of the ECG hardware to discriminate abnormalities in simulated ECG signals (Section 5.3.2)

c) To examine the performance of the Java-based ECG viewer and data logger (Section Appendix I)

2. To evaluate the accuracy and reliability of the e-textile electrode response to external factors:

a) To examine the response of the smart ECG vest and the textile electrodes to repeated washing (Section 5.4.1)

b) To determine the compression pressure that needs to be applied by the smart ECG vest onto the user (Section 5.4.2)

5.3. Evaluating the accuracy and reliability of the e-textile based EASI 12-lead equivalent ECG prototype electronics hardware module

5.3.1. Response of the ECG hardware to known inputs

5.3.1.1. Specific objectives

The specific objectives of the research were to study the response of the ECG hardware to known inputs such as ADS129X specific built-in test signals, and to a simulated ECG signal from the ProSim 3.0 Vital Signs Simulator.

5.3.1.2. Methods

Testing the ECG hardware based on ProSim 3.0 Vital Signs Simulator

It is customary to use an artificial signal of known magnitude and frequency to calibrate and test the performance of an ECG monitor (Ueno et al., 2007, Andreoni et al., 2013, Lin et al., 2013, Zhou et al., 2013, Wang et al., 2015, Caldara et al., 2017a, Li et al., 2017). In this regard, the signal reception and fidelity of the proposed ECG monitor were evaluated based on a number of simulated ECG signals generated from the ProSim 3.0 Vital Signs Simulator from Fluke Biomedical (Fluke Biomedical, n.d.). The test protocols are presented below.

ECG hardware design parameters

a. Internal test signal

b. Intrinsic noise test

c. Sampling rate (samples per second): 500sps, 1Ksps, 2Ksps, 4Ksps, 8Ksps, 16Ksps

d. Noise: 50Hz noise, baseline wander, respiration

Physiological parameters

a. Different ECG amplitude: [0.5 - 5.5] mV

b. Different HR: [40 - 200] bpm

Data comparison techniques

Summarized below are the quantitative measures and techniques used for the component level testing and analysis of the textile-based 12-lead ECG monitor.

Signal to noise ratio

Signal to Noise Ratio (SNR) is a measure of relative power between the desired signal and unwanted interference. SNR is one of the parameters used extensively in signal processing (Cheng et al., 2008, Lee et al., 2008, Loewe et al., 2011, Kannaian et al., 2013, Rattfält, 2013, Atallah et al., 2014, Takamatsu et al., 2015, Wang et al., 2015, Cho et al., 2016, Trindade et al., 2016, Li et al., 2017, Sun et al., 2017).

SNR1 is defined in equation 5.1 (Alfaouri and Daqrouq, 2008, Raeiatibanadkooki et al., 2014, Sundar et al., 2016):

$$SNR1 = 10 * \log_{10}\left(\frac{\sum_{i=1}^{N}(\bar{x}(i))^2}{\sum_{i=1}^{N}(x(i)-\bar{x}(i))^2}\right), \qquad [5.1]$$

$Where\ x(i)$: the raw ECG signal

$\bar{x}(i)$: the filtered ECG signal

SNR2 based on normalized mean square error (Sundar et al., 2016) is given in equation 5.2:

$$SNR2 = 10 * \log_{10}\left(\frac{\sum_{i=1}^{N}(\bar{x}(i))^2}{\frac{\sum_{i=1}^{N}(x(i)-\bar{x}(i))^2}{\sum_{i=1}^{N}(x(i))^2}}\right), \qquad [5.2]$$

SNR3 based on mean normalized ECG and normalized mean square error is defined in equation 5.3:

$$SNR3 = 10 * \log_{10}\left(\frac{\dfrac{\sum_{i=1}^{N}(\bar{x}(i) - x)^2}{\sum_{i=1}^{N}(x(i) - \bar{x}(i))^2}}{\sum_{i=1}^{N}(x(i))^2}\right), \qquad [5.3]$$

Where x: the mean of the clean ECG signal

Another qualitative term used to measure signal quality along with SNR is the Peak Signal to Noise Ratio (PSNR) defined in equation 5.4. In a noisy environment, the mean absolute error is the preferred way of measuring error (Willmott and Matsuura, 2005). Hence, mean absolute error is used in calculating the PSNR.

$$PSNR = 20 * \log_{10}\frac{\max(x(i))}{MAE} \qquad [5.4]$$

Where $\max(x(i))$: the peak value of the raw ECG signal

MAE: Mean absolute error

Two additional parameters used to measure signal quality were percentage root mean square differences (PRD1 and PRD2) as defined in equation 5.5 (Alfaouri and Daqrouq, 2008, Kim et al., 2009, Abo-Zahhad et al., 2012):

$$PRD1 = \sqrt{\frac{\sum_{i=1}^{N}(x(i) - \bar{x}(i))^2}{\sum_{i=1}^{N}(x(i))^2}} * 100, \quad PRD2 = \sqrt{\frac{\sum_{i=1}^{N}(x(i) - \bar{x}(i))^2}{\sum_{i=1}^{N}(x(i) - \mu)^2}} * 100 \qquad [5.5]$$

Where μ: the mean of the raw ECG signal

The higher the value, the better the energy content in the e-textile ECG. For example, a lower SNR requires complex signal processing algorithms to reduce noise (Phukpattaranont, 2014).

Power spectral density

The power spectral density (PSD) is a frequency domain parameter widely used to study ECG signal power content and distribution across the frequency spectrum of interest (Bourdon et al., 2005, Scilingo et al., 2005, Stoica and Moses, 2005, Puurtinen et al., 2006, Merritt, 2008, Bianchi and Mendez, 2010, Marozas et al., 2011, Chamadiya et al., 2013). The formula used to calculate PSD is given in equation 5.6 (Kaur and Singh, 2011, The MathWorks Inc., c2020a):

$$PSD = \frac{1}{fsN} \left| \sum_{n=1}^{N} x(n) e^{-j(2\Pi f / fs)n} \right|^2 \quad [5.6]$$

Where $x(n)$: the signal

fs: sampling frequency

N: number of data points

Data analysis

MATLAB 2017a was used to analyse the acquired ECG.

5.3.1.3. Results

ADS129X built-in test signals

Internal test signal

It is possible to study how an electronic circuit responds if a well-defined electrical signal is applied at its input terminals. In this regard, an internally generated $1mV_{pp}$ square wave test signal was used to study the ability of the ADS1294 ECG module to reproduce the applied input signal. Figure 5.1 depicts the response to the $1mV_{PP}$ internal test signal.

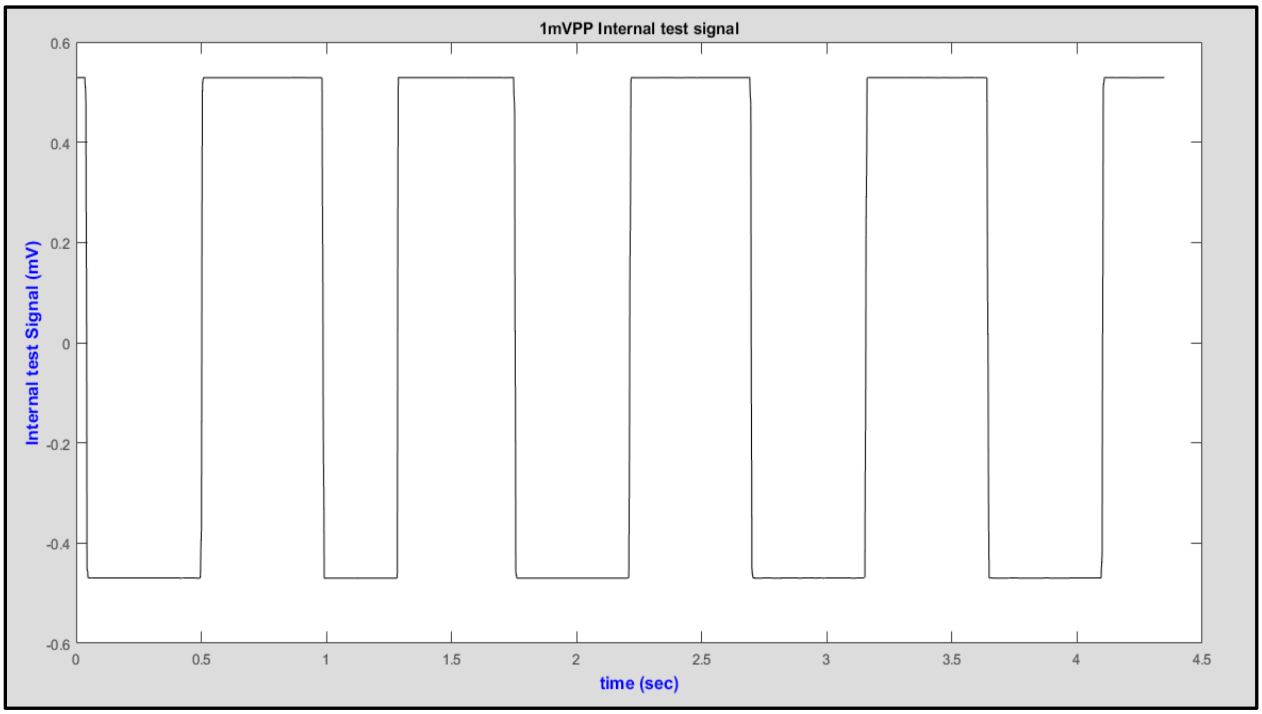

Figure 5.1: Response of the ECG hardware for $1mV_{PP}$ internal test signal (Based on the ADS1294, input = $1.0mV_{PP}$, output = $1.000994mV_{PP}$)

Intrinsic noise test

Each channel of the ADS1294 consists of positive and negative terminals. The two terminals were short-circuited to assess the internal noise generated due to the electronics components. An internal short circuit test was conducted to ascertain that the ECG hardware satisfies the recommended fundamental noise level stated by the manufacturer of the ADS1294 (5µVpp) (Texas Instruments, 2015, p. 14). As depicted in Figure 5.2, the intrinsic noise level was around 10µVpp.

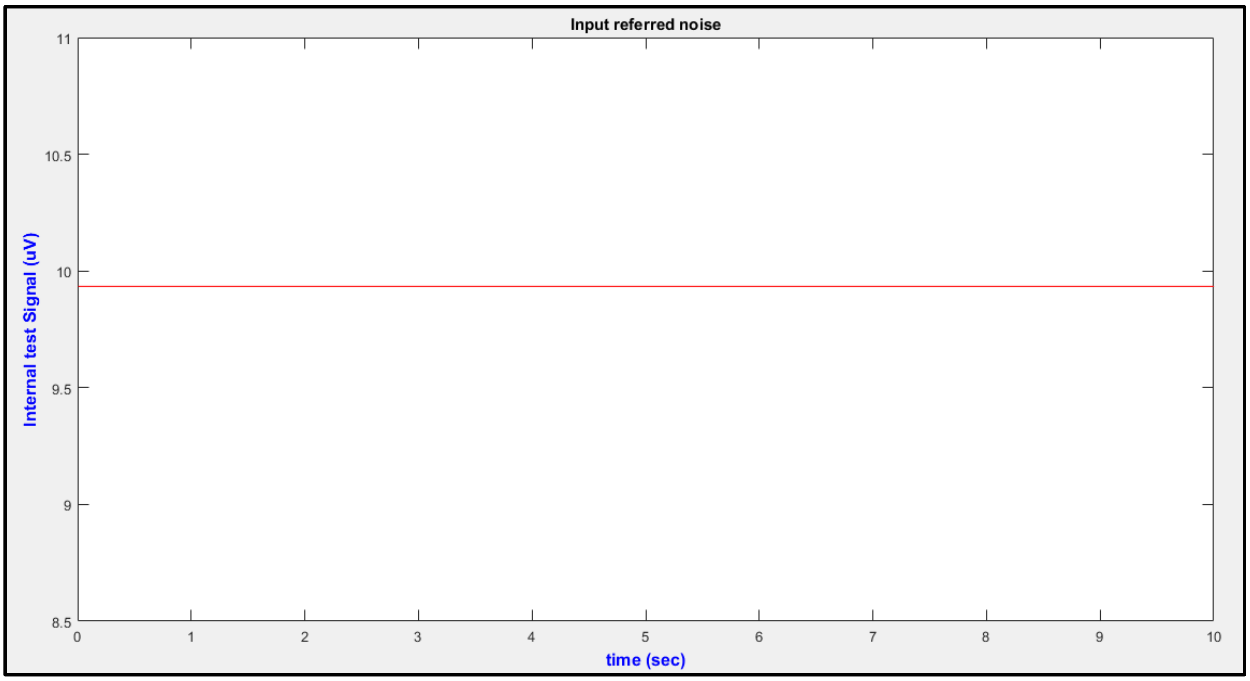

Figure 5.2: Input-referred noise from the ADS1294 based ECG hardware (CH1: 500sps, 4.0V reference voltage).

Test results based on ProSim 3.0 ECG Simulator

A ProSim 3.0 Vital Signs Simulator from Fluke Biomedical (Fluke Biomedical, n.d.) was used to test the performance of the ECG hardware and software.

Twelve-lead ECG

The ECG hardware successfully acquired 12-lead standard simulated ECGs at 250, 500, 1K, 2K, 4K, and 8Ksps. Higher sampling frequencies showed an increased level of noise in the acquired ECG signal. After 12 hours of continuous ECG retrieval, sampling frequencies higher than ~4Ksps resulted in increased noise in the signal. However, this problem did not happen with the final prototype, due to careful design and assembly of the ECG hardware. Figure 5.3 depicts different leads acquired from ProSim 3.0 Vital Signs Simulator at 500 and 8Ksps.

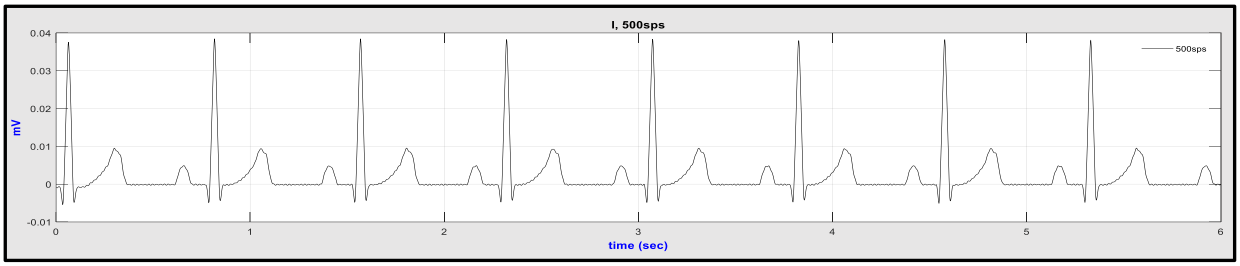

a) Lead-I, 500sps

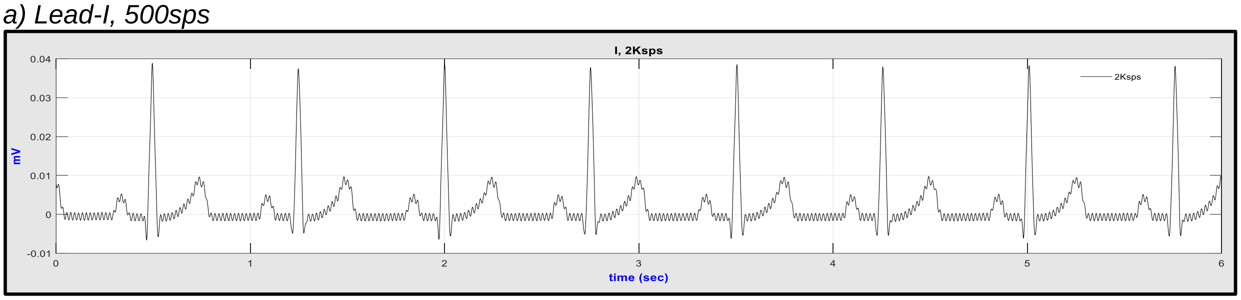

b) Lead-I, 2Ksps

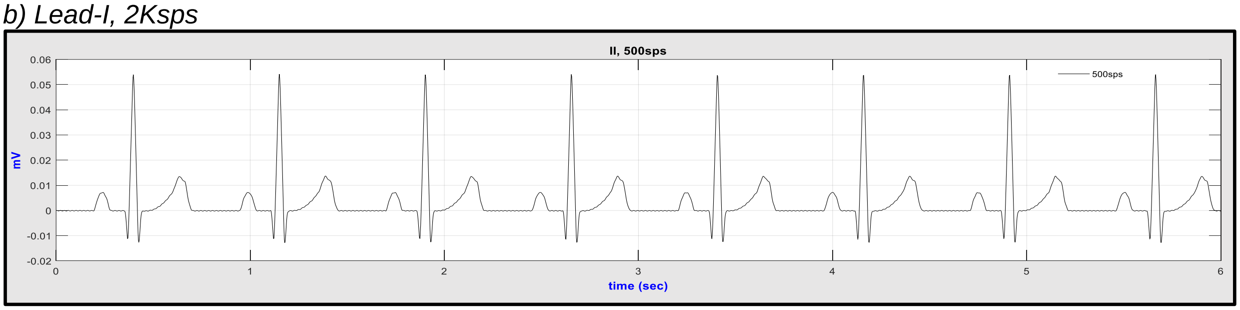

c) Lead-II, 500sps

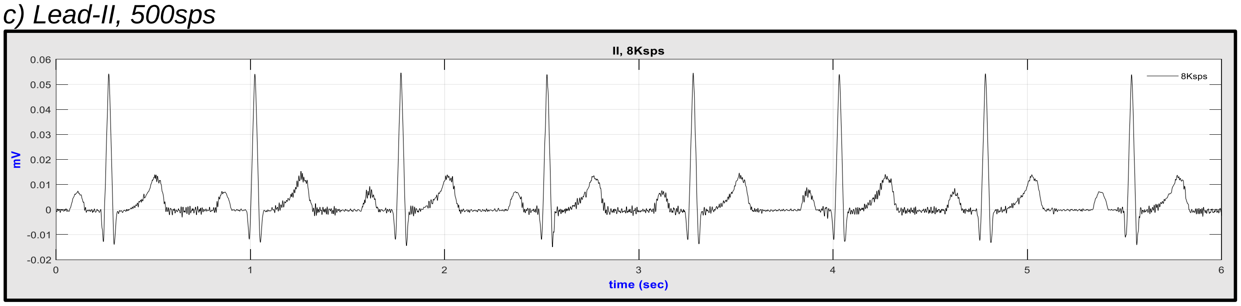

d) Lead-II, 8Ksps

Figure 5.3: ECG acquired from ProSim 3.0 Vital Signs Simulator with ADS1298 AFE.

At 8Ksps, the SNR of the lead-I ECG was reduced by 73% and the SNR of lead-II was reduced by 56% compared to the SNR at 500sps. Table 5.1 summarises the SNR calculated on lead-I and lead-II ECG signals.

Table 5.1: Effect of sampling rate on channel performance

ECG lead	Sampling rate (SPS)	SNR (dB)	Difference (dB)	% Decrease in SNR
Lead-I	500	8.3581	6.0911	73
	8000	2.2670		
Lead-II	500	7.8019	4.3812	56
	8000	3.4207		

EASI electrode placement

The next available ECG acquisition option on the ECG hardware is 12-lead equivalent ECG from EASI electrode configuration. Unfortunately, the ProSim 3.0 Vital Sign Simulator has no EASI electrode configuration options. Hence, lead-I and lead-II in the standard ECG (RA, LA, and LL) were used to acquire the EASI configuration base signals (V_{AI}, V_{ES}, and V_{AS}). A transformation matrix developed by Feild et al. (2002) was used to convert the EASI signals to the standard 12-lead ECG. Moreover, least-square regression was used to generate new coefficients based on equation 5.7 (Feild et al., 2002) and 72 hours of ECG from the MIT-BIH arrhythmia database (Goldberger et al., 2000).

$$l = \alpha Vai + \beta Ves + \gamma Vas \qquad [5.7]$$

Where l : any of the ECG leads

α, β, γ : coefficients

Appendix H illustrates the three base ECG signals (V_{AI}, V_{ES}, and V_{AS}) acquired at 1K, 2K, 4K, 8K, and 16Ksps, respectively.

Real-time digital filters

This section presents the performance of the real-time digital filters (the smoothing filters and the IIR Butterworth filters described in Chapter 1, section 4.4.8.2) evaluated based on ECG acquired from a ProsSim 3.0 Vital Sign Simulator. The ProSim 3.0 Vital Sign Simulator has various built-in real-life noise functions, including 50Hz power line interference (PLI), an artefact from breathing, and baseline wander.

Smoothing filters

In the design, various smoothing filters, including a single variable Kalman filter (Li et al., 2008, Moradi et al., 2014), Savitzky Golay filter (Press and Teukolsky, 1990, Hargittai, 2005, Awal et al., 2011, Schafer, 2011), and moving average (Chen and Chen, 2003, Łęski and Henzel, 2005) filters were implemented (see Sections 4.6.3). To test the filter performances, a reference ECG signal with no smoothing filters was acquired from the ProSim 3.0 Vital Sign Simulator. The reference signal was passed through each filter individually and in combination, and the filtered signal was compared to the reference signal using the PSNR, SNR and PRD methods described earlier in section 5.3.1.2. Performances were compared (Table 5.2).

Table 5.2: Quantitative comparison of the smoothing filters rounded to three decimal places

No.	Smoothing filter	Raw ECG (SNR, dB)	PSNR (dB)	SNR1 (dB)	SNR2 (dB)	SNR3 (dB)	PRD1	PRD2
1.	Kalman filter (KF)	8.0958	60.687	17.684	48.677	48.104	14.380	15.637
2.	SG filter (2^{nd} order - 5 points)	8.104	57.879	11.249	42.250	41.684	31.345	34.077
3.	SG filter (2^{nd} order - 7 points)	8.122	53.109	16.706	47.699	47.102	16.561	18.011
4.	SG filter (2^{nd} order - 9 points)	8.111	55.394	15.603	46.600	45.992	18.471	20.078
5.	SG filter (2^{nd} order - 11 points)	8.108	64.189	10.650	41.744	41.110	31.583	34.345
6.	SG filter (4^{th} order - 7 points)	8.100	59.443	13.519	44.513	43.951	24.192	26.309
7.	SG filter (4^{th} order - 9 points)	8.111	56.392	15.500	46.493	45.922	19.220	20.899
8.	SG filter (4^{th} order - 11 points)	8.117	54.640	14.998	45.992	45.407	20.261	22.036
9.	SG filter (4^{th} order - 15 points)	8.098	63.733	9.261	40.272	39.676	38.375	41.776
10.	A moving average (3 - points)	8.104	52.278	12.799	43.795	43.159	25.360	27.589
11.	A moving average (5 - points)	8.103	53.423	13.589	44.594	43.858	21.586	23.492
12.	A moving average (7 - points)	8.108	59.883	10.618	41.615	40.803	27.669	30.103
13.	KF and SG filter (2^{nd} order - 5 points)	8.117	53.786	5.381	36.375	35.795	61.742	67.148
14.	KF and SG filter (2^{nd} order - 7 points)	8.119	51.797	10.587	41.598	40.997	33.557	36.485
15.	KF and SG filter (2^{nd} order - 9 points)	8.101	52.848	14.782	45.779	45.155	20.318	22.107
16.	KF and SG filter (2^{nd} order - 11 points)	8.093	58.792	13.414	44.411	43.767	23.057	25.086
17.	KF and SG (4th order - 7 points)	8.122	54.895	11.042	42.039	41.471	32.256	35.063
18.	KF and SG (4th order - 9 points)	8.141	53.165	15.685	46.682	46.096	18.834	20.492
19.	KF and SG (4th order - 11 points)	8.165	52.191	15.343	46.354	45.753	19.502	21.231
20.	KF and SG (4th order - 15 points)	8.146	58.839	14.943	45.954	45.352	20.001	21.775
21.	KF and A moving average (3 - points)	8.167	50.966	17.275	48.268	47.630	15.173	16.499
22.	KF and A moving average (5 - points)	8.132	51.943	15.386	46.379	45.645	17.605	19.143
23.	KF and A moving average (7 - points)	8.116	76.849	8.642	39.740	38.912	34.772	37.806

NB: SNR, SNR1, SNR2, SNR3: *Signal to Noise Ratio;* ***PSNR****: Peak Signal to Noise Ratio;* ***PRD1, PRD2:*** *Percentage Root Mean Square Differences;* ***SG filter****: Savitzky Golay filter*

Power line interference (PLI) test

The 50Hz anti-hum filter was used to reduce power line interference. Figure 5.4 depicts the acquired real-time lead-II ECG signal filtered by the 50Hz notch filter.

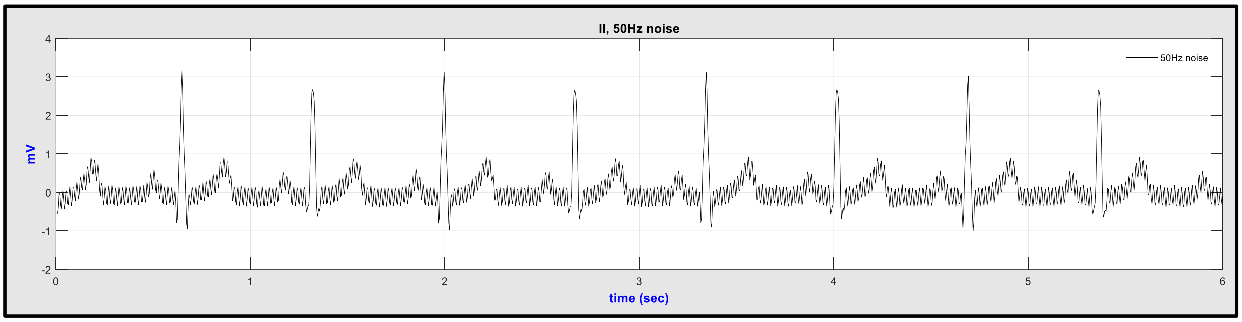

a) 50Hz noise in lead-II ECG

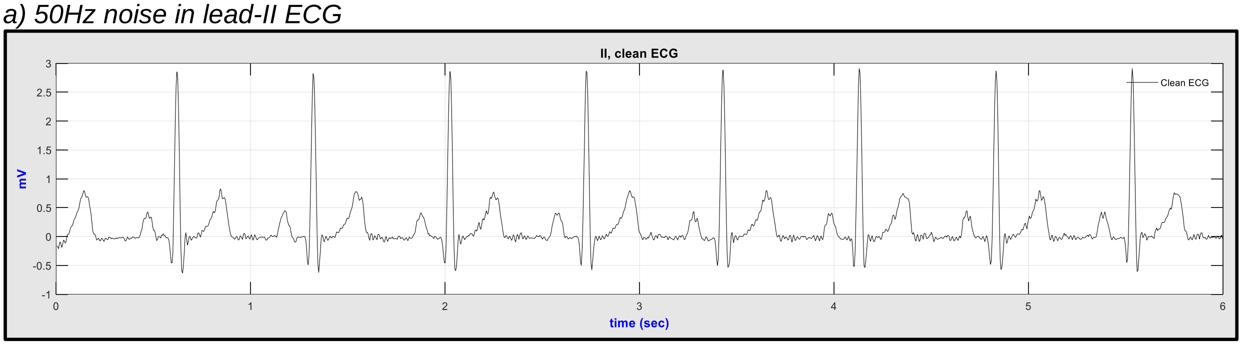

b) Clean lead-II ECG

Figure 5.4: ProSim 3.0 Vital Sign Simulator generated 50Hz noise-contaminated (top) and clean lead-II ECG signal (bottom) based on the real-time Java-based anti-hum filter.

Baseline wander and respiration noise

In an effort to remove baseline wander and respiration noise from the acquired ECG signal, a 4th order high pass (F_c = 0.5Hz) and low pass (Fc = 150Hz), Butterworth filter was implemented. Figure 5.5 compares the baseline wander and respiration noise-contaminated ECG signal and the filtered ECG signals.

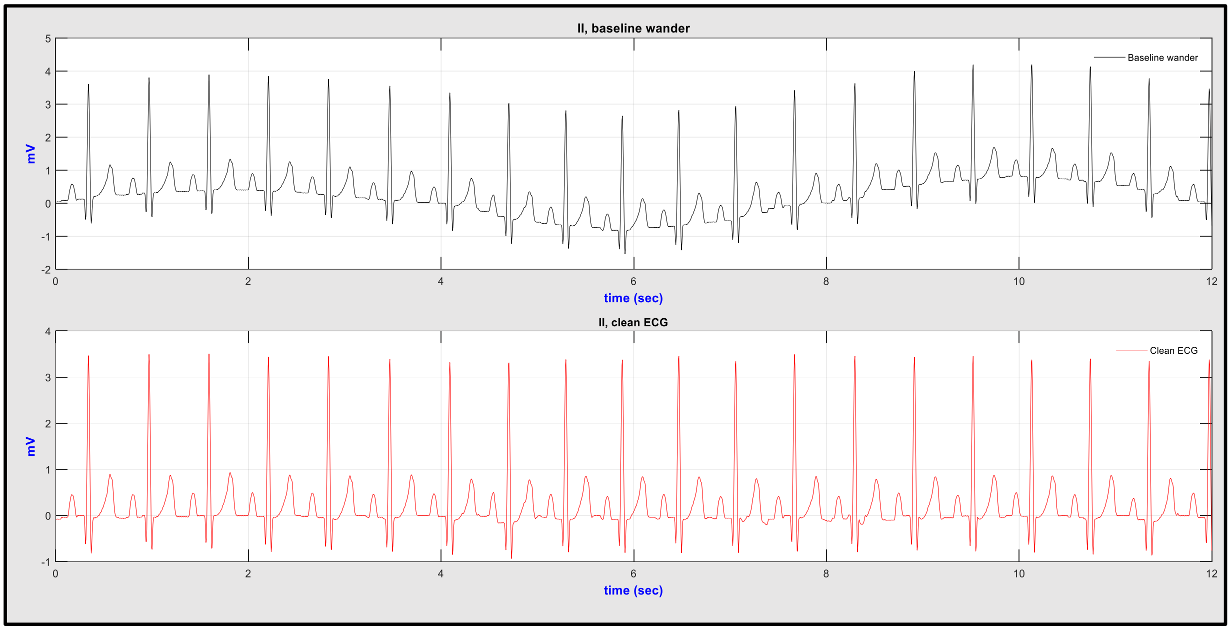

a) Baseline wander contaminated lead-II ECG (top - black) and clean ECG (bottom - red)

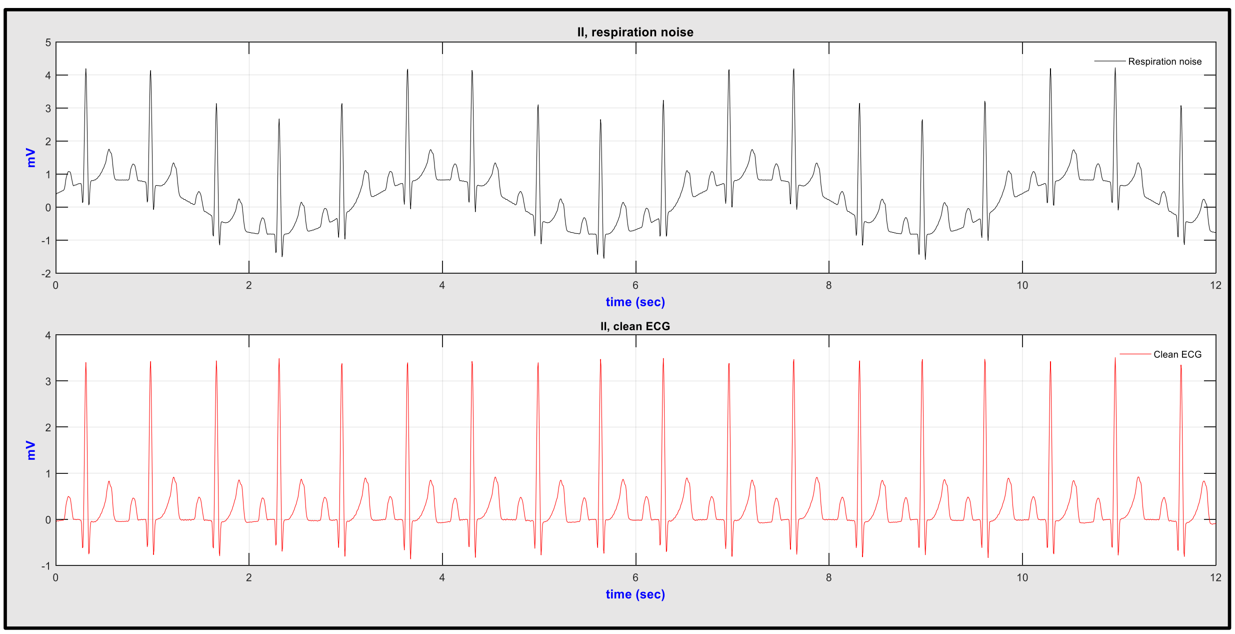

b) Respiration noise contaminated lead-II ECG (top - black) and clean ECG (bottom - red)

Figure 5.5: Comparison between baseline wander and respiration contaminated lead-II ECGs (black) and clean lead-II ECGs (red), signal source – ProSim 3.0 Vital Sign Simulator.

Quantitative comparison

Table 5.3 presents the quantitative comparison of the noisy and filtered ECG signals based on SNR and PRD.

Table 5.3: Quantitative indexes of the filtered lead-II ECG signal

No.	Noise source	Calculated values					
		PSNR	SNR1	SNR2	SNR3	PRD1	PRD2
1.	**50Hz PLI noise**	97.562	9.642	42.023	41.330	31.295	33.610
2.	**Baseline wander**	43.788	4.980	40.893	40.320	48.423	51.840
3.	**Respiration**	56.303	11.200	28.795	28.795	26.376	26.376

Power spectral density

The ECG waveform represents the ECG signal in the time domain. On the other hand, the PSD is a useful tool to visualize the frequency components affected by the respective noise sources. In this regard, the PSD of the noise sources and the individual filtered signals were plotted (Figure 5.6) using MATLAB R217a.

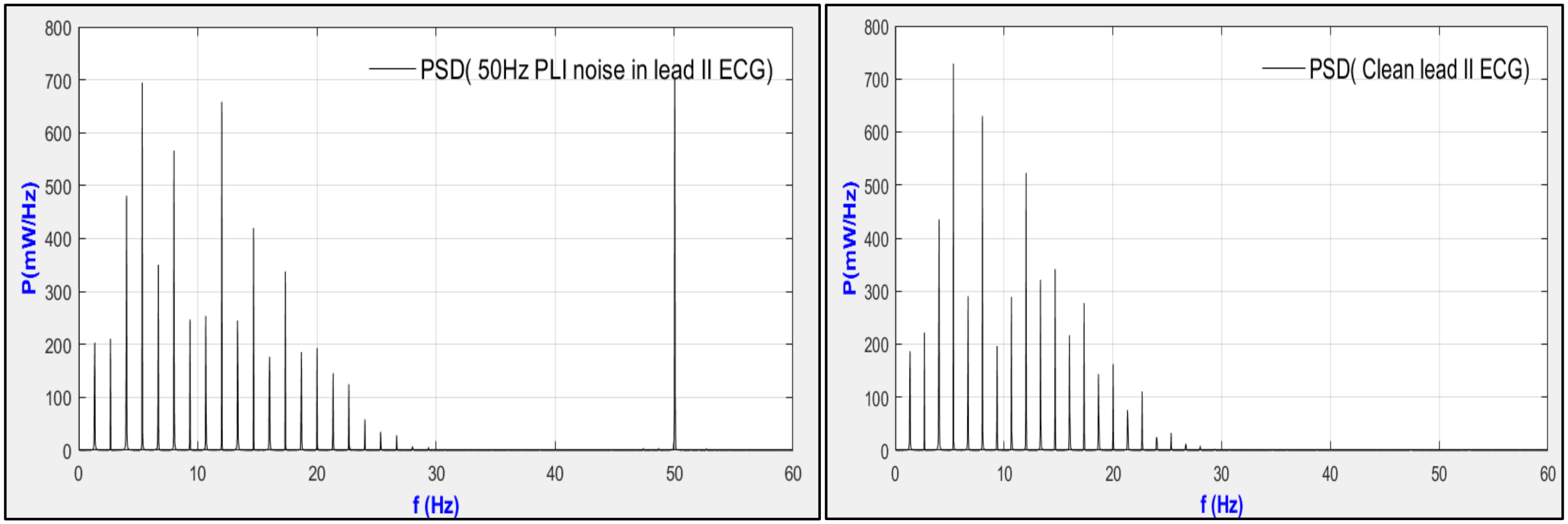

a) 50Hz PLI interference in lead-II ECG (left) and clean lead-II ECG (right)

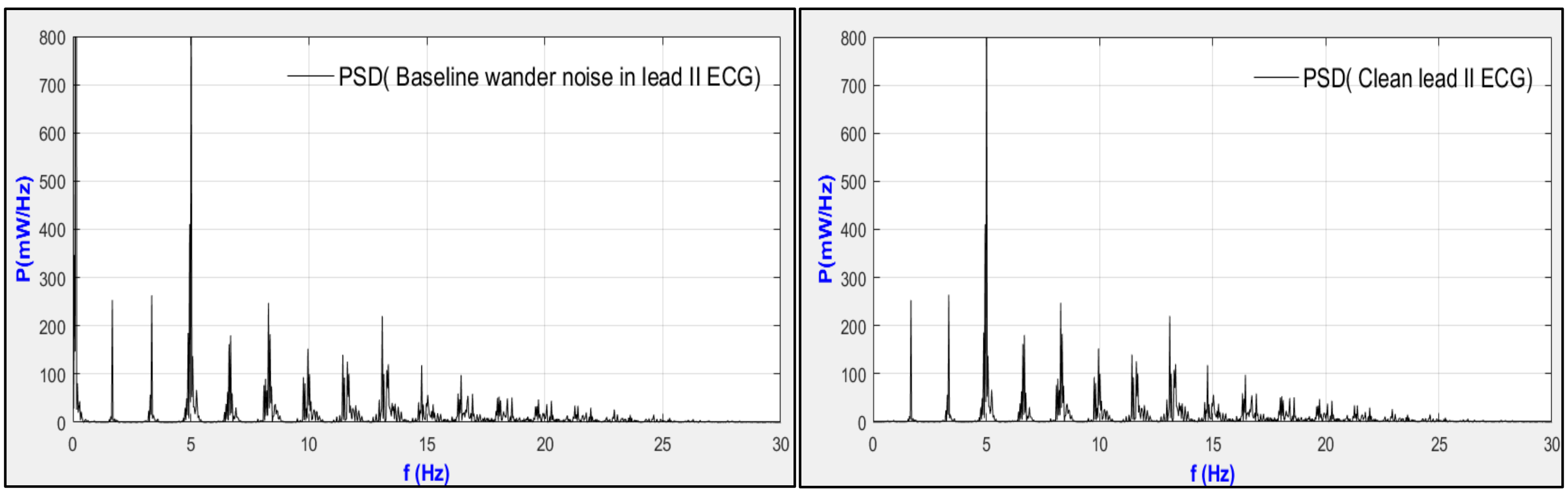

b) Baseline wander in lead-II ECG (left) and clean lead-II ECG (right)

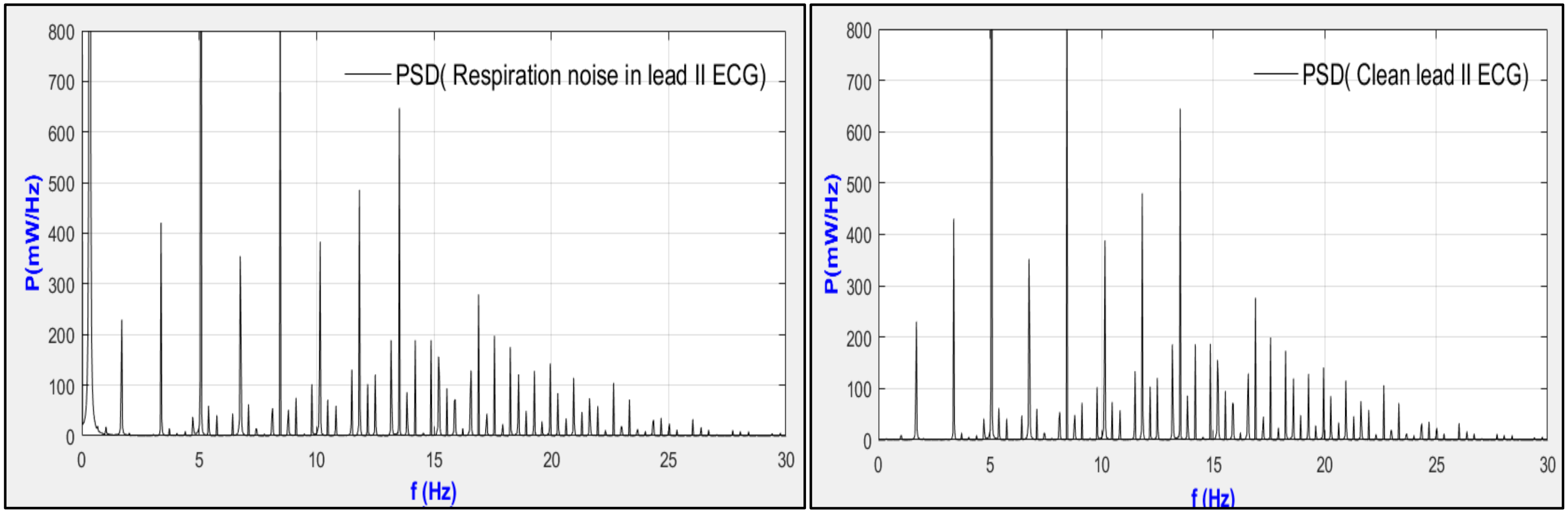

c) Respiration noise in lead-II ECG (left) and clean lead-II ECG (right)

Figure 5.6: Power spectral density of lead-II ECG.

Hardware response for different amplitude ECG signals

Different amplitude ECG signals from the ProSim 3.0 Vital Sign Simulator were investigated to study the ability of the ECG hardware to acquire signals of varying amplitudes (from 0.5 to 5.5mV). Figure 5.7 depicts the different amplitude ECG signals obtained from the ECG hardware, while Table 5.4 presents peak amplitudes of the input and output ECG signals and the percentage difference.

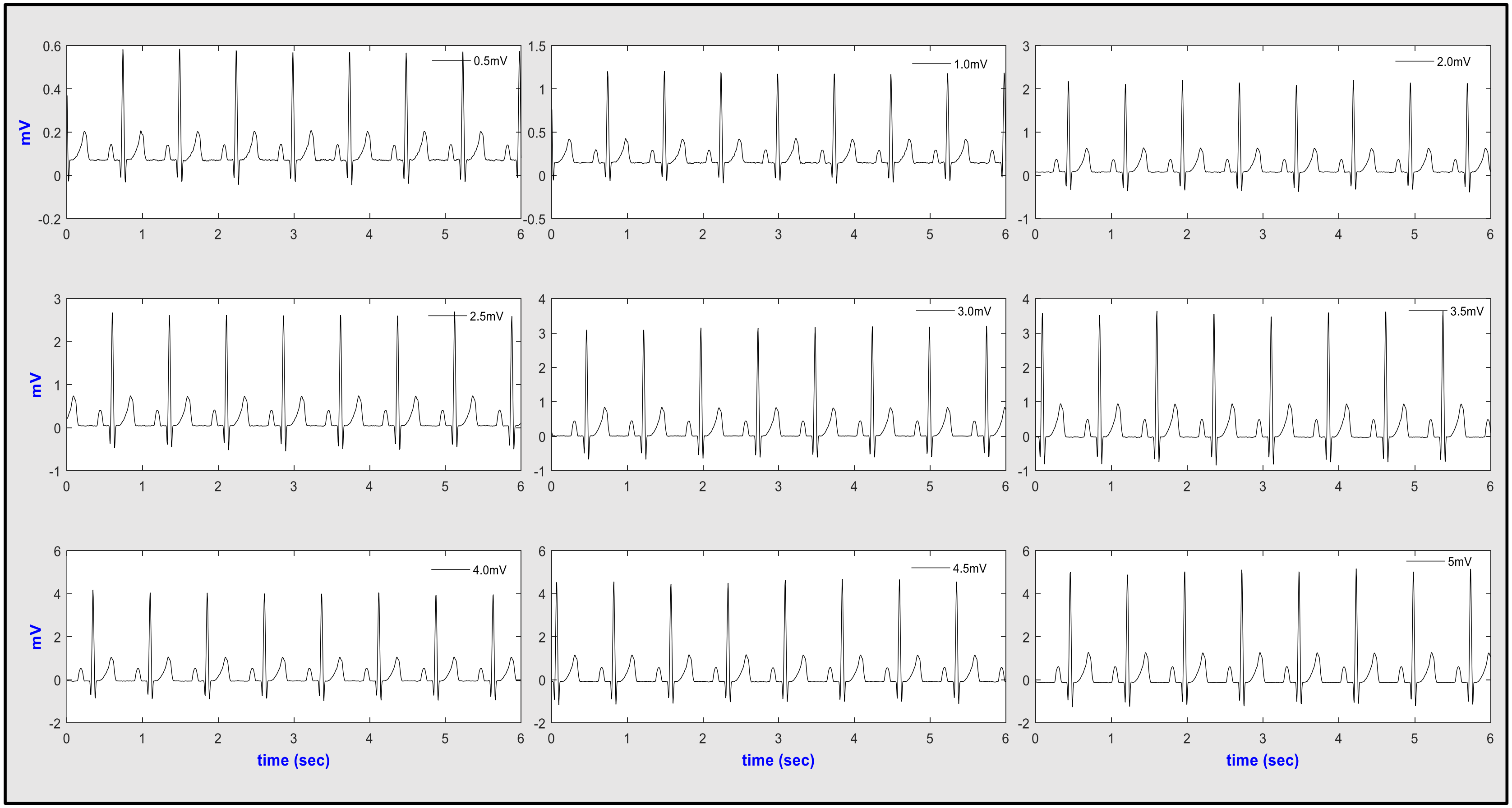

Figure 5.7: ECG hardware response for variable amplitude inputs (1Ksps).

Table 5.4: Comparison between the input and output ECG R amplitudes

No.	Input ECG R amplitude (mV)	Output ECG R amplitude (mV)	Difference (%) = [abs (Inp - Outp)/Inp] *100
1.	0.5	0.4820	3.60
2.	1.0	0.9115	8.85
3.	2.0	1.9831	0.84
4.	2.5	2.4879	0.48
5.	3.0	2.9780	0.73
6.	3.5	3.4907	0.26
7.	4.0	3.9858	0.35
8.	4.5	4.4572	1.60
9.	5.0	4.9147	1.70

Increased baseline wander was observed for lower amplitude ECG signals (<=1mV) as it was affected by the internal noise of the ECG hardware generated by the hardware components. As a result, lower amplitude input signals showed a higher percentage difference compared to the respective output ECG (Table 5.4). To remove the effect of the baseline wander, an off-line MATLAB based zero-phase shift Butterworth 2nd order high-pass filter was used to clean the signal acquired from the 1mV input. The results showed that the R-peak amplitude was 0.9914mV (Figure 5.8). Moreover, the percentage difference was reduced to 0.86% once the baseline was removed.

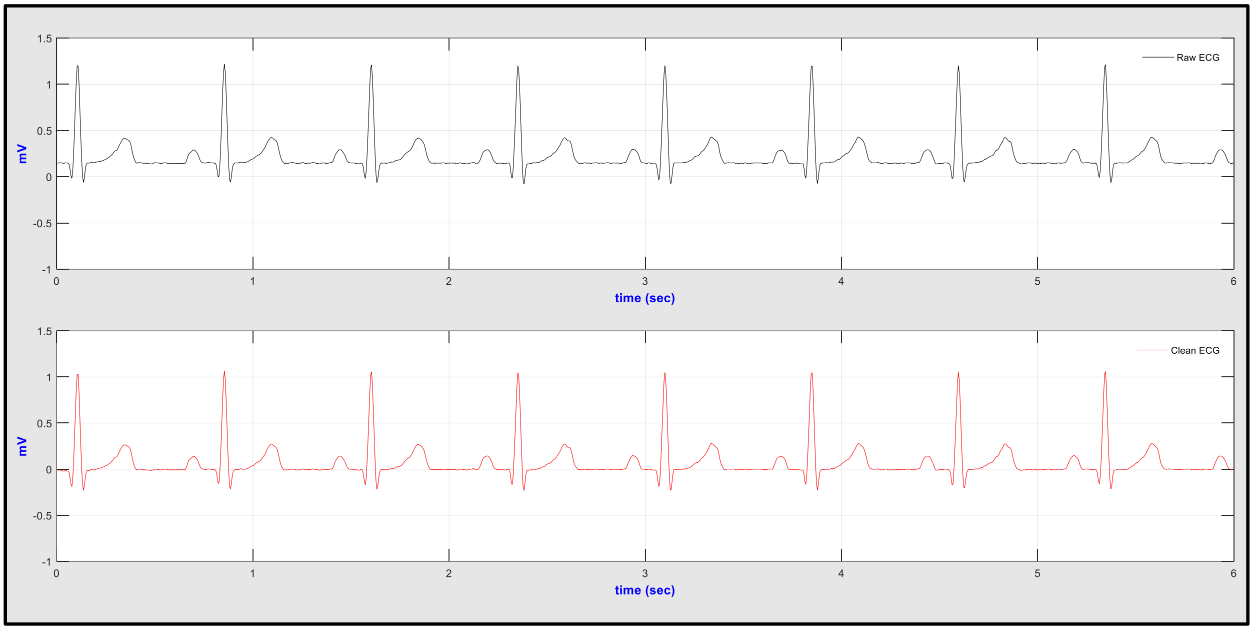

Figure 5.8: ECG from 1mV input signal; black – raw ECG; red – after the baseline wander was removed by a 2nd order zero-phase shift MATLAB based Butterworth high pass filter.

Hardware response for different beats per minute (bpm)

One of the design parameters for ECG hardware design is the ability to detect different HRs. In this regard, the response of the ECG hardware to varying the HR between 40bpm and 200bpm of a 3mV simulated ECG signal was studied. The test results revealed that the ECG hardware is capable of reliably detecting different HRs, as required by the design specification in Chapter 1, section 4.3.1. Table 5.5 compares the input HR from the ProSim 3.0 Vital Sign Simulator and the measured HR by the proposed ECG hardware. Representative signals at each HR over six seconds are shown in Figure 5.9.

Table 5.5: Comparison of the input HR from ProSim 3.0 vital sign simulator and measured HR by the ECG hardware

No.	ProSim 3.0 vital sign simulator (bpm)	HR Measured by the ECG hardware (bpm)
1.	40	40
2.	60	60
3.	80	80
4.	120	120
5.	140	140
6.	180	180
7.	200	200

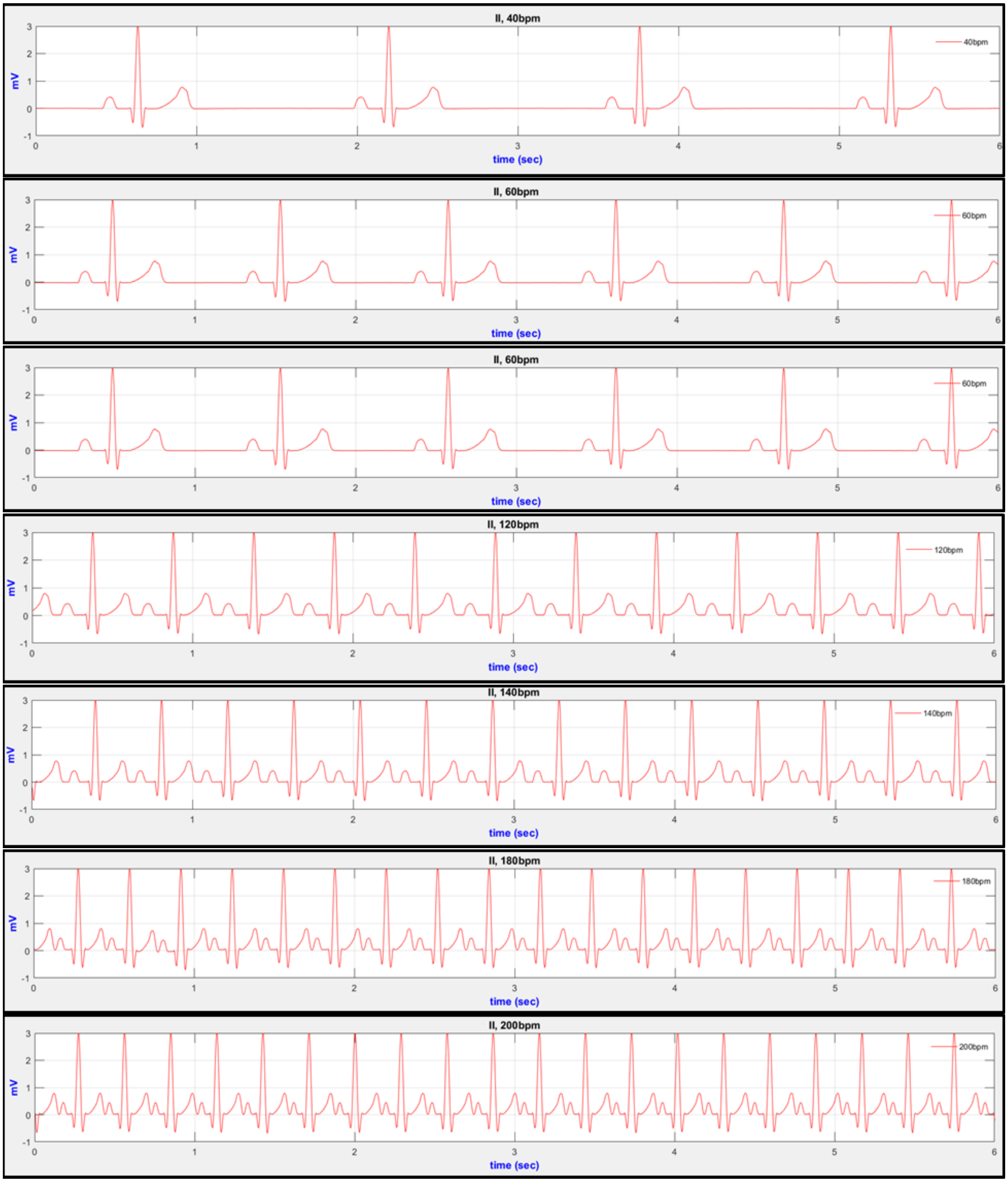

Figure 5.9: Representative ECG acquired at different beats per minutes (Signal source: ProSim 3.0 Vital Sign Simulator, 3mV ECG at 1Ksps)

5.3.1.4. Discussion

Short circuit and internal noise test

One of the measures for the successful implementation of ECG hardware based on the ADS1294 was to compare the results against the electrical characteristics stated by the manufacturer. Hence, the first test was based on an internally generated 1mVpp signal. The ECG hardware successfully reproduces the 1mVpp input signal with minimal distortion.

The internal noise was measured in the respective channels by shortcircuiting the input terminals. The results revealed that the noisy channel output was around $10\mu V_{PP}$, almost double the magnitude stated by the manufacturer. The noise level ($5\mu V_{PP}$) quoted by the manufacturer is based on a 3.3V supply and 2.4V reference voltage (Texas Instruments Incorporated, 2015). However, the e-textile ECG hardware used a 5V supply and 4V reference voltage. A higher reference voltage increases the dynamic range of the ECG hardware. The downside is an increased level of intrinsic noise. Therefore, the 10µVpp is acceptable, considering the 5V power supply and the noise introduced by the external components (connecting wires, passive filters, patient protection circuit, the linear voltage regulator, and the Bluetooth module). Moreover, the internal noise satisfies the design criteria ($<30\mu V_{PP}$) stated in Chapter 1, section 4.3.1.

Digital filters

Regarding the smoothing filters, the majority of the proposed combinations showed roughly similar results, as shown in Chapter 5 (Table 5.2). However, the combination of the single variable Kalman Filter (Woods and Radewan, 1977, Simon, 2001, Mneimneh et al., 2006, Sameni et al., 2007) and a 3-point moving average filter (Chen and Chen, 2003, Hu et al., 2011, Kaur and Singh, 2011, Azami et al., 2012) showed a relatively better SNR (Table 5.2: *SNR1 = 17.275 dB, SNR2 = 48.268dB, SNR3 = 47.630dB*). Therefore, the final prototype of the Java-based real-time filter was implemented based on a single variable smoothing filter and a 3-point moving average filter.

According to previous studies, a higher sampling rate and lower order of the IIR filters showed minimal distortion and better performance (Piskorowski, 2009, Sørensen et al., 2010, Chandrakar et al., 2013, Joshi et al., 2013, Bhogeshwar et al., 2014, Biswas and Maniruzzaman, 2014). In this regard, only fourth order IIR filters were used in the final implementation. Looking at the SNR calculations (Table 5.3) and the PSDs (Figure 5.6) showed that the proposed digital filters effectively removed the 50Hz power line interference, the baseline wanders and respiration induced noise.

ECG hardware response for different inputs

Different amplitude ECG signals from the ProSim 3.0 vital sign simulator were acquired to study the response of the ECG hardware for the respective signals. Results showed that ECG hardware reproduces the ECG with minimal error. However, at lower inputs (<1mV) there was a higher artefact level due to the internally generated noise. On the other hand, an input voltage higher than 5mV showed clipping of the output voltage as shown in Figure 5.10. Therefore, a variable gain control was integrated into the ECG viewer and data logger to avoid saturation of the ADS1294 and clipping of the collected ECG signal.

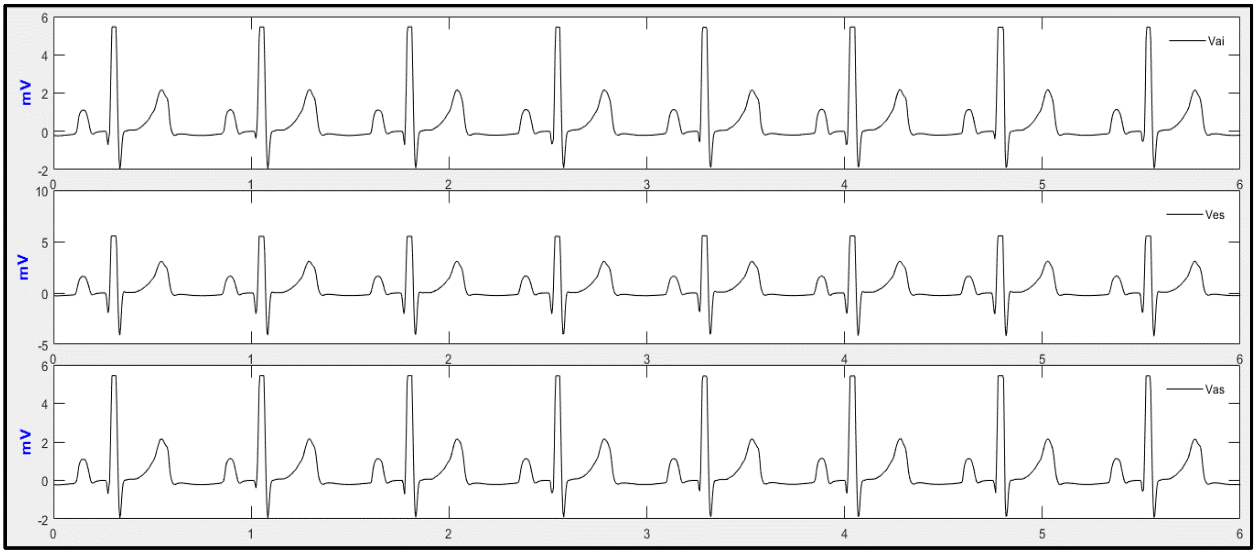

Figure 5.10: Clipping of the ECG output for higher input signal higher than 5mV

Regarding varying HRs, the ECG hardware successfully acquired ECG signals of variable heart rates from 40 to 240bpm.

5.3.2. Response of the ECG hardware to cardiac abnormalities

5.3.2.1. Specific objectives

The specific objectives of the study were to examine the ability of the ECG hardware to discriminate abnormalities in simulated ECG signals.

5.3.2.2. Methods

The ability of the ECG hardware to acquire several different cardiac abnormalities from the ProSim 3.0 Vital Sign Simulator was investigated. Abnormalities included:

supraventricular arrhythmias, premature contraction of the cardiac chambers and ventricular arrhythmias. The CP 200™ 12-Lead Resting Electrocardiograph (Welch Allyn, Inc., Skaneateles Falls, New York, Figure 5.11) was used to compare the simulation results of the proposed ECG hardware.

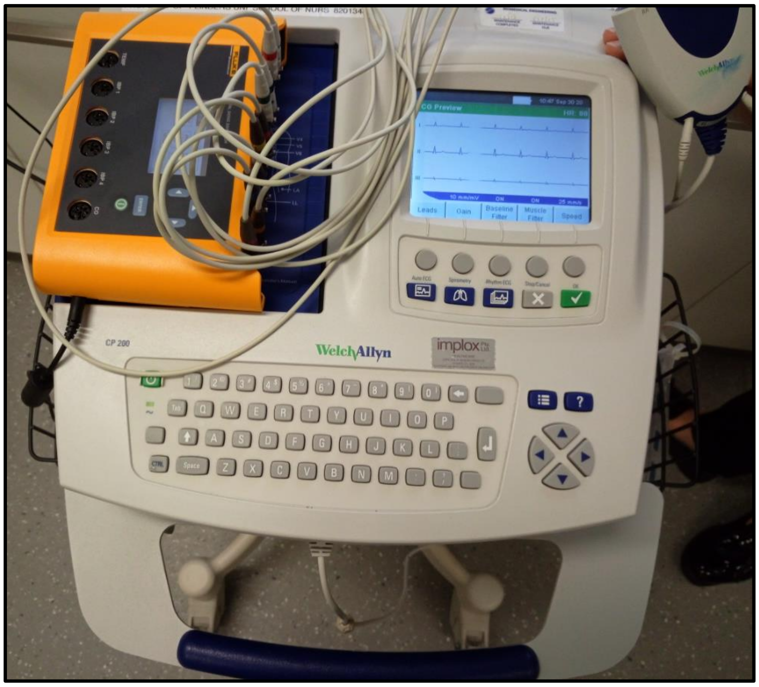

Figure 5.11: The reference CP 200™ 12-Lead Resting ECG and the Prosim 3.0 Vital Sign Simulator (yellow) in a laboratory setup

5.3.2.3. Results

Supraventricular (SV) Arrhythmias

Supraventricular arrhythmias, also known as atrial arrhythmias, occur in the upper chambers of the heart (Texas Heart Institute). Figure 5.12 shows the test results from both the CP 200™ 12-Lead Resting Electrocardiograph and the developed ECG hardware for the common arrhythmias of the atria.

***a) Atrial flutter in lead-II ECG**; **top -** captured by the reference Resting ECG, 25mm/s, 10mm/mv, R_{peak} = ~2.8mV); **bottom -** captured by the proposed ECG hardware*

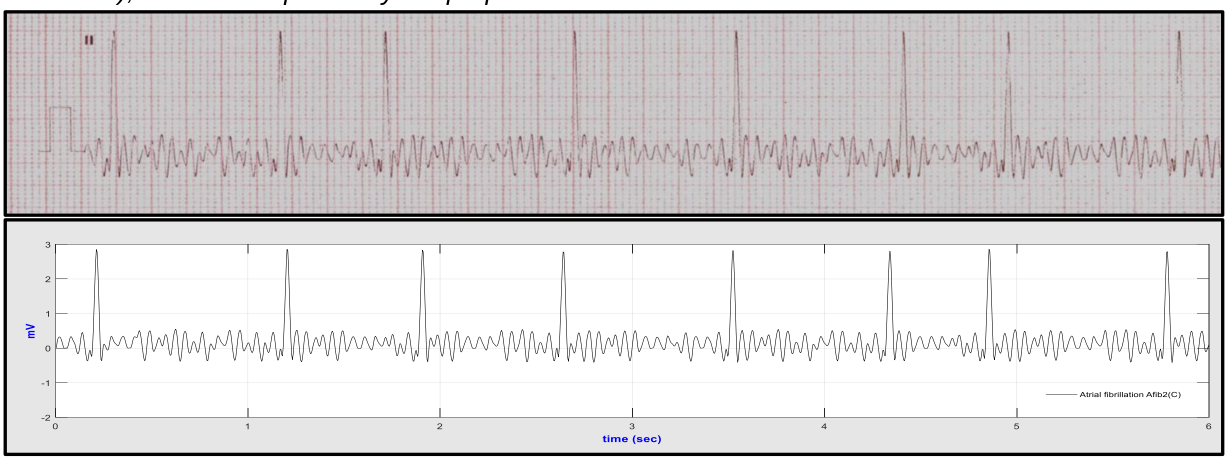

***b) Atrial fibrillation Afib2(C) in lead-II ECG**; **top -** captured by the reference Resting ECG, 25mm/s, 10mm/mv, R_{peak} = ~2.8mV; **bottom -** captured by the proposed ECG hardware*

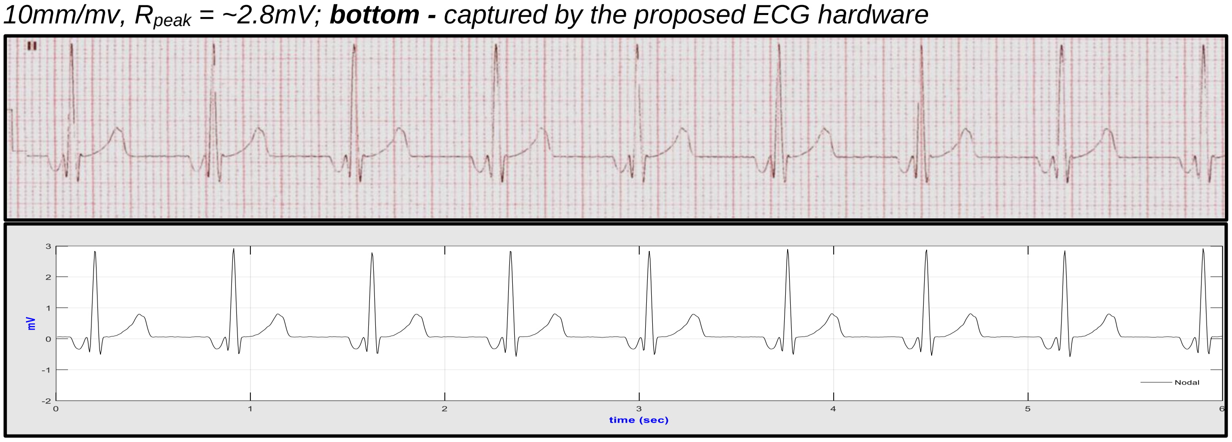

***c) Nodal in lead II ECG; top -** captured by the reference Resting ECG, 25mm/s, 10mm/mv, R_{peak} = ~2.8mV; **bottom -** captured by the proposed ECG hardware*

Figure 5.12: Examples of the Supraventricular arrhythmia captured by the reference and the proposed ECG monitor

Premature contraction of the cardiac chambers

Three cardiac abnormalities were simulated during the test: premature contraction of the atria, which happens when the atria contracts “too soon”, and premature ventricular contraction, due to the early contraction of the left and right ventricle. The occurrence of either or both premature contractions results in an irregular heartbeat (Texas Heart Institute). Figure 5.13 illustrates the simulation results captured by the reference Resting ECG and the proposed ECG hardware.

Ventricular arrhythmia

Ventricular arrhythmias are abnormalities of the lower chambers of the heart. The ECG hardware reproduced the following ventricular defects; trigeminy, ventricular tachycardia and asystole as shown in Figure 5.14.

a) Premature atrial contraction in lead-II ECG; top - *captured by the reference Resting ECG, 25mm/s, 10mm/mv,* R_{peak} *= ~2.8mV;* ***bottom -*** *captured by the proposed ECG hardware*

b) Premature ventricular contraction (PVC1-LV Early) in lead-II ECG; top - *captured by the reference Resting ECG, 25mm/s, 10mm/mv,* R_{peak} *= ~2.8mV;* ***bottom -*** *captured by the proposed ECG hardware*

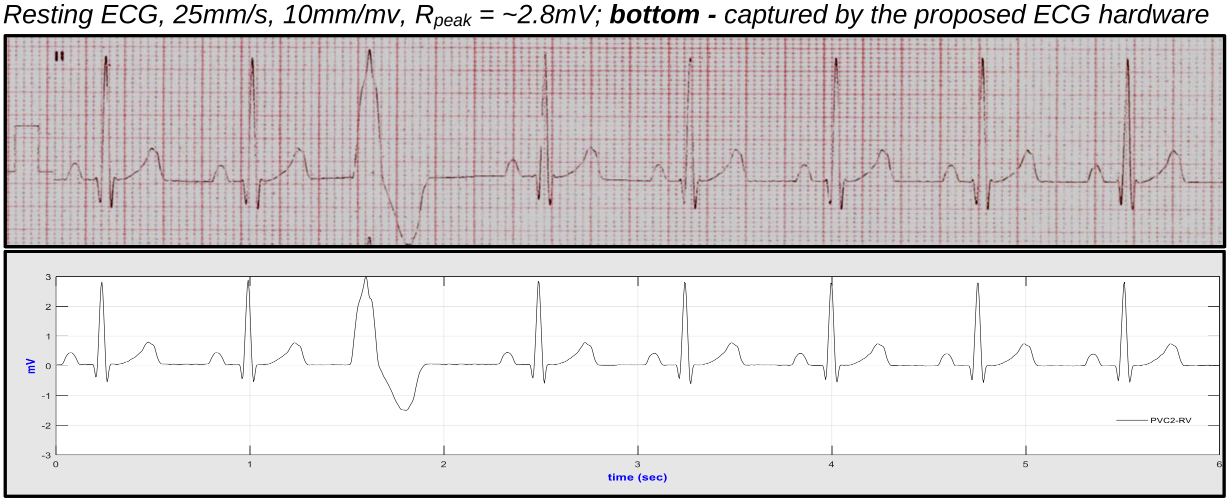

c) Premature ventricular contraction (PVC2-RV) in lead-II ECG; top - *captured by the reference Resting ECG, 25mm/s, 10mm/mv,* R_{peak} *= ~2.8mV;* ***bottom -*** *captured by the proposed ECG hardware*

Figure 5.13: Sample premature contractions of the cardiac chambers

b) Trigeminy in lead-II ECG; top - *captured by the reference Resting ECG, 25mm/s, 10mm/mv, R_{peak} = ~2.8mV;* ***bottom -*** *captured by the proposed ECG hardware*

d) Ventricular tachycardia; top *- captured by the reference Resting ECG, 25mm/s, 10mm/mv, R_{peak} = ~ [-2.4, 1.6mV];* ***bottom -*** *captured by the proposed ECG hardware*

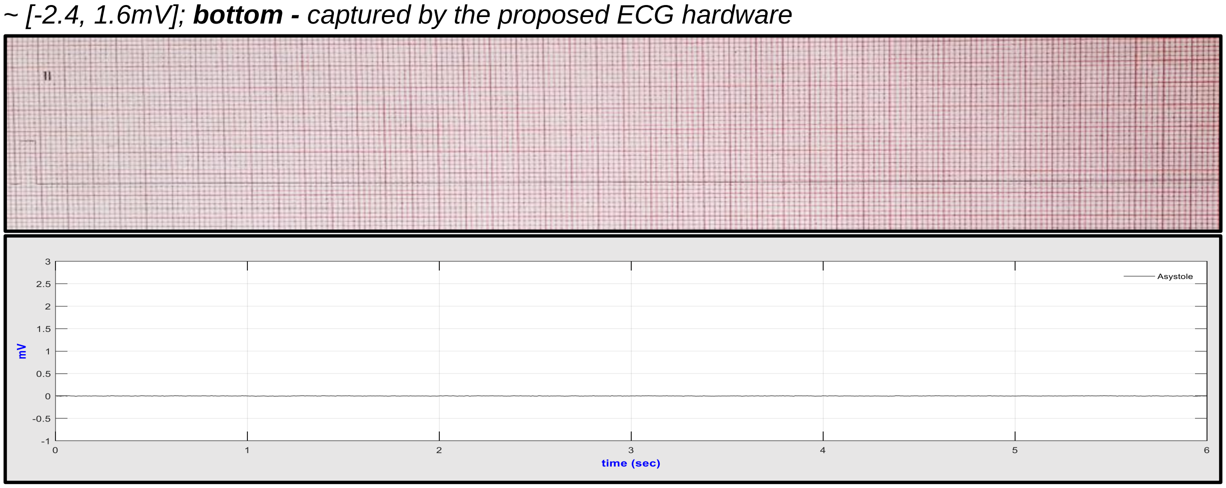

f) Asystole in lead-II ECG; top *- captured by the reference Resting ECG, 25mm/s, 10mm/mv;* ***bottom - captured by the proposed ECG hardware***

Figure 5.14: Sample ventricular abnormalities

5.3.2.4. Discussion

In this section, the ability of the ECG hardware to reproduce cardiac abnormalities from the ProSim 3.0 Vital Sign Simulator was studied. Compared to the reference ECG, the proposed ECG hardware reproduced several cardiac arrhythmias as specified in the design section Chapter 1, section 4.3.1. The limitation of the study is that the comparison was qualitative. The cardiac abnormalities from the reference CP 200™ 12-Lead Resting Electrocardiograph were printed on thermal paper. The scanned images of the respective cardiac abnormalities from the reference ECG had to be compared visually to the temporal plots of the corresponding cardiac episodes from the proposed ECG hardware. Therefore the peaks don't align completely in the figures (Figure 5.12, Figure 5.13, and Figure 5.14). For future experiment, it is recommended to export ECG abnormalities from the reference ECG to an external mass storage and compare the results in the digital domain using MATLAB or Python.

Appendix I presents performance analysis of the ECG viewer and data logger.

5.4. Evaluating the accuracy and reliability of the smart ECG vest and e-textile electrodes response to external factors

5.4.1. Response of the smart ECG vest and the textile electrodes to repeated washing

5.4.1.1. Specific objective

The specific objective of the study was to examine the response of the smart ECG vest and the textile electrodes to repeated washing.

5.4.1.2. Methods

Response to repeated washing

The proposed ECG vest and textile electrodes are washable. According to the AS/NZS ISO 10535:2011 (Standards Australia Limited/Standards New Zealand, 2011, p. 38) section 8.3, test standard for nonrigid body support, "the nonrigid body support, device that is manufactured from flexible materials and which adapts to the body shape, shall be cleaned and dried ten (10) times" and thoroughly inspected for damage. In this regard, the ECG vest and textile electrodes were washed and dried 10 times using an LG WDC1475NCW 7.5kg/4kg Washer Dryer.

During the experiment, a washing cycle consisted of 10 minutes of moderate machine washing at room temperature using Surf 5 Herbal Extracts Washing Liquid, two minutes of rinsing with clean water, and drying at a temperature of not more than 40°C (Low Temp setting on the washing machine). The shortest drying cycle available was around 30 minutes. Hence the washing machine was stopped two minutes into the drying cycle.

The weakest link between the connecting wires and the snap fastener is the soldering point where it was postulated it could break as a result of repeated washing. A simple continuity test was performed after each wash cycle to affirm the integrity of the embedded wires in the ECG vest.

Consecutive resistance and continuity measurement

To evaluate the response of the textile electrodes after washing, a resistance measurement after each cycle was performed. This is important because, washing degrades the electrode conductivity and hence increases the electrical resistance (Schwarz et al., 2011, Tsukada et al., 2019).

5.4.1.3. Results

Effect of washing on the ECG vest

Table 5.6 presents the consecutive continuity test.

Table 5.6: Wash response of the embedded wires

Wash cycle	JST XH 5 pin, 2.0 mm pitch male adapter to ECG lead	Continuity test (Yes/No/ Intermittent)	Remark
1, 2, 3, 4	***R, I, E, S, A***	Yes	No noticeable defect detected
5.	***R, I***	Yes	The connection between the **E** electrode and the respective pin of the **JST XH** connector was intermittent. Wiggling the wire at the **E**-electrode position, it was possible to bridge the connection problem.
	E	Intermittent	
	S	Yes	
	A	Yes	
6.	***R, I***	Yes	Intermittent connection at the **E** electrode position
	E	Intermittent	
	S, A	Yes	
7.	***R***	Yes	After the seventh wash cycle, both the **I** and **A** electrodes connection became intermittent while the tracing of the **E** electrode completely failed. The **E** electrode position broke at the soldering point.
	I	Intermittent	
	E	No	
	S	Yes	
	A	Intermittent	
8.	***R***	Yes	On top of the **E** electrode, **A,** and **I** failed after the eighth wash cycle. The wire connecting the electrode was slightly shorter and broken due to tension while the **I** electrode tracing failed at the solder point.
	I	No	
	E	No	
	S	Yes	
	A	No	
9.	***R***	Yes	The connections of the **S** and **R** electrodes to the **JST XH** connector withstood ten cycles of washing and were continuous after the end of the tenth wash cycle.
	I	No	
	E	No	
	S	Yes	
	A	No	
10.	***R***	Yes	
	I, E	No	
	S	Yes	
	A	No	

Referring to Table 5.6, electrodes **A**, **E** and **I** became unstable and broke at the solder point after eight washing cycles indicating a limit on the potential for repeated washing.

Effect of washing on the textile electrodes

Ten cycles of washing were performed on the textile electrodes. The test results are presented in Table 5.7. No noticeable change in resistance was observed.

Table 5.7: Washing cycle and the measured resistance value of the textile ECG electrode

<table>
<tr><th colspan="3">Initial resistance value R_i = 0.4 Ω</th></tr>
<tr><th>Wash cycle</th><th>Resistance measured (Ω)</th><th>Remark</th></tr>
<tr><td>1st cycle</td><td>0.4</td><td rowspan="10">No noticeable difference was observed</td></tr>
<tr><td>2nd cycle</td><td>0.4</td></tr>
<tr><td>3rd cycle</td><td>0.4</td></tr>
<tr><td>4th cycle</td><td>0.4</td></tr>
<tr><td>5th cycle</td><td>0.4</td></tr>
<tr><td>6th cycle</td><td>0.4</td></tr>
<tr><td>7th cycle</td><td>0.4</td></tr>
<tr><td>8th cycle</td><td>0.4</td></tr>
<tr><td>9th cycle</td><td>0.4</td></tr>
<tr><td>10th cycle</td><td>0.4</td></tr>
</table>

5.4.1.4. Discussion

The primary problem identified after washing the smart ECG vest was the breakage of the connection between the electrode site and the JST XH connector at the soldering point. Heat-shrink tubing (Jaycar Electronics, n.d.) was suggested to curb the stated problem in the final prototype, where all the connections were intact after five washing cycles.

Moreover, 10 washing cycles were performed on the textile electrodes according to the AS/NZS ISO standard 10535:2011. However, there was no significant difference in the electrical properties of the textile electrodes, considering the washing setup given in section 5.4.1.2. This result aligns with another study conducted on textile electrodes (Schwarz et al., 2011) using silver and copper-based el2-yarns. The electrodes were washed for 40 minutes at 40ºC and for 25 washing cycles to study the effect of washing on the electrical characteristics of the textile electrodes. After 25 cycles of washing, the silver-based textile electrodes did not show a significant change in resistance while the electrical resistance of the copper-based electrodes degraded by 30%. Our electrodes were made of silver-based fabrics (section 4.5.3) and hence ten cycles of washing were not enough to degrade the electrical properties of the textile electrodes.

In contrast, Cho et al. (2007) used Cu/Ni electrodes plated Ripstop and Mesh textile electrodes to study the effect of washing on the electrical characteristics of the electrodes. There were two groups of electrodes regarding waterproofing, polyurethane (PU)-sealed and unsealed. The electrodes were washed ten times at 20ºC water temperature. The authors reported that the resistance of the unsealed textile electrodes increased by more than five times to the unwashed value after the first washing cycle. This might be due to the methods and materials used to prepare the textile electrodes. For example, the double PU sealed textile electrodes showed more resistance to washing compared to the untreated textile electrodes. In a similar study, Ankhili et al. (2018) studied the effect of washing on three textile electrodes made of cotton, polyamide and polyester coated with Poly(3,4-ethylene dioxythiophene):poly(styrene sulfonate) (PEDOT:PSS). After 50 washing cycles, the electrical resistance of the textile electrodes made up of polyester textile electrodes was around 60 times of the pre-washed value while the electrical resistance of the polyamide electrodes was nine times and the cotton electrodes was five times of the respective pre-washed resistance values.

As a result of this study, it is recommended that silver-based textile electrodes are more resilient for washing and hence could be used for long term ambulatory ECG monitoring and washed repeatedly (possibly more than 10 times) without significant signal distortion.

5.4.2. Estimating the compression pressure that needs to be applied by the smart ECG vest onto the user

As the textile electrodes are not firmly attached to the skin, the slightest motion of the wearer changes the electrodes' site of attachment to the wearer's skin contributing significantly to motion artefact (Teferra et al., 2019b). Hence acquiring quality ECG from the smart vest requires a stable skin-electrode interface.

Previous studies have reported a tight T-shirt, garment, or a vest to provide a secure electrode site (Nag and Sharma, 2006, Di Rienzo et al., 2010, Lopez et al., 2010, Di Rienzo et al., 2013, Abtahi et al., 2015, Cai et al., 2017, Sun et al., 2017, Yu et al., 2017, Balsam et al., 2018, Catarino et al., 2012). Cömert et al. (2013) conducted a pilot study on a single lead ECG and concluded that ECG from textile electrodes showed higher quality where the applied pressure is between 15mmHg and 20mmHg. However, as a critical parameter, the magnitude of the compression pressure applied to the wearer's skin by a 12-lead e-textile ECG vest is yet to be reported. Thus, the pressure required to collect a quality ECG tracing from the proposed smart vest was experimentally determined.

5.4.2.1. Calibrating the Forse-sensing Resistor sensor

A force-sensing resistor (FSR) was chosen to measure the pressure under the textile electrode. FSRs are straightforward and inexpensive pressure sensors that have been used in numerous studies (Schultz, 1993, Pitei et al., 1996, Bathiche, 2007, King et al., 2009, Rana, 2009, Stephanou et al., 2015, Schofield et al., 2016) to measure applied pressure. An FSR pressure sensor estimates the compressive force applied on a surface area based on the principle of differential resistance. In this study, a flexible circular thin-film pressure sensor (RP-C18.3-ST) from DFRobot was used.

With an FSR, the force-resistance relation is nonlinear and requires a proper calibration (Schofield et al., 2016). In the study, the FSR sensor was calibrated prior to use at room temperature and on a flat surface using a sphygmomanometer (Figure 5.15). A ramp pressure from zero to 300mmHg with a 10mmHg increment was applied. The voltage reading from the Arduino Mega 2560 for the corresponding applied pressure was collected at 100 samples per second and transferred to a desktop PC, running a Java-based application platform.

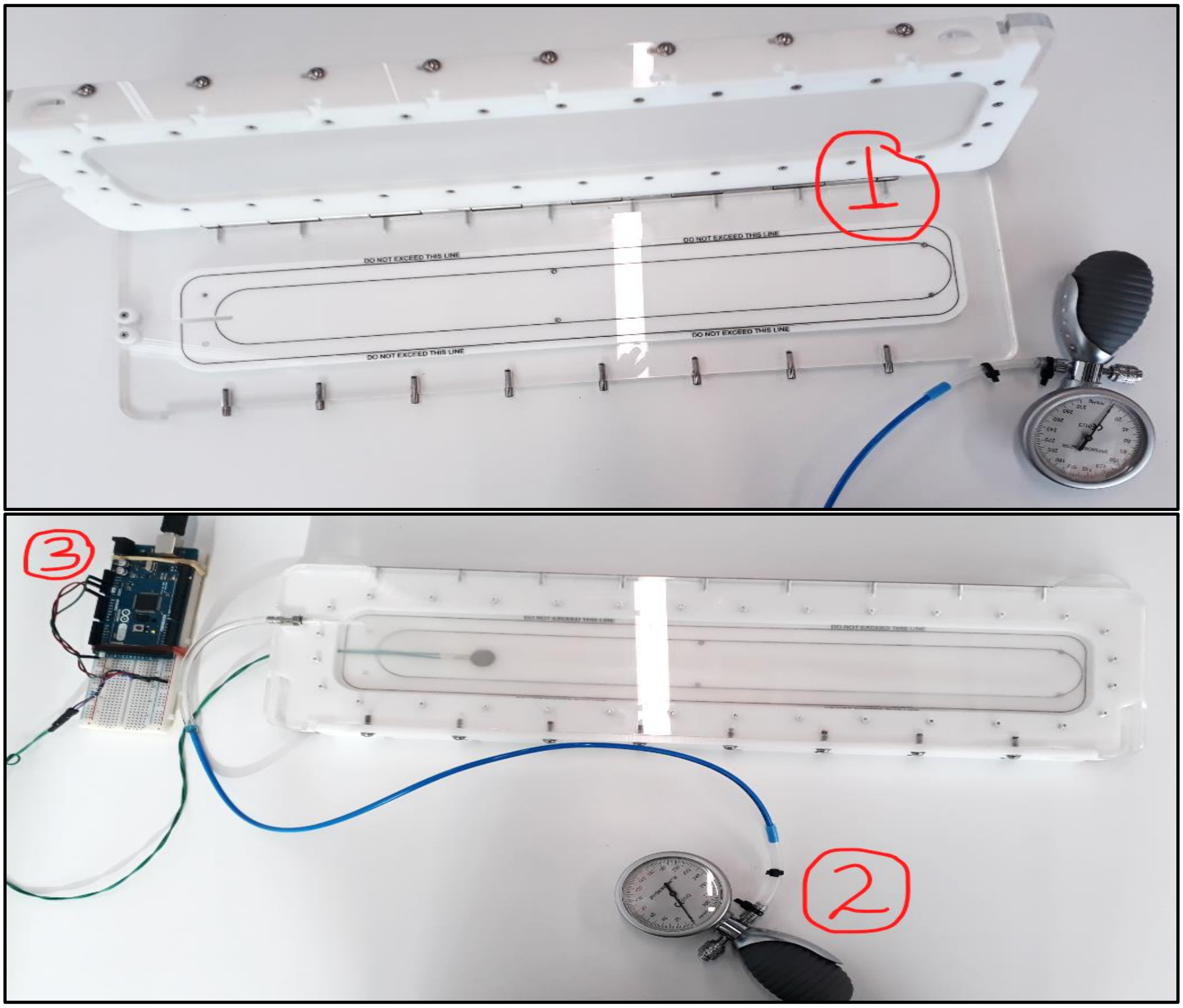

Figure 5.15: Calibration pressure chamber (1) with a sphygmomanometer (2) and Arduino Mega 2560 (3)

5.4.2.2. Calibration results

An inverse logarithmic curve (equation 5.8), as recommended by Schofield et al. (2016), was fitted to the FSR voltage-pressure relation using nonlinear regression.

$$P = a.e^{b.V} + c$$
$$\text{Where} \quad \begin{aligned} P &= pressure\ (mmHg), \\ V &= Voltage\ (mV), \\ a,b,c &= constants\ to\ be\ determined\ from\ the\ experiment \end{aligned} \qquad [5.8]$$

To account for the effect of dead weight and hysteresis properties (Hollinger and Wanderley, 2006) of the FSR sensor on the calibration curve, two methods for FSR sensor calibration were employed. During the first calibration cycle (case-I), continuous pressure was applied in 10mmHg steps without withdrawing the applied pressure. Figure 5.16 depicts the acquired data, the model function based on nonlinear regression and the residue.

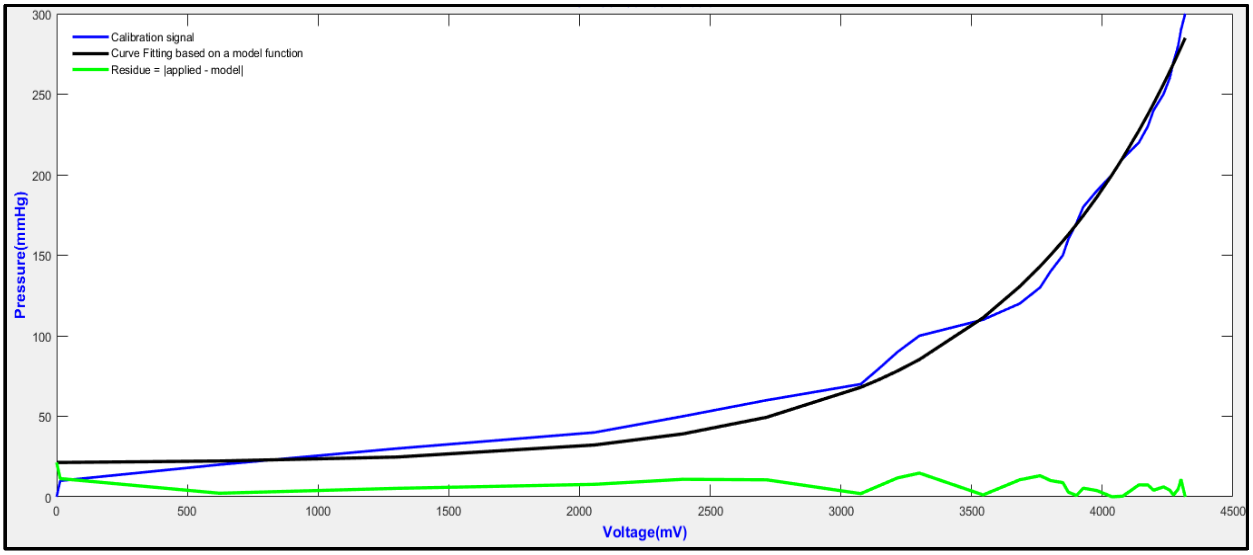

Figure 5.16: Case-I calibration results (FSR sensor not relaxing between measurements); model function (*$P = 0.66742*e^{0.0013855*V} + 20.663$, R^2= 0.99, root mean square error = 9.24)*

In the second method (case-II), a ramped pressure was applied at a step of 10mmHg. According to (Hollinger and Wanderley, 2006), the maximum settling-time required for the FSR sensor is 800 seconds. Therefore, for every pressure point, a calibration signal was collected for about 1000 seconds and the average over 1000 seconds was calculated. Then, the applied pressure was removed, and the FSR sensor was allowed to relax for 800 seconds before the next higher pressure was applied. Figure 5.17 shows the acquired calibration signal, a model function (nonlinear regression), and the discrepancy between the calibration signal and the model function.

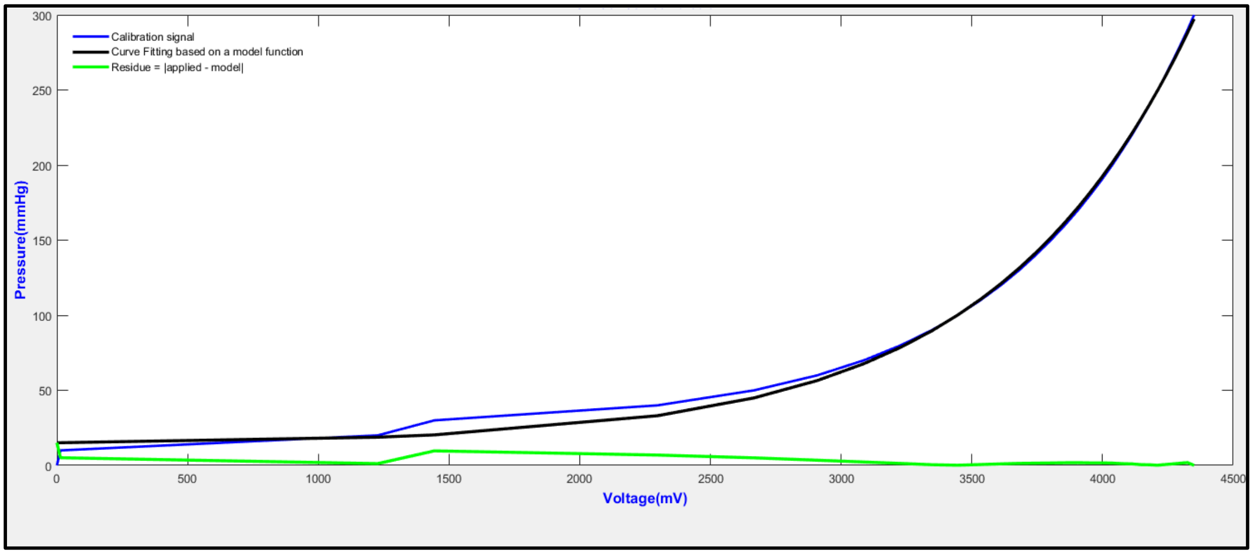

Figure 5.17: Case-II calibration results (FSR sensor relaxing between measurements); model function ($P = 0.91422 * e^{0.0013185 * V} + 14.183$, $R^2 = 0.998$, *root mean square error = 4.15*)

5.4.2.3. Specific objective

The specific objective of the study was to determine the compression pressure that needs to be applied by the smart ECG vest onto the user for acceptable ECG acquisition by the textile electrodes.

5.4.2.4. Materials and method for data collection

Four pre-calibrated FSRs were wrapped in material cut from a bedsheet from Kmart (Kmart Australia, n.d.) as shown in Figure 5.18 to minimize the effect of sweating and attached to the vest on a flat backing plate to reduce any error due to curvature (Boutry et al., 2015, Schofield et al., 2016).

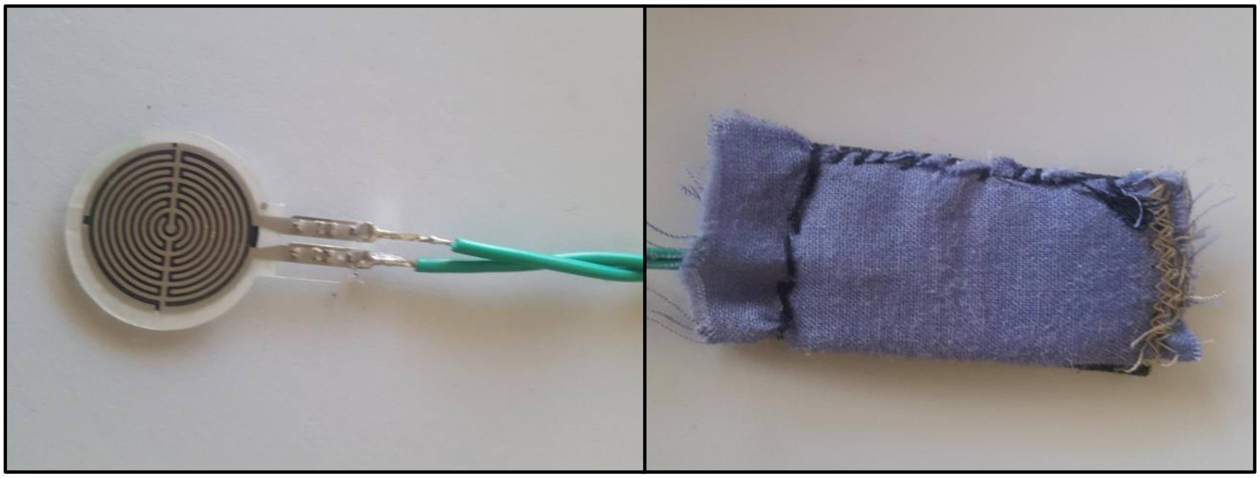

Figure 5.18: FSR sensor (left), FSR sensor wrapped with textile (right)

A healthy male volunteer subject (age 34, BMI 23.4 Kg/m^2) participated in the experiment. The participant wore the ECG vest to evaluate the maximum and minimum compressive pressure that resulted in an acceptable ECG tracing. While the voltage corresponding to the applied pressure was measured, a simultaneous real-time ECG was acquired. The four FSR sensors were positioned to measure the pressure at four anatomical landmarks (Figure 5.19); at the top and the bottom of the sternum (P1 and P3) and left and right mid-axillary lines (P2 and P4). Each pressure point corresponds to the respective electrodeposition in the EASI configuration.

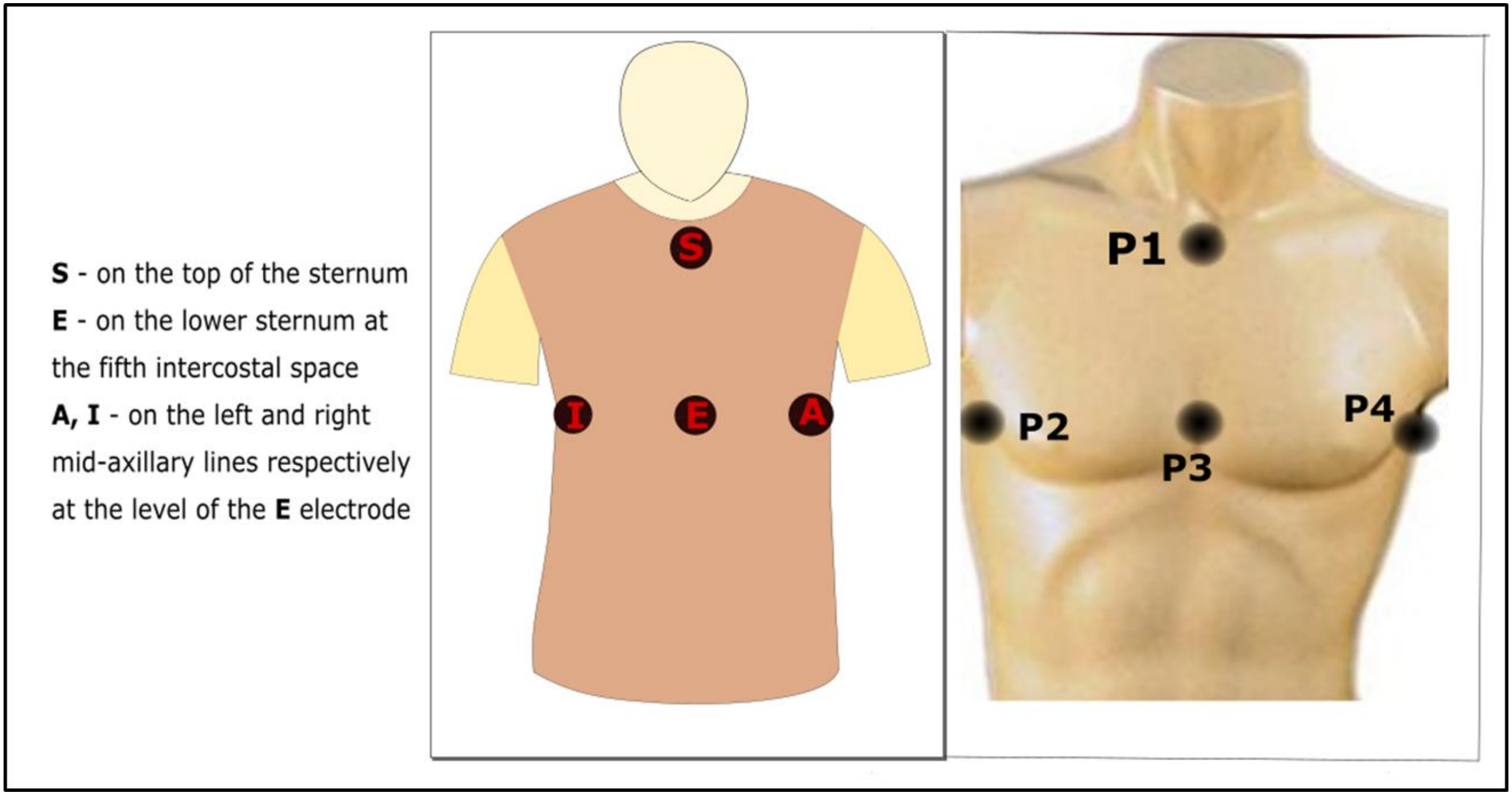

Figure 5.19: Anatomical landmarks for pressure measurement (test points – right; the equivalent electrodes in the EASI lead system – left)

5.4.2.5. Results

The maximum compression pressure for acceptable ECG tracing

At every test point, more than 25 minutes of data were collected. However, only 100,000 representative samples were used to reduce computation overload.

The highest average voltage reading was recorded at point ***P3*** (the ***E*** – electrode site on the smart ECG vest; 2149.40mV – day one; 2101.90mV – day two) followed by the test point ***P1*** (the ***S*** – electrode site on the smart-ECG garment; 1881.70mV – day one; 1761.10mV – day two). Relatively similar mean voltage readings were measured at the two axillary test points point ***P2*** (the ***I*** – electrode site on the smart ECG vest; 1282.30mV – day one; 1221.60mV – day two) and ***P4*** (the ***A*** – electrode site on the smart ECG vest; 1313.00mV – day one; 1242.10mV – day two).

Based on the measurements, the estimated maximum compression pressures were computed at each test point (*P1, case-I = 29.11 ± 0.63 mmHg and case-II = 24.41 ± 0.75 mmHg; P2, case-I = 24.73 ± 0.15 mmHg and case-II = 19.27 ± 0.18 mmHg; P3, case-I = 33.53 ± 0.31 mmHg and case-II = 29.45 ± 0.36 mmHg; P4, case-I = 24.73 ± 0.19 mmHg and case-II = 19.28 ± 0.22 mmHg*) using the calibration equations developed in section 5.4.2.1. Table 5.8 summarises the voltage readings and the corresponding estimated pressures.

Table 5.8: Summary of mean measured voltage and mean calculated compression pressure.

Test point		Mean measured voltage (mV)	Mean calculated pressure (mmHg)	
			Case-I (nonrelaxing)	Case-II (relaxing)
P1 (S)	Day 1	1881.70	29.77	25.17
	Day 2	1761.10	28.46	23.66
	Average	1821.40	29.11	24.41
P2 (I)	Day 1	1282.30	24.88	19.46
	Day 2	1221.60	24.58	19.09
	Average	1251.95	24.73	19.27
P3 (E)	Day 1	2149.40	33.85	29.82
	Day 2	2101.90	33.22	29.09
	Average	2125.65	33.53	29.45
P4 (A)	Day 1	1313.00	24.92	19.51
	Day 2	1242.10	24.54	19.06
	Average	1277.55	24.73	19.28

Estimating the minimum compression pressure

The compression pressure presented in the previous section item was the maximum applied pressure for a quality ECG transduction. In this section, the minimum compression pressure for a readable ECG collection was determined.

The applied pressure at the individual test points was determined by averaging 100,000 representative samples.

Table 5.9: Minimum compression pressure for a readable ECG tracing

Test point	Mean measured voltage (mV)	Mean calculated pressure (mmHg)	
		Case-I (Nonrelaxing)	Case-II (Relaxing)
P1 (S)	1668.50	27.66	22.72
P2 (I)	481.57	21.98	15.92
P3 (E)	1736.20	28.59	23.79
P4 (A)	564.89	22.14	16.13

Table 5.9 presents the minimum compression pressure. It was no longer possible to reliably acquire ECG if the contact pressure applied was lower than these values.

5.4.2.6. Discussion

A preliminary test to estimate the pressure required of the smart vest for a readable ECG tracing was conducted. The pressure was measured at four different anatomical landmarks (test points), each spot corresponding to the electrode positions on the smart ECG vest (E, A, S, and I). During the trial, two methods of calibration were employed to generate a close estimate and best fit of the voltage – pressure curve. The second calibration scenario (case – II) showed a better statistical result (*R^2 = 0.998, root mean square error = 4.15*) compared to the first calibration method (*case – I; R^2 = 0.99, root mean square error = 9.24*). However, a higher residue between the calibration results and the model function was observed in both graphs, especially around the lower region of the curves. At all times, the second method produced better pressure estimation compared to the previous study by Cömert et al. (2013). Moreover, the estimated pressure in both cases agrees with a previous study conducted by Beckmann et al. (2010) on various textile electrodes (2.5cm by 9.5cm) and skin dummy made up of agar-agar of 29.3μScm^{-1} conductivity, distilled water, disinfection agent and salt, where the authors recommended a compressive pressure of up to 10 Newton (~31mmHg) for stable and comfortable long-term applications.

In general, the measured voltage and hence, the computed maximum pressure value oscillates between the higher and lower limits modulated by the breathing cycle. The compression pressure at the test point ***P3*** (the ***E*** – electrode site on the smart ECG vest) was the sum of pressure applied by the Velcro loop along the chest line and the two Velcro straps from the left and the right side of the neck. The experiment revealed that the higher estimated pressure was observed at the test point ***P3*** (*29.45 ± 0.36 mmHg*). The main contributor to the compression pressure at the test point ***P1*** was the two Velcro straps from either side of the neck. Additionally, the Velcro along the chest line affected the test point ***P1*** where the next highest-pressure reading was recorded ***P1*** (*24.41 ± 0.75 mmHg*).

5.5. Conclusion

This chapter presented the module level testing and evaluation of a 12-lead textile-based ECG monitor, an initial procedure to study the response of the respective modules for known inputs. Testing the ECG hardware revealed that the individual modules of the proposed ECG monitor are capable of reproducing simulated input signals representing a variety of common cardiac abnormalities without significant deviation. The washing of the smart ECG vest affected the connection points after eight washing cycles, while ten cycles of washing did not alter the electrical properties of the textile electrodes. Moreover, the maximum and minimum applied pressure by the vest on the textile electrodes for acceptable ECG tracing was experimentally determined. To the best of our knowledge, this is the first pilot study that experimentally estimated the numerical values of the applied pressure by the smart ECG vest at the respective electrode sites.

This page is left blank intentionally

Chapter 6. Electronic textile-based ECG monitor: system-level test and evaluation

6.1. Introduction

This chapter presents system-level testing and assessments of the 12-lead e-textile based ECG monitor in general and the effects of textile electrodes and vest design on signal reception in particular. First, the effect of the textile electrode characteristics on signal quality was studied. Second, the effects of vest design and electrode position on the acquired ECG were studied. Third, the signal quality between ECG acquired from dry / or wet textile electrodes was compared to the ECG obtained using commercial wet-gel sensors using the developed wearable ECG monitor. Finally, the ECG from the textile-based 12-lead ECG monitor was compared to a reference ECG from a traditional Holter monitor.

6.2. General objective and research questions

6.2.1. General objective

The objective of the tests presented in this chapter was to evaluate the accuracy and reliability of an e-textile based 12-lead ECG monitor prototype (system-level testing).

6.2.2. Research questions

1. Is ECG quality affected by the area and the thickness of the textile electrodes? (Section 6.4)
2. How does the smart vest design affect ECG quality? How close and where on the body should the e-textile sensors be placed for optimal performance? Do the methods used to connect the textile electrodes to the smart vest affect signal quality? (Section 6.5)
3. Does sweating affect ECG quality? (Section 6.6.1)
4. Do the textile electrodes result in an acceptable ECG tracing compared to the commercial wet-gel electrodes? (Section 6.6.2)
5. Is there a significant difference in performance between the proposed textile-based ECG monitor and the traditional Holter monitor when ECG is acquired during different body movements and activities of daily living? (Section 6.7)

6.3. Methods

6.3.1. Data collection protocol

During the first stage of each experiment to address Research Questions 1-4, the novel e-textile based ECG monitor outlined in Chapter 1 was used to collect 25 minutes of ECG data. Following this, the following set of movements were undertaken during the acquisition: i) yawning, ii) deep breathing, iii) coughing, iv) sideways (shoulder adduction-abduction – moving the hands sideways and moving them back to the midline horizontally) and v) up (shoulder flexion-extension – raising arms above the head and moving them back).

In addition, ECGs during activities of daily living (sitting, sitting/standing from a chair, lying on a bed in a supine position, writing on a keyboard, making a call from a mobile phone and climbing stairs) were collected to compare the signal quality from the proposed textile ECG monitor and the standard Holter monitor. Each body movement or activity of daily living was recorded for five minutes, and there were two minutes intervals between each recording.

6.3.2. Participants

Ethics approval to collect ECG based on the data collection protocol outlined in section 6.3.1 from healthy adult participants was obtained from the Flinders University Social and Behavioural Research Ethics Committee (SBREC: project code – 8490). However, due to COVID 19, it was impossible to proceed with the trial, and therefore the study was restricted to just one person. Hence, all ECG acquisitions described in this chapter were obtained from a single healthy male volunteer (age 34, BMI 22.5 Kg/m^2).

6.3.3. Signal quality parameters

The following parameters were defined to evaluate the accuracy and reliability of the developed textile-based ECG monitor.

Relative power - Signal to signal ratio (SSR)

The relative power contained within the ECG measurements (signal to signal ratio (SSR), equation 6.1) refers to the ratio of the power contained within two ECG measurements in decibel scale:

$$SSR = 20 * \log_{10}\left(\frac{(RMS(ECG1)}{RMS(ECG2)}\right),$$

$$\begin{aligned} &\textit{Where } ECG1 \ : \text{ the first ECG signal} \\ &\qquad ECG2 \ : \text{ the second ECG signal to be compared} \end{aligned} \qquad [6.1]$$

And

$$RMS = \sqrt{\frac{\sum_{i=1}^{N} (X(i) - mean(X))^2}{N}}$$

Positive values refer to a higher power content within ECG1 compared to ECG2, while negative values signify the converse is true.

Power spectral density

The PSD was used to study the collected ECG in the frequency domain and is defined in Chapter 5, section 5.3.1.2. Throughout the experiment, the PSD was computed over a pre-defined frequency profile (low-frequency noise: f <1Hz) of the acquired ECG.

Approximate entropy

Approximate entropy (ApEn) is a statistical method used to determine the dynamic nature (randomness) of a noisy time-series signal (Pincus, 1995, Moody, 2015, Montesinos et al., 2018). Given the variable nature of the ECG signal, the ApEn (equation 6.2) of the collected data was used to study irregularities in the acquired ECG (Pincus, 1991, Pincus and Goldberger, 1994, Pincus, 1995, Moody, 2015).

$$ApEn(S_N, m, r) = \ln\left(\frac{C_m(r)}{C_{m+1}(r)}\right)$$

$$\begin{aligned} \textit{Where} \quad C_m(r)&: \text{ the prevalance of repetitive patterns of length } m \textit{ in } S_N \\ \mathrm{S_N}&: \text{ Sequence of length N} \\ m&: \text{ Pattern length} \\ r&: \text{ Similarity criteria} \end{aligned} \qquad [6.2]$$

The ApEn is interpreted differently in different disciplines. For example, lower ApEn of HRV analysis might be an indicator of underlying pathology. However, the ApEn in the context of this study refers to the complexity and randomness of the acquired ECG, where a higher ApEn value signifies increased noise (Pincus and Goldberger, 1994). The ApEn analysis was conducted for a minimum of 1,000 data points based on similarity criteria of 0.2 and a pattern length of two, as recommended by Pincus and Goldberger (1994).

The beat detection signal quality index

Various ECG delineation algorithms are affected by noise differently. Therefore, it is possible to use different QRS detection algorithms to devise a quantitative ECG signal quality matrix (Friesen et al., 1990). One such technique used widely to quantify ECG quality is the beat detection signal quality index, ***bSQI*** (Friesen et al., 1990, Li et al., 2008, Clifford et al., 2012, Johnson et al., 2015). The bSQI of the kth ECG beat is defined as follows in equation 6.3 (Li et al., 2008):

$$bSQI(k) = \frac{N_{matched}(k,w)}{N_{all}(k,w)},$$

$$\begin{aligned} &where \quad \text{w = the ECG length = 10sec} \\ &N_{matched} = number \text{ of matched beats detected by all algorithms} \\ &N_{all} = total\ number \text{ of beats} \end{aligned} \qquad [6.3]$$

In the experiment, three peak detection algorithms (Pan and Tompkins (Pan and Tompkins, 1985), State-Machine (Sedghamiz, 2013), Multilevel Teager Energy Operator (MTEO) (Sedghamiz and Santonocito, 2015)) from BioSigKit, a MATLAB toolkit for Bio-Signal analysis (Sedghamiz, 2018), were used to detect the R waves. Then the locations of the respective peaks were used to compute the F1 scores (signal quality measures) of the bSQI.

Two statistical terms used to calculate F1 values are sensitivity (Se - correct detection of true positive, possibly with no false negative) and positive prediction value (PPV – accurate identification with no false positive) (Trevethan, 2017). If an ECG peak (P, R and T) is identified correctly along with the standard intervals of the temporal ECG, it is a True-Positive (TP); missing a peak is a False-Negative (FN). Correct detection of a missed peak is a True-Negative (TN), and false detection of a maximum is a False-Positive (FP). The total number of peaks detected is the sum of the TP and the FP. The total number of missed peaks is the sum of TN and the FN. Therefore, a clear definition of F1 is given in equation 6.4 (Johnson et al., 2015).

$$F1 = 2 * \frac{Se * PPV}{Se + PPV}$$

$$where, \mathrm{Se} = \frac{TP}{TP + FN}, PPV = \frac{TP}{TP + FP} \qquad [6.4]$$

$$F1 = 2 * \frac{Se * PPV}{Se + PPV} = \frac{2TP}{2TP + FP + FN}$$

Referring to the bSQI (F1) values of the acquired ECG signal from the e-textile based ECG vest and the Holter monitor, it is possible to determine if different QRS detectors can identify individual cardiac events. An F1 value higher than 0.95 was considered a good level of accurate identification.

The power signal quality index

The power signal quality index (pSQI) is a measure of the relative ECG power. It is calculated as the ratio of the ECG power contained within the QRS complex (Power calculated from 5Hz to 15Hz) to the total ECG power computed between 5Hz and 50Hz (Li et al., 2008, Clifford et al., 2012). The accepted values are between 0.5 and 0.8, where extreme pSQI signifies the prevalence of increased motion artefact in the collected ECG (Li et al., 2008).

The baseline power signal quality index

The baseline power signal quality index (basSQI (equation 6.5)) is used to examine the ECG noise artefact in the low-frequency region (f<=1Hz) as a result of deep breathing, coughing, yawning and various body movements (Clifford et al., 2012). The higher the value of the basSQI, the better the signal quality. Clifford et al. (2012) showed that a good quality signal had a basSQI value of 0.996 while a poor-quality ECG signal scored a basSQI value of 0.5. Therefore, a basSQI greater than or equal to 0.95 was considered the minimum acceptable baseline low-frequency noise in this study.

$$\text{basSQI}=1-\frac{\int_0^1 P(f)df}{\int_0^{40} P(f)df} \quad [6.5]$$

6.3.4. Visual inspection

Representative ECG temporal tracing and the PSD plot in the frequency domain were used as additional sources to assess the signal quality and compare different ECGs.

6.3.5. Data analysis

ECG from the proposed textile system was sampled at 4,000 samples per second (sps), recorded at 200sps with a frequency range from zero to 100 Hz at -3 dB level, and wirelessly transmitted to a host PC. Data analysis was based on MATLAB ™ 2017Ra software (The MathWorks Inc., Natick, MA, U.S.), the MedCalc® Version 19.0.4.0 (MedCalc Software Ltd, Ostend, Belgium) and IBM SPSS Statistics 25.0.2 (Armonk, New York, U.S.).

Lead-II ECG has a good view of the P wave and it is commonly used as a reference lead to analyse cardiac activities (Meek and Morris, 2002). A previous study on the effect of change in body position on ischemia monitoring (Adams and Drew, 1997) suggested that V4 ECG showed the greatest deviation within the ST segment and QRS complex. V4 ECG showed higher accuracy on the classification of myocardial infarction (Baloglu et al.,

2019) and a better estimate to quantify the interval between the start of the Q wave to the end of the T wave (QT) Prolongation (Sadanaga et al., 2006). Therefore, lead II and V4 ECGs were chosen to evaluate the performance of the proposed ECG monitor characteristics throughout the analysis.

On the other hand, looking at the SEER light user manual (GE Healthcare, c2009), channel one (modified V5, mV5) was the recommended reference signal for the commercial Holter monitor used in the trial. Therefore, the performance analysis of the proposed textile-based ECG monitor against the reference ambulatory monitor was based on the V5 ECG.

6.3.6. Statistical analysis

Wilcoxon Signed-Rank Test is the non-parametric form of the paired-sample t-test used to analyse samples where the data has unknown distribution. The Wilcoxon Test ranks the absolute values of the differences between the paired data in the two samples. It computes statistical values based on the number of negative and positive differences. If the resulting p-value is small ($p<0.05$), it is safe to assume that the two samples have different distributions and reject the null-hypothesis (Altman, 1990). In cardiac research, there are previous studies (Budgell and Polus, 2006, Di Rienzo et al., 2013, Reinhard et al., 2013) that validated the Wilcoxon Signed-Rank Test as a practical statistical tool to analyse ECG. As a result, the Wilcoxon Signed-Rank Test was used to compare results throughout the experiment. A p-value of less than 0.05 was considered statistically significant.

6.4. Textile electrode characteristics

6.4.1. Specific objective

This section aims to address Research Question 1: is ECG quality affected by the area and the thickness of the textile electrodes? The specific objective of the study was to examine the effect of the area and thickness of the textile electrodes on signal quality.

6.4.2. Effect of electrode area on signal quality

Different physiological signals and motion artefacts generated from various sources share the low amplitude (V_{ECG}< 20mV) and bandwidth (f < 200Hz) of the ECG. Of the factors affecting ECG signal quality, the electrode surface area (Puurtinen et al., 2006, Ueno et al., 2007, Marozas et al., 2011) was considered in the following experiments.

6.4.2.1. ECG from equal size EASI configuration textile electrodes

Specific objective

The specific objective was to examine the effect of electrode area (electrode size) on signal quality.

Materials and methods

ECGs were acquired from equal size textile sensors (first from 40mm^2 EASI electrodes, followed by 60mm^2 EASI electrodes, and finally from 70mm^2 EASI electrodes) to investigate the effect of electrode surface area on signal quality. The thickness of the electrodes was kept at 3mm throughout this study. For data collection, the subject performed a series of movements and daily living routines outlined in the data collection protocol section 6.3.1. Before the start of the next experiment, the participant rested for two minutes. Then, a higher area textile electrode (starting from 40mm^2 to 70mm^2) was attached to each electrode site. The built-in digital high pass filter (f_c = 0.5Hz) was turned off to capture the low-frequency noise components introduced by body movement.

Resting ECG

Results

Figure 6.1 depicts six seconds strips of the ECG acquired from 40mm^2, 60mm^2, and 70mm^2 textile electrodes (from top to bottom), respectively. These were collected with the participant resting quietly. As can be seen from the sample tracing in Figure 6.1, all three sizes of textile electrodes capture the important ECG features (QRS complex, R, and T waves).

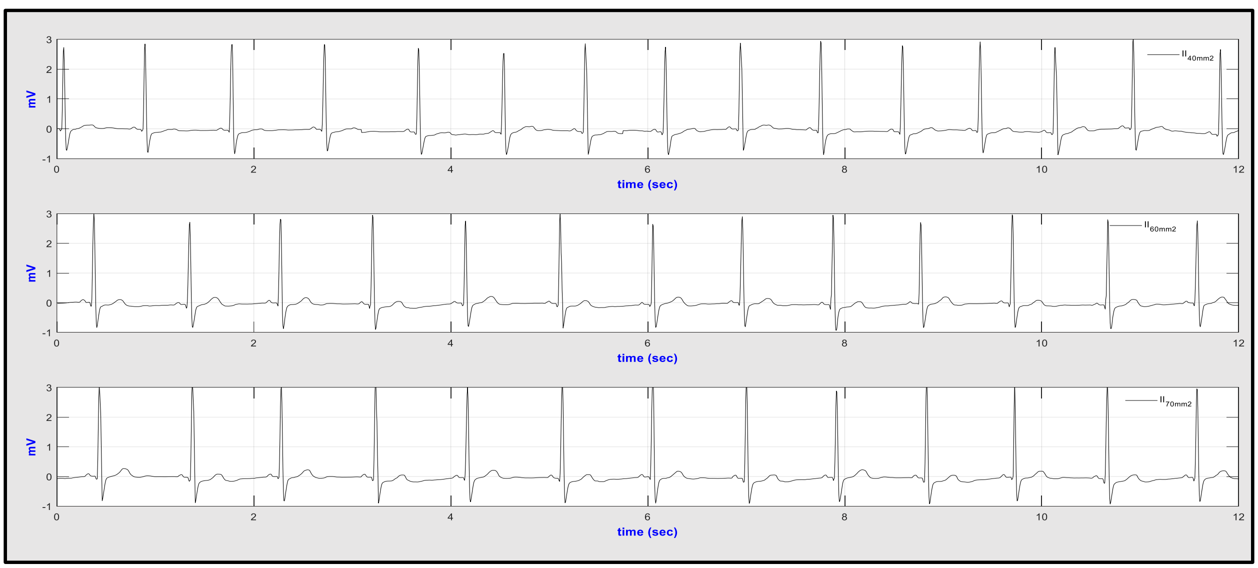

Figure 6.1: Lead-II representative ECG strips from different size textile sensors (***top*** – ECG from 3mm thick, 40mm^2 textile electrodes; ***middle*** – ECG from 3mm thick, 60mm^2 textile electrodes and ***bottom*** – ECG from 3mm thick, 70mm^2 textile electrodes)

Table 6.1 presents SSR and peak PSD of ECG acquired from different size textile electrodes while Table 6.2 summarises the results of the Wilcoxon Signed-Rank Test based on ApEn calculated for every 1,000 data points of a representative ECG strip as recommended by Pincus (1991).

Table 6.1: Comparison of the SSR and peak PSD of lead-II and V4 ECG collected from different size ($40mm^2$, $60mm^2$ and $70mm^2$) textile sensors.

ECG lead	**SSR (dB) = 10*log$_{10}$(Px)**			**PSD**				
	Px = (P_{70mm^2}/ P_{40mm^2})	**Px = P_{70mm^2}/P_{60mm^2})**	**Px = (P_{60mm2}/ P_{40mm^2})**	**Electrode size**	**Peak PSDN (mW/Hz)**	**f_{PSD} (Hz)**	**Peak PSD_{QRS} (mW/Hz)**	**f_{QRSpsd} (Hz)**
II	2.5450	1.6338	0.9112	$40mm^2$	12.25	0.514	65.27	6.028
				$60mm^2$	12.67	0.028	58.88	9.8286
				$70mm^2$	17.78	0.514	90.45	12.142
V4	1.3125	1.0659	1.1131	$40mm^2$	34.12	0.175	47.57	7.562
				$60mm^2$	17.99	0.437	42.19	6.750
				$70mm^2$	11.8	0.500	50.60	8.825

***Note: Peak PSD_N** – the maximum noise PSD within the low-frequency range **$f<1Hz$; f_{PSD}** – the frequency at which the max noise PSD occurred; **Peak PSD_{QRS}** – the peak PSD of the QRS complexes; **f_{QRSpsd}** – the frequency at which the max QRS-complex PSD occurred along with the QRS frequency spectrum **f = [5 - 15] Hz**; **PSD** – power spectral density*

Table 6.2: Statistical summary of the ApEn computed from ECG acquired through different size textile electrodes.

ECG lead	**ApEn Descriptive Statistics**					
	$40mm^2$ textile electrodes		**$60mm^2$ textile electrodes**		**$70mm^2$ textile electrodes**	
	Mean±SD	**50th Percentiles (Median)**	**Mean±SD**	**50th Percentiles (Median)**	**Mean±SD**	**50th Percentiles (Median)**
II	0.0688±0.0078	0.0667	0.0613±0.0104	0.0584	0.0502±0.0064	0.0509
V4	0.0938±0.0181	0.0954	0.0808±0.0163	0.0775	0.0671±0.0073	0.0682
ECG lead	**ApEn Test Statistics**					
	$70mm^2$ Vs $60mm^2$		**$70mm^2$ Vs $40mm^2$**		**$60mm^2$ Vs $40mm^2$**	
II	Z	-3.0101	Z	-3.4084	Z	-2.4422
	p	0.0026*	p	0.0006*	p	0.0145
V4	Z	-2.1582	Z	-3.0669	Z	-2.1014
	p	0.0309	p	0.0021*	p	0.0356

***Note**: ApEn – Approximate entropy; * – statistically significant*

A Wilcoxon signed-rank test presented in Table 6.2 showed that the ECG collected from the $70mm^2$ textile electrodes scored a statistically significant lower approximate entropy compared to the ECG acquired from the 40mm^2 textile electrodes (lead-II: Z = -3.4084, $p = 0.0006$; V4: Z = -3.0669, $p = 0.0021$).

Table 6.3 compares the power quality index (pSQI) and the baseline power quality index (basSQI).

Table 6.3: Comparison of the signal quality indexes; pSQI accepted [0.5-0.8]; higher pSQI indicates increased motion artefact in the QRS complex. Higher values of basSQI indicate better signal quality.

ECG lead	Electrode area					
	40mm^2		60mm^2		70mm^2	
	pSQI	basSQI	pSQI	basSQI	pSQI	basSQI
II	0.6394	0.9776	0.6757	0.9910	0.6897	0.9870
V4	0.6369	0.9569	0.7127	0.9875	0.7250	0.9812

***Note: pSQI** – power signal quality index; **basSQI** – baseline power signal quality index*

The ECG acquired from the 70mm^2 textile electrodes showed better signal quality, looking at the SSR values, the peak QRS PSD and the ApEn. On the other hand, the signal quality indexes given in Table 6.3 found no difference between the SQI values for ECGs acquired from the different size textile electrodes (40mm^2, 60mm^2 and 70mm^2) for resting ECG.

Effect of electrode area on ECG during movement and activities of daily living

Various noise sources affect ECG signal acquisition. However, the focus of this experiment was the low-frequency noises due to patient movement. Noise in ECG caused by movement artefact has a frequency span of mainly less than 1Hz but can be a few Hz for exercise ECG (Pandit, 1996, Bailón et al., 2006, Gacek and Pedrycz, 2011). The relation between the noise introduced during a series of controlled movements and the textile electrodes surface area was studied. The influence of the textile electrode surface area on ECG signal quality for given activities of daily living was therefore examined. The standard EASI electrode configuration was used throughout the experiment and each experiment was conducted once a day in the morning on three different days.

Results

Table 6.4 compares the lead-II and V4 ECG SSR results of experiments conducted to investigate the effect of electrode surface area on motion artefact.

Table 6.4: SSR from different size textile electrodes (40mm^2, 60mm^2 and 70mm^2)

SSR (dB) = 10*log$_{10}$(Px)			
ECG lead	**II**		
Body movement / activities	**Px = ($P_{70mm}{}^2$/ $P_{40mm}{}^2$)**	**Px = ($P_{70mm}{}^2$/$P_{60mm}{}^2$)**	**Px = ($P_{60mm}{}^2$/ $P_{40mm}{}^2$)**
Yawning	0.4075	-0.2396	0.6519
Deep Breath	1.2201	0.5898	0.6388
Coughing	1.1251	0.6559	0.5236
Sideways	1.5188	0.0053	1.4054
Up	1.9799	-0.0300	2.0275
Writing on a Keyboard	-0.7068	-0.5018	-0.2050
Sitting / Standing activities	0.2239	0.3963	-0.1317
Stairs	0.1031	0.6921	-0.8102
ECG lead	**V4**		
Body movement / activities	**Px = ($P_{70mm}{}^2$/ $P_{40mm}{}^2$)**	**Px = ($P_{70mm}{}^2$/$P_{60mm}{}^2$)**	**Px = ($P_{60mm}{}^2$/ $P_{40mm}{}^2$)**
Yawning	-0.1737	-0.6880	0.6012
Deep Breath	0.6083	0.5036	0.1143
Coughing	0.4408	0.5040	0.0240
Sideways	-0.9847	-0.7768	-0.2489
Up	1.2008	0.0201	1.3026
Writing on a Keyboard	-1.7167	-1.5650	-0.0711
Sitting / Standing activities	-0.0295	0.3291	-0.3125
Stairs	-0.1710	0.4425	-0.7125

Note: *SSR – Signal to Signal Ratio*

Looking at the SSR values presented in Table 6.4, the lead-II ECG collected from the 70mm^2 textile electrodes showed higher signal power compared to the ECG from the 40mm^2 except during writing on a keyboard. In contrast, the power contained within the lead-II ECG collected from the 60mm^2 textile electrodes was higher compared to the ECG from the 70mm^2 textile electrodes during yawning, up movement, and writing on a keyboard. However, it is difficult to decide the quality of the ECG from the SSR values alone as higher power might be a result of noise in the ECG signal. Therefore, the ApEn (Table 6.5) was computed to further understand the ECG signals.

Referring to Table 6.5, the ECG from the 70mm^2 textile electrodes showed significantly lower ApEn during yawning, deep breathing, up movement and writing on a keyboard. In contrast, the ECG from the 60mm^2 textile electrodes showed lower ApEn during coughing. The ECG acquired from the 70mm^2 and 60mm^2 textile electrodes did not show significant ApEn difference during sideways movement, sitting/standing from a chair and climbing stairs.

Table 6.5: Statistical summary of lead-II ECG approximate entropy during different movements (yawning, deep breathing, coughing, sideways – moving the hands sideways and moving them back to the midline horizontally; up – raise arms above the head and moving them back) and daily activities (writing on a keyboard at 40 words / minute, sitting / standing from a chair, and climbing stairs).

Body movement / activities	**Approximate entropy (ApEn) Descriptive Statistics**					
	40mm² textile electrodes		**60mm² textile electrodes**		**70mm² textile electrodes**	
	Mean±SD	**50th Percentiles (Median)**	**Mean±SD**	**50th Percentiles (Median)**	**Mean±SD**	**50th Percentiles (Median)**
Yawning	0.0628±0.0081	0.0633	0.0486±0.0049	0.0461	0.0426±0.0030	0.0413
Deep Breathing	0.0483±0.0078	0.0473	0.0457±0.0067	0.0446	0.0407±0.0040	0.0402
Coughing	0.0483±0.0081	0.0486	0.0360±0.0067	0.0344	0.0442±0.0039	0.0436
Sideways	0.0606±0.0063	0.0581	0.0547±0.0080	0.0544	0.0549±0.0055	0.0545
Up	0.1981±0.0251	0.1943	0.1206±0.0182	0.1219	0.0984±0.0155	0.0982
Writing on a Keyboard	0.0536±0.0035	0.0535	0.0467±0.0059	0.0452	0.0383±0.0045	0.0365
Sitting / Standing activities	0.0485±0.0057	0.0482	0.0459±0.0063	0.0460	0.0429±0.0029	0.0435
Stairs	0.0599±0.0091	0.0581	0.0458±0.0063	0.0444	0.0454±0.0029	0.0454
Body movement / activities	**ApEn Test Statistics**					
	70mm² Vs 60mm²		**70mm² Vs 40mm²**		**60mm² Vs 40mm²**	
Yawning	Z	-2.6299	Z	-3.0594	Z	-3.0594
	p	0.0085*	p	0.0022*	p	0.0022*
Deep Breathing	Z	-2.2758	Z	-2.5887	Z	-1.1558
	p	0.0228	p	0.0096*	p	0.2477
Coughing	Z	-2.9025	Z	-1.8042	Z	-2.9821
	p	0.0037*	p	0.0711	p	0.0028*
Sideways	Z	0.0000	Z	-2.0396	Z	-2.4318
	p	1.0000	p	0.0413	p	0.0150
Up	Z	-2.5887	Z	-3.0594	Z	-3.0594
	p	0.0096	p	0.0022*	p	0.0022*
Writing on a keyboard	Z	-2.7466	Z	-3.0594	Z	-2.5102
	p	0.0060*	p	0.0022*	p	0.0120
Sitting / standing activities	Z	-1.5302	Z	-2.5112	Z	-1.2551
	p	0.1259	p	0.0120	p	0.2094
Stairs	Z	-0.4708	Z	-3.0605	Z	-3.0594
	p	0.6377	p	0.0022*	p	0.0022*

Note*: ApEn – Approximate entropy; * – statistically significant*

The signal quality indices were computed and presented in Table 6.6 to understand the acquired signal quality.

Table 6.6: Results of SQI analysis based on lead-II from different size textile electrodes (40mm^2, 60mm^2 and 70mm^2)

Body movement / activities	**Electrode area**					
	40mm^2		**60mm^2**		**70mm^2**	
	pSQI	**basSQI**	**pSQI**	**basSQI**	**pSQI**	**basSQI**
Yawning	0.6468	0.9661	0.6750	0.9312	0.6852	0.9946
Deep Breath	0.6441	0.9791	0.7013	0.9780	0.6857	0.9840
Coughing	0.6498	0.9950	0.6988	0.9920	0.6996	0.9692
Sideways	0.6504	0.9852	0.7024	0.9880	0.6979	0.9876
Up	0.6139	0.7760	0.6984	0.9895	0.6781	0.9937
Writing on a Keyboard	0.6490	0.9816	0.6875	0.9953	0.6928	0.9931
Sitting / Standing activities	0.6438	0.9812	0.7011	0.9921	0.7001	0.9943
Stairs	0.6523	0.9828	0.6994	0.9968	0.7070	0.9921

***Note: Light blue** – lower to moderate level of baseline drift; **Red** – intense low-frequency noise (poor signal quality); **pSQI** – power signal quality index; **basSQI** – baseline power signal quality index*

The frequency domain is the best way to visualize the low-frequency noise embedded in the acquired ECG. Based on the pSQI values in Table 6.6, there was no significant noise artefact within the QRS complex of the acquired ECG. However, the main challenge for textile-based ECG monitoring was noise artefact within the low-frequency range (f<1Hz) due to an unstable skin-electrode interface. Therefore, Table 6.7 compares the peak noise values of the PSD analysis of the ECGs obtained from textile electrodes of three-different surface areas (40mm^2, 60mm^2, 70mm^2).

Table 6.7: Summary of the peak noise PSD and the corresponding frequency for ECG acquired from 40mm^2, 60mm^2 and 70mm^2 textile electrodes.

Body movement / activity	II											
	40mm^2 Textile electrodes				60mm^2 Textile electrodes				70mm^2 Textile electrodes			
	Peak PSD_N (mW/Hz)	f_{PSD} (Hz)	Peak PSD_{ECG} (mW/Hz)	f_{ECGPsd} (Hz)	Peak PSD_N (mW/Hz)	f_{PSD} (Hz)	Peak PSD_{ECG} (mW/Hz)	f_{ECGPsd} (Hz)	Peak PSD_N (mW/Hz)	f_{PSD} (Hz)	Peak PSD_{ECG} (mW/Hz)	f_{ECGPsd} (Hz)
Yawning	50.4	0.2170	63.50	9.933	290.7	0.400	116.8	1.217	2.9	0.317	93.6	8.467
Deep breathing	44.0	0.300	55.8	1.150	53.7	0.317	79.0	1.117	53.3	0.267	97.8	1.133
Coughing	4.9	0.583	84.5	1.350	10.6	0.55	72.5	9.067	123.5	0.517	150.6	8.533
Sideways	5.2	0.35	74.2	3.450	9.3	0.483	82.9	11.783	21.4	0.583	221.8	3.283
Up	367.8	0.017	59.4	7.700	19.3	0.633	168.5	1.250	14.3	0.600	494.7	3.500
Writing on a keyboard	56.0	0.567	107.2	2.467	7.0	0.517	103.4	3.650	9.7	0.550	185.9	1.083
Sitting / standing	58.6	0.583	206.1	6.15	9.5	0.550	154.2	4.217	21.0	0.45	228.5	2.867
Stairs	24.0	0.667	131.7	11.517	9.4	0.717	185.2	3.883	14.8	0.683	261.1	3.817

Body movement / activity	V4											
	40mm^2 Textile electrodes				60mm^2 Textile electrodes				70mm^2 Textile electrodes			
	Peak PSD_N (mW/Hz)	f_{PSD} (Hz)	Peak PSD_{ECG} (mW/Hz)	f_{ECGPsd} (Hz)	Peak PSD_N (mW/Hz)	f_{PSD} (Hz)	Peak PSD_{ECG} (mW/Hz)	f_{ECGPsd} (Hz)	Peak PSD_N (mW/Hz)	f_{PSD} (Hz)	Peak PSD_{ECG} (mW/Hz)	f_{ECGPsd} (Hz)
Yawning	57.9	0.217	37.5	12.7	51.0	0.400	66.7	1.217	3.300	0.167	53.0	8.467
Deep breathing	13.2	0.300	54.5	1.15	84.8	0.317	56.2	1.117	19.9	0.300	92.6	1.133
Coughing	13.9	0.533	40.2	10.35	10.6	0.550	38.7	9.067	61.5	0.517	83.6	8.533
Sideways	170.9	0.817	112.2	1.083	27.8	0.683	71.1	1.150	17.5	0.800	109.6	3.283
Up	1425.0	0.083	171.8	1.250	45.4	0.667	152.7	1.250	9.7	0.567	284.3	1.167
Writing on a keyboard	32.7	0.583	37.9	9.983	5.9	0.517	60.1	1.167	9.1	0.550	150.0	1.083
Sitting / standing	38.3	0.467	108.5	6.15	34.8	0.550	70.7	8.400	28.6	0.450	122.3	1.433
Stairs	192.1	0.650	68.0	11.517	14.1	0.750	99.8	1.283	14.6	0.683	139.1	1.283

Note: Peak PSD_N *– the maximum noise PSD within the low-frequency range* $f<1Hz$*;* f_{PSD} *– the frequency at which the max noise PSD occurred;* ***Peak*** PSD_{ECG} *– the peak PSD of the ECG signal;* f_{ECGPsd} *– the frequency at which the max ECG PSD occurred;* ***Light blue*** *– increased baseline wander;* ***Red*** *– intense baseline wander;* ***Green*** *– prominent peak ECG Power*

During yawning, the lead-II ECG from the 60mm^2 showed increased baseline drift while the V4 ECG from the 40mm^2 and 60mm^2 textile electrodes resulted in nearly equal noise levels. The V4 ECG collected during deep breathing from the 60mm^2 showed more than four times peak noise power compared to the V4 ECGs from the 40mm^2 and 70mm^2 textile electrodes. Acquiring ECG through the 70mm^2 textile sensors during coughing showed increased noise power compared to the smaller area textile electrodes. An extreme low-frequency interference was observed within the V4 ECG acquired from 40mm^2 textile electrodes during sideways movement. As can be seen from Figure 6.2 (a), the ECG tracing is heavily affected by the noise distributed across the entire length of the signal. The continuous shifting of the textile electrodes due to the sideways movement could be the main reason for the significant motion artefact. As a first step to minimise induced noise, a HR-based sliding cut off frequency Butterworth high pass filter and median filters were designed and implemented in MATLAB. Figure 6.2 (b) illustrates the clean V4 ECG. The filtered V4 ECG showed an improved signal to noise ratio (SNR = 16.05dB).

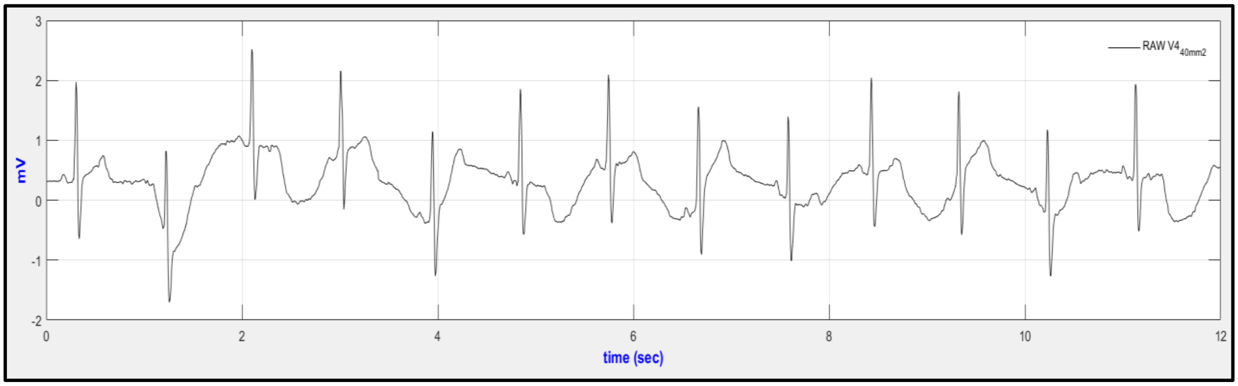

a) Raw V4 ECG

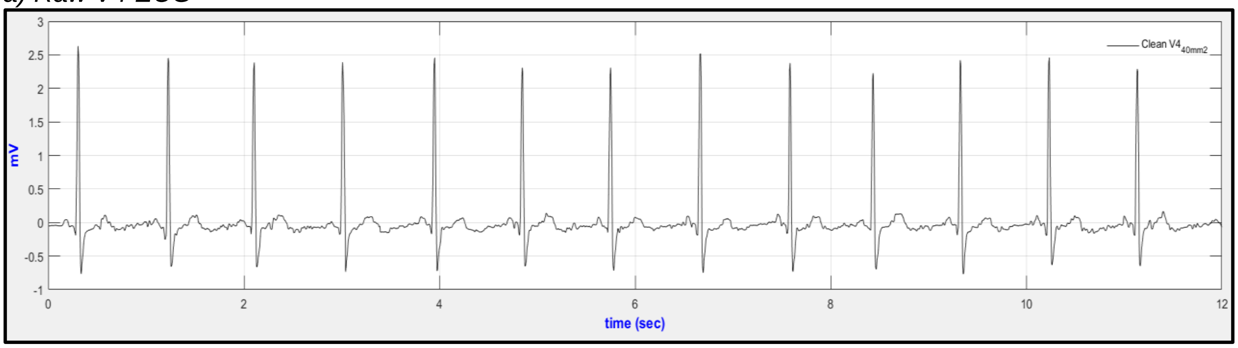

b) Clean V4 ECG filtered by a HR-based sliding cut-off frequency Butterworth high pass and median filters

Figure 6.2: V4 ECG from $40mm^2$ textile electrodes during sideways movement.

The SSR analysis (Table 6.4), the ApEn (Table 6.5), SQI analysis results (Table 6.6) and the PSD analysis (Table 6.7) revealed that the $70mm^2$ textile electrodes performed relatively better than the $40mm^2$ and $60mm^2$ textile electrodes. The ECGs from the $40mm^2$ textile electrodes during the up movement was affected by an intensive baseline wander (lead-II: peak noise PSD = 367.8mW/Hz at 0.017Hz; V4: peak noise PSD = 1425.0mW/Hz at 0.083Hz; Table 6.7). Throughout the study, no increased muscle artefact that affected the QRS complex was observed and the pSQI results across the experiment were within the acceptable limit (pSQI = [0.5 – 0.8], Table 6.6).

6.4.2.2. Combining the 40mm^2 and 70mm^2 textile electrodes to acquire ECG

The size of the textile electrodes affected the signal quality as shown in section 6.4.2.1 where the 70mm^2 textile electrodes showed better signal quality. According to previous studies on sternum length (Jit et al., 1980, Laurin et al., 2012) and stature estimation (Menezes et al., 2011, Marinho et al., 2012), it has been reported that the shortest sternum could be less than 13cm, especially for women. As a result, using 70mm^2 ES electrodes to acquire ECG is impossible as the two electrodes touch each other considering the standard EASI electrode placement where the 'S' electrode is placed at the top of the sternum and the 'E' electrode is placed at the bottom of the sternum. Moreover, to the best of our knowledge, no previous study is reported that acquire ECG from different size textile electrodes. The only exception was (Fuhrhop et al., 2009) where the authors reported a larger size reference electrode (250cm^2). Therefore, in this section, we examined the effect of electrode size difference on signal quality.

Specific objective

The specific objective was to study the effect of using two different size electrodes on ECG quality.

Materials

During the experiments, 40mm^2 and 70mm^2 square textile electrodes were used to collect ECG from the standard EASI configuration. First, 70mm^2 ‘A’ and ‘I’ electrodes were combined with 40mm^2 ‘E’ and ‘S’ electrodes. Then, the AI electrodes were switched to 40mm^2 and the ES to 70mm^2.

Resting ECG

Results

Figure 6.3 shows lead-II and V4 ECGs from the combined textile electrodes. The temporal plot indicates the possibility of low-frequency noise within the ECG collected from 40mm^2 AI electrodes. Referring to Table 6.8, the ECG from the 40mm^2 AI electrodes showed a higher baseline wander. Lead-II ECG from the 40mm^2 ES and the 70mm^2 EASI electrodes resulted in relatively equal power distribution. In contrast, ECG collected from the 40mm^2 AI textile sensors displayed more average ECG power content than the ECG acquired of the 40mm^2 ES and 70mm^2 EASI sensors. However, the higher power content was not supported by the approximate entropy as the 40mm^2 AI ECG resulted in a higher ApEn in both leads (II and V4, Figure 6.4).

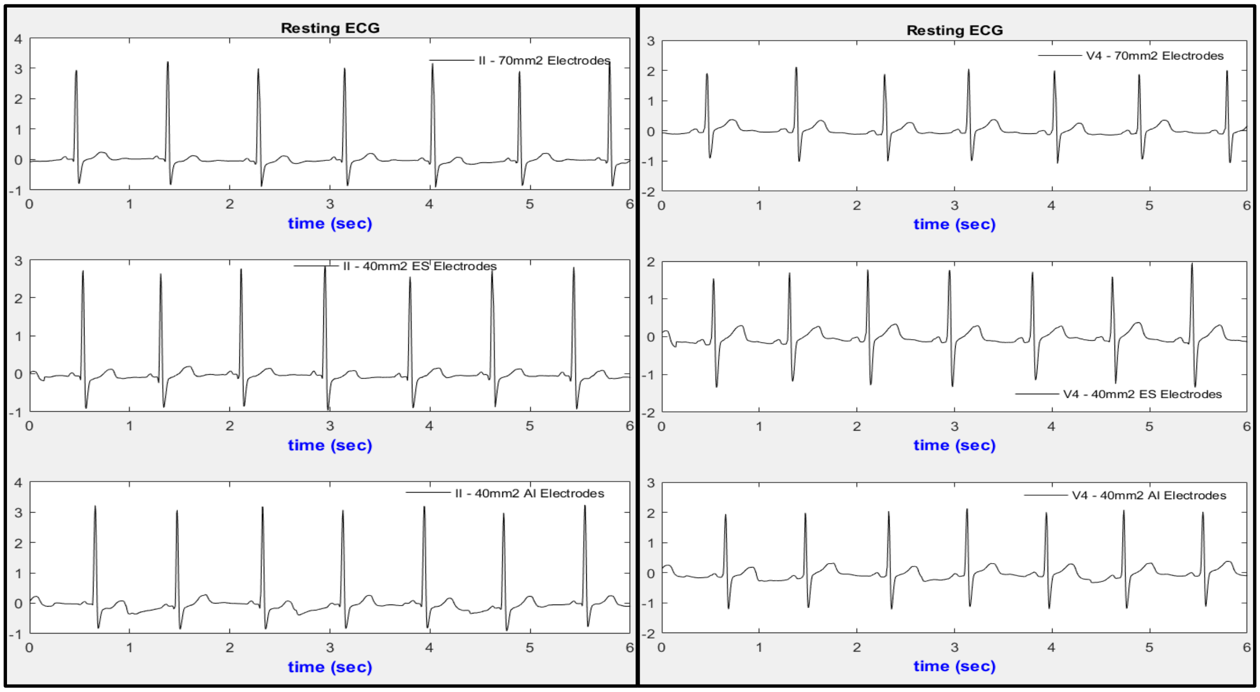

Figure 6.3: ECG acquired by combining the different area of textile electrodes (left – lead-II and right – V4; (top – ECG from 70mm^2 textile sensors; middle – ECG from 40mm^2 ES electrodes and 70mm^2 AI textile sensors and bottom – ECG from 40mm^2 AI and 70mm^2 ES textile sensors).

Power quality indexes were computed. As can be seen from Table 6.8, the ECG from the 40mm^2 AI electrodes showed higher noise in the low-frequency region.

Table 6.8: Comparison of SSR from the mixed area (40mm^2 and 70mm^2) textile electrodes

ECG leads	SSR (dB) = 10*log$_{10}$(Px)			basSQI 70mm^2 EASI electrodes	basSQI 40mm^2 ES electrodes	basSQI 40mm^2 AI electrodes
	Px = (P$_{70mm^2\ electrodes}$/ P$_{40mm^2\ ES\ electrodes}$)	Px = (P$_{70mm^2\ electrodes}$/ P$_{40mm^2\ AI\ electrodes}$)	Px = (P$_{40mm^2\ AI\ electrodes}$/ P$_{40mm^2\ ES\ electrodes}$)			
II	0.0021	-1.2430	1.2451	0.9912	0.9941	0.9774
V4	-1.2202	-1.9225	0.7022	0.9850	0.9905	0.9752

Note: *70mm^2 – the* ***EASI*** *electrodes were 70mnm^2, 40mm^2* ***ES*** *– the* ***E*** *and* ***S*** *electrodes were 40mm^2 while the* ***A*** *and* ***I*** *electrodes were 70mm^2, 40mm^2* ***AI*** *– the* ***A*** *and* ***I*** *electrodes were 40mm^2 and the* ***E*** *and* ***S*** *electrodes were 70mm^2*

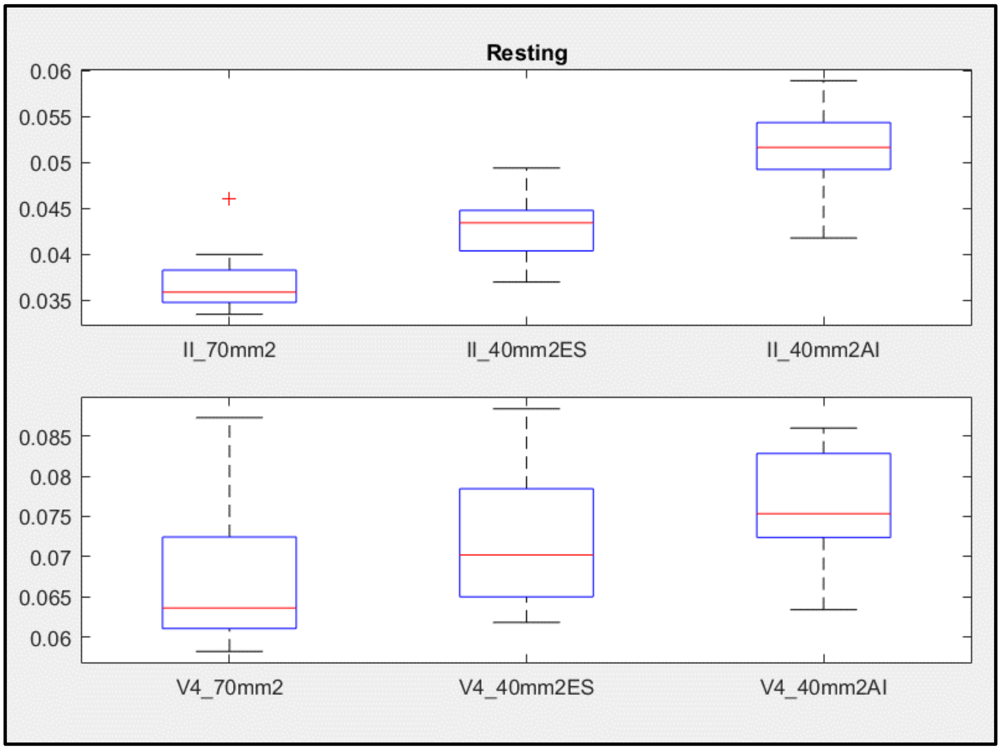

Figure 6.4: Approximate entropy from combined electrode area (resting ECG; top – lead-II; bottom – V4; 70mm^2 – the **EASI** electrodes were 70mnm^2, 40mm^2 **ES** – the **E** and **S** electrodes were 40mm^2 while the **A** and **I** electrodes were 70mm^2, 40mm^2 **AI** – the **A** and **I** electrodes were 40mm^2 and the **E** and **S** electrodes were 70mm^2)

ECG during body movements and from daily living

Results

The power contained within the collected ECGs were compared, and results are presented in Table 6.9.

Table 6.9: SSR values of ECG acquired from simultaneous 40mm^2 and 70mm^2 textile sensors.

SSR (dB) = 10*log$_{10}$(Px), Lead-II ECG			
Body movement / activities	**Px = ($P_{70mm^2\ electrodes}$/ $P_{40mm^2\ ES\ electrodes}$)**	**Px = ($P_{70mm^2\ electrodes}$/ $P_{40mm^2\ AI\ electrodes}$)**	**Px = ($P_{40mm^2\ ES\ electrodes}$/ $P_{40mm^2\ AI\ electrodes}$)**
Sideways	0.7192	-1.2505	-1.9697
Up	0.6674	-1.7189	-2.3863
Sitting / Standing activities	0.1243	-1.0778	-1.2021
Stairs	0.3830	-0.5170	-0.9000
SSR (dB) = 10*log$_{10}$(Px), Lead-V4 ECG			
Body movement / activities	**Px = ($P_{70mm^2\ electrodes}$/ $P_{40mm^2\ ES\ electrodes}$)**	**Px = ($P_{70mm^2\ electrodes}$/ $P_{40mm^2\ AI\ electrodes}$)**	**Px = ($P_{40mm^2\ ES\ electrodes}$/ $P_{40mm^2\ AI\ electrodes}$)**
Sideways	-0.2033	-3.1824	-2.9791
Up	-0.4202	-2.2000	-1.7798
Sitting / Standing activities	-0.4922	-1.5067	-1.0144
Stairs	-0.3806	-0.8228	-0.4422

Note: *70mm^2 – the **EASI** electrodes were 70mnm^2, 40mm^2 **ES** – the **E** and **S** electrodes were 40mm^2 while the **A** and **I** electrodes were 70mm^2, 40mm^2 **AI** – the **A** and **I** electrodes were 40mm^2 and the **E** and **S** electrodes were 70mm^2*

For all body movements and daily activities, the lead-II ECGs from the 70mm^2 textile electrodes showed higher power content compared to the ECGs from the 40mm^2 ES electrodes. On the other hand, using the 40mm^2 AI textile sensors to acquire ECG produced more power at all times.

Three more quantitative parameters (SQI, PSD and ApEn) were used to understand the effect of motion on the acquired ECG and to examine the reason for the increased power shown in Table 6.9.

According to the SQI results presented in Table 6.10, the 40mm^2 AI electrodes performed poorly, primarily in the V4 ECG (Sideways - basSQI = 0.7366). At the same time, sideways V4 ECG from the 40mm^2 AI electrodes showed a spike in the frequency of interest (peak noise PSD = 2231.0mW/Hz). The PSD analysis of the ECGs collected from the 40mm^2 AI textile sensors during the up movement (peak noise PSD = 217.52mW/Hz), sitting / standing from a chair (peak noise PSD = 162.04mW/Hz) and climbing stairs (peak noise PSD = 53.12mW/Hz) revealed more lower-frequency interference in lead-II ECGs.

Table 6.10: Summary of the ECG PSD analysis and Signal quality index based on ECG acquired from combined 40mm^2 and 70mm^2 textile electrodes.

Body movement / activity	II											
	70 mm^2 Textile electrodes				40mm^2 ES and 70mm^2 AI Textile electrodes				40mm^2 AI and 70mm^2 ES Textile electrodes			
	Peak PSD_N (mW/Hz)	P_{av} (mW)	pSQI	basSQI	Peak PSD_N (mW/Hz)	P_{av} (mW)	pSQI	basSQI	Peak PSD_N (mW/Hz)	P_{av} (mW)	pSQI	basSQI
Sitting	26.0	217.8	0.6897	0.9912	10.3	191.7	0.6995	0.9941	55.0	261.6	0.6617	0.9774
Sideways	22.3	221.1	0.6979	0.9921	129.6	187.3	0.6818	0.9973	19.0	294.9	0.6303	0.9957
Up	14.7	213.8	0.6781	0.9942	5.1	183.4	0.6998	0.9975	217.5	317.7	0.6476	0.9857
Sitting / standing	11.3	270.3	0.7001	0.9953	31.4	262.7	0.6956	0.9917	162.0	346.5	0.6473	0.9553
Stairs	15.2	265.0	0.7070	0.9926	21.0	242.7	0.6931	0.9933	53.1	298.5	0.6525	0.9924

Body movement/ activity	V4											
	70 mm^2 Textile electrodes				40mm^2 ES and 70mm^2 AI Textile electrodes				40mm^2 AI and 70mm^2 ES Textile electrodes			
	Peak PSDN (mW/Hz)	Pav (mW)	pSQI	basSQI	Peak PSDN (mW/Hz)	Pav (mW)	pSQI	basSQI	Peak PSDN (mW/Hz)	Pav (mW)	pSQI	basSQI
Sitting	12.9	115.3	0.7250	0.9850	9.2	122.1	0.7476	0.9905	28.9	140.4	0.6481	0.9752
Sideways	23.2	119.4	0.7483	0.9744	44.9	125.2	0.7708	0.9885	2231.0	248.5	0.6555	0.7366
Up	11.0	117.4	0.7417	0.9942	37.3	129.3	0.7798	0.9878	233.8	194.8	0.6718	0.8941
Sitting / standing	8.0	139.3	0.7309	0.9951	26.8	156.1	0.7374	0.9890	182.7	197.1	0.6364	0.9086
Stairs	15.0	140.8	0.7165	0.9906	19.6	153.7	0.7293	0.9918	49.7	170.2	0.6368	0.9784

Note: Peak PSD_N *– the maximum noise PSD within the low-frequency range **$f<1Hz$**; **P_{av}** – the average total power within the ECG signal; **pSQI** – power signal quality index; **basSQI** – the baseline signal quality index; **Light blue** – increased baseline wander; **Red** – intense baseline wander; **Green** – higher power content within the ECG acquired; 70mm^2 – the **EASI** electrodes were 70mnm^2, 40mm^2 **ES** – the **E** and **S** electrodes were 40mm^2 while the **A** and **I** electrodes were 70mm^2, 40mm^2 **AI** – the **A** and **I** electrodes were 40mm^2 and the **E** and **S** electrodes were 70mm^2*

Table 6.11: Statistical summary of the ApEn computed on lead-II and V4 ECG acquired combining 40mm^2 and 70mm^2 textile electrodes.

Body movement / activities	Approximate entropy (ApEn) Descriptive Statistics – lead II					
	70mm^2 textile electrodes		40mm^2 ES and 70mm^2 AI Textile electrodes		40mm^2 AI and 70mm^2 ES Textile electrodes	
	Mean±SD	50th Percentiles (Median)	Mean±SD	50th Percentiles (Median)	Mean±SD	50th Percentiles (Median)
Sideways	0.0549±0.0055	0.0545	0.0596±0.0041	0.0599	0.0539±0.0044	0.0536
Up	0.0984±0.0155	0.0982	0.1329±0.0237	0.1323	0.1540±0.0290	0.1415
Sitting/ Standing activities	0.0429±0.0029	0.0435	0.0521±0.0042	0.0525	0.0454±0.0029	0.0454
Stairs	0.0521±0.0031	0.0526	0.0646±0.0078	0.0626	0.0528±0.0047	0.0520
Body movement / activities	**ApEn Test Statistics – lead II**					
	70mm^2 Vs 40mm^2 ES & 70mm^2 AI		70mm^2 Vs 40mm^2 AI & 70mm^2 ES		40mm^2 ES&70mm^2 AI Vs 40mm^2 AI & 70mm^2 ES	
Sideways	Z	-1.7258	Z	0.0000	Z	-2.3150
	p	0.0843	p	1.0000	p	0.0206
Up	Z	-2.5887	Z	-2.9809	Z	-1.9611
	p	0.0096*	p	0.0028*	p	0.0498
Sitting / standing activities	Z	-2.9821	Z	-3.0594	Z	-3.0594
	p	0.0028*	p	0.0022*	p	0.0022*
Stairs	Z	-3.0594	Z	-2.9821	Z	-0.4706
	p	0.0022*	p	0.0028*	p	0.6378
Body movement/ activities	**Approximate entropy (ApEn) Descriptive Statistics – V4**					
	70mm^2 textile electrodes		40mm^2 ES and 70mm^2 AI Textile electrodes		40mm^2 AI and 70mm^2 ES Textile electrodes	
	Mean±SD	50th Percentiles (Median)	Mean±SD	50th Percentiles (Median)	Mean±SD	50th Percentiles (Median)
Sideways	0.0900±0.0080	0.0891	0.1027±0.0064	0.1012	0.1263±0.0128	0.1221
Up	0.1611±0.0166	0.1639	0.1018±0.0066	0.1007	0.1897±0.0189	0.1884
Sitting / Standing activities	0.0683±0.0051	0.0672	0.0871±0.0050	0.0865	0.0722±0.0046	0.0719
Stairs	0.0855±0.0049	0.0856	0.0938±0.0064	0.0925	0.0907±0.0057	0.0904
Body movement/ activities	**ApEn Test Statistics – V4**					
	70mm^2 Vs 40mm^2 ES & 70mm^2 AI		70mm^2 Vs 40mm^2 AI & 70mm^2 ES		40mm^2 ES&70mm^2 AI Vs 40mm^2 AI & 70mm^2 ES	

Sideways	Z	-2.7456	Z	-2.5504	Z	-0.1568
	p	0.0060*	p	0.0107	p	0.8753
Up	Z	-2.9809	Z	-3.0594	Z	-2.9025
	p	0.0028*	p	0.0022*	p	0.0037*
Sitting / standing activities	Z	-3.0594	Z	-3.0594	Z	-2.3935
	p	0.0022*	p	0.0022*	p	0.0166
Stairs	Z	-3.0594	Z	-3.0594	Z	-2.1180
	p	0.0022*	p	0.0022*	p	0.0341

***Note**: ApEn – Approximate entropy; 70mm^2 – the **EASI** electrodes were 70mnm^2, 40mm^2 **ES** – the **E** and **S** electrodes were 40mm^2 while the **A** and **I** electrodes were 70mm^2, 40mm^2 **AI** – the **A** and **I** electrodes were 40mm^2 and the **E** and **S** electrodes were 70mm^2; * – statistically significant*

The ApEn analysis results (Table 6.11) aligned with the SQI values (Table 6.10) where the ECG from the 40mm^2 AI textile sensors scored higher ApEn for all body movements and daily living activities except sideways.

As an additional measure of data comparison, 12 seconds of representative V4 ECG were plotted for visual inspection (Figure 6.5).

a) *Left - sideways movement and right - up movement (top – V4 ECG from 70mm^2 textile sensors; middle – V4 ECG from 40mm^2 ES electrodes and 70mm^2 AI textile sensors and bottom – V4 ECG from 40mm^2 AI and 70mm^2 ES textile sensors)*

b) *Left – sitting / standing from a chair and right - climbing stairs (top – V4 ECG from 70mm^2 textile sensors; middle – V4 ECG from 40mm^2 ES electrodes and 70mm^2 AI textile sensors and bottom – V4 ECG from 40mm^2 AI and 70mm^2 ES textile sensors)*

Figure 6.5: V4 representative ECG traces acquired by combining the 40mm^2 and 70mm^2 textile sensors during different body movements and activities of daily living.

6.4.2.3. Discussion

The relation between the size of the electrodes and the ECG quality was studied. Results showed the bigger the size of the textile electrodes, the better the signal quality and the lower the approximate entropy (randomness of the signal). The finding matches with a previous study by Ueno et al. (2007).

Comparing different size electrodes (40mm^2, 60mm^{2,} and 70mm^2), the ECG acquired from the 70mm^2 textile electrodes show a higher Signal to Signal Ratio (SSR) and lower approximate entropy.

Additionally, the 40mm^2 and 70mm^2 square textile electrodes were combined to collect ECG using the standard EASI configuration.

Throughout the experiment, the ECG from the 70mm^2 resulted in a higher peak ECG signal for all body movements and daily activities except for yawning where the ECG collected via the 60mm^2 textile electrodes showed more prominent ECG PSD (Table 6.7). On the other hand, the ECGs acquired from the combined (40mm^2 ES and 70mm^2 AI) and the 70mm^2 EASI textile electrodes did not show a significant quality difference. However, the ECG collected from the combined 40mm^2 AI and 70mm^2 ES textile electrodes resulted in an increased baseline drift in the precordial ECG lead (V4), especially during sideways, up movement and sitting / standing from a chair. In contrast, the power contained within the ECG collected through the combined 40mm^2 AI and 70mm^2 ES textile electrodes resulted in higher ECG power but higher low-frequency noise (Table 6.10). The decrease in ECG quality from the combined area textile electrodes could be explained as follows. First, the lower area textile electrodes showed higher low-frequency noise. As a result, the quality of the ECGs measured from the AI textile electrodes were affected. Second, in the EASI textile electrode configuration, three base ECG values are measured (V_{AI}, V_{AS} and V_{ES}) where a transformation matrix is used to generate the equivalent 12-lead ECG signals. Due to the location of the 'AI' electrodes on the body, V_{AI} and V_{AS} are the dominant ECGs compared to V_{ES}. Therefore, the ECG acquired from the combined textile electrodes (40mm^2 AI and 70mm^2 ES) showed lower signal quality. Another explanation would be lowering the size of the textile electrode area increased the skin-electrode impedance and hence decreased the ECG quality.

The increased ECG amplitude and higher signal power for an increased electrode area align with previous studies (Puurtinen et al., 2006, Marozas et al., 2011, Wu et al., 2018).

6.4.3. Effect of electrode thickness (electrode padding) on signal quality

6.4.3.1. Specific objective

The specific objective was to study the effect of textile electrode thickness on signal quality.

6.4.3.2. Materials for data collection

The developed textile electrodes are of 3mm thickness. However, a 60mm^2 conductive textile fabric was sewn onto a 5mm and a 10mm thick Statfree® conductive polyurethane foam to examine the effect of electrode thickness (padding of the textile electrodes) on ECG signal transduction. The standard EASI electrode configuration was used throughout the experiment.

6.4.3.3. Resting ECG

Results

Figure 6.6 presents six seconds of 12-lead ECG tracing acquired from 5mm and 10mm thick textile ECG electrodes.

To better understand the influence of electrode thickness on signal quality, the signal to signal ratio (Table 6.12) and the approximate entropy (Table 6.13) of the two ECG leads (II and V4) were computed over five minutes of ECG data. The five minutes of data were divided into 60 segments of 1,000 samples each to calculate the approximate entropy values.

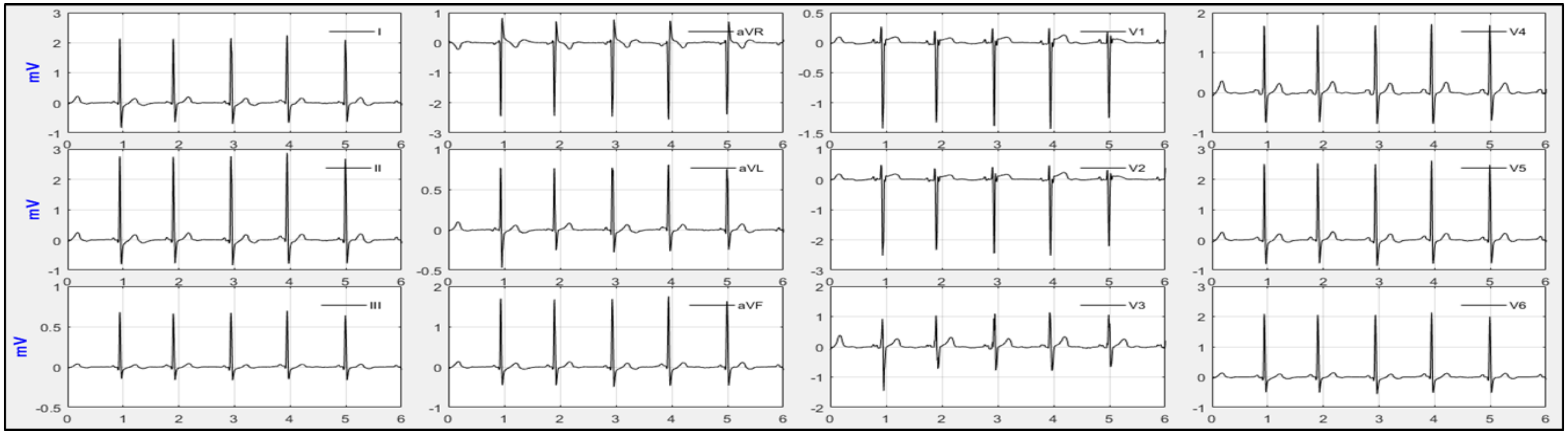

a. ECG from 5mm thick textile electrodes

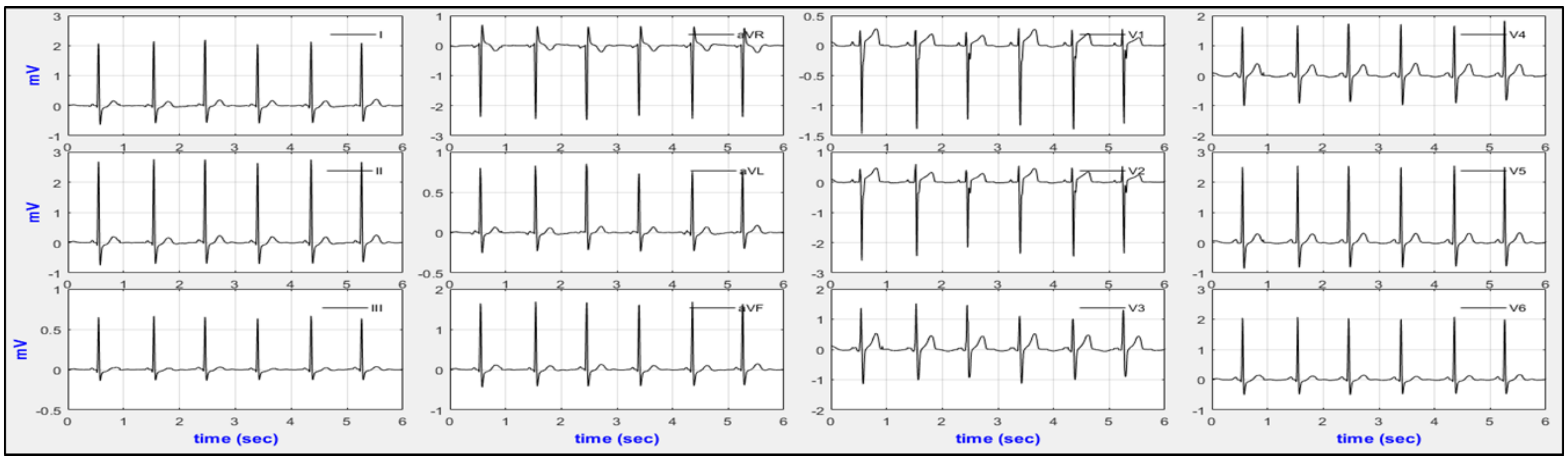

b. ECG from 10mm thick textile electrodes

***Note*:** Raw 1 (top): ECG leads I, aVR, V1 and V4, raw 2 (middle): II, aVL, V2 and V5; raw 3 (bottom): III, aVF, V3 and V6

Figure 6.6: Twelve lead representative resting ECG from single (5mm) and doubles (10mm) filling of the textile electrodes

Table 6.12: Comparison of the SSR and peak PSD analysis of the lead-II and V4 ECG acquired from 3mm, 5mm and 10mm thick textile electrodes.

ECG lead	SSR (dB) = 10*log$_{10}$(Px)		PSD				
	Px = (P_{3mm}/P_{5mm})	Px = P_{5mm}/P_{10mm})	Electrode thickness	Peak PSDN (mW/Hz)	f_{PSD} (Hz)	Peak PSD_{QRS} (mW/Hz)	f_{QRSpsd} (Hz)
II	0.7523	0.5184	3mm	26.77	0.5333	99.39	7.6167
			5mm	64.09	0.0133	79.30	7.4133
			10mm	243.44	0.0133	45.95	7.6533
V4	1.9316	2.5120	3mm	47.97	0.0333	59.07	7.6167
			5mm	34.54	0.4133	41.08	7.4133
			10mm	60.15	0.0133	21.09	11.9467

***Note: Peak PSD_N** – the maximum noise PSD within the low-frequency range **f<1Hz**; **f_{PSD}** – the frequency at which the max noise PSD occurred; **Peak PSD_{QRS}** = the peak PSD of the QRS complexes; **f_{QRSpsd}** – the frequency at which the max QRS-complex PSD occurred along with the QRS frequency spectrum **f = [5 - 15] Hz**; **PSD** – power spectral density; **Red** – intense low-frequency noise; **Green** – higher QRS power*

Table 6.13: Statistical summary of the ApEn; ECGs were collected from 3mm, 5mm and 10mm thick textile electrodes.

ECG lead	ApEn Descriptive Statistics					
	3mm textile electrodes		5mm textile electrodes		10mm textile electrodes	
	Mean±SD	50th Percentiles (Median)	Mean±SD	50th Percentiles (Median)	Mean±SD	50th Percentiles (Median)
II	0.0306±0.0030	0.0297	0.0323±0.0041	0.0326	0.0444±0.0040	0.0440
V4	0.0579±0.0089	0.0549	0.0692±0.0087	0.0674	0.0804±0.0098	0.0786
ECG lead	**ApEn Test Statistics**					
	3mm Vs 5mm		**3mm Vs 10mm**		**5mm Vs 10mm**	
II	Z	-2.6357	Z	-6.7361	Z	-6.728
	p	0.0083*	p	0.0000*	p	<0.0000*
V4	Z	-5.7495	Z	-6.5813	Z	-5.5366
	p	<0.0000*	p	<0.0000*	p	<0.0000*

***Note**: ApEn – Approximate entropy; * – statistically significant*

To further examine the ECG acquired in the frequency domain, the PSD from lead II and V4 ECG were computed over five minutes of ECG data, as shown in Table 6.12.

Referring to Table 6.12, reducing the textile electrode thickness by half from 10mm to 5mm almost doubled the power content in the acquired ECG. The peak PSD analysis (Table 6.12) further confirms the higher power content in the ECG obtained from the 3mm and 5mm thick textile electrodes. The ApEn (Table 6.13) revealed that the ECG from the

10mm thick ECG showed more unpredictable behaviour and significantly higher ApEn compared to the ECGs collected from 3mm and 5mm thick textile electrodes. Therefore, the 3mm and 5mm thick textile electrodes are preferred over the 10mm thick textile electrodes to acquire resting ECG.

6.4.3.4. Effect of electrode thickness on ECG acquired during participant movements and activities of daily living

Results

The SSR and SQI parameters were computed to examine the influence of electrode thickness on the ECG signal quality during different body movements and activities of daily living.

As can be seen in Table 6.14, the ECG collected from the 10mm thick textile electrodes performed poorly for all movements and activities in both lead-II and V4. The only exception was the V4 ECG during the sideways movement. The ECG acquired during climbing stairs was worst for the 10mm thick textile electrodes. For the 5mm thick textile sensors, the V4 ECG showed lower baseline drift (higher basSQI values) compared to the lead-II ECG; the only time the lead-II ECG recorded higher basSQI was during the sideways movement.

Referring to the ApEn analysis (Table 6.15), the results supported the power quality matrix analysis, as the ECG from the 10mm thick textile electrodes showed higher ApEn at all times.

Table 6.14: Quantitative signal comparison matrix based on the thickness of the textile electrodes (3mm, 5mm and 10mm)

Signal to signal ratio (SSR, dB) = $10*\log_{10}Px$				
Body movement / activity	**Px = ($P_{3\,mm}$/ P_{5mm})**		**Px = ($P_{5\,mm}$/ P_{10mm})**	
	ECG lead			
Yawning	**II**	**V4**	**II**	**V4**
Deep Breath	3.2672	3.5964	1.2343	0.8103
Coughing	1.0665	0.7634	0.8583	0.5793
Sideways	1.3667	1.1964	1.0606	0.7436
Up	0.5202	-0.4750	0.8088	0.5697
Writing on a keyboard	0.4150	0.0306	1.1958	0.8582
Phone call	-0.8730	-0.5300	0.8361	-0.0160
Sitting / Standing	0.9764	0.5324	0.7965	0.1660
Stairs	0.5675	0.2845	0.8640	0.6132

Textile electrode thickness												
Body movement / activity	**ECG from 3mm thick sensors**				**ECG from 5mm thick sensors**				**ECG from 10mm thick sensors**			
	II		**V4**		**II**		**V4**		**II**		**V4**	
	pSQI	**basSQI**	**pSQI**	**basSQI**	**pSQI**	**basSQI**	**pSQI**	**basSQI**	**pSQI**	**basSQI**	**pSQI**	**basSQI**
Yawning	0.6890	0.9680	0.6745	0.9554	0.6864	0.9624	0.7284	0.9803	0.7059	0.9138	0.7518	0.9064
Deep Breath	0.6857	0.9863	0.6597	0.9782	0.6854	0.9655	0.7247	0.9828	0.7079	0.9182	0.7338	0.9282
Coughing	0.6996	0.9709	0.6481	0.9695	0.6855	0.9559	0.7094	0.9772	0.7036	0.8619	0.7031	0.8564
Sideways	0.6979	0.9921	0.6902	0.9744	0.6922	0.9655	0.7354	0.8808	0.7068	0.8074	0.7616	0.9149
Up	0.6781	0.9942	0.6850	0.9942	0.6958	0.9712	0.7459	0.9959	0.7156	0.9279	0.7784	0.9029
Writing on a keyboard	0.6927	0.9934	0.6669	0.9883	0.6984	0.9702	0.7179	0.9728	0.7100	0.9417	0.7116	0.9030
Phone call	0.6807	0.9909	0.6502	0.9781	0.6831	0.9606	0.7066	0.9689	0.7085	0.9191	0.7283	0.8930
Sitting / Standing	0.7001	0.9953	0.6785	0.9951	0.6868	0.9743	0.7085	0.9747	0.7155	0.8727	0.7284	0.8662
Stairs	0.7070	0.9926	0.6566	0.9906	0.6991	0.9692	0.7222	0.9693	0.7226	0.8028	0.7311	0.7898

***Note: Light blue** – light to moderate baseline wander; **Red** – higher low-frequency interference; **pSQI** – power signal quality index; **basSQI** – baseline power signal quality index; **sideways** – moving the hands sideways and moving them back to the midline horizontally; **up** – raising arms above the head and moving them back; **writing on a keyboard** - writing on a keyboard at 40 words / minute; **sitting / standing** – sitting / standing from a chair; **stairs** – climbing stairs*

Table 6.15*:* ApEn of ECG (lead-II and V4) from 3mm, 5mm and 10mm thick textile electrodes

Body movement / activities	Approximate entropy (ApEn) Descriptive Statistics – II					
	3mm thick textile electrodes		5mm thick textile electrodes		10mm thick textile electrodes	
	Mean±SD	50th Percentiles (Median)	Mean±SD	50th Percentiles (Median)	Mean±SD	50th Percentiles (Median)
Yawning	0.0426±0.0030	0.0413	0.0481±0.0075	0.0480	0.0534±0.0065	0.0538
Deep Breathing	0.0402±0.0039	0.0397	0.0500±0.0055	0.0492	0.0540±0.0061	0.0528
Coughing	0.0426±0.0048	0.0426	0.0487±0.0050	0.0488	0.0744±0.0096	0.0729
Sideways	0.0544±0.0057	0.0527	0.0608±0.0068	0.0609	0.0796±0.0077	0.0820
Up	0.0962±0.0202	0.0982	0.1461±0.0205	0.1473	0.1748±0.0316	0.1750
Writing on a Keyboard	0.0387±0.0045	0.0369	0.0474±0.0046	0.0475	0.0603±0.0047	0.0603
Sitting / Standing activities	0.0421±0.0031	0.0426	0.0533±0.0043	0.0523	0.0812±0.0102	0.0817
Stairs	0.0457±0.0025	0.0454	0.0563±0.0043	0.0562	0.1236±0.0158	0.1301
Body movement/activities	**ApEn Test Statistics – II**					
	3mm Vs 5mm		**3mm Vs 10mm**		**5mm Vs 10mm**	
Yawning	Z	-2.3533	Z	-3.0594	Z	-1.9611
	p	0.0186	p	0.0022*	p	0.0498
Deep Breathing	Z	-2.7859	Z	-3.0594	Z	-1.5695
	p	0.0053*	p	0.0022*	p	0.1165
Coughing	Z	-2.3159	Z	-3.0605	Z	-3.0594
	p	0.0205	p	0.0022*	p	0.0022*
Sideways	Z	-1.8042	Z	-3.0594	Z	-3.0594
	p	0.0711	p	0.0022*	p	0.0022*
Up	Z	-2.9809	Z	-3.0594	Z	-2.8240
	p	0.0028*	p	0.0022*	p	0.0047*
Writing on a keyboard	Z	-2.8240	Z	-3.0605	Z	-2.9809
	p	0.0047*	p	0.0022*	p	0.0028*
Sitting / standing activities	Z	-2.9809	Z	-3.0594	Z	-3.0594
	p	0.0028*	p	0.0022*	p	0.0022*
Stairs	Z	-3.0594	Z	-3.0594	Z	-3.0594
	p	0.0022*	p	0.0022*	p	0.0022*
	Approximate entropy (ApEn) Descriptive Statistics – V4					

Body movement/activities	3mm thick textile electrodes		5mm thick textile electrodes		10mm thick textile electrodes	
	Mean±SD	50th Percentiles (Median)	Mean±SD	50th Percentiles (Median)	Mean±SD	50th Percentiles (Median)
Yawning	0.0801±0.0055	0.0809	0.0908±0.0049	0.0916	0.1148±0.0094	0.1166
Deep Breathing	0.0792±0.0073	0.0821	0.0883±0.0065	0.0900	0.1141±0.0072	0.1144
Coughing	0.0812±0.0056	0.0818	0.0841±0.0100	0.0880	0.1217±0.0077	0.1205
Sideways	0.0903±0.0081	0.0892	0.1015±0.0090	0.1012	0.1299±0.0092	0.1308
Up	0.1238±0.0162	0.1209	0.1527±0.0183	0.1544	0.2069±0.0308	0.2132
Writing on a Keyboard	0.0626±0.0029	0.0633	0.0846±0.0085	0.0833	0.1160±0.0086	0.1148
Sitting / Standing activities	0.0656±0.0068	0.0662	0.0911±0.0068	0.0892	0.1155±0.0088	0.1160
Stairs	0.0725±0.0046	0.0723	0.0961±0.0047	0.0974	0.1410±0.0142	0.1457
Body movement/activities	**ApEn Test Statistics – V4**					
	The thickness of textile electrodes					
	3mm Vs 5mm		**3mm Vs 10mm**		**5mm Vs 10mm**	
Yawning	Z	-3.0594	Z	-3.0594	Z	-3.0605
	p	0.0022*	p	0.0022*	p	0.0022*
Deep Breathing	Z	-2.3542	Z	-3.0594	Z	-3.0594
	p	0.0185	p	0.0022*	p	0.0022*
Coughing	Z	-0.6275	Z	-3.0594	Z	-3.0605
	p	0.5302	p	0.0022*	p	0.0022*
Sideways	Z	-1.8042	Z	-3.0594	Z	-3.0605
	p	0.0711	p	0.0022*	p	0.0022*
Up	Z	-3.0594	Z	-2.9809	Z	-2.9809
	p	0.0022*	p	0.0028*	p	0.0028*
Writing on a keyboard	Z	-3.0594	Z	-3.0594	Z	-3.0605
	p	0.0022*	p	0.0022*	p	0.0022*
Sitting / standing activities	Z	-3.0594	Z	-3.0594	Z	-2.9809
	p	0.0022*	p	0.0022*	p	0.0028*
Stairs	Z	-3.0605	Z	-3.0594	Z	-3.0594
	p	0.0022*	p	0.0022*	p	0.0022*

***Note: SSR** – a signal to signal ratio; **ApEn** – approximate entropy; **sideways** – moving the hands sideways and moving them back to the midline horizontally; **up** – raising arms above the head and moving them back; **writing on a keyboard** - writing on a keyboard at 40 words / minute; **sitting / standing** – sitting / standing from a chair; **stairs** – climbing stairs; * – statistically significant*

Table 6.16: Lead-II and V4 ECG PSD comparison between ECG acquired from 3mm, 5mm and 10mm thick Textile electrodes.

Body movement/ activity	**II**											
	3mm thick textile electrodes				**5mm thick textile electrodes**				**10mm thick textile electrodes**			
	Peak PSD_N (mW/Hz)	**f_{PSD} (Hz)**	**Peak PSD_{ECG} (mW/Hz)**	**f_{ECGPsd} (Hz)**	**Peak PSD_N (mW/Hz)**	**f_{PSD} (Hz)**	**Peak PSD_{ECG} (mW/Hz)**	**f_{ECGPsd} (Hz)**	**Peak PSD_N (mW/Hz)**	**f_{PSD} (Hz)**	**Peak PSD_{ECG} (mW/Hz)**	**f_{ECGPsd} (Hz)**
Yawning	43.70	0.267	113.30	10.067	93.9	0.25	51.20	15.2830	112.90	0.500	77.8	1.233
Deep breathing	67.00	0.267	99.10	1.133	127.3	0.267	120.6	3.683	168.40	0.267	71.8	1.267
Coughing	132.00	0.517	150.60	8.533	55.50	0.617	102.8	3.750	218.00	0.517	66.60	6.867
Sideways	22.60	0.583	221.80	3.283	82.10	0.517	184.50	3.450	491.60	0.517	75.90	3.700
Up	15.20	0.600	495.40	3.500	86.20	0.517	146.50	1.183	143.30	0.467	88.40	3.650
Writing on a keyboard	10.20	0.550	188.70	1.083	214.90	0.517	163.40	1.133	141.50	0.483	82.50	1.167
Sitting/standing	11.70	0.583	108.60	4.133	72.20	0.517	105.90	2.833	294.90	0.533	147.7	3.050
Stairs	15.60	0.683	261.50	3.817	166.0	0.483	102.20	3.700	626.20	0.800	781.00	1.600
Body movement/ activity	**V4**											
	3mm thick textile electrodes				**5mm thick textile electrodes**				**10mm thick textile electrodes**			
	Peak PSD_N (mW/Hz)	**f_{PSD} (Hz)**	**Peak PSD_{ECG} (mW/Hz)**	**f_{ECGPsd} (Hz)**	**Peak PSD_N (mW/Hz)**	**f_{PSD} (Hz)**	**Peak PSD_{ECG} (mW/Hz)**	**f_{ECGPsd} (Hz)**	**Peak PSD_N (mW/Hz)**	**f_{PSD} (Hz)**	**Peak PSD_{ECG} (mW/Hz)**	**f_{ECGPsd} (Hz)**
Yawning	13.32	0.266	61.30	10.067	20.70	0.250	52.00	1.300	58.54	0.2670	106.1	1.233
Deep breathing	25.20	0.300	93.80	1.133	35.90	0.267	133.80	1.233	56.20	0.250	116.8	1.267
Coughing	65.70	0.517	83.60	8.533	15.50	0.583	129.50	1.250	92.40	0.517	52.40	1.367
Sideways	18.90	0.633	109.30	3.283	310.20	0.567	267.10	1.167	76.90	0.517	133.80	1.200
Up	10.70	0.567	288.20	1.167	5.80	0.500	282.10	1.183	99.30	0.467	125.30	1.167
Writing on a keyboard	9.70	0.550	152.60	1.083	68.70	0.517	209.70	1.133	110.20	0.483	115.00	1.167
Sitting/standing	8.30	0.583	52.80	9.067	42.40	0.517	80.20	1.367	143.60	0.517	125.50	1.533
Stairs	15.40	0.683	140.60	1.283	180.80	0.750	107.60	1.250	311.20	0.800	425.60	1.600

***Note: Peak PSD_N** – the maximum noise PSD within the low-frequency range **$f<1Hz$**; **f_{PSD}** – the frequency at which the max noise PSD occurred; **Peak PSD_{ECG}** – the peak PSD of the QRS-complexes / the ECG; **f_{ECGPsd}** – the frequency at which the max ECG PSD occurred; **Red** – intense baseline wander; **Green** – prominent peak ECG Power*

For identification of baseline wander in the frequency domain, the lead-II and V4 ECG PSD analyses were conducted, and the results are presented in Table 6.16. Looking at the PSD analysis (Table 6.16), the low-frequency interference in the 10mm thick textile electrodes were higher compared to the ECG from the 3mm and 5mm thick textile electrodes during sitting / standing and climbing stairs. In contrast, the ECG from the 10mm thick textile electrodes showed higher peak ECG PSD during sitting / standing from a chair and climbing stairs. The increased ECG power especially during climbing stairs might be the result of the intense low-frequency interference (II: basSQI = 0.8028; and V4: basSQI = 0.7898, Table 6.14) that extends to the ECG region. The temporal plot presented in Figure 6.7 further confirms the poor quality and lower amplitude ECG from the 10mm textile electrodes during climbing stairs.

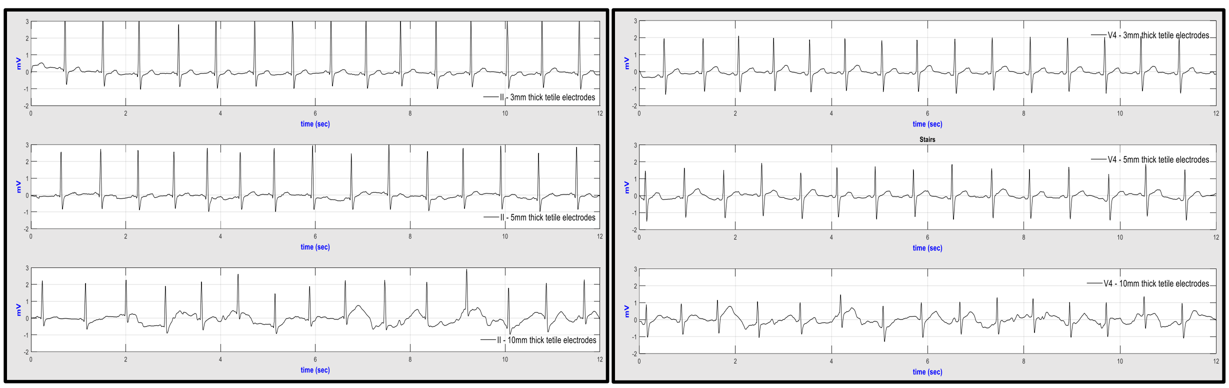

Left – led-II and right – V4 (top – ECG from 3mm, middle ECG from 5mm and bottom – ECG from 10mm thick electrodes)

Figure 6.7: Representative lead-II and V4 ECG tracings from 3mm, 5mm and 10mm thick textile electrodes collected during climbing stairs.

6.4.3.5. Discussion

In a previous study, Cömert and Hyttinen (2015) used a 4mm thick cushion padding structure to support the textile electrodes. The authors showed that the electrode support structure and padding increased the stability of the skin-electrode interface and distributed the compressive force uniformly across the electrode. Moreover, a soft support structure has been shown to produce less noise as it allows the textile electrode to follow the underlying anatomy (Cömert and Hyttinen, 2015). In this study, 3mm, 5mm and 10mm thick textile electrodes were constructed using a soft support structure made of Statfree® conductive polyurethane foam.

Throughout the trial, ECGs from the 3mm and 5mm textile electrodes showed higher signal power, lower randomness and decreased motion artefact aligning with Comert and Hyttinen's 2015 study (Cömert and Hyttinen, 2015) where they showed a positive relation between electrode padding and signal quality using a 4mm thick padding. In another study (Cömert et al., 2013) examined the effect of different thicknesses and types of padding using 6mm, 9mm, 13mm, 14mm and 16mm thick electrodes where the padding was made of two different grades of SunMate memory foam and Poron XRD impact protection cushion. The authors reported the positive effect of padding on signal quality. However, the padding that resulted in the best ECG quality was not clearly stated.

In the study presented in this thesis, increasing the padding thickness beyond 5mm showed decreased signal quality. For example, during climbing stairs, the ECG from the 10mm thick textile sensors performed poorly (Figure 6.7). This may be a result of the thicker textile electrodes (thicker padding, e.g., 10mm thick textile electrodes) shifting position and sliding when subjected to movement more so than the thinner (e.g., 3mm and 5mm) textile electrodes. Moreover, Cömert et al. (2013) used a different technique to acquire the ECG (electrode was placed on the upper arm and was subjected to different magnitude pressure from 5mmHg to 25mmHg) and a different material to make the support structure. In our experiment, the electrodes were placed along the EASI configuration and the support structure was made of Statfree® conductive polyurethane foam. Hence, it was difficult to compare the results directly.

6.4.4. Conclusion

For resting ECG, changes in electrode size did not produce a significant quality difference. In contrast, for ECGs collected during different body movements and activities of daily living, ECGs from the 70mm^2 textile electrodes showed better signal quality compared to the ECGs acquired from the 40mm^2 and 60mm^2 textile electrodes. Moreover, the ECGs collected from unequal area (40mm^2 AI and 70mm^2 ES) textile electrodes showed higher signal power but increased lower-frequency motion artefact compared to the ECGs acquired from the equal-size (70mm^2 EASI) textile electrodes.

In conclusion, increased signal quality was observed for an increased area of the textile electrodes. However, an increased electrode size might be subject to motion artefact from EMG signals in the high-frequency spectrum (f>100Hz) affecting the ability of the acquired ECG to diagnose acute myocardial ischemia and myocardial infarction.

Regarding textile electrode thickness, it is known that padding the textile electrodes lowers motion artefact. In this experiment, 3mm, 5mm and 10mm thick textile electrodes were considered. The ECG from the 3mm and 5mm textile electrodes showed better signal quality while the ECG from the 10mm textile electrodes were subject to increased motion artefact. In conclusion, the 3mm and 5mm thick textile electrodes could be an ideal option for textile-based cardiac long-term ambulatory monitoring. Further experiments on more participants are required to confirm the optimum electrode size, thickness, and padding material.

6.5. Vest design and electrode position

6.5.1. Specific objectives

This section aims to address Research Question 2: how does the smart vest design affect ECG quality? How close and where on the body should the e-textile sensors be placed for optimal performance? Do the methods used to connect the textile electrodes to the smart vest affect signal quality?

The specific objectives of the study were:

a. To study the effect of the smart ECG vest design on ECG quality.

b. To investigate the optimal electrode placement that results in better signal quality.

c. To examine the different methods used to connect the textile electrodes to the smart ECG vest and their effect on signal quality.

6.5.2. The smart ECG vests

6.5.2.1. Specific objective

The specific objective was to study the effect of the smart ECG vest design on ECG quality.

6.5.2.2. Materials

The two prototype ECG vests (sECGVest1 and sECGVest2) discussed in Chapter 4, section 4.5.2.2, were used for data collection. The digital high pass filter was turned off to capture the low-frequency noise components. From section 6.4, the 3mm thick, 70mm^2 textile electrodes showed better signal quality. As a result, the 3 mm thick, 70mm^2 textile electrodes placed at the standard EASI electrode configuration were used.

6.5.2.3. Resting ECG

Results

Table 6.17 compares the SSR values computed from resting lead-II and V4 ECGs acquired from the two ECG vests (sECGVest1 and sECGVest2). Approximate entropy is presented in Table 6.18.

Table 6.17: Comparison of SSR based on the ECG acquired from the two ECG vests (sECGVest1 and sECGVest2)

SSR (dB) = 10*log$_{10}$(P$_{sECGVest1}$/P$_{CsECGVest2}$)	**ECG lead**	
	II	**V4**
	0.1352	0.0930

Table 6.18: Statistical summary of the approximate entropy (resting ECG) based on the two variations of the smart ECG vest design.

ECG lead	ApEn Descriptive Statistics				ApEn Test Statistics	
	sECGVest1		sECGVest2		sECGVest1 Vs sECGVest2	
	Mean±SD	50^{th} Percentiles (Median)	Mean±SD	50^{th} Percentiles (Median)		
II	0.0383± 0.0040	0.0383	0.0461±0.0033	0.0462	Z	-3.060589
					p	0.0022*
V4	0.0461±0.0033	0.0462	0.0712±0.0081	0.0712	Z	-3.0594
					p	0.0022*

***Note**: ApEn – Approximate entropy; * – statistically significant*

Looking at the SSR (Table 6.17) and the ApEn analysis summary (Table 6.18), sECGVest1 performed slightly better than the second smart ECG vest (sECGVest2) for resting ECG.

6.5.2.4. ECG during body movement and activities of the daily living

ECGs were collected while the participant wore each of the smart ECG vests and performed a series of movements and activities of daily living. Then the results from the two vest designs were compared.

Results

Table 6.19 compares the SSR values, while the SQI results of the ECG acquired from the two alternative smart ECG vest designs are presented in Table 6.20. Table 6.21 shows the statistical summary of the approximate entropy (ApEn), while Table 6.22 illustrates the ECG response in the frequency domain. Table 6.23 presents the power characteristics of lead-II and V4 ECG acquired from sECGVest1 and sECGVest2.

Table 6.19: Lead-II and V4 ECG SSR based on two alternate smart ECG vest designs.

SSR (dB) = 10*log$_{10}$(P$_{sECGVest1}$/P$_{sECGVest2}$)		
Body movement / activities	**ECG lead**	
	II	**V4**
Yawning	0.2608	0.0072
Deep Breathing	0.3468	0.1600
Sideways	0.0413	0.5522
Up	0.2337	-0.0300
Writing on a keyboard	-0.6029	-0.3450
Making a phone call	-0.1654	0.0060
Sitting / Standing activities	-0.8661	-0.3686
Stairs	-0.9264	-0.4961

Note: P$_{sECGVest1}$ *– power within the ECG acquired from the first smart ECG vest and* ***P$_{sECGVest2}$*** *– power within the ECG obtained from the second smart ECG vest;* ***sideways*** *– moving the hands sideways and moving them back to the midline horizontally;* ***up*** *– raising arms above the head and moving them back;* ***writing on a keyboard*** *– writing on a keyboard at 40 words / minute;* ***sitting / standing*** *– sitting / standing from a chair;* ***stairs*** *– climbing stairs*

The SQI presented in Table 6.20, showed that there is no significant difference between vest designs in terms of pSQI and baseline interference. However, the V4 ECG from the first smart vest design (sECGVest1) performed poorly for sideways movements (sECGVest1-basSQI = 0.7636). In contrast, the second alternative design (sECGVest2) V4 ECG showed a moderate level of low-frequency noise during sideways and up movements and using a mobile phone.

Table 6.20: ECG SQI based on the two alternative smart ECG vest designs.

Body movement / activity	**Smart ECG vest design**							
	sECGVest1				**sECGVest2**			
	II		**V4**		**II**		**V4**	
	pSQI	**basSQI**	**pSQI**	**basSQI**	**pSQI**	**basSQI**	**pSQI**	**basSQI**
Yawning	0.7060	0.9709	0.7625	0.9642	0.6719	0.9800	0.7393	0.9619
Deep Breathing	0.7038	0.9766	0.7024	0.9659	0.6741	0.9885	0.7427	0.9810
Sideways	0.7025	0.9933	0.7726	0.7636	0.6743	0.9614	0.7543	0.9125
Up	0.7191	0.9758	0.7283	0.9649	0.6762	0.9668	0.7536	0.9376
Writing on a keyboard	0.6967	0.9783	0.6871	0.9686	0.6999	0.9986	0.7615	0.9944
Phone call	0.7043	0.9960	0.7395	0.9882	0.6900	0.9844	0.7499	0.9308
Sitting / standing	0.7036	0.9785	0.6927	0.9694	0.7073	0.9759	0.7763	0.9828
Stairs	0.6995	0.9932	0.7446	0.9886	0.6868	0.9850	0.7336	0.9708

Note: Light blue *– lower to moderate level of baseline wander;* ***Red*** *– a higher level of baseline wander;* ***pSQI*** *– power signal quality index;* ***basSQI*** *– baseline power signal quality index*

Table 6.21: Lead-II ApEn comparison from the two alternative smart ECG vest designs.

Body movement / activity	ApEn Descriptive Statistics				ApEn Test Statistics	
	sECGVest1		sECGVest2		sECGVest1 Vs. sECGVest2	
	Mean±SD	50th Percentiles (Median)	Mean±SD	50th Percentiles (Median)		
Yawning	0.0480±0.0035	0.0480	0.0449±0.0081	0.0470	Z	-1.0198
					p	0.3078
Deep Breathing	0.0466±0.0041	0.0433	0.0422±0.0074	0.0404	Z	-2.1973
					p	0.0279
Sideways	0.0613±0.0073	0.0604	0.0501±0.0073	0.0481	Z	-2.4318
					p	0.0150
Up	0.1292±0.0191	0.1284	0.1551±0.0192	0.1533	Z	-2.4318
					p	0.0150
Writing on a keyboard	0.0476±0.0044	0.0488	0.0449±0.0029	0.0454	Z	-1.5689
					p	0.1166
Phone call	0.0519±0.0057	0.0522	0.0432±0.0051	0.0398	Z	-2.8240
					p	0.0047*
Sitting / standing	0.0484±0.0056	0.0473	0.0432±0.0051	0.0420	Z	-2.0396
					p	0.0413
Stairs	0.0387±0.0040	0.0392	0.0327±0.0037	0.0324	Z	-2.5504
					p	0.0107

Note: ApEn *– approximate entropy;* ***sideways*** *– moving the hands sideways and moving them back to the midline horizontally;* ***up*** *- raising arms above the head and moving them back;* ***writing on a keyboard*** *– writing on a keyboard at 40 words / minute;* ***sitting / standing*** *– sitting / standing from a chair;* ***stairs*** *– climbing stairs; * – statistically significant*

Table 6.22: Comparison of lead-II and V4 ECGs PSD from the two variations of the smart ECG vest designs

Body movement / activity	II							
	sECGVest1				sECGVest2			
	Peak PSD_N (mW/Hz)	f_{PSD} (Hz)	Peak PSD_{ECG} (mW/Hz)	f_{ECGPsd} (Hz)	Peak PSD_N (mW/Hz)	f_{PSD} (Hz)	Peak PSD_{ECG} (mW/Hz)	f_{ECGPsd} (Hz)
Yawning	20.40	0.067	122.80	8.467	319.70	0.400	111.10	1.217
Deep breathing	113.50	0.250	222.20	1.200	579.90	0.067	77.30	9.883
Sideways	16.00	0.450	106.80	3.850	26.60	0.517	117.70	1.333
Up	76.20	0.667	132.50	1.283	105.40	0.583	76.60	1.350
Writing on a keyboard	542.50	0.083	172.90	3.600	4.60	0.117	131.60	1.250
Phone call	5.70	0.133	93.50	8.617	649.30	0.083	206.60	1.217
Sitting / standing	23.20	0.450	228.90	2.867	1381.2	0.100	267.40	1.483
Stairs	12.60	0.567	137.30	3.783	68.90	0.100	120.70	1.067
Body movement / activity	**V4**							
	sECGVest1				**sECGVest2**			
	Peak PSD_N (mW/Hz)	**f_{PSD} (Hz)**	**Peak PSD_{ECG} (mW/Hz)**	**f_{ECGPsd} (Hz)**	**Peak PSD_N (mW/Hz)**	**f_{PSD} (Hz)**	**Peak PSD_{ECG} (mW/Hz)**	**f_{ECGPsd} (Hz)**
Yawning	5.70	0.133	71.40	8.467	55.20	0.400	72.30	1.217
Deep breathing	77.50	0.250	227.80	1.200	289.20	0.117	47.20	9.883
Sideways	717.00	0.433	123.10	1.250	204.10	0.533	94.30	1.333
Up	43.20	0.533	151.10	1.267	151.50	0.600	50.60	2.683

Writing on a keyboard	267.30	0.083	220.40	1.183	7.00	0.550	76.40	1.250
Phone call	15.30	0.133	60.80	1.167	384.20	0.083	112.70	1.217
Sitting / standing	31.90	0.450	123.80	1.433	466.40	0.100	111.60	2.967
Stairs	9.70	0.583	80.50	1.267	18.30	0.100	154.70	1.067

Note: Peak PSD_N *– the maximum noise PSD within the low-frequency range* ***f<1Hz****;* f_{PSD} *– the frequency at which the max noise PSD occurred;* ***Peak*** PSD_{ECG} *– the peak PSD of the QRS-complexes / the ECG;* f_{ECGPsd} *– the frequency at which the max ECG PSD occurred;* ***Red*** *– intense baseline wander*

Table 6.23: Summary of mean R-waves amplitude and average ECG power for ECGs acquired from the two alternative smart ECG vest designs.

Body movement / activity	Smart ECG vest design							
	sECGVest1				sECGVest2			
	II		V4		II		V4	
	V_{Ravg} (mV)	P_{av} (mW)	V_{Ravg} (mV)	P_{av} (mW)	V_{Ravg} (mV)	P_{av} (mW)	V_{Ravg} (mV)	P_{av} (mW)
Yawning	2.43	167.00	1.51	99.00	2.23	140.50	1.50	81.60
Deep Breath	2.74	197.70	1.67	104.80	2.42	248.00	1.62	133.70
Sideways	2.61	193.1	1.60	159.30	2.51	189.10	1.71	118.10
Up	2.81	222.90	1.60	119.70	2.65	207.60	1.77	121.60
Writing on a keyboard	2.78	341.50	1.32	169.60	2.99	242.00	1.93	129.70
Phone call	2.72	194.90	1.67	110.50	2.82	317.10	1.69	177.30
Sitting / standing	2.72	224.60	1.65	120.20	2.91	633.80	1.81	235.90
Stairs	2.76	202.10	1.64	115.90	3.03	235.50	1.99	122.90

Note: V_{Ravg} *– average R amplitude;* P_{av} *– average ECG power;* ***Green*** *– higher average ECG power*

Looking at the SSR results (Table 6.19), SQI (Table 6.20), the ApEn (Table 6.21), the PSD analysis (Table 6.22) and the power characteristics summary (Table 6.23), the first smart ECG vest (sECGVest2) produced slightly better signal quality for most of the body movements and daily living activities. The only activity where the ECGs from the sECGVest2 showed reduced lower-frequency noise compared to the ECG obtained from the sECGVest1 was during writing on a keyboard (Table 6.22).

6.5.2.5. Discussion

Two alternative smart ECG vests (sECGVest1 and sECGVest2) were tested to investigate the impact of vest design on motion artefact. The ECG vest has two main parts, the anterior and posterior components, as presented in the design and implementation chapter (Chapter 1, Section 4.5.2). sECGVest1 contains both posterior and anterior components, while sECGVest2 was based on a minimalist approach using the anterior segment alone. Based on the ApEn results (Table 6.21), there was no statistically significant quality difference between the ECGs acquired from the two designs. However, looking at the power characteristics summary (Table 6.23), for ECG during sitting / standing from a chair activity, the power contained within the ECG from sECGVest2 was more than double compared to ECG from sECGVest1. The increased power of the ECG during sitting / standing might be due to the intense noise artefact in the low-frequency region. Therefore, a second-order Butterworth high pass filter (f_c=0.67Hz) was used to denoise the signal and the power was computed. The power calculated from the denoised signal was reduced by half (P_{avRaw_II} = 633.8mW, $P_{avClean\_II}$ = 307.3mW; P_{avRaw_V4} = 235.9mW, $P_{avClean\_V4}$ = 146.7mW). Therefore, higher power contained within the acquired ECG from the sECGVest2 during sitting / standing from a chair activity was indeed due to noise in the low-frequency region (f<1Hz).

The minimalist approach used to design the second smart ECG vest (sECGVest2) did not produce a significant noise reduction in the acquired ECG. This may be due to the following reasons. As an integral part of the vest design, similar techniques were used to connect the ECG vests to the textile electrodes (12mm snap fastener) and the ECG vest to the ECG hardware (JST XH 5 pin, 2.0 mm pitch male adapter) in both smart ECG vests. As a determinant factor, the same method (Velcro fasteners) was used to apply pressure to create a stable textile electrode-skin interface. Moreover, the textile electrodes used in both smart ECG vests had the same characteristics (3mm thick and

$70mm^2$ surface area) and were placed at the standard EASI electrode configuration positions.

6.5.3. Electrode placement

Optimal electrode placement remains an active area of research in cardiac monitoring (Huigen et al., 2002, Finlay et al., 2008b, Maan et al., 2011, Albert, 2015, Teferra et al., 2019b). In this study, ECGs were acquired to examine the effect of electrode placement on signal quality. Additionally, the impact of electrode placement on motion artefact was analysed based on a series of controlled movements introduced during the ECG acquisition as outlined in section 6.3.1.

6.5.3.1. Specific objective

The specific objective was to investigate the optimal electrode placement that results in better signal quality.

Specific objectives

a. To study the effect of modifying the 'A' and 'I' electrodes placement (from the standard EASI configuration) on signal quality
b. To examine the effect of modifying the 'E' and 'S' electrodes placement (from the standard EASI configuration) on signal quality

6.5.3.2. Modified A and I electrodes placement

Specific objective

The objective was to study the effect of modifying the 'A' and 'I' electrodes placement (from the standard EASI configuration) on signal quality.

Method

Feild et al. (2002) recommended the following electrode placement for an ECG EASI configuration:

I. Electrode 'E' on the lower sternum at the fifth intercostal space
II. Electrodes 'A' and 'I' on the same level as the ‘E’ electrode. 'A' electrode placed on the left mid-axillary line and 'I' on the right mid-axillary line.
III. Electrode 'S' at the top of the sternum, on the manubrium

The two textile sensors ('A' and 'I') were placed at the three positions - anterior axillary lines, mid-axillary lines, and the posterior-axillary lines - while keeping the 'E' and 'S' electrodes at their defined positions to examine the effect of 'AI' electrodes placement on signal quality. Throughout the experiment, 70mm^2 textile electrodes of 3mm thickness were used.

Resting ECG

Results

Table 6.24 compares the SSR among the ECG signal collected from the three positions, while Table 6.25 presents the approximate entropy.

Table 6.24: Comparison of energy contained within the lead-II and V4 ECG based on variations in the placement of the 'A' and 'I' electrodes

ECG lead	SSR (dB) = 10*log$_{10}$(Px), Lead-II ECG		
	Px = ($P_{Anterior}$ / P_{Medial})	**Px = ($P_{Anterior}$ / $P_{Posterior}$)**	**Px = (P_{Medial} / $P_{Posterior}$)**
II	3.1139	5.5494	2.4355
V4	1.4891	2.5788	1.0897

Note: $P_{Anterior}$ *– power in the ECG signal acquired when the 'A' and 'I' electrodes placed at the anterior – axillary position;* ***P_{Midial}*** *– 'A' and 'I' electrodes placed at the medial-axillary position;* ***$P_{Posterior}$*** *– 'A' and 'I' electrodes placed at the posterior-axillary position*

Table 6.25: Approximate entropy of a representative lead-II and V4 ECG for the three axillary positions of the 'A' and 'I' electrodes

ECG lead	ApEn Descriptive Statistics					
	AI electrode placement					
	Anterior		Medial		Posterior	
	Mean±SD	50th Percentiles (Median)	Mean±SD	50th Percentiles (Median)	Mean±SD	50th Percentiles (Median)
II	0.0470±0.0046	0.0454	0.0508±0.0046	0.0498	0.0598±0.0069	0.0579
V4	0.0733±0.0120	0.0675	0.0792±0.0147	0.0750	0.0779±0.0137	0.0744
ECG lead	**ApEn Test Statistics**					
	Anterior Vs. Medial		**Anterior Vs Posterior**		**Medial Vs. Posterior**	
II	Z	-2.0734	Z	-3.2941	Z	-3.2373
	p	0.0381	p	0.0009*	p	0.0012*
V4	Z	-1.4767	Z	-1.1645	Z	-0.4543
	p	0.1397	p	0.2441	p	0.6495

Note*: ApEn – Approximate entropy; * – statistically significant*

Looking at Table 6.24, placing the electrodes at the anterior axillary position resulted in roughly double power (~3dB) compared to the mid-axillary electrode placement and four times (~6dB) relative to the electrodes placed at the posterior-axillary position. The ApEn presented in Table 6.25, confirms that the ECG acquired placing the 'A' and 'I' textile sensors on the anterior axillary lines showed significantly lower randomness compared to the posterior placement in the lead-II ECG (Anterior Vs. Posterior, lead-II: Z = -3.2941, p = *0.0009*). In conclusion, the anterior axillary electrode placement resulted in better resting ECG quality compared to the medial-axillary and posterior-axillary electrode placements.

The modified 'A' and 'I' electrodes placement and motion artefact

Results

From the SSR analysis of the data recorded during the outlined series of movements and activities of daily living, it is evident that placing the 'A' and ‘I’ electrodes on the anterior axillary line resulted in higher power content, as shown in Table 6.26.

Table 6.26: SSR from ECG acquired from various 'A' and 'I' electrodes placement.

SSR (dB) = 10*log$_{10}$(Px), Lead-II ECG			
Body movement	**Px = ($P_{Anterior}$/ P_{Medial})**	**Px = ($P_{Anterior}$/$P_{Posterior}$)**	**Px = (P_{Medial}/ $P_{Posterior}$)**
Yawning	2.8310	4.9173	2.0864
Deep Breath	2.8450	5.2868	2.4418
Coughing	2.5087	4.5904	2.0817
Sideways	1.7885	3.8478	2.0593
Up	1.9777	3.8616	1.8839
Daily living			
Writing on a Keyboard	2.0473	5.9097	3.8625
Making a phone call	2.6990	4.6346	1.9356
Sitting / Standing activities	2.2765	4.3689	2.0924
Stairs	2.2527	4.4235	2.1707
SSR (dB) = 10*log$_{10}$(Px), Lead-V4 ECG			
Body movement	**Px = ($P_{Anterior}$/ P_{Medial})**	**Px = ($P_{Anterior}$/$P_{Posterior}$)**	**Px = (P_{Medial}/ $P_{Posterior}$)**
Yawning	1.2393	1.9660	0.7267
Deep Breath	1.3542	2.4328	1.0786
Coughing	1.3053	1.8315	0.5262
Sideways	***-0.6815***	***0.2664***	***0.9479***
Up	0.8806	1.3608	0.4802
Daily living			
Writing on a Keyboard	1.0736	3.6851	2.6115
Making a phone call	1.2557	1.7653	0.5096
Sitting / Standing activities	1.2749	1.9205	0.6456
Stairs	1.2026	1.7602	0.5575

Note: ***$P_{Anterior}$*** *– power within the ECG signal when the 'A' and 'I' electrodes placed on the left and right anterior-axillary lines, respectively;* ***P_{Medial}*** *– on the left and right medial-axillary lines, respectively;* ***$P_{Posterior}$*** *– on the left and right posterior-axillary lines, respectively*

The calculated SSR of the ECG collected from the anterior-axillary electrode placement is roughly double the magnitude of ECG SSR acquired placing the 'A' and 'I' electrodes on the medial-axillary position across all movements for lead-II ECGs. When the 'A' and 'I' textile sensors are located at the posterior-axillary lines, the power contained in the collected signal was around one-quarter of the ECG power compared to the anterior-axillary electrode (lead-II) placement. The power contained within the V4 ECG collected when the 'A' and 'I' electrodes were placed at the anterior axillary lines was slightly higher than the ECG power when the 'A' and 'I' electrodes were placed at the medial and posterior axillary lines, except during sideways movement.

SQI, average R-peak amplitude and average ECG power were calculated to assess the power characteristics of the acquired ECG and are summarised in Table 6.27.

Placing the textile electrodes far from the heart, on the posterior-axillary lines, reduced the amplitude of the collected ECG. Therefore, even though the medial placement showed higher noise in the low-frequency range, the pSQI and basSQI were better compared to the posterior placement (Table 6.27).

Table 6.27: Summary of ECG characteristics based on **AI** electrodes placement.

Body movement / activity	**Electrode placement**											
	Anterior				**Medial**				**Posterior**			
	pSQI	**basSQI**	**V_{Ravg} (mV)**	**P_{av} (mW)**	**pSQI**	**basSQI**	**V_{Ravg} (mV)**	**P_{av} (mW)**	**pSQI**	**basSQI**	**V_{Ravg} (mV)**	**P_{av} (mW)**
Yawning	0.6827	0.9900	3.08	269.1	0.7194	0.9859	1.89	105.3	0.7192	0.8717	1.13	41.3
Deep Breathing	0.6845	0.9878	3.15	258.1	0.7153	0.9872	2.01	105.4	0.6588	0.9230	1.23	40.6
Coughing	0.6858	0.9949	3.27	304.6	0.7122	0.9979	2.12	140.5	0.6569	0.9923	1.35	59.1
Sideways	0.7136	0.9916	3.04	221.1	0.7084	0.9899	2.07	110.20	0.6675	0.9651	1.26	43.20
Up	0.6951	0.9926	2.89	228.80	0.6759	0.9921	1.93	119.60	0.6613	0.9639	1.24	49.40
Writing on a Keyboard	0.6990	0.9928	3.08	236.70	0.7091	0.9842	2.00	197.10	0.6858	0.9888	1.35	44.00
Making a phone call	0.6943	0.9966	3.07	293.20	0.7135	0.9878	2.17	145.70	0.6821	0.9768	1.36	62.10
Sitting / Standing	0.7047	0.9979	3.16	275.30	0.7224	0.9841	2.26	138.40	0.6646	0.9721	1.38	55.50
Stairs	0.7145	0.9980	3.08	269.1	0.7261	0.9914	1.89	105.3	0.6814	0.9811	1.13	41.3

Note:* V_{Ravg}** *– average R amplitude**; P_{av}** – average ECG power;* ***pSQI *– power signal quality index;* ***basSQI*** *– baseline power signal quality index;* ***Green*** *– higher R amplitude / ECG power;* ***Red*** *– intense low-frequency interference**; Light blue** – lower to moderate level of baseline wander;* ***sideways*** *– moving the hands sideways and moving them back to the midline horizontally;* ***up*** *– raising arms above the head and moving them back;* ***writing on a keyboard*** *– writing on a keyboard at 40 words / minute;* ***sitting / standing*** *– sitting / standing from a chair;* ***stairs*** *- climbing stairs*

ApEn analysis was conducted to confirm that the higher power content of the ECG acquired from the anterior axillary lines is, in fact, mostly from the ECG signal, and the results are summarised in Table 6.28. The anterior axillary electrode placement resulted in lower randomness in the acquired signal for the entire experiment. On the other hand, the ECG obtained from the medial-axillary lines showed a higher noise level for every test involving hand movement (sideways, up, writing on a keyboard, sitting / standing from a chair and stairs). As the 'A' and 'I' electrodes are placed under the arm, moving the hands might introduce higher noise compared to the off-centre electrode placement.

The acquired data were subjected to frequency domain analysis and the PSD analysis was summarised in Table 6.29.

The PSD analysis revealed a higher noise level in the low-frequency spectrum of the ECGs acquired from the medial-axillary locations during sideways movement, sitting / standing from a chair and climbing stairs.

Figure 6.8 presents the temporal plots of lead-II ECG acquired during sideways movement and climbing stairs for visual inspection. The ECG showed reduced R-wave amplitude when the 'AI' electrodes were moved from the anterior to the medial axillary lines and finally from the medial to the posterior axillary lines.

Table 6.28: Lead-II ECG ApEn of ECG collected under different body movements and activities of daily living based on different 'AI' electrodes placement.

Body movement / activities	ApEn Descriptive Statistics					
	Anterior AI electrode placement		Medial AI electrode placement		Posterior AI electrode placement	
	Mean±SD	50th Percentiles (Median)	Mean±SD	50th Percentiles (Median)	Mean±SD	50th Percentiles (Median)
Yawning	0.0388±0.0091	0.0344	0.0436±0.0106	0.0410	0.0603±0.0084	0.0600
Deep Breathing	0.0388±0.0050	0.0372	0.0436±0.0066	0.0439	0.0562±0.0086	0.0570
Coughing	0.0318±0.0047	0.0316	0.0376±0.0050	0.0361	0.0623±0.0060	0.0614
Sideways	0.0393±0.0039	0.0392	0.1587±0.0346	0.1609	0.1392±0.0311	0.1377
Up	0.0736±0.0110	0.0717	0.3842±0.0585	0.4010	0.1676±0.0266	0.1730
Writing on a Keyboard	0.0386±0.0048	0.0381	0.1061±0.0326	0.0978	0.1050±0.0177	0.1009
Sitting / Standing activities	0.0394±0.0051	0.0399	0.0667±0.0114	0.0640	0.0652±0.0094	0.0676
Stairs	0.0384±0.0044	0.0395	0.0867±0.0127	0.0902	0.0738±0.0056	0.0739
Body movement / activities	**ApEn Test Statistics**					
	Anterior Vs. Medial		**Anterior Vs. Medial**		**Anterior Vs. Medial**	
Yawning	Z	-1.4120	Z	-3.0605	Z	-2.8251
	p	0.1579	p	0.0022*	p	0.0047*
Deep Breathing	Z	-1.9226	Z	-3.0594	Z	-3.0605
	p	0.0545	p	0.0022*	p	0.0022*
Coughing	Z	-2.9809	Z	-3.0594	Z	-3.0594
	p	0.0028*	p	0.0022*	p	0.0022*
Sideways	Z	-3.0594	Z	-3.0594	Z	-1.8827
	p	0.0022*	p	0.0022*	p	0.0597
Up	Z	-3.0594	Z	-3.0594	Z	-3.0594
	p	0.0022*	p	0.0022*	p	0.0022*
Writing on a keyboard	Z	-3.0594	Z	-3.0594	Z	-0.1568
	p	0.0022*	p	0.0022*	p	0.8753
Sitting/standing activities	Z	-3.0605	Z	-3.0594	Z	-0.4706
	p	0.0022*	p	0.0022*	p	0.6378
Stairs	Z	-3.0594	Z	-3.0594	Z	-2.1965
	p	0.0022*	p	0.0022*	p	0.0280

***Note: ApEn** – approximate entropy; **Anterior** – AI electrodes placed at the left and right anterior axillary lines respectively; **Medial** – AI electrodes placed at the left and right medial axillary lines respectively; **Posterior** – AI electrodes placed at the left and right posterior axillary lines respectively; **Red** – higher ApEn; * – statistically significant*

Table 6.29: PSD analysis of lead-II and V4 ECGs acquired during experiments involving hand movement placing the 'A' and 'I' textile electrodes on the left and right anterior-axillary lines, on the left and right medial-axillary lines, and the left and right posterior-axillary lines, respectively.

Body movement/ activity	II											
	Anterior AI electrode placement				Medial AI electrode placement				Posterior AI electrode placement			
	Peak PSD_N (mW/Hz)	f_{PSD} (Hz)	Peak PSD_{ECG} (mW/Hz)	f_{ECGPsd} (Hz)	Peak PSD_N (mW/Hz)	f_{PSD} (Hz)	Peak PSD_{ECG} (mW/Hz)	f_{ECGPsd} (Hz)	Peak PSD_N (mW/Hz)	f_{PSD} (Hz)	Peak PSD_{ECG} (mW/Hz)	f_{ECGPsd} (Hz)
Yawning	31.60	0.273	106.80	10.073	22.30	0.255	45.60	3.873	40.90	0.236	15.10	2.782
Deep breathing	29.20	0.109	151.60	3.764	5.40	0.945	56.40	1.200	71.80	0.236	18.10	8.309
Coughing	34.10	0.491	121.20	11.909	6.80	0.509	87.40	2.927	50.10	0.073	44.80	3.145
Sideways	13.30	0.527	245.90	4.382	172.20	0.109	66.00	3.345	12.80	0.218	21.80	1.200
Up	20.40	0.600	139.90	1.255	15.60	0.636	40.10	3.673	23.60	0.636	38.60	1.200
Writing on a keyboard	10.50	0.564	234.90	1.164	35.90	0.073	81.20	1.145	2.30	0.109	39.00	1.055
Sitting / standing	5.30	0.527	291.40	2.909	404.60	0.073	98.80	2.818	23.70	0.545	48.00	1.527
Stairs	11.40	0.764	140.80	4.000	41.30	0.764	78.80	1.255	8.90	0.818	27.20	6.60

Body movement/ activity	V4											
	Anterior AI electrode placement				Medial AI electrode placement				Posterior AI electrode placement			
	Peak PSD_N (mW/Hz)	f_{PSD} (Hz)	Peak PSD_{ECG} (mW/Hz)	f_{ECGPsd} (Hz)	Peak PSD_N (mW/Hz)	f_{PSD} (Hz)	Peak PSD_{ECG} (mW/Hz)	f_{ECGPsd} (Hz)	Peak PSD_N (mW/Hz)	f_{PSD} (Hz)	Peak PSD_{ECG} (mW/Hz)	f_{ECGPsd} (Hz)
Yawning	8.40	0.273	57.10	10.073	3.50	0.255	24.10	12.055	10.30	0.455	33.80	1.364
Deep breathing	25.90	0.109	62.20	3.764	15.60	0.236	45.10	1.200	56.90	0.236	41.20	1.145
Coughing	4.30	0.491	61.00	11.909	24.10	0.509	27.40	2.927	8.10	0.582	43.50	1.564
Sideways	258.80	0.545	135.70	1.109	426.00	0.600	142.30	1.145	380.50	0.600	35.40	1.200
Up	55.10	0.618	133.60	1.255	43.20	0.091	25.20	1.200	6.60	0.600	117.10	1.200
Writing on a keyboard	14.20	0.164	131.90	1.164	55.60	0.073	70.60	1.145	3.80	0.127	120.30	1.055
Sitting / standing	88.00	0.527	118.30	8.709	232.50	0.073	44.00	2.818	10.80	0.273	68.60	1.527
Stairs	7.00	0.782	71.10	9.855	111.70	0.764	65.20	1.255	9.80	0.800	65.90	1.255

Note: Peak PSD_N *– the maximum noise PSD within the low-frequency range **$f<1Hz$**; **f_{PSD}** – the frequency at which the max noise PSD occurred; **Peak PSD_{ECG}** – the peak PSD of the ECG signal; **f_{ECGPsd}** – the frequency at which the max ECG PSD occurred; **Red** – intense low-frequency noise; **Green** – prominent peak ECG Power*

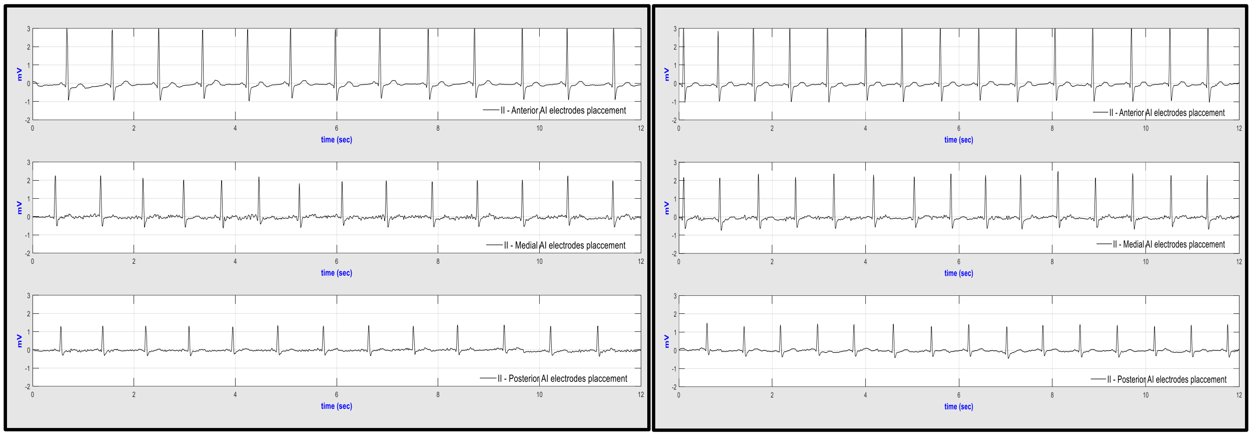

Figure 6.8: Comparison of lead-II ECGs acquired during sideways movement (left) and climbing stairs (right) based on different **AI** electrodes placements (top – anterior, middle – medial and bottom – posterior electrode placement)

Discussion

Optimal electrode placement for quality ECG transduction is a significant challenge to be addressed (Finlay et al., 2008a, Jiang et al., 2009, Cho and Lee, 2015).

Based on the EASI configuration, placing the 'A' and 'I' electrodes at the anterior axillary line showed a lower ApEn (Table 6.28). At the same time, during sideways, up movement and writing on a keyboard, the medial axillary and posterior 'AI' placement showed higher randomness (an increased ApEn) in the acquired ECG. As the hands were moved side to side (sideways) and raised above the head and then moved back (up movement), there was a high chance of the arms touching the electrodes placed under the armpit and on the posterior axillary lines, resulting in an unstable skin-electrode interface. The continuous impedance-change induced low-frequency interference in the acquired ECGs. Moreover, moving the electrodes from the anterior-axillary to the posterior-axillary line, diminished the overall ECG amplitude. As quantitative evidence for the decreased magnitude, the average amplitude of the R-waves was computed based on a thresholding peak detection algorithm. Again, the average power contained within the collected ECG was calculated. As a result, placing the 'AI' electrodes at the posterior axillary locations reduced both the R waves amplitude and the power contained within the acquired ECG. The ECG collected from electrodes placed away from the heart (electrodes placed at the posterior axillary position) showed increased low-frequency noise (Table 6.27).

Regardless of the higher noise in the ECG signal, the power contained within the acquired ECG from the medial axillary lines is higher than the ECG collected from the posterior-axillary lines (Table 6.26). From the electrophysiology perspective, where the body is assumed to be a volume conductor (Malmivuo and Plonsey, 1995), the further the sensors from the source (the heart), the higher the impedance of the volume conductor (Malmivuo and Plonsey, 1995, Gacek and Pedrycz, 2011). Therefore, it is unsurprising that the amplitude of the ECG collected when the two electrodes (AI) are at the medial axillary point is greater than the ECG collected, placing the 'A' and 'I' electrodes at the left and right posterior axillary lines, respectively.

6.5.3.3. Modified 'S' and modified 'E' electrode placement

Specific objective

The objective was to examine the effect of modifying the 'E' and 'S' electrodes placement (from the standard EASI configuration presented in section 6.5.3.2) on signal quality.

Method and materials

In section 6.5.3, the effect of modifying the 'A' and 'I' electrodes position on signal quality was examined. To further understand the influence of electrode placement, the 'S' electrode was first placed above the jugular notch of the sternum (neck). In the second stage, the 'E' electrode position was modified, and the 'E' electrode was placed at the lower tip of the sternum (Xiphoid process), keeping the rest of the electrodes at the respective EASI standard configuration positions. The 3mm thick, 70mm^2 textile electrodes were used in the study.

Results

The quality of the ECG signal acquired during modified 'S' and 'E' electrode positions was assessed against the ECG obtained from the standard EASI electrode placement outlined in section 6.5.3.2. Table 6.30 compares the SSR, while Table 6.31 summarises the ApEn.

Table 6.30: SSR comparison of ECG acquired between the standard EASI configuration versus modified 'S' and modified 'E' electrode placement.

SSR (dB) = $10*\log_{10}(Px)$, II		
Body movement	**$Px = (P_{Standard} / P_{ModS})$**	**$Px = (P_{Standard} / P_{ModE})$**
Sitting	1.2376	-0.2794
Sideways	1.1186	-0.5347
Up	0.3789	-0.3522
Sitting / standing	0.6484	0.2058
Stairs	-0.0587	-1.0346
SSR (dB) = $10*\log_{10}(Px)$, V4		
Body movement	**$Px = (P_{Standard} / P_{ModS})$**	**$Px = (P_{Standard} / P_{ModE})$**
Sitting	0.5753	-1.0213
Sideways	-2.5058	-0.9879
Up	-2.4487	-0.8649
Sitting / standing	0.1712	-0.6964
Stairs	-0.8464	-1.2341

Note: ***$P_{Standard}$*** *– power in the ECG signal acquired from standard electrode placement,* ***P_{ModS}*** *– Modified 'S' and* ***P_{ModE}*** *– modified 'E' electrode placement;* ***sideways –*** *moving the hands sideways and moving them back to the midline horizontally;* ***up*** *– raising arms above the head and moving them back;* ***sitting / standing*** *– sitting / standing from a chair;* ***stairs*** *– climbing stairs*

Table 6.31: Statistical summary of ApEn of lead-II and V4 ECG acquired from modified 'S' and modified 'E' electrode placement.

Lead – II						
Body movement/activities	**ApEn Descriptive Statistics**					
	Standard EASI		**Modified S**		**Modified E**	
	Mean±SD	**50^{th} Percentiles (Median)**	**Mean±SD**	**50^{th} Percentiles (Median)**	**Mean±SD**	**50^{th} Percentiles (Median)**
Sitting	0.0371±0.0034	0.0365	0.0460±0.0030	0.0453	0.0488±0.0039	0.0483
Sideways	0.0783±0.0059	0.0794	0.0687±0.0044	0.0682	0.0648±0.0051	0.0658
Up	0.1292±0.0191	0.1284	0.1660±0.0205	0.1677	0.1616±0.0260	0.1626
Sitting / standing	0.0394±0.0051	0.0399	0.0527±0.0031	0.0523	0.0541±0.0035	0.0540
Stairs	0.0525±0.0056	0.0518	0.0530±0.0027	0.0527	0.0530±0.0045	0.0531
Body movement/activities	**ApEn Test Statistics**					
	Standard EASI Vs. Modified S		**Standard EASI Vs Modified E**		**Modified S Vs Modified E**	
Sitting	Z	-2.9809	Z	-3.0594	Z	-1.8827
	p	0.0028	p	0.0022	p	0.0597
Sideways	Z	-2.9809	Z	-3.0594	Z	-1.8848
	p	0.0028	p	0.0022	p	0.0594
Up	Z	-2.5897	Z	-2.8240	Z	-0.7844
	p	0.0096	p	0.0047	p	0.4327
Sitting/standing	Z	-3.0594	Z	-3.0605	Z	-0.7071
	p	0.0022	p	0.0022	p	0.4795
Stairs	Z	-0.4706	Z	-0.4710	Z	-0.1568
	p	0.6378	p	0.6376	p	0.8753
V4						
Body movement/activities	**ApEn Descriptive Statistics**					
	Standard EASI		**Modified S**		**Modified E**	
	Mean±SD	**50^{th} Percentiles (Median)**	**Mean±SD**	**50^{th} Percentiles (Median)**	**Mean±SD**	**50^{th} Percentiles (Median)**
Sitting	0.0671±0.0098	0.0625	0.0774±0.0085	0.0760	0.0596±0.0098	0.0567
Sideways	0.1083±0.0072	0.1076	0.1062±0.0127	0.1081	0.0754±0.0041	0.0763
Up	0.1611±0.0217	0.1570	0.1525±0.0166	0.1555	0.1508±0.0157	0.1478
Sitting / standing	0.0766±0.0052	0.0762	0.1068±0.0070	0.1046	0.0690±0.0041	0.0684

Stairs	0.0902±0.0057	0.0881	0.1200±0.0090	0.1219	0.0666±0.0053	0.0670
Body movement/activities	**ApEn Test Statistics**					
	Standard EASI Vs. Modified S		**Standard EASI Vs Modified E**		**Modified S Vs Modified E**	
Sitting	Z	-2.3542	Z	-1.7657	Z	-3.0605
	p	0.0185	p	0.0774	p	0.0022*
Sideways	Z	-0.2353	Z	-3.0594	Z	-2.9855
	p	0.8139	p	0.0022*	p	0.0028*
Up	Z	-1.1766	Z	-0.9413	Z	-0.4706
	p	0.2393	p	0.3465	p	0.6378
Sitting/standing	Z	-3.0617	Z	-2.9821	Z	-3.0594
	p	0.0022*	p	0.0028*	p	0.0022*
Stairs	Z	-3.0594	Z	-3.0605	Z	-3.0594
	p	0.0022*	p	0.0022*	p	0.0022*

Note: ApEn *– approximate entropy;* ***Standard*** *– AI electrodes placed at the standard electrode positions;* ***Modified S*** *– Modified 'S' and* ***Modified E*** *– Modified 'E' electrode placements; * – statistically significant*

The modified 'S' and 'E' electrode placement affected the limb-lead ECG (e.g., II) and the precordial ECG (e.g., V4) differently, as shown in Table 6.30 and Table 6.31. It was challenging to create a stable skin-electrode interface for the altered 'S' electrode position due to its location. The modified 'S' electrode was placed at the neck. As a result, it was difficult to apply the necessary compressive pressure as increasing the pressure tends to compress blood vessels in the neck that induced reduced blood supply to the brain. Hence, there was little to no improvement in signal quality compared to the standard electrode placement. However, modifying the 'E' electrode position from the usual electrode placement resulted in higher signal power and lowered approximate entropy, especially in the V4 ECG (Table 6.31) during sideways movement (Standard EASI Vs modified 'E': $Z = -3.0594$, $p = 0.0022$), sitting / standing from a chair (Standard EASI Vs modified 'E': $Z = -2.9821$, $p = 0.0028$) and climbing stairs (Standard EASI Vs modified 'E': $Z = -3.0605$, $p = 0.0022$).

The SSR (Table 6.30) during the up movement in lead-II ECG is not supported by the ApEn (Table 6.31).

The ECG from the modified ‘E’ electrode position has shown slightly higher power and noise levels. Therefore, the peak noise PSD in the low-frequency spectrum and the total average power were computed and presented in Table 6.32. To minimise the noise contribution to the ECG power estimation, the average noise power was extracted from the acquired ECG based on a cut-off frequency computed from the average HR. The dominant features (P, QRS and T) of the ECG signal occurred at a frequency equal to higher to the HR. If the HR is higher than 60bpm, the cut-off frequency was set to 1Hz.

Table 6.32: Summary of peak noise PSD and total average power within lead-II and V4 ECG acquired from modified 'S' and 'E' electrodes placements.

Body movement / activities	II											
	Electrode placement											
	Standard EASI				Modified S				Modified E			
	Peak PSD_N (mW/Hz)	f_{PSD} (Hz)	P_{av} (mW)	P^*_{av} (mW)	Peak PSD_N (mW/Hz)	f_{PSD} (Hz)	P_{av} (mW)	P^*_{av} (mW)	Peak PSD_N (mW/Hz)	f_{PSD} (Hz)	P_{av} (mW)	P^*_{av} (mW)
Sitting	25.6	0.533	223.0	220.1	10.6	0.933	159.0	157.6	12.9	0.117	233.5	231.2
Sideways	211.2	0.483	221.3	211.6	317.5	0.017	194.1	153.7	7.7	0.550	253.1	252.6
Up	72.7	0.667	224.9	218.1	554.3	0.017	267.3	185.9	5.0	0.517	243.9	242.7
Sitting / standing	4.8	0.500	295.1	294.3	7.9	0.017	246.1	244.6	7.0	0.017	278.7	277.5
Stairs	21.7	0.500	212.4	209.7	20.0	0.883	209.1	207.9	36.3	0.017	297.8	293.0

Body movement / activities	V4											
	Electrode placement											
	Standard EASI				Modified S				Modified E			
	Peak PSD_N (mW/Hz)	f_{PSD} (Hz)	P_{av} (mW)	P^*_{av} (mW)	Peak PSD_N (mW/Hz)	f_{PSD} (Hz)	P_{av} (mW)	P^*_{av} (mW)	Peak PSD_N (mW/Hz)	f_{PSD} (Hz)	P_{av} (mW)	P^*_{av} (mW)
Sitting	20.3	0.050	121.7	116.6	15.0	0.933	96.9	94.3	16.2	0.117	164.0	162.1
Sideways	15.4	0.483	114.9	113.0	5032.9	0.550	414.1	123.3	4.0	0.033	183.2	182.1
Up	41.7	0.533	121.6	115.8	3781.3	0.533	319.0	155.2	6.9	0.583	184.3	183.1
Sitting / standing	68.6	0.533	147.5	142.0	22.2	0.733	140.3	136.7	8.2	0.483	205.6	204.3
Stairs	48.6	0.767	116.2	112.5	1222.7	0.883	176.5	128.9	27.8	0.017	216.3	211.1

Note: Peak PSD_N *– the maximum noise PSD within the low-frequency range* ***f<1Hz; f_{PSD}*** *– the frequency at which the max noise PSD occurred;* ***P_{av}*** *– the average total power within the ECG signal;* ***P^*_{av}*** *– the average total power within the ECG signal less the lower and high-frequency noise power;* ***sideways*** *– moving the hands sideways and moving them back to the midline horizontally;* ***up*** *– raising arms above the head and moving them back;* ***sitting / standing*** *- sitting / standing from a chair;* ***stairs*** *– climbing stairs*

Despite a higher value of ApEn (Table 6.31), the frequency domain analysis of the lead-II and V4 ECG acquired from a modified 'E' electrode during the up movement showed less noise (Table 6.32) in the low-frequency region (f<1Hz) where the body movement is a major contributing factor of motion artefact in the ECG signal. In this regard, the higher power content of the lead-II ECG during the up movement from the modified 'E' electrode placement was not due to increased noise in the low-frequency spectrum, but due to the better quality of the ECG signal.

Table 6.33: Lead-II ECG SQI based on modified 'S' and 'E' electrodes placements.

Body movement / activities	Electrode placement					
	Standard		Modified S		Modified E	
	pSQI	basSQI	pSQI	basSQI	pSQI	basSQI
Sitting	0.6878	0.9861	0.6689	0.9841	0.7039	0.9901
Sideways	0.7230	0.9555	0.6710	0.7916	0.6961	0.9980
Up	0.7191	0.9696	0.6639	0.6956	0.6862	0.9952
Sitting / Standing	0.7047	0.9974	0.6726	0.9936	0.6848	0.9958
Stairs	0.7190	0.9870	0.6881	0.9942	0.6938	0.9837

Note: Red *– increased low-frequency noise;* ***pSQI*** *– power signal quality index;* ***basSQI*** *– baseline power signal quality index;* ***sideways*** *– moving the hands sideways and moving them back to the midline horizontally;* ***up*** *– raising arms above the head and moving them back;* ***sitting / standing*** *– sitting / standing from a chair;* ***stairs*** *– climbing stairs*

In line with the SSR and PSD analyses, the SQI computation (Table 6.33) revealed that the modified 'E' electrode placement showed lower baseline drift compared to the standard EASI electrode configuration and the modified 'S' electrode placement. For visual inspection, the V4 ECGs are presented in Figure 6.9 based on 12 seconds representative ECG strips.

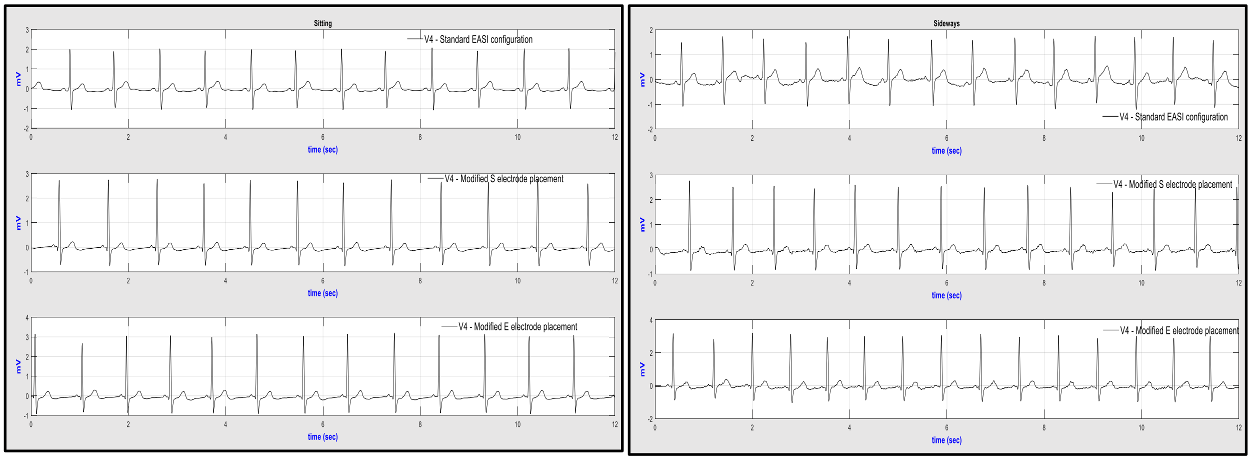

a) *Left – sitting and right - sideways (top – standard EASI, middle – modified S and bottom – modified E electrode placement)*

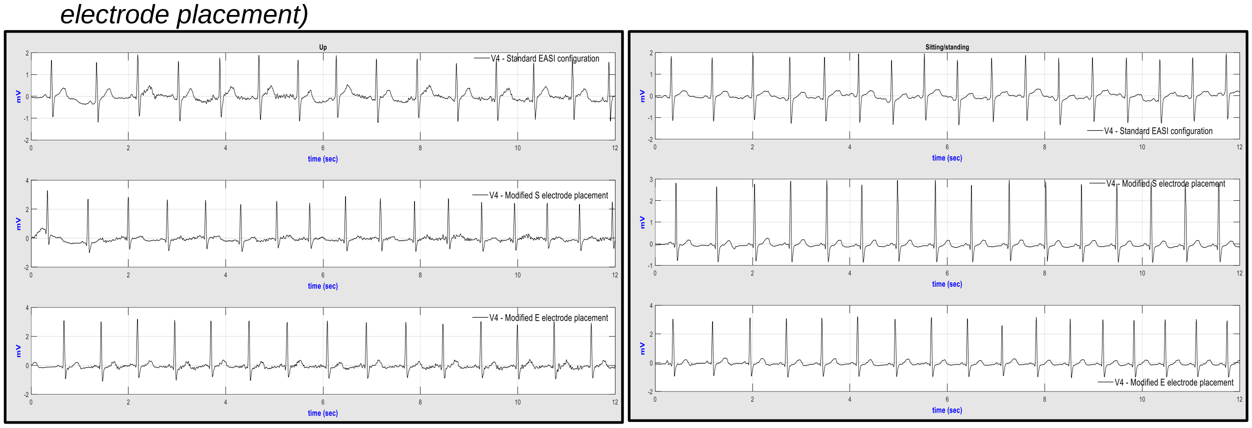

b) *Left - up movements and right - sitting / standing from a chair (top – standard EASI, middle – modified S and bottom – modified E electrode placement)*

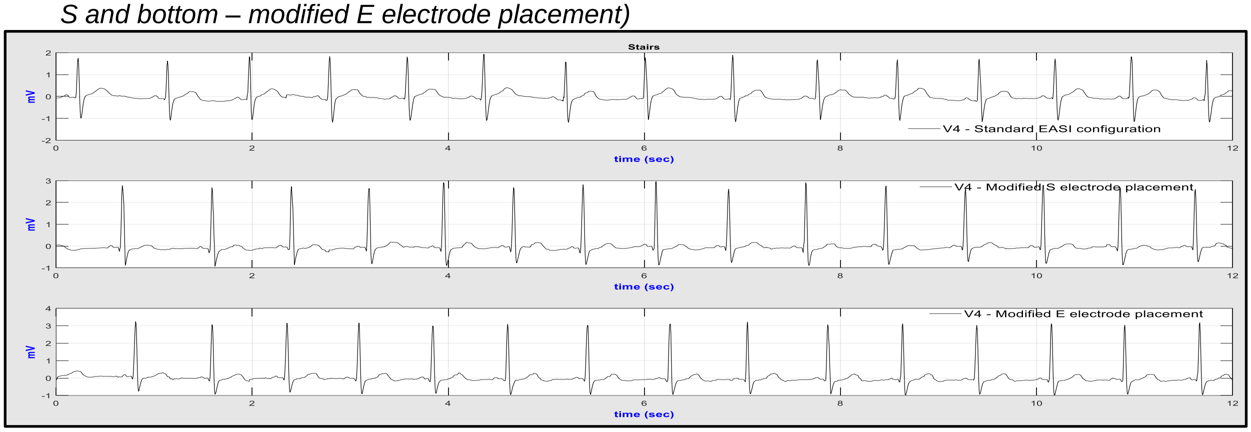

c) *Climbing stairs (top – standard EASI, middle – modified S and bottom – modified E electrode placement)*

Figure 6.9: Comparison of the representative V4 ECG acquired from standard EASI configuration and modified 'S' and modified 'E' textile electrode placement.

Referring to Figure 6.9, there was a slight morphological difference between the V4 ECG acquired from the standard EASI configuration and the modified 'E' and 'S' electrodes placement. The ECG from the standard EASI placement showed more prominent S-wave deflection. However, the morphological difference might not have a significant impact on the diagnosis as both waveforms are accepted normal V4 variations (Lilly and Braunwald, 2012).

Discussion

The 'S' and 'E' electrodes positions were individually modified from the standard EASI configuration and ECG was collected. Table 6.32 revealed that the modified 'E' electrode position resulted in lower peak noise PSD and higher average ECG power. Additionally, the V4 acquired from the modified 'S' sensor placement showed intense low-frequency motion artefact during sideways (Peak PSD_N = 5032.9mW/Hz, f= 0.550Hz), up movement (Peak PSD_N = 3781.3mW/Hz, f= 0.533Hz) and climbing stairs activities (Peak PSD_N = 1222.7mW/Hz, f= 0.883Hz).

As an additional signal quality parameter, it is possible to tell the intensity of the low-frequency noise by comparing ECG power from the clean ECG to the ECG power from the raw ECG. For instance, for the modified 'S' electrode placement, the ECG power calculated filtering the noise component was one-quarter (P^*_{av} = 123.3mW, Table 6.32) of the total power calculated from the raw ECG (Pav = 414.1mW, Table 6.32) during the sideways movement.

The increased low-frequency interference within the ECG collected from the newly proposed 'S' position in the lower ECG frequency spectrum could be related to continuous slipping of the 'S' electrode under body motion.

6.5.4. Textile electrode attachment

One of the design aspects of the wearable ECG monitor is the interconnection between the textile electrodes and the analogue front-end hardware. In the proposed wearable ECG monitor, the smart vest is at the heart of the interconnection, where wires are embedded into the vest linking the female component of an interlocking disc at each sensor placement site of the EASI configuration to the ECG hardware. The textile sensors themselves are not an integral part of the smart ECG vest. Electrodes are attached to the garment via a snap fastener at the connection site. The concept of removable electrodes increases the usability of the smart ECG vest and simplifies the replacement of textile sensors.

One of the requirements for successful ECG transduction is a stable skin-electrode interface (Gacek and Pedrycz, 2011). In the proposed wearable ECG monitor, the stability of textile electrodes is provided through the careful design of the smart ECG vest. In the standard vest design, the electrodes are removable and will be attached at the respective electrode position as shown in Figure 6.10.

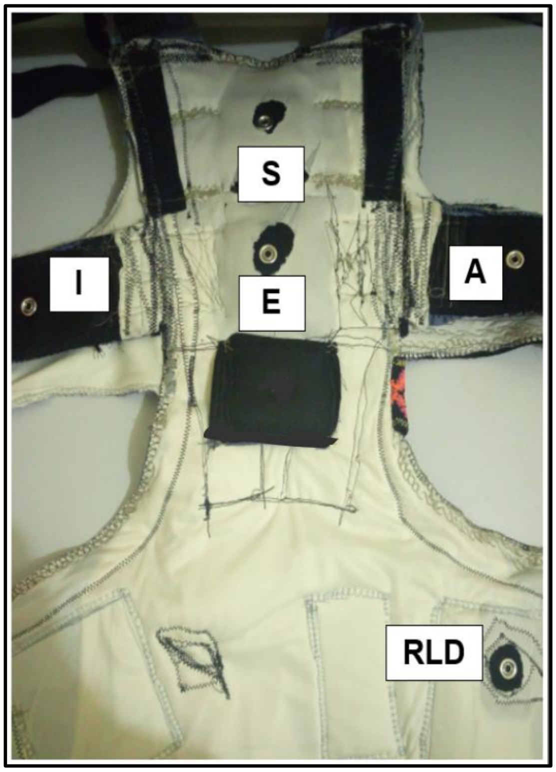

Figure 6.10: The EASI electrode attachment site on the smart ECG vest (RLD – the reference Right Leg Drive electrode)

As an additional measure of the steady impedance requirement, two alternative approaches were used: taping the textile electrodes to the wearer's body and the use of embedded textile electrodes to the smart ECG vest. Therefore, the aim of this experiment was twofold: first, it investigated the signal quality for the three types of electrode attachments (removable, taped to the user's skin and embedded in the garment); second, the study examined the versatility of the proposed smart ECG vest.

6.5.4.1. Effect of electrode attachment on signal quality

Specific objective

The specific objective was to examine the different methods used to connect the textile electrodes to the smart ECG vest and their effect on signal quality.

Method

During the first stage of the experiment, 3mm thick, $70mm^2$ textile electrodes were attached at the respective electrode sites (Figure 6.10). In the second phase, Scotch tape was used to tape the 3mm thick, $70mm^2$ textile electrodes to the wearer's body at the EASI electrode positions. In the third round, 3mm thick, $70mm^2$ textile electrodes were sewn into the smart ECG vest at the individual electrode sites (E, A, S, and I) to acquire ECG. During the experiments, the standard EASI electrode placement was used.

Results

Table 6.34 summarises the SSR analysis results between the ECG obtained from the detachable (removable) textile electrodes and taped textile electrodes / or embedded textile electrodes.

Table 6.34: Comparison of SSR based on ECG from removable textile electrodes and taped textile electrodes / or embedded textile electrodes.

SSR (dB) = 10*log$_{10}$(Px), II		
Body movement	**Px = ($P_{Removable}$ / P_{Taped})**	**Px = ($P_{Removable}$ / $P_{Embedded}$)**
Yawning	0.7094	1.5627
Deep breathing	0.9997	1.2340
Sideways	-0.1888	-0.0012
Up	0.3713	0.4078
Sitting / standing	0.1858	0.9275
Stairs	0.3612	1.0996
SSR (dB) = 10*log$_{10}$(Px), V4		
Body movement	**Px = ($P_{Removable}$ / P_{Taped})**	**Px = ($P_{Removable}$ / $P_{Embedded}$)**
Yawning	0.1492	0.1018
Deep breathing	0.2085	-0.1077
Sideways	-5.4765	-1.5232
Up	-0.8912	-0.3718
Sitting / standing	-0.1877	0.0669
Stairs	-0.2007	-0.1127

Note: *$P_{Removable}$ – power in the ECG signal acquired from removable textile electrodes, P_{Taped} – from taped textile electrodes and $P_{Embedded}$ – from embedded textile electrodes*

According to Table 6.34, ECG acquired from the regular removable textile electrodes showed higher signal power within the limb lead ECG (lead-II) relative to the ECG from the taped and fixed textile electrodes in five of the six movements.

Sixty-seven percent of the body movements (n=4) in the ECG collected from the taped and embedded textile sensors resulted in higher SSR compared to the V4 ECG collected via the removable textile electrodes. Moreover, the V4 ECG obtained from the taped textile electrodes showed a very high SSR value (5.5dB) relative to the V4 ECG collected from the removable textile electrodes during the sideways movement. To further understand the reasons for the differences between the SSR values within lead-II and V4 ECG, the randomness (ApEn) of the collected signals was computed and is presented in Table 6.35.

Table 6.35: Lead-II and V4 ECG ApEn based on textile electrode attachment.

Lead – II						
Body movement / activities	**ApEn Descriptive Statistics**					
	Removable electrodes		**Taped to the skin**		**Embedded electrodes**	
	Mean±SD	**50th Percentiles (Median)**	**Mean±SD**	**50th Percentiles (Median)**	**Mean±SD**	**50th Percentiles (Median)**
Yawning	0.0388±0.0091	0.0344	0.0382±0.0081	0.0360	0.0605±0.0040	0.0616
Deep breathing	0.0388±0.0050	0.0372	0.0388±0.0043	0.0384	0.0522±0.0046	0.0524
Sideways	0.0393±0.0039	0.0392	0.0581±0.0042	0.0575	0.0713±0.0072	0.0738
Up	0.0736±0.0110	0.0717	0.1365±0.0198	0.1354	0.1281±0.0205	0.1247
Sitting/standing	0.0394±0.0051	0.0399	0.0439±0.0066	0.0449	0.0658±0.0029	0.0665
Stairs	0.0384±0.0044	0.0395	0.0461±0.0037	0.0467	0.0593±0.0036	0.0595
Body movement / activities	**ApEn Test Statistics**					
	Removable Vs Taped electrodes		**Removable Vs Embedded electrodes**		**Taped Vs Embedded electrodes**	
Sitting	Z	-0.2746	Z	-3.0605	Z	-3.0594
	p	0.7835	p	0.0022*	p	0.0022*
Deep breathing	Z	-0.6275	Z	-3.0594	Z	-3.0594
	p	0.5302	p	0.0022*	p	0.0022*
Sideways	Z	-3.0605	Z	-3.0594	Z	-2.7456
	p	0.0022*	p	0.0022*	p	0.0060*
Up	Z	-3.0594	Z	-3.0594	Z	-1.0198
	p	0.0022*	p	0.0022*	p	0.3078
Sitting / standing	Z	-2.1581	Z	-3.0594	Z	-3.0605
	p	0.0309	p	0.0022*	p	0.0022*
Stairs	Z	-2.9036	Z	-3.0641	Z	-3.0594
	p	0.0036*	p	0.0021*	p	0.0022*
V4						
Body movement / activities	**ApEn Descriptive Statistics**					
	Removable electrodes		**Taped to the skin**		**Embedded electrodes**	
	Mean±SD	**50th Percentiles (Median)**	**Mean±SD**	**50th Percentiles (Median)**	**Mean±SD**	**50th Percentiles (Median)**
Yawning	0.0633±0.0082	0.0611	0.0815±0.0077	0.0816	0.0939±0.0069	0.0944
Deep breathing	0.0647±0.0080	0.0669	0.0808±0.0060	0.0788	0.0804±0.0071	0.0824
Sideways	0.0885±0.0116	0.0888	0.0983±0.0069	0.0991	0.0984±0.0083	0.0969

Up	0.1085±0.0093	0.1096	0.1604±0.0149	0.1588	0.1445±0.0129	0.1415
Sitting / standing	0.0766±0.0052	0.0762	0.0833±0.0069	0.0830	0.0909±0.0033	0.0905
Stairs	0.0696±0.0066	0.0713	0.0865±0.0065	0.0857	0.0888±0.0030	0.0895
Body movement / activities	**ApEn Test Statistics**					
	Removable Vs Taped electrodes		**Removable Vs Embedded electrodes**		**Taped Vs Embedded electrodes**	
Yawning	Z	-3.0594	Z	-3.0594	Z	-2.5887
	p	0.0022*	p	0.0022*	p	0.0096*
Deep breathing	Z	-3.0594	Z	-3.0594	Z	-0.2353
	p	0.0022*	p	0.0022*	p	0.8139
Sideways	Z	-2.0396	Z	-2.0403	Z	-0.0784
	p	0.0413	p	0.0413	p	0.9374
Up	Z	-3.0594	Z	-3.0594	Z	-2.0403
	p	0.0022*	p	0.0022*	p	0.0413
Sitting / standing	Z	-1.8827	Z	-3.0594	Z	-2.6682
	p	0.0597	p	0.0022*	p	0.0076*
Stairs	Z	-3.0594	Z	-3.0594	Z	-1.1766
	p	0.0022*	p	0.0022*	p	0.2393

Note: ApEn *– approximate entropy;* ***Removable*** *– ECG from the removable textile electrodes,* ***Taped*** *– from taped textile electrodes and* ***Embedded*** *– from embedded textile electrodes, respectively; * – statistically significant*

Referring to Table 6.35, ECG from the removable textile electrodes showed less randomness. However, the ApEn presented in Table 6.35 did not explain enough of the difference in power content between the lead-II and V4 ECG and especially the large increase in the SSR value of the V4 ECG during the sideways movement. As a result, PSD analysis was conducted to examine the signal in the frequency domain. The peak noise PSD in the low-frequency region and the total ECG power was computed for comparison and presented in Table 6.36.

Looking at the PSD summary presented in Table 6.36, ECG from the taped textile electrodes showed a higher noise level in the low-frequency region (f<1Hz) in both leads, especially during yawning, sideways and up movements.

Table 6.36: Summary of the power characteristics of lead-II and V4 ECGs collected from the three types of textile electrode attachments (removable, taped to the user's body and embedded into the smart garment) during various body movements and activities of daily living.

Body movement / activities	II								
	Electrode attachment								
	Removable electrodes			Taped to the user's skin			Embedded into the smart ECG vest		
	Peak PSD_N (mW/Hz)	f_{PSD} (Hz)	P^*_{av} (mW)	Peak PSD_N (mW/Hz)	f_{PSD} (Hz)	P^*_{av} (mW)	Peak PSD_N (mW/Hz)	f_{PSD} (Hz)	P^*_{av} (mW)
Yawning	49.6	0.267	267.0	147.3	0.233	211.0	27.0	0.217	160.8
Deep breathing	38.9	0.283	254.9	12.0	0.467	190.4	65.1	0.267	169.1
Sideways	11.9	0.6	219.2	130.0	0.500	189.8	47.4	0.450	180.0
Up	23.4	0.017	227.1	139.6	0.65	196.5	28.2	0.467	191.3
Sitting / standing	4.8	0.500	292.6	15.2	0.600	277.9	201.9	0.433	220.1
Stairs	10.1	0.767	274.7	31.0	0.800	244.5	53.1	0.017	199.4

Body movement / activities	V4								
	Electrode attachment								
	Removable electrodes			Taped to the user's skin			Embedded into the smart ECG vest		
	Peak PSD_N (mW/Hz)	f_{PSD} (Hz)	P^*_{av} (mW)	Peak PSD_N (mW/Hz)	f_{PSD} (Hz)	P^*_{av} (mW)	Peak PSD_N (mW/Hz)	f_{PSD} (Hz)	P^*_{av} (mW)
Yawning	15.6	0.267	128.0	62.6	0.25	114.1	10.4	0.167	111.4
Deep breathing	13.2	0.283	122.1	36.1	0.017	110.7	33.9	0.267	115
Sideways	192.8	0.533	114.4	9299.9	0.517	108.4	32.0	0.450	128.0
Up	48.3	0.617	119.5	960.3	0.650	120.9	8.0	0.450	129.9
Sitting / standing	68.6	0.533	140.5	51.7	0.300	153.5	137.5	0.433	141.6
Stairs	7.6	0.767	135.6	105.2	0.800	141.8	78.6	0.050	148.3

***Note: Peak PSD_N** – the maximum noise PSD within the low-frequency range **$f<1Hz$; f_{PSD}** – the frequency at which the max noise PSD occurred; **P^*_{av}** – the average total power within the ECG signal less the lower and high-frequency noise power; **Red** – intense low-frequency noise; **sideways** – moving the hands sideways and moving them back to the midline horizontally; **up** – raising arms above the head and moving them back; **sitting / standing** – sitting / standing from a chair; **stairs** – climbing stairs*

Table 6.37: Lead-II and V4 ECG SQI based on textile electrodes attachment (vest-electrode and electrode-skin interface)

Body movement / activity	**Electrode attachment**					
	II					
	Removeable		**Taped**		**Embedded**	
	pSQI	**basSQI**	**pSQI**	**basSQI**	**pSQI**	**basSQI**
Yawning	0.6835	0.9921	0.6885	0.9882	0.6674	0.9877
Deep Breathing	0.6845	0.9879	0.6842	0.9905	0.6737	0.9845
Sideways	0.7136	0.9916	0.6995	0.9917	0.6668	0.9902
Up	0.6951	0.9926	0.7008	0.9934	0.6822	0.9903
Sitting / Standing	0.7047	0.9979	0.6738	0.9945	0.6817	0.9771
Stairs	0.7145	0.9980	0.6947	0.9939	0.6744	0.9871
Body movement / activity	**V4**					
	Removeable		**Taped**		**Embedded**	
	pSQI	**basSQI**	**pSQI**	**basSQI**	**pSQI**	**basSQI**
Yawning	0.7275	0.9951	0.7299	0.9866	0.7349	0.9928
Deep Breathing	0.7122	0.9842	0.7204	0.9791	0.7231	0.9882
Sideways	0.7705	0.8906	0.7616	0.5198	0.7332	0.9936
Up	0.7608	0.9751	0.7593	0.7025	0.7392	0.9950
Sitting / Standing	0.7395	0.9650	0.6924	0.9528	0.7168	0.9719
Stairs	0.7521	0.9954	0.7029	0.9717	0.6890	0.9836

***Note: Light blue** – low to moderate level of baseline wander; **Red** – intensive low-frequency interference; **pSQI** – power signal quality index; **basSQI** – baseline power signal quality index; **sideways** – moving the hands sideways and moving them back to the midline horizontally; **up** –- raising arms above the head and moving them back; **sitting / standing** – sitting / standing from a chair; **stairs** – climbing stairs*

As can be seen from Table 6.37, the removable electrodes were not inferior to the embedded textile electrodes. However, the taped textile electrodes performed poorly, especially in the V4 ECG. The sideways and up movements introduced intense low-frequency noise in the ECGs acquired from the taped textile electrodes, and hence the temporal plot followed a sinusoidal pattern (Figure 6.11).

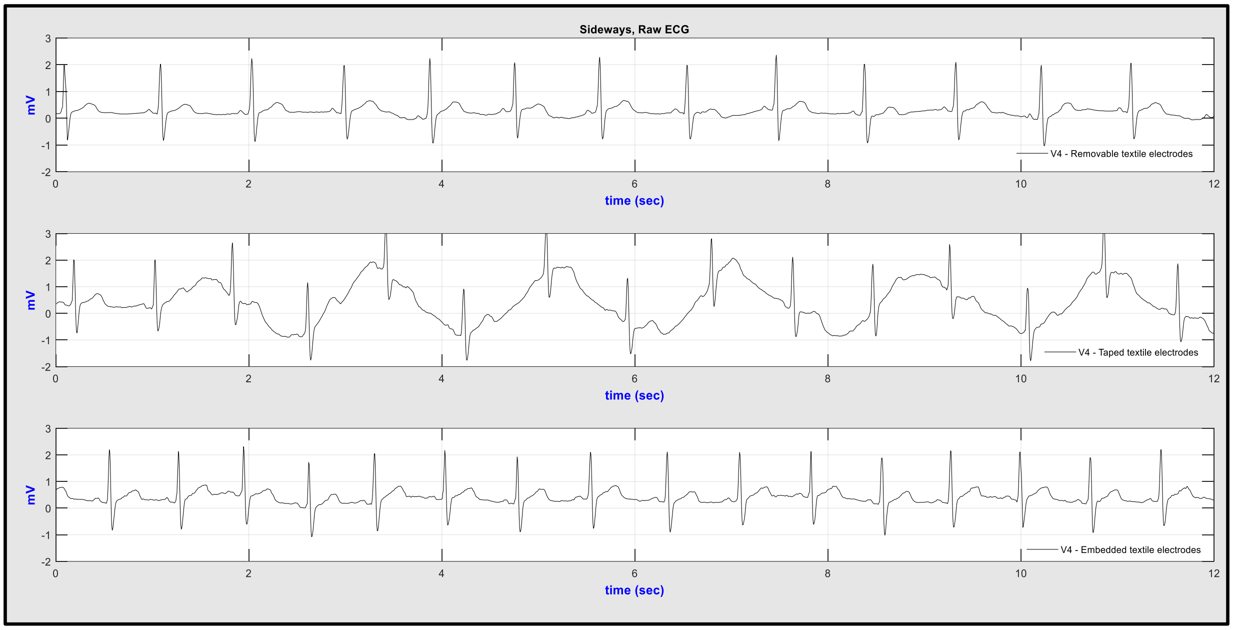

a) Sideways ECG (top – removable; middle – taped and bottom – embedded electrodes)

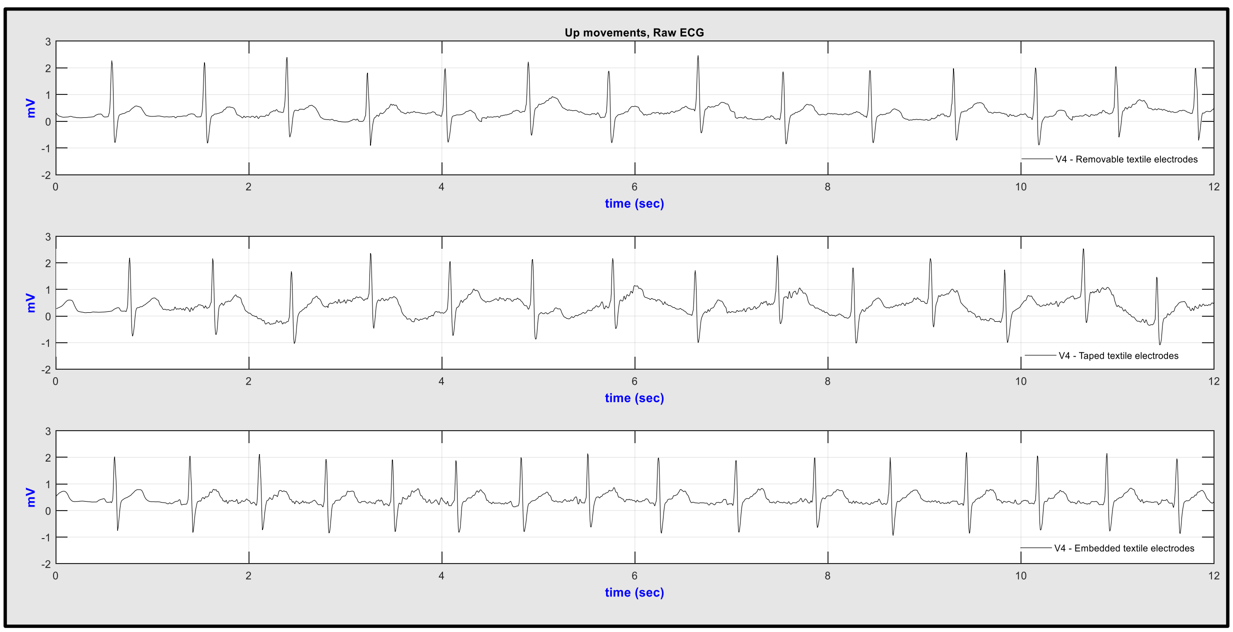

b) Up movements ECG (top – removable; middle – taped and bottom – embedded electrodes)

Figure 6.11: Representative V4 ECG temporal plots

Discussion

In the proposed textile-based ECG monitor, the electrodes are removable and connected to the smart ECG vest through 12.5mm snap fasteners at the respective EASI electrode sites. In the experiment, three alternative textile electrodes were considered: removable textile electrodes, textile electrodes taped to the user's skin and textile electrodes embedded in the smart ECG vest.

The ECG collected from the removable textile electrodes resulted in higher average power. The V4 ECG from the taped textile electrodes during sideways and up movements showed an increased low-frequency motion artefact. Despite the intense noise level, the motion artefact can be removed with minimal distortion of the original signal by applying a high pass filter of 0.67Hz corner frequency at -3dB, which is a fundamental prerequisite for monitoring ECG hardware (Marozas et al., 2011). For example, Figure 6.12 illustrates the clean ECG after a bidirectional 2nd order zero phase shift Butterworth high pass filter (fc=0.67Hz) and a median filter has been applied in MATLAB.

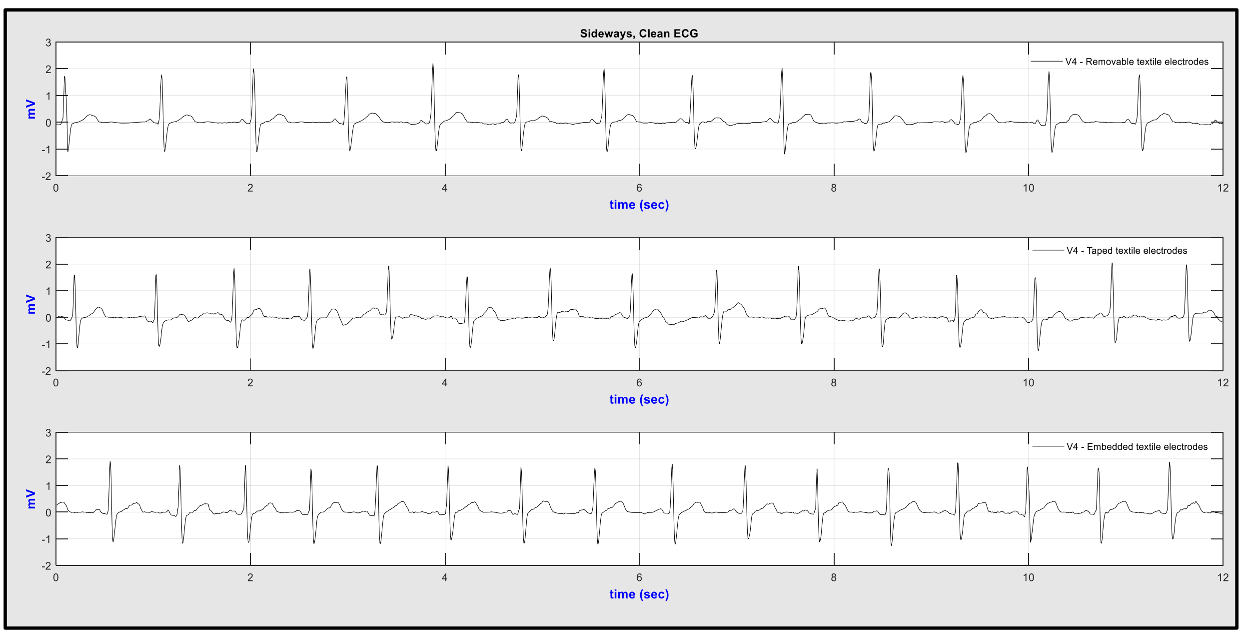

a) Sideways clean ECG (top – removable; middle – tapped and bottom – embedded electrodes)

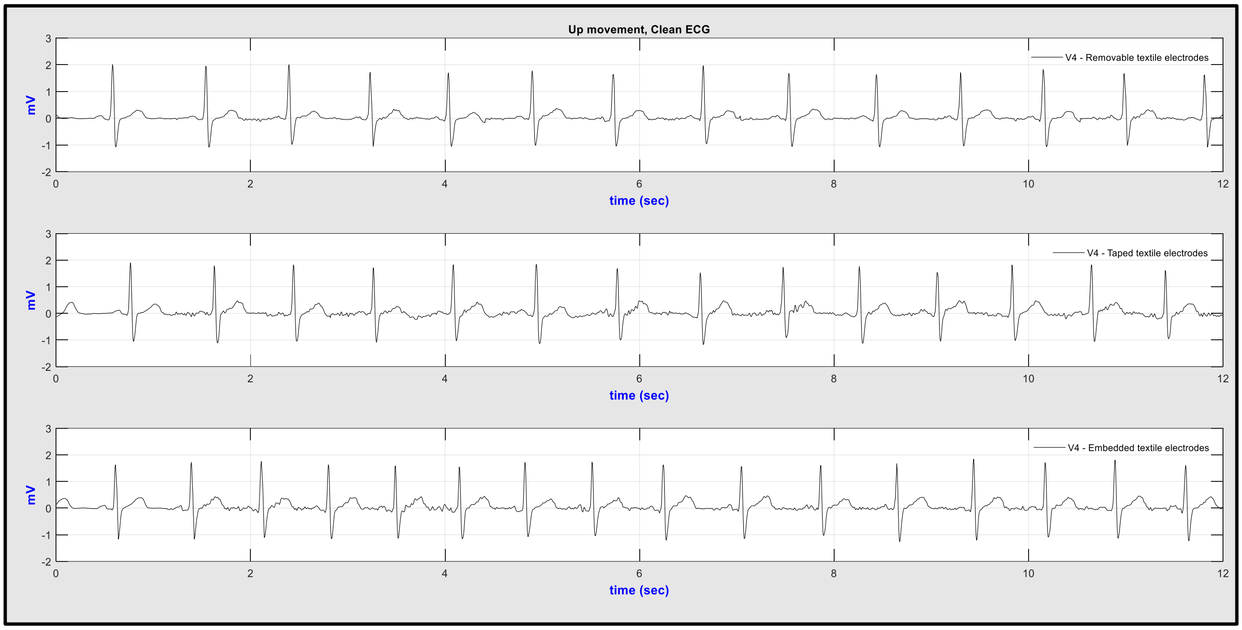

b) Up clean ECG (top – removable; middle – tapped and bottom – embedded electrodes)

Figure 6.12: Representative V4 ECG acquired from different textile electrode attachment.

The textile electrodes taped to the skin showed higher baseline wander during sideways and up movements. As the textile electrodes are fixed on the wearer's skin while connected to the smart vest, moving the arms sideways or upwards pulled the textile electrodes. The pulling of the fixed textile electrodes, in turn, decreases the active contact area and hence increases the impedance at the skin-electrode interface. The continuous decrease / increase of the impedance during hand movements was reflected within the time domain ECG tracings, as shown in Figure 6.11.

The increased noise artefact in the ECG acquired from the taped, or embedded textile electrodes might be due to the pulling of the electrodes by the vest during body movement. The textile sensors are taped around the edges and connected to the smart vest through the snap fastener located at the electrode's centre. The embedded textile sensors are integrated into the smart garment. In this regard, intense body movement tends to stretch the ECG vest. Moving the vest, in turn, affects the stability of the textile electrodes inducing an unstable skin-electrode interface and hence increased noise.

6.5.5. Conclusion

Regarding the vest design, two alternative vest prototypes were implemented and ECG during different body movements and activities of daily living were acquired. The results of the experiment revealed that the minimalist approach used to implement the second ECG vest (sECGVest2) did not produce an observable ECG quality difference compared to the ECG acquired from the first ECG vest (sECGVest1) given similar interconnection techniques, electrode characteristics, electrode placement and pressure applying mechanisms used in both designs.

Electrode placement affected the acquired ECG quality. The results showed that moving the 'A' and 'I' electrode position from the standard EASI configuration to left and right anterior-axillary lines respectively resulted in better signal quality and higher R-wave amplitude. In contrast, the standard EASI electrode placement (the 'AI' electrodes were placed at the medial axillary lines), showed lower signal quality, especially during sideways, up movements and writing on a keyboard. In conclusion, the anterior axillary line is the optimal 'AI' electrode position and recommended for ambulatory monitoring based on the EASI electrode placement. Moreover, changing the 'E' electrodes from the initially proposed location resulted in a better-quality ECG, especially in the V4 ECG. In conclusion, the newly proposed 'E' electrode placement resulted in relatively better signal quality compared to the standard EASI electrode placement, and it is recommended for future practice.

As far as electrode attachment is concerned, the removable textile electrodes are as good as the embedded textile electrodes. However, the removable textile electrodes increase the versatility of the smart ECG vest as they are more easily replaced.

6.6. Electrode condition

6.6.1. Effect of sweating on signal quality

ECG measured from commercial wet-gel electrodes has shown decreased quality over time, especially for long-term ambulatory monitoring (Marozas et al., 2011). However, ECG from textile electrodes has been shown to demonstrate improvement over an extended period of application, due to the positive effect of sweating on signal quality (Bourdon et al., 2005, Di Rienzo et al., 2013, Trindade et al., 2016).

6.6.1.1. Specific objective

This section aims to address Research Question 3: does sweating affect ECG quality? The specific objective of this study was to examine the effect of sweating on signal quality.

6.6.1.2. Methods

An experiment was conducted to investigate the effect of moisture from sweating on the signal quality. During the first phase, resting ECG from the dry textile and wet textile electrodes was acquired. The ECG obtained during the first five minutes of the test was considered as being measured by dry textile electrodes since the effect of sweating was minimal over this time.

Once ECG acquisition from the dry textile electrodes was complete, the volunteer performed casual walking for five minutes wearing the smart ECG vest to induce sweating. Five minutes of ECG was collected from the ‘wet’ textile electrodes to study the effect of sweating.

Finally, a series of body movements were performed, while ECG was acquired. Before the start of each experiment, the subject was rested for five minutes and given a fresh hand towel to use to dry body sweating. Then, the textile electrodes used in the previous test were replaced with new dry textile electrodes.

For the entire duration of the test, the standard EASI configuration and 3mm thick, 70mm^2 textile electrodes were used to collect ECG.

6.6.1.3. Resting ECG

Results

Figure 6.13 presents a typical 12-lead ECG six seconds strip before casual walking (dry textile electrodes) and after casual walking (wet textile electrodes). Compared to the ECGs acquired from the 'wet' textile electrodes, the ECGs from the dry textile electrodes showed a lower amplitude (e.g., V_{II_wet} = ~3mV, V_{II_dry} = ~ 2mV).

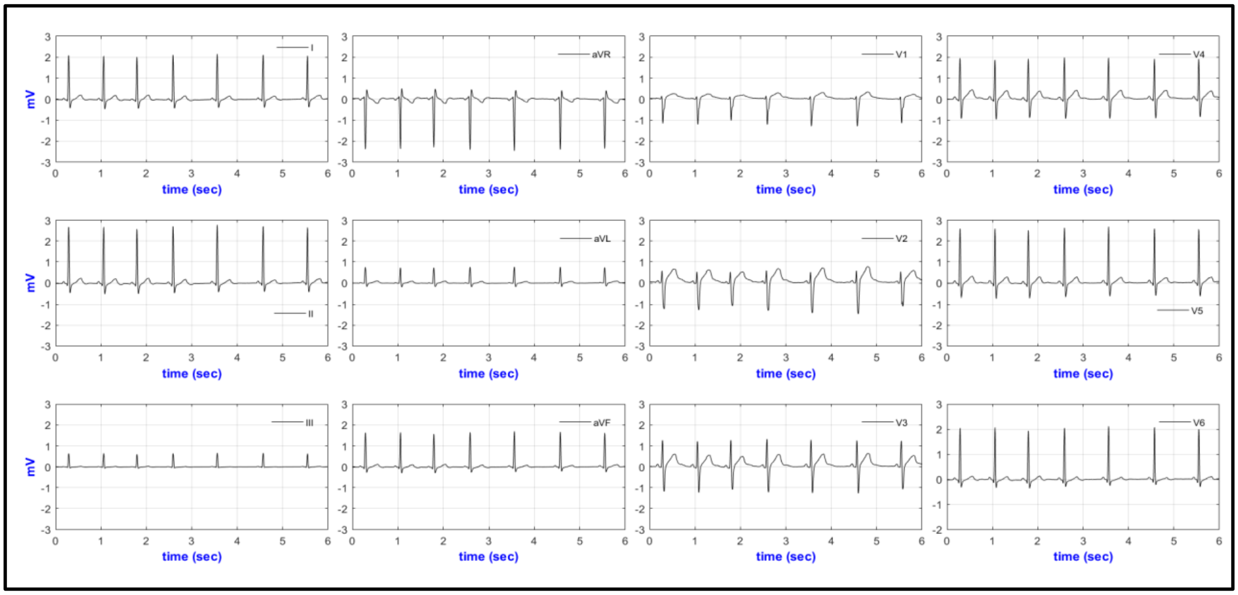

***a) ECG from wet textile electrodes** (raw 1 (top): ECG leads I, aVR, V1 and V4, raw 2 (middle): II, aVL, V2 and V5; raw 3 (bottom): III, aVF, V3 and V6)*

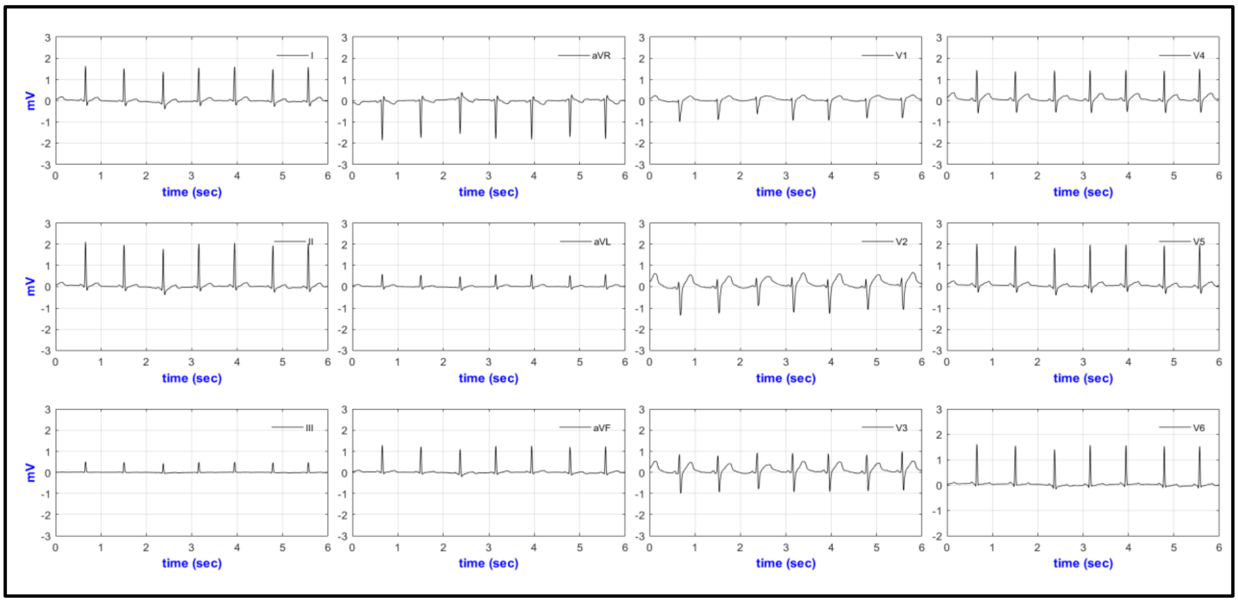

***b) ECG from dry textile electrodes (**raw 1 (top): ECG leads I, aVR, V1 and V4, raw 2 (middle): II, aVL, V2 and V5; raw 3 (bottom): III, aVF, V3 and V6)*

Figure 6.13: Twelve lead ECG from wet textile electrodes (top) and dry textile ECG electrodes (bottom)

Table 6.38 presents the SSR calculated from the ECG acquired through dry and wet textile ECG electrodes. In both ECG leads (lead-II and V4), the ECG power within the wet textile ECG showed higher power compared to the ECG from the dry textile electrodes.

Table 6.38: Signal-to-signal ratio (ECG from wet textile electrodes vs. ECG from dry textile electrodes)

SSR (dB) = 10*log$_{10}$(Px), L-I ECG Px = ($P_{Wet\_textile\_electrodes}$/ $P_{Dry\_textile\_electrode}$)	
ECG lead	**SSR**
II	1.4491
V4	2.4999

The box and whisker plot (Figure 6.14) compares the approximate entropy computed on lead-II and V4 ECG.

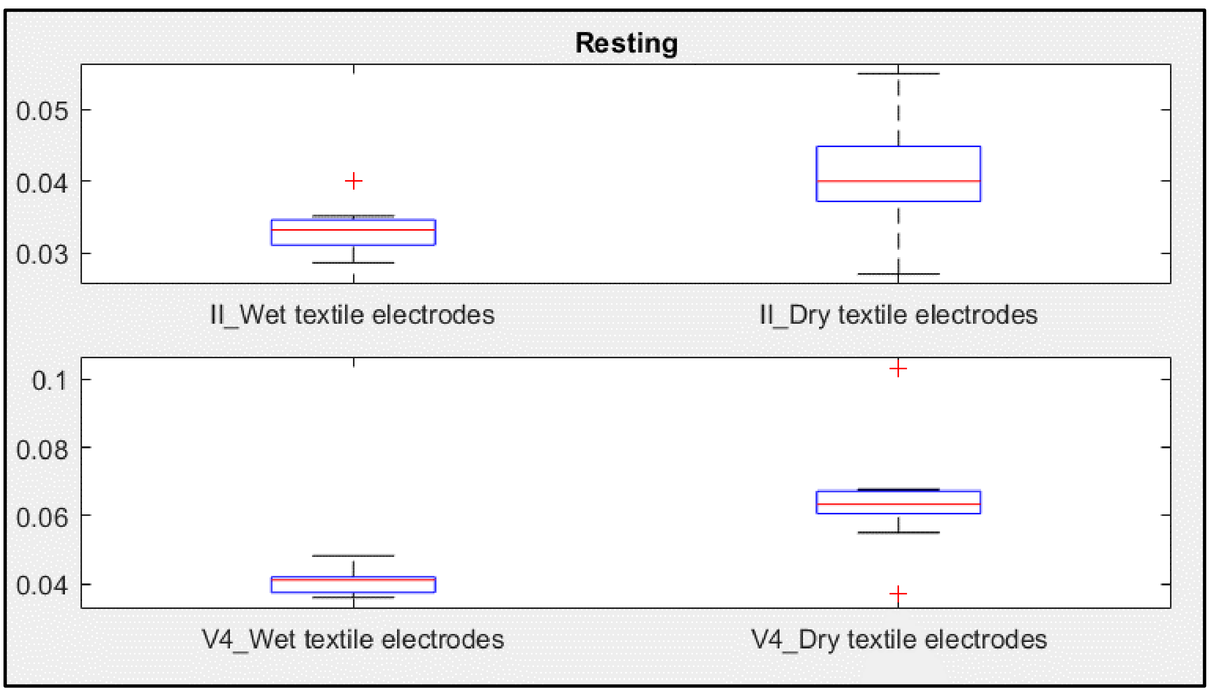

Figure 6.14: Lead-II (top) and V4 (bottom) resting ECG approximate entropy.

The ApEn analysis indicates that the wet textile electrodes showed lower randomness and hence performed better compared to the dry counterpart.

6.6.1.4. Influence of sweating on motion artefact

Results

Table 6.39: SSR based on ECG acquired from wet and dry textile electrodes.

SSR (dB) = 10*log$_{10}$(Px), Px = (P$_{Wet_textile\ _electrodes}$/ P$_{Dry_textile_\ electrode}$)		
Body movement / activities	**ECG lead**	
	II	**V4**
Yawning	0.2417	-0.2705
Deep breathing	1.2744	1.9280
Sideways	0.9639	-1.0119
Up	0.8967	-1.2360
Writing on a keyboard	0.5825	-0.0967
Making a phone call	0.3123	-0.3766
Sitting / standing	-0.8912	-0.7743
Stairs	0.1075	-3.0843

***Note: SSR** – Signal to signal ratio; **sideways** – moving the hands sideways and moving them back to the midline horizontally; **up** - raising arms above the head and moving them back; **writing on a keyboard** - writing on a keyboard at 40 words / minute; **sitting / standing** – sitting / standing from a chair; **stairs** – climbing stairs*

The SSR values presented in Table 6.39 showed that the lead-II ECG from wet textile electrodes resulted in more power except for sitting / standing from a chair. In contrast, the energy contained within the V4 ECG from the dry textile electrodes was higher, with ECG during deep breathing the only exception. The SSR value by itself does not tell too much about the quality of the signal. Therefore, time-domain (ApEn and SQI) and frequency domain analysis were conducted to better understand the acquired ECG signal.

Table 6.40: Comparison of the ApEn calculated from wet and dry textile electrodes in lead-II ECGs.

Body movement / activity	**ApEn Descriptive Statistics**				**ApEn Test Statistics**	
	Wet textile electrodes		**Dry textile electrodes**			
	Mean±SD	**50th Percentiles (Median)**	**Mean±SD**	**50th Percentiles (Median)**	**Wet Vs. Dry textile electrodes**	
Yawning	0.0382±0.0055	0.0378	0.0588± 0.004	0.0583	Z	-3.0594
					p	0.0022*
Deep Breathing	0.0466±0.0041	0.0467	0.0505±0.0062	0.0502	Z	-1.6473
					p	0.0994
Sideways	0.0454±0.0045	0.0447	0.0573±0.007	0.0562	Z	-3.0594
					p	0.0022*
Up	0.0941±0.0115	0.0925	0.1812±0.0188	0.1783	Z	-3.0594
					p	0.0022*
Writing on a keyboard	0.0419±0.0028	0.0426	0.04810±0.0042	0.0468	Z	-3.0605
					p	0.0022*
Phone call	0.0403±0.0044	0.0407	0.0488±0.0090	0.0479	Z	-2.1965
					p	0.0280
Sitting / standing	0.0519±0.0057	0.0522	0.0672±0.0064	0.0665	Z	-3.0594
					p	0.0022*
Stairs	0.0618±0.0052	0.0606	0.0748±0.0046	0.0750	Z	-3.0605
					p	0.0022*

Note: ApEn *– approximate entropy;* ***sideways*** *– moving the hands sideways and moving them back to the midline horizontally;* ***up*** *- raising arms above the head and moving them back;* ***writing on a keyboard*** *– writing on a keyboard at 40 words / minute;* ***sitting / standing*** *– sitting / standing from a chair;* ***stairs*** *– climbing stairs; * – statistically significant*

The ApEn analysis results presented in Table 6.40 revealed that the ECG from the dry textile electrodes exhibited higher randomness compared to the ECG from the wet textile sensors.

Table 6.41: SQI, ECG collected from wet and dry textile electrodes.

Body movement / activity	II							
	ECG from wet textile electrodes				ECG from dry textile electrodes			
	pSQI	basSQI	Peak PSD_{noise} (mW/Hz)	f_{PSD} (Hz)	pSQI	basSQI	Peak PSD_{noise} (mW/Hz)	f_{PSD} (Hz)
Yawning	0.6314	0.9932	74.18	0.0167	0.6275	0.9051	117.73	0.30
Deep Breathing	0.6602	0.9750	113.52	0.25	0.6574	0.9060	410.67	0.2333
Sideways	0.6419	0.9958	64.72	0.0833	0.6155	0.9858	344.73	0.1000
Up	0.6246	0.9732	88.15	0.6167	0.6189	0.9633	66.86	0.5000
Writing on a keyboard	0.6442	0.9950	59.99	0.0833	0.6344	0.9919	114.82	0.5833
Making a phone call	0.6265	0.9885	10.57	0.1667	0.6261	0.9894	12.99	0.4500
Sitting / standing	0.6429	0.9780	23.21	0.4500	0.6467	0.9044	300.76	0.5333
Stairs	0.6470	0.9675	162.37	0.2167	0.6441	0.9313	263.13	0.8167
Body movement / activity	V4							
	ECG from wet textile electrodes				ECG from dry textile electrodes			
	pSQI	basSQI	Peak PSD_{noise} (mW/Hz)	f_{PSD} (Hz)	pSQI	basSQI	Peak PSD_{noise} (mW/Hz)	f_{PSD} (Hz)
Yawning	0.6771	0.9879	33.81	0.0167	0.7154	0.9829	17.94	0.2667
Deep Breathing	0.6537	0.9638	77.49	0.25	0.7456	0.8960	249.5	0.2333
Sideways	0.6717	0.9860	16.56	0.4833	0.7098	0.8707	602.77	0.55
Up	0.6672	0.9819	58.66	0.6333	0.7231	0.8194	833.7	0.6167
Writing on a keyboard	0.6519	0.9855	105.76	0.0833	0.6770	0.9459	141.93	0.5833
Making a phone call	0.6284	0.9726	11.01	0.10	0.6910	0.8013	59.82	0.5000
Sitting / standing	0.6253	0.9686	31.88	0.4500	0.6924	0.7400	627.26	0.6000
Stairs	0.6713	0.9337	293.51	0.7167	0.6989	0.5026	3092.8	0.8333

Note: Peak PSD_{noise} *– the maximum PSD value within the range of f<1Hz;* ***f_{PSD},*** *the frequency at which the peak PSD_{noise} occurred****, Light blue*** *– low to moderate baseline drift;* ***Red*** *– extreme baseline wander;* ***pSQI*** *– power signal quality index;* ***basSQI*** *- baseline power signal quality index;* ***sideways*** *– moving the hands sideways and moving them back to the midline horizontally;* ***up*** *– raising arms above the head and moving them back;* ***writing on a keyboard*** *– writing on a keyboard at 40 words / minute;* ***sitting / standing*** *– sitting / standing from a chair;* ***stairs*** *– climbing stairs*

Table 6.41 presents the SQI and PSD computation results of the ECG from dry and wet textile electrodes. Referring to Table 6.41, the ECG acquired from the wet textile electrodes showed reduced noise in the low-frequency region. The V4 ECGs obtained through the dry textile electrodes during sideways, sitting / standing from a chair and climbing stairs were affected by intense baseline interference. The peak noise power within the ECG acquired from the dry textile electrodes during a phone call was 59.82mW/Hz. However, the lower baseline SQI (basSQI = 0.8013) is due to the multiple noise peaks distributed across the frequency range (f<1Hz, Figure 6.15).

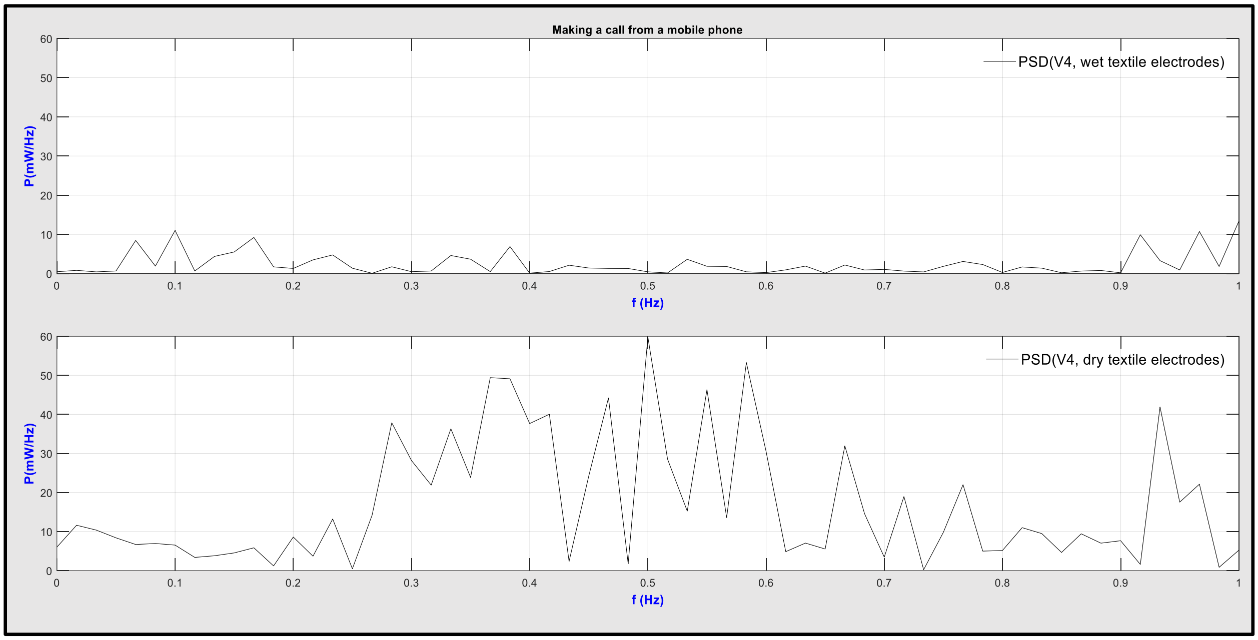

Figure 6.15: PSD plot to visualize and compare the low-frequency noise induced in the V4 ECG acquired from wet and dry textile electrodes during a phone call (top-ECG from wet textile electrodes and bottom – ECG from dry textile electrodes).

The power characteristics were computed and summarized in Table 6.42 to compare the influence of sweating on signal quality during various body movements and activities of daily living.

Before the power analysis was undertaken, the power quality indexes (pSQI>0.8 and basSQI<0.95) were used to determine if there was a need to denoise the collected ECG. In this regard, one of the algorithms that has been identified as useful to discriminate noise from a non-stationary, nonlinear signal like ECG is empirical mode decomposition (EMD) (Huang et al., 1998, Liang et al., 2000, Salisbury and Sun, 2004, Blanco-Velasco et al., 2008, Kopsinis and McLaughlin, 2008, Suchetha et al., 2017). In this technique, the ECG is decomposed into resultant intrinsic mode functions (IMF), and the Hilbert transform (Huang et al., 1998) of the individual IMFs is computed. Based on the Hilbert transform, the magnitude and instantaneous frequency spectrum are calculated. Most of the QRS energy is concentrated between 5Hz and 15Hz (Li et al., 2008, Clifford et al., 2012). Hence IMFs with a frequency component higher than 15Hz might contain a higher-order motion artefact from the EMG signal. Therefore, for this study, 15Hz was chosen to be the threshold frequency (f_{trsh}) indicating the need for a bandpass filter. If a maximum frequency (f_{max}) higher than f_{trsh} was detected across the IMF's frequency spectrum, the corresponding IMF contributes to the high-frequency noise, and it was passed through a bidirectional second-order band pass filter (f_{c_lower} = 0.67Hz and f_{c_upper} = 40Hz). On the other hand, if f_{max} was lower than f_{trsh}, the frequency f_{peak} where the peak noise PSD occurs between the absolute direct current (DC, f = 0Hz) and f = (minimum HR/60) Hz was calculated. Then a bidirectional second-order Butterworth high pass filter ($f_c = f_{peak}$) was used to remove the low-frequency noise. Figure 6.16 presents the workflow of the EMD based selective filter. The algorithm was implemented in MATLAB.

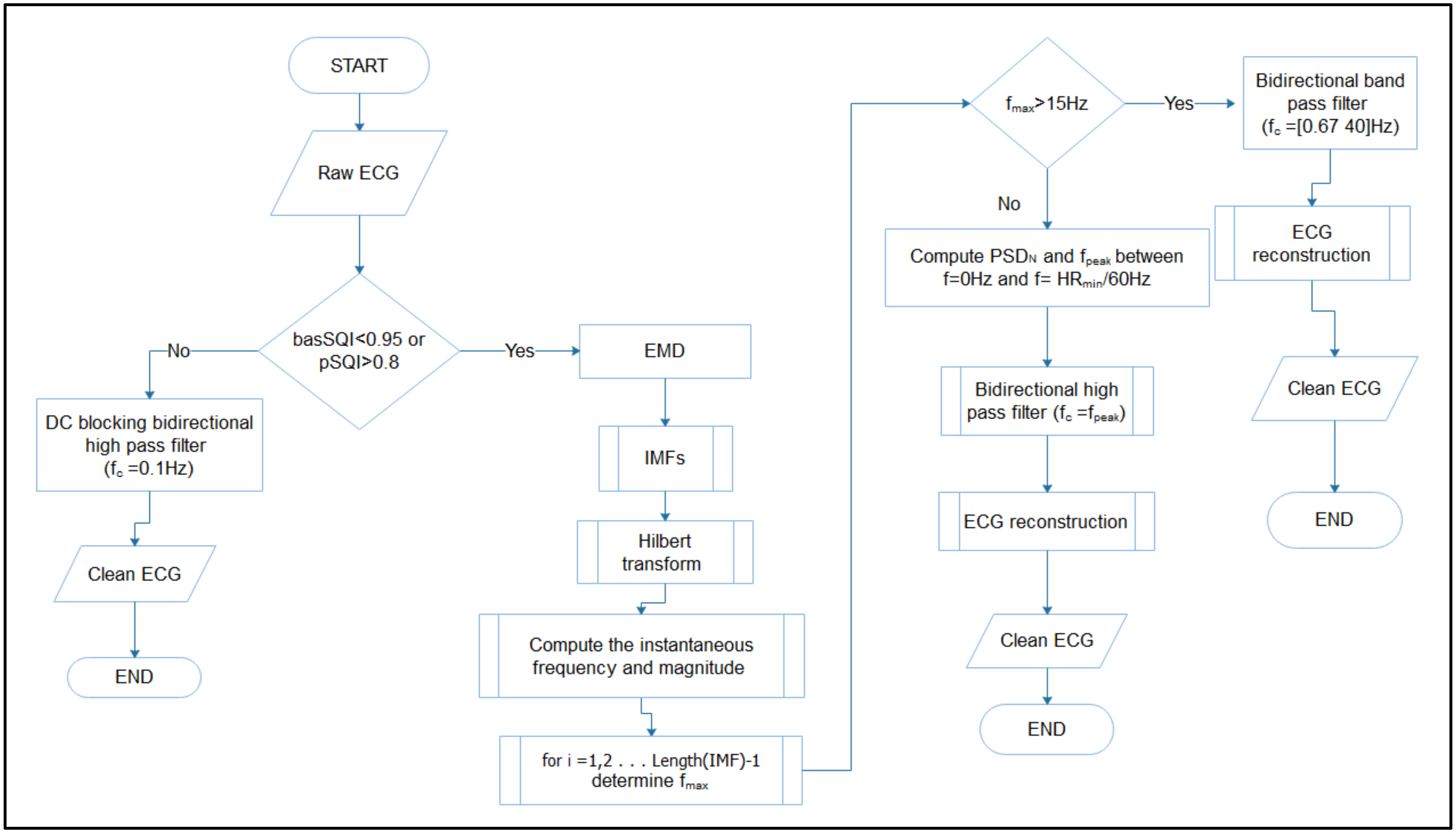

Figure 6.16: EMD based selective filter flow chart

Reconstructing the signal from the selectively filtered IMFs, a three-point median filter was used to smooth the clean ECG, and finally, the average power (***P^*_{av}***) was computed. Referring to Table 6.42, the power contained within the lead-II ECG acquired from the wet textile electrodes is higher at all times compared to the ECGs from the dry textile electrodes. However, V4 ECG average power during climbing stairs was higher for the dry textile electrodes; hence, the average power within the clean ECG (V4: ***P^*_{av}* =** 118.4mW, Table 6.42) was less than the average power within the raw ECG signal (V4: ***P_{av}* =** 278.1mW, Table 6.42) which indicates the intense low-frequency noise within the acquired ECG. The average power in the V4 ECG from the dry textile electrodes collected during deep breathing was the lowest (***P^*_{av}*** = 51.1mW, Table 6.42). In summary, the dry textile electrodes performed poorly compared to the wet electrodes, especially in the V4 ECG.

Table 6.42: Summary of the lead-II and V4 ECG power characteristics

	Wet textile Electrodes (lead-II)							**Dry textile Electrodes (lead-II)**						
Body movement / activities	**Raw ECG**			**Clean ECG**			**PD (%)**	**Raw ECG**			**Clean ECG**			**PD (%)**
	Peak PSD_N (mW/Hz)	**f_{PSD} (Hz)**	**P_{av} (mW)**	**Peak* PSD_N (mW/Hz)**	**f^*_{PSD} (Hz)**	**P^*_{av} (mW)**		**Peak PSD_N (mW/Hz)**	**f_{PSD} (Hz)**	**P_{av} (mW)**	**Peak* PSD_N (mW/Hz)**	**f^*_{PSD} (Hz)**	**P^*_{av} (mW)**	
Yawning	109.7	0.067	171.8	5.5	0.800	170.4	0.815	170.7	0.283	162.5	6.4	0.833	125.3	22.892
Deep breathing	113.5	0.250	191.9	4.7	0.950	189.9	1.042	410.7	0.233	143.1	9.7	0.933	113.5	20.685
Sideways	64.7	0.083	248.2	4.0	0.950	245.6	1.047	344.7	0.100	198.8	12.6	0.550	197.5	0.653
Up	88.2	0.617	243.9	15.2	0.617	241.2	1.107	66.9	0.500	198.4	10.2	0.633	196.6	0.654
Writing on a keyboard	114.8	0.083	239.8	5.4	0.650	237.0	1.167	60.0	0.583	209.7	7.4	0.583	208.1	0.763
Phone call	10.6	0.167	220.5	5.9	0.917	216.9	1.632	13.0	0.450	205.2	2.0	0.767	203.2	0.975
Sitting / standing	23.2	0.450	221.7	6.1	0.817	218.0	1.669	300.8	0.533	272.2	7.6	0.900	208.5	23.402
Stairs	162.4	0.217	249.4	38.6	0.717	245.7	1.483	263.1	0.817	243.3	69.3	0.867	185.1	23.921
	Wet textile Electrodes (V4)							**Dry textile Electrodes (V4)**						
Body movement / activities	**Raw ECG**			**Clean ECG**			**PD (%)**	**Raw ECG**			**Clean ECG**			**PD (%)**
	Peak PSD_N (mW/Hz)	**f_{PSD} (Hz)**	**P_{av} (mW)**	**Peak* PSD_N (mW/Hz)**	**f^*_{PSD} (Hz)**	**P^*_{av} (mW)**		**Peak PSD_N (mW/Hz)**	**f_{PSD} (Hz)**	**P_{av} (mW)**	**Peak* PSD_N (mW/Hz)**	**f^*_{PSD} (Hz)**	**P^*_{av} (mW)**	
Yawning	31.8	0.067	91.8	4.0	0.900	90.7	1.198	22.6	0.267	97.7	12.8	0.983	74.1	24.156
Deep breathing	77.5	0.250	100.7	6.0	0.950	98.8	1.886	249.5	0.233	64.6	0.9	0.967	51.1	20.588
Sideways	16.6	0.483	113.2	3.0	0.933	111.1	1.855	602.8	0.550	142.9	7.2	0.933	108.2	24.283
Up	58.7	0.633	129.7	13.0	0.633	127.3	1.850	833.7	0.617	172.4	10.1	0.917	104.0	36.675
Writing on a keyboard	141.9	0.083	119.9	5.1	0.650	117.2	2.252	105.8	0.583	122.6	8.5	0.900	89.9	26.672
Phone call	16.8	0.167	114.8	7.3	0.967	110.4	3.100	64.3	0.500	125.2	14.5	0.917	90.2	27.955
Sitting / standing	31.9	0.450	115.8	5.3	0.917	113.7	1.813	627.3	0.600	138.4	9.3	0.883	103.1	25.506
Stairs	293.5	0.717	136.7	21.2	0.950	104.5	23.555	3092.8	0.833	278.1	1130.2	0.833	118.4	57.425

Note: Peak PSD_N *– the maximum noise PSD within raw ECG and* ***Peak* PSD_N (mW/Hz)*** *– the maximum noise PSD within clean ECG across the low-frequency range* ***f<1Hz*** *of the raw ECG;* ***f_{PSD}*** *– the frequency at which the max noise PSD occurred within the raw ECG;* ***f^*_{PSD}*** *– the frequency at which the max noise PSD occurred within the clean ECG;* ***P_{av}*** *– the average total power within the raw ECG;* ***P^*_{av}*** *– the average total power within the ECG signal less the lower and high-frequency noise power;* ***pSQI*** *– power signal quality index;* ***PD(%) = (abs(P_{av} - P^*_{av})/ P_{av})*100%,*** *SSR based on* ***P^*_{av}; sideways*** *– moving the hands sideways and moving them back to the midline horizontally;* ***up*** *– raising arms above the head and moving them back;* ***writing on a keyboard*** *– writing on a keyboard at 40 words / minute;* ***sitting / standing*** *– sitting / standing from a chair;* ***stairs*** *– climbing stairs*

6.6.1.5. Discussion

The fact that the pSQI calculated from both ECGs (lead-II and V4) falls within the accepted range (pSQI = [0.5 - 0.8], Table 6.41) indicates that there was no significant muscle artefact induced into the QRS complex. However, the difference between the ECGs from the wet and dry textile electrodes was mainly because of the elevated motion artefact in the ECGs acquired from the dry textile electrodes in the low-frequency spectrum (f<1Hz) as the dry textile electrodes move easily under motion. The effect of sweating on the signal quality resembles the effect of the interfacing gel used in the wet-gel commercial electrodes, which reduced the electrode-skin impedance. Besides sweating probably exhibited the behaviour of the sticky surface around the commercial ECG electrodes contributing to the overall stability of the textile electrode-skin interface. Our results are supported by previous studies that reported the positive impact of sweating (Lee et al., 2014, Pani et al., 2015) in particular and wetting the textile electrodes (Puurtinen et al., 2006) in general, on signal quality.

6.6.2. Comparison between the textile electrodes and the disposable wet-gel electrodes

6.6.2.1. Specific objective

This section aims to address Research Question 4: do the textile electrodes result in an acceptable ECG tracing compared to the commercial wet-gel electrodes? The specific objective was to study the difference between the signal acquired from the textile electrodes and the signal acquired from the commercial wet-gel electrodes using the smart ECG vest.

6.6.2.2. Resting ECG

Materials and methods

ECGs from wet-gel electrodes (Nissha Medical Technologies, n.d.) and 3mm thick textile electrodes (40mm^2, 60mm^2, and 70mm^2) were collected using the developed textile-based ECG monitor. The 'A' and 'I' electrodes were placed on the left and right anterior-axillary lines, respectively, and at the level of the 'E' electrode. No change was made from the standard EASI placement regarding the 'E' and 'S' electrodes.

Results

Figure 6.17 presents a representative 12-lead ECG from the commercial wet-gel electrodes and ECG from 70mm^2 textile electrodes.

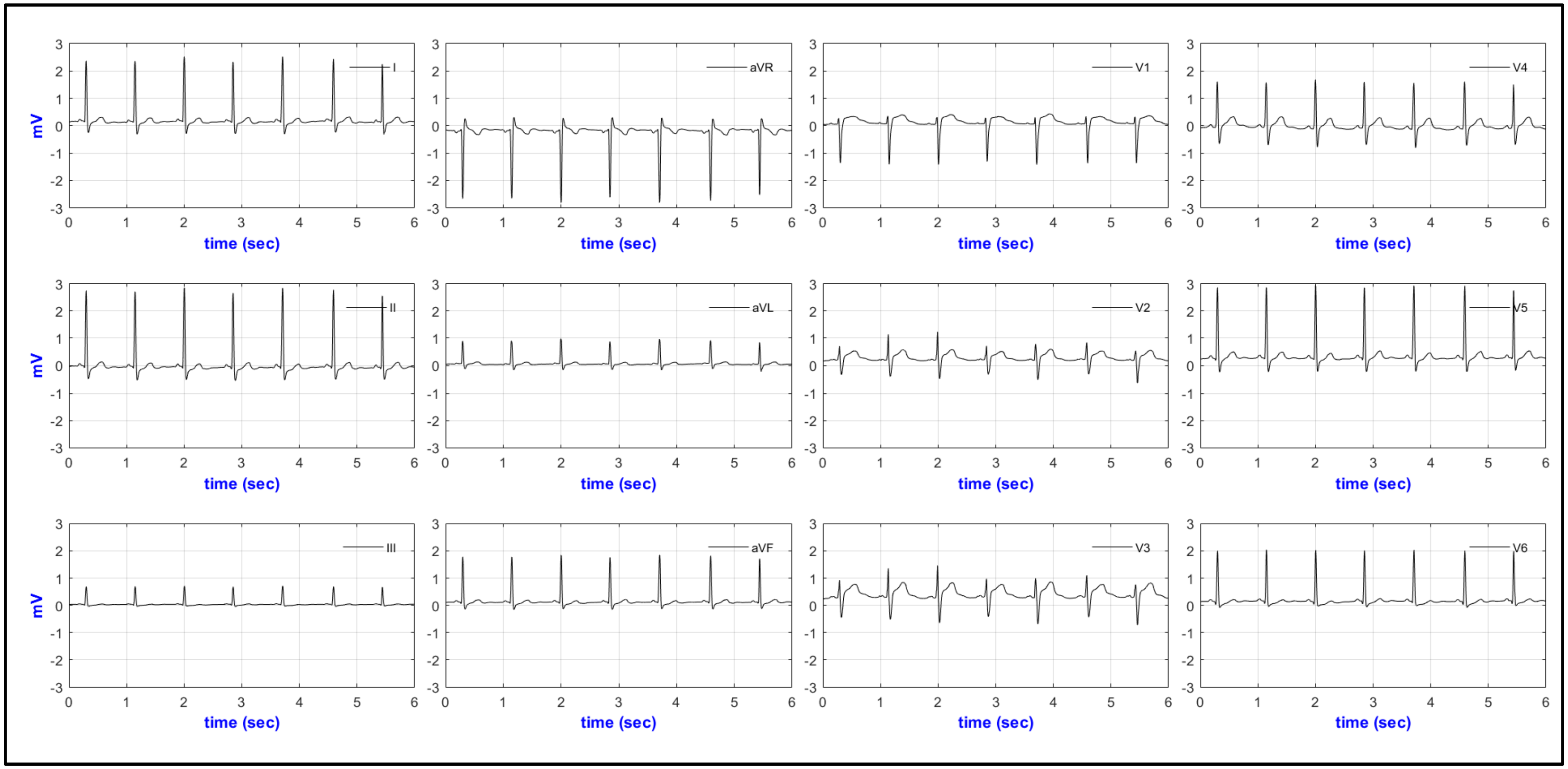

a) ECG from wet-gel commercial electrodes (*raw 1 (top): ECG leads I, aVR, V1 and V4, raw 2 (middle): II, aVL, V2 and V5; raw 3 (bottom): III, aVF, V3 and V6)*

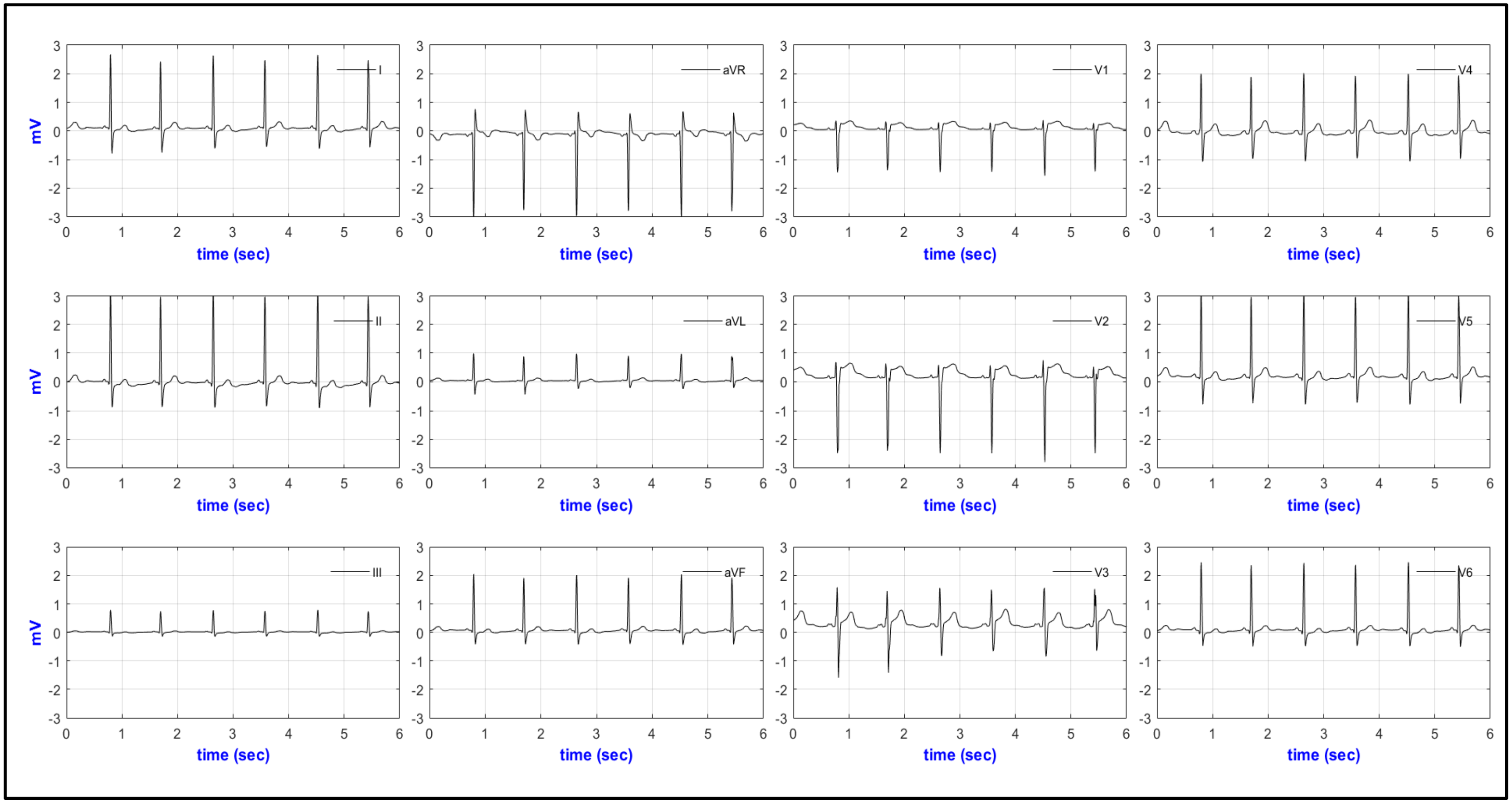

b) ECG from 3mm thick, 70mm^2 textile electrodes (*raw 1 (top): ECG leads I, aVR, V1 and V4, raw 2 (middle): II, aVL, V2 and V5; raw 3 (bottom): III, aVF, V3 and V6)*

Figure 6.17: Twelve lead resting ECG from the commercial wet-gel electrodes (a) and textile electrodes (b) using the proposed textile-based ECG monitor

Looking at Figure 6.17, the ECGs from the 70mm^2 textile electrodes showed higher ECG amplitude compared to the ECGs from the wet-gel commercial electrodes. To better understand the discrepancies between the ECGs acquired from the wet-gel commercial electrodes and the textile electrodes, the SSR from lead-II and V4 ECGs were computed, and the results are presented in Table 6.43.

Table 6.43: Comparison of power content in different leads acquired from textile sensors and the commercial wet-gel electrodes.

SSR (dB) = 10*log$_{10}$(Px), lead-II ECG		
Px = ($P_{Wet\text{-}gel\ electrode}$ /P_{40mm^2})	**Px = ($P_{Wet\text{-}gel\ electrode}$/$P_{60mm^2}$)**	**Px = ($P_{Wet\text{-}gel\ electrode}$ /P_{70mm^2})**
0.9114	0.000018093	-1.6336
SSR (dB) = 10*log$_{10}$(Px), V4 ECG		
Px = ($P_{Wet\text{-}gel\ electrode}$ /P_{40mm^2})	**Px = ($P_{Wet\text{-}gel\ electrode}$/$P_{60mm^2}$)**	**Px = ($P_{Wet\text{-}gel\ electrode}$ /P_{70mm^2})**
-0.6138	-0.8603	-1.9263

In line with the ECG tracing presented in Figure 6.17, the ECG acquired from the 70mm^2 textile electrodes showed a higher signal power compared to the commercial wet-gel commercial electrode. Regarding the lead-II ECGs collected from the 60mm^2 textile electrodes, there was no observable difference in signal power compared to the lead-II ECGs from the wet-gel commercial electrodes (SSR = 0DB, Table 6.43).

Table 6.44 compares the approximate entropy of lead-II and V4 acquired from various textile electrodes as well as the commercial wet-gel electrodes.

Table 6.44: Comparison of approximate entropy from lead-II and V4 representative ECG strips collected from three different textile electrodes (40mm^2,60mm^2,70mm^2) and the commercial wet-gel ECG electrodes.

ECG lead	ApEn Descriptive Statistics							
	Textile electrodes						Commercial ECG electrodes	
	40mm^2 textile electrodes		60mm^2 textile electrodes		70mm^2 textile electrodes			
	Mean±SD	50th Percentiles (Median)	Mean±SD	50th Percentiles (Median)	Mean±SD	50th Percentiles (Median)	Mean±SD	50th Percentiles (Median)
II	0.0688±0.0078	0.0667	0.0613±0.0104	0.0584	0.0502±0.0064	0.0509	0.0600±0.0094	0.0564
V4	0.0938±0.0181	0.0954	0.0808±0.0163	0.0775	0.0671±0.0073	0.0682	0.0831±0.0143	0.0820
ECG lead	ApEn Test Statistics							
	40mm^2 Vs. Commercial		60mm^2 Vs. Commercial		70mm^2 Vs. Commercial		60mm^2 Vs. 70mm^2	
II	Z	-1.9310	Z	-0.1135	Z	-2.8966	Z	-3.0101
	p	0.0534	p	0.9095	p	0.0037*	p	0.0026*
V4	Z	-1.5334	Z	-0.2839	Z	-3.2380	Z	-2.1582
	p	0.1251	p	0.7764	p	0.0012*	p	0.0309

Note: *ApEn – Approximate entropy; * – statistically significant*

The SSR (Table 6.43) and ApEn (Table 6.44) analyses based on the ECG acquired from the 40mm^2 and 70mm^2 textile electrodes resulted in slightly different values compared to the ECG obtained from the commercial wet-gel sensors. However, the ECG from the 60mm^2 textile electrodes showed a better match to the ECG acquired from the commercial wet-gel electrodes in both leads (lead-II and V4).

6.6.2.3. ECG motion artefact

Materials and methods

ECGs from wet-gel electrodes (Nissha Medical Technologies, n.d.) and 3mm thick 60mm^2 textile electrodes were collected using the proposed textile-based ECG monitor during different body movements (yawning, deep breathing, sideways and up movements) and activities of daily living (sitting / standing from a chair and climbing stairs). The 'A' and 'I' electrodes were placed on the left and right anterior-axillary lines, respectively and at the level of the 'E' electrode. No change was made from the standard EASI placement regarding the 'E' and 'S' electrodes.

Results

The lead-II ECG acquired during the respective body movements and activities of daily living are presented in Figure 6.18 for visual inspection.

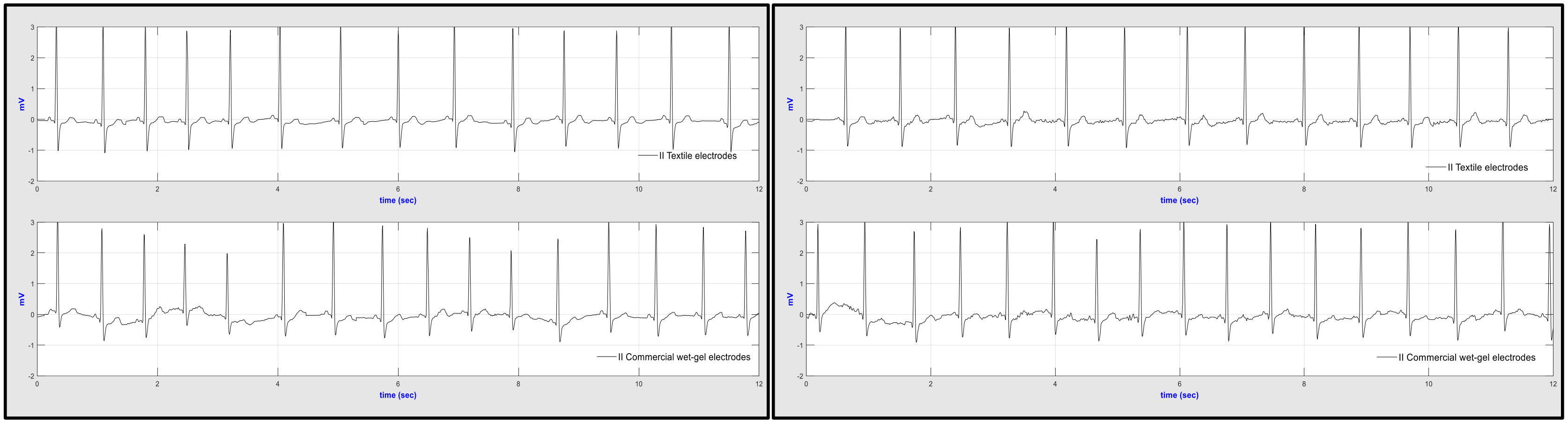

***a) Left - ECG during yawning and right - ECG during Sideways** (top – ECG from 60mm² textile electrodes and bottom – ECG from commercial wet-gel electrodes)*

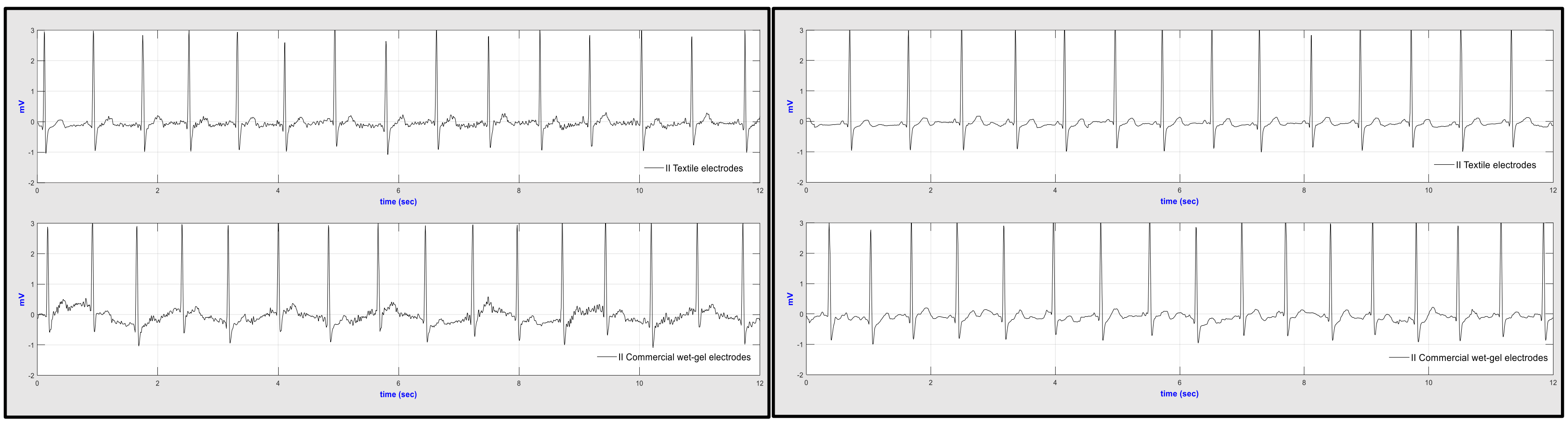

***b) Left - ECG during up movements and right - ECG during climbing stairs** (top – ECG from 60mm² textile electrodes and bottom – ECG from commercial wet-gel electrodes)*

Figure 6.18: Representative lead-II ECGs from 3mm thick, 60mm² textile and disposable commercial wet-gel electrodes.

Table 6.45: Comparison of ApEn for ECG collected from the commercial wet-gel electrodes and textile electrodes using the proposed textile-based ECG monitor.

Lead-II						
Body movement / activity	**ApEn Descriptive Statistics**				**ApEn Test Statistics**	
	Wet textile electrodes		**Commercial wet-gel electrodes**			
	Mean±SD	**50th Percentiles (Median)**	**Mean±SD**	**50th Percentiles (Median)**	**Wet textile Vs. Commercial wet-gel electrodes**	
Yawning	0.0426±0.0030	0.0413	0.0577±0.0054	0.0577	Z	-3.0594
					p	0.0022*
Deep Breathing	0.0407±0.0040	0.0402	0.0391±0.0061	0.0382	Z	-0.8629
					p	0.3881
Sideways	0.0549±0.0055	0.0545	0.0610±0.0104	0.0598	Z	-1.3733
					p	0.1696
Up	0.0984±0.0155	0.0982	0.1859±0.0185	0.1882	Z	-3.0594
					p	0.0022*
Sitting / standing	0.0429±0.0029	0.0435	0.0629±0.0102	0.0612	Z	-3.0605
					p	0.0022*
Stairs	0.0454±0.0029	0.0454	0.0590±0.0068	0.0590	Z	-2.9809
					p	0.0028
V4						
Body movement / activity	**ApEn Descriptive Statistics**				**ApEn Test Statistics**	
	Wet textile electrodes		**Commercial wet-gel electrodes**			
	Mean±SD	**50th Percentiles (Median)**	**Mean±SD**	**50th Percentiles (Median)**	**Wet textile Vs. Commercial wet-gel electrodes**	
Yawning	0.0802±0.0054	0.0809	0.0978±0.0082	0.0998	Z	-2.9809
					p	0.0028*
Deep Breathing	0.0788±0.0072	0.0801	0.0747±0.0049	0.0738	Z	-1.1766
					p	0.2393
Sideways	0.0900±0.0080	0.0891	0.0967±0.0085	0.0949	Z	-1.8042
					p	0.0711
Up	0.1263±0.0128	0.1221	0.2073±0.0207	0.2062	Z	-3.0594
					p	0.0022*
Sitting / standing	0.0683±0.0051	0.0672	0.0962±0.0126	0.0940	Z	-3.0605
					p	0.0022*
Stairs	0.0722±0.0046	0.0719	0.1084±0.0069	0.1082	Z	-3.0594
					p	0.0022*

Note: ApEn *– approximate entropy;* ***sideways*** *– moving the hands sideways and moving them back to the midline horizontally;* ***up*** *– raising arms above the head and moving them back;* ***sitting / standing*** *– sitting / standing from a chair;* ***stairs*** *– climbing stairs; * – statistically significant*

Looking at the temporal plots (Figure 6.18), the ECG from the textile electrodes showed a lower baseline interference as opposed to the ECG from the disposable wet-gel electrodes. Quantitative signal quality parameters, including ApEn (Table 6.45), SSR, signal quality indices and PSD (Table 6.46), were computed to support the evidence illustrated within the time domain ECG traces. The ECGs from the commercial wet-gel electrodes exhibited higher randomness (ApEn) within both lead-II and V4 ECGs (Table 6.45).

Table 6.46: SQI analysis results of lead-II ECG from textile electrodes and commercial wet-gel electrodes using the proposed ECG monitor.

SSR (dB) = 10*log$_{10}$($P_{Wet\_textile\_electrodes}$ /$P_{commercial\_wet\_gel\_electrodes}$)									
Body movement / activities	**SSR**	**Wet textile electrodes**				**Wet-gel commercial electrodes**			
		pSQI	**basSQI**	**Peak PSD_{noise} (mW/Hz)**	**f_{PSD}**	**pSQI**	**basSQI**	**Peak PSD_{noise} (mW/Hz)**	**f_{PSD}**
Yawning	-0.5933	0.6891	0.9822	275.30	0.217	0.7409	0.9614	56.50	0.333
Deep Breath	-0.2530	0.6857	0.9900	23.8	0.273	0.7587	0.9860	27.5	0.3270
Sideways	-1.1300	0.6980	0.9932	20.4	0.5820	0.7580	0.9701	137.0	0.5270
Up	-1.5730	0.6781	0.9944	17.1	0.6000	0.7370	0.9447	262.3	0.5820
Sitting / standing	-1.0940	0.7001	0.9953	13.7	0.582	0.7439	0.9581	94.7	0.4360
Stairs	-0.9800	0.7070	0.9926	15.18	0.6833	0.7376	0.9733	60.57	0.8833

Note: Peak PSD_{noise} *– the maximum PSD value within the range of f<1Hz;* ***fPSD,*** *the frequency at which the peak PSDnoise occurred;* ***Light blue*** *– low to a moderate level low-frequency noise;* ***Red*** *– intense low-frequency noise;* ***SSR*** *– signal to signal ratio;* ***pSQI*** *– power signal quality index;* ***basSQI*** *- baseline power signal quality index;* ***sideways*** *– moving the hands sideways and moving them back to the midline horizontally;* ***up*** *– raising arms above the head and moving them back;* ***sitting / standing*** *– sitting / standing from a chair;* ***stairs*** *– climbing stairs*

According to Table 6.46, the low-frequency interference was higher within the ECG acquired from the commercial wet-gel electrodes. However, ECG obtained from neither sensor showed signs of increased noise in the QRS complex as the pSQI throughout the experiments fall within the generally accepted range (pSQI = [0.5 0.8]). The fact that most of the SSR values are negative signifies the higher power contained within the ECG collected through the commercial wet-gel electrodes. In this regard, further analysis was conducted to examine if the increased low-frequency motion artefact within the ECGs acquired from the disposable wet-gel electrodes contributed to the higher power. Based on the pSQI and basSQI values, the need for an EMD filter was determined. Similar filtering procedures to those outlined in Figure 6.16 were used to denoise the ECG. Finally, the average ECG power was computed, and the results of the analysis are summarised in Table 6.47.

Table 6.47: Summary of lead-II and V4 ECG power parameters

Body movement / activities	II								
	Wet textile electrodes				Commercial wet-gel electrodes				SSR*
	pSQI	basSQI	P_{av} (mW)	P^*_{av} (mW)	pSQI	basSQI	P_{av} (mW)	P^*_{av} (mW)	
Yawning	0.6891	0.9822	198.1	195.2	0.7409	0.9614	227.1	175.8	0.4546
Deep breathing	0.6857	0.9900	219.7	217.9	0.7587	0.9860	232.9	185.7	0.6945
Sideways	0.6980	0.9932	213.6	212.6	0.7580	0.9701	277.1	210.0	0.0534
Up	0.6781	0.9944	211.5	210.3	0.7370	0.9447	303.8	219.3	-0.1820
Sitting / standing	0.7001	0.9953	280.0	278.6	0.7439	0.9581	360.2	276.0	0.0407
Stairs	0.7070	0.9926	272.8	271.2	0.7376	0.9733	342.3	262.8	0.1366

Body movement / activities	V4								
	Wet textile electrodes				Commercial wet-gel electrodes				SSR*
	pSQI	basSQI	P_{av} (mW)	P^*_{av} (mW)	pSQI	basSQI	P_{av} (mW)	P^*_{av} (mW)	
Yawning	0.7290	0.9754	111.8	86.8	0.7788	0.9421	117.2	89.1	-0.1136
Deep breathing	0.7166	0.9843	117.7	116.5	0.7925	0.9747	110.5	91.6	1.0443
Sideways	0.7484	0.9781	114.1	86.7	0.7950	0.9791	143.7	112.7	-1.1390
Up	0.7418	0.9945	115.5	89.3	0.7839	0.9406	168.3	127.0	-1.5295
Sitting / standing	0.7309	0.9951	142.3	110.3	0.7802	0.9517	171.7	128.4	-0.6599
Stairs	0.7165	0.9906	142.1	141.4	0.7730	0.9665	172.1	135.6	0.1819

***Note: basSQI** – baseline-power signal quality index; **pSQI** – power signal quality index; P_{av} – **P_{av} -** average ECG power, P^*_{av} – the average total power within the ECG signal less the low and high-frequency noise power; $SSR^* = 10*\log_{10}(P^*_{avTextile} / P^*_{avCommercial})$, SSR based on P^*_{av}; **Light blue** – low to a moderate level low-frequency noise; **sideways** – moving the hands sideways and moving them back to the midline horizontally; **up** – raising arms above the head and moving them back; **sitting / standing** -– sitting / standing from a chair; **stairs** – climbing stairs*

Looking at Table 6.47, the textile ECGs (ECG from 60mm^2 textile electrodes) showed higher basSQI values compared to the ECGs from the disposable wet-gel ECG electrodes for a given body movement and activities of daily living. The fact that the denoising algorithm (EMD filter) profoundly affected the magnitude of the average power within the commercial wet-gel sensors indicates an increased noise artefact.

After the low and high-frequency motion artefacts were removed, the ECG from the textile electrodes resulted in a slightly higher power, and hence an improved SSR against the ECG acquired from the conventional commercial ECG sensors. Figure 6.19 illustrates the time-domain and frequency-domain representation of V4 ECG collected during climbing stairs before and after the noise was suppressed.

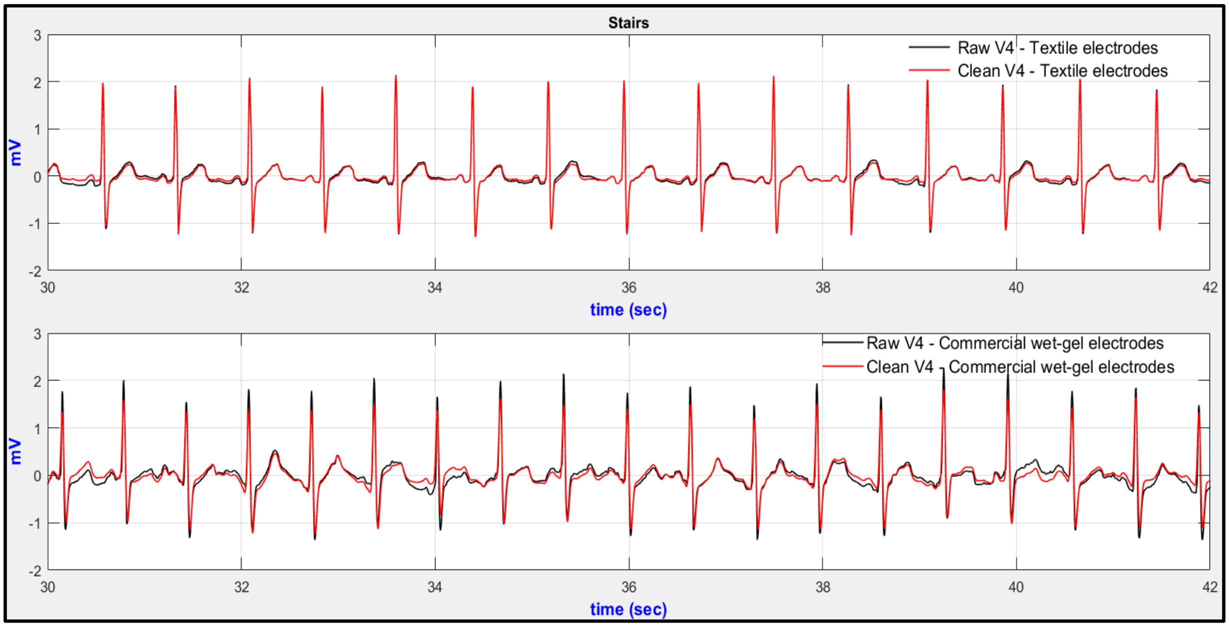

a) Top *– raw (black) and clean (red) V4 ECG from textile electrodes; bottom – raw (black) and clean (red) V4 ECG from commercial electrodes*

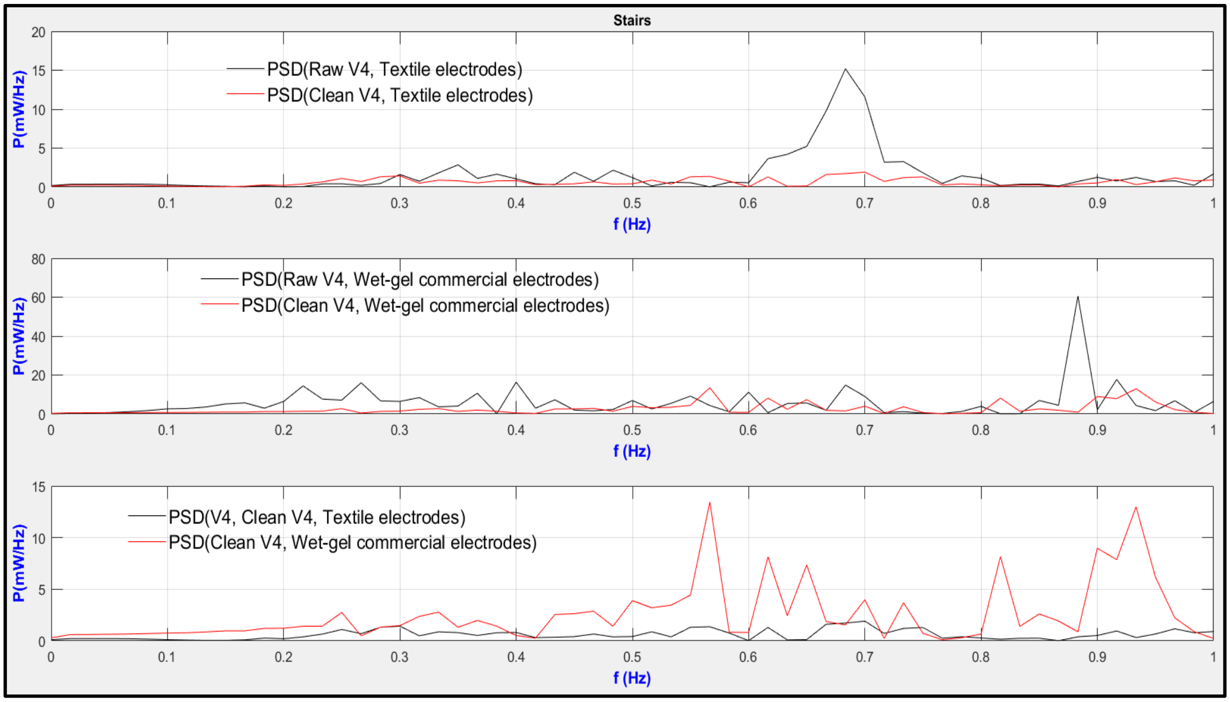

***b) Top** – PSD for the raw (black) and clean (red) V4 ECG from textile electrodes; **middle** – PSD for the raw (black) and clean (red) V4 ECG from commercial electrodes and **bottom** – PSD for the clean V4 ECG from textile electrodes (black) and the clean V4 ECG from commercial electrodes (red)*

Figure 6.19: Comparison of raw and clean V4 ECG acquired during climbing stairs; a) time-domain and b) frequency-domain representation.

As can be seen from Figure 6.19, the V4 ECG from the commercial ECG sensors showed a higher noise in the low-frequency spectrum (f<1Hz).

6.6.2.4. Discussion

ECG was collected from the textile electrodes and the commercial wet-gel electrodes. Considering resting ECG, the disposable wet-gel electrodes and the 60mm^2 textile electrodes yielded relatively similar results. The 70mm^2 textile electrodes resulted in higher power content and lower-approximate entropy.

ECG collected during body movements and daily activities were based on the 3mm thick, $60mm^2$ textile electrodes. Compared to the disposable wet-gel electrodes, the textile electrodes showed decreased low-frequency noise (higher basSQI, Table 6.46). However, ECG from the commercial ECG sensors resulted in a higher power. The pSQI values from the disposable ECG sensors were higher and near to the maximum threshold value (pSQI max = 0.8) that signals the possibility of increased motion artefact within the QRS complex.

Previous studies support these results. In a similar study, Pani et al. (2015) compared the performance of wet textile electrodes with commercial wet-gel electrodes during resting and under motion. Evaluating the collected ECG based on a QRS detector, the authors reported that the ECG from wet textile electrodes resulted in better outcomes compared to the ECG from the commercial silver / silver chloride gel electrodes.

In another study, (Marozas et al., 2011) compared textile electrodes and commercial silver / silver chloride gel electrodes during exercise ECG. The authors reported that the textile electrodes showed higher baseline drift, while the ECG from commercial silver / silver chloride gel electrodes exhibited an increased estimate of the broadband noise power spectrum.

6.6.3. Conclusion

In conclusion, wetting the textile electrodes for instance, during sweating, increased ECG signal quality acquired from the textile electrodes. Therefore, the textile electrodes could be ideal candidates to acquire ECG especially for long-term ambulatory monitoring of cardiac patients.

The ECG from the commercial wet-gel electrodes showed an increased low-frequency noise, and hence slightly lower basSQI values that might be a result of the unstable skin-electrode interface due to a pull from the smart ECG vest under motion. In the case of the textile electrodes, the relatively larger surface area compared to the commercial wet-gel sensors might guarantee adequate skin-electrodes contact under an increased pull from the vest. Moreover, the textile electrodes were not fixed. Therefore, the textile electrodes had a relative degree of freedom of movement to adjust accordingly to the pulling of the smart ECG vest and to follow the change within the underlying anatomy.

6.7. Comparison between the proposed textile-based ECG monitor and the commercial Holter monitor

6.7.1. Specific Objective

This section aims to address Research Question 5: is there a significant difference in performance between the proposed textile-based ECG monitor and the traditional Holter monitor when ECG is acquired during different body movements and activities of daily living? The specific objective of the study was to compare the performance of the proposed e-textile based ECG monitor against the traditional Holter monitor.

6.7.2. Methods

6.7.2.1. Data collection

ECG was acquired simultaneously from the proposed e-textile 12-lead ECG monitor and from a reference standard 3-leads Holter monitor (SEER light ambulatory ECG from General Electric). The SEER light Holter monitor operator’s manual was utilized to place the seven electrodes as outlined in the 'preparing the patient' section. According to the user’s documentation, channel one is the reference lead and used to acquire modified V5 (mV5), and a modified V1 (mV1) is obtained through channel two. It is possible to collect either modified V3 (mV3), modified aVF (maVF), or modified Z (mZ) ECG based on the lead placement connected to channel three (GE Healthcare, c2009). The modified maVF arrangement was selected as the lead placement during the maVF ECG does not coincide with any of the EASI ECG electrode positions.

The experiment was divided into two phases. During the first stage, the volunteer performed i) coughing, ii) deep breathing, iii) sideways (shoulder adduction-abduction – moving the hands sideways and moving them back to the midline horizontally) and iv) up (shoulder flexion-extension – raising arms above the head and moving them back). In the latter phase, i) sitting, ii) sitting / standing from a chair, iii) lying on a bed, iv) making a call from a mobile phone, and v) walking up and down on stairs were performed. On top of the five minutes resting ECG (during sitting on a chair), two minutes of ECG were collected for the respective body movements and daily activities. Before the start of each experiment, the subject was rested for two minutes of recovery time to minimize the influence of the previous stage on the ensuing test.

6.7.2.2. Holter ECG pre-processing

Upon completion of the experiments, the ECG collected from the SEER Holter monitor was exported to MIT Signal Format. The data were then converted to an excel file (CSV UTF comma delimited - *.csv) and Text (Tab delimited - *.txt) format using a MATLAB script for ease of manipulation. According to the header file, the ECG from the Holter monitor was recorded at 125Hz. However, the proposed textile ECG monitor has a recording frequency of 200 samples per second. Therefore, the Holter EC was resampled to match the 200Hz rate.

To retain as much low-frequency noise as possible while removing the DC offset from the inadequate skin-electrode interface and the electrode half-cell potential (Lee and Kruse, 2008), a first-order Butterworth high pass filter (Fc = 0.067Hz) was used to block the zero-frequency interference into the acquired ECG signal.

6.7.2.3. Short term heart rate variability analysis

There is increasing evidence that supports the influence of the autonomous nervous system on the onset of cardiac arrhythmia. HRV analysis has become an essential experimental tool that provides quantitative evidence (Electrophysiology, 1996, Zipes et al., 2019). Therefore, the short-term HRV analysis was used to examine the performance of the proposed textile-based ECG against the traditional Holter monitor.

The calculated HRV values lead to a better understanding of any pathophysiology that may exist (Malik, 1996, Antelmi et al., 2004, Tan et al., 2011, Xhyheri et al., 2012). This study intended to compare the commonly reported HRV parameters from the Holter ECG and the textile-based ECG monitor. Both linear (mean RR – the mean of the RR intervals (ms), STDRR / STDNN - Standard deviation of all normal RR intervals (ms), RMSSD - Root mean square of successive RR interval differences (ms), STDHR – standard deviation of instantaneous HR values (bpm), TP – Total power (ms^2), LF - Power in LF range (ms^2), HF - Power in HF range (ms^2), LF:HF - Ratio LF [ms^2]/HF[ms^2]) and nonlinear (SD1 - Poincaré plot standard deviation perpendicular to the line of identity (ms) and SD2 - Poincaré plot standard deviation along the line of identity (ms)) HRV parameters were used. A good match is achieved when the percentage difference between the HRV parameters from the commercial ambulatory ECG and the textile-based ECG monitor is ten percent or less. The percentile difference is defined in equation 6.6.

$$
\begin{aligned}
&\mathrm{pD}(\%)=\left|\frac{(H_{hrv}-T_{hrv})}{H_{hrv}}\right|*100 \\
&\textit{Where}, \mathrm{pD} \quad - \text{ percentage difference} \\
&\qquad H_{hrv} - \text{HRV parameter from the reference Holter } \textit{monitor} \\
&\qquad T_{hrv} - \text{HRV parameter from the textile } \textit{ECG monitor}
\end{aligned}
\qquad [6.6]
$$

Frequency domain HRV analysis

Fast Fourier transform (FFT) and Autoregressive (AR) analysis (Malliani et al., 1991, Electrophysiology, 1996) were used during the frequency domain HRV analysis. The MATLAB '*pwelch*' (The MathWorks Inc., c2020b) and '*pyulear*' (The MathWorks Inc., c2020c) functions were utilized to calculate the FFT and AR response, respectively.

6.7.2.4. QRS duration and QT intervals

The clinical relevance of the QRS duration (Shamim et al., 2002, Wang et al., 2008, Gold et al., 2012) and QT intervals (Mandyam et al., 2013, Trinkley et al., 2013, Ambhore et al., 2014, Brieger et al., 2018) to diagnose and predict possible cardiac abnormalities are well-established concepts. Therefore, accurate delineation of the QRS duration and QT intervals were used to compare the performance of the textile-based ECG against the reference Holter monitor.

6.7.2.5. Bland-Altman method

The Bland–Altman method (Brazdzionyte and Macas, 2007, Myles and Cui, 2007, Preiss and Fisher, 2008, Bunce, 2009, Parker et al., 2009, Giavarina, 2015, Doğan, 2018) is used to examine the level of agreement between two models and has been used widely in clinical research. Therefore, the Bland–Altman method was used to investigate the similarity of the measures from the commercial Holter monitor to the proposed textile-based ECG monitor.

6.7.3. Results

6.7.3.1. Visual inspection

Twelve seconds of representative ECG strips from the Holter and textile-based ECG are presented in Figure 6.20. Increased body movement (e.g., sitting / standing) forced the ECG to drift away from the isoelectric line. However, the ECG traces alone are not enough to compare the signal quality. Therefore, it is imperative to extend the results of the temporal plot to a more comprehensive time and frequency domain analysis.

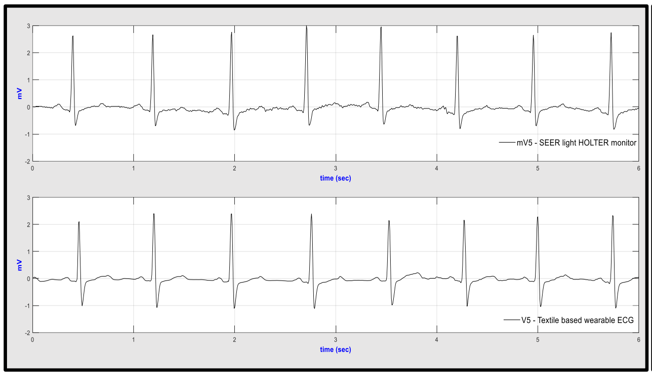

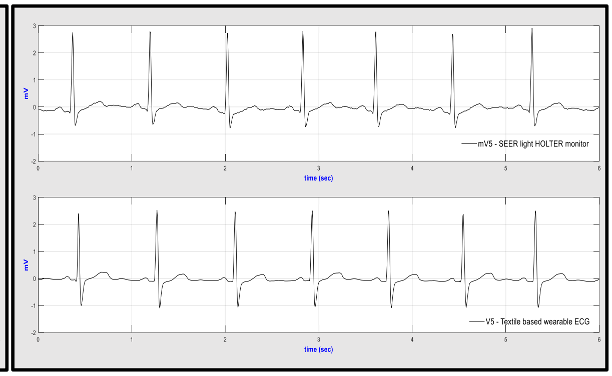

a) ***Deep breathing*** *(top – ECG from the Holter monitor and bottom – ECG from the proposed textile-based ECG monitor)*

b) ***Up movements*** *- (top – ECG from the Holter monitor and bottom – ECG from the proposed textile-based ECG monitor)*

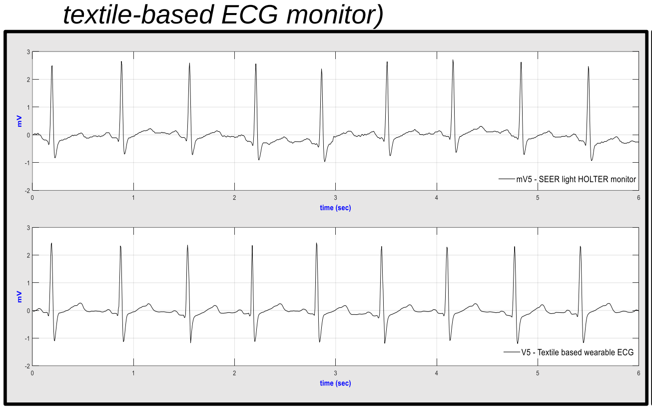

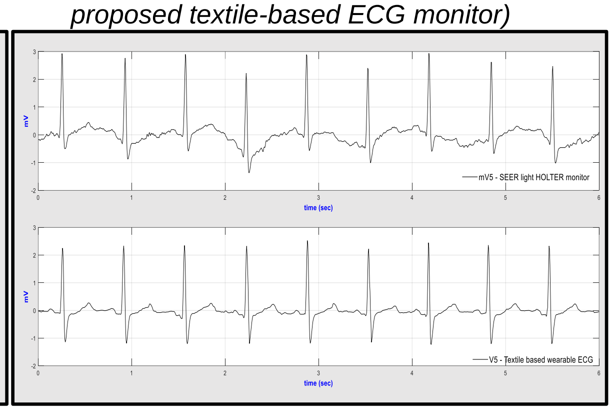

c) ***Sitting / standing from a chair*** *(top – ECG from the Holter monitor and bottom – ECG from the proposed textile-based ECG monitor)*

d) ***Climbing stairs*** *(top – ECG from the Holter monitor and bottom – ECG from the proposed textile-based ECG monitor)*

Figure 6.20: Sample ECG traces from the reference Holter monitor and the textile-based ECG monitor.

6.7.3.2. ECG power characteristics and Signal quality indexes

Table 6.48 compares the quantitative signal quality parameters. The power contents within the Holter monitor are higher for the entire experiments except for deep breathing (-0.3734dB). Conversely, the Holter ECG revealed an increased interference in the low-frequency region of the ECG acquired, especially during sitting / standing activities (*basSQI = 0.8067*), lying on a bed (*basSQI = 0.8687*), climbing stairs (*basSQI = 0.8874*) and making a phone call from a mobile phone (*basSQI = 0.9325*). The significantly higher ApEn values of the ECGs from the reference ambulatory monitor (Table 6.49) supported the increased randomness of the Holter ECGs compared to the ECGs from the proposed textile-based ECG monitor. As an additional measure to examine the frequency response of the collected ECGs in the frequency domain, the PSD in the low-frequency region (F<1Hz), was computed and the results are presented in Table 6.48.

Table 6.48: Comparison of the SSR, PSD and SQI between the reference Holter ECG and ECG from the proposed textile ECG monitor collected during different body movements and activities of daily living.

Body movement / activities	SSR	Reference Holter ECG (mV5)				Textile based ECG (V5)			
		pSQI	basSQI	Peak PSD_N (mW/Hz)	f_{PSD} (Hz)	pSQI	basSQI	Peak PSD_N (mW/Hz)	f_{PSD} (Hz)
Deep Breath	-0.3734	0.6171	0.9818	32.60	0.404	0.6226	0.9898	36.20	0.408
Coughing	0.9772	0.6195	0.9639	171.20	0.667	0.6227	0.9890	72.20	0.675
Sideways	0.4284	0.6287	0.9896	23.00	0.742	0.6273	0.9904	17.10	0.425
Up	0.1170	0.6418	0.9862	69.80	0.400	0.6300	0.9911	15.60	0.417
Sitting	0.4151	0.6354	0.9896	213.60	0.456	0.6403	0.9867	14.00	0.112
A phone call	0.1804	0.6303	0.9300	132.10	0.850	0.6318	0.9920	107.90	0.100
Sitting / Standing	1.0068	0.6229	0.8067	131.80	0.521	0.6161	0.9287	136.60	0.471
Lying on a bed	1.0426	0.6374	0.8687	158.30	0.434	0.6303	0.9924	3.20	0.500
Stairs	1.1038	0.6283	0.8874	127.00	0.742	0.6274	0.9970	8.50	0.742

SSR *– signal to signal ratio;* ***SSR = 10*log10(P_{Holter}/$P_{Textile}$);*** ***ApEn –*** *approximate entropy;* ***pSQI –*** *power signal quality;* ***basSQI –*** *baseline power signal quality;* ***Peak PSD_N*** *– the maximum noise PSD within the low-frequency range* ***f<1Hz; f_{PSD}*** *– the frequency at which the max noise PSD occurred;* ***Light blue*** *– low to a moderate level low-frequency noise;* ***Red –*** *intense low-frequency noise*

Body movement / activities	bSQI – Reference Holter ECG (mV5)				bSQI –Textile based ECG (V5)			
	F1PS	F1PM	F1SM	F1(F1PS|F1PM|F1SM)	F1PS	F1PM	F1SM	F1(F1PS|F1PM|F1SM)
Deep Breath	1.0	0.9985	0.9985	1.0	1.0	1.0	1.0	1.0
Coughing	1.0	1.0	1.0	1.0	1.0	1.0	1.0	1.0
Sideways	1.0	1.0	1.0	1.0	1.0	0.9967	0.9967	1.0
Up	1.0	1.0	1.0	1.0	1.0	1.0	1.0	1.0
Sitting	1.0	1.0	1.0	1.0	1.0	0.9981	0.9981	1.0
A phone call	0.9816	1.0	0.9816	1.0	0.9940	0.9940	1.0	1.0
Sitting / Standing	0.9936	1.0	0.9936	1.0	0.9937	0.9937	1.0	1.0
Lying on a bed	1.0	1.0	1.0	1.0	1.0	1.0	1.0	1.0
Stairs	0.9938	1.0	0.9938	1.0	1.0	1.0	1.0	1.0

Note: pSQI – *power signal quality index;* ***basSQI -*** *baseline power signal quality index;* ***bSQI*** *– beat detection signal quality,* ***F1*** *– bSQI score based on matched detection of the RR-intervals between the two peak detection algorithms;* ***F1PS*** *– F1 score based on the Pan-Tompkins Algorithm and RST State-Machine algorithm,* ***F1PM*** *– F1 score based on the Pan-Tompkins Algorithm and MTEO algorithm,* ***F1SM*** *– F1 score based on the RST State-Machine algorithm vs. MTEO algorithm;* ***sideways*** *– moving the hands sideways and moving them back to the midline horizontally;* ***up*** *– raising arms above the head and moving them back;* ***sitting / standing*** *– sitting / standing from a chair;* ***stairs*** *– climbing stairs*

Table 6.49: ApEn statistical summary of ECG acquired from the reference Holter monitor and the Textile based ECG monitor.

Body movement / activity	ApEn Descriptive Statistics				ApEn Test Statistics	
	Holter monitor		Textile based ECG		Holter Vs. Textile based ECG	
	Mean±SD	50th Percentiles (Median)	Mean±SD	50th Percentiles (Median)		
Deep Breath	0.1385±0.0245	0.1383	0.1268±0.0126	0.1263	Z	-3.0461
					p	0.0023*
Coughing	0.1590±0.0197	0.1616	0.1328±0.0093	0.1319	Z	-5.9298
					p	0.0000*
Sideways	0.1665± 0.0520	0.1492	0.1459±0.0329	0.1341	Z	-2.6263
					p	0.0086
Up	0.1138±0.0114	0.1123	0.1097±0.0063	0.1107	Z	-1.4464
					p	0.1480
Sitting	0.1294 ±0.0274	0.1171	0.1143±0.0102	0.1116	Z	-2.8616
					p	0.0042*
A phone call	0.1842± 0.0191	0.1885	0.1244±0.0156	0.1225	Z	-6.0356
					p	0.0000*
Sitting / standing	0.1803±0.0353	0.1674	0.1400±0.0184	0.1378	Z	-5.9341
					p	0.0000*
Lying on a bed	0.1442±0.0222	0.1417	0.1126±0.0052	0.1147	Z	-6.0368
					p	0.0000*
Stairs	0.17871±0.0224	0.1804	0.1268±0.0126	0.1263	Z	-6.0318
					p	0.0000*

***Note: ApEn** – approximate entropy; **sideways** – moving the hands sideways and moving them back to the midline horizontally; **up** – raising arms above the head and moving them back; **Sitting** – Sitting on a chair, **sitting / standing** – sitting / standing from a chair; **stairs** – climbing stairs; * – statistically significant*

As there was no significant nose induced within the QRS complexes that corrupt the ECG signal (Table 6.48), the PSD was focused on the low-frequency spectrum (f<1Hz). The PSD analysis (Table 6.48) further confirmed the higher baseline drifts within the reference Holter monitor during the two activities (lying on a bed and climbing stairs) compared to the ECG acquired from the proposed textile-based ECG monitor during the same sequence of body movements. However, the PSD analysis of ECGs collected during sitting / standing from a chair showed comparable noise levels in the low-frequency spectrum of both systems (the reference Holter monitor and the textile-based ECG monitor).

Therefore, an EMD based selective filter (Figure 6.16) was used to denoise the signals. Once the ECGs from the reference ambulatory monitor and the textile-based ECG monitor were passed through an EMD based selective filter, the signal quality indexes (pSQI and basSQI), the average power and the SSR were computed again (Table 6.50).

Table 6.50: Summary of ECG power characteristics

Body movement / activities	Holter Monitor (mV5)				Textile Based ECG (V5)				SSR*
	pSQI	basSQI	P_{av} (mW)	P^*_{av} (mW)	pSQI	basSQI	P_{av} (mW)	P^*_{av} (mW)	
Deep Breath	0.6171	0.9818	170.4	167.7	0.6226	0.9898	185.7	183.8	-0.3981
Coughing	0.6195	0.9639	213.9	211.5	0.6227	0.9890	170.8	169.9	0.9512
Sideways	0.6287	0.9896	183.1	181.3	0.6273	0.9904	165.9	164.6	0.4197
Up	0.6418	0.9862	165.6	163.7	0.6300	0.9911	161.2	159.8	0.1047
Sitting	0.6354	0.9896	115.2	114.0	0.6403	0.9867	104.7	103.4	0.4151
A phone call	0.6303	0.9300	184.3	125.2	0.6318	0.9920	176.8	175.6	-1.4692
Sitting / Standing	0.6229	0.8067	237.3	140.5	0.6161	0.9287	188.2	129.1	0.3675
Lying on a bed	0.6374	0.8687	205.7	133.8	0.6303	0.9924	161.8	160.5	-0.7902
Stairs	0.6283	0.8874	235.7	153.1	0.6274	0.9970	182.8	182.4	-0.7605

Note: basSQI *– baseline-power signal quality index;* ***pSQI*** *– power signal quality index;* P_{av} *– average ECG power,* P^*_{av} *– the average total power within the ECG signal less the lower and high-frequency noise power;* ***SSR**** $= 10*\log_{10}(P^*_{av\_Holter} / P^*_{av\_Text})$*, SSR based on* P^*_{av}*,* ***Red –*** *intense low-frequency noise,* ***Light blue –*** *low to moderate level of baseline wander,* ***Yellow –*** *significant difference between the* P_{av} *and* P^*_{av}*;* ***sideways*** *– moving the hands sideways and moving them back to the midline horizontally;* ***up*** *– raising arms above the head and moving them back;* ***sitting / standing*** *– sitting / standing from a chair, and* ***stairs*** *– climbing stairs*

Referring to Table 6.50, the average power from the Holter monitor during a phone call, sitting / standing from a chair, lying on a bed, and climbing stairs was reduced once the EMD based selective filter was applied. The power contained within the ECG from the textile ECG monitor during sitting / standing from a chair was Appendix J presents the IMFs of the EMD decomposed ECG from the Holter monitor acquired during sideways movement. The basSQI values presented in Table 6.51 revealed that the filtering techniques applied reduced the low-frequency interference and improved the baseline-power signal quality index.

Table 6.51: Comparison of the ***basSQI*** before and after the ***EMD*** based selected filter.

Body movement / activities	Holter Monitor (mV5)			Textile Based ECG (V5)		
	basSQI	basSQI*	pD(%)	basSQI	basSQI*	pD(%)
A phone call	0.9300	0.9988	7.39	0.9920	0.9920	0
Sitting / Standing	0.8067	0.9857	22.19	0.9287	0.9813	5.66
Lying on a bed	0.8687	0.9953	14.57	0.9924	0.9924	0
Stairs	0.8874	0.9963	12.27	0.9970	0.9970	0

Note: basSQI** – baseline-power signal quality index; **basSQI – baseline-power signal quality index of the clean ECG; **pD** – the percentage difference, **Red** – intense low-frequency noise; **Light blue** – low to moderate level of baseline wander*

On the other hand, the power analysis (power quality index, pSQI) presented in Table 6.48 showed that the pSQI of the ECG collected from the reference ambulatory ECG and the textile ECG fall within the accepted ranges (pSQI >=0.5 and pSQI <=0.8). Moreover, the bSQI F1 scores were calculated by taking the higher values returned, comparing the three peak-detection algorithms (Pan-Tompkins Algorithm, RST State-Machine algorithm and MTEO algorithm). As a result, the bSQI analysis displayed a 100% delineation rate of the QRS complexes in both ECG monitors for all activities.

6.7.3.3. Short term HRV analysis

There is increasing evidence that supports the influence of the autonomous nervous system on the onset of cardiac arrhythmia. HRV analysis has become an essential experimental tool that provides quantitative evidence (Electrophysiology, 1996, Zipes et al., 2019). Therefore, the short-term HRV analysis was used to examine the performance of the proposed textile-based ECG against the traditional Holter monitor.

Table 6.52 summarizes the short-term HRV analysis results based on ECGs acquired from the Holter monitor and the proposed textile-based wearable ECG monitor. Despite the increased number of studies on HRV, the accepted values for "normal/abnormal" diagnosis remains unsolved. Nunan et al. (2010) and Dantas et al. (2018) reported the normative values for some of the commonly reported short-term HRV parameters and are used as a baseline. In a systematic quantitative review, Nunan et al. (2010) mapped the available evidence and summarised the normal range of HRV values. Regarding Dantas et al. (2018), the authors conducted a longitudinal study on healthy adults in Brazil and proposed an age-dependent reference short-term HRV values based on 10 minutes resting ECG. For comparison purposes, the minimum and maximum values were defined based on the 2.5th and 97.5th percentile of the HRV parameters, respectively.

Table 6.52: Summary of the commonly reported HRV measures based on the Holter and textile-based ECG (AR model order = 16). Suggested normal values based on previous study (Nunan et al., 2010): mean RR = 785 – 1,160 (ms); STDNN = 32 – 93(ms); RMSSD = [19 – 75](ms); LF = [193 – 1,009](ms^2); HF = [82 – 3,630](ms^2);and LF:HF = [1.1 – 11.6]; and (Dantas et al., 2018): mean HR = [50 – 86](1/min).

Body movement / activity	HRV Measures	Holter monitor	CV	Textile based ECG	CV	pD (%)
Deep breathing	Mean RR (ms)	717*		711.6*		0.75
	STDRR(STDNN) (ms)	52.5	7.32	52.9	7.37	0.76
	RMSSD (ms)	21.9	-	23	-	5.02
	Mean HR (1/min)	84.6		85.2		0.71
	STD HR (1/min)	6.1	7.21	6.3	7.39	3.27
	TP (ms^2)	1315		1322		0.53
	LF [0.04 0.15] Hz (ms^2)	325		331		1.84
	HF [0.15 0.4] Hz (ms^2)	120		129		0.77
	LF: HF	2.7083		2.5659		5.25
	SD1 (ms)	15.2		16.0		5.26
	SD2 (ms)	71.8		72.9		1.53
Coughing	Mean RR (ms)	750.4*		744.7*		0.76
	STD RR(STDNN) (ms)	47.9	6.38	47.5	6.37	0.83
	RMSSD (ms)	29.5		29.8	-	1.01
	Mean HR (1/min)	80.7		81.3		0.74
	STD HR (1/min)	5.2	6.44	5.3	6.51	1.92

Body movement / activity	HRV Measures	Holter monitor	CV	Textile based ECG	CV	pD (%)
	TP (ms^2)	1049		998		4.86
	LF [0.04 0.15] Hz (ms^2)	617		614		0.48
	HF [0.15 0.4] Hz (ms^2)	201		189		5.97
	LF: HF	3.0697		3.2487		5.83
	SD1 (ms)	21.6		21.0		2.77
	SD2 (ms)	64.2		63.6		0.93
Sideways	Mean RR (ms)	806.9	8.44	790.3	8.44	2.05
	STD RR(STDNN) (ms)	68.1		66.7		2.05
	RMSSD (ms)	33.6		33	-	1.78
	Mean HR (1/min)	75.3	8.36	76.9	8.32	2.14
	STD HR (1/min)	6.3		6.4		1.58
	TP (ms^2)	2195		2066		5.87
	LF [0.04 0.15] Hz (ms^2)	861		812		5.69
	HF [0.15 0.4] Hz (ms^2)	165		151		8.48
	LF: HF	5.2182		5.3775		3.05
	SD1 (ms)	23.9		22.9		4.18
	SD2 (ms)	93.1		91.1		2.14
Up	Mean RR (ms)	848.5	6.70	841.3	6.63	0.84
	STD RR(STDNN) (ms)	56.9		55.8		1.93
	RMSSD (ms)	34.4		34.6	-	0.58
	Mean HR (1/min)	71.5	6.99	72.2	6.78	0.97
	STD HR (1/min)	5		4.9		2
	TP (ms^2)	1467		1365		6.95
	LF [0.04 0.15] Hz (ms^2)	692		648		6.36
	HF [0.15 0.4] Hz (ms^2)	127		124		2.36
	LF: HF	5.4488		5.2258		4.09
	SD1 (ms)	23.1		23.5		1.73
	SD2 (ms)	77.3		75.4		2.45
Sitting	Mean RR (ms)	860.1	5.65	853.3	5.61	0.79
	STD RR(STDNN) (ms)	48.6		47.9		1.44
	RMSSD (ms)	39.7		39.9	-	0.50
	Mean HR (1/min)	70.4	5.68	71.1	5.62	0.99
	STD HR (1/min)	4.0		4.0		0
	TP (ms^2)	3806		3732		1.94
	LF [0.04 0.15] Hz (ms^2)	913		940		2.95
	HF [0.15 0.4] Hz (ms^2)	166		170		2.41
	LF: HF	5.5		5.5294		0.53
	SD1 (ms)	24.8		26.5		6.85
	SD2 (ms)	130.7		130.1		0.45

Body movement / activity	HRV Measures	Holter monitor	CV	Textile based ECG	CV	pD (%)
Sitting / standing	Mean RR (ms)	753.5*		746.9*		0.87
	STD RR(STDNN) (ms)	99.1**	13.14	98.6**	13.2	0.50
	RMSSD (ms)	31.1		30.8	-	0.96
	Mean HR (1/min)	81.3		82		0.86
	STD HR (1/min)	9.6	11.81	9.7	11.83	1.04
	TP (ms^2)	4402		4533		2.97
	LF [0.04 0.15] Hz (ms^2)	1372**		1321**		3.71
	HF [0.15 0.4] Hz (ms^2)	247		252		2.02
	LF: HF	5.5547		5.2421		5.62
	SD1 (ms)	25.1		24.6		1.99
	SD2 (ms)	137.8		145.2		5.37
Lying on a bed	Mean RR (ms)	835.9		823.9		1.43
	STD RR(STDNN) (ms)	53.2	6.36	51.2	6.21	3.76
	RMSSD (ms)	35.3		37.2	-	4.81
	Mean HR (1/min)	72.5		73.6		1.52
	STD HR (1/min)	4.7	6.48	4.7	6.38	0
	TP (ms^2)	1239		1136		8.31
	LF [0.04 0.15] Hz (ms^2)	686		664		3.20
	HF [0.15 0.4] Hz (ms^2)	268		233		13.06
	LF: HF	2.5597		2.8498		11.33
	SD1 (ms)	27.1		26.3		2.95
	SD2 (ms)	70.5		66.8		5.25
Making a phone call	Mean RR (ms)	722.7*		718.5		0.58
	STD RR(STDNN) (ms)	84.5	11.69	83.8	11.66	0.83
	RMSSD (ms)	31.4		31.3	-	0.32
	Mean HR (1/min)	84.6		85.1		0.59
	STD HR (1/min)	9.8	11.58	9.9	11.63	1.02
	TP (ms^2)	3230		3175		1.70
	LF [0.04 0.15] Hz (ms^2)	858		879		2.44
	HF[0.15 0.4]Hz (ms^2)	208		233		12.02
	LF: HF	4.125		3.7725		8.54
	SD1 (ms)	21.5		22.6		5.11
	SD2 (ms)	116.6		115		1.37
Stairs	Mean RR (ms)	743		742.8		0.02
	STD RR(STDNN) (ms)	74.1	9.97	75	10.09	1.21
	RMSSD (ms)	22.6		24.8	-	9.73
	Mean HR (1/min)	82		82		0
	STD HR (1/min)	7.6	9.27	7.7	9.39	1.31
	TP (ms^2)	2756		2766		0.36
	LF [0.04 0.15] Hz (ms^2)	360		354		1.67

Body movement / activity	HRV Measures	Holter monitor	CV	Textile based ECG	CV	pD (%)
	HF [0.15 0.4] Hz (ms^2)	115		116		0.89
	LF: HF	3.1304		3.0517		2.51
	SD1 (ms)	17.2		18.0		4.65
	SD2 (ms)	104.0		104.9		0.86

Note: STDRR** – standard deviation of the RR intervals; **RMSSD** – The square root mean square of differences between adjacent RR intervals; **HR** – heart rate; **STD HR** – standard deviation of the heart rate; **TP** – Total power; **LF** – low-frequency spectral power; **HF** – high-frequency spectral power; **LF: HF** – the ratio of low-frequency power to high-frequency power; **nu** – normalized units; **CV** – coefficient of variation = (Standard deviation/mean × 100); **SD1** – Poincaré plot standard deviation perpendicular to the line of identity; **SD2** – Poincaré plot standard deviation along the line of identity; **n/a** – not available; **pD** – percentage difference (**pD** = abs(Holter – Textile)/Holter*100%); ** lower than the minimum of the reference value; ****** higher than the maximum of the reference value; **sideways** – moving the hands sideways and moving them back to the midline horizontally; **up** – raising arms above the head and moving them back; **sitting / standing** – sitting / standing from a chair; **stairs** – climbing stairs*

The HRV measures from the proposed textile-based ECG monitor strictly follow the HRV parameters from the reference ambulatory monitor (percentage difference (pD) <= 10%) for all time-domain HRV values (Table 6.52). According to the coefficient of variation, the Holter monitor, and the textile-based ECG showed nearly equal dispersion of the respective RR intervals and the observed HRs (Table 6.52).

In the frequency domain, the percentage difference is lower than 10% except for lying on a bed and climbing stairs. During lying on a bed, the high-frequency component from the Holter ECG was higher, and the LF to HF ratio was lower (Holter ECG: HF = 268ms^2, textile ECG: HF = 233ms^2, pD = 13.06%, and Holter ECG: LF: HF = 2.5597; textile ECG: LF:HF = 2.8498, pD = 11.33%). Conversely, the reference ambulatory monitor scored lower HF power (HF = 208ms^2) compared to the textile ECG monitor (HF = 233 ms^2, pD = 12.02%) while making a phone call activity.

The ECG acquired from the Holter monitor during laying on a bed showed relatively higher LF and HF power. Hence the LF to HF ratio was lower compared to the textile-based

ECG. Looking into the frequency spectrum of the ECG collected during laying on a bed, the ECG from the Holter monitor exhibits higher PSD (f=< 0.4Hz, Figure 6.21).

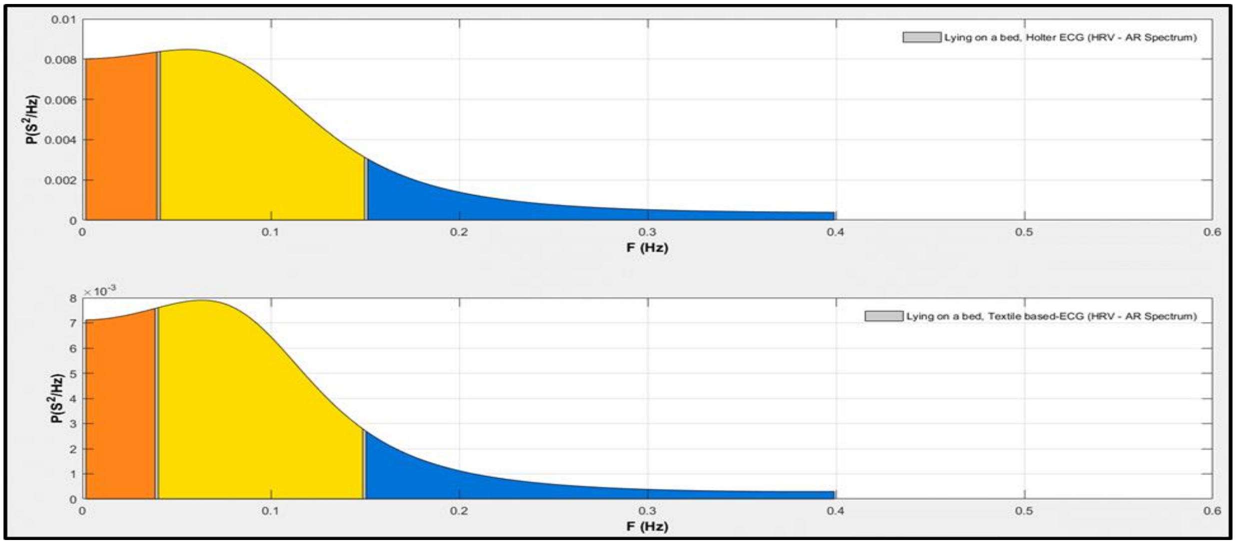

a) AR spectrum, AR model order = 16 (top – Holter ECG and bottom – textile ECG)

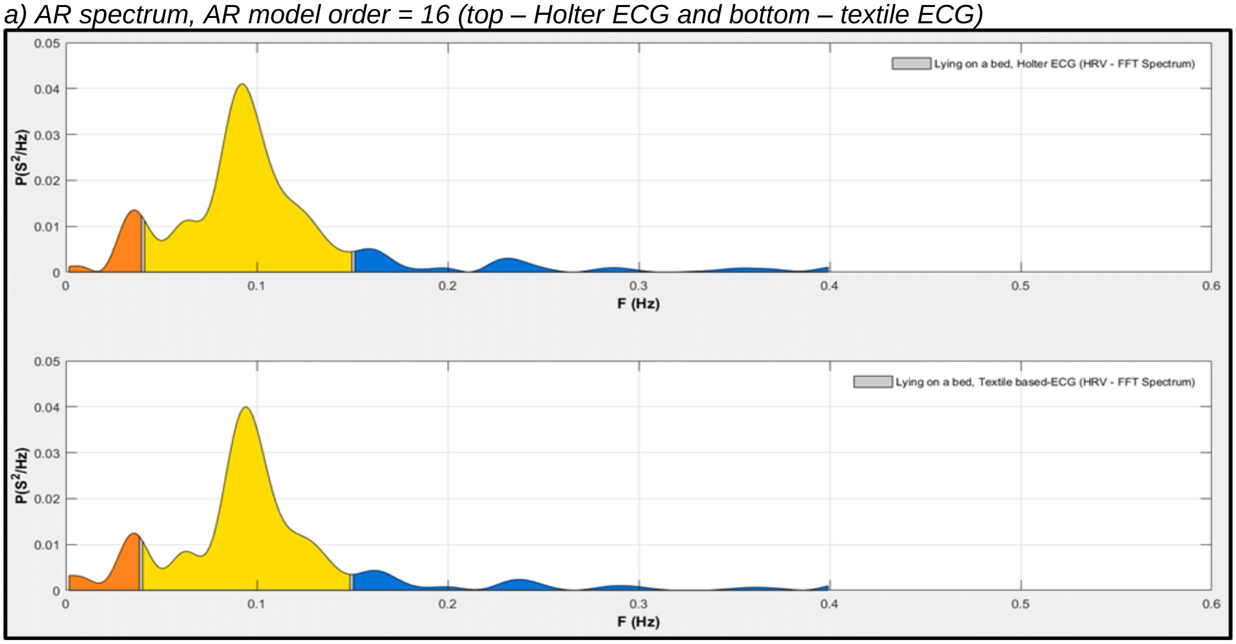

b) FFT, Welch's periodogram: 256 samples window with 50% overlap (top – Holter ECG and bottom – textile ECG)

Figure 6.21: Frequency domain HRV analysis of the ECG acquired while lying on a bed in a supine position (***Red*** – VLF; ***Yellow*** – LF and ***Blue*** – HF).

At the same time, sitting on a chair resulted in a relatively higher power with a pronounced VLF component (Figure 6.22) in both Holter monitor and textile-based ECG monitor (Holter ECG: VLF = 2827ms^2, LF = 913ms^2, LF = 166ms^2; textile ECG: VLF = 2622ms^2, LF = 940ms^2, LF = 170ms^2).

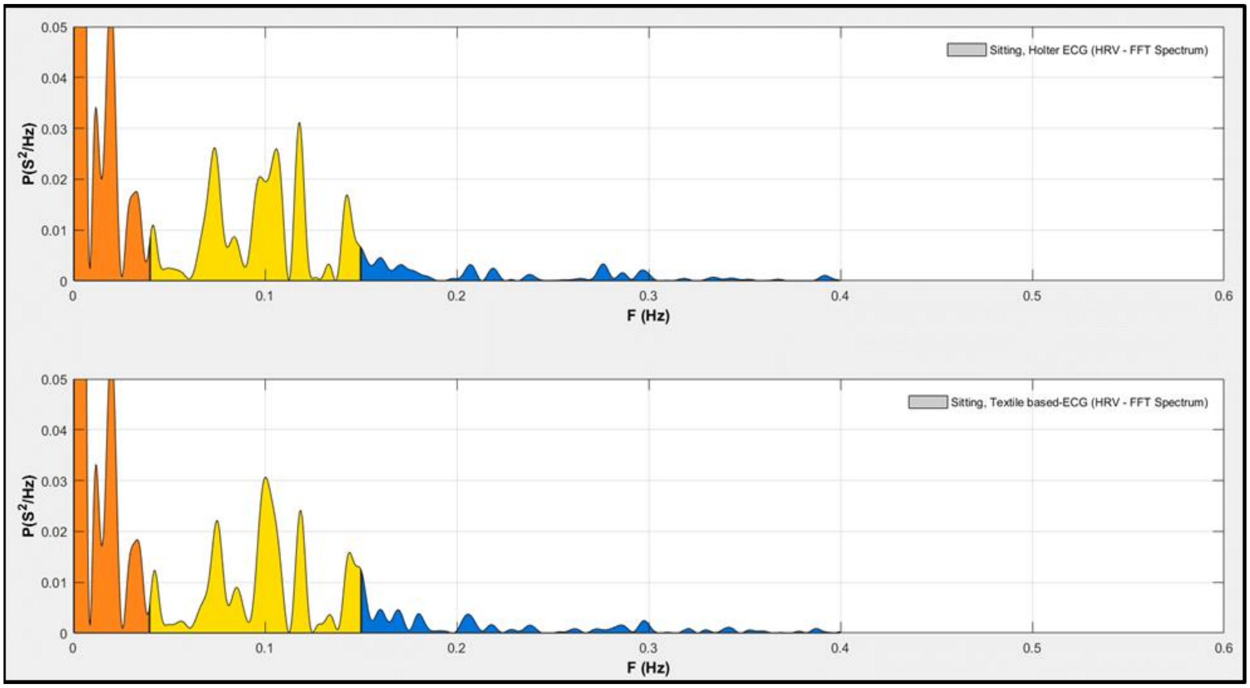

Top – Holter ECG and bottom – textile ECG)

Figure 6.22: Frequency spectrum of the HRV analysis of ECG acquired while sitting on a chair (FFT, Welch's periodogram: 256 samples window with 50% overlap)

The full pictorial representation of the FFT and AR spectrum is presented in Appendix K.

6.7.3.4. QRS duration and QTc intervals

Another time-based ECG analysis used for the diagnosis of cardiac patients is the measurement of QRS duration and QT intervals. The clinical importance of the QRS duration (Iuliano et al., 2002, Shamim et al., 2002, Shenkman et al., 2002, Wang et al., 2008, Gold et al., 2012) and QT intervals (Mandyam et al., 2013, Trinkley et al., 2013, Ambhore et al., 2014, Brieger et al., 2018) to diagnose and predict possible cardiac abnormalities are well-established concepts. In this regard, for an ECG monitor to have a diagnostic application, it should be able to acquire a signal of QRS duration and QT intervals equivalent to the standard ECG (Zipes et al., 2019). In the study, the QRS period and the corrected QT interval (QT_C) were used to evaluate the performance of the textile ECG monitor against the reference Holter monitor. The QT_C was calculated based on the following formula (equation 6.7) (Zipes et al., 2019, p. 125).

$$QTc = \frac{QT}{\sqrt{RR}} \quad [6.7]$$

Table 6.53 summarizes the QRS duration and QTc based on ECG collected from the reference Holter monitor and the proposed textile-based ECG monitor.

Table 6.53: Summary of the QRS duration and QT_C intervals of ECG from the Holter monitor and textile-based ECG monitor during different body movements and activities of the daily living.

Body movement / activities	Reference Holter ECG (mV5)					Textile based ECG (V5)				
	QRS duration		QTc			QRS duration		QTc		
	NQRS	LQRS	NQT_C	SQT_C	LQT_C	NQRS	LQRS	NQT_C	SQT_C	LQT_C
Deep Breath	333	0	332	1	0	333	0	333	0	0
Coughing	159	0	159	0	0	159	0	159	0	0
Sideways	147	0	146	1	0	147	0	146	0	1
Up	140	0	140	0	0	140	0	140	0	0
Sitting	261	1	202	1	58	262	0	261	0	0
A phone call	82	0	79	3	0	82	0	82	0	0
Sitting / Standing	78	0	77	1	0	78	0	77	0	1
Lying on a bed	70	0	70	0	0	70	0	69	1	0
Stairs	160	0	158	0	2	160	0	160	0	0

***Note: QTc** – corrected QT interval, **NQRS** – number of the normal and **LQRS** – short **QRS** durations, **NQT_C** number of the normal, **SQT_C** – short and **LQT_C** – long **QT_C** intervals, respectively*

Regarding the ECG acquired from the Holter monitor while the participant was sitting on a chair, 58 of the 262 QT_C intervals were identified as long QT_C, and one was a short QT_C

interval. However, 261 of the 262 QT_C intervals of the textile-based ECG were detected as normal QT_C intervals. In both the Holter monitor and the textile-based ECG, one QT_C interval was missing (Table 6.53). The ECG was then denoised by the EMD based selective filter (Figure 6.16) to recover the missed T-wave and to ascertain that the long QT_C intervals from the reference Holter monitor were not due to the motion artefact. Once the noise was suppressed, the QT_C intervals were computed again. The 58 QT_C intervals identified as long QT_C within the reference ambulatory monitor were due to motion artefact and hence after the Holter ECG was denoised, all of the 58 long QT_C intervals were classified as normal QT_C. Moreover, the missed T-wave was recovered in both the Holter and textile ECGs. The results are presented in Table 6.54.

Table 6.54: Effect of motion artefact on the ***QTc*** intervals for an ECG collected while sitting on a chair.

Body movement / activities	Reference Holter ECG (mV5)						Textile based ECG (V5)					
	QTc before the selective EMD filter was applied											
	QRS duration		QTc				QRS duration		QTc			
	NQRS	***LQRS***	***NQT$_C$***	***SQT$_C$***	***LQT$_C$***	***Missed***	***NQRS***	***LQRS***	***NQT$_C$***	***SQT$_C$***	***LQT$_C$***	***Missed***
Sitting	261	1	202	1	58	1	262	0	261	0	0	1
Body movement / activities	**QTc after the ECG was denoised using a selective EMD filter**											
	Reference Holter ECG (mV5)						**Textile based ECG (V5)**					
	NQRS	***LQRS***	***NQT$_C$***	***SQT$_C$***	***LQT$_C$***	***Missed***	***NQRS***	***LQRS***	***NQT$_C$***	***SQT$_C$***	***LQT$_C$***	***Missed***
Sitting	262	0	261	1	0	0	262	0	262	0	0	0

Note: QT$_C$ *– corrected QT interval,* ***NQRS*** *– number of the normal and* ***LQRS*** *-short* ***QRS*** *durations,* ***NQT$_C$*** *number of the normal,* ***SQT$_C$*** *– short and* ***LQT$_C$*** *– long* ***QT$_C$*** *intervals, respectively*

6.7.3.5. Bland–Altman analysis

The Bland-Altman analysis was used to evaluate the level of agreement between the ECGs collected from the reference ambulatory Holter monitor and the proposed textile-based ECG monitor. The most commonly reported beat-to-beat measure that has been evaluated using Bland Altman analysis is based on RR intervals (Gamelin et al., 2006, Weippert et al., 2010b) since for ECGs of increased low-frequency noise, detecting the low amplitude ECG waves (P, Q, S and T) is challenging. However, including the P, Q, S, and T waves on top of the dominant R wave in the analysis may provide additional information to augment the comparison.

During the study, the PP, QQ, RR, SS and TT intervals were extracted and imported to the MedCalc® Version 19.0.4.0 (MedCalc Software Ltd). For the individual body movements and daily activities considered in the experiment, a Bland Altman analysis was performed based on the intervals of the respective ECG wave intervals (PP, QQ, RR, SS and TT intervals).

Table 6.55 presents the statistical summary of the mean difference, limits of agreement (95% confidence of interval, CI) and the associated p-values.

Table 6.55: Bland–Altman analysis summary statistics

Body movement / activities	Statistical measures	Method A: Holter monitor; Method B: Textile based ECG				
		ECG wave intervals				
		PP	QQ	RR	SS	TT
Deep breathing	Mean difference	3.26	3.47	3.47	3.49	4.95
	SD of bias	49.95	48.99	48.9552	48.96	64.79
	95% CI limits of agreement	-103.96 and 110.49	-101.58 and 108.53	-101.493 and 108.44	101.49 and 108.46	-133.98 and143.89
	P (H_0: Mean=0)	0.2386	0.1961	0.1957	0.1938	0.1638
Coughing	Mean difference	6.63	6.23	5.28	6.26	6.67
	SD of bias	48.97	44.82	43.38	44.94	56.44
	95% CI limits of agreement	-102.61 and 115.88	-93.63 and 106.08	91.43 and 102.00	-93.87 and 106.38	-119.15 and 132.50
	P (H_0: Mean=0)	0.0926	0.0817	0.1278	0.0810	0.1391
Sideways	Mean difference	16.56	10.72	9.61	11.21	10.95
	SD of bias	172.85	82.12	82.46	79.30	81.33
	95% CI limits of agreement	-371.53 and 404.65	-173.39 and 194.86	-175.54 and 194.76	-166.59 and 189.02	171.65 and 193.57
	P (H_0: Mean=0)	0.2572	0.1191	0.1686	0.0919	0.1119
Up	Mean difference	5.87	2.35	2.35	3.17	7.17
	SD of bias	66.26	72.91	72.85	66.86	53.77
	95% CI limits of agreement	-143.17 and 154.92	-161.43 and 166.15	-161.30 and 166.01	147.02 and 153.38	-113.60 and 127.96
	P (H_0: Mean=0)	0.3011	0.7027	0.7025	0.5747	0.1165
Sitting	Mean difference	7.62	7.22	7.10	7.10	7.15
	SD of bias	77.15	64.94	64.85	64.98	70.71
	95% CI limits of agreement	-166.09 and 181.35	-138.86 and 153.31	-138.70 and 152.90	-139.00 and 153.20	-151.90 and 166.21
	P (H_0: Mean=0)	0.2526	0.1950	0.2005	0.2014	0.2384
Sitting /	Mean difference	-6.18	-6.62	-6.62	-6.62	-3.7013
	SD of bias	204.63	87.51	87.53	87.47	114.11

Body movement / activities	Statistical measures	Method A: Holter monitor; Method B: Textile based ECG				
		ECG wave intervals				
		PP	QQ	RR	SS	TT
standing	95% CI limits of agreement	-487.52 and 475.15	-212.23 and 198.99	-212.29 and 199.05	-212.14 and 198.90	-271.82 and 264.41
	P (H_0: Mean=0)	0.7929	0.5086	0.5087	0.5084	0.7767
Lying on a bed	Mean difference	9.92	11.21	12.04	11.21	11.97
	SD of bias	59.69	52.24	52.58	52.82	68.02
	95% CI limits of agreement	-131.89 and 151.75	-112.57 and 135.00	-112.38 and 136.46	-113.96 and 136.38	-149.00 and 172.94
	P (H_0: Mean=0)	0.1749	0.0769	0.0577	0.0801	0.1426
Making a phone call	Mean difference	5.67	3.02	3.29	3.39	2.90
	SD of bias	276.66	32.66	31.93	32.22	93.52
	95% CI limits of agreement	-641.55 and 652.91	-73.40 and 79.45	-71.34 and 77.92	-72.00 and 78.79	-215.89 and 221.69
	P (H_0: Mean=0)	0.8539	0.4072	0.3533	0.3459	0.7808
Stairs	Mean difference	0.3822	0.59	0.21	0.56	0.5346
	SD of bias	54.17	42.10	41.81	41.73	67.15
	95% CI limits of agreement	-120.42 and 121.18	-93.22 and 94.41	-92.92 and 93.35	-92.42 and 93.56	-149.11 and 150.18
	P (H_0: Mean=0)	0.9297	0.8582	0.9473	0.8644	0.9202

***Note: SD** – standard deviation; **CI** – confidence of interval; **H_0** – null hypothesis*

6.7.4. Discussion

The objective of the research was to design, implement and test a textile-based 12-leads ambulatory ECG of diagnostic quality. The usability of such a system depends on its competitive performance compared to a traditional Holter monitor.

In the pilot study, ECG was collected simultaneously from the SEER light Holter monitor from GE Healthcare and the proposed textile-based ECG monitor. Different techniques were used to assess the performance of the proposed wearable ECG monitor against the traditional Holter monitor, including visual inspection, signal quality indexes, short-term HRV analysis, the study of QRS duration and QT_C intervals and the Bland-Altman analysis.

Visual inspection

The first comparison employed was a visual inspection of the representative ECG tracings. In the time domain plots, there was no significant difference between the ECGs acquired from the Holter monitor and the textile-based ECG monitor. Even from the noisy recording, it was possible to identify the QRS complexes. The main problem seen on the time traces were baseline drift.

ECG power characteristics and Signal quality indexes

To further evaluate the performance of the textile-based ECG monitor, signal quality indexes were computed. For both the textile ECG and the Holter ECGs, the pSQI values fall within the accepted range (pSQI = [0.5-0.8]), which indicates a minimal noise artefact within the QRS complex. The F1 scores of the bSQI were calculated based on three-beat detection algorithms, and a 100% beat detection rate in both the textile-based ECG and Holter monitor was achieved. The SSR values revealed that the textile-based ECG resulted in a lower average power except during deep breathing and a phone call. On the other hand, the ECGs from the Holter monitor showed an increased low-frequency noise, and hence lower basSQI values during a phone call, sitting / standing from a chair, lying on a bed, and climbing stairs.

In summary, compared to the body movements (e.g., deep breathing), the daily activities (e.g., sitting / standing from a chair) resulted in greater low-frequency interference within the ECG acquired from the Holter monitor. The reference ambulatory monitor and the smart ECG vest were used simultaneously. In this regard, for an increased activity like sitting / standing from a chair, the smart ECG vest might be touching the Holter lead wires and hence introducing an increased noise within the Holter ECG.

Short term HRV analysis

Both temporal and frequency-domain parameters were analysed. The comparison was based on a percentage difference. The time-domain parameters showed a lower percentage difference and coefficient of variation for all body movements and activities of daily living. At the same time, there was no significant difference seen regarding the frequency parameters except for a few discrepancies during lying on a bed and making a phone call where the percentage difference was higher than the threshold value (10%). In line with a previous study, coughing and deep breathing resulted in a shorter RR interval and showed an increased HR (Sroufe, 1971, Kotani et al., 2007).

Different studies examine the effect of noise artefact on the estimation of HRV. Both time and frequency domain parameters will be affected (Albrecht and Cohen, 1988, Berntson and Stowell, 1998). The overall impact of increased noise in the low-frequency domain will be a high power within the respective HRV frequency bands.

In the pilot study, coughing (Holter ECG: TP = 1049ms^2, textile ECG: TP = 998ms^2) and deep breathing (Holter ECG: TP = 1315ms^2, textile ECG: TP = 1322ms^2) showed lower total power. The upright position of the volunteer during the experiment might be the reason for the lower TP during deep breathing (Shields Jr, 2009). Conversely, ECG during sitting / standing from a chair, where there was an increased low-frequency interference, resulted in a higher total power (Holter ECG: TP = 4402ms^2, textile ECG: TP = 4533ms^2). The non-linear HRV analysis is another method that provides both quantitative and qualitative beat-to-beat study. It is reported in different studies (Mourot et al., 2004, Gamelin et al., 2006, Libbus et al., 2017, Choi and Shin, 2018). Regarding the quantitative beat-to-beat analysis (SD1 and SD2), there was no significant difference between the ECG acquired from the reference Holter monitor and the proposed textile-based ECG monitor (Table 6.52).

Compared to the normative values proposed by Nunan et al. (2010), the short-term analysis from the reference Holter monitor and the textile-based ECG monitor resulted in a close match. Nevertheless, the HRV analysis of the textile and Holter ECGs acquired during sitting / standing from a chair showed a slightly lower mean RR interval, higher SDNN and higher LF power. No information regarding the participants' characteristics was mentioned in the reference study (Nunan et al., 2010) except the volunteers were healthy and 18 years old and above. However, activity level (Sandercock et al., 2007, Hautala et al., 2010), ethnicity / race (Choi et al., 2006, Hill et al., 2015), the presence / absence of risk factor modifiers (Kupari et al., 1993, Karason et al., 1999, Greiser et al., 2009), gender and age (Zhang, 2007, Koskinen et al., 2009, Voss et al., 2015) contribute to inter-individual variations in the expected short term HRV values. Moreover, the data considered in this preliminary experiment were shorter than the standard five minutes. Therefore, the slight discrepancies between the short-term HRV values from the textile and Holter ECG and the normative short-term HRV values presented in the systematic review might be due to the above reasons.

In summary, the results of the short-term HRV analysis showed that the textile-based ECG was not inferior to the reference Holter monitor.

QRS duration and QTc intervals

The accurate detection of the QRS duration and QT interval is of prime importance for ECG analysis. In this regard, the QRS duration and the QT_C were computed. The results revealed that there was no significant difference between the results of the Holter monitor and the textile-based ECG monitor except for the resting ECG. Regarding the ECG acquired while the participant was sitting on a chair, the textile-based ECG was lightly affected by low-frequency noise and hence showed better performance (99.6% accuracy of QT_C detection rate) compared to the traditional Holter monitor (77.5% accuracy of QT_C detection rate).

Bland–Altman analysis

The data sets showed a lower difference mean, standard deviation and relatively closer limits of agreements. The error from the PP intervals showed more variability (SD = 204.63ms) and wider limits of agreement (95% CI = [-487.52 - 475.15]) during sitting / standing activities. The P-wave is low in amplitude and is easily affected by low-frequency noise. As a result, P-wave detection is prone to error and the correct delineation requires a complex peak detection algorithm. Moreover, the increased low-frequency noise within the Holter ECG might further contribute to the incorrect detection of the R-peaks and hence resulting in a wider limit of agreement compared to the ECG from the proposed textile-based ECG monitor. On the other hand, climbing stairs resulted in the best agreement between the Holter monitor and the textile-based ECG (Table 6.55); minimal difference means, lower deviation, and higher p-values in all of the intervals considered (PP, RR, QQ, SS and TT). The worst agreement was during laying on a bed in terms of mean difference and sitting / standing from a chair considering the wider limit of agreement. The Bland-Altman analysis on the ECG acquired during coughing and lying on a bed resulted in lower p-values.

6.7.5. Conclusion

In conclusion, the performance of the proposed textile-based ECG monitor was compared against a reference ambulatory monitor. The evaluation and testing results presented in section 6.7.3 revealed that the performance of the proposed textile-based ECG monitor is comparable to the reference Holter monitor and therefore the device could be used for ambulatory monitoring of cardiac patients, subject to confirming these observations through a much larger clinical trial on a cardiac population.

6.8. Limitations of the study

Source of errors between the measurements of the reference Holter monitor and the proposed textile-based ECG monitor

Even if the results from the proposed textile-based ECG monitor is acceptable as a pilot study, a further experiment based on a diverse population is imperative for an objective comparison of the proposed e-textile based ECG monitor against the standard ECG. Moreover, there are technical differences between the textile ECG and the reference Holter monitor, including the default data format, the recording frequency, and ECG lead placement. The ECG from the Holter monitor was saved as a SIG/RAW format. The application program that opens the SIG format comes with the Holter monitor is called the MARS system and does not allow further data analysis and manipulation except the GE Healthcare approved reporting format. Therefore, the Holter ECG was converted from the SIG format to the common data formats (.txt and .csv) using MATLAB. The limitation is the lower recording frequency of the Holter monitor (125Hz), while the MATLAB script is designed for a higher sampling frequency, typically 256Hz and above. Moreover, the MATLAB script usually works best with lead-II data instead of modified V5.

Regarding the data rate, the reference ambulatory monitor has a recording rate of 125sps. In contrast, the textile-based ECG records at 200Hz. Therefore, the ECG from the Holter monitor was up-sampled to 200Hz for comparison purposes. However, complete synchronization was not achieved.

Another source of error was the ECG leads considered for comparison. The recommended reference ECG in the traditional Holter monitor is channel one (modified V5). Hence the comparison was between the modified V5 from the Holter monitor and the derived V5 from the proposed textile-based ECG. Therefore, ECGs collected from a different location, mechanism, and input sensors (commercial wet-gel electrodes of the Holter monitor vs. the textile ECG electrodes of the textile-based ECG monitor) might contribute to the discrepancies between the time and frequency domain HRV parameters. Finally, the peak detection algorithm could be an additional source of error that resulted in the broader limit of agreements during the Bland-Altman analysis and variations in the results of the HRV analysis. In a previous study, Weippert et al. (2010a) explained the effect of the peak detection algorithm on short-term HRV. Comparing three ECG RR interval measuring devices, the authors argued that the underlying algorithm used to detect the RR intervals might be the contributing factor for the disagreements seen among the inter-beat intervals acquired from the three ECG devices.

Shorter duration of ECG

The major limitation of the study is that the results were obtained from a single participant over a relatively limited time period. Although ethics approval to collect ECG from healthy volunteers was obtained from the Flinders University Social and Behavioural Research Ethics Committee (SBREC: project code – 8490), the study was limited to only one subject due to the outbreak of the COVID-19 pandemic. Further trials will be required to investigate the effect of subject variability more fully.

The proposed textile-based ECG system is designed for long-term ambulatory monitoring of cardiac patients. Ten different experiments were designed and implemented grouped in to four themes:

- Characteristics of the textile electrodes:
    - Size of textile electrodes: equal size, different size textile electrodes
    - Thickness of textile electrodes
- Vest design and electrode position:
    - Vest design
    - Electrode position: modified AI, modified ES electrodes
    - Electrode attachment
- Electrode condition:
    - Effect of sweating: dry textile electrodes vs wet textile electrodes
    - Textile electrodes vs commercial wet-gel electrodes
- Textile based ECG monitor vs reference Holter monitor.

Approximately seven hours of ECG data were collected (25 minutes of resting ECG + 5 minutes of ECG * (8 activities / experiment) * 10 experiments = 425 minutes or 7 hours and 5 minutes). Further data collection from a diverse population over a longer duration (48 or 72 hours) is imperative for an objective comparison of the proposed e-textile based ECG monitor against the standard Holter monitor.

Clinically, silent ventricular dysrhythmias are the major factors that induce cardiac abnormalities including heart failure, stroke, and cardiac death (Jahrsdoerfer et al., 2005).

Therefore, long-term cardiac monitoring is recommended to record the onset of these silent and infrequent cardiac ischaemic events (Decker et al., 2003). Hingorani et al. (2016) studied 24-hours Holter ECGs from 1273 health volunteers (male =1000; female = 273; age = 18 - 65 years). The authors reported that supraventricular arrhythmias (n = 60.8%) and ventricular arrhythmias (n = 43.4%) were observed compared to the baseline where all participants showed normal screening ECGs. In a similar study, (Grond et al., 2013) compared 24-hour and 78-hour Holter monitoring to detect silent atrial fibrillation based on ECGs from 1135 patients (mean age = 67 ± 13.1 years, 45% women). Higher number of patients were diagnosed with atrial fibrillation from the 72-hours of Holter ECGs (n = 49) compared to the 24-hours Holter ECGs (n = 29). In view of this, the experiments considered in this thesis were conducted for a much shorter duration than the standard 24-hours of Holter ECG. Therefore, as a limitation of the study it was not possible to study or detect the occurrence of infrequent cardiac episodes. Furthermore, the ability of the device to collect and store data over this time period has not been tested.

6.9. Chapter summary

In this chapter, system-level testing and evaluation of the proposed textile-based ECG monitor were described and results were presented.

Regarding the electrode characteristics, the size and thickness of the textile electrodes were considered in the trial. The ECG from $70mm^2$, and 3mm and 5mm thick textile electrodes showed relatively better signal quality. The next factor considered was the electrode placement. Placing the 'A' and 'I' electrodes on the left and right anterior axillary lines, respectively, and the 'E' electrode below the lower sternum resulted in higher signal quality. Compared to the dry textile electrodes, the ECG from the wet textile electrodes showed higher basSQI and lower baseline wander.

The performance of the proposed ECG monitor was compared to the traditional Holter monitor. The temporal plot revealed that the ECG tracing from the textile-based ECG monitor showed lower baseline drift compared to the ECG from the Holter monitor. Referring to the signal quality indexes, the ECG from the Holter monitor showed higher signal power and lower basSQI values. Hence the basSQI values supported the increased low-frequency interference within the Holter monitor. ECGs from the Holter monitor showed significantly higher ApEn compared to the proposed textile-based ECGs. The fact that the pSQI values were within the accepted range (0.5 – 0.8) indicates that there was no increased motion artefact within the ECG acquired from both methods.

The time-domain HRV parameters from the proposed textile-based ECG monitor resulted in a smaller percentage difference (<10%) compared to the ECG from the reference ambulatory ECG. In the case of the frequency domain values, the ECG collected during laying on a bed showed higher discrepancies in the HF power and LF:HF ratio. Referring to the QRS durations and QT_C intervals, there was no significant difference except during sitting on a chair activity where there were 58 long QT_C and one missed QT_C intervals among 262 QT_C intervals from Holter ECG. However, 261 of the 262 from the textile-based ECG was identified as normal QT_C intervals. Therefore, the QT_C detection accuracy of the textile-based ECG monitor (99.6% accuracy of QTc detection rate) was higher compared to the traditional Holter monitor (77.5% accuracy of QT_C detection rate).

According to the Bland-Altman analysis, the worst agreement was during coughing and lying on a bed, where intervals of the respective ECG waves showed a lower p-value. However, the ECG wave intervals during sitting / standing from a chair showed a wider limit of agreements despite the higher p-values. On the other hand, the best agreement was during climbing stairs where the individual ECG waves displayed narrow limit of agreements, lower difference errors and higher p-values.

A limitation of the study is that the results were driven by a single participant. Although an ethics approval to collect ECG from healthy volunteers was obtained from the Flinders University Social and Behavioural Research Ethics Committee (SBREC: project code – 8490), the results have been limited to only one subject due to the outbreak of the COVID-19 pandemics.

This page is left blank intentionally

Chapter 7. Thesis summary and contribution to the field

7.1. Introduction

A twelve-lead electrocardiogram (ECG) is the gold standard for clinical diagnostics of cardiac abnormalities that provides complete information from 12 different leads (viewpoints) (Denes, 1992, Malmivuo and Plonsey, 1995, HEARTe, c2018). The 12-lead ECG has three independent and nine redundant leads assuming the heart as a dipole electrical source (Malmivuo and Plonsey, 1995). The availability of redundant leads is ideal, especially for e-textile based cardiac monitoring, where motion artefact is a common problem reported across numerous studies. Twelve lead ECG has superior dependability and less prone to data loss due to noise and bad electrode-skin contact (Clifford et al., 2006, Di Rienzo et al., 2013). In this regard, the design, construction, and testing of 12-lead equivalent e-textile based ambulatory monitoring based on the EASI electrode configuration (5 electrodes) was presented in the previous chapters of this thesis. In contrast, this chapter presents the overall summary of the thesis. It discusses the limitations of the research and highlights recommendations for future research. Finally, it concludes that *the proposed textile-based EASI 12-lead equivalent ECG monitor could be a viable option for long-term real-time monitoring of cardiac activities, and a clinical trial is recommended based on a population with a known cardiac disease to validate and produce clinically significant results.*

7.2. Thesis summary

Wearable technology and electronic textiles are contemporary fields of research, where their application extends to medicine, rehabilitation, sporting and many more. In the field of rehabilitation, the emergence of smart fabrics and miniaturised electronics has led to the integration of sensors and control system to deliver wearable home-based monitoring of the commonly reported vital signs, including ECG, EEG, EMG, respiration, oxygen saturation, temperature and blood pressure (Angelidis, 2010a, López et al., 2010, Zhang et al., 2011, Löfhede et al., 2012, Lee et al., 2013). In the last two decades, there has been increased research on the application of textiles and wearable technology for the monitoring of cardiac patients. Chapter 2 presented a systematic scoping review conducted to map the available evidence and identify the knowledge gap in electronic textile-based cardiac monitoring.

This scoping review determined that a 12-lead, personalized, HBCR monitor, using fully textile-integrated electronics and circuit wiring with diagnostic capability, has yet to be reported. Even though there has been increased research on e-textile cardiac monitoring, noise artefact remains the major challenge. The scoping review concluded that there is a need for further research into home-based cardiac monitoring. Chapter 3, in this regard, presents the research methodology used to design, develop, implement, and test such a system.

There is a growing demand for continuous follow-up for individual's physiological activities at home or while they are working (Bonato, 2010, p. 25), especially for patients with chronic diseases (Bonato, 2003, p. 18). Moreover, the unprecedented rate at which technology is advancing (Tao, 2001, p. 1, Van Langenhove, 2007, p. 3) together with the increasing possibilities for manufacturing highly miniaturized components to micro and nanoscales, drive increased possibilities for wearable electronics or systems (Bonato, 2003, p. 18).

The remainder of the thesis described the design, analysis, implementation, and testing of a 12-lead diagnostic level textile-based ECG monitor. The work successfully implemented and prototyped a wearable ECG capable of acquiring 12-lead equivalent ECG from an EASI ECG lead system. The system is comprised of miniature ECG hardware, a versatile smart ECG vest and textile electrodes and a Java-based ECG real-time ECG viewer. The ADS129X integrated circuit from Texas Instrument is the best option for low-power high-quality wearable ECG applications as confirmed by previous studies (Zhang et al., 2012, Caldara et al., 2017b) and was used to implement the analogue front end circuit of the ECG hardware.

Multiple wearable ECGs have been proposed with two or more electrodes embedded along with the Mason-Likar electrode placement (Jourand et al., 2010, Morrison et al., 2014, Boehm et al., 2016, Yu et al., 2017) or at new electrode positions (Di Rienzo et al., 2006b, Coyle et al., 2010, Cho et al., 2011, Wang et al., 2015) to acquire ECG. However, ECG collected from a newly electrode placement might require correlation analysis between the acquired ECG and any of the standard 12-lead ECGs to generate clinically relevant data. The smart ECG vest proposed in this thesis is easy to wear and utilizes four textile electrodes placed on well know anatomical landmarks based on the EASI electrode configuration. The 'E' and 'S' electrodes are situated at the bottom and top of the sternum, and the 'A' and 'I' electrodes on the left and right medial axillary lines, respectively.

Both active (Merritt et al., 2009, Paul et al., 2015, Boehm et al., 2016, Dai et al., 2016) and passive (Pola and Vanhala, 2007, Xu et al., 2008, Yapici et al., 2015) textile ECG electrodes are proposed. The former requires integrated circuitry within the textile electrodes and could not be washed repeatedly. The latter is simply made up of conductive fabrics. The passive electrodes were chosen to reduce circuit complexity and power consumption.

Once the electronic textile-based ECG monitor was realized, the next step was testing and evaluating based on prior testing and data analysis protocols. Chapter 5 and Chapter 6 detailed the module level and system-level testing and evaluation of the proposed textile-based ECG monitor. The module-level pilot study presented in Chapter 5 confirmed that the proposed ECG monitor satisfied the general design requirements of a wearable ECG: long term sensors, wireless connectivity, hardware stability for long term applications, comfortable and intuitive design.

The ProSim 3.0 Vital Sign Simulator was used to test the ECG module based on artificial power line interference, respiration noise, variable amplitude and variable heartbeat ECG inputs and finally cardiac abnormalities such as supraventricular arrhythmias, premature contraction of the cardiac chambers and ventricular arrhythmias. The ECG hardware successfully reproduced the applied inputs and cardiac abnormalities as confirmed by the reference CP 200™ 12-Lead Resting Electrocardiograph (Welch Allyn, Inc., Skaneateles Falls, New York). The vest and textile electrodes were subjected to 10 cycles of washing as per section 8.3 of the AS/NZS ISO standard 10535:2011. Washing the vest revealed that the joint connecting the snap fastener and the integrated wires was the weakest point which started to fail after eight washing cycles. This is a result of the wires being soldered to the snap fasteners and becoming hard and brittle due to the intermetallic compounds formed during the soldering process (Tegehall, 2006). An alternative solution could be to integrate the snap fasteners with holes to the vest using conductive thread. Another option would be to use a crimp tool to connect the wires to the snap fasteners and then cover the joints with a heat shrink tube. Regarding the textile electrodes, ten cycles of washing did not alter the mechanical and electrical properties of the textile electrodes sufficiently to produce a noticeable loss of signal quality.

One of the determinant factors for quality ECG transduction using a wearable ECG monitor is the applied pressure that keeps the textile electrodes in place. The minimum and maximum compressive pressure applied by the vest on the user's skin was determined experimentally using FSR sensors ('AI' = [16.0mmHg, 19.3mmHg]; 'S' = [22.7mmHg, 24.4mmHg] and 'E' = [23.8mmHg, 29.4mmHg]). Our results are close to the results reported by Cömert et al. (2013). The authors placed two textile electrodes along the thorax and the reference electrode on the right upper arm using an elastic band. The pressure applied on the upper arm was varied from 5mmHg to 25mmHg and measured by the PicoPress pressure monitor (Microlab, Padua, Italy) while the pressure along the thorax was fixed at 15mmHg. They concluded that the recommended applied pressure for quality ECG transduction is between 15mmHg and 25mmHg. Two main reasons contributed to the difference between our results and the results reported in the study. The first difference was due to the sensors used to measure the applied pressure. The FSR sensors are known to be inaccurate whereas the PicoPress pressure monitor produces accurate pressure measurement results (McLaren et al., 2010, Chi et al., 2018). Moreover, in the previous study (Cömert et al., 2013), the applied pressure variation was applied only on the electrode placed on the upper arm, while in our study the pressure variation affected four of the EASI electrodes. In this regard, it is not possible to compare the results directly.

Chapter 6 presented the prototype testing and evaluation of the proposed textile-based ECG monitor as a system. Several experiments were conducted to evaluate the performance of the textile-based ECG monitor based on a series of body movements and activities of daily living. During the first set of experiments, the effect of the textile electrode characteristics (area and thickness) on signal quality was studied. Marozas et al. (2011) showed that 40mm^2 was the smallest textile electrode area that could be used to acquire ECG without significant distortion. Therefore, three different textile area electrodes (40mm^2, 60mm^2, and 70mm^2) were considered in the experiment. The overall signal quality from the 70mm^2 textile electrodes was better compared to the smaller areas. Another characteristic studied in the experiment was the textile electrode thickness; hence 3mm, 5mm and 10mm thick textile electrodes were considered. Padding is important to distribute the applied compressive pressure evenly across the textile electrode. The 3mm and 5mm textile electrodes showed good quality ECGs; however, increasing the thickness of the textile electrodes to 10mm resulted in decreased ECG quality during body movements and activities of daily living.

The effect of the vest design and textile electrodes to vest attachment on signal quality was studied. Two alternative designs (sECGVest1 and sECGVest2) prototypes were proposed. The difference is the minimal approach used to implement the second vest (sECGVest2). The ECG vests are unisex and adjustable to fit any size. Based on the experiment there was no significant difference in signal quality. Two possible reasons are suggested. First, the minimal approach used to implement the second smart ECG vest (sECGVest2) alone might not be enough to acquire an ECG of significant quality compared to the ECG collected from the first ECG vest (sECGVest1). Second, the data was acquired from one person, and hence, maybe it requires more than a single participant to understand the effect of the vest design on signal quality. Therefore, further clinical trial based on volunteers of different size and gender is recommended to examine the effect of vest design on signal quality.

Three methods to connect the textile electrodes were proposed and the effect on signal quality was studied; removable textile electrodes, textile electrodes taped to the user's skin and embedded textile electrodes into the ECG vest. The taped textile electrodes performed poorly compared to the removable and embedded textile electrodes. No significant quality difference was seen between the removable and embedded textile electrodes. However, the removable textile electrodes increased the versatility of the ECG vest and could be easily replaced. To the best of our knowledge, this is the first study that examined the effect of the three types of textile electrode connections on signal quality.

Another factor affecting long-term textile-based ambulatory monitoring was sweating. Wet textile electrodes (from sweating) were compared to dry counterparts and were found to perform better as the dry textile electrodes drift easily and change position and are susceptible to motion artefact during physical activities. Moreover, the performance of the wet textile electrodes was comparable to that of commercial wet-gel electrodes. Our results are supported by previous studies. Pani et al. (2015) Poly (3,4-ethylene dioxythiophene): poly (styrene sulfonate) textile electrodes to compare the dry textile electrodes, wet textile electrodes, and commercial Ag/AgCl electrodes during different daily activities. The authors showed that the dry textile electrodes performed poorly especially during physical activities. However, the wet textile electrodes were as good as the Ag/AgCl commercial electrodes. When evaluated based on a QRS detector, the wet textile electrodes performed better than the commercial Ag/AgCl electrodes. Marozas et al. (2011) compared the commercial Ag/AgCl electrodes to the wet textile electrodes in exercise ECG. The authors concluded that the textile electrodes showed significant noise in the low-frequency band (0 - 0.67Hz) while textile electrodes are less prone to the broadband noise (0 - 250Hz) compared to the Ag/AgCl electrodes. The results of the low-frequency noise could not be directly applied to our textile-based ECG monitor as we did not experiment on exercise ECG. Also, the authors experimented on three electrodes placed on the thorax area 25cm apart where in our case we used the EASI electrode configuration. However, we believe that the careful design of the analogue front-end component of the ECG hardware could minimize the low-frequency distortion of the signal due to the textile electrodes. Our ECG hardware was carefully designed to minimize such effect and that might be the reason that we did not observe intense low-frequency noise from the wet textile electrodes.

Finally, the performance of the proposed textile-based ECG monitor was compared against the traditional Holter monitor. Channel one (modified V5) from the Holter monitor and the V5 ECG from the textile-based ECG monitor were used to analyse the data. The visual inspection of the temporal plot from the reference Holter monitor showed increased low-frequency noise for increased activities. This was supported by the significantly higher approximate entropy of the ECGs collected from the Holter monitor. In both the Holter monitor and the textile-based ECG monitor the motion artefact within the QRS band (5 – 15Hz) was minimal as confirmed by the power signal quality index values. As a result, the F1 scores of the bSQI were 100% for both the Holter and the textile-based ECGs.

The ability of the proposed system to measure HRV parameters was also assessed. Short-term HRV analysis is becoming a valuable tool to study the effect of the autonomic nervous system on the cardiovascular system (Balocchi et al., 2006). We aimed to implement a diagnosis-level textile-based ECG and hence it is inevitable that the ECG collected from our ECG monitor should be able to generate accurate information based on the HRV analysis. Both time and frequency domain HRV parameters were considered. Based on the analysis results, the HRV parameters from the textile-based ECG monitor closely followed the HRV values from the Holter monitor.

The precise delineation of the QRS duration and QT_C interval is important to detect cardiac episodes. In this regard, the QRS durations and the QT_C intervals were extracted from the Holter ECGs and the textile-based ECGs, and results were compared. Based on the analysis, there was no significant difference between the Holter monitor and the textile-based ECG monitor. However, the textile-based ECG monitor showed higher accuracy compared to the Holter monitor for the ECG collected when the participant was sitting quietly. This might be due to the increased low-frequency noise within the Holter ECG that affected the lower amplitude Q and T waves. The peak detection algorithm might be an additional contributing factor (Weippert et al., 2010a, Marozas et al., 2011). A Bland–Altman analysis was conducted to study the agreements between the ECGs of the Holter monitor and the textile-based ECG monitors. The PP, QQ, RR, SS and TT intervals were extracted from the ECGs and imported to MedCalc® Version 19.0.4.0 (MedCalc Software Ltd). The analysis results revealed that the ECGs during climbing stairs showed the best agreement with a minimum standard deviation of the errors and higher p-values. In conclusion, there was no significant quality difference between the ECG acquired from the textile ECG monitor and the reference Holter monitor.

7.3. Summary of contribution to textile-based cardiac monitoring

The findings of the thesis are relevant to wearable ECG in general and to textile-based ambulatory cardiac monitoring in particular. Summarized below are the key contributions:

(1) Wearable and electronic textile-based ECG is an integrative approach aimed at solving the growing demand for long term ambulatory monitoring. So far, various studies have been conducted on different aspects of the textile-based ECG. In an attempt to identify the knowledge gap and map the available evidence on textile-based cardiac monitoring, a systematic scoping review (Teferra et al., 2019b) was conducted based on a prior protocol (Teferra et al., 2019a).

(2) A miniature ECG hardware capable of acquiring diagnostic level 12-lead equivalent ECG from the EASI configuration (5 electrodes) was proposed, implemented, and tested. The ECG hardware showed an internal noise level of less than 10µVpp at 4V reference voltage and capable of handling all requirements of a wearable ECG.

(3) The focus of the research being textile-based ambulatory cardiac monitoring, a textile-based smart ECG vest based on the EASI configuration and with the following features, was designed, successfully implemented, and tested.

(a) The smart ECG vest is easy to use and could be worn for seamless ambulatory monitoring. The intuitive design will significantly reduce the time needed to train the users. No assistance is required to put on / off the smart ECG vest end therefore, it will also lower diagnosis errors due to misplaced electrodes.

(b) Due to its unique and flexible all in one design concepts, it is possible to accommodate different user groups without the need for a separate smart ECG vest.

(c) As an extra option, the smart ECG vest incorporates a feature that enables the acquisition of diagnostic level 12-lead ECG either from textile electrodes or the conventional wet-gel electrodes.

(d) For the proposed smart ECG vest, the necessary compression pressure for the stable-skin electrode interface was experimentally determined.

(4) Optimal electrodeposition remains an active area of research for quality ECG transduction. In this regard, the best electrodeposition for the EASI configuration was studied where the results could be extended for the traditional EASI lead system ECG. Placing the 'A' and 'I' electrodes on the left and right anterior axillary point respectively, the 'E' electrode slightly lower than the lower sternum (xiphoid process) showed higher signal quality compared to the standard EASI electrode placement.

(5) In a pilot study, the type of connections between the textile electrodes and smart ECG vest and their impact on ECG quality was explored. It recommends that there was no significant signal quality difference between the ECG collected from the removable and the embedded textile electrodes. However, removable textile electrodes are one step ahead as they could be swapped without affecting the integrity of the smart ECG vest. Moreover, the removable textile electrodes increase the flexibility of the proposed smart ECG vest.

(6) The performance of the proposed electronic-textile-based ECG monitor was compared against a traditional reference Holter monitor. The results showed that the textile-based ECG is as good as the reference ambulatory monitor. However, further research based on a diverse cardiac population is recommended to validate and produce clinically significant results.

7.4. Limitations and recommendations

7.4.1. Limitations

The major limitation of the research resulted from the outbreak of the COVID 19. Even though ethics approval was obtained from the Flinders University Social and Behavioural Research Ethics Committee (SBREC: project code – 8490), it was not possible to collect data from participants. Moreover, COVID 19 made the access policy of the Flinders Cardiac centre stricter and the logistics of borrowing the reference Holter monitor and getting the copy of the data took longer. Therefore, the data analysis was restricted to a single participant, and the ability of the proposed textile-based ECG monitor to discriminate against severe arrhythmias, such as sustained ventricular tachycardia from a cardiac population, was not able to be studied. However, the developed ECG hardware successfully reproduced cardiac abnormalities from the Prosim 3.0 Vital Sign Simulator.

7.4.2. Recommendations for further research

The proposed textile-based 12-lead equivalent ECG monitor was developed based on the EASI configuration. There are three distinct modules: the ECG hardware, the smart ECG vest, and the ECG viewer.

The proposed ECG hardware can handle the necessary input-output requirements. However, it could be further miniaturized for seamless integration into the smart ECG-vest.

The smart ECG vest achieved the stable skin-electrode interface through a specially designed hook and loop. For a quality ECG transduction, the applied compression pressure is a crucial factor. In the pilot study, the compression pressure at the respective electrodeposition was experimentally determined based on FSR sensors. In the future, the pressure distribution along the entire length of the Velcro loop and with a more accurate sensor (for example PicoPress® from Microlab, Padua, Italy) needs to be measured, which results in a better approximation of the required pressure.

Additionally, the smart ECG vest prototype is unisex and could be used for both males and females. Therefore, more tests need to be conducted to examine the usability of the vest based on male and female participants of a diverse population.

7.4.3. Recommendations for clinical practice

The pilot study could be useful for medicine, health science and sports where ECG monitoring is essential. In the field of cardiology, long-term ambulatory ECG monitoring is becoming critical to identify the underlying problems for the onset of arrhythmia and stroke (Mathes and Halhuber, 2012, Rosero et al., 2013, Roth et al., 2017a, Teferra et al., 2019b). The pilot study revealed that there was no significant signal quality difference between the traditional Holter monitor and the proposed textile-based ECG monitor. Moreover, the intuitive and straightforward design of the proposed textile-based ECG monitor could bolster the long-term ambulatory monitoring of cardiac patients with increased comfort and minimal description of daily living. The wearable and wireless features augment the usability of the ECG monitor and increase access to CR via telemonitoring. In this regard, further research is suggested to validate these issues; a set of experiments based on healthy volunteers followed by the cardiac population. In the proposed clinical studies, three experimental scenarios could be considered: resting ECG (lying on bed and sitting) for approximately 5 - 10 minutes each, and ambulatory ECG (at casual walking pace) for 10 minutes. Then 24 hours of ambulatory ECG from a standard Holter monitor and the textile-based ECG will be collected, simultaneously. Finally, a survey form could be used to collect information about the user's experience with the smart ECG vest.

7.5. Conclusion

In conclusion, the standard ambulatory monitor utilizes sticky wet-gel electrodes where the ECG quality deteriorates over time due to the drying of the gel-interface. Moreover, the ECG lead wires reduced the comfort of the users. On the other hand, the proposed textile-based ECG monitor has embedded wires and textile electrodes. The smart ECG vest is easy to use and could be worn for seamless ambulatory monitoring. The intuitive design significantly reduced the time need to train the users. Therefore, the proposed textile-based EASI 12-lead equivalent monitor could be a viable option for long-term real-time monitoring of cardiac activities, and a clinical trial is recommended based on a population with a known cardiac disease to validate and produce clinically significant results.

This page is left blank intentionally

Appendices

Appendix A. Search strategy

Ovid MEDLINE(R) Epub Ahead of Print, In-Process & Other Non-Indexed Citations, Ovid MEDLINE(R) Daily, Ovid MEDLINE and Versions(R) <1946 to April 18 2018>

Date of search: initial search 6 September 2017, secondary/follow-up search 29 March 2018

S. No.	Searches
1	Textiles/
2	textile*.tw.
3	(e-textile* or etextile* or textile-based).tw.
4	((smart adj2 fabric) or (smart adj2 fabrics) or (smart adj2 garment*) or (smart adj2 cloth*) or (sensori?ed adj2 garment*) or (conductive adj2 fabric) or (conductive adj2 fabrics) or (conductive adj2 textile*) or electronic cloth* or e-cloth* or ecloth* or e-fabric* or efabric* or e-garment* or egarment*).tw.
5	(textronics or fibertronics or Vivometrics LifeShirt system or textro or e-shirt or eshirt or h-shirt or MagIC-SCG or (embed* adj3 electronics)).tw.
6	or/1-5
7	Electrocardiography/ or Electrocardiography, Ambulatory/
8	(electrocardio* or ECG or EKG).tw.
9	(Holter* or cardiac event monitor* or loop recorder*).tw.
10	or/7-9
11	Rehabilitation/ or Cardiac Rehabilitation/
12	rehabilitation.tw.
13	or/11-12
14	10 or 13
15	6 and 14
16	limit 15 to yr="2000 -Current"

CINAHL

Date of search: initial search 6 September 2017, secondary/follow-up search 29 March 2018

S. No.	Query
S1	(MH "Textiles")
S2	TI textile* OR AB textile*
S3	TI (((smart N2 fabric) or (smart N2 fabrics) or (smart N2 garment*) or (smart N2 cloth*) or (sensori?ed N2 garment*) or (conductive N2 fabric) or (conductive N2 fabrics) or (conductive N2 textile*) or "electronic cloth*" or e-cloth* or ecloth* or e-fabric* or efabric* or e-garment* or egarment*)) OR AB (((smart N2 fabric) or (smart N2 fabrics) or (smart N2 garment*) or (smart N2 cloth*) or (sensori?ed N2 garment*) or (conductive N2 fabric) or (conductive N2 fabrics) or (conductive N2 textile*) or electronic cloth* or e-cloth* or ecloth* or e-fabric* or efabric* or e-garment* or egarment*))
S4	TI ((textronics or fibertronics or "Vivometrics LifeShirt system" or textro or e-shirt or eshirt or h-shirt or "MagIC-SCG" or (embed* N3 electronics))) OR AB ((textronics or fibertronics or "Vivometrics LifeShirt system" or textro or e-shirt or eshirt or h-shirt or "MagIC-SCG" or (embed* N3 electronics)))
S5	TI ((e-textile* or etextile* or textile-based)) OR AB ((e-textile* or etextile* or textile-based))
S6	S1 OR S2 OR S3 OR S4 OR S5
S7	(MH "Electrocardiography") OR (MH "Electrocardiography, Ambulatory")
S8	TI ((Holter* or cardiac event monitor*)) OR AB ((Holter* or cardiac event monitor*))
S9	TI ((electrocardio* or ECG or EKG or “loop recorder*”)) OR AB ((electrocardio* or ECG or EKG or “loop recorder*”))
S10	S7 OR S8 OR S9
S11	(MH "Rehabilitation") OR (MH "Rehabilitation, Cardiac")
S12	TI rehabilitation OR AB rehabilitation
S13	S11 OR S12
S14	S10 OR S13
S15	S6 AND S14

WoS

Date of search: initial search 6 September 2017, secondary/follow-up search 29 March 2018

TS=(textile* OR e-textile* OR etextile* OR textile-based OR (smart NEAR/2 fabric) OR (smart NEAR/2 fabrics) OR (smart NEAR/2 garment*) OR (smart NEAR/2 cloth*) OR (sensori*ed NEAR/2 garment*) OR (conductive NEAR/2 fabric) OR (conductive NEAR/2 fabrics) OR (conductive NEAR/2 textile*) OR "electronic clothing" OR e-cloth* OR ecloth* OR e-fabric* OR efabric* OR e-garment* OR egarment* OR textronics OR fibertronics OR "Vivometrics LifeShirt system" OR textro OR e-shirt OR eshirt OR h-shirt OR MagIC-SCG OR (embed* NEAR/3 electronics)) AND TS=(electrocardio* OR ECG OR EKG OR Holter* OR "cardiac event monitors" OR "cardiac event monitor" OR “loop recorder*” OR rehabilitation)

Cochrane

Date of search: initial search 6 September 2017, secondary/follow-up search 29 March 2018

(textile* OR e-textile* OR etextile* OR "textile-based" OR (smart NEAR/2 fabric) OR (smart NEAR/2 fabrics) OR (smart NEAR/2 garment*) OR (smart NEAR/2 cloth*) OR (sensori*ed NEAR/2 garment*) OR (conductive NEAR/2 fabric) OR (conductive NEAR/2 fabrics) OR (conductive NEAR/2 textile*) OR "electronic clothing" OR "e-cloth*" OR ecloth* OR "e-fabric*" OR efabric* OR "e-garment*" OR egarment* OR textronics OR fibertronics OR "Vivometrics LifeShirt system" OR textro OR "e-shirt" OR eshirt OR "h-shirt" OR "MagIC-SCG" OR (embed* NEAR/3 electronics)) AND (ECG OR EKG OR Holter* OR "cardiac event monitor" OR "cardiac event monitors" OR “loop recorder*” OR rehabilitation)

Scopus

Date of search: initial search 6 September 2017, secondary/follow-up search 29 March 2018

(TITLE-ABS-KEY(textile* OR e-textile* OR etextile* OR textile-based OR (smart W/2 fabric) OR (smart W/2 fabrics) OR (smart W/2 garment*) OR (smart W/2 cloth*) OR (sensori?ed W/2 garment*) OR (conductive W/2 fabric) OR (conductive W/2 fabrics) OR (conductive W/2 textile*) OR "electronic clothing" OR e-cloth* OR ecloth* OR e-fabric* OR efabric* OR e-garment* OR egarment* OR textronics OR fibertronics OR "Vivometrics LifeShirt system" OR textro OR e-shirt OR eshirt OR h-shirt OR MagIC-SCG OR (embed* W/3 electronics))) AND (TITLE-ABS-KEY(electrocardio* OR ECG OR EKG OR Holter* OR "cardiac event monitor*" OR “loop recorder*” OR rehabilitation))AND PUBYEAR > 1999

PubMed

Date of search: initial search 6 September 2017, secondary/follow-up search 29 March 2018

((textile*[tiab] OR "e-textile*"[tiab] OR etextile*[tiab] OR "textile-based"[tiab] OR (smart AND fabric)[tiab] OR (smart AND fabrics)[tiab] OR (smart[tiab] AND garment*[tiab]) OR (smart[tiab] AND cloth*[tiab]) OR (sensori*[tiab] AND garment*[tiab]) OR (conductive[tiab] AND fabric[tiab]) OR (conductive[tiab] AND fabrics[tiab]) OR (conductive[tiab] AND textile*[tiab]) OR "electronic clothing"[tiab] OR "e-cloth*"[tiab] OR ecloth*[tiab] OR "e-fabric*"[tiab] OR efabric*[tiab] OR "e-garment*"[tiab] OR egarment*[tiab] OR textronics[tiab] OR fibertronics[tiab] OR "Vivometrics LifeShirt system"[tiab] OR textro[tiab] OR "e-shirt"[tiab] OR eshirt[tiab] OR "h-shirt"[tiab] OR "MagIC-SCG"[tiab] OR (embed*[tiab] AND electronics[tiab]) AND (electrocardio*[tiab] OR ECG[tiab] OR EKG[tiab] OR Holter*[tiab] OR "cardiac event monitor"[tiab] OR "cardiac event monitors"[tiab] OR “loop recorder*”[tiab] OR rehabilitation[tiab]) NOT medline)

Informit

Date of search: initial search 6 September 2017, secondary/follow-up search 29 March 2018

(("e-textile*" OR etextile* OR "textile-based" OR (smart %2 fabric) OR (smart %2 fabrics) OR (smart %2 garment*) OR (smart %2 cloth*) OR (sensori* %2 garment*) OR (conductive %2 fabric) OR (conductive %2 fabrics) OR (conductive %2 textile*) OR "electronic clothing" OR "e-cloth*" OR ecloth* OR "e-fabric*" OR efabric* OR "e-garment*" OR egarment* OR textronics OR fibertronics OR "Vivometrics LifeShirt system" OR textro OR "e-shirt" OR eshirt OR "h-shirt" OR "MagIC-SCG" OR (embed* %3 electronics)) AND (electrocardio* OR ECG OR EKG OR Holter* OR "cardiac event monitor" OR "cardiac event monitors" OR “loop recorder*” OR rehabilitation))

Proquest

Date of search: initial search 6 September 2017, secondary/follow-up search 29 March 2018

all(textile* OR "e-textile*" OR etextile* OR "textile-based" OR (smart NEAR/2 fabric) OR (smart NEAR/2 fabrics) OR (smart NEAR/2 garment*) OR (smart NEAR/2 cloth*) OR (sensori* NEAR/2 garment*) OR (conductive NEAR/2 fabric) OR (conductive NEAR/2 fabrics) OR (conductive NEAR/2 textile*) OR "electronic clothing" OR "e-cloth*" OR ecloth* OR "e-fabric*" OR efabric* OR "e-garment*" OR egarment* OR textronics OR fibertronics OR "Vivometrics LifeShirt system" OR textro OR "e-shirt" OR eshirt OR "h-shirt" OR "MagIC-SCG" OR (embed* NEAR/3 electronics)) AND all(electrocardio* OR ECG OR EKG OR Holter* OR "cardiac event monitor" OR "cardiac event monitors" OR “loop recorder*” OR rehabilitation)

Academic ASAP

Date of search: initial search 6 September 2017, secondary/follow-up search 29 March 2018

Search Terms: Document Title (textile* Or "e-textile" Or "e-textiles" Or etextile* Or "textile-based" Or (smart N2 fabric) Or (smart N2 fabrics) Or (smart N2 garment*) Or (smart N2 cloth*) Or (sensori?ed N2 garment*) Or (conductive N2 fabric) Or (conductive N2 fabrics) Or (conductive N2 textile*) Or "electronic clothing" Or "e-clothing") And Basic Search (electrocardio* Or ECG Or EKG Or Holter* Or "cardiac event monitor" Or "cardiac event monitors" Or “loop recorder*” Or rehabilitation)

IEEE Xplore (basic search structure)

Date of search: initial search 6 September 2017, secondary/follow-up search 29 March 2018

(eclothing OR "e-fabric" OR "e-fabrics" OR efabric* OR "e-garment" OR "e-garments" OR egarment* OR textronics OR fibertronics OR "Vivometrics LifeShirt system" OR textro OR "e-shirt" OR eshirt OR "h-shirt" OR "MagIC-SCG" OR (embed* N3 electronics)) AND (electrocardio* OR ECG OR EKG OR Holter* OR "cardiac event monitor" OR "cardiac event monitors" OR “loop recorder” OR “loop recorders” OR rehabilitation)

SPORTDiscus

Date of search: initial search 6 September 2017, secondary/follow-up search 29 March 2018

S. No.	Query
S1	TI textile* OR AB textile*
S2	TI (((smart N2 fabric) or (smart N2 fabrics) or (smart N2 garment*) or (smart N2 cloth*) or (sensori?ed N2 garment*) or (conductive N2 fabric) or (conductive N2 fabrics) or (conductive N2 textile*) or "electronic cloth*" or e-cloth* or ecloth* or e-fabric* or efabric* or e-garment* or egarment*)) OR AB (((smart N2 fabric) or (smart N2 fabrics) or (smart N2 garment*) or (smart N2 cloth*) or (sensori?ed N2 garment*) or (conductive N2 fabric) or (conductive N2 fabrics) or (conductive N2 textile*) or electronic cloth* or e-cloth* or ecloth* or e-fabric* or efabric* or e-garment* or egarment*))
S3	TI ((textronics or fibertronics or "Vivometrics LifeShirt system" or textro or e-shirt or eshirt or h-shirt or "MagIC-SCG" or (embed* N3 electronics))) OR AB ((textronics or fibertronics or "Vivometrics LifeShirt system" or textro or e-shirt or eshirt or h-shirt or "MagIC-SCG" or (embed* N3 electronics)))
S4	TI ((e-textile* or etextile* or textile-based)) OR AB ((e-textile* or etextile* or textile-based))
S5	S1 OR S2 OR S3 OR S4
S6	TI ((Holter* or cardiac event monitor*)) OR AB ((Holter* or cardiac event monitor*))
S7	TI ((electrocardio* or ECG or EKG or “loop recorder*”)) OR AB ((electrocardio* or ECG or EKG or “loop recorder*”))
S8	S6 OR S7
S9	TI rehabilitation OR AB rehabilitation
S10	S8 OR S9
S15	S5 AND S10

Appendix B. Studies ineligible follow the full-text review

Abtahi F, Ji G, Lu K, Rodby K, Seoane F. A knitted garment using intarsia technique for Heart Rate Variability biofeedback: Evaluation of initial prototype. Conference Proceedings: Annual International Conference of the IEEE Engineering in Medicine & Biology Society. 2015; 2015: 3121-4.
Reason for exclusion: Healthy subjects are used. The whole concept is the performance of garment for heart rate variability (HRV) biofeedback; hence it violates both participant and concept inclusion criteria.

Ahmari S. Design and implementation of advanced sensing platform for wearable biomedical applications development: California State University, Long Beach; 2015.
Reason for exclusion: As the central point of the research is design and implementation of advanced sensing platform for wearable biomedical applications; nothing specific to e-textile based cardiac electrocardiogram (ECG) monitoring; it does not satisfy the concept criteria

Ambrosio R, Guevara C, Silva C, Heredia A, Moreno M. Electrical characterization of textile electrodes for an ECG acquisition system; 2014.
Reason for exclusion: Applied on a healthy subject (no prior history of cardiovascular disease). Moreover, it is the study of electrical properties of the textile electrode.

Andreoni G, Fanelli A, Witkowska I, Perego P, Fusca M, Mazzola M, et al. Sensor validation a for a wearable monitoring system in ambulatory monitoring: application to textile electrodes. Proceedings of the 2013 7th International Conference on Pervasive Computing Technologies for Healthcare and Workshops. International Conference on Pervasive Computing Technologies for Healthcare2013. p. 169-75.
Reason for exclusion: Conducted on ten healthy subjects, the study is a general effectiveness study of textile electrodes.

Arcelus A, Sardar M, Mihailidis A. Design of a capacitive ECG sensor for unobtrusive heart rate measurements. 2013 IEEE International Instrumentation and Measurement Technology Conference (I2MTC); 2013 6-9 May 2013.
Reason for exclusion: It is the study of capacitive textile electrode development.

Atallah L, Serteyn A, Meftah M, Schellekens M, Vullings R, Bergmans JW, et al. Unobtrusive ECG monitoring in the NICU using a capacitive sensing array. Physiological Measurement. 2014; 35(5): 895-913.
Reason for exclusion: Focused on capacitive textile electrodes embedded in a mattress.

Baig MM, Gholamhosseini H, Connolly MJ. A comprehensive survey of wearable and wireless ECG monitoring systems for older adults. Medical & Biological Engineering & Computing. 2013; 51(5): 485-95.
Reason for exclusion: It is a review of ECG monitoring systems.

Balogová L, Babušiak B, Gála M. Biopotential sensing with electroconductive fabrics. Vlakna a Textil. 2014; 21(3): 8-10.
Reason for exclusion: Not in English.

Beckmann L, Neuhaus C, Medrano G, Jungbecker N, Walter M, Gries T, et al. Characterization of textile electrodes and conductors using standardized measurement setups. Physiological Measurement. 2010; 31(2): 233-47.
Reason for exclusion: The paper is about the characterization of textile electrodes and conductors using standardized measurement setups; it was tested on a skin dummy made up of agar instead of humans with known cardiac abnormalities.

Bifulco P, Gargiulo G, Romano M, Fratini A, Cesarelli M. Bluetooth portable device for continuous ECG and patient motion monitoring during daily life. IFMBE Proc: Springer; 2007. p. 369-72.
Reason for exclusion: Ineligible population.

Boehm A, Yu X, Neu W, Leonhardt S, Teichmann D. A novel 12-lead ECG T-shirt with active electrodes. Electronics (Switzerland). 2016; 5(4).
Reason for exclusion: Tested on healthy volunteers; ineligible population.

Liu B, Zhang Y, Liu Z. Wearable monitoring system with multiple physiological parameters. Medical Devices and Biosensors, 2008 ISSS-MDBS 2008 5th International Summer School and Symposium on; 2008: IEEE.
Reason for exclusion: Review article.

Büssen A, Büddefeld J, Neukirch B. Sensoric textiles in sports and medicine. DWI Reports. 2006; (130).
Reason for exclusion: The paper is focused on the textile electrode design.

Bystricky T, Moravcova D, Kaspar P, Soukup R, Hamacek A, Ieee. A Comparison of embroidered and woven textile electrodes for continuous measurement of ECG. In 2016 39th International Spring Seminar on Electronics Technology. International Spring Seminar on Electronics Technology ISSE. 2016. p. 7-11.
Reason for exclusion: The paper is a comparative study between embroidered and woven textile electrodes for continuous measurement of ECG.

Caldara M, Comotti D, Gaioni L, Pedrana A, Pezzoli M, Re V, et al. Development of a multi-lead ECG wearable sensor system for biomedical applications; 2017.
Reason for exclusion: Tested on a healthy subject.

Catarino A, Carvalho H, Dias MJ, Pereira T, Postolache O, Pedro S G. Continuous health monitoring using E-textile integrated biosensors; 2012.
Reason for exclusion: Further data are required about the type and number of participants. The authors responded in the second round, tested on healthy subjects.

Chamadiya B, Mankodiya K, Wagner M, Hofmann UG. Textile-based, contactless ECG monitoring for non-ICU clinical settings. Journal of Ambient Intelligence and Humanized Computing. 2013; 4(6): 791-800.
Reason for exclusion: Further data are required about the type and number of participants. The system was tested on healthy volunteers.

Chi YM, Patrick N, Cauwenberghs G. Wireless non-contact ECG and EEG biopotential sensors. Transactions on Embedded Computing Systems. 2013; 12(4).
Reason for exclusion: The system was tested on a healthy 21 years old male subject; hence, ineligible population.

Chiarugi F, Karatzanis I, Zacharioudakis G, Meriggi P, Rizzo F, Stratakis M, et al. Measurement of heart rate and respiratory rate using a textile-based wearable device in heart failure patients; 2008.
Reason for exclusion: A descriptive paper about the signal acquisition and processing system, based on a wearable textile-based device.

Chiu CC, Shyr TW, Chu HC, Chung YC, Lan CY. A wearable e-health system with multi-functional physiological measurement; 2007.
Reason for exclusion: Further data are required about the type and number of participants. The authors responded and tested on healthy subjects.

Cho H, Lim H, Cho S. Efficacy research of electrocardiogram and heart rate measurement following the structure of the textile electrodes. Fibers and Polymers. 2016; 17 2069+.
Reason for exclusion: The paper is focused on the structure of textile electrodes.

Cho H, Lee JH. A Study on the Optimal Positions of ECG Electrodes in a Garment for the Design of ECG-Monitoring Clothing for Male. J Med Syst. 2015; 39(9): 95.
Reason for exclusion: The paper is a study of optimal electrode positioning.

Cleland I, Nugent C, Finlay D, Burns W, Bougourd J, Armitage R. Assessment of custom-fitted heart rate sensing garments whilst undertaking everyday activities. 2012. p. 124-31.
Reason for exclusion: Authors studied the efficiency of the textile electrode in two configurations.

Comert A, Honkala M, Aydogan B, Vehkaoja A, Verho J, Hyttinen J. Comparison of Different Structures of Silver Yarn Electrodes for Mobile Monitoring. In: VanderSloten J, Verdonck P, Nyssen M, Haueisen J, editors. In 4th European Conference of the International Federation for Medical and Biological Engineering. IFMBE Proceedings. vol. 22. 2009. p. 1204-7.
Reason for exclusion: The paper is about the comparison of different structures of silver yarn electrodes for mobile monitoring.

Comert A, Hyttinen J. Investigating the possible effect of the electrode support structure on motion artefact in wearable bioelectric signal monitoring. Biomed Eng Online. 2015; 14: 44.
Reason for exclusion: The paper presents the effect of the electrode support structure for motion artefact reduction.

Comstock J. HealthWatch seeks FDA clearance for its 12-lead ECG T-shirt. [Internet]. 2014 [cited 2017 April 6]. Available from: http://www.mobihealthnews.com/32774/healthwatch-seeks-fda-clearance-for-its-12-lead-ecg-tshirt
Reason for exclusion: A report on a hWear t-shirts.

Coyle S, Lau KT, Moyna N, O'Gorman D, Diamond D, Di Francesco F, et al. BIOTEX--biosensing textiles for personalised healthcare management. IEEE Trans Inf Technol Biomed. 2010; 14(2): 364-70.
Reason for exclusion: The central point of the paper is multi-parameter sensing; nothing specific to e-textile ECG monitoring.

Dai M, Xiao X, Chen X, Lin H, Wu W, Chen S. A low-power and miniaturized electrocardiograph data collection system with smart textile electrodes for monitoring of cardiac function. Australasian Physical & Engineering Sciences in Medicine. 2016; 39(4): 1029-40.
Reason for exclusion: Tested on six healthy adult male participants.

Das PS, Park JY. A flexible touch sensor based on conductive elastomer for biopotential monitoring applications. Biomedical Signal Processing and Control. 2017; 33: 72-82.
Reason for exclusion: This paper proposes a novel flexible touch sensor based on conductive elastomer for biomedical applications.

De Rossi D, Carpi F, Lorussi F, Mazzoldi A, Paradiso R, Scilingo EP, et al. Electroactive fabrics and wearable biomonitoring devices. AUTEX Research Journal. 2003; 3(4): 180-5.
Reason for exclusion: A literature review on a smart garment for vital sign monitoring.

Deng YM, Yan NN, Zhang H. Analysis of influencing factors of accuracy on ECG monitoring clothing and apparel design elements; 2014.
Reason for exclusion: The paper is an analysis of influencing factors of accuracy on ECG monitoring clothing and apparel design elements.

Di Rienzo M, Vaini E, Castiglioni P, Merati G, Meriggi P, Parati G, et al. Wearable seismocardiography: towards a beat-by-beat assessment of cardiac mechanics in ambulant subjects. Autonomic Neuroscience-Basic & Clinical. 2013; 178(1-2): 50-9.
Reason for exclusion: Two healthy male subjects were included for the study. Besides, the method investigated here is seismocardiogram (SCG) instead of ECG.

Di Rienzo M, Vaini E, Castiglioni P, Lombardi P, Meriggi P, Rizzo F. A textile-based wearable system for the prolonged assessment of cardiac mechanics in daily life. Conference Proceedings: Annual International Conference of the IEEE Engineering in Medicine & Biology Society. 2014; 2014 6896-8.

Reason for exclusion: First, the focus is not ECG rather SCG and again, the data sets are derived from healthy subjects.

Dias R, Da Silva JM. A flexible wearable sensor network for bio-signals and human activity monitoring; 2014.
Reason for exclusion: Tested on healthy subjects; hence, ineligible population.

Dimov A. Wireless shirt for ECG and Respiration [Internet]. BIOPAC Systems, Inc.; n.d. [cited 2017 April 6]. Available from: http://www.measuringbehavior.org/mb2016/wireless-shirt-ecg-and-respiration.html
Reason for exclusion: News on wireless shirt for ECG and respiration.

Ding H, Sarela A, Helmer R, Mestrovic M, Karunanithi M. Evaluation of ambulatory ECG sensors for a clinical trial on outpatient cardiac rehabilitation; 2010.
Reason for exclusion: This study only evaluated the performance of two ECG sensors/electrodes.

Dittmar A, Axisa F, Delhomme G, Gehin C. New concepts and technologies in a home care and ambulatory monitoring. Studies in Health Technology & Informatics. 2004; 108 9-35.
Reason for exclusion: Review paper - it narrates the new possibilities for home care and ambulatory monitoring.

Dittmar A, Lymberis A, Ieee. Smart clothes and associated wearable devices for biomedical ambulatory monitoring; 2005. 221-7 p.
Reason for exclusion: Review - it highlights the opportunities and challenges for smart clothes and associated wearable devices for Biomedical ambulatory monitoring.

Fleury A, Sugar M, Chau T. E-textiles in Clinical Rehabilitation: A Scoping Review. Electronics. 2015; 4(1): 173-203.
Reason for exclusion: The paper is a scoping review of e-textiles for rehabilitation.

Gargiulo GD, Gunawardana U, apos, Loughlin A, Sadozai M, Varaki ES, et al. A wearable contactless sensor suitable for continuous simultaneous monitoring of respiration and cardiac activity. Journal of Sensors. 2015.
Reason for exclusion: Authors contacted; authors responded in the second round, tested on healthy subjects between the ages of 22 and 27.

Gi SO, Lee YJ, Koo HR, Khang S, Kim KN, Kang SJ, et al. Application of a textile-based inductive sensor for the vital sign monitoring. Journal of Electrical Engineering and Technology. 2015; 10(1): 364-71.
Reason for exclusion: Included 'five male subjects in their twenties, all of whom were in good health', and the focus is the development of textile-based inductive electrodes.

Gi SO, Lee YJ, Koo HR, Khang SA, Park HJ, Kim KS, et al. An analysis on the effect of the shape features of the textile electrode on the non-contact type of sensing of cardiac activity based on the magnetic-induced conductivity priciple. Transactions of the Korean Institute of Electrical Engineers. 2013; 62(6): 803-10.
Reason for exclusion: Study of textile electrodes.

Gonzales L, Walker K, Keller K, Beckman D, Goodell H, Wright G, et al. Textile Sensor System for Electrocardiogram Monitoring. 2015 Virtual Conference on Application of Commercial Sensors. 2015.
Reason for exclusion: The authors contacted; the system was tested on 4 healthy volunteers.

Green RB. Bluetooth telemetry system for a wearable electrocardiogram. 2013.
Reason for exclusion: Not e-textile-based ECG system.

Guo JS, Deng QK. The design of a wearable ECG and respiration sensor vest and its monitoring system. Zhongguo Yiliao Qixie Zazhi. 2006; 30(5): 341-4.
Reason for exclusion: Not in English.

Guttke S, Laukner M, Weber P, Iop. Cross sensitivity of different electrode types for impedance plethysmography under motion conditions. In Xv International Conference on Electrical Bio-Impedance. Journal of Physics Conference Series. vol. 434. 2013.
Reason for exclusion: A comparative study of cross-sensitivity of different electrode types for impedance plethysmography.

Hanic M, Sladek Lu, Horinek F, Jagelka M, Donoval M, Daricek M, et al. BIO-monitoring system with conductive textile electrodes integrated into t-shirt. Radioelektronika (RADIOELEKTRONIKA), 2014 24th International Conference; 2014: IEEE.
Reason for exclusion: The aim of this article is to simply describe the electronic and mechanical design of the system.

Hughes M. Development grant for HealthVest. Medical Textiles. 2007; (DEC.): 5-6.
Reason for exclusion: A literature about the grant to build Smartlife in the UK.

Hung K, Lee CC, Chan WM, Choy SO, Kwok P. Development of a wearable system integrated with novel biomedical sensors for ubiquitous healthcare. Conference proceedings: Annual International Conference of the IEEE Engineering in Medicine and Biology Society IEEE Engineering in Medicine and Biology Society Annual Conference. 2012; 2012 5802-5.
Reason for exclusion: A laboratory report of sensors development for wearable systems.

Jeon YJ, Shin SC, Jang YW, Kim SH. Development and verification of the system for heart rate detection during exercise. Transactions of the Korean Institute of Electrical Engineers. 2007; 56(9): 1688-93.
Reason for exclusion: Not in English.

Joseph J. Clothes show. Engineering. 2008; 249(7): 16-8.
Reason for exclusion: A literature review.

Joshi AS, Sharma K, Wagh D, Pareek D. Development of E-health monitoring garment. Man-Made Textiles in India. 2011; 39(8): 279-85.
Reason for exclusion: Literature review.

Jourand P, De Clercq H, Corthout R, Puers R. Textile Integrated Breathing and ECG Monitoring System; 2009.
Reason for exclusion: The primary aim of the paper is the construction of textile integrated breathing and ECG monitoring system and testing the modules in the laboratory.

Joutsen AS, Kaappa ES, Karinsalo TJ, Vanhala J. Dry electrode sizes in recording ECG and heart rate in wearable applications; 2017.
Reason for exclusion: The paper detailed the size of dry electrodes in recording ECG and heart rate for wearable applications.

Ishijima M. Acquisition of long-term cardiac signals for chronodiagnostic utility. Frontiers of Medical & Biological Engineering. 2000; 10(3): 261-7.
Reason for exclusion: The focus is textile electrodes for resting ECG; it is not e-textile-based ECG monitoring.

Kaappa ES, Joutsen AS, Vanhala J. Performance analysis of novel flexible electrodes for wearable ECG/heart rate monitoring; 2017.
Reason for exclusion: A performance analysis of novel flexible electrodes.

Kannaian T, Neelaveni R, Thilagavathi G. Design and development of embroidered textile electrodes for continuous measurement of electrocardiogram signals. Journal of Industrial Textiles. 2013; 42(3): 303-18.
Reason for exclusion: It is focused on the design and development of textile electrodes.

Kang T-H. Textile -embedded sensors for wearable physiological monitoring systems [Ph.D.]. Ann Arbor: North Carolina State University; 2006.
Reason for exclusion: Review section (have to search for studies from this review).

Kawashima M, Nakamura T, Hata K. Construction of healthcare network based on proposed ECG and physical-activity sensor adopting energy-harvesting technologies. Healthcom; 2013 9-12 Oct. 2013.
Reason for exclusion: A literature review on healthcare network based on proposed ECG and physical-activity sensors.

Khosla A. Smart garments in chronic disease management: Progress and challenges; 2012.
Reason for exclusion: It is a narrative paper on challenges and progresses in smart garments in chronic disease management.

Kim S, Leonhardt S, Zimmermann N, Kranen P, Kensche D, Muller E, et al. Influence of contact pressure and moisture on the signal quality of a newly developed textile ECG sensor shirt2008. 175-+ p.
Reason for exclusion: The paper explained the influence of contact pressure and moisture on the signal quality.

Kim H, Kim T, Joo M, Yi S, Yoo C, Lee K, et al. Design of a calorie tracker utilizing heart rate variability obtained by a nanofiber technique-based wellness wear system. Appl Math Inf Sci. 2011; 5(SUPPL.2): 171S-7S.
Reason for exclusion: The central point is software applied in calorie tracker.

Kim HS, Varanasi V, Mehta G, Zhang H, Choi TY, Namuduri K, et al. Circuits, systems, and technologies for detecting the onset of sudden cardiac death through EKG analysis. IEEE Circuits and Systems Magazine. 2013; 13(4): 10-25.
Reason for exclusion: This article discusses the circuits, systems, and technologies that can be put together to design an electronic vest that is capable of recognizing cardiac events and alerting emergency services personnel.

Kirsh D. This new 'smart shirt' can monitor your vital signs. [Internet]. 2017 [cited 2017 6 April]. Available from: https://www.medicaldesignandoutsourcing.com/this-smart-shirt-monitors-key-vital-signs/.
Reason for exclusion: Review of the smart shirt developed by Holst Center.

Kumar P, Rai P, Oh S, Harbaugh RE, Varadan VK. Smart e-textile-based nanosensors for cardiac monitoring with smartphone and wireless mobile platform. Springer Tracts in Mechanical Engineering2014. p. 387-401.
Reason for exclusion: Study of smart fabrics, textile electrodes for ECG application.

Kuroda T. Evaluation of NISHIJIN ECG e-Textile [Internet]. 2016 [cited 2018 22 April]. Available from: https://upload.umin.ac.jp/cgi-open-bin/ctr_e/ctr_view.cgi?recptno=R000027138
Reason for exclusion: The goal of the clinical trial is to validate the textile electrode produced by NISHIJIN.

Kuroda T, Hirano K, Sugimura K, Adachi S, Igarashi H, Ueshima K, et al. Applying NISHIJIN historical textile technique for e-Textile. Conf Proc IEEE Eng Med Biol Soc. 2013; 2013 1226-9.
Reason for exclusion: It is focused on textile production technology.

Lanatà A, Scilingo EP, Francesconi R, De Rossi D. Bi-modal transducer-based wearable system for cardiac monitoring; 2006.
Reason for exclusion: The paper is about transducer used as an ultrasound transceiver and passive acoustic sensor.

Lee IB, Shin SC, Jang YW, Song YS, Jeong JW, Kim S. Comparison of conductive fabric sensor and Ag-AgCl sensor under motion artefacts. Conf Proc IEEE Eng Med Biol Soc; 2008 20-25 Aug. 2008.

Reason for exclusion: It is a comparative study between the conductive fabric sensor and the Ag-AgCl sensor under motion artefacts; also, participants of no cardiac abnormalities are used.

Lee YJ, Lee JW, Yang HK, Lee JH, Kang DH, Cho HS, et al. Development of miniaturized textile electrode for measuring heart electric activity. Trans Korean Inst Electr Eng. 2009; 58(6): 1186-93.
Reason for exclusion: Not in English.

Leichman K. A T-shirt that monitors your heart. [Internet]. 2014 [cited 2018 6 April]. Available from: https://www.israel21c.org/a-t-shirt-that-monitors-your-heart/.
Reason for exclusion: A report on a hWear t-shirts.

Lim CY, Jang KJ, Kim HW, Kim YH. A wearable healthcare system for cardiac signal monitoring using conductive textile electrodes. Conf Proc IEEE Eng Med Biol Soc. 2013; 2013 7500-3.
Reason for exclusion: MIT-BIH Arrhythmia Database is used to validate the result.

Lim CY, Kim K. A Study on a Healthcare System Using Smart Clothes. JEET. 2014; 9(1): 372-7.
Reason for exclusion: MIT-BIH Arrhythmia Database is used to validate the result.

Linz T, Kallmayer C, Aschenbrenner R, Reichl H. Fully untegrated EKG shirt based on embroidered electrical interconnections with conductive yarn and miniaturized flexible electronics. Int Conf Wearable Implant Body Sens Netw; 2006: IEEE.
Reason for exclusion: This work is different from other research in the field as it focuses more on advanced interconnection and integration technologies for electronics in textiles rather than on the ECG shirt as functionality.

Lin Y-D, Chien Y-H, Wang S-F, Tsai C-L, Chang H-H, Lin K-P. Implementation of multiple-channel capacitive ECG measurement based on conductive fabric. Biomed Eng (Singapore). 2013; 25(06): 1350052.
Reason for exclusion: The overall idea is multiple channel ECG electrodes; six volunteer healthy college students were included.

Liu J, Zhou Y. Design of a novel portable ECG monitor for heart health. ISCID; 2013: IEEE.
Reason for exclusion: The authors used a simulator to generate an ECG signal to test the stability of the hardware. The algorithm results have been evaluated on the MITBIH Arrhythmia Database.

Liu GD, Guo W, Li SY, Cai J, Bao ZM, Sun XY. Wearable system for continuously monitoring physiological parameters. Jilin Daxue Xuebao 2011; 41(3): 771-5.
Reason for exclusion: Not in English.

Liu Y-L. Hardware Implementation of Wearable Electrocardiograph and Development of Nonlinear Analysis for Physiological Signals: Feng Chia University; 2003.
Reason for exclusion: Not in English does not fulfill the language requirement.

Lobodzinski SS, Laks MM. Comfortable textile-based electrocardioram systems for very long-term monitoring. Cardiol J. 2008; 15(5): 477-80.
Reason for exclusion: The paper is mainly a literature review; In this work, continuous health monitoring for disabled or elderly people is proposed using textile integrated electrodes for ECG measurement.

Lokare N, Gonzalez L, Lobaton E. Comparing wearable devices with wet and textile electrodes for activity recognition. 2016 38th Annual International Conference of the IEEE Engineering in Medicine and Biology Society (EMBC); 2016 16-20 Aug. 2016.
Reason for exclusion: The focus is activity identification, and again it is further narrowed down to comparison of wet and textile electrodes.

Luprano J, Sola J, Dasen S, Koller JM, Chetelat O, Ieee Computer SOC. Combination of Body Sensor Networks and On-Body Signal Processing Algorithms: The practical case of MyHeart project; 2006.
Reason for exclusion: The primary aim of the project is a case study on the combination of Body Sensor Networks and On-Body Signal Processing Algorithms for MyHeart project.

Luprano J. Bio-sensing textile for medical monitoring applications. 2008; 57: 257-65.
Reason for exclusion: The focus is on textile sensors for Bio-sensing measurement - a literature review.

Lymberis A, Olsson S. Intelligent biomedical clothing for personal health and disease management: state of the art and future vision. Telemedicine Journal and e-health. 2003; 9(4): 379-86.
Reason for exclusion: A review of the exciting features of smart textiles.

Ma YC, Chao YP, Tsai TY. Smart-clothes 2014; Prototyping of a health monitoring platform. 2013 IEEE Third International Conference on Consumer Electronics. Berlin (ICCE-Berlin); 2013 9-11 Sept.
Reason for exclusion: A report on the wearable platform.

Malliopoulos C, Milsis A, Vavouras T, Paradiso R, Alonso A, Cianflone D. Continuous mobile services for healthcare: the HealthWear project. Journal on Information Technology in Healthcare. 2008; 6(5): 344-55.
Reason for exclusion: A review paper (evaluating health-monitoring services based on wearable garments).

Marozas V, Petrenas A, Daukantas S, Lukosevicius A. A comparison of conductive textile-based and silver/silver chloride gel electrodes in exercise electrocardiogram recordings. J Electrocardiol. 2011; 44(2): 189-94.
Reason for exclusion: A comparative study between conductive textile-based and silver/silver chloride gel electrodes in exercise ECG recordings.

McCann J. Smart medical textiles in rehabilitation. In Smart textiles for medicine and healthcare: Materials, systems and applications. 2007. p. 166-82.
Reason for exclusion: General review paper about e-textile in rehabilitation.

Meinander H. Haptic sensing in intelligent textile development; 2008.
Reason for exclusion: It details the importance and advantages of haptic properties for the intelligent garment.

Milsis A, Katsaras T, Saoulis N, Varoutaki E, Vontetsianos A. Clinical Effectiveness of the "Healthwear" Wearable System in the Reduction of COPD Patients' Hospitalization. International Conference on Wireless Mobile Communication and Healthcare; 2011: Springer.
Reason for exclusion: The focus is on the chronic obstructive pulmonary disease (COPD) instead of cardiac abnormalities.

Morrison, T., Silver, J. & Otis, B. A single-chip encrypted wireless 12-lead ECG smart shirt for continuous health monitoring. 2014 Symposium on VLSI Circuits Digest of Technical Papers, 2014. IEEE, 1-2.
Reason for exclusion: Data acquired from a healthy participant.

Muhlsteff J, Such O, Ieee. Dry electrodes for monitoring of vital signs in functional textiles. In Proceedings of the 26th Annual International Conference of the Ieee Engineering in Medicine and Biology Society, Vols 1-7. Proceedings of Annual International Conference of the Ieee Engineering in Medicine and Biology Society. vol. 26. 2004. p. 2212-5.
Reason for exclusion: The paper explains the dry electrodes for monitoring of vital signs in functional textiles.

Muthu Kumar N, Thilagavathi G. Textile electrodes for ECG and EEG monitoring. JTA. 2013; 74(2): 81-6.
Reason for exclusion: A review of textile electrodes.

Nag S, Sharma DK, Ieee. Wireless e-jacket for multiparameter biophysical monitoring and telemedicine applications; 2006.
Reason for exclusion: A report on the wearable platform.

Ogasawara T, Ono K, Matsuura N, Yamaguchi M, Watanabe J, Tsukada S. Development of applications for a wearable electrode embedded in inner shirt. NTT Technical Review. 2015; 13(1).
Reason for exclusion: The paper explains the development of applications for a wearable electrode embedded in a shirt.

Ottenbacher J, Romer S, Kunze C, Großmann U, Stork W. Integration of a bluetooth based ECG system into clothing. Wearable Computers, 2004 ISWC 2004 Eighth International Symposium on; 2004: IEEE.
Reason for exclusion: The central point of the research was to show that the possibility of creating smart clothes with integrated components using commercially available materials.

Ozkaraca O, Guler I. Denoising and remote monitoring of ECG signal with real-time extended Kalman filter in a wearable system. Biomed Eng (Singapore). 2014; 27(01): 1550009.
Reason for exclusion: Centred on de-noising and remote monitoring of ECG signal with real-time extended Kalman filter; additionally, data was derived from the MIT-BIH arrhythmia database.

Pandian PS, Mohanavelu K, Safeer KP, Kotresh TM, Shakunthala DT, Gopal P, et al. Smart Vest: Wearable multi-parameter remote physiological monitoring system. Med Eng Phys. 2008; 30(4): 466-77.
Reason for exclusion: A literature review about advances in the field of textile sensing.

Pani D, Achilli A, Bassareo PP, Cugusi L, Mercuro G, Fraboni B, et al. Fully-textile polymer-based ECG electrodes: Overcoming the limits of metal-based textiles. Comput Cardiol; 2016: IEEE.
Reason for exclusion: The study is about textile electrodes, and they used the CAM-14 ECG module from GE to acquire the ECG signal.

Paradiso R, De Rossi D. Advances in textile sensing and actuation for e-textile applications. Conf Proc IEEE Eng Med Biol Soc; 2008. p. 3629.
Reason for exclusion: A literature review about advances in the field of textile sensing.

Paradiso R, Gemignani A, Scilingo E, De Rossi D. Knitted bioclothes for cardiopulmonary monitoring. Conf Proc IEEE Eng Med Biol Soc; 2003: IEEE.
Reason for exclusion: A review of the WEALTHY system, which is, developed as the integration of several functional modules.

Paradiso R, Loriga G, Taccini N. Wearable system for vital signs monitoring. Stud Health Technol Inform. 2004; 108 253-9.
Reason for exclusion: A review article.

Paradiso R, Belloc C, Loriga G, Taccini N. Wearable healthcare systems, new frontiers of e-textile. Stud Health Technol Inform. 2005; 117 9-16.
Reason for exclusion: Authors were contacted to request further data; authors reposed in the second round. The system was tested on healthy subjects.

Paradiso R, Caldani L, Pacelli M. Knitted Electronic Textiles. In Wearable Sensors: Fundamentals, Implementation and Applications. 2014. p. 153-74.
Reason for exclusion: The paper is focused on knitted electronic textile sensors.

Paul G. Screen printed textile-based wearable biopotential monitoring [Ph.D.]. Ann Arbor: University of Southampton (United Kingdom); 2014.
Reason for exclusion: The concept addressed is screen printed textile-based wearable biopotential monitoring, not specific to ECG.

Peltokangas M, Verho J, Vehkaoja A. Night-time EKG and HRV monitoring with bed sheet integrated textile electrodes. IEEE Trans Inf Technol Biomed. 2012; 16(5): 935-42.
Reason for exclusion: Data acquired from healthy participants.

Peng M, Wang T, Hu G, Zhang H. A wearable heart rate belt for ambulant ECG monitoring. 2012; 371-4.
Reason for exclusion: Not e-textile based ECG monitoring; also, six healthy male subjects were included.

Peng Y, Qin ZG. The design of a portable wireless remote ECG monitor system. 2013. p. 2375-9.
Reason for exclusion: The paper provides a portable ECG monitoring system which is not e-textile based; Also, no cardiac patients were involved.

Pereira T, Carvalho H, Catarino AP, Dias MJ, Postolache O, Girao PS, et al. Wearable Biopotential Measurement Using the TI ADS1198 Analog Front-End and Textile Electrodes Signal conditioning and signal quality assessment. IEEE Int Symp Med Meas Appl; 2013.
Reason for exclusion: Authors were contacted to request further data; healthy participants were included in the study.

Pérez-Villacastín J, Gaeta E. Smart Clothes to Take Care of People or Smart People Who Use Clothes to Take Care of Themselves? Rev Esp Cardiol. 2015; 68(07): 559-61.
Reason for exclusion: Review.

Perego P, Andreoni G, Tarabini M. Textile Performance Assessment for Smart T-Shirt Development, Mechanical and electrical study for conductive yarn. Proceedings of the eTELEMED. 2016.
Reason for exclusion: A performance assessment of e-textiles.

Periyaswamt T, DP A. Ambulatory monitoring of ECG signals using textile electrodes. 2013.
Reason for exclusion: Authors were contacted to request further data; authors responded in the second round, tested on healthy college students.

Postolache G, Carvalho H, Catarino A, Postolache OA. Smart Clothes for Rehabilitation Context: Technical and Technological Issues. In Sensors for Everyday Life. Springer; 2017. p. 185-219.
Reason for exclusion: Review; the paper presents the technical and technological issues related to smart clothes for rehabilitation context.
Rai P, Kumar PS, Oh S, Kwon H, Mathur GN, Varadan VK. Printable low-cost sensor systems for healthcare smart textiles. Nanosensors, Biosensors, and Info-Tech Sensors and Systems 2011; 2011: International Society for Optics and Photonics.
Reason for exclusion: The paper details printable low-cost sensor systems.

Rai P, Oh S, Shyamkumar P, Ramasamy M, Harbaugh RE, Varadan VK. Nano- Bio- Textile Sensors with Mobile Wireless Platform for Wearable Health Monitoring of Neurological and Cardiovascular Disorders. Journal of the Electrochemical Society. 2014; 161(2): B3116-B50.
Reason for exclusion: The central point of the paper is to develop a hybrid Nanostructured Textile Bioelectrode for Unobtrusive Health Monitoring

Rai P. Hybrid Nanostructured Textile Bioelectrode for Unobtrusive Health Monitoring [Ph.D.]. Ann Arbor: University of Arkansas; 2013.
Reason for exclusion: The central point of the paper is to develop a hybrid Nanostructured Textile Bioelectrode for Unobtrusive Health Monitoring, focused on an e-textile based sensor.

Rienzo MD, Rizzo F, Meriggi P, Castiglioni P, Mazzoleni P, Ferrarin M, et al. MagIC: a Textile System for Vital Signs Monitoring. Advancement in Design and Embedded Intelligence for Daily Life Applications. Conf Proc IEEE Eng Med Biol Soc; 2007 22-26 Aug.
Reason for exclusion: The primary purpose of the paper is to augment features of the MagIC for daily activity follow-up of healthy subjects.

Pieter. Smart T-shirt with removable electronics is next step in wearable health. [Internet]. 2015 [cited 2018 6 April]. Available from: https://www.healthtechevent.com/sensor/smart-t-shirt-with-removable-electronics-is-next-step-in-wearable-health/.
Reason for exclusion: News report.

Rathnayake AS. Development of the core technology for the creation of electronically-active, smart yarn [Ph.D.]. Ann Arbor: Nottingham Trent University (United Kingdom); 2015.
Reason for exclusion: The idea investigated is the development of the core technology for the creation of electronically-active, smart yarn – not specific to e-textile based ECG monitoring.

Rattfalt L, Ahlstrom C, Berglin L, Linden M, Hult P, Ask P, et al. A canonical correlation approach to heart beat detection in textile ECG measurements; 2006.
Reason for exclusion: It is about an algorithm, a canonical correlation approach to detect a heartbeat in textile ECG. Additionally, a heartbeat detector is used for evaluation.

Rattfalt L, Linden M, Hult P, Berglin L, Ask P. Electrical characteristics of conductive yarns and textile electrodes for medical applications. Med Biol Eng Comput. 2007; 45(12): 1251-7.
Reason for exclusion: The paper is about the electrical characterization of textile electrodes.

Rattfält L. Smartware electrodes for ECG measurements: Design, evaluation and signal processing: Linköping University Electronic Press; 2013.
Reason for exclusion: Focused on textile electrodes.

Rawcliffe N. Conductive textiles already revolutionising our lives. Technical Textiles International : TTI. 2001; 10(7):25-6.
Reason for exclusion: The paper review textiles with electrically conductive property

Sarda RM. ECG signal detection using conducting polymer fibers as sensors [M.S.]: Northern Illinois University; 2010.
Reason for exclusion: The thesis that explains the design of an e-textile sensor.

Shiozawa N. Measurement of electrocardiogram with the textile electrode. Trans Jpn Soc Med Biol Eng. 2016; 54(3): 135-8.
Reason for exclusion: Not in English.

Shyamkumar P. Dry Electrodes for ECG and Pulse Transit Time for Blood Pressure: A Wearable Sensor and Smartphone Communication Approach: University of Arkansas; 2011.
Reason for exclusion: The central point is dry Electrodes; data acquired from two healthy subjects.

Spulber I, Chen YM, Papi E, Anastasova-Ivanova S, Bergmann J, McGregor AH, et al. Live Demonstration: Wearable Electronics for a Smart Garment Aiding Rehabilitation. In ISSCS. IEEE International Symposium on Circuits and Systems. 2015. p. 1912.
Reason for exclusion: The concept investigated is osteoarthritis rehabilitation management, data acquired from healthy participants.

Sung M, Jeong K, Cho G. Suggestion for optimal location of textile-based ECG electrodes on an elastic shirt considering clothing pressure of the shirt. Proc Int Symp Wearable Comput; 2008: IEEE.
Reason for exclusion: The paper presents an optimal location of textile-based ECG electrodes on an elastic shirt considering the clothing pressure of the shirt. Five men between 20 to 25 years old without any history of heart disease were included.

Steltenkamp S, Becher K, Doerge T, Ruff R, Hoffmann KP. Electrode structures for acquisition and neural stimulation controlling the cardiovascular system. Conf Proc IEEE Eng Med Biol Soc. 2009; 5478-81.
Reason for exclusion: The paper is about electrode structures for acquisition and neural stimulation controlling the cardiovascular system.

Tada Y, Inoue M, Tokumaru T. A Characteristic Evaluation of an Undershirt for Measurement of Bioelectricity Using Conductive Ink Wires. JTE. 2013; 59(6): 141-8.
Reason for exclusion: Not in English.

Tada Y, Amano Y, Sato T, Saito S, Inoue M. A smart shirt made with conductive ink and conductive foam for the measurement of electrocardiogram signals with unipolar precordial leads. Fibers. 2015; 3(4): 463-77.
Reason for exclusion: The central concept is the e-textile electrode, and they are using a Holter monitor to collect the signal.

Tae-Ho K, Merritt C, Karaguzel B, Wilson J, Franzon P, Pourdeyhimi B, et al. Sensors on Textile Substrates for Home-Based Healthcare Monitoring. Transdisciplinary Conference on D2H2 2006 2-4 April.
Reason for exclusion: The paper is about electrode development.

Taji B, Shirmohammadi S, Groza V, Bolic M. An ECG monitoring system using conductive fabric. IEEE Int Symp Med Meas Appl; 2013: IEEE.
Reason for exclusion: The central point of the paper is the types of electrodes and optimal positioning for ECG signal measurement; the authors contacted; data acquired from healthy subjects.
Taji B. Reconstruction of ECG Signals Acquired with Conductive Textile Electrodes: Université d'Ottawa/University of Ottawa; 2013.
Reason for exclusion: The central point is a signal reconstruction; the authors contacted; data acquired from healthy subjects.

Taji B, Shirmohammadi S, Groza V. Measuring skin-electrode impedance variation of conductive textile electrodes under pressure. 2014 IEEE International Instrumentation and Measurement Technology Conference (I2MTC) Proceedings; 2014/05: IEEE; 2014.
Reason for exclusion: The concept presented here is a measure of skin-electrode impedance of conductive textile electrodes. Authors were contacted to request further data; healthy adults between 30 and 36 years old were recruited to acquire ECG signals.

Takahashi K, Suzuki K, Ieee. An ECG Monitoring System Through Flexible Clothes with Elastic Material. IEEE Healthcom 2015; 305-10.
Reason for exclusion: The central concept addressed is the application of smart clothing for autism spectrum disorders.

Takamatsu S, Lonjaret T, Crisp D, Badier JM, Malliaras GG, Ismailova E. Direct patterning of organic conductors on knitted textiles for long-term electrocardiography. Sci Rep. 2015; 5 15003.
Reason for exclusion: The authors presented a direct patterning of organic conductors on knitted textiles for long-term electrocardiography.

Tsai TY, You KM, Ma YC, Chao YP. CGU smart clothes platform - Development of a gateway device and real-time mobile display; 2014.
Reason for exclusion: Doesn't satisfy the “P” criteria; data collected from a healthy 24 years old male subject.

Tsukada S, Kasai N, Kawano R, Takagahara K, Fujii K, Sumitomo K. Electrocardiogram Monitoring Simply by Wearing a Shirt—For Medical, Healthcare, Sports, and Entertainment. NTT Technical Review. 2014; 12(4): 1-7.
Reason for exclusion: The central concept is the textile electrodes.

Van Langenhove L. Advances in Smart Medical Textiles: Treatments and Health Monitoring; 2015. 1-279 p.
Reason for exclusion: Book about the advances in Smart Medical Textiles: Treatments and Health Monitoring.

Varadan VK. An EKG in your underwear: Nanostructured sensors, smartphones, and cloud computing promise a new platform for everyday medical monitoring. Mechanical Engineering-CIME. 2011 2011/10//:34+.
Reason for exclusion: It is a news report on the promising futures of Nanostructured sensors, smartphones, and cloud computing

Varadan VK, Kumar PS, Oh S, Kegley L, Rai P. e-bra with nanosensors for real-time cardiac health monitoring and smartphone communication. J Nanotechnol Eng Med. 2011; 2(2).
Reason for exclusion: Does not satisfy the "P" criteria; two healthy subjects included.

Vehkaoja A, Verho J, Cömert A, Honkala M, Lekkala J. Wearable system for EKG monitoring - Evaluation of night-time performance. 2012. p. 119-26.
Reason for exclusion: Does not satisfy the "P" criteria; data acquired from four subjects without known medical conditions.

Vojtech L, Bortel R, Neruda M, Kozak M. Wearable Textile Electrodes for ECG Measurement. AEEE. 2013; 11(5): 410-4.
Reason for exclusion: The focal point of the paper is a textile electrode for ECG measurement.

Wang J, Lin C-C, Yu Y-S, Yu T-C. Wireless sensor-based smart-clothing platform for ECG monitoring. Comput Math Methods Med. 2015.
Reason for exclusion: An ECG signal generator (KL-79106 ECG simulator) to study the SNR and MIT database to examine the performance of the QRS detection algorithm; ineligible population.

Weber JL, Blanc D, Dittmar A, Comet B, Corroy C, Noury N, et al. VTAM-A new «biocloth» for ambulatory telemonitoring. Proceedings of the IEEE/EMBS Region 8 International Conference on Information Technology Applications in Biomedicine, ITAB; 2003.
Reason for exclusion: The central point of the paper is not ECG and ineligible population, as data was acquired from persons in a normal state of health.

Weder M, Hegemann D, Amberg M, Hess M, Boesel LF, Abacherli R, et al. Embroidered electrode with silver/titanium coating for long-term ECG monitoring. Sensors. 2015; 15(1): 1750-9.
Reason for exclusion: Design and development of an embroidered electrode with silver/titanium coating for long-term ECG monitoring is discussed in the paper.

Wijesiriwardana R. Novel knitted fibre-meshed transducers [Ph.D.]. Ann Arbor: The University of Manchester (United Kingdom); 2005.
Reason for exclusion: The central idea is fibre-meshed (e-textile) transducers.

Windmiller JR, Wang J. Wearable electrochemical sensors and biosensors: a review. Electroanalysis. 2013; 25(1): 29-46.
Reason for exclusion: A review paper on wearable electrochemical and biosensors.

Wright B. Inovatica develops ECG smart T-shirt | Apparel Industry News [Internet]. 2017 [cited 2018 17 April]. Available from: https://www.just-style.com/news/inovatica-develops-ecg-smart-t-shirt_id129800.aspx.
Reason for exclusion: News about smart shirt developed by Inovatica.

Wu T-K, Lin C-C, Ku W-Y, Liou Y-S, Yang C-Y, Lee M-Y, et al. The study of the Enhanced External Counterpulsation system based on smart clothes. IEEE Int Conf Connect Health Appl Syst Eng Technol; 2016: IEEE.
Reason for exclusion: MIT-BIH database is used instead of a real subject with known cardiac abnormalities.

Xianxiang Chen X, Lv Y, Fang RRZ, hong Xia S, Li H, Tian L. A wireless non-contact ECG detection system based on capacitive coupling. Healthcom; 2012: IEEE.
Reason for exclusion: Authors were contacted to request further data, data derived from healthy subjects.

Xie L, Yang G, Xu L, Seoane F, Chen Q, Zheng L. Characterization of dry biopotential electrodes. Conf Proc IEEE Eng Med Biol Soc. 2013; 2013 1478-81.
Reason for exclusion: The central idea is a comparative study of electrodes. Hence, the authors studied the features of each type of electrodes, and they also addressed the suitable application scenario.

Xu PJ, Liu H, Zhang H, Tao XM, Wang SY. Electrochemical Modification of Silver Coated Multifilament for Wearable ECG Monitoring Electrodes. In: Qian XM, Liu HW, editors. In Advanced Textile Materials, Pts 1-3. Advanced Materials Research. vol. 332-334. 2011. p. 1019-+.
Reason for exclusion: The paper addresses the methodological framework for the fabrication of textile electrodes for wearable ECG measurement.

Yang B, Dong Y. Capacitive coupled non-contact electrodes and ECG signal acquisition. Yi Qi Yi Biao Xue Bao/Chinese Journal of Scientific Instrument. 2015; 36(5): 1072-8.
Reason for exclusion: Not in English.

Yapici MK, Alkhidir TE. Intelligent medical garments with graphene-functionalized smart-cloth ECG sensors. Sensors. 2017; 17(4): 875.
Reason for exclusion: Commercially available DAQ (Power Lab 26T, AD Instruments, Dunedin, New Zealand); Additionally, healthy subjects were used.

Yi WJ, Park KS, Ieee, Ieee, Ieee. Derivation of respiration from ECG measured without subject's awareness using wavelet transform. In Second Joint Embs-Bmes Conference 2002, Vols 1-3, Conference Proceedings: Bioengineering - Integrative Methodologies, New Technologies. Proceedings of Annual International Conference of the Ieee Engineering in Medicine and Biology Society. 2002. p. 130-1.
Reason for exclusion: The main idea is respiration signals (EDR) calculation by reconstructing the detail signal of 9th decomposition from wavelet transform; nothing specific to e-textile based cardiac monitoring.

Yoon SW, Shin HS, Min SD, Lee M. Adaptive motion artefacts reduction algorithm for ECG signal in the textile wearable sensor. IEICE Electronics Express. 2007; 4(10): 312-8.
Reason for exclusion: The focus is a de-noising algorithm.

Zelle D, Fiedler P, Haueisen J. Artefact reduction in multichannel ECG recordings acquired with textile electrodes. Biomedizinische Technik. 2012; 57(SUPPL. 1 TRACK-F): 171-4.
Reason for exclusion: Algorithm; Principal Component Analysis and Independent Component Analysis in time and frequency domain using FastICA and Temporal Decorrelation Source Separation, were employed respectively on ECG signal acquired from textile electrodes.

Zhou Y, Ding X, Hu JY, Duan YR. PPy/Cotton Fabric Composite Electrode for Electrocardiogram Monitoring. Adv Mat Res; 2014: Trans Tech Publ.
Reason for exclusion: The authors applied PPy/cotton fabric composite electrode for electrocardiogram monitoring.

Zięba J, Frydrysiak M, Tesiorowski Ł, Tokarska M. Textronic clothing to ECG measurement. IEEE Int Symp Med Meas Appl; 2011: IEEE.
Reason for exclusion: Focused on electrodes.

Hexoskin Smart Shirts - Cardiac, Respiratory, Sleep & Activity Metrics [Internet]. n.d. [cited 2018 18 April]. Available from: https://www.hexoskin.com/.
Reason for exclusion: An overview of a Hexoskin smart shirt

Holst Centre demonstrates a smart shirt monitoring key vital signs for medical and fitness applications [Internet]. 2017 Available from: https://www.holstcentre.com/news---press/2016/vital-sign-shirt/.
Reason for exclusion: An overview of a smart shirt designed by Holst centre.

ECG Shirt Design - ECE Senior Design - NC State University [Internet]. n.d. [cited 2018 19 April]. Available from: https://research.ece.ncsu.edu/seniordesign/project/ecg-shirt-design/.
Reason for exclusion: Highlight on ECG shirt design.

Overview - Fit Vital Signs Monitoring Shirt [Internet]. 2016 [cited 2018 19 April]. Available from: https://www.maximintegrated.com/en/solutions/fit-shirt/index.mvp
Reason for exclusion: Highlight on Fit vital sign monitor.

Omsignal Smart-Shirt to Wirelessly Measure your Vitals [Internet]. [cited 2018 19 April]. Available from: http://thefutureofthings.com/5137-omsignal-smart-shirt-to-wirelessly-measure-your-vitals/.
Reason for exclusion: Review on a wearable healthcare system project report.

New uses for wearable textile-based health monitoring technology. Textile Outlook International. 2008; (135): 87-8.
Reason for exclusion: It is the review of the attractive the attractive futures of e-textile technology and conclude that: Overall, the outlook for wearable textile-based health monitoring systems is positive.

Award-winning developments for apparel textiles take honours. Technical Textiles International. 2005; 14: 15-8.
Reason for exclusion: Newspaper report

Health-tracking clothing and other machine-to-machine technologies. PT in Motion. 2012 2012/03//:38+.
Reason for exclusion: An overview of machine-to-machine (M2M) technology on health care application.

Appendix C. Studies excluded due to no response from the author

Bianchi AM, Mendez MO. Automatic detection of sleep macrostructure based on a sensorized T-shirt. Conference Proceedings: Annual International Conference of the IEEE Engineering in Medicine & Biology Society. 2010; 2010 3606-9.
Reason for exclusion: The study aimed at the classification of the sleep macrostructure, nothing specific to textile-based ECG monitoring of cardiac patients. Additionally, authors were contacted to request missing information but did not respond on time.

Cai Z, Luo K, Liu C, Li J. Design of a smart ECG garment based on the conductive textile electrode and flexible printed circuit board. Technology & Health Care. 2017; 25(4): 815-21.
Reason for exclusion: Further data are required about the type and number of participants; authors were contacted but no response.

Chen W, Hu J, Bouwstra S, Oetomo SB, Feijs L. Sensor integration for perinatology research. International Journal of Sensor Networks. 2011; 9(1): 38-49.
Reason for exclusion: Focused on premature babies, but the characteristics are not mentioned. The primary authors of the paper were contacted to clear doubts, and they did not respond.

Cheng MH, Chen LC, Hung YC, Chang MY, Tzu LY. A real-time heart-rate estimator from steel textile ECG sensors in a wireless vital wearing system; 2008.
Reason for exclusion: The focus is the real-time heart-rate estimator from ECG data of the system using an adaptive notch filter. Moreover, the authors were contacted to request additional data and did not respond.

Cho HS, Koo SM, Lee J, Cho H, Kang DH, Song HY, et al. Heart monitoring garments using textile electrodes for healthcare applications. Journal of Medical Systems. 2011; 35(2): 189-201.
Reason for exclusion: Further data are required about the type and number of participants; no response from authors.

Fuhrhop S, Lamparth S, Heuer S. A textile integrated long-term ECG monitor with capacitively coupled electrodes; 2009.
Reason for exclusion: Authors were contacted to request further data but did not respond.

Gnecchi JAG, De Jesus Valencia Herrejon A, Del Carmen Tellez Anguiano A, Patino AM, Espinoza DL. Advances in the construction of ECG wearable sensor technology: The ECG-ITM-05 ehealth data acquisition system; 2012.
Reason for exclusion: Authors were contacted to request further data but did not respond.

Huang WT, Chen CH, Chang YJ, Chen YY, Huang JL, Yang CM, et al. Exquisite textiles sensors and wireless sensor network device for home health care. Conference proceedings: Annual International Conference of the IEEE Engineering in Medicine and Biology Society IEEE Engineering in Medicine and Biology Society Annual Conference. 2008; 2008 546-9.
Reason for exclusion: Authors were contacted to request further data but did not respond.

Lee YD, Chung WY. Wireless sensor network based wearable smart shirt for ubiquitous health and activity monitoring. Sensors and Actuators, B: Chemical. 2009; 140(2): 390-5.
Reason for exclusion: Authors were contacted to request further data but did not respond.

Li H, Chen X, Cao L, Zhang C, Tang C, Li E, et al. Textile-based ECG acquisition system with capacitively coupled electrodes. T I MEAS CONTROL. 2017;39(2):141-8.

Reason for exclusion: Authors were contacted to request further data but did not respond.

Loriga G, Taccini N, De Rossi D, Paradiso R. Textile sensing interfaces for cardiopulmonary signs monitoring. Conf Proc IEEE Eng Med Biol Soc. 2005; 7 7349-52.
Reason for exclusion: The paper focuses on the textile electrodes and signal quality; authors were contacted to request further data but did not respond.

Merritt CR. Electronic textile-based sensors and systems for long-term health monitoring [Ph.D.]. Ann Arbor: North Carolina State University; 2008.
Reason for exclusion: The central point is the development of a textile sensor system for health care application; authors were contacted to request further data; no response from authors.

Paradiso R, De Rossi D. Advances in textile technologies for unobtrusive monitoring of vital parameters and movements. Conf Proc IEEE Eng Med Biol Soc. 2006; 1 392-5.
Reason for exclusion: The present the sensors in the t-shirt. The authors were contacted to clarify doubts; they did not respond.

Rai P, Shyamkumar P, Oh S, Kwon H, Mathur GN, Varadan VK, et al. Smart healthcare textile sensor system for unhindered-pervasive health monitoring. Proc SPIE Int Soc Opt Eng; 2012.
Reason for exclusion: Focused on e-textile electrodes; authors were contacted to request further data but did not respond.

Shen CL, Kao T, Huang CT, Lee JH, Ieee Computer SOC. Wearable band using a fabric-based sensor for exercise ECG monitoring 2006. 143-+ p.
Reason for exclusion: Authors were contacted to request further data but did not respond.

Sun F, Yi C, Li W, Li Y. A wearable H-shirt for exercise ECG monitoring and individual lactate threshold computing. Computers in Industry. 2017 12 July 2017 92:1-11.
Reason for exclusion: Authors were contacted to request further data but did not respond.

Sun F, Zhao Z, Fang Z, Du L, Chen D. Design and implementation of a highly integrated non-contact ECG monitoring belt. JFBI. 2015; 8(1): 37-46.
Reason for exclusion: Authors were contacted to request further data but did not respond.

Taccini N, Loriga G, Pacelli M, Paradiso R. Wearable monitoring system for chronic cardio-respiratory diseases. Conf Proc IEEE Eng Med Biol Soc. 2008; 2008 3690-3.
Reason for exclusion: Authors were contacted to request further data; all healthy volunteers participated.

Trindade IG, Martins F, Dias R, Oliveira C, da Silva JM. Novel textile systems for the continuous monitoring of vital signals: design and characterization. Conf Proc IEEE Eng Med Biol Soc: IEEE; 2015. p. 3743-6.
Reason for exclusion: Authors were contacted to request further data but did not respond.

Ueno A, Akabane Y, Kato T, Hoshino H, Kataoka S, Ishiyama Y. Capacitive sensing of electrocardiographic potential through cloth from the dorsal surface of the body in a supine position: a preliminary study. IEEE Trans Biomed Eng. 2007; 54(4): 759-66.
Reason for exclusion: Authors were contacted to request further data but did not respond.

Ulbrich M, Muhlsteff J, Sipila A, Kamppi M, Koskela A, Myry M, et al. The IMPACT shirt: textile integrated and portable impedance cardiography. Physiol Meas. 2014; 35(6): 1181-96.
Reason for exclusion: The method is ICG instead of ECG. Again, the authors were contacted to request further data but did not respond.

Zhou P, Li Z, Wang F, Jiao H. Portable wireless ECG monitor with fabric electrodes; 2013.
Reason for exclusion: Authors were contacted to request further data but did not respond.

Appendix D. Characteristics summary of the included studies (n = 17)

Author, year, and country	Aims, purpose or objectives	Sample size population	Physiological parameters Monitored	# of leads	ECG acquired	Context	Key findings
(Balsam et al., 2018), Poland	This study aims to show the utility of biomedical shirt-based ECG monitoring of patients with CVD in different clinical situations using the Nuubo ECG (nECG) system.	220 adults and neonates MI	• ECG	3	• Resting ECG • Ambulatory ECG	Out-patient	• Continuous ECG monitoring during daily activities • High quality of ECG recordings, as well as the assurance of a proper adherence due to adequate comfort of wearing the shirt.
(Bourdon et al., 2005), Italy & France	The purpose was to verify that the ECG data generated by the WEALTHY device are reliable and satisfactory for physicians compared with those achievable with standard clinical telemetry devices.	5 adult cardiac patients	• ECG, • Respiration	5	• Resting ECG • Ambulatory ECG	In hospital	• In healthy subjects, WEALTHY gave a signal as good as the reference system in 82.6 ± 4.1 % of the time for ECG and 88.4 ± 1.5 % of the time for respiration (RESP). • Sweating makes the signal acquired from the textile electrodes better.
(Coli et al., 2006), Spain	Successful real-time ECG recording and transmission in cardiac patients with a wearable system based on smart textiles: first clinical experience of the WEALTHY project.	15 adult male Cardiac patients	• ECG, • Respiration	5	• Resting ECG • Exercise ECG	In hospital	• ECG quality score was not different between the WEALTHY system and the standard telemetry system. • ECG quality modestly decreased during exercise. • V5 performed significantly better than V2.
(Coosemans et al., 2006), Belgium (Europe)	Garment embedded patient monitoring system, including wireless communication and inductive powering for beat-to-beat heart rate detection, is presented in the paper.	2 Neonates Sudden Infant Death Syndrome (SIDS)	• ECG	1	• Resting ECG	In hospital	• Textile electrodes (Textile electrodes) are knitted on the elastic belt and connected to the printed circuit board (PCB) through three press-studs. • As power is provided through an inductive link, no battery is required. • Testing the prototype at rest, using textile electrodes and conventional electrodes, they

Author, year, and country	Aims, purpose or objectives	Sample size population	Physiological parameters Monitored	# of leads	ECG acquired	Context	Key findings
							found out the signal collected from the textile electrodes exhibits more low-frequency baseline drift.
.(Di Rienzo et al., 2005), Italy	A Textile-Based Wearable System for Vital Sign Monitoring: Applicability in Cardiac Patients - MagIC has been tested in freely moving subjects at work, at home, while driving and cycling. The applicability of the system in a clinical setting is now under evaluation.	14 adult cardiac patients	• ECG, • Respiration	1	• Resting ECG • Exercise ECG	In hospital	• The MagIC System is composed of a vest, including textile sensors and a portable electronic board with the typical size and weight of a small cell phone - which is placed on the vest through a velcro strip. • MagIC provided readable signals for more than 99% and 97% of the time while the subjects were lying supine and on the cycloergometer, respectively.
(Di Rienzo et al., 2006a), Italy	In this study, the MagIC System has been used to monitor vital signs: In cardiac inpatients in bed and during physical exercise.	31 adult cardiac patients	• ECG, • Respiration	1	• Resting ECG • Ambulatory ECG • Exercise ECG	In hospital	• MagIC provided readable signals (namely, adequate to detect the QRS complex) for more than 99% and 97% of the time in cardiac inpatients while lying supine and pedalling on the cycloergometer, respectively. • Signals from MagIC also allowed correct identification of the targeted rhythm aberrances.
(Di Rienzo et al., 2010), Italy	The paper presents the device, named Maglietta Interattiva Computerizzata (MagIC), which was used for the home monitoring of cardiac patients.	3 adult cardiac patients	• ECG, • Respiration	1	• Not mentioned	Out-patient	• The results of this study indicated that the system behaved correctly in 85 out of 90 sessions (94%). In contrast, in five cases, a second session was required due to the Universal Mobile Telecommunications System (UMTS) traffic congestion.

Author, year, and country	Aims, purpose or objectives	Sample size population	Physiological parameters Monitored	# of leads	ECG acquired	Context	Key findings
							• They assume that the patients might not be familiar with the technology. Thus, they adopted several solutions to simplify the patient's interaction with the technological aspects of the service.
(Di Rienzo et al., 2013), 2013, Italy	Evaluation of a textile-based wearable system for the electrocardiogram monitoring in cardiac patients; Applications of a Textile-Based Wearable System in clinics exercise and under gravitational stress; Clinical evaluation of MagIC.	40 adult cardiac inpatients	• ECG, • Respiration	1	• Resting ECG • Ambulatory ECG • Exercise ECG	In hospital	• At rest, the artefact rates observed with MagIC and Trad-ECG were virtually identical (1.4% of the registered signal). • During physical exercise, the artefact rate observed with MagIC was much lower than with Traditional ECG (4.07 vs. 17.31%). • Recordings from MagIC allowed correct identification of the type of rhythm in the vast majority of patients (92.5%) and estimation of PQ interval and QRS duration similar to Traditional ECG (<0.016 s). • MagIC displayed a good performance in detecting arrhythmias, with only 14 misclassified events out of 3618 and both specificity and sensitivity being above 99%. • No practical difference was observed in the estimation of the beat-by-beat RR interval by the two methods. • Thirty-eight out of 40 patients found the vest comfortable during activity and preferable to the standard technique.

Author, year, and country	Aims, purpose or objectives	Sample size population	Physiological parameters Monitored	# of leads	ECG acquired	Context	Key findings
(Hsiao et al., 2015), 2015, Taiwan	The primary objective is to design and develop a wearable heart rate monitoring system and prediction tool that can measure the patient's heart rate parameters, allow him/her to move around easily, and which can effectively improve the medical personnel's working efficiency.	31 adult cardiac patients	• ECG	Not mentioned	• Resting ECG	In hospital	• This research proposes a system that can effectively support clinical prognosis through a smart textile integrated with heart rate measurement function to support important characteristics such as comfortable wearing, heart rate recording, wireless transmission, and constraint-free when the patient is hospitalized for observation. • The future architecture of this system is to enable all the hospitalized patients to download the app on their smartphones to perform the measurement, and to transmit data to the physician's computer at the same time to save hardware cost.
(Kakria et al., 2015), Thailand	A Real-Time Health Monitoring System for Remote Cardiac Patients Using Smartphone and Wearable Sensors; This study develops a remote monitoring diagnostic framework to detect underlying heart conditions in real-time, which helps to avoid potential heart diseases and rehabilitation of the patients recovering from cardiac diseases.	40 adult cardiac patients	• ECG, • BP, • Temperature	Not mentioned	• Not mentioned	Not mentioned	• A web interface that enables several physicians, doctors, and medical centres to view and diagnose patients' medical status simultaneously; Alarming Messages is proposed. • The use of a 3G network provides a wide coverage area as compared to the existing system. • The system uses wearable sensors that are physically comfortable for wearing.
	The objective of this paper is to present the results of the LOBIN platform, which provides remote location and						• The performance of the whole system was tested through a pilot scheme in the cardiology

Author, year, and country	Aims, purpose or objectives	Sample size population	Physiological parameters Monitored	# of leads	ECG acquired	Context	Key findings
(Lopez et al., 2010) , Spain	healthcare-monitoring support for hospital environments based on the combination of e-textile and Wireless sensor network (WSN) technologies. This paper presents the architecture, system deployment as well as validation results from both laboratory tests and a pilot scheme developed with real users in collaboration with the Cardiology Unit at La Paz Hospital, Madrid, Spain.	5 adult cardiac patients	• ECG, • HR, • Temperature, • location of patients	1	• Not mentioned	In hospital	unit at La Paz Hospital; Battery life for the Wearable data-acquisition device (WDAD) is 7-8 hours and 2 days for location Wireless transmission board (WTB) while the doctors approve the quality of the ECG signal. • The system is a substitute for the commercial telemetry systems
(Olmos et al., 2014), Spain	The paper aims to assess the accuracy of the Nuubo system in the diagnosis of patients with reflex syncope; To evaluate this point, they compared the results obtained with the Nuubo system with those obtained utilizing a conventional monitoring system during a tilt table test.	31 adult with clinical suspicion of reflex syncope	• ECG	1	• Resting ECG	In hospital	• The device enables remote, continuous, non-invasive and long-lasting monitoring. • The elastic textile adapts to the patients' movements, permitting them to carry out daily physical activities without the limitation of wires. • The device has a built-in 3-axis accelerometer that measures the position and inclination of the patient at every moment, which is another useful tool when syncope is analysed.
(Pandian and Srinivasa, 2016), 2016, India	The paper discusses the preliminary results of a prototype wearable physiological monitoring system to monitor physiological parameters such as ECG, HR, EEG and Body Temperature.	Numbers not clearly stated. Adult cardiac patients	• ECG, • EEG, • Temperature	1	• Not mentioned	Not mentioned	• There is a baseline wander due to the modulation of the respiratory waveform over the ECG signals induced by the breathing of the subject. • The motion artefact is caused due to the involuntary contractions of the muscles and also the relative motion of electrodes with the movement of the subject. • Power line interference is removed by a digital notch filter.

Author, year, and country	Aims, purpose or objectives	Sample size population	Physiological parameters Monitored	# of leads	ECG acquired	Context	Key findings
(Perez De Isla et al., 2011), Spain	The paper aims to assess the feasibility of using the Nuubo system during exercise echocardiography and to compare the results obtained with the Nuubo system with the results obtained using the conventional treadmill system.	31 adult cardiac patients	• ECG	1	• Exercise ECG	In hospital	• Nuubo's dynamic ECG can obtain similar results to the conventional treadmill system during exercise tests and allows to obtain echocardiographic images but more easily and comfortably.
(Romagnoli et al., 2014), Spain	The paper aims to compare the time between heartbeats and HRV parameters obtained with a smart textile system (GOW; Weartech sl., Spain) and an electrocardiogram machine commonly used in hospitals during continuous cycling tests.	12 adult acute myocardial infarction	• ECG	Not mentioned	• Exercise ECG	Not mentioned	• There were no-wide discrepancies in the limits of agreement (LoAs) of the RR intervals recorded by the two systems: ○ Mean RR, SDNN (standard deviation normal) and SD2 (long-term heart rate variability (HRV)) present excellent LoAs for absolute and relative values. ○ The square root of the differences of successive NN intervals (RMSSD), high-frequency (HF), low-frequency (LF)/HF, HF power in normalized units (HFnu) and SD1 showed a worse agreement between systems. • In conclusion, the GOW system is a valid tool for controlling HR while performing physical activity, although its use as a clinical tool for HRV cannot be supported.
							• ECG raw signals, acquired with the data acquisition (DAT) unit,

Author, year, and country	Aims, purpose or objectives	Sample size population	Physiological parameters Monitored	# of leads	ECG acquired	Context	Key findings
							were obtained with three subjects in standing and walking states.
(Trindade et al., 2016), Portugal	This article addresses the design, development, and evaluation of T-shirt prototypes that embed novel textile sensors for the capture of cardio and respiratory signals.	8 adult cardiac patients	• ECG	4	• Not mentioned	In hospital	• In both states of the subject, wander interference caused by the respiration activity is present, most severely in the walking condition. • The skin-contact electrodes simultaneously capture the respiratory signals, which can be useful to minimize the number of sensors to integrate into the monitoring garment. • The waveforms processed by the MATLAB program (lead L2 and lead V1) clearly show that the signals obtained with the subject in the walking state exhibit higher noise amplitude than those corresponding to the standing state. • The signal to noise ratio (SNR) of the ECG signal from the walking subject is affected by motion artefact interference, characterized by a decrease of SNR amplitude caused by the degradation of electrical electrode-skin contact
(Yu et al., 2017), Germany	In this paper, the authors present the application and evaluation of a T-shirt in a clinical study, during which they obtained 422 hours of data from five subjects.	5 adult cardiac subjects	• ECG	12	• Resting ECG • Ambulatory ECG	Out-patient	• The ECG T-shirt is based on a commercially available men's fitness T-shirt (Nike Legend, Nike, Beaverton, OR, USA); • Reference data was unavailable for this study since the large impact of a simultaneously recorded conventional 12-lead Holter-

Author, year, and country	Aims, purpose or objectives	Sample size population	Physiological parameters Monitored	# of leads	ECG acquired	Context	Key findings
							ECG on the subjects' daily life would be impractical. • Temporal coverage for individual ECG leads ranges from 16.3% up to 74.8% and mean values from 20.9% to 56.3% depending on the subject. • The simple temporal fusion of all ECG-leads increases coverage, depending on the subject, by 40% to 80% compared to the independent analysis of single ECG leads.

Appendix E. Summary of technical specifications (n = 17)

Author, year, and country	Number and type of Sensors	Data storage	Electronic - textile integration	Frequency response (Hz)	Wireless protocol	Area of application	Platform	Recommendations and Limitations
(Balsam et al., 2018), Poland	4 textile electrodes plus 1 neutral electrode	Memory card (Size not specifically mentioned)	• No electronic integration except the textile electrodes (attachable wireless device, nECG MINDER)	• Not mentioned	• Bluetooth	• Monitoring	Compute r-based	• Few studies evaluating such wearable systems, • Short battery life, • Dependence on the user adherence and presence of artefacts during recordings, • Implementing the Nuubo ECG monitoring in the children's population may provide some challenges. • Moreover, the detection of asymptomatic AF with new technologies, such as wearable shirts, has not yet been formally evaluated as an arrhythmia detection method
(Bourdon et al., 2005), Italy & France	5 ECG textile electrodes, 4 impedance pneumography sensor	Not specifically mentioned	• No electronics integration except the textile electrodes, separate portable patient unit (PPU)	• Not mentioned	• GPRS communicat ion under TCP/IP protocol	• Monitoring	Compute r-based	• The general performance of the WEALTHY system could be enhanced by post-processing as well as by customization of the WEALTHY garment to the subject/patient
(Coli et al., 2006), Spain	5 ECG textile electrodes, 4 impedance pneumography sensor	The data is transmitted and stored on a computer; nothing is given about intermediate data storage	• No electronics integration except the textile electrodes, separate portable patient unit (PPU)	• Not mentioned	• GPRS communicat ion under TCP/IP protocol	• Monitoring	Compute r-based	• Not published as a full article but just an abstract presented at a conference

Author, year, and country	Number and type of Sensors	Data storage	Electronic - textile integration	Frequency response (Hz)	Wireless protocol	Area of application	Platform	Recommendations and Limitations
(Coosemans et al., 2006), Belgium (Europe)	3 knitted and woven stainless-steel textile ECG electrodes	Not specifically mentioned	• Embedded electronics	• 0.5–150	• Not mentioned	• Continuous ECG monitoring	Not clearly mentione d	• The signal collected from the textile electrodes exhibits more low-frequency baseline drift than the signal collected using the standard commercial electrodes. • Higher CMMR circuit configuration tends to saturate the amplifier, and they did not report or proposed possible solutions. • The suggested PCB is not washable. • Nothing has been discussed how the user is electrically insulated from the PCB, the inductive coil and electrodes are knitted on the garment. • Nothing is said about how the data is presented to the user. • No clear information is provided about the maximum allowable distance. The user can travel from the power source as power is provided wirelessly via an inductive link.
(Di Rienzo et al., 2005), Italy	2 textile ECG electrodes	Data stored on PDA or computers disk; nothing is mentioned about intermediate data storage	• No electronics integration except the textile electrodes (portable electronic board)	• Not mentioned	• Not mentioned	• Monitoring	Compute r / Personal digital assistant (PDA)	• The issue of motion artefact and the effect of capacitive coupling has not been addressed. • A single lead configuration and hence reduced dynamic range in the acquired signal. • Given the current integrated technology, their system especially the cell phone-size portable electronic board seems outdated

Author, year, and country	Number and type of Sensors	Data storage	Electronic - textile integration	Frequency response (Hz)	Wireless protocol	Area of application	Platform	Recommendations and Limitations
(Di Rienzo et al., 2006a), Italy	2 textile ECG electrodes	Data stored on PDA or computers disk; nothing is mentioned about intermediate data storage	• No electronics integration except the textile electrodes (portable electronic board)	• Not mentioned	• Bluetooth	• Monitoring	Computer / Personal digital assistant (PDA)	• Motion artefact
(Di Rienzo et al., 2010), Italy	2 textile ECG electrodes	Stored locally on the Memory card	• No electronics integration except the textile electrodes (portable electronic board)	• Not mentioned	• WiFi or universal mobile telecommunications system (UMTS) connections	• Monitoring	Computer-based	• The main challenge was motion artefact and hence they accepted recordings containing at least 50% of the valid signal. • Thermal discomfort of the subject
(Di Rienzo et al., 2013), Italy	2 textile ECG electrodes,	Stored locally on the Memory card	• No electronics integration except the textile electrodes (portable electronic board)	• Not mentioned	• Bluetooth	• Monitoring	Computer-based	• The vest embeds two electrodes and thus only one ECG lead is available: the implicit limitation of this choice is that no reliable information can be guaranteed on the ischemic changes in the ST segment. • The experiment was performed on males only because the female version of the vest was not yet available at the moment of the data collection. • System capability of recognizing other kinds of severe arrhythmias, such as sustained ventricular tachycardia, Torsade de point, is not yet investigated
(Hsiao et al., 2015), Taiwan	Not mentioned	Not specifically mentioned	• Not clearly stated.	• Not mentioned	• Bluetooth	• Monitoring	Computer-based	• The back-end analysis software is based on MATLAB which is technical by its nature. • Nothing has been discussed about the number of electrodes,

Author, year, and country	Number and type of Sensors	Data storage	Electronic - textile integration	Frequency response (Hz)	Wireless protocol	Area of application	Platform	Recommendations and Limitations
								available leads and how and where the electrodes are attached to the body. • Power requirement and data security issues are not addressed. • Signal quality is left untouched.
(Kakria et al., 2015), Thailand	Not clearly mentioned, they used Zephyr HxM Bluetooth (BT) Wireless Heart Rate Sensor, Monitor; Omron wireless upper arm blood pressure monitor; G plus, Bluetooth based temperature sensor	Micro Secure Digital (SD) memory card	• Not clearly stated.	• Not mentioned	• Bluetooth low energy and GPRS/WiFi/ 3G	• Monitoring	Android Mobile & Compute r-based	• It is focused more on the software part (IT platform) for the commercially available systems Zephyr BT (heart rate sensor), Omron wireless upper arm blood pressure monitor, and G plus Bluetooth based temperature sensor. • Possibility of false alarms due to the battery issues of sensors and smartphone
(Loriga et al., 2006), Spain	2 textile ECG electrodes, 3 axis accelerometers, and a thermometer	Data stored in the management subsystem (Management server- PC)	• No electronics integration except the textile electrodes (the data acquisition and processing PCB are not integrated into the t-shirt)	• 0.5 - 125	• IEEE 802.15.4 (Low-Rate Wireless Personal Area Networks)	• Monitoring	Compute r-based	• Single lead configuration. • Too many subsystems • To be able to do a reliable measure of ST-segment descent, it should operate at 0.05 Hz frequency
(Olmos et al., 2014), Spain	2 textile ECG electrodes plus 1 neutral electrode	Stored on micro–Secure Digital (SD) card and computer hard disk	• No electronics integration except the textile electrodes (attachable wireless device, nECG MINDER)	• 0.5 - 100	• Bluetooth	• Monitoring	Compute r-based	• Single lead configuration • To be able to do a reliable measure of ST-segment descent, it should operate at 0.05 Hz frequency
								• Further work is been carried out

Author, year, and country	Number and type of Sensors	Data storage	Electronic - textile integration	Frequency response (Hz)	Wireless protocol	Area of application	Platform	Recommendations and Limitations
(Pandian and Srinivasa, 2016), India	3 textile ECG electrodes 2 textile EEG electrodes 1 temperature sensor (thermistor)	Data stored in the PC, no intermediate storage	• Embedded electronics	• 0.5-100	• ZigBee wireless communication	• Monitoring	Computer-based	on the signal processing section of the system to remove tremors and motion artefact from the ECG signal at the remote monitoring station. • The hardware must be miniaturized and packaged, and more testing needs to be carried out. • The issue of electrical safety and data security needs to be addressed
(Perez De Isla et al., 2011), Spain	2 textile ECG electrodes plus 1 neutral electrode	Stored on micro–Secure Digital (SD) card and computer hard disk	• No electronics integration except the textile electrodes (attachable wireless device, nECG MINDER)	• 0.5 - 100	• Bluetooth	• Monitoring	Computer-based	• The main limitation of the tested device is the fact that it works from the 0.5 Hz frequency to 100 Hz frequency. • To be able to do a reliable measure of ST-segment descent, it should operate at 0.05 Hz frequency. • Therefore, Nuubo's devices that were tested in this study were not suitable for measuring with diagnostic precision ST-segment descents or variations
(Romagnoli et al., 2014), Spain	4 textile ECG electrodes	Data stored in the GOW module	• No electronics integration except the textile electrodes, separate GOW module	• Not mentioned	• Not mentioned	• Monitoring	Not mentioned	• The results of the present study show that the measurement error of the GOW system is too large to accept the HRV data during exercise and, therefore, does not meet the requirements as a clinical tool.
(Trindade et al., 2016), Portugal	5 textile ECG electrodes (RA, LA, LL, V1 and a reference electrode)	Data recorded on a Smartphone, and further processed on a PC	• Embedded electronics	• 0.05 - 100	• Bluetooth	• Monitoring	Mobile-based	• Motion artefact interference, mainly caused by friction between the textile electrodes and the skin, and considerably limited the performance of the prototypes in mobile contexts.

Author, year, and country	Number and type of Sensors	Data storage	Electronic - textile integration	Frequency response (Hz)	Wireless protocol	Area of application	Platform	Recommendations and Limitations
(Yu et al., 2017), Germany	10 textile ECG electrodes	Micro Secure Digital (SD) card with a 64GB	• No electronics integration except the textile electrodes	• Not mentioned	• Not mentioned	• Monitoring	Not mentione d	• There are ECG segments with artefacts with a signal to noise ratio (SNR) higher than the threshold. • In the future they recommended compression T-shirts to increase contact pressure and therefore to improve signal quality;

Appendix F. Design for band stop filter

The first digital filter implemented on the microcontroller was anti hum filter. The design procedures are discussed below:

Step 1:

Type of filter – Butterworth band-stop anti hum filter

The following are the filter specifications:

- Filter order – $N_{bsp} = 4$;
- Sampling frequency – fs = 250Hz; and
- Passband cut-off frequency – f_{c1} = 48Hz, f_{c2}=52Hz.

Step 2:

Based on the IIR filter design outlined in (Milivojevic, 2009), the transfer function of the Butterworth reference analog prototype filter has no zeros. Hence only poles are calculated as follows:

$$S_K = e^{j\pi(\frac{1}{2}+\frac{2K+1}{2N})} \quad \textit{Where } \text{K=0,1,2,. . . N-1 and N = Filter order}$$

$$S_K = \cos(\pi(\frac{1}{2}+\frac{2K+1}{2N})) + j\sin(\pi(\frac{1}{2}+\frac{2K+1}{2N}))$$

For a band-stop IIR filter of order N, the reference analog filter has half of the required filter order. Hence the order is N = N_{bsp} / 2 = 2. Then the poles are:

$$S_1 = \cos(\pi(\frac{1}{2}+\frac{1}{2*2})) + j\sin(\pi(\frac{1}{2}+\frac{1}{2*2})) = \cos(\pi(\frac{1}{2}+\frac{1}{4})) + j\sin(\pi(\frac{1}{2}+\frac{1}{4}))$$

$$= \cos(\frac{3\pi}{4}) + j\sin(\frac{3\pi}{4}) = -0.7071 + j0.7071$$

$$S_2 = \cos(\pi(\frac{1}{2}+\frac{2*1+1}{2*2})) + j\sin(\pi(\frac{1}{2}+\frac{2*1+1}{2*2})) = \cos(\pi(\frac{1}{2}+\frac{3}{4})) + j\sin(\pi(\frac{1}{2}+\frac{3}{4}))$$

$$= \cos(\frac{5\pi}{4}) + j\sin(\frac{5\pi}{4}) = -0.7071 - j0.7071$$

$$S_1 = -0.7071 + j0.7071, \quad S_2 = -0.7071 - j0.7071$$

Hence, the transfer function to the prototype analog filter is given as follows.

$$H_a = \frac{1}{\text{s-(-0.7071 + j0.7071)+s-(-0.7071 - j0.7071)}}$$

$$= \frac{1}{\text{(s + 0.7071 - j0.7071) + (s + 0.7071 + j0.7071)}}$$

Step 3:

The analog filter cut-off frequency Ωc:

$$\Omega_{c1} = \tan(\pi\frac{f_{c1}}{f_s}) = \tan(\pi\frac{48}{250}) = 0.688824$$

$$\Omega_{c2} = \tan(\pi\frac{f_{c2}}{f_s}) = \tan(\pi\frac{52}{250}) = 0.7656645$$

$$\Omega_0 = \sqrt{\Omega_{c1} * \Omega_{c2}} = \sqrt{0.688824 * 0.7656645} = 0.72623$$

$$\Omega_c = \frac{\Omega_{c1}}{\Omega_0^2 - \Omega_{c1}^2} = \frac{0.688824}{0.72623^2 - 0.688824^2} = \frac{0.688824}{0.52741 - 0.47448} = 13.04$$

Analog filter transfer function from the transfer function of the reference analog prototype filter:

$$H(s) = H_0 \frac{1}{(-\Omega_c)^{N-M}} \frac{\prod_{k=1}^{M} z_k}{\prod_{k=1}^{N} p_k} (s - j\Omega_0)^{N-M} (s + j\Omega_0)^{N-M} \frac{\prod_{k=1}^{M} (s - \frac{1-\sqrt{1-4\Omega_c^2 z_k^2 \Omega_0^2}}{2\Omega_0^2 z_k})(s - \frac{1+\sqrt{1-4\Omega_c^2 z_k^2 \Omega_0^2}}{2\Omega_0^2 z_k})}{\prod_{k=1}^{N} (s - \frac{1-\sqrt{1-4\Omega_c^2 p_k^2 \Omega_0^2}}{2\Omega_0^2 p_k})(s - \frac{1+\sqrt{1-4\Omega_c^2 p_k^2 \Omega_0^2}}{2\Omega_0^2 p_k})}$$

Butterworth reference prototype filter has no zeros, then:

$$H(s) = \frac{1}{(\Omega_c)^2 p_1 . p_2} \frac{(s - j\Omega_0)^2 (s + j\Omega_0)^2}{(s - \frac{1-\sqrt{1-4\Omega_c^2 p_1^2 \Omega_0^2}}{2\Omega_c p_1})(s - \frac{1+\sqrt{1-4\Omega_c^2 p_1^2 \Omega_0^2}}{2\Omega_c p_1}) * (s - \frac{1-\sqrt{1-4\Omega_c^2 p_2^2 \Omega_0^2}}{2\Omega_c p_2})(s - \frac{1+\sqrt{1-4\Omega_c^2 p_2^2 \Omega_0^2}}{2\Omega_c p_2})}$$

$$= \frac{1}{(13.04)^2 \ (-0.7071 + j0.7071) * (-0.7071 - j0.7071)} * \frac{(s - j0.72623)^2 (s + j0.72623)^2}{\exp r}$$

$$\exp r = (s - \frac{1-\sqrt{1-4(13.04)^2(-0.7071 + j0.7071)^2 \ 0.72623^2}}{2 * 13.04(-0.7071 + j0.7071)})(s - \frac{1+\sqrt{1-4(13.04)^2(-0.7071 + j0.7071)^2 \ 0.72623^2}}{2 * 13.04(-0.7071 + j0.7071)}) *$$
$$(s - \frac{1-\sqrt{1-4(13.04)^2(-0.7071 - j0.7071)^2 \ 0.72623^2}}{2 * 13.04(-0.7071 - j0.7071)})(s - \frac{1+\sqrt{1-4(13.04)^2(-0.7071 - j0.7071)^2 \ 0.72623^2}}{2 * 13.04(-0.7071 - j0.7071)})$$

$$H(s) = \frac{1}{170.0383} * \frac{(s - j0.72623)^2 (s + j0.72623)^2}{(s + 0.0261 - j0.6991)(s + 0.0281 + j0.7533)) * (s + 0.0261 + j0.6991)(s + 0.0281 - j0.7533))}$$

Step 4:

Bilinear transformation is used to convert the analog transfer function to the digital filter.

$$s = \frac{1 - z^{-1}}{1 + z^{-1}}$$

Then,

$$H(z) = H_0 (-1)^{N-M} \frac{\prod_{k=1}^{M} (1 - z_k)}{\prod_{k=1}^{N} (1 - p_k)} (1 + z^{-1})^{N-M} \frac{\prod_{k=1}^{M} (1 - \frac{1 - z_k}{1 + z_k}) z^{-1}}{\prod_{k=1}^{N} ((1 - \frac{1 - p_k}{1 + p_k}) z^{-1})}$$

$$= \frac{(1 - j0.72623)(1 - j0.72623)(1 + j0.72623)(1 + j0.72623)}{(1.0261 - j0.6991)(1.0281 + j0.7533)(1.0261 + j0.6991)(1.0281 - j0.7533)} *$$

$$\frac{(1 - \frac{1 - j0.72623}{1 + j0.72623} z^{-1}).(1 - \frac{1 - j0.72623}{1 + j0.72623} z^{-1}).(1 - \frac{1 + j0.72623}{1 - j0.72623} z^{-1}).(1 - \frac{1 + j0.72623}{1 - j0.72623} z^{-1})}{(1 - \frac{1.0261 - j0.6991}{0.9739 + j0.6991} z^{-1}).(1 - \frac{1.0281 + j0.7533}{0.9719 - j0.7533} z^{-1}).(1 - \frac{1.0261 + j0.6991}{0.9739 - j0.6991} z^{-1}).(1 - \frac{1.0281 - j0.7533}{0.9719 + j0.7533} z^{-1})}$$

$$= \frac{2.333}{2.5043} \frac{(1 - (0.3094 - j0.9509) z^{-1})^2 * (1 - (0.3094 + j0.9509) z^{-1})^2}{(1 - (0.3552 - j0.9731) z^{-1}).(1 - (0.2855 + j0.9964) z^{-1}).(1 - (0.3552 + j0.9731 z^{-1}).(1 - (0.2855 - j0.9964) z^{-1})}$$

$$= \frac{2.333}{2.5043} \frac{(1 - 0.6188 z^{-1} + 0.9999 z^{-2})^2}{(1 - 0.7104 z^{-1} + 1.0731 z^{-2})(1 - 0.571 z^{-1} + 1.0743 z^{-2})}$$

$$H(z) = \frac{0.9314 - 1.1527 z^{-1} + 2.2194 z^{-2} - 1.1529 z^{-3} + 0.9314 z^{-4}}{1 - 1.1937 z^{-1} + 2.5530 z^{-2} - 1.1127 z^{-3} + 1.1028 z^{-4}}$$

Appendix G. External short circuit test (ADS1298)

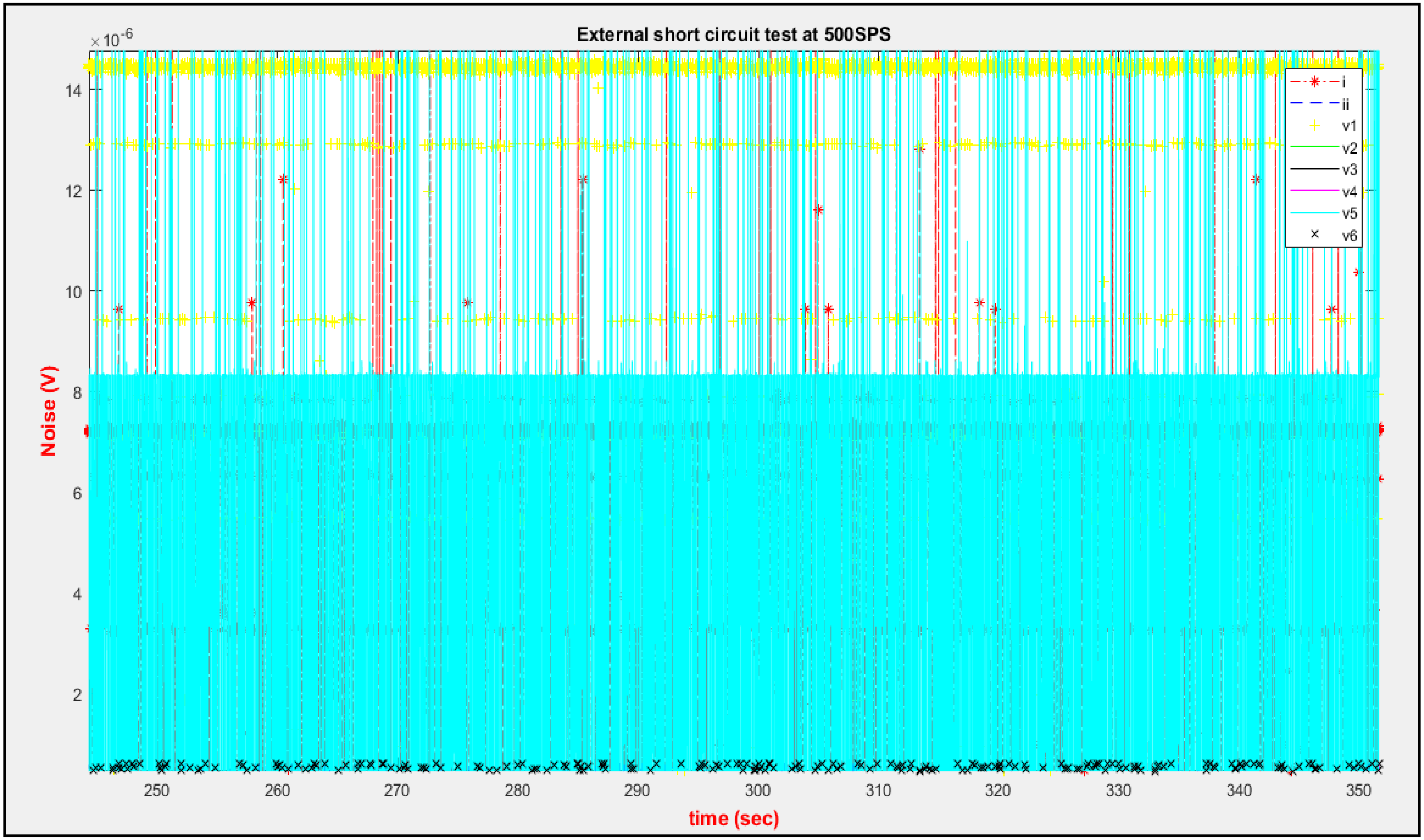

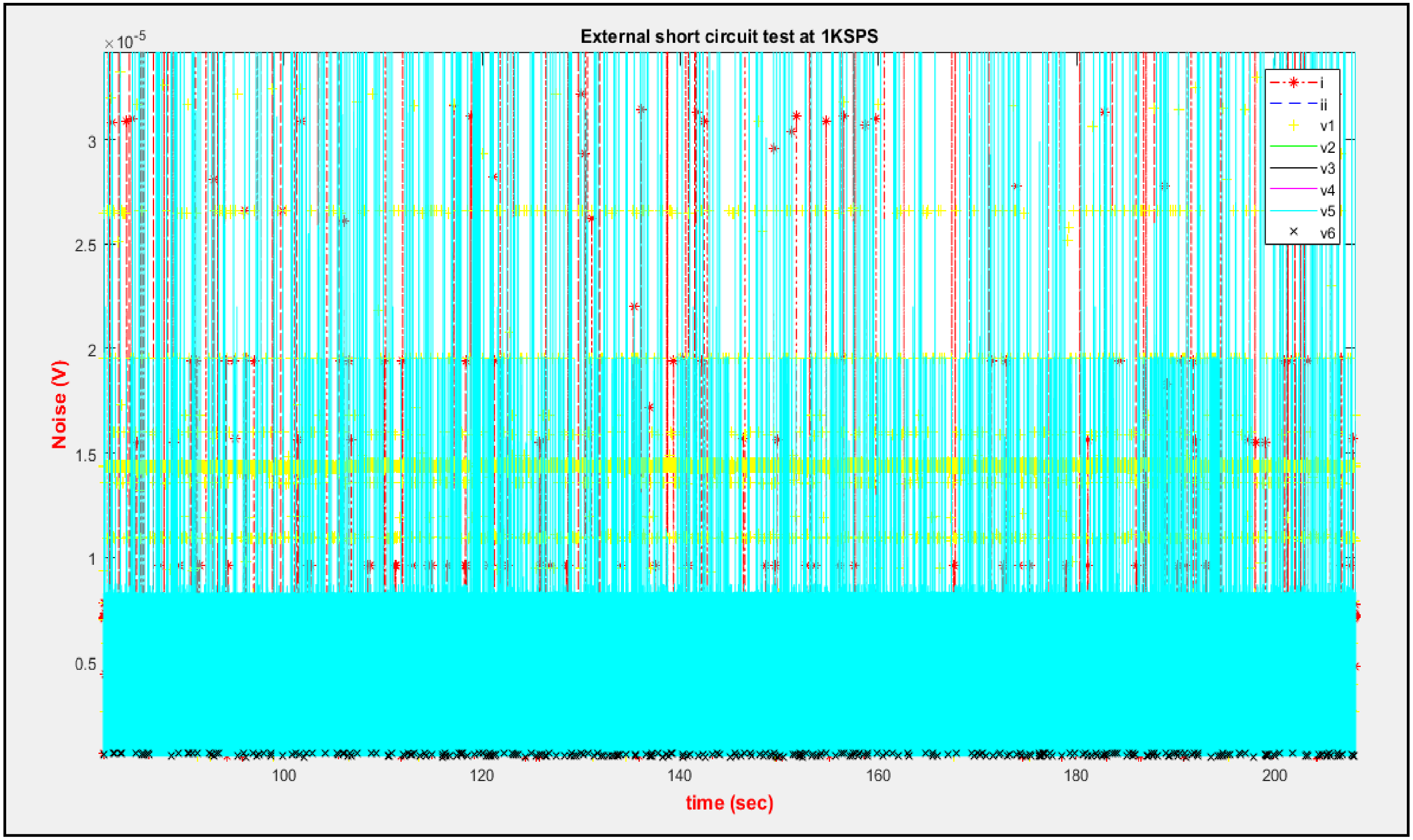
External short circuit test at 1KSPS
× 10^-5
3
2.5
2
1.5
1
0.5
Noise (V)
100
120
140
160
180
200
time (sec)
i
ii
v1
v2
v3
v4
v5
v6

Appendix H. EASI base ECG leads (V_{AI}, V_{ES}, and V_{AS}) - acquired from the ProSim 3.0 Vital Signal Simulator, the vertical axis in mV.

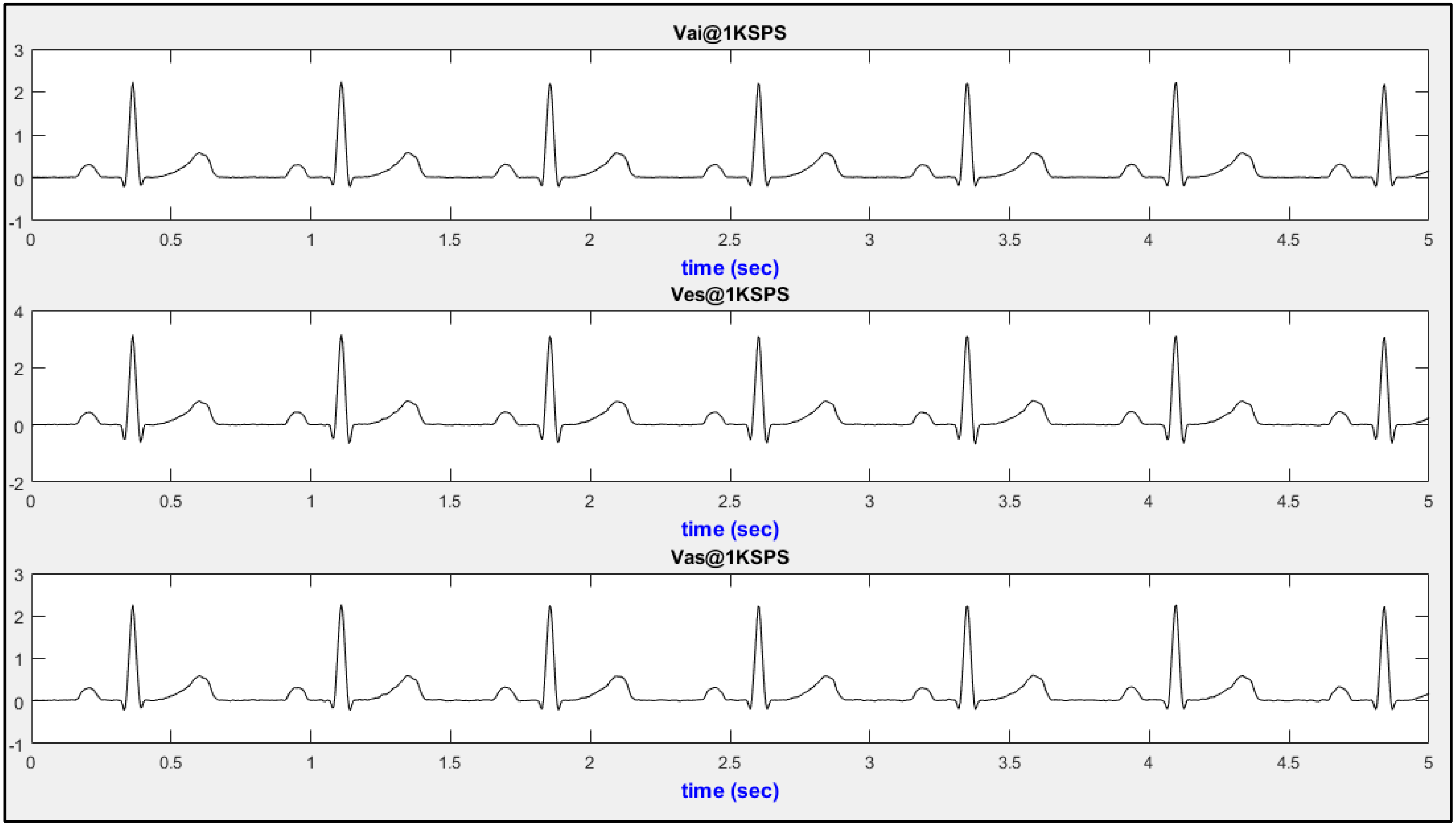

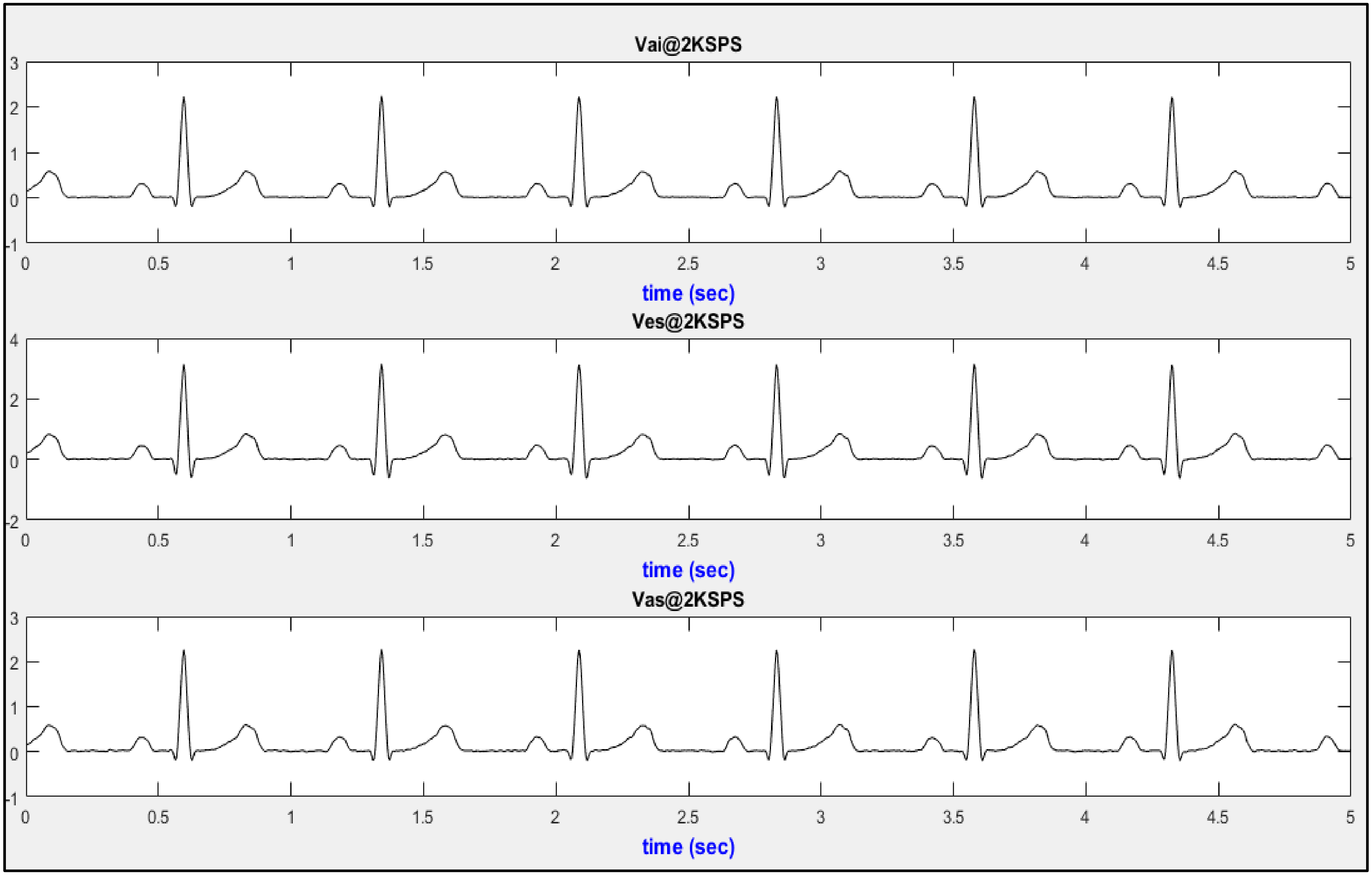
Vai@2KSPS
3
2
1
0
-1
0 0.5 1 1.5 2 2.5 3 3.5 4 4.5 5
time (sec)
Ves@2KSPS
4
2
0
-2
0 0.5 1 1.5 2 2.5 3 3.5 4 4.5 5
time (sec)
Vas@2KSPS
3
2
1
0
-1
0 0.5 1 1.5 2 2.5 3 3.5 4 4.5 5
time (sec)

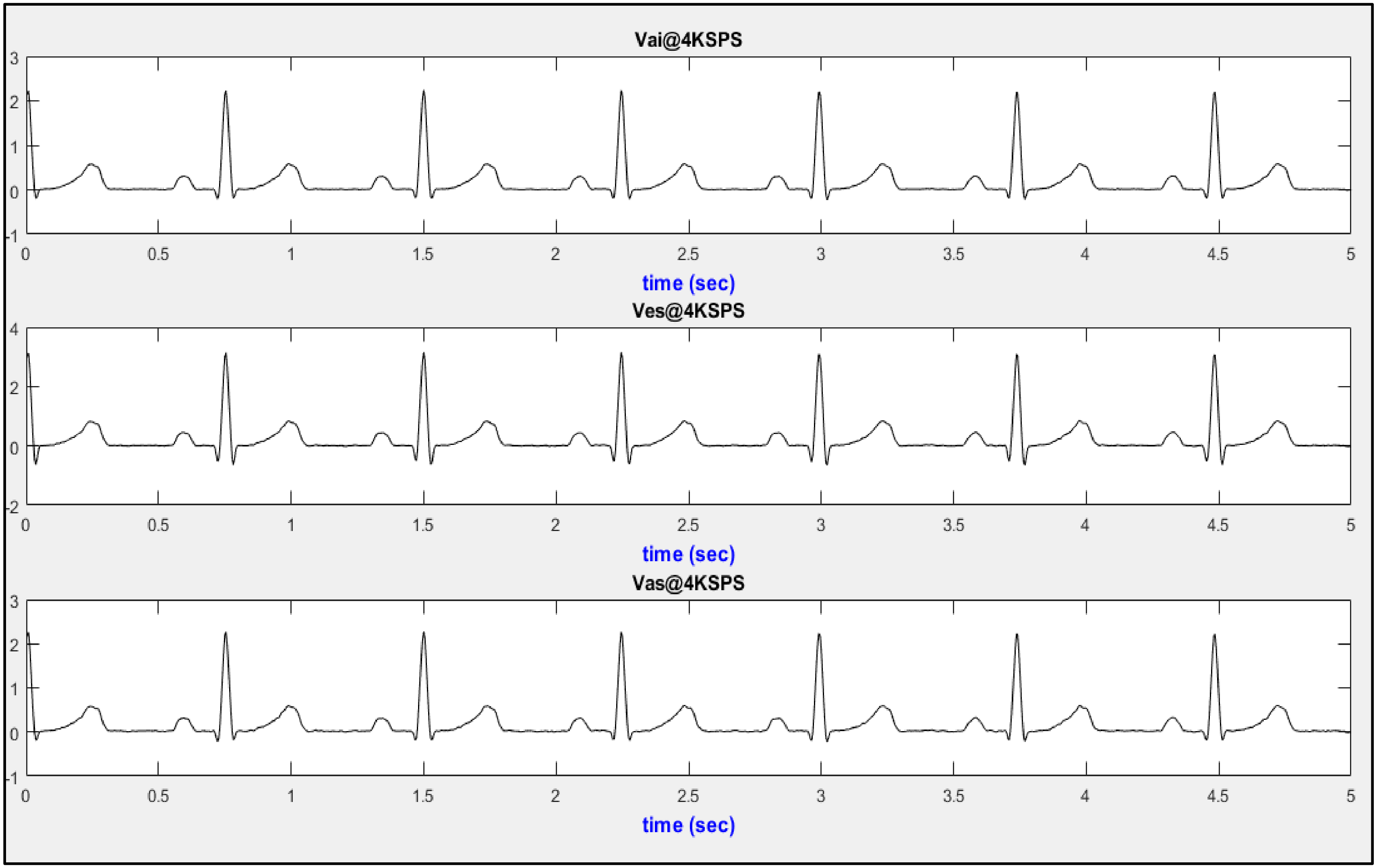
Vai@4KSPS
time (sec)
Ves@4KSPS
time (sec)
Vas@4KSPS
time (sec)

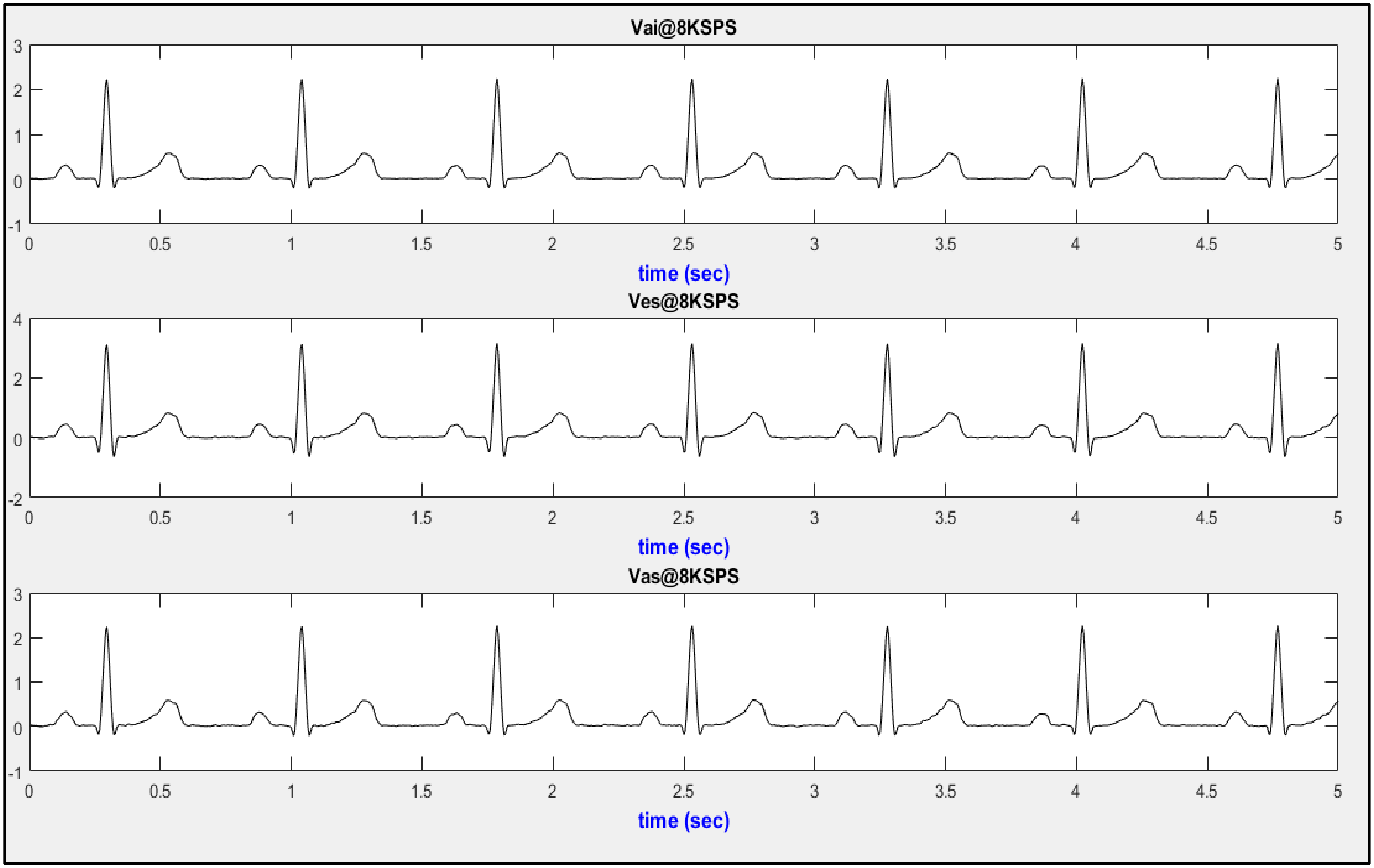
Vai@8KSPS
time (sec)
Ves@8KSPS
time (sec)
Vas@8KSPS
time (sec)

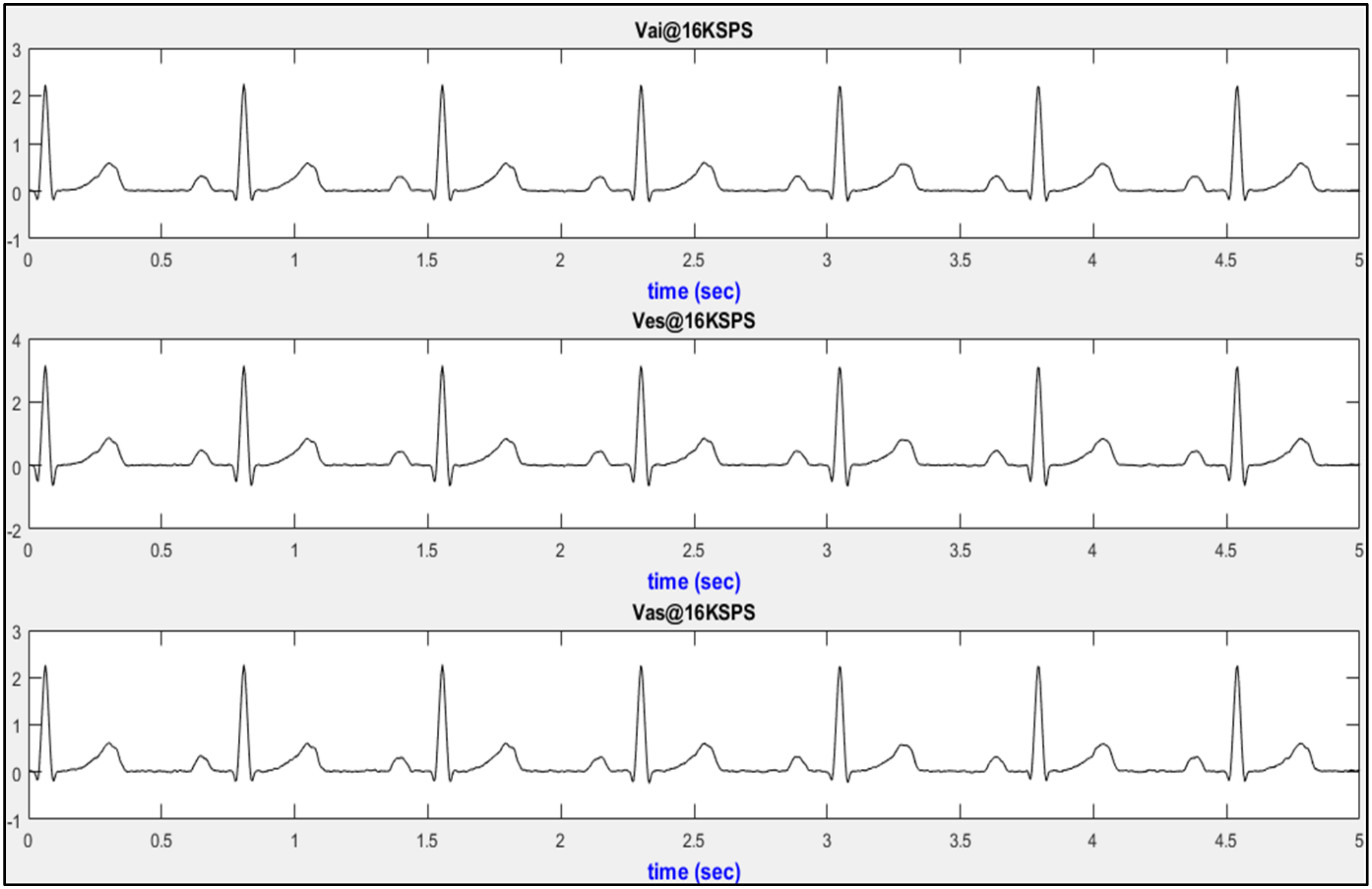
Vai@16KSPS
3
2
1
0
-1
0
0.5
1
1.5
2
2.5
3
3.5
4
4.5
5
time (sec)
Ves@16KSPS
4
2
0
-2
0
0.5
1
1.5
2
2.5
3
3.5
4
4.5
5
time (sec)
Vas@16KSPS
3
2
1
0
-1
0
0.5
1
1.5
2
2.5
3
3.5
4
4.5
5
time (sec)

Appendix I. Performance analysis of the ECG viewer and data logger

Specific objective

The specific objective was to examine the performance of the Java-based ECG viewer and data logger.

Methods

The performance of the Java-based program is measured against memory consumption and run-time taken. There are two primary memories in the Java Virtual Machine (JVM): the heap that holds all objects and classes created in Java, and the stack, the run time memory. Efficient memory management is possible in Java through consecutive garbage collection, where unused memory is freed and make available for later use (Oracle, 2019). Hence, a memory leak test was performed to test the performance of the Java-based ECG viewer and data logger.

Results

A trial of the ECG viewer and data logger commenced on the 15th of April 2019. Real-time single-lead ECG (lead-I) was successfully received and plotted on the computer screen for 10 minutes. The test was repeated for each lead individually. However, buffering multiple ECG leads resulted in the freezing of the Java program in particular and the host computer in general.

In an attempt to identify the errors in the ECG viewer and data logger, the Java virtual memory analyzer (VisualVM 1.4.2) (Oracle Corporation, n.d.) was used to monitor live garbage collection in action as depicted in Figure I.1.

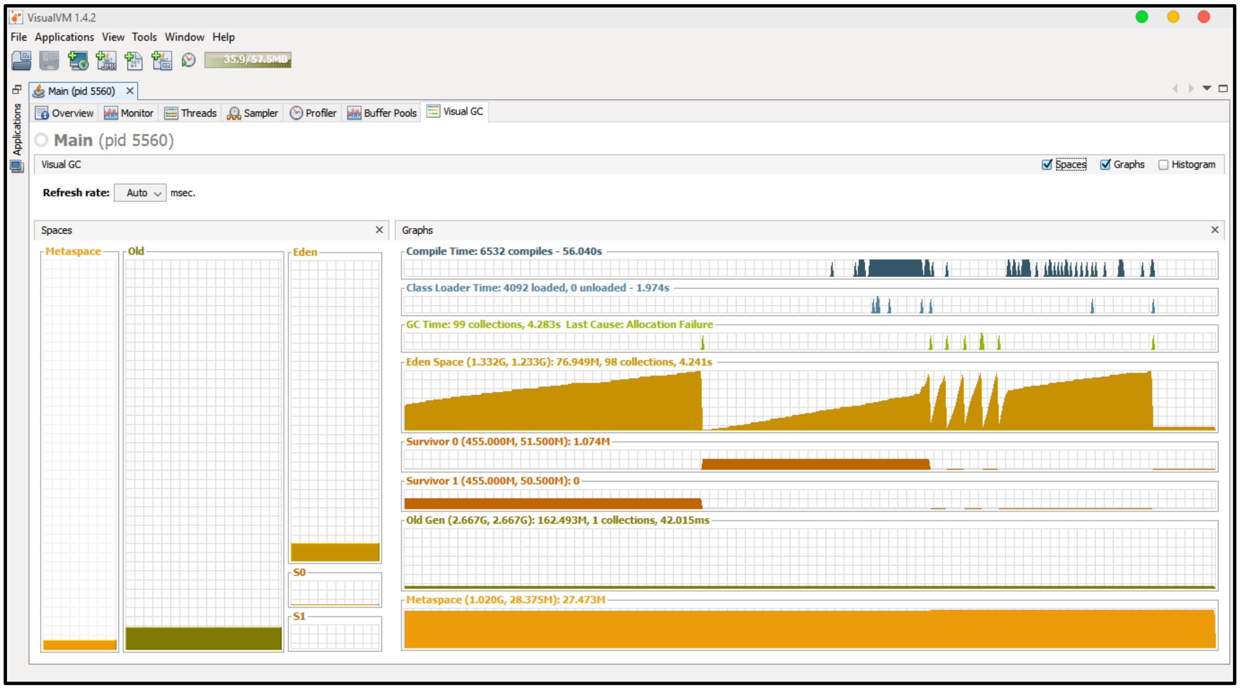

Figure I.1: Snapshot of the Garbage Collection in action

After 10 minutes of live streaming, the Java heap memory was full, and the host computer stopped working and required a restart. This was an indication of a possible memory leak in the Java threads. Eclipse Memory Analyzer-1.8.1.2 (Eclipse Foundation, n.d.) was used for hunting for a memory leak. The hunt revealed a memory leak caused by a time-based method invocation referenced to a static object within the ECG datasets. Following correction of the possible source of error that consumed the heap memory and clogged the CPU of the host PC, multiple lead ECG streaming was conducted for about 11 hours. Figure I.2 presents the collection report in action. The top right figure illustrates (B) the Java virtual memory (the light blue represents the used heap (1GB) of the total 3G heap memory). On the other hand, the top left figure (A - the CPU profiler) illustrates the time taken by the CPU to execute the Java threads (20%).

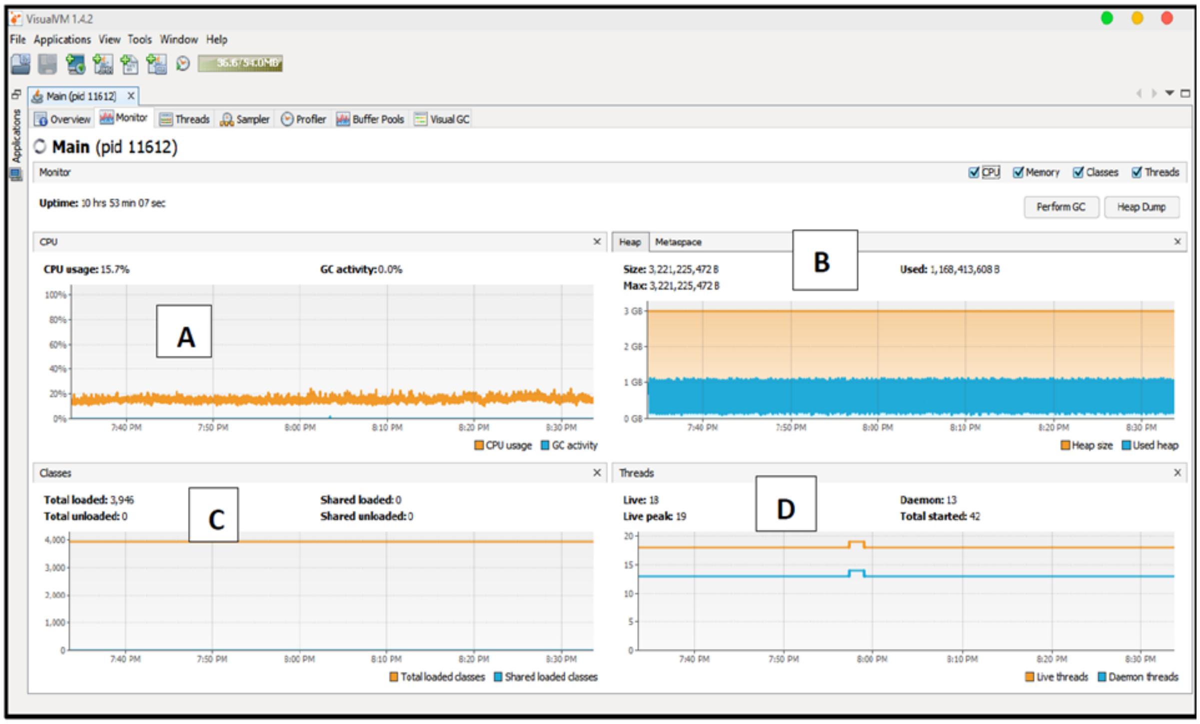

***Note: A)** the CPU profiler - illustrates the time taken by the CPU to execute the Java threads (currently at 20%), **B)** The total heap memory available for dynamic objects (the light blue represents the used heap (1GB) of the total 3G heap memory)), **C)** The number of Java classes used by the application and **D)** Illustrates the number of running threads*

Figure I.2: VisualVM monitor report after the memory leak was fixed (Uptime = 10hrs and 53 minutes of continuous ECG streaming from PrsoSim 3.0 vital sign simulator).

Discussion

During the initial assessment, a single-lead ECG was buffered successfully to the host PC. However, multiple lead ECG transfer was challenging. The first finding was data rate mismatch among the ADS1294, the Arduino Mega, and the serial port. After a thorough investigation, the timing requirements for the respective components were fixed. The firmware was updated accordingly.

Additionally, after 10 minutes of data streaming, the host PC was clogged and needed a restart. A memory leak in the Java threads of the ECG viewer and data logger was identified. The Java virtual memory analyser was efficient in visualizing the garbage collection in action. At the same time, the Eclipse Memory Analyzer (Maxwell et al., 2010, Weninger et al., 2018) spotted the primary source of the problem in the running Java thread. Then, the Java thread responsible for taking up the heap memory was fixed. Eleven hours of continuous ECG signals from multiple leads were collected after the issue mentioned above was addressed to confirm that there was no further memory leakage in the Java threads.

Appendix J. EMD of Holter ECG during sideways movement

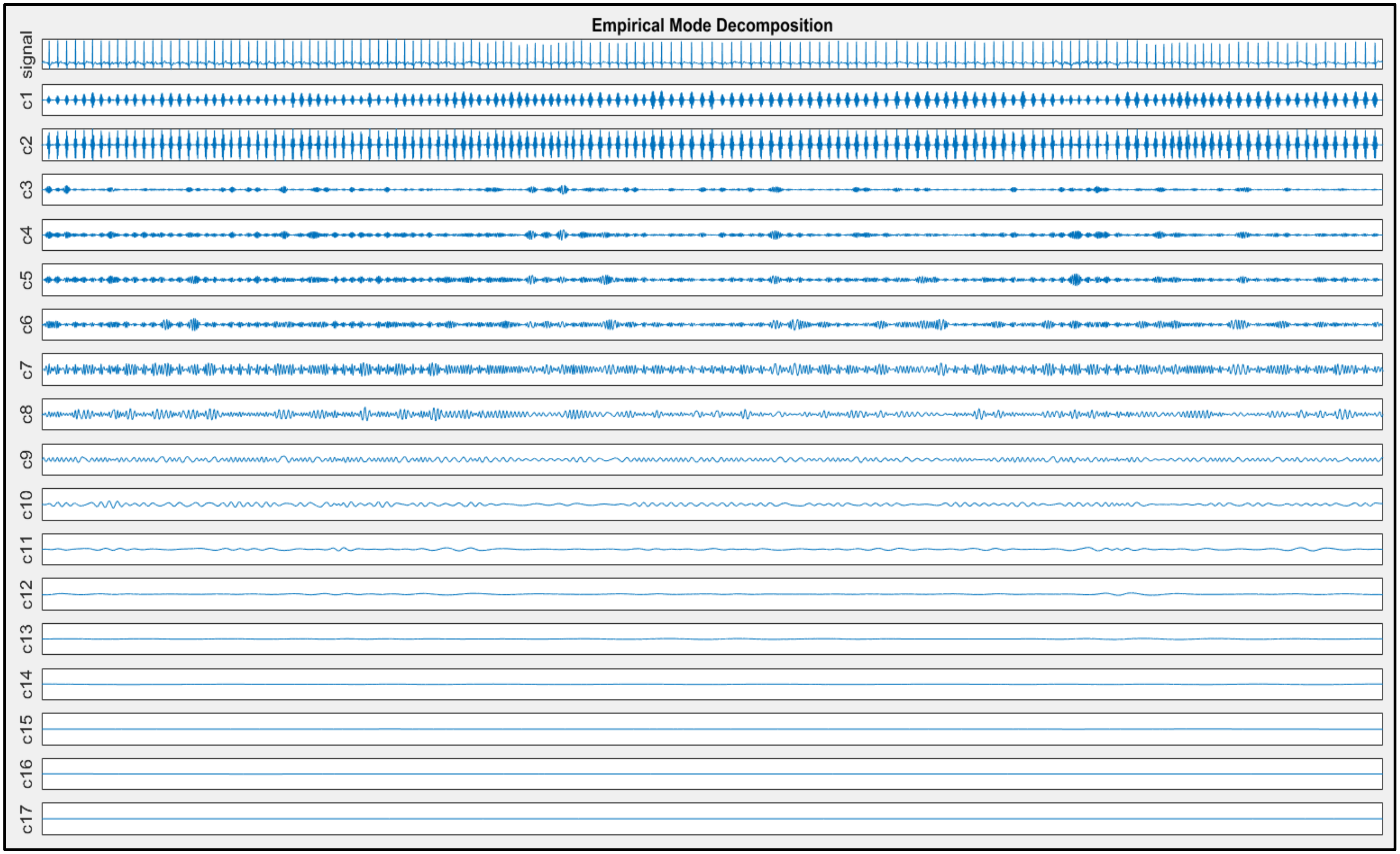

a) Intrinsic mode functions (IMFs) of the EMD

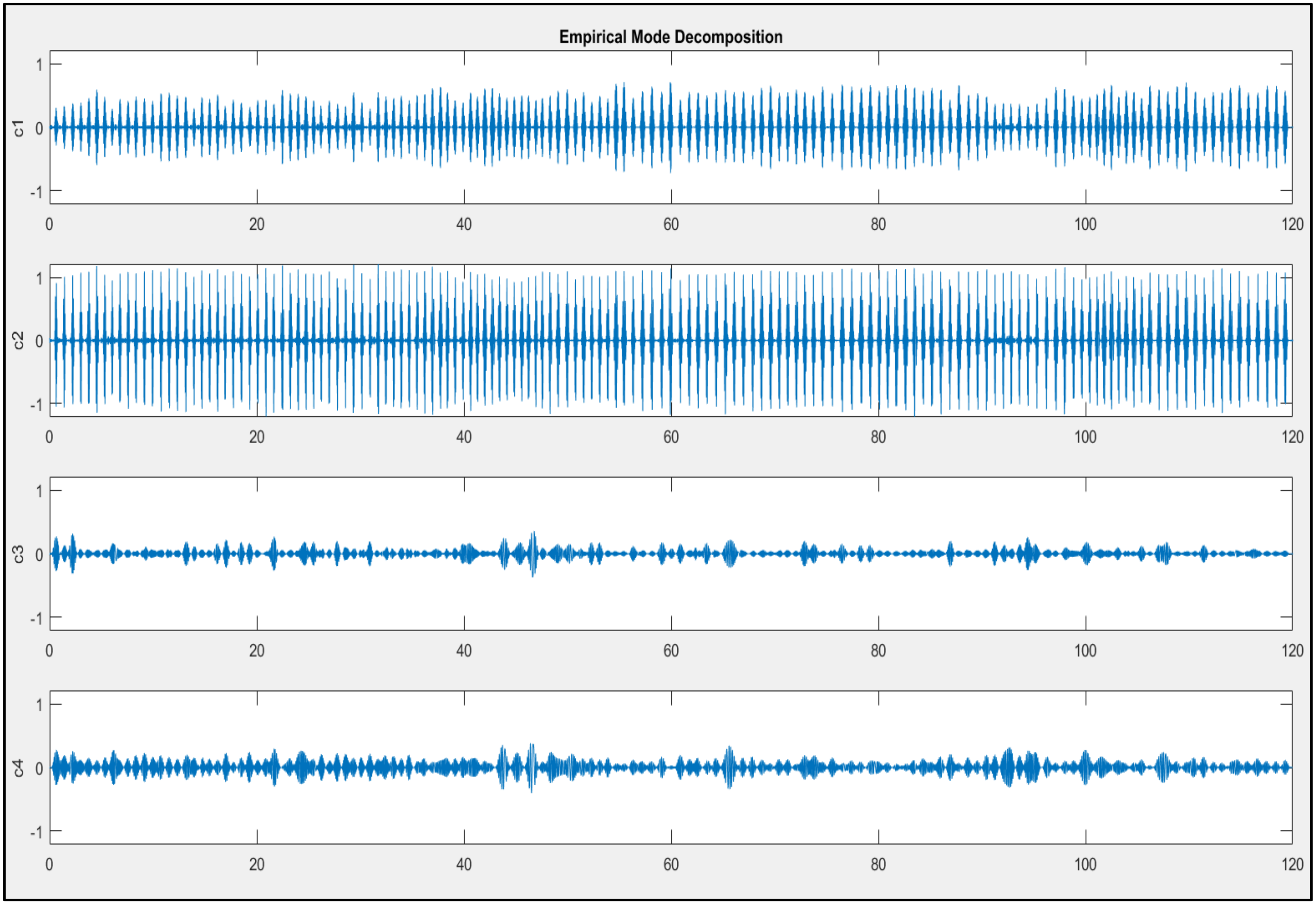
Empirical Mode Decomposition
c1
c2
c3
c4
1
0
-1
0
20
40
60
80
100
120

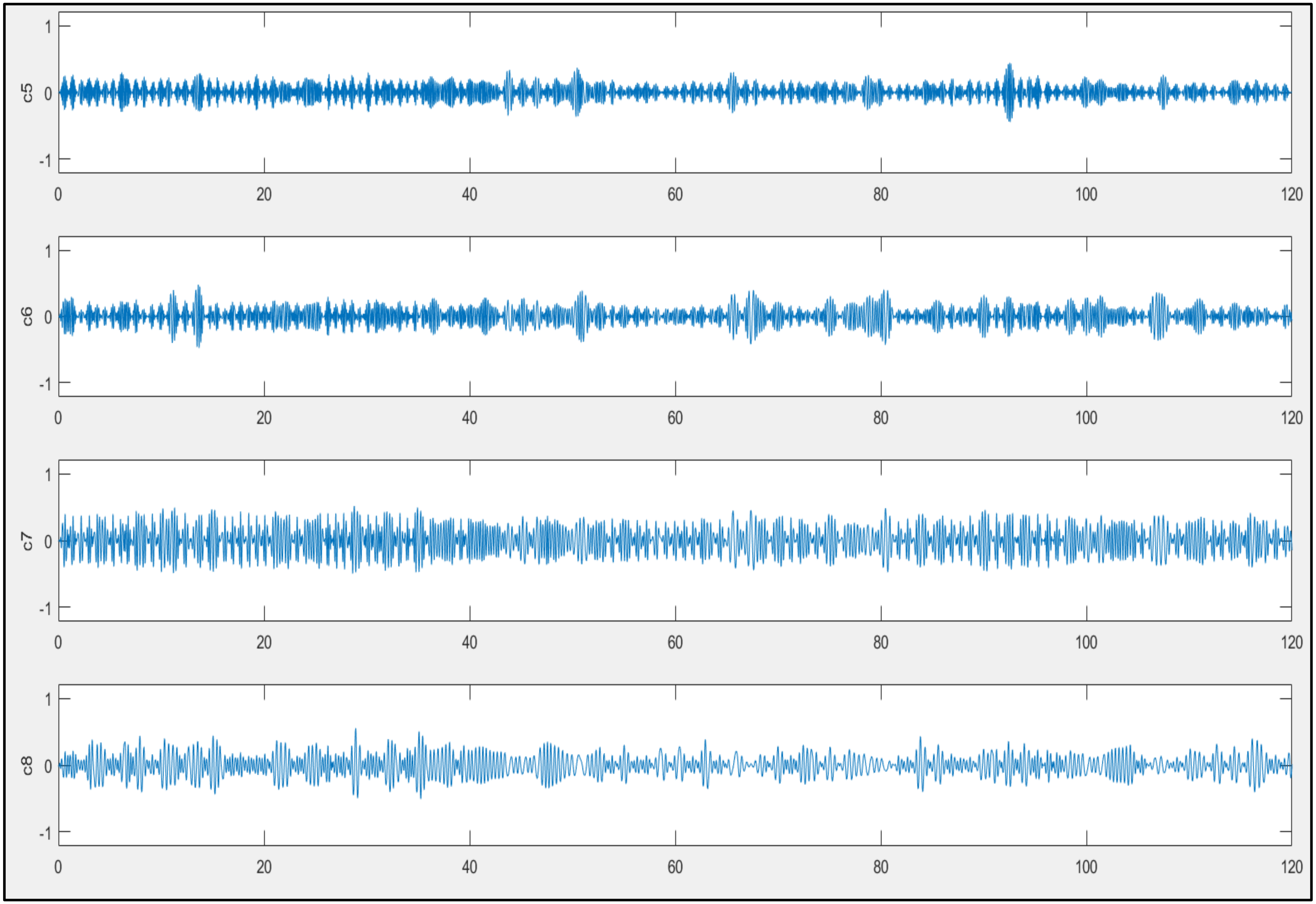

b) Zoomed version of the first eight IMFs

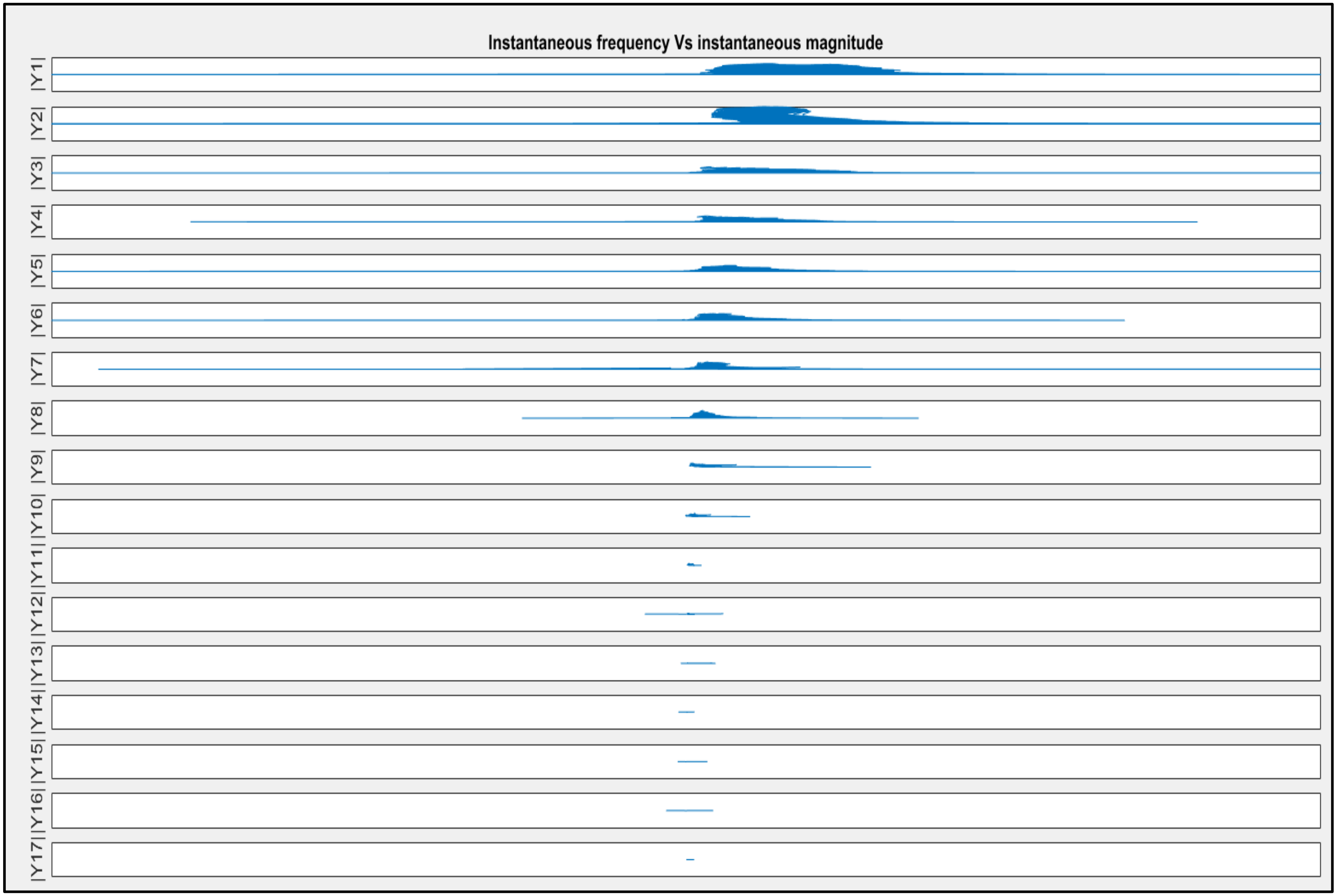

c) IMFs frequency spectrum based on the EMD-Hilbert transformation

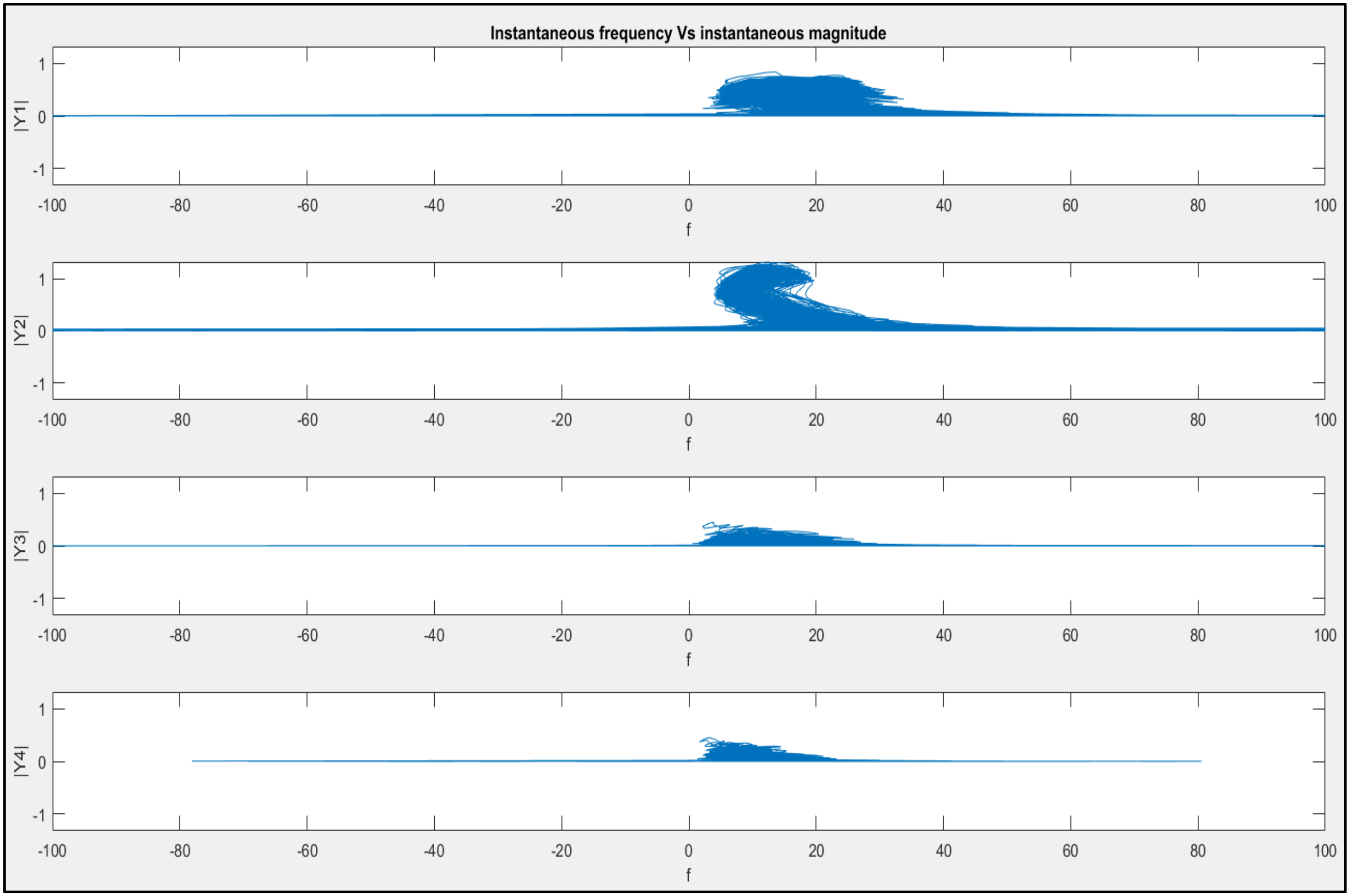
Instantaneous frequency Vs instantaneous magnitude
|Y1|
|Y2|
|Y3|
|Y4|
f
1
0
-1
-100
-80
-60
-40
-20
0
20
40
60
80
100

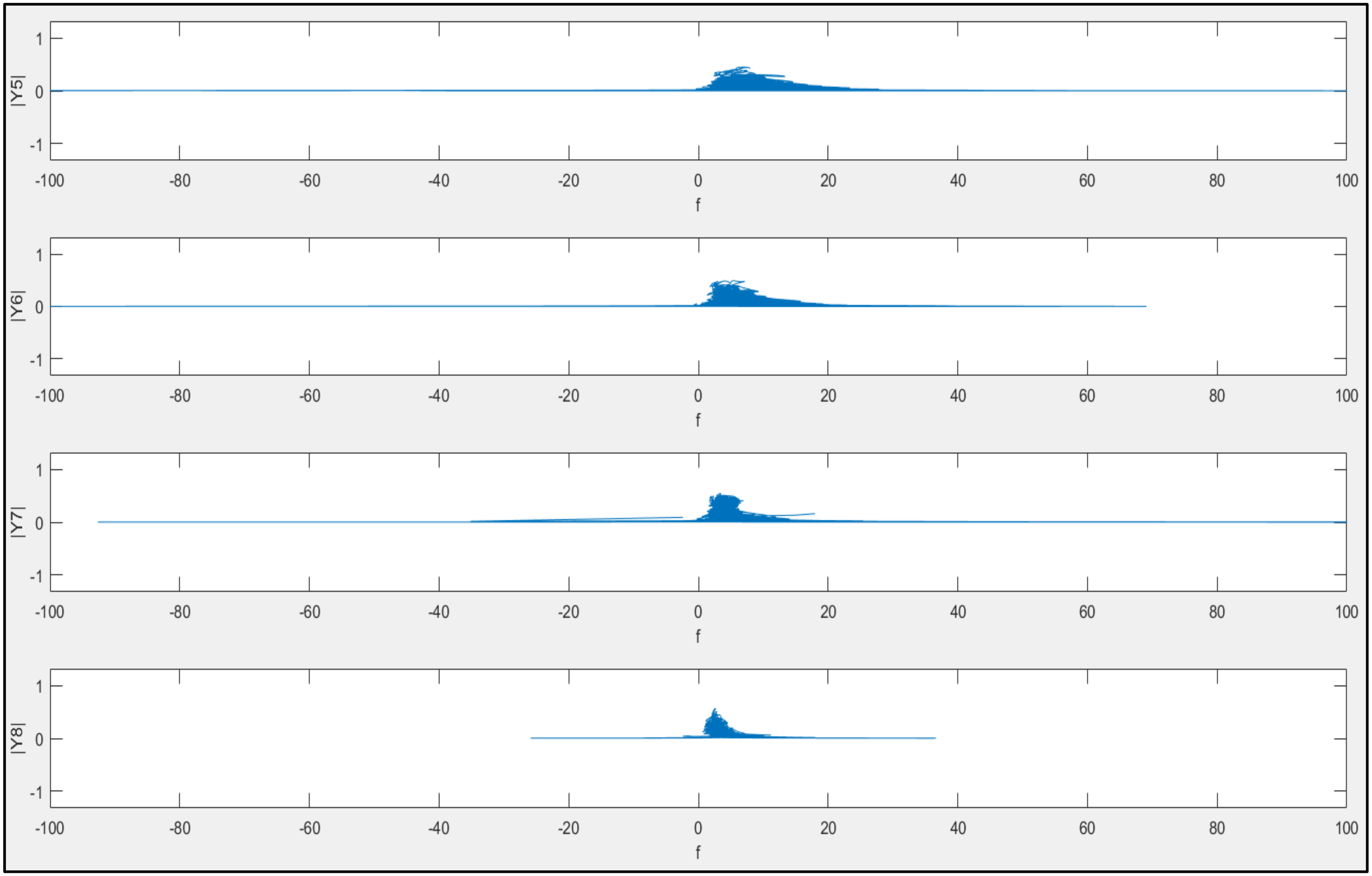

d) Zoom into the frequency spectrum of the eight higher-order IMFs (IMF1 – IMF8)

Appendix K.K. The FFT and AR spectrum representation of the short term HRV analysis

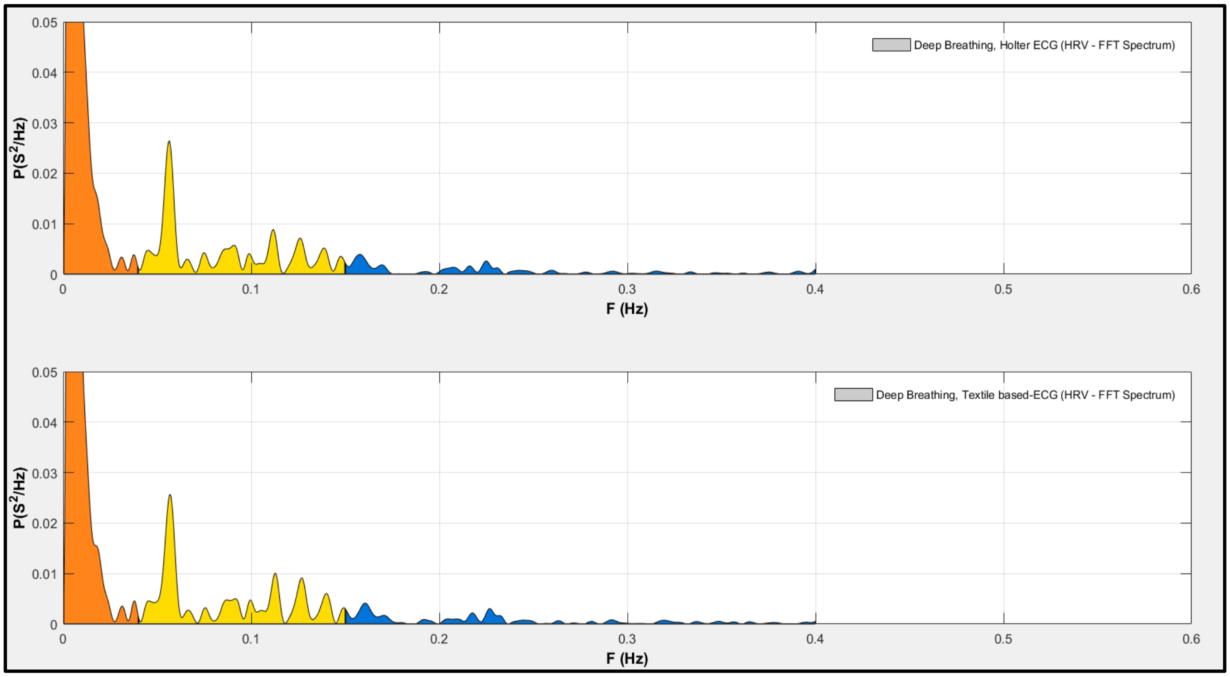

a) Deep Breathing – FFT spectrum (top – Holter monitor; bottom – textile-based ECG monitor)

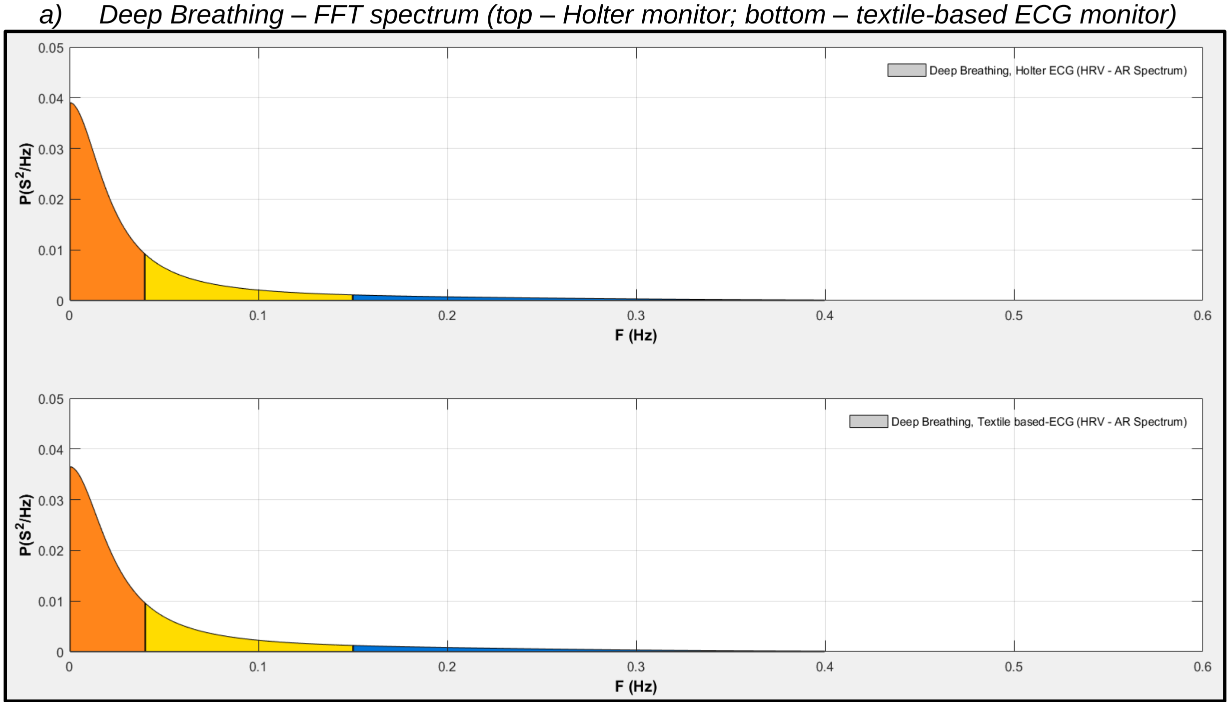

b) Deep Breathing – AR spectrum (top – Holter monitor; bottom – textile-based ECG monitor)

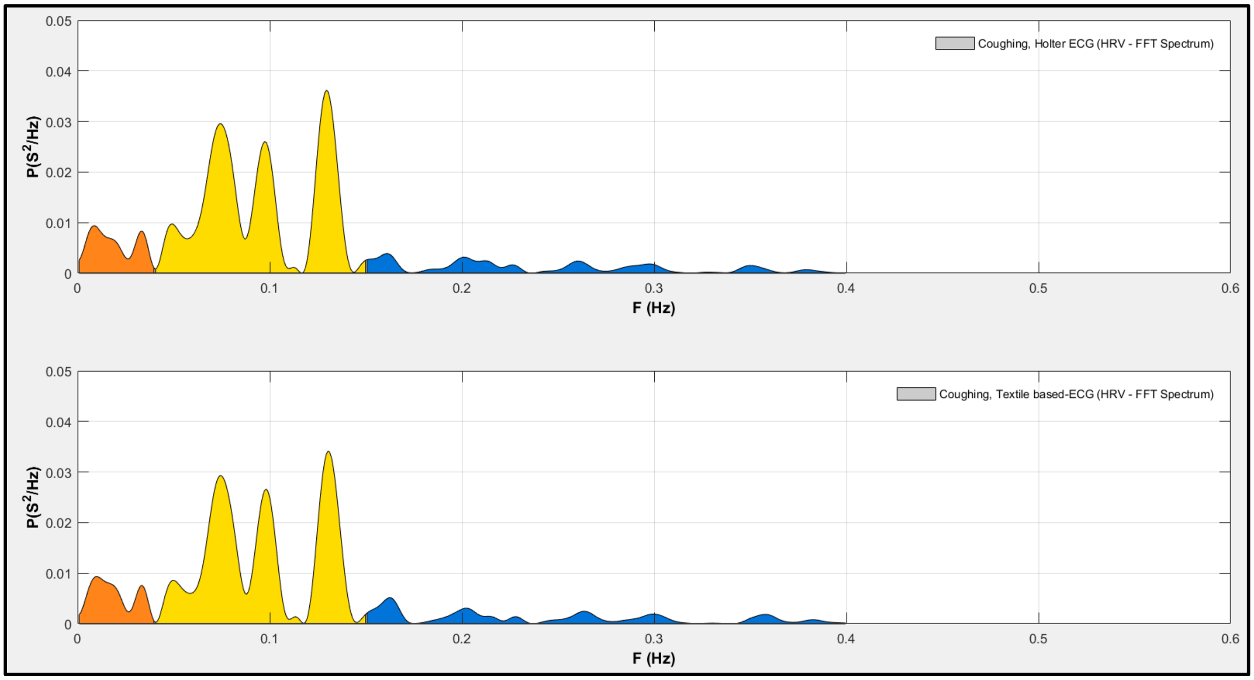

c) *Coughing – FFT spectrum (top – Holter monitor; bottom – textile-based ECG monitor)*

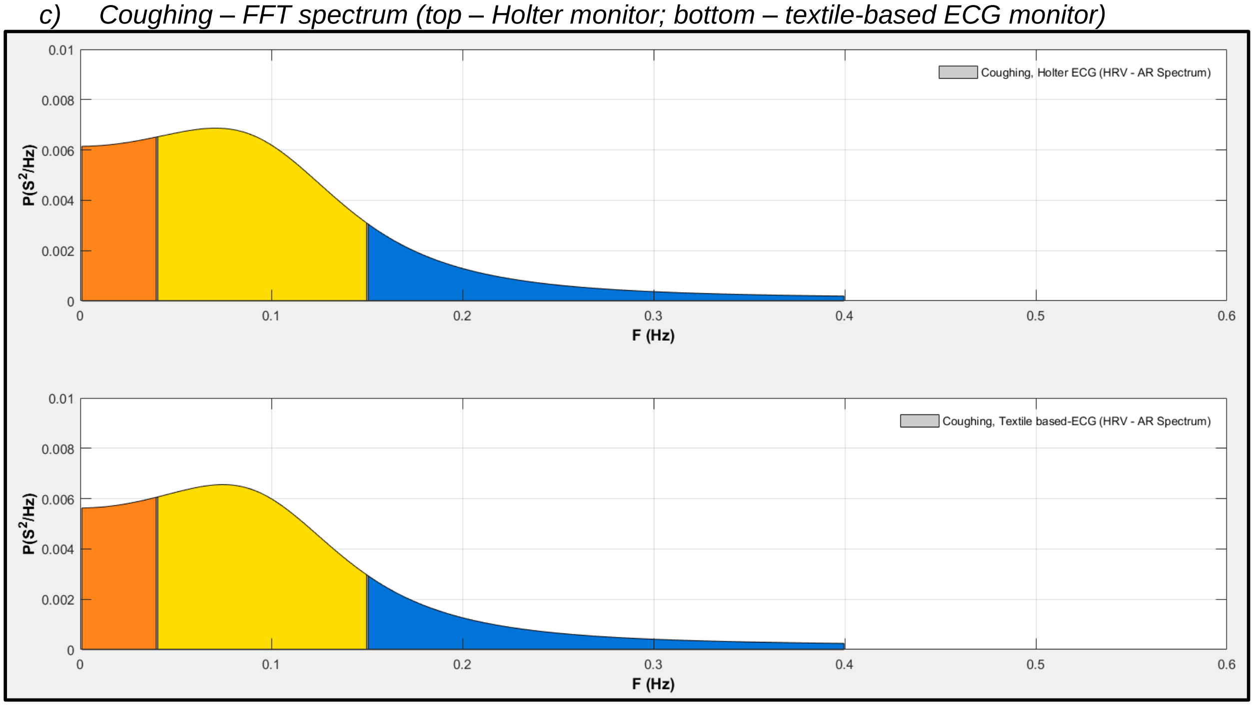

d) *Coughing – AR spectrum (top – Holter monitor; bottom – textile-based ECG monitor)*

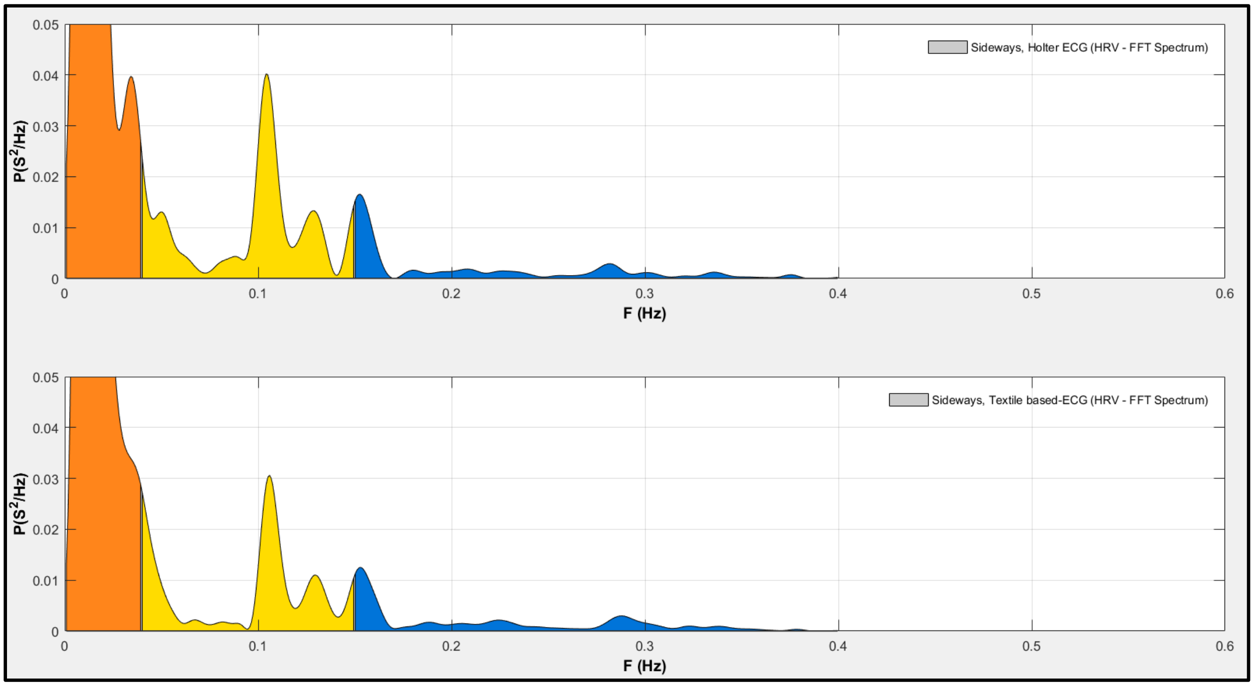

e) *Sideways – FFT spectrum (top – Holter monitor; bottom – textile-based ECG monitor)*

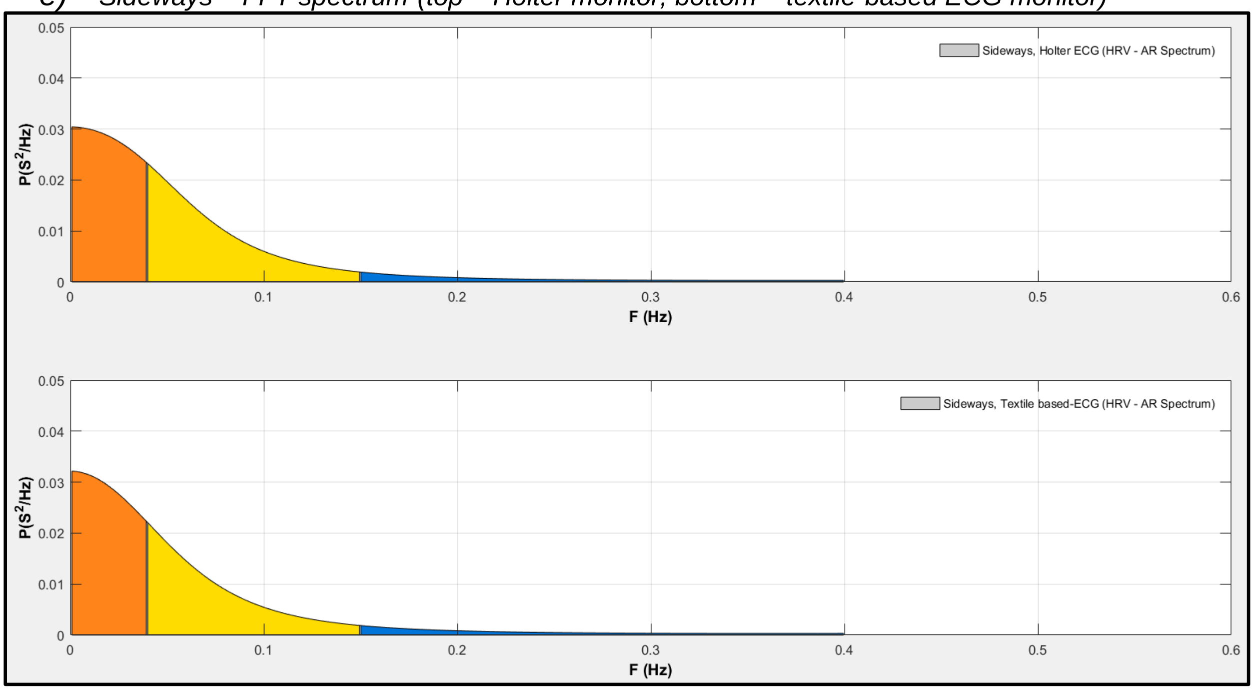

f) *Sideways – AR spectrum (top – Holter monitor; bottom – textile-based ECG monitor)*

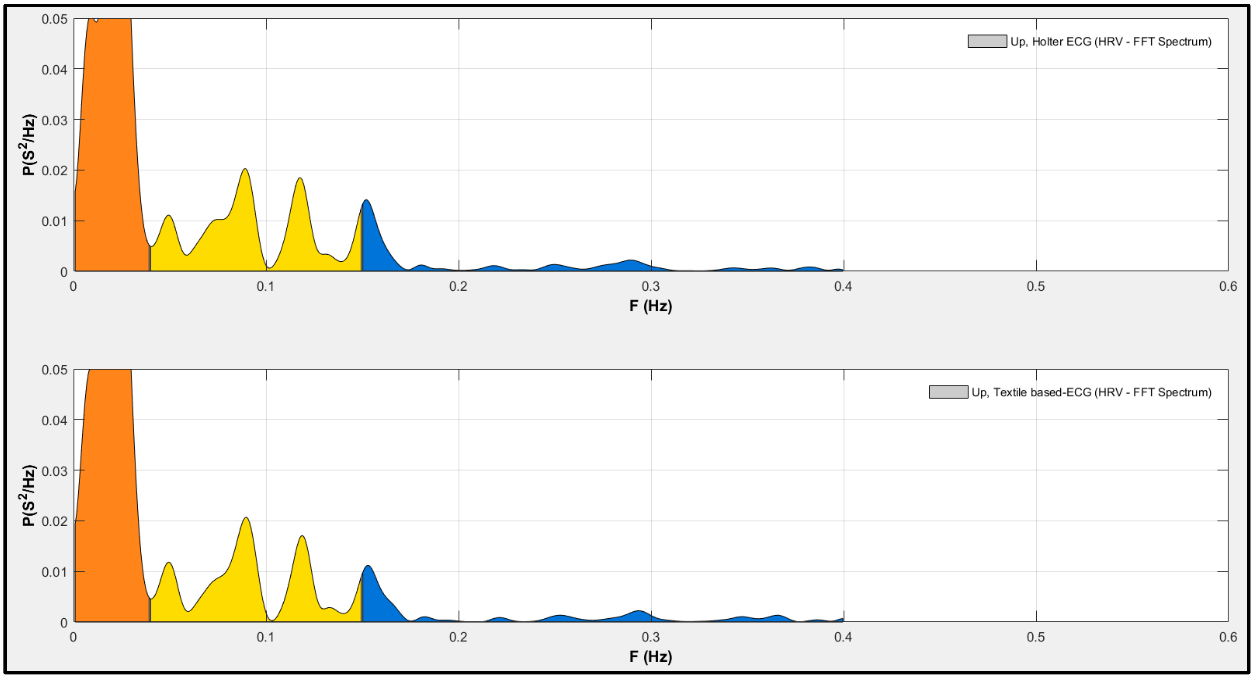

g) Up movement – FFT spectrum (top – Holter monitor; bottom – textile-based ECG monitor)

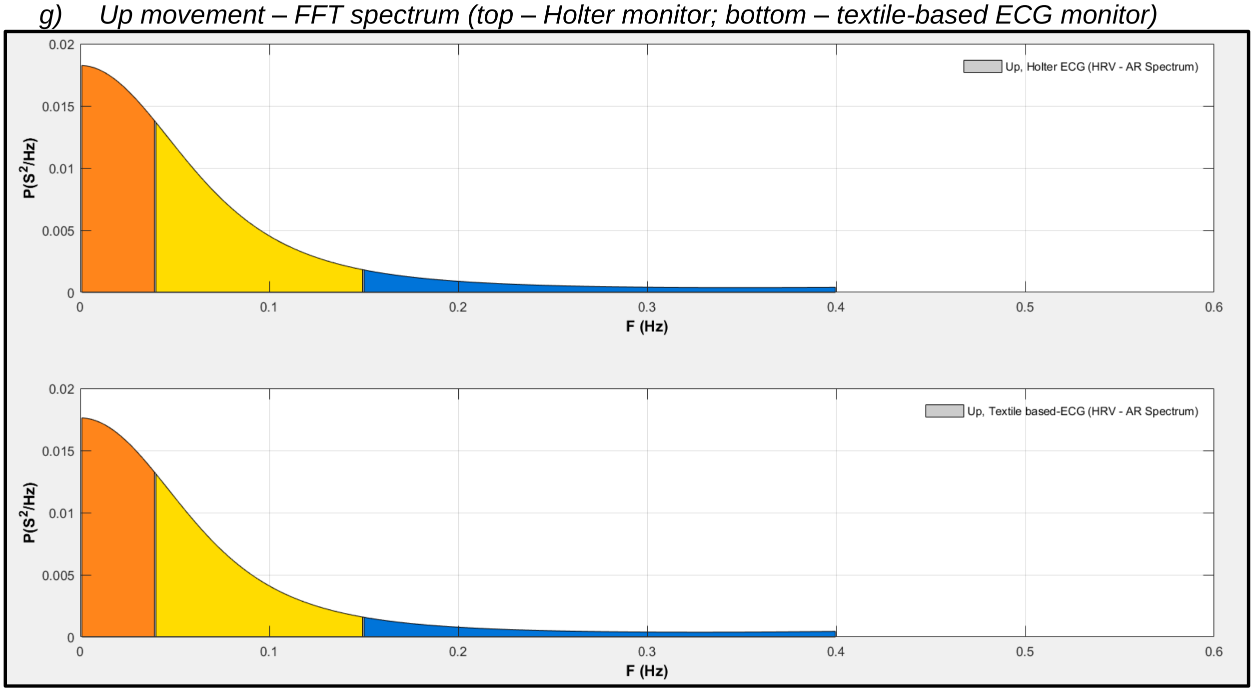

h) Up movement – AR spectrum (top – Holter monitor; bottom – textile-based ECG monitor)

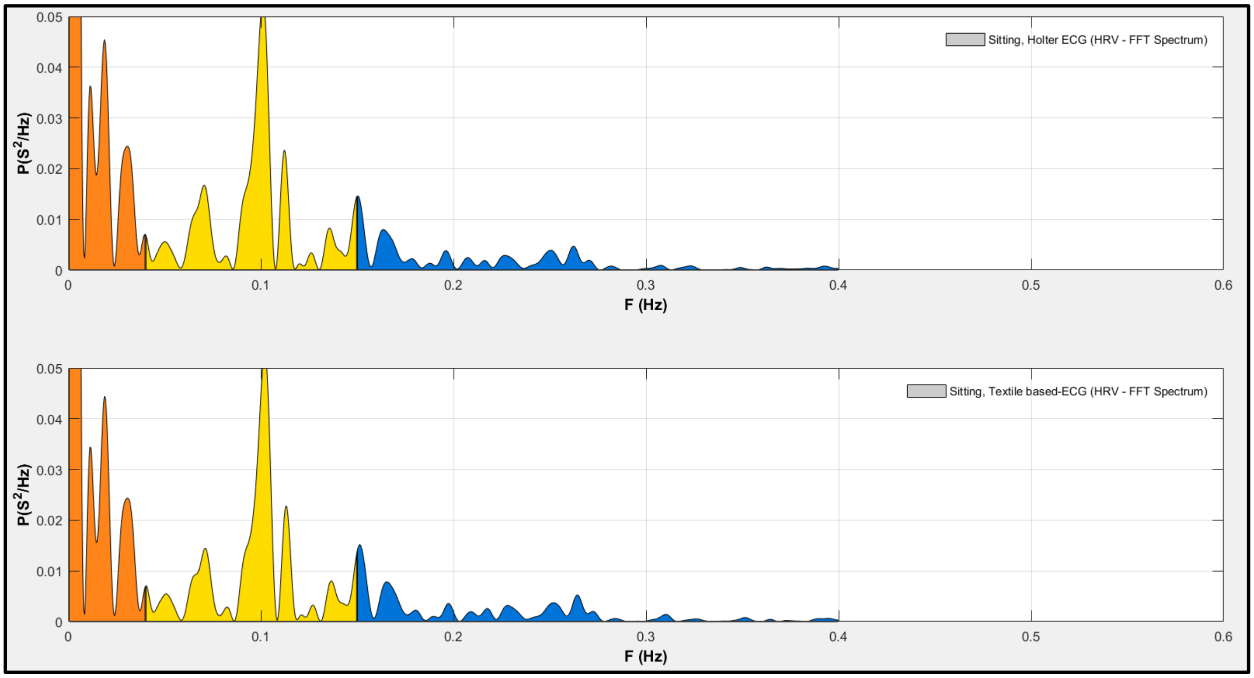

i) Sitting – FFT spectrum (top – Holter monitor; bottom – textile-based ECG monitor)

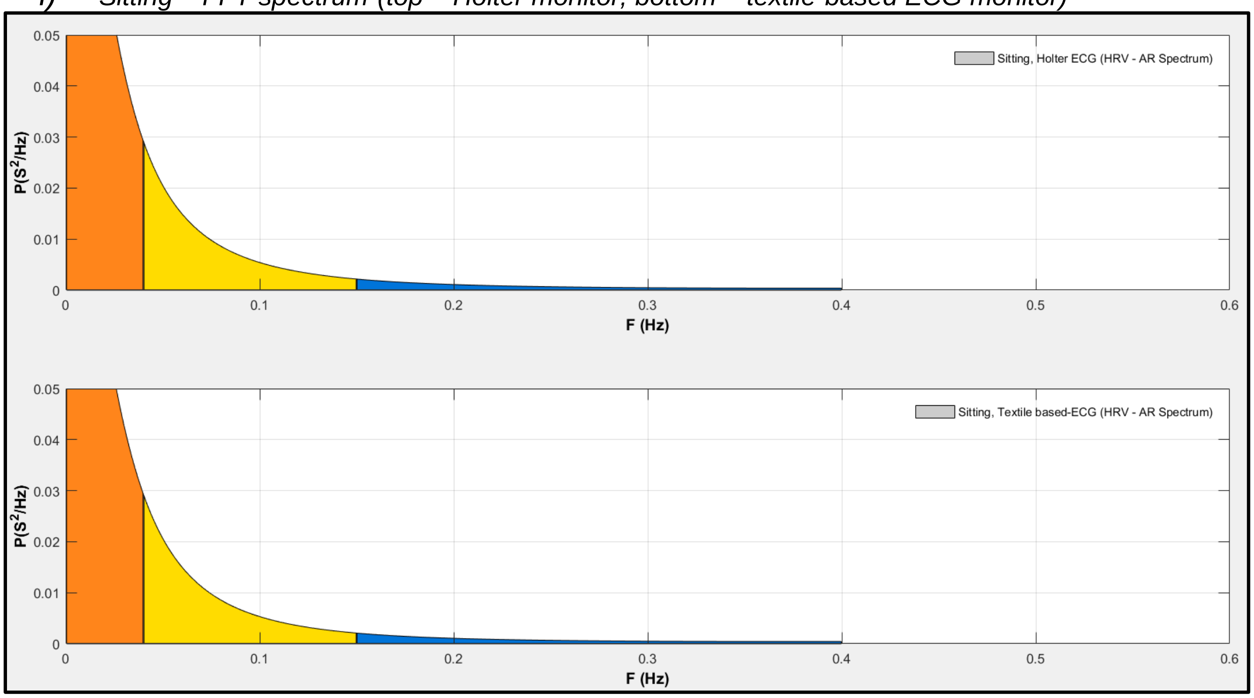

j) Sitting – AR spectrum (top – Holter monitor; bottom – textile-based ECG monitor)

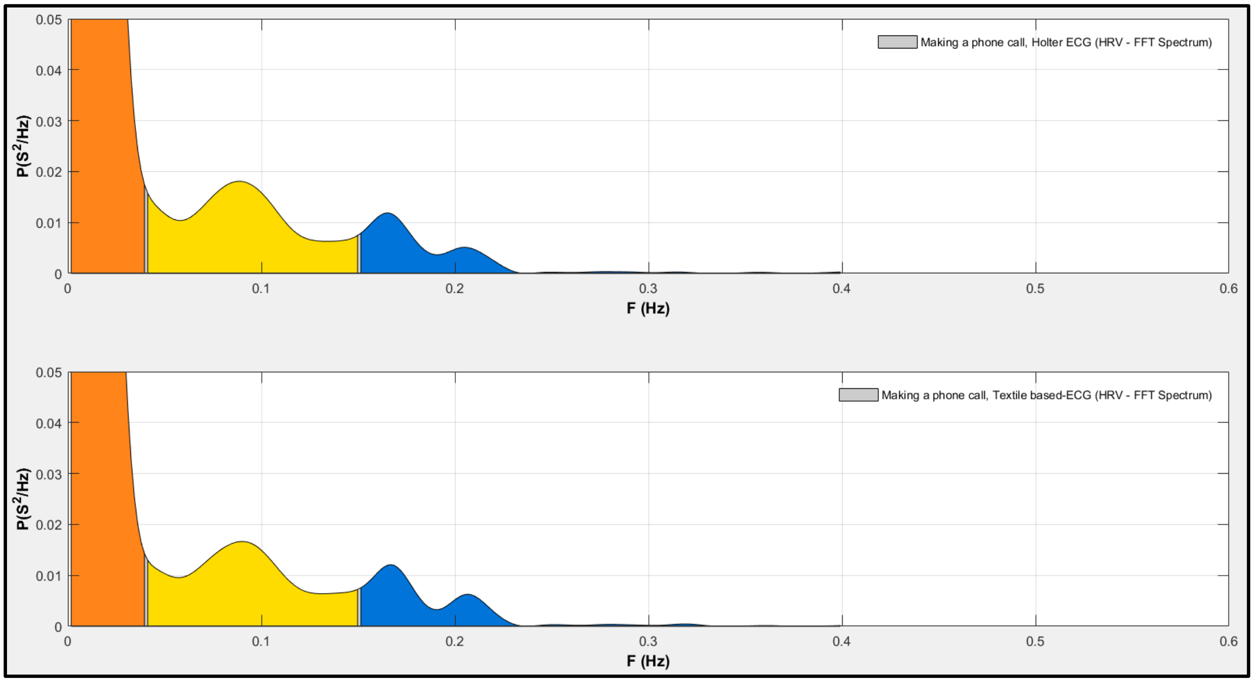

k) Making a phone call – FFT spectrum (top – Holter monitor; bottom – textile-based ECG monitor)

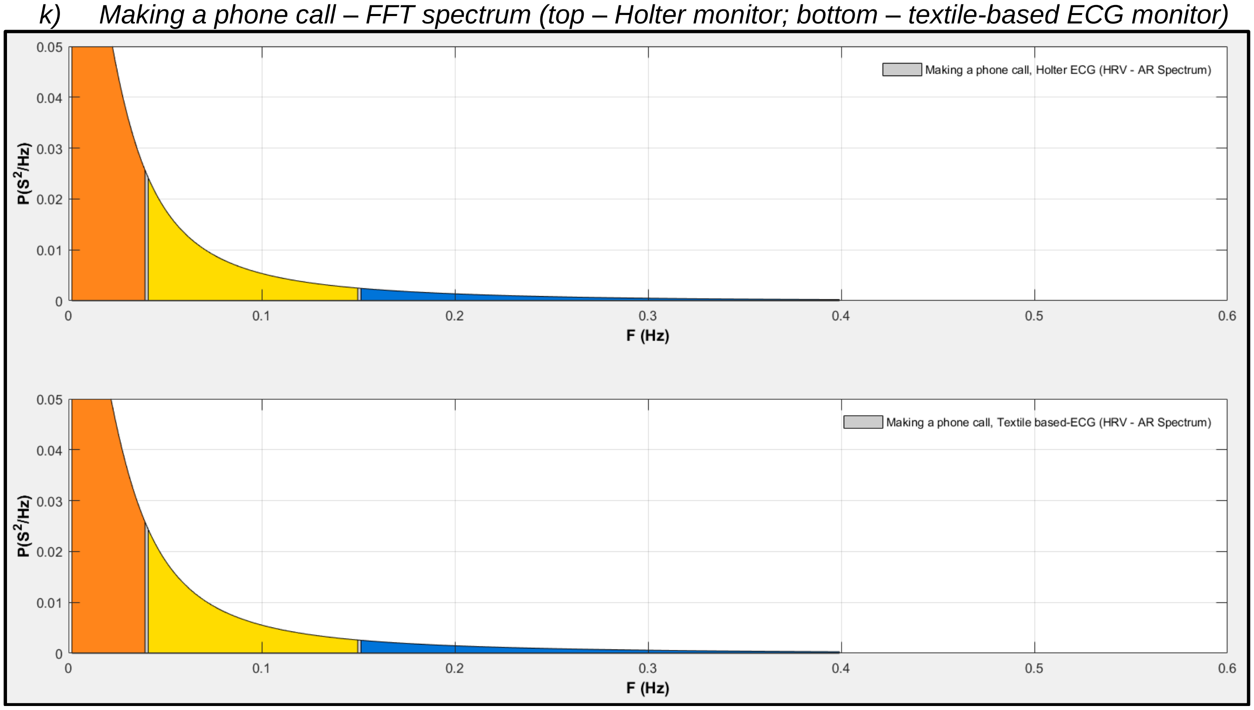

l) Making a phone call – AR spectrum (top – Holter monitor; bottom – textile-based ECG monitor)

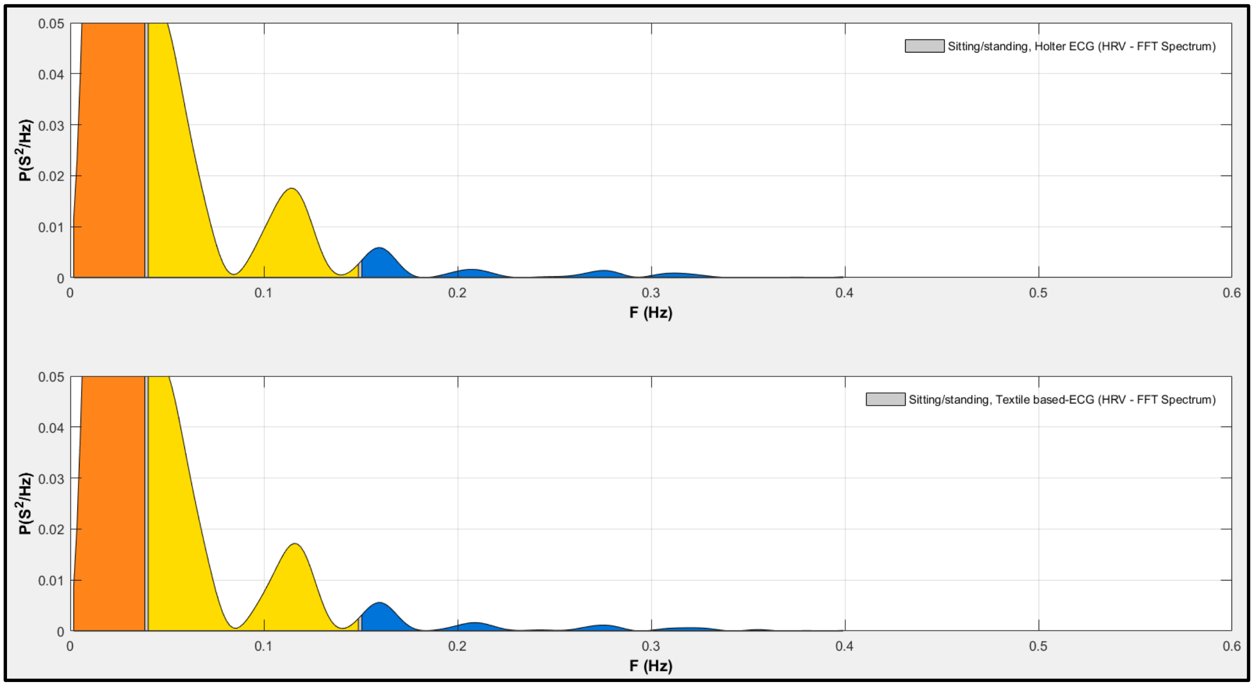

m) Sitting / standing – FFT spectrum (top – Holter monitor; bottom – textile-based ECG monitor)

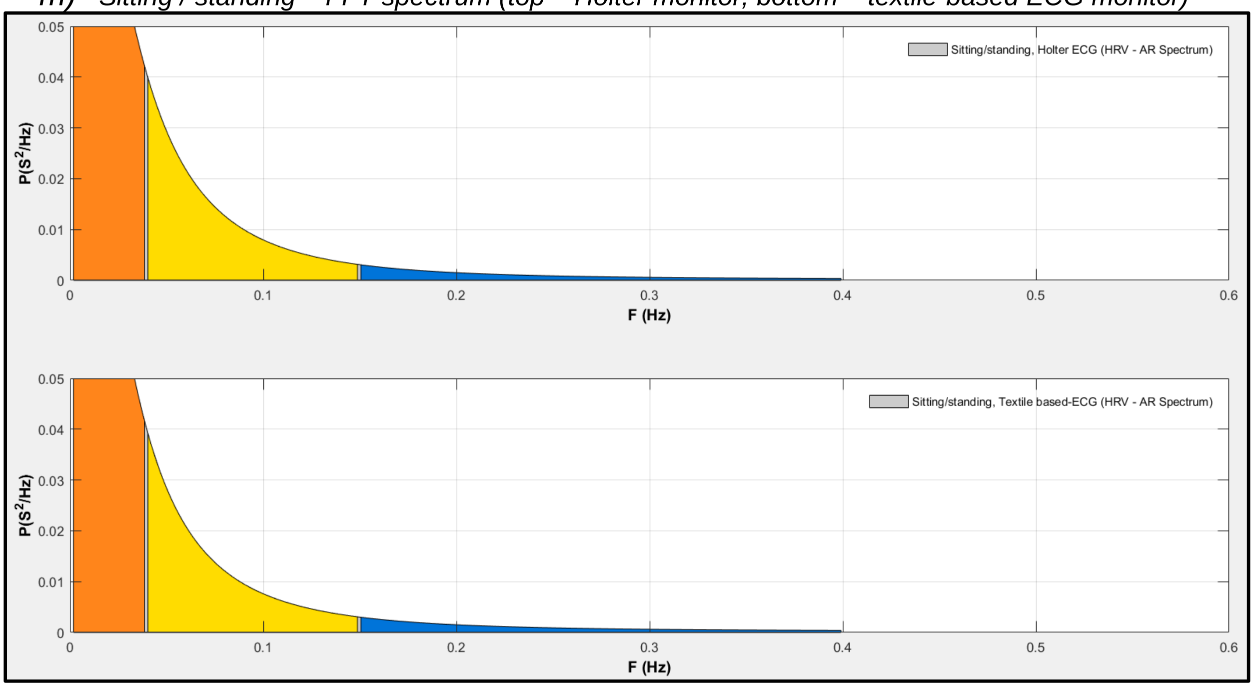

n) Sitting / standing – AR spectrum (top – Holter monitor; bottom – textile-based ECG monitor)

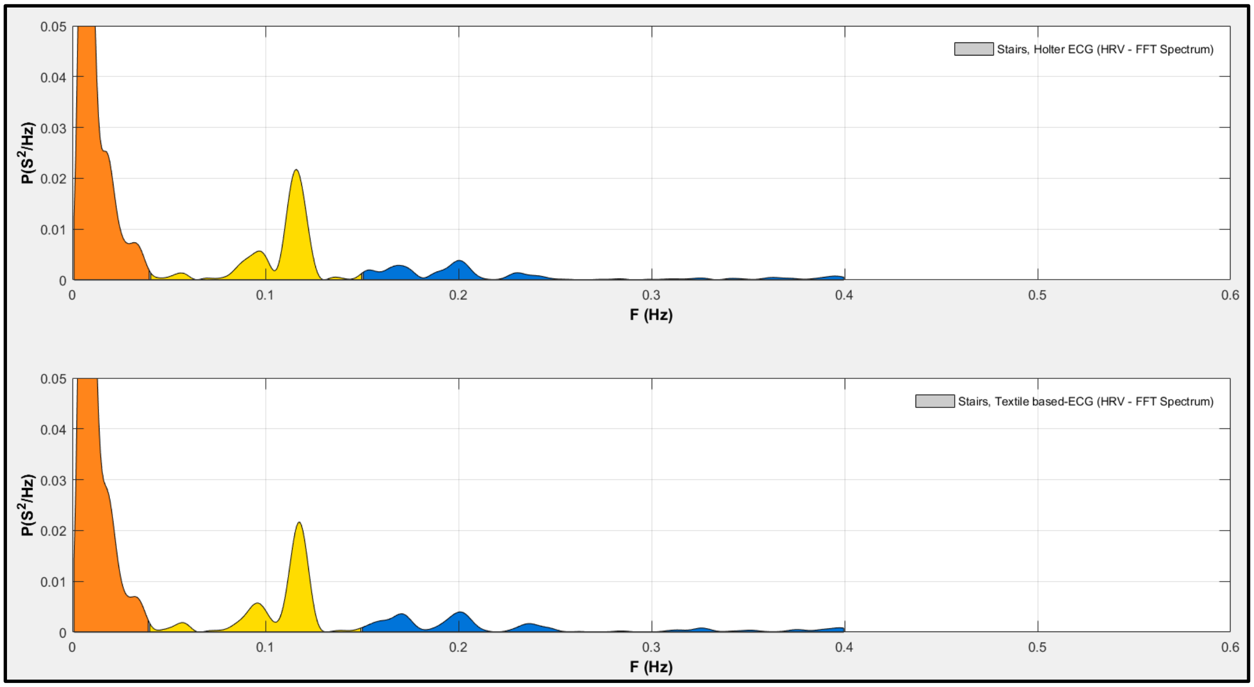

o) Climbing stairs – FFT spectrum (top – Holter monitor; bottom – textile-based ECG monitor)

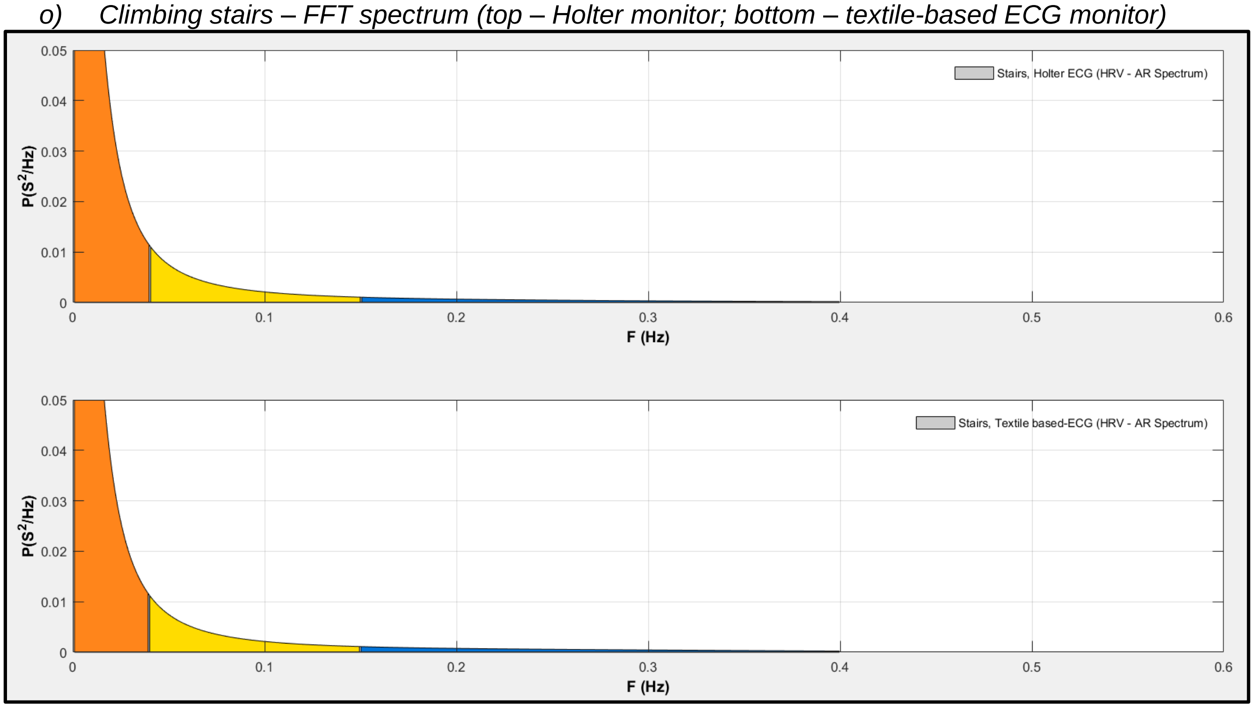

p) Climbing stairs – AR spectrum (top – Holter monitor; bottom – textile-based ECG monitor)

This page is left blank intentionally

Reference lists

2019a. Single Lead Electrocardiography (ECG) Equipment - Global Market Outlook (2017-2026).

2019b. Smart Fabrics Market Size, Share & Trends Analysis Report By Product (Active, Very Smart), By End Use (Defense & Military, Sports & Fitness), By Functionality (Sensing, Energy Harvesting), And Segment Forecasts, 2019 - 2025.

2019c. Wearable Devices Market by Product Type (Smartwatch, Earwear, Eyewear, and others), End-Use Industry (Consumer Electronics, Healthcare, Enterprise and Industrial, Media and Entertainment), Connectivity Medium, and Region - Global Forecast to 2025.

c2017. *Bluetooth Transceiver Module HC-06* [Online]. Media Wiki. Available: http://wiki.sunfounder.cc/index.php?title=Bluetooth_Transceiver_Module_HC-06 [Accessed 6 Septembe 2019].

Abo-Zahhad, M., Ahmed, S. M. & Zakaria, A. 2012. An efficient technique for compressing ECG signals using QRS detection, estimation, and 2D DWT coefficients thresholding. *Modelling and simulation in engineering,* 2012**,** 51.

Abtahi, F., Ji, G., Lu, K., Rodby, K. & Seoane, F. 2015. A knitted garment using intarsia technique for Heart Rate Variability biofeedback: Evaluation of initial prototype. *Conf Proc IEEE Eng Med Biol Soc.,* 2015**,** 3121-4.

Abuhav, I. 2018. *ISO 13485: 2016: a complete guide to quality management in the medical device industry*, CRC Press.

Adafruit. n.d. *PowerBoost 1000 Charger - Rechargeable 5V Lipo USB Boost @ 1A - 1000C* [Online]. Adafruit. Available: https://www.adafruit.com/product/2465 [Accessed 20 April 2019].

Adams, M. G. & Drew, B. J. 1997. Body position effects on the ECG: implication for ischemia monitoring. *Journal of electrocardiology,* 30**,** 285-291.

Ahtinen, A., Mattila, E., Vaatanerr, A., Hynninen, L., Salminen, J., Koskinen, E. & Laine, K. User experiences of mobile wellness applications in health promotion: User study of Wellness Diary, Mobile Coach and SelfRelax. Int Conf Pervasive Comput Technol Healthc, 2009. IEEE, 1-8.

Albert, D. E. 2015. Methods and systems for electrode placement. Google Patents.

Albrecht, P. & Cohen, R. J. Estimation of heart rate power spectrum bands from real-world data: dealing with ectopic beats and noisy data. Proceedings. Computers in Cardiology 1988, 1988. IEEE, 311-314.

Alfaouri, M. & Daqrouq, K. 2008. ECG signal denoising by wavelet transform thresholding. *American Journal of applied sciences,* 5**,** 276-281.

AlMahamdy, M. & Riley, H. B. 2014. Performance study of different denoising methods for ECG signals. *Procedia Computer Science,* 37**,** 325-332.

Altium Limited. n.d. *ALTIUM DXP DEVELOPER* [Online]. Altium Limited. Available: https://www.altium.com/altium-dxp/overview [Accessed 26 September 2018].

Altman, D. G. 1990. *Practical statistics for medical research*, CRC press.

Ambhore, A., Teo, S.-G., Omar, A. R. B. & Poh, K.-K. 2014. ECG series. Importance of QT interval in clinical practice. *Singapore Med J,* 55**,** 607.

American Association of Cardiovascular Pulmonary Rehabilitation 2013. *Guidelines for Cardia Rehabilitation and Secondary Prevention Programs-(with Web Resource)*, Human Kinetics.

Amsterdam, E. A., Wenger, N. K., Brindis, R. G., Casey, D. E., Ganiats, T. G., Holmes, D. R., Jaffe, A. S., Jneid, H., Kelly, R. F. & Kontos, M. C. 2014. 2014 AHA/ACC guideline for the management of patients with non–ST-elevation acute coronary syndromes: a report of the American College of Cardiology/American Heart Association Task Force on Practice Guidelines. *Journal of the American College of Cardiology,* 64**,** e139-e228.

Anderson, L., Sharp, G. A., Norton, R. J., Dalal, H., Dean, S. G., Jolly, K., Cowie, A., Zawada, A. & Taylor, R. S. 2017. Home-based versus centre-based cardiac rehabilitation. *Cochrane database of systematic reviews*.

Andes , C. B. 1983. Hospital telemetry monitoring systems. *J Clin Eng,* 8**,** 195 - 199.

Andreoni, G., Fanelli, A., Witkowska, I., Perego, P., Fusca, M., Mazzola, M. & Signorini, M. G. Sensor validation for wearable monitoring system in ambulatory monitoring: Application to textile electrodes. Int Conf Pervasive Comput Technol Healthc, 2013. 169-175.

Angelidis, P. A. 2010a. Personalised physical exercise regime for chronic patients through a wearable ICT platform. *International journal of electronic healthcare,* 5**,** 355-370.

Angelidis, P. A. 2010b. Personalised physical exercise regime for chronic patients through a wearable ICT platform. *IJEH,* 5**,** 355-370.

Ankhili, A., Tao, X., Cochrane, C., Coulon, D. & Koncar, V. 2018. Washable and reliable textile electrodes embedded into underwear fabric for electrocardiography (ECG) monitoring. *Materials,* 11**,** 256.

Antelmi, I., De Paula, R. S., Shinzato, A. R., Peres, C. A., Mansur, A. J. & Grupi, C. J. 2004. Influence of age, gender, body mass index, and functional capacity on heart rate variability in a cohort of subjects without heart disease. *The American journal of cardiology,* 93**,** 381-385.

Arduino. n.d.-a. *ARDUINO MEGA 2560 REV3* [Online]. Arduino. Available: https://store.arduino.cc/usa/arduino-uno-rev3 [Accessed 12 October 2018].

Arduino. n.d.-b. *ARDUINO UNO REV3* [Online]. Arduino. Available: https://store.arduino.cc/usa/arduino-uno-rev3 [Accessed 21 September 2018].

Arena, R., Williams, M., Forman, D. E., Cahalin, L. P., Coke, L., Myers, J., Hamm, L., Kris-Etherton, P., Humphrey, R. & Bittner, V. 2012. Increasing referral and participation rates to outpatient cardiac rehabilitation: the valuable role of healthcare professionals in the inpatient and home health settings: a science advisory from the American Heart Association. *Circulation,* 125**,** 1321-1329.

Aromataris, E. & Munn, Z. 2017. *Joanna Briggs Institute Reviewer's Manual* [Online]. The Joanna Briggs Institute. Available: https://reviewersmanual.joannabriggs.org/ [Accessed].

Arthur C. Guyton & Hall, J. E. 2006. *Text book of Medical Physiology,* Philadelphia, Elsevier Inc.

Arthur, H. M., Smith, K. M., Kodis, J. & McKelvie, R. 2002. A controlled trial of hospital versus home-based exercise in cardiac patients. *Medicine & Science in Sports & Exercise,* 34**,** 1544-1550.

Atallah, L., Serteyn, A., Meftah, M., Schellekens, M., Vullings, R., Bergmans, J. W., Osagiator, A. & Oetomo, S. B. 2014. Unobtrusive ECG monitoring in the NICU using a capacitive sensing array. *Physiol Meas,* 35**,** 895-913.

Australian Family Physician. 2011. Ambulatory blood pressure monitoring *Australian Family Physician* [Online], 40. Available: http://www.racgp.org.au/afp/2011/november/ambulatory-blood-pressure-monitoring/ [Accessed 16 March 2017].

Australian Institute of Health and Welfare 2011a. Cardiovascular disease : Australian facts. Canberra: Australian Institute of Health and Welfare.

Australian Institute of Health and Welfare 2011b. Cardiovascular disease: Australian facts 2011. Canberra: Australian Institute of Health and Welfare.

Australian Institute of Health and Welfare. 2015. *Chronic diseases* [Online]. Australian Institute of Health and Welfare Available: http://www.aihw.gov.au/chronic-diseases/ [Accessed 20 January 2017 2016].

Australian Institute of Health and Welfare 2016. Australia's health 2016. Canberra: Australian Institute of Health and Welfare.

Awal, M. A., Mostafa, S. S. & Ahmad, M. 2011. Performance analysis of Savitzky-Golay smoothing filter using ECG signal. *International Journal of Computer and Information Technology,* 1**,** 24.

Azami, H., Mohammadi, K. & Bozorgtabar, B. 2012. An improved signal segmentation using moving average and Savitzky-Golay filter.

Bailón, R., Sornmo, L. & Laguna, P. 2006. A robust method for ECG-based estimation of the respiratory frequency during stress testing. *IEEE transactions on biomedical engineering,* 53**,** 1273-1285.

Bakhshayeh, S., Sarbaz, M., Kimiafar, K., Vakilian, F. & Eslami, S. 2019. Barriers to participation in center-based cardiac rehabilitation programs and patients' attitude toward home-based cardiac rehabilitation programs. *Physiotherapy theory and practice***,** 1-11.

Balocchi, R., Cantini, F., Varanini, M., Raimondi, G., Legramante, J. M. & Macerata, A. 2006. Revisiting the potential of time-domain indexes in short-term HRV analysis. *Biomedical Engineering/Biomedizinische Technik,* 51**,** 190-193.

Baloglu, U. B., Talo, M., Yildirim, O., San Tan, R. & Acharya, U. R. 2019. Classification of myocardial infarction with multi-lead ECG signals and deep CNN. *Pattern Recognition Letters,* 122**,** 23-30.

Balsam, P., Lodzinski, P., Tyminska, A., Ozieranski, K., Januszkiewicz, L., Glowczynska, R., Wesolowska, K., Peller, M., Pietrzak, R., Ksiazczyk, T., Borodzicz, S., Koltowski, L., Borkowski, M., Werner, B., Opolski, G. & Grabowski, M. 2018. Study design and rationale for biomedical shirt-based electrocardiography monitoring in relevant clinical situations: ECG-shirt study. *Cardiol J,* 25**,** 52-59.

Bathiche, S. N. 2007. Computer keyboard with quantitatively force-sensing keys. Google Patents.

Batzel, J. J., Kappel, F., Schneditz, D. & Iran, H. T. 2007. *Cardiovascular and Respiratory Systems: Modeling, Analysis, and Control,* Philadelphia, Society for Industrial and Applied Mathematics.

Beckmann, L., Neuhaus, C., Medrano, G., Jungbecker, N., Walter, M., Gries, T. & Leonhardt, S. 2010. Characterization of textile electrodes and conductors using standardized measurement setups. *Physiological measurement,* 31**,** 233.

Bennett, P. 2012. Cardiovascular Rehabilitation. *In:* KENNEDY, P. (ed.) *The Oxford Handbook of Rehabilitation Psychology*

BERNINA Australia. n.d. *BERNINA 350 PE: Stylish sewing from the first stitch to the last* [Online]. BERNINA Australia Pty Ltd. Available: https://www.bernina.com/en-AU/Machines-AU/Series-Overview/BERNINA-3-Series/BERNINA-350-PE [Accessed 21 May 2019].

Berntson, G. G. & Stowell, J. R. 1998. ECG artifacts and heart period variability: don't miss a beat! *Psychophysiology,* 35**,** 127-132.

Bhogeshwar, S. S., Soni, M. & Bansal, D. Design of Simulink Model to denoise ECG signal using various IIR & FIR filters. 2014 International Conference on Reliability Optimization and Information Technology (ICROIT), 2014. IEEE, 477-483.

Bianchi, A. M. & Mendez, M. O. 2010. Automatic detection of sleep macrostructure based on a sensorized T-shirt. *Conf Proc IEEE Eng Med Biol Soc.,* 2010**,** 3606-9.

Biswas, U. & Maniruzzaman, M. Removing power line interference from ECG signal using adaptive filter and notch filter. 2014 international conference on electrical engineering and information & communication technology, 2014. IEEE, 1-4.

Blanco-Velasco, M., Weng, B. & Barner, K. E. 2008. ECG signal denoising and baseline wander correction based on the empirical mode decomposition. *Computers in biology and medicine,* 38**,** 1-13.

Boehm, A., Yu, X., Neu, W., Leonhardt, S. & Teichmann, D. 2016. A novel 12-lead ECG T-shirt with active electrodes. *Electronics,* 5**,** 75.

Bonato, P. 2003. Wearable sensors/systems and their impact on biomedical engineering: An Overview from the Guest Editor. *IEEE Engineering in Medicine and Biology* [Online]. Available: http://www.bu.edu/bostonroc/files/2011/04/2003-IEEE-EMBS-Bonato-editorial2.pdf [Accessed October 19, 2015].

Bonato, P. 2010. Wearable Sensors and Systems from enabling technology to Clinical applications. *IEEE Engineering in Medicine and Biology magazine* [Online]. Available: http://www.researchgate.net/profile/Paolo_Bonato2/publication/45365464_Wearable_sensors_and_systems._From_enabling_technology_to_clinical_applications/links/00b7d52cde32125c05000000.pdf [Accessed August 31, 2015].

Bourdon, L., Coli, S., Loriga, G., Taccini, N., Gros, B., Gemignani, A., Cianflone, D., Chapotot, F., Dittmar, A. & Paradiso, R. 2005. First results with the wealthy garment electrocardiogram monitoring system. *Comput Cardiol.* IEEE.

Boutry, C. M., Nguyen, A., Lawal, Q. O., Chortos, A., Rondeau-Gagné, S. & Bao, Z. 2015. A sensitive and biodegradable pressure sensor array for cardiovascular monitoring. *Advanced Materials,* 27**,** 6954-6961.

Bouwstra, S., Chen, W., Oetomo, S. B., Feijs, L. M. & Cluitmans, P. J. Designing for reliable textile neonatal ECG monitoring using multi-sensor recordings. 2011 Annual International Conference of the IEEE Engineering in Medicine and Biology Society, 2011. IEEE, 2488-2491.

Brazdzionyte, J. & Macas, A. 2007. Bland-Altman analysis as an alternative approach for statistical evaluation of agreement between two methods for measuring hemodynamics during acute myocardial infarction. *Medicina,* 43**,** 208-214.

Brieger, D., Amerena, J., Attia, J. R., Bajorek, B., Chan, K. H., Connell, C., Freedman, B., Ferguson, C., Hall, T. & Haqqani, H. M. 2018. National Heart Foundation of Australia and Cardiac Society of Australia and New Zealand: Australian clinical guidelines for the diagnosis and management of atrial fibrillation 2018. *Medical Journal of Australia,* 209**,** 356-362.

Buchwald, H. WE-PM-3 Tutorial lab experiences with IEC 60601-1-2 4 th Edition. 2017 IEEE International Symposium on Electromagnetic Compatibility & Signal/Power Integrity (EMCSI), 2017. IEEE, 1-50.

Budgell, B. & Polus, B. 2006. The effects of thoracic manipulation on heart rate variability: a controlled crossover trial. *Journal of manipulative and physiological therapeutics,* 29**,** 603-610.

Bullock, J., Boyle, J. & Wang, M. B. 2001. *NMS (National Medical Series for Independent Study) Physiology,* London, Lippincott Williams &Wilkins.

Bunce, C. 2009. Correlation, agreement, and Bland–Altman analysis: statistical analysis of method comparison studies. *American journal of ophthalmology,* 148**,** 4-6.

Bunnings. n.d. . *1200 x 900 x 3mm Black PVC Foam Board Sheet* [Online]. Available: https://www.bunnings.com.au/1200-x-900-x-3mm-black-pvc-foam-board-sheet_p1010816 [Accessed 12 April 2019].

Burdea, G., Richard, P. & Coiffet, P. 1996. Multimodal virtual reality: Input-output devices, system integration, and human factors. *International Journal of Human-Computer Interaction,* 8**,** 5-24.

Burdea, G. C. & Coiffet, P. 2003. *Virtual reality technology*, John Wiley & Sons.

Burger, H. & Van Milaan, J. 1943. Measurements of the specific resistance of the human body to direct current. *Acta Medica Scandinavica,* 114**,** 584-607.

Cai, Z., Luo, K., Liu, C. & Li, J. 2017. Design of a smart ECG garment based on conductive textile electrode and flexible printed circuit board. *Technology and Health Care,* 25**,** 815-821.

Caldara, M., Comotti, D., Gaioni, L., Pedrana, A., Pezzoli, M., Re, V. & Traversi, G. Development of a multi-lead ECG wearable sensor system for biomedical applications. 2017 7th IEEE International Workshop on Advances in Sensors and Interfaces (IWASI), 2017a. IEEE, 207-212.

Caldara, M., Comotti, D., Gaioni, L., Pedrana, A., Pezzoli, M., Re, V. & Traversi, G. Wearable sensor system for multi-lead ECG measurement. 2017 IEEE 14th International Conference on Wearable and Implantable Body Sensor Networks (BSN), 2017b. IEEE, 137-140.

Caplan, L. R. & Sumner, A. J. 2006. *Stroke,* New York, American Academy of Neurology Press.

Carlson, J. J., Johnson, J. A., Franklin, B. A. & VanderLaan, R. L. 2000. Program participation, exercise adherence, cardiovascular outcomes, and program cost of traditional versus modified cardiac rehabilitation. *The American journal of cardiology,* 86**,** 17-23.

Carvalho, H., Catarino, A. P., Rocha, A. & Postolache, O. 2014. Health monitoring using textile sensors and electrodes: an overview and integration of technologies. *IEEE Int Symp Med Meas Appl.* IEEE.

Catarino, A., Carvalho, H., Dias, M. J., Pereira, T., Postolache, O. & Pedro S, G. Continuous health monitoring using E-textile integrated biosensors., 2012. 605-609.

Chakraborty, M. & Das, S. 2012. Determination of signal to noise ratio of electrocardiograms filtered by band pass and Savitzky-Golay filters. *Procedia Technology,* 4**,** 830-833.

Chamadiya, B., Mankodiya, K., Wagner, M. & Hofmann, U. G. 2013. Textile-based, contactless ECG monitoring for non-ICU clinical settings. *J Ambient Intell Humaniz Comput,* 4**,** 791-800.

Chandrakar, B., Yadav, O. & Chandra, V. 2013. A survey of noise removal techniques for ECG signals. *International Journal of Advanced Research in Computer and Communication Engineering,* 2**,** 1354-1357.

Chatzitofis, A., Monaghan, D., Mitchell, E., Honohan, F., Zarpalas, D., O'Connor, N. E. & Daras, P. HeartHealth: a cardiovascular disease home-based rehabilitation system. Procedia Comput Sci, 2015. Elsevier B.V., 340-347.

Chaudhuri, S., Duttagupta, S. & Pawar, T. D. 2009. Ambulation Analysis in Wearable ECG. Springer.

Chen, H. & Chen, S.-W. A moving average based filtering system with its application to real-time QRS detection. Computers in Cardiology, 2003, 2003. IEEE, 585-588.

Cheng, M. H., Chen, L. C., Hung, Y. C., Chang, M. Y. & Tzu, L. Y. 2008. A real-time heart-rate estimator from steel textile ecg sensors in a wireless vital wearing system. 1339-1342.

Chew, D. P., Scott, I. A., Cullen, L., French, J. K., Briffa, T. G., Tideman, P. A., Woodruffe, S., Kerr, A., Branagan, M. & Aylward, P. E. 2016. National Heart Foundation of Australia and Cardiac Society of Australia and New Zealand: Australian clinical guidelines for the management of acute coronary syndromes 2016. *Medical Journal of Australia,* 205**,** 128-133.

Chi, Y.-W., Tseng, K.-H., Li, R. & Pan, T. 2018. Comparison of piezoresistive sensor to PicoPress® in in-vitro interface pressure measurement. *Phlebology,* 33**,** 315-320.

Cho, H.-S., Koo, S.-M., Lee, J., Cho, H., Kang, D.-H., Song, H.-Y., Lee, J.-W., Lee, K.-H. & Lee, Y.-J. 2011. Heart Monitoring Garments Using Textile Electrodes for Healthcare Applications. *J Med Syst,* 35**,** 189-201.

Cho, H. & Lee, J. H. 2015. A study on the optimal positions of ECG electrodes in a garment for the design of ECG-monitoring clothing for male. *Journal of medical systems,* 39**,** 95.

Cho, H., Lim, H. & Cho, S. 2016. Efficacy research of electrocardiogram and heart rate measurement in accordance with the structure of the textile electrodes. *Fibers and Polymers,* 17**,** 2069-2077.

Cho, J., Moon, J., Jeong, K. & Cho, G. 2007. Application of PU-sealing into Cu/Ni electroless plated polyester fabrics for e-textiles. *Fibers and Polymers,* 8**,** 330-334.

Choi, A. & Shin, H. 2018. Quantitative analysis of the effect of an ectopic beat on the heart rate variability in the resting condition. *Frontiers in physiology,* 9**,** 922.

Choi, J.-B., Hong, S., Nelesen, R., Bardwell, W. A., Natarajan, L., Schubert, C. & Dimsdale, J. E. 2006. Age and ethnicity differences in short-term heart-rate variability. *Psychosomatic medicine,* 68**,** 421-426.

Clifford, G., Behar, J., Li, Q. & Rezek, I. 2012. Signal quality indices and data fusion for determining clinical acceptability of electrocardiograms. *Physiol Meas,* 33**,** 1419.

Clifford, G. & Oefinger, M. B. 2006. ECG acquisition, storage, transmission, and representation. *Advanced Methods and Tools for ECG Data Analysis***,** 27-53.

Clifford, G. D., Azuaje, F. & McSharry, P. 2006. *Advanced methods and tools for ECG data analysis*, Artech house Boston.

Coli, S., Grassi, F., Taccini, N., Loriga, G., Calori, G., Gemignani, A., Ghelarducci, B. & Cianflone, D. 2006. Successful real time ECG recording and transmission in cardiac patients with a wearable system based on smart textiles: first clinical experience of the WEALTHY project. *Eur Heart J,* 27**,** 871.

Cömert, A., Honkala, M. & Hyttinen, J. 2013. Effect of pressure and padding on motion artifact of textile electrodes. *Biomedical engineering online,* 12**,** 26.

Cömert, A. & Hyttinen, J. 2015. Investigating the possible effect of electrode support structure on motion artifact in wearable bioelectric signal monitoring. *Biomedical engineering online,* 14**,** 1-18.

CONSORT transparent reporting of trials. n.d. *CONSORT 2010* [Online]. CONSORT. Available: http://www.consort-statement.org/consort-2010 [Accessed 14 December 2017].

Coosemans, J., Hermans, B. & Puers, R. 2006. Integrating wireless ECG monitoring in textiles. *Sens Actuators A Phys,* 130-131**,** 48-53.

Coyle, S., Lau, K. T., Moyna, N., O'Gorman, D., Diamond, D., Di Francesco, F., Costanzo, D., Salvo, P., Trivella, M. G., De Rossi, D. E., Taccini, N., Paradiso, R., Porchet, J. A., Ridolfi, A., Luprano, J., Chuzel, C., Lanier, T., Revol-Cavalier, F., Schoumacker, S., Mourier, V., Chartier, I., Convert, R., De-Moncuit, H. & Bini, C. 2010. BIOTEX--biosensing textiles for personalised healthcare management. *IEEE Trans Inf Technol Biomed,* 14**,** 364-70.

Crassidis, J. L. 2017. Introduction to the special issue on the Kalman filter and its aerospace applications. American Institute of Aeronautics and Astronautics.

Dai, M., Xiao, X., Chen, X., Lin, H., Wu, W. & Chen, S. 2016. A low-power and miniaturized electrocardiograph data collection system with smart textile electrodes for monitoring of cardiac function. *Australas Phys Eng Sci Med,* 39**,** 1029-1040.

Dalal, H. M., Zawada, A., Jolly, K., Moxham, T. & Taylor, R. S. 2010. Home based versus centre based cardiac rehabilitation: Cochrane systematic review and meta-analysis. *BMJ,* 340**,** b5631.

Dantas, E. M., Kemp, A. H., Andreão, R. V., da Silva, V. J. D., Brunoni, A. R., Hoshi, R. A., Bensenor, I. M., Lotufo, P. A., Ribeiro, A. L. P. & Mill, J. G. 2018. Reference values for short-term resting-state heart rate variability in healthy adults: Results from the Brazilian Longitudinal Study of Adult Health—ELSA-Brasil study. *Psychophysiology,* 55**,** e13052.

Dawson, D., Yang, H., Malshe, M., Bukkapatnam, S. T., Benjamin, B. & Komanduri, R. 2009. Linear affine transformations between 3-lead (Frank XYZ leads) vectorcardiogram and 12-lead electrocardiogram signals. *Journal of electrocardiology,* 42**,** 622-630.

Decker, W. W., Prina, L. D., Smars, P. A., Boggust, A. J., Zinsmeister, A. R. & Kopecky, S. L. 2003. Continuous 12-lead electrocardiographic monitoring in an emergency department chest pain unit: an assessment of potential clinical effect. *Annals of emergency medicine,* 41**,** 342-351.

Deighana, C., Michalovaa, L., Pagliarib, C., Elliotta, J., Taylora, L. & Ranaldia, H. c2017. The Digital Heart Manual: A pilot study of an innovative cardiac rehabilitation program developed for and with users. *Patient Educ Couns*.

Denes, P. 1992. The importance of derived 12-lead electrocardiography in the interpretation of arrhythmias detected by Holter recording. *American heart journal,* 124**,** 905-911.

Dhaker, P. 2018. *Introduction to SPI Interface* [Online]. Analog Devices, Inc. Available: https://www.analog.com/en/analog-dialogue/articles/introduction-to-spi-interface.html [Accessed 7 April, 2019].

Di Rienzo, M., Meriggi, P., Rizzo, F., Castiglioni, P., Lombardi, C., Ferratini, M. & Parati, G. 2010. Textile technology for the vital signs monitoring in telemedicine and extreme environments. *IEEE Trans Inf Technol Biomed,* 14**,** 711-7.

Di Rienzo, M., Racca, V., Rizzo, F., Bordoni, B., Parati, G., Castiglioni, P., Meriggi, P. & Ferratini, M. 2013. Evaluation of a textile-based wearable system for the electrocardiogram monitoring in cardiac patients. *Europace,* 15**,** 607-612.

Di Rienzo, M., Rizzo, F., Meriggi, P., Bordoni, B., Brambilla, G., Ferratini, M. & Castiglioni, P. 2006a. Applications of a textile-based wearable system for vital signs monitoring. *Conf Proc IEEE Eng Med Biol Soc.*

Di Rienzo, M., Rizzo, F., Parati, G., Brambilla, G., Ferratini, M. & Castiglioni, P. MagIC system: A new textile-based wearable device for biological signal monitoring. Applicability in daily life and clinical setting. 2005 IEEE Engineering in Medicine and Biology 27th Annual Conference, 2006b. IEEE, 7167-7169.

Di Rienzo, M., Rizzo, F., Parati, G., Ferratini, M., Brambilla, G. & Castiglioni, P. 2005. A textile-based wearable system for vital sign monitoring: applicability in cardiac patients. *Comput Cardiol.* IEEE.

Dias, T. (ed.) 2015. *Electronic Textiles: Smart Fabrics and Wearable Technology,* Cambridge: Woodhead Publishing.

Doğan, N. Ö. 2018. Bland-Altman analysis: A paradigm to understand correlation and agreement. *Turkish journal of emergency medicine,* 18**,** 139-141.

Dower, G. E., Yakush, A., Nazzal, S. B., Jutzy, R. V. & Ruiz, C. E. 1988. Deriving the 12-lead electrocardiogram from four (EASI) electrodes. *Journal of electrocardiology,* 21**,** S182-S187.

Drew, B. J., Pelter, M. M., Brodnick, D. E., Yadav, A. V., Dempel, D. & Adams, M. G. 2002. Comparison of a new reduced lead set ECG with the standard ECG for diagnosing cardiac arrhythmias and myocardial ischemia. *Journal of electrocardiology,* 35**,** 13-21.

Drew, B. J., Pelter, M. M., Wung, S.-F., Adams, M. G., Taylor, C., Evans Jr, G. T. & Foster, E. 1999. Accuracy of the EASI 12-lead electrocardiogram compared to the standard 12-lead electrocardiogram for diagnosing multiple cardiac abnormalities. *Journal of electrocardiology,* 32**,** 38-47.

Dunn, S. L., Dunn, L. M., Buursma, M. P., Clark, J. A., Vander Berg, L., DeVon, H. A. & Tintle, N. L. 2017. Home-and hospital-based cardiac rehabilitation exercise: the important role of physician recommendation. *Western journal of nursing research,* 39**,** 214-233.

eBay Inc. n.d. *Korea Vintage Cotton Minky Fabric* [Online]. eBay Inc. . Available: https://www.ebay.com/str/koreavintagecottonminkyfabric [Accessed 19 June 2019].

Eclipse Foundation. n.d. *Memory Analyzer (MAT)* [Online]. the Eclipse Foundation. Available: https://www.eclipse.org/org/ [Accessed].

Electrophysiology, T. F. o. t. E. S. o. C. t. N. A. S. o. P. 1996. Heart rate variability: standards of measurement, physiological interpretation, and clinical use. *Circulation,* 93**,** 1043-1065.

Eric P. Widmaier, Hershel Raff & Strang, K. T. 2014. Vander's Human Physiology: The Mechanisms of Body Function. 13 ed. New York: The McGraw-Hill Companies, Inc.

Falco, V. 2012. *vinniefalco/DSPFilters* [Online]. GitHub, Inc. Available: https://github.com/vinniefalco/DSPFilters/blob/master/shared/DSPFilters/source/Documentation.cpp [Accessed].

Farahbod, F. 2018. *Telemetry Viewer v0.5* [Online]. Farrell Farahbod. Available: http://farrellf.com/ [Accessed 12 April 2019].

Fawcus, R. 2000. *Stroke Rehabilitation: A Collaborative Approach*, Blackwell Science Ltd.

Feild, D. Q., Feldman, C. L. & Hor, B. M. 2002. Improved EASI coefficients: their derivation, values, and performance. *Journal of electrocardiology,* 35**,** 23-33.

Feldman, C. L., Milstein, S. Z., Neubecker, D., Underhill, B. K., Moyer, E., Glumm, S., Womble, M., Auer, J., Maynard, C. & Serra, R. K. 2005. Comparison of the Five-Electrode–Derived EASI Electrocardiogram to the Mason Likar Electrocardiogram in the Prehospital Setting. *The American journal of cardiology,* 96**,** 453-456.

Finlay, D. D., Nugent, C. D., Donnelly, M. P. & Black, N. D. 2008a. Selection of optimal recording sites for limited lead body surface potential mapping in myocardial infarction and left ventricular hypertrophy. *Journal of electrocardiology,* 41**,** 264-271.

Finlay, D. D., Nugent, C. D., Donnelly, M. P., McCullagh, P. J. & Black, N. D. 2008b. Optimal electrocardiographic lead systems: practical scenarios in smart clothing and wearable health systems. *IEEE Transactions on Information Technology in Biomedicine,* 12**,** 433-441.

Fleury, A., Sugar, M. & Chau, T. 2015. E-textiles in Clinical Rehabilitation: A Scoping Review. *Electronics,* 4**,** 173-203.

Fluke Biomedical. n.d. *ProSim 2 and 3 Vital Sign Simulators* [Online]. Fluke. Available: https://www.flukebiomedical.com/products/biomedical-test-equipment/patient-monitor-simulators/prosim-2-3-vital-signs-patient-simulators [Accessed 21 May 2019].

Franco, S. 2015. *Design with operational amplifiers and analog integrated circuits,* New York, McGraw-Hill Education

Friesen, G. M., Jannett, T. C., Jadallah, M. A., Yates, S. L., Quint, S. R. & Nagle, H. T. 1990. A comparison of the noise sensitivity of nine QRS detection algorithms. *IEEE Transactions on biomedical engineering,* 37**,** 85-98.

Fuhrhop, S., Lamparth, S. & Heuer, S. A textile integrated long-term ECG monitor with capacitively coupled electrodes. 2009 IEEE Biomedical Circuits and Systems Conference, 26-28 Nov. 2009 2009. 21-24.

Gacek, A. & Pedrycz, W. 2011. *ECG signal processing, classification and interpretation: a comprehensive framework of computational intelligence*, Springer Science & Business Media.

Gamelin, F.-X., Berthoin, S. & Bosquet, L. 2006. Validity of the polar S810 heart rate monitor to measure RR intervals at rest.

GE Healthcare. c2009. *SEERLight Ambulatory Recorder/Controller Operator's Manual* [Online]. GE Healthcare. Available: https://www.udh.med.sa/advices/2040604-012D_S_L_E_OM_Eng.pdf [Accessed 10 March 2020].

Giavarina, D. 2015. Understanding bland altman analysis. *Biochemia medica: Biochemia medica,* 25**,** 141-151.

Gold, M. R., Thébault, C., Linde, C., Abraham, W. T., Gerritse, B., Ghio, S., St. John Sutton, M. & Daubert, J.-C. 2012. Effect of QRS duration and morphology on cardiac resynchronization therapy outcomes in mild heart failure: results from the Resynchronization Reverses Remodeling in Systolic Left Ventricular Dysfunction (REVERSE) study. *Circulation,* 126**,** 822-829.

Goldberger, A. L., Amaral, L. A., Glass, L., Hausdorff, J. M., Ivanov, P. C., Mark, R. G., Mietus, J. E., Moody, G. B., Peng, C.-K. & Stanley, H. E. 2000. PhysioBank, PhysioToolkit, and PhysioNet: components of a new research resource for complex physiologic signals. *Circulation,* 101**,** e215-e220.

Greiser, K. H., Kluttig, A., Schumann, B., Swenne, C. A., Kors, J. A., Kuss, O., Haerting, J., Schmidt, H., Thiery, J. & Werdan, K. 2009. Cardiovascular diseases, risk factors and short-term heart rate variability in an elderly general population: the CARLA study 2002–2006. *European journal of epidemiology,* 24**,** 123.

Grond, M., Jauss, M., Hamann, G., Stark, E., Veltkamp, R., Nabavi, D., Horn, M., Weimar, C., Köhrmann, M. & Wachter, R. 2013. Improved detection of silent atrial fibrillation using 72-hour Holter ECG in patients with ischemic stroke: a prospective multicenter cohort study. *Stroke,* 44**,** 3357-3364.

Guyton, A. C. & Hall, J. E. 2006. *Text book of Medical Physiology,* Philadelphia, Elsevier Inc.

Hall, J. E. 2010. *Guyton and Hall textbook of medical physiology e-Book*, Elsevier Health Sciences.

Hargittai, S. Savitzky-Golay least-squares polynomial filters in ECG signal processing. Computers in Cardiology, 2005, 2005. IEEE, 763-766.

Harvey, A. C. 1990. *Forecasting, structural time series models and the Kalman filter*, Cambridge university press.

Hautala, A. J., Karjalainen, J., Kiviniemi, A. M., Kinnunen, H., Makikallio, T. H., Huikuri, H. V. & Tulppo, M. P. 2010. Physical activity and heart rate variability measured simultaneously during waking hours. *American Journal of Physiology-Heart and Circulatory Physiology,* 298**,** H874-H880.

HEARTe. c2018. *Cardiac Investigations: Electrocardiography* [Online]. Chest Heart & Stroke Scotland and The University of Edinburgh. Available: https://www.heartelearning.org/labyrinths?id=47637 [Accessed 29 April 2018].

Hill, L. K., Hu, D. D., Koenig, J., Sollers III, J. J., Kapuku, G., Wang, X., Snieder, H. & Thayer, J. F. 2015. Ethnic differences in resting heart rate variability: a systematic review and meta-analysis. *Psychosomatic medicine,* 77**,** 16.

Hingorani, P., Karnad, D. R., Rohekar, P., Kerkar, V., Lokhandwala, Y. Y. & Kothari, S. 2016. Arrhythmias seen in baseline 24-hour Holter ECG recordings in healthy normal volunteers during phase 1 clinical trials. *The Journal of Clinical Pharmacology,* 56**,** 885-893.

Hollinger, A. & Wanderley, M. M. Evaluation of commercial force-sensing resistors. Proceedings of the International Conference on New Interfaces for Musical Expression, Paris, France, 2006. 4-8.

Hsiao, C. C., Lee, R. G., Tien, S. C., Feng, Y. Y. & Huang, S. F. 2015. Early clinical prognosis for high-risk chest pain patients using smart textiles. *Biomed Eng,* 27**,** 1550057.

Hu, X., Xiao, Z. & Zhang, N. 2011. Removal of baseline wander from ECG signal based on a statistical weighted moving average filter. *Journal of Zhejiang University SCIENCE C,* 12**,** 397-403.

Huang, N. E., Shen, Z., Long, S. R., Wu, M. C., Shih, H. H., Zheng, Q., Yen, N.-C., Tung, C. C. & Liu, H. H. 1998. The empirical mode decomposition and the Hilbert spectrum for nonlinear and non-stationary time series analysis. *Proceedings of the Royal Society of London. Series A: mathematical, physical and engineering sciences,* 454**,** 903-995.

Huigen, E., Peper, A. & Grimbergen, C. 2002. Investigation into the origin of the noise of surface electrodes. *Medical and biological engineering and computing,* 40**,** 332-338.

Iancu-Constantin, R., Serbanati, L. D., Chera, C., Gheorghe-Pop, I.-D. & Ertl, B. An E-health approach for remote cardiac rehabilitation. 2015 20th International Conference on Control Systems and Computer Science, 2015. IEEE, 205-210.

Iliev, I. T., Tabakov, S. D. & Krasteva, V. T. 2008. Combined high-pass and power-line interference rejecter filter for ecg signal processing. *Proceedings of the Technical University-Sofia, Bugaria,* 58**,** 7-13.

Iuliano, S., Fisher, S. G., Karasik, P. E., Fletcher, R. D., Singh, S. N. & Failure, D. o. V. A. S. T. o. A. T. i. C. H. 2002. QRS duration and mortality in patients with congestive heart failure. *American heart journal,* 143**,** 1085-1091.

Jahrsdoerfer, M., Giuliano, K. & Stephens, D. 2005. Clinical usefulness of the EASI 12-lead continuous electrocardiographic monitoring system. *Critical Care Nurse,* 25**,** 28-37.

Jaworek, J. & Augustyniak, P. A cardiac telerehabilitation application for mobile devices. 2011 Computing in Cardiology, 2011. IEEE, 241-244.

Jaycar Electronics. n.d. *5.0mm Black Heatshrink Tubing* [Online]. Jaycar Electronics. Available: https://www.jaycar.com.au/5-0mm-black-heatshrink-tubing/p/WH5533 [Accessed 12 April 2019].

Jiang, Y., Qian, C., Hanna, R., Farina, D. & Doessel, O. Optimization of electrode positions of a wearable ECG monitoring system for efficient and effective detection of acute myocardial infarction. 2009 36th Annual Computers in Cardiology Conference (CinC), 2009. IEEE, 293-296.

Jit, I., Jhingan, V. & Kulkarni, M. 1980. Sexing the human sternum. *American Journal of Physical Anthropology,* 53**,** 217-224.

John Bullock, Joseph Boyle & Wang, M. B. 2001. NMS (National Medical Series for Independent Study) Physiology. 4 ed. London: Lippincott Williams &Wilkins.

Johnson, A. E., Behar, J., Andreotti, F., Clifford, G. D. & Oster, J. 2015. Multimodal heart beat detection using signal quality indices. *Physiological measurement,* 36**,** 1665.

Jolly, K., Lip, G. Y., Taylor, R. S., Raftery, J., Mant, J., Lane, D., Greenfield, S. & Stevens, A. 2009. The Birmingham Rehabilitation Uptake Maximisation study (BRUM): a randomised controlled trial comparing home-based with centre-based cardiac rehabilitation. *Heart,* 95**,** 36-42.

Jolly, K., Taylor, R., Lip, G., Greenfield, S., Raftery, J., Mant, J., Lane, D., Jones, M., Lee, K. & Stevens, A. 2007. The Birmingham Rehabilitation Uptake Maximisation Study (BRUM). Home-based compared with hospital-based cardiac rehabilitation in a multi-ethnic population: cost-effectiveness and patient adherence. *Health Technology Assessment (Winchester, England),* 11**,** 1.

Jones, M., Jolly, K., Raftery, J., Lip, G. Y. & Greenfield, S. 2007. 'DNA'may not mean 'did not participate': a qualitative study of reasons for non-adherence at home-and centre-based cardiac rehabilitation. *Family practice,* 24**,** 343-357.

Jones, M., Martin, T., Nakad, Z., Shenoy, R., Sheikh, T., Lehn, D., Edmison, J. & Chandra, M. 2003. Analyzing the use of e-textiles to improve application performance. *Vehicular Technology Conference.* IEEE.

Joshi, S. L., Vatti, R. A. & Tornekar, R. V. A survey on ECG signal denoising techniques. 2013 International Conference on Communication Systems and Network Technologies, 2013. IEEE, 60-64.

Jourand, P., De Clercq, H. & Puers, R. 2010. Robust monitoring of vital signs integrated in textile. *Sensors and Actuators A: Physical,* 161**,** 288–296

Kakria, P., Tripathi, N. K. & Kitipawang, P. 2015. A real-time health monitoring system for remote cardiac patients using smartphone and wearable sensors. *Int J Telemed Appl,* 2015**,** 8.

Kannaian, T., Neelaveni, R. & Thilagavathi, G. 2013. Design and development of embroidered textile electrodes for continuous measurement of electrocardiogram signals. *Journal of Industrial Textiles,* 42**,** 303-318.

Karason, K., Mølgaard, H., Wikstrand, J. & Sjöström, L. 1999. Heart rate variability in obesity and the effect of weight loss. *The American journal of cardiology,* 83**,** 1242-1247.

Kaur, M. & Singh, B. Comparison of different approaches for removal of baseline wander from ECG signal. Proceedings of the International Conference & Workshop on Emerging Trends in Technology, 2011. 1290-1294.

Keteyian, S. J., Mellett, P. A., Fedel, F. J., McGowan, C. M. & Stein, P. D. 1995. Electrocardiographic monitoring during cardiac rehabilitation. *Chest,* 107**,** 1242-1246.

Kim, C., Moon, C. J. & Lim, M. H. 2012. Safety of monitoring exercise for early hospital-based cardiac rehabilitation. *Ann Rehabil Med,* 36**,** 262-267.

Kim, H., Yazicioglu, R. F., Merken, P., Van Hoof, C. & Yoo, H.-J. 2009. ECG signal compression and classification algorithm with quad level vector for ECG holter system. *IEEE Transactions on Information Technology in Biomedicine,* 14**,** 93-100.

Kim, Y. & Bang, H. 2018. Introduction to Kalman Filter and Its Applications. *Introduction and Implementations of the Kalman Filter.* IntechOpen.

King, M., Baragwanath, A., Rosamond, M., Wood, D. & Gallant, A. 2009. Porous PDMS force sensitive resistors. *Procedia Chemistry,* 1**,** 568-571.

Klabunde, R. E. 2012. *Cardiovascular physiology concepts,* Baltimore, Lippincott Williams & Wilkins.

Klein, M. D., Key-Brothers, I. & Feldman, C. L. Can the vectorcardiographically derived EASI ECG be a suitable surrogate for the standard ECG in selected circumstances. Computers in Cardiology 1997, 1997. IEEE, 721-724.

Kligfield, P., Gettes, L. S., Bailey, J. J., Childers, R., Deal, B. J., Hancock, E. W., Van Herpen, G., Kors, J. A., Macfarlane, P. & Mirvis, D. M. 2007. Recommendations for the standardization and interpretation of the electrocardiogram: part I: the electrocardiogram and its technology a scientific statement from the American Heart Association Electrocardiography and Arrhythmias Committee, Council on Clinical Cardiology; the American College of Cardiology Foundation; and the Heart Rhythm Society endorsed by the International Society for Computerized Electrocardiology. *Journal of the American College of Cardiology,* 49**,** 1109-1127.

Klootwijk, P., Meij, S., Es, G. v., Müller, E., Umans, V., Lenderink, T. & Simoons, M. 1997. Comparison of usefulness of computer assisted continuous 48-h 3-lead with 12-lead ECG ischaemia monitoring for detection and quantitation of ischaemia in patients with unstable angina. *European heart journal,* 18**,** 931-940.

Kmart Australia. n.d. *180 Thread Count Sheet Set - Single Bed, Mid Blue* [Online]. Kmart. Available: https://www.kmart.com.au/product/180-thread-count-sheet-set---single-bed,-mid-blue/114554 [Accessed 15 March 2019].

Kopsinis, Y. & McLaughlin, S. 2008. Empirical mode decomposition based denoising techniques. *1st International Work-shop on Cognitive Information Processing (CIP)*.

Koskinen, T., Kähönen, M., Jula, A., Laitinen, T., Keltikangas-Järvinen, L., Viikari, J., Välimäki, I. & Raitakari, O. T. 2009. Short-term heart rate variability in healthy young adults: the Cardiovascular Risk in Young Finns Study. *Autonomic Neuroscience,* 145**,** 81-88.

Kotani, K., Tachibana, M. & Takamasu, K. 2007. Investigation of the influence of swallowing, coughing and vocalization on heart rate variability with respiratory-phase domain analysis. *Methods of Information in Medicine,* 46**,** 179-185.

Kraus, W. & Keteyian, S. 2007. *Cardiac rehabilitation*, Springer Science & Business Media.

Kupari, M., Virolainen, J., Koskinen, P. & Tikkanen, M. J. 1993. Short-term heart rate variability and factors modifying the risk of coronary artery disease in a population sample. *The American journal of cardiology,* 72**,** 897-903.

Laidler, P. 1994. *Stroke Rehabilitation: Structure and Strategy,* San Diego, Singular Publishing Group Inc.

Laks, M. M., Arzbaecher, R., Bailey, J. J., Geselowitz, D. B. & Berson, A. S. 1996. Recommendations for safe current limits for electrocardiographs: a statement for healthcare professionals from the Committee on Electrocardiography, American Heart Association. *Circulation,* 93**,** 837-839.

Lancia, L., Toccaceli, A., Petrucci, C., Romano, S. & Penco, M. 2018. Continuous ECG monitoring in patients with acute coronary syndrome or heart failure: EASI versus gold standard. *Clinical nursing research,* 27**,** 433-449.

Laurin, L.-P., Jobin, V. & Bellemare, F. 2012. Sternum length and rib cage dimensions compared with bodily proportions in adults with cystic fibrosis. *Canadian respiratory journal,* 19.

Lee, I. B., Shin, S. C., Jang, Y. W., Song, Y. S., Jeong, J. W. & Kim, S. 2008. Comparison of conductive fabric sensor and Ag-AgCl sensor under motion artifacts. *Conf Proc IEEE Eng Med Biol Soc.*

Lee, J. S., Heo, J., Lee, W. K., Lim, Y. G., Kim, Y. H. & Park, K. S. 2014. Flexible capacitive electrodes for minimizing motion artifacts in ambulatory electrocardiograms. *Sensors,* 14**,** 14732-14743.

Lee, S., Ahn, Y., Prabu, A. & Kim, K. 2013. Piezoelectric polymer and piezocapacitive nanoweb based sensors for monitoring vital signals and energy expenditure in smart textiles. *Journal of Fiber Bioengineering and Informatics,* 6**,** 369-381.

Lee, S. & Kruse, J. 2008. Biopotential electrode sensors in ECG/EEG/EMG systems. *Analog Devices,* 200**,** 1-2.

Łęski, J. M. & Henzel, N. 2005. ECG baseline wander and powerline interference reduction using nonlinear filter bank. *Signal processing,* 85**,** 781-793.

Li, H., Chen, X., Cao, L., Zhang, C., Tang, C., Li, E., Feng, X. & Liang, H. 2017. Textile-based ECG acquisition system with capacitively coupled electrodes. *T I MEAS CONTROL,* 39**,** 141-148.

Li, Q., Mark, R. G. & Clifford, G. D. 2008. Robust heart rate estimation from multiple asynchronous noisy sources using signal quality indices and a Kalman filter. *Physiological measurement,* 29**,** 15.

Liang, H., Lin, Z. & McCallum, R. 2000. Artifact reduction in electrogastrogram based on empirical mode decomposition method. *Medical and Biological Engineering and Computing,* 38**,** 35-41.

Libbus, I., Nearing, B. D., Amurthur, B., KenKnight, B. H. & Verrier, R. L. 2017. Quantitative evaluation of heartbeat interval time series using Poincaré analysis reveals distinct patterns of heart rate dynamics during cycles of vagus nerve stimulation in patients with heart failure. *Journal of Electrocardiology,* 50**,** 898-903.

Lilly, L. S. & Braunwald, E. 2012. *Braunwald's heart disease: a textbook of cardiovascular medicine*, Elsevier Health Sciences.

Lim, C. Y. & Kim, K. 2014. A Study on a Healthcare System Using Smart Clothes. *Journal of Electrical Engineering and Technology,* 9**,** 372-377.

Lin, Y.-D., Chien, Y.-H., Wang, S.-F., Tsai, C.-L., Chang, H.-H. & Lin, K.-P. 2013. Implementation of multiple-channel capacitive ECG measurement based on conductive fabric. *Biomed Eng (Singapore),* 25**,** 1350052.

Loewe, A., Schulze, W. H., Jiang, Y., Wilhelms, M. & Dössel, O. Determination of optimal electrode positions of a wearable ECG monitoring system for detection of myocardial ischemia: a simulation study. 2011 Computing in Cardiology, 2011. IEEE, 741-744.

Löfhede, J., Seoane, F. & Thordstein, M. 2012. Textile electrodes for EEG recording—A pilot study. *Sensors,* 12**,** 16907-16919.

Lopez, G., Custodio, V. & Moreno, J. I. 2010. LOBIN: E-textile and wireless-sensor-network-based platform for healthcare monitoring in future hospital environments. *IEEE Trans Inf Technol Biomed,* 14**,** 1446-58.

López, G., Custodio, V. & Moreno, J. I. 2010. LOBIN: E-textile and wireless-sensor-network-based platform for healthcare monitoring in future hospital environments. *IEEE Transactions on Information Technology in Biomedicine,* 14**,** 1446-1458.

Loreto, L., Andrea, T., Lucia, D., Carla, L., Cristina, P. & Silvio, R. 2016. Accuracy of EASI 12-lead ECGs in monitoring ST-segment and J-point by nurses in the Coronary Care Units. *Journal of clinical nursing,* 25**,** 1282-1291.

Loriga, G., Taccini, N., De Rossi, D. & Paradiso, R. Textile sensing interfaces for cardiopulmonary signs monitoring. Engineering in Medicine and Biology Society, 2005. IEEE-EMBS 2005. 27th Annual International Conference of the, 2006. IEEE, 7349-7352.

Lorimer, A. R. & Hillis, W. S. 1985. *Cardiovascular Disease*, Springer-Verlag Berlin Heidelberg.

Loue, S. & Sajatovic, M. 2012. *Encyclopedia of Immigrant Health,* New York, Springer Science and Business Media, LLC.

Lu, T.-H., Lin, H.-C., Lee, Y.-H., Chen, R.-R., Chen, H.-L., Chang, S.-Y., Chen, J.-D., Wu, B.-R. & Wu, T.-H. 2012. A motion-sensing enabled personalized exercise system for cardiac rehabilitation. *IEEE*

14th International Conference on e-Health Networking, Applications and Services (Healthcom). IEEE.

Lynn, P. 1971. Recursive digital filters for biological signals. *Medical & biological engineering,* 9**,** 37-43.

Maan, A. C., van Zwet, E. W., Man, S., Oliveira-Martens, S. M., Schalij, M. J. & Swenne, C. A. Assessment of signal quality and electrode placement in ECGs using a reconstruction matrix. 2011 Computing in Cardiology, 2011. IEEE, 289-292.

Mackay, J. & Mensah, G. A. 2004. The Atlas of Heart Disease and Stroke. World Health Organization.

Majumder, S., Mondal, T. & Deen, M. 2017. Wearable sensors for remote health monitoring. *Sensors,* 17**,** 130.

Malik, M. 1996. Heart rate variability: Standards of measurement, physiological interpretation, and clinical use: Task force of the European Society of Cardiology and the North American Society for Pacing and Electrophysiology. *Annals of Noninvasive Electrocardiology,* 1**,** 151-181.

Malliani, A., Pagani, M., Lombardi, F. & Cerutti, S. 1991. Cardiovascular neural regulation explored in the frequency domain. *Circulation,* 84**,** 482-492.

Malmivuo, J. & Plonsey, R. 1995. *Bioelectromagnetism: principles and applications of bioelectric and biomagnetic fields*, Oxford University Press, USA.

Mandyam, M. C., Soliman, E. Z., Alonso, A., Dewland, T. A., Heckbert, S. R., Vittinghoff, E., Cummings, S. R., Ellinor, P. T., Chaitman, B. R. & Stocke, K. 2013. The QT interval and risk of incident atrial fibrillation. *Heart rhythm,* 10**,** 1562-1568.

Marinho, L., Almeida, D., Santos, A. & Cardoso, H. F. 2012. Is the length of the sternum reliable for estimating adult stature? A pilot study using fresh sterna and a test of two methods using dry sterna. *Forensic science international,* 220**,** 292. e1-292. e4.

Mark Jones, Tom Martin, Zahi Nakad & Ravi Shenoy 2003. Towards a design framework for wearable electronic textiles *Wearable computers.* IEEE

Marozas, V., Petrenas, A., Daukantas, S. & Lukosevicius, A. 2011. A comparison of conductive textile-based and silver/silver chloride gel electrodes in exercise electrocardiogram recordings. *J Electrocardiol,* 44**,** 189-194.

Martínez, J. P., Laguna, P., Olmos, S., Pahlm, O., Pettersson, J. & Sörnmo, L. 2007. Assessment of QT-measurement accuracy using the 12-lead electrocardiogram derived from EASI leads. *Journal of electrocardiology,* 40**,** 172-179.

Mathes, P. & Halhuber, M. l. (eds.) 2012. *Controversies in Cardiac Rehabilitation*: Springer Science & Business Media.

Maxwell, E. K., Back, G. & Ramakrishnan, N. Diagnosing memory leaks using graph mining on heap dumps. Proceedings of the 16th ACM SIGKDD international conference on Knowledge discovery and data mining, 2010. 115-124.

McGrath, B. P. 2002. Ambulatory blood pressure monitoring. *Medical Journal of Australia,* 176**,** 588-592.

McLaren, J., Helmer, R., Horne, S. & Blanchonette, I. 2010. Preliminary development of a wearable device for dynamic pressure measurement in garments. *Procedia Engineering,* 2**,** 3041-3046.

McLellan, A. & Mohamed, U. 2011. Ambulatory electrocardiographic monitoring. *Australian family physician,* 40**,** 596.

Meau, Y. P., Ibrahim, F., Narainasamy, S. A. & Omar, R. 2006. Intelligent classification of electrocardiogram (ECG) signal using extended Kalman Filter (EKF) based neuro fuzzy system. *Computer Methods and Programs in Biomedicine,* 82**,** 157-168.

Meek, S. & Morris, F. 2002. ABC of clinical electrocardiography: introduction. I—Leads, rate, rhythm, and cardiac axis. *BMJ: British Medical Journal,* 324**,** 415.

Mehmann, A., Varga, M. & Tröster, G. 2017. Reversible Contacting for Smart Textiles. *Smart Textiles.* Springer.

Meinhold, R. J. & Singpurwalla, N. D. 1983. Understanding the Kalman filter. *The American Statistician,* 37**,** 123-127.

Meissimilly, G., Cartaya, M., Valles, J., Guerra, A. & Botana, G. 2009. 8-Patient ECG Telemetry System Intended for Cardiac Rehab. *World Congress on Medical Physics and Biomedical Engineering, September 7-12, 2009, Munich, Germany.* Springer.

Menezes, R. G., Nagesh, K., Monteiro, F. N., Kumar, G. P., Kanchan, T., Uysal, S., Rao, P. J., Rastogi, P., Lobo, S. W. & Kalthur, S. G. 2011. Estimation of stature from the length of the sternum in South Indian females. *Journal of forensic and legal medicine,* 18**,** 242-245.

Merritt, C. R. 2008. Electronic textile-based sensors and systems for long-term health monitoring.

Merritt, C. R., Nagle, H. T. & Grant, E. 2009. Fabric-based active electrode design and fabrication for health monitoring clothing. *IEEE Transactions on information technology in biomedicine,* 13**,** 274-280.

Meyer-Sabellek, W., Anlauf, M., Gotzen, R. & Steinfeld, L. 1990. *Blood Pressure Measurements: New Techniques in Automatic and 24-hour Indirect Monitoring*, Springer-Verlag New York.

Meziane, N., Yang, S., Shokoueinejad, M., Webster, J., Attari, M. & Eren, H. 2015. Simultaneous comparison of 1 gel with 4 dry electrode types for electrocardiography. *Physiological measurement,* 36**,** 513.

Mihelj, M., Novak, D. & Beguš, S. 2014. Virtual Reality Technology and Applications. Dordrecht: Springer Science+Business Media BV.

Milivojevic, Z. 2009. Digital Filter Design. 1 ed.: mikroElektronika.

Min, M. 2011. *Cardiac Pacemakers - Biological Aspects, Clinical Applications and Possible Complications,* Janeza Trdine, InTech.

Mneimneh, M., Yaz, E., Johnson, M. & Povinelli, R. An adaptive Kalman filter for removing baseline wandering in ECG signals. 2006 Computers in Cardiology, 2006. IEEE, 253-256.

Montesinos, L., Castaldo, R. & Pecchia, L. 2018. On the use of approximate entropy and sample entropy with centre of pressure time-series. *Journal of neuroengineering and rehabilitation,* 15**,** 116.

Montrose, M. I. 1996. *Printed circuit board design techniques for EMC compliance*, Citeseer.

Moody, G. B. M. 2015. *Approximate Entropy (ApEn)* [Online]. PHYSIONET. Available: https://archive.physionet.org/physiotools/ApEn/ [Accessed 26 August 2019].

Moradi, M., Rad, M. A. & Khezerloo, R. B. 2014. ECG signal enhancement using adaptive Kalman filter and signal averaging. *International journal of cardiology,* 173**,** 553-555.

Morrison, T., Silver, J. & Otis, B. A single-chip encrypted wireless 12-lead ECG smart shirt for continuous health monitoring. 2014 Symposium on VLSI Circuits Digest of Technical Papers, 2014. IEEE, 1-2.

Mourot, L., Bouhaddi, M., Perrey, S., Cappelle, S., Henriet, M. T., Wolf, J. P., Rouillon, J. D. & Regnard, J. 2004. Decrease in heart rate variability with overtraining: assessment by the Poincare plot analysis. *Clinical physiology and functional imaging,* 24**,** 10-18.

Mukhopadhyay, S. C. 2015. *Wearable Electronics Sensors: For Safe and Healthy Living*, Springer

Myles, P. S. & Cui, J. 2007. I. Using the Bland–Altman method to measure agreement with repeated measures. Oxford University Press.

Nag, S. & Sharma, D. K. Wireless E-Jacket for Multiparameter Biophysical Monitoring and Telemedicine Applications. 3rd IEEE/EMBS International Summer School on Medical Devices and Biosensors, 3 April 2017 2006. IEEE, 40-44.

Naghavi, M., Abajobir, A. A., Abbafati, C., Abbas, K. M., Abd-Allah, F., Abera, S. F., Aboyans, V., Adetokunboh, O., Afshin, A. & Agrawal, A. 2017. Global, regional, and national age-sex specific mortality for 264 causes of death, 1980–2016: a systematic analysis for the Global Burden of Disease Study 2016. *The Lancet,* 390**,** 1151-1210.

National Heart Foundation of Australia. n.d. *Heart disease in Australia* [Online]. National Heart Foundation of Australia. Available: https://www.heartfoundation.org.au/about-us/what-we-do/heart-disease-in-australia [Accessed 10 November 2019].

National Heart Foundation of Australia, C. S. o. A. a. N. Z. 2012. Reducing risk in heart disease: an expert guide to clinical practice for secondary prevention of coronary heart disease. Melbourne: National Heart Foundation of Australia.

National Instruments. 2015. *IIR Filters and FIR Filters* [Online]. National Instruments. Available: http://zone.ni.com/reference/en-XX/help/370858M-01/genmaths/genmaths/calc_filterfir_iir/ [Accessed 9 April 2019].

Nelwan, S. 2005. Evaluation of 12-Lead Electrocardiogram Reconstruction Methods for Patient Monitoring. MarkWouters.

Nissha Medical Technologies. n.d. *Swaromed ECG Electrodes* [Online]. Graphic Controls Holdings. Available: https://vermed.co.uk/Electrodes/Swaro.aspx [Accessed 16 September 2019].

Nunan, D., Sandercock, G. R. & Brodie, D. A. 2010. A quantitative systematic review of normal values for short-term heart rate variability in healthy adults. *Pacing and clinical electrophysiology,* 33**,** 1407-1417.

Oerkild, B., Frederiksen, M., Hansen, J. F. & Prescott, E. 2012. Home-based cardiac rehabilitation is an attractive alternative to no cardiac rehabilitation for elderly patients with coronary heart disease: results from a randomised clinical trial. *BMJ open,* 2**,** e001820.

Olmos, C., Franco, E., Suárez-Barrientos, A., Fortuny, E., Martín-García, A., Viliani, D., Macaya, C. & Pérez De Isla, L. 2014. Wearable wireless remote monitoring system: An alternative for prolonged electrocardiographic monitoring. *International Journal of Cardiology,* 172**,** e43-e44.

Oracle. 2019. *Fusion Middleware Performance and Tuning for Oracle WebLogic Server* [Online]. Oracle Available: https://docs.oracle.com/cd/E15523_01/web.1111/e13814/jvm_tuning.htm#PERFM150 [Accessed 23 June 2019].

Oracle Corporation. n.d. *VisualVM: All-in-One Java Troubleshooting Tool* [Online]. Oracle Corporation and/or its affiliates. Available: https://visualvm.github.io/index.html [Accessed 22 March 2019].

Oster, J., Behar, J., Sayadi, O., Nemati, S., Johnson, A. E. & Clifford, G. D. 2015. Semisupervised ECG ventricular beat classification with novelty detection based on switching Kalman filters. *IEEE Transactions on Biomedical Engineering,* 62**,** 2125-2134.

Pahlm, O., Pettersson, J., Thulin, A., Feldman, C. L., Feild, D. Q. & Wagner, G. S. 2003. Comparison of waveforms in conventional 12-lead ECGs and those derived from EASI leads in children. *Journal of electrocardiology,* 36**,** 25-31.

Pan, J. & Tompkins, W. J. 1985. A real-time QRS detection algorithm. *IEEE transactions on biomedical engineering***,** 230-236.

Pandian, P. S. & Srinivasa, M. G. 2016. A ZigBee-wireless wearable remote physiological monitoring system. *2016 International Conference on Signal Processing and Communication (ICSC)* IEEE.

Pandit, S. ECG baseline drift removal through STFT. Proceedings of 18th Annual International Conference of the IEEE Engineering in Medicine and Biology Society, 1996. IEEE, 1405-1406.

Pani, D., Dessì, A., Saenz-Cogollo, J. F., Barabino, G., Fraboni, B. & Bonfiglio, A. 2015. Fully textile, PEDOT: PSS based electrodes for wearable ECG monitoring systems. *IEEE Trans Biomed Eng,* 63**,** 540-549.

Papouchado, M., Walker, P., James, M. & Clarke, L. 1987. Fundamental differences between the standard 12–lead electrocardiograph and the modified (Mason—Likar) exercise lead system. *European heart journal,* 8**,** 725-733.

Paradiso, R., Loriga, G. & Taccini, N. 2005. A wearable health care system based on knitted integrated sensors. *IEEE Trans Inf Technol Biomed.,* 9**,** 337-344.

Parker, M., Goodwin, D., Eager, R. A., Redhead, E. S. & Marlin, D. J. 2009. Comparison of Polar® heart rate interval data with simultaneously recorded ECG signals in horses. *Comparative Exercise Physiology,* 6**,** 137-142.

Paul, G., Torah, R., Beeby, S. & Tudor, J. 2015. Novel active electrodes for ECG monitoring on woven textiles fabricated by screen and stencil printing. *Sensors and Actuators A: Physical,* 221**,** 60-66.

PCBWay. n.d. *PCB Prototype the Easy Way* [Online]. PCBWay. Available: https://www.pcbway.com [Accessed 16 August 2018].

Peltokangas, M., Verho, J. & Vehkaoja, A. 2012. Night-time EKG and HRV monitoring with bed sheet integrated textile electrodes. *IEEE Trans Inf Technol Biomed.,* 16**,** 935-42.

Pereira, T., Carvalho, H., Catarino, A. P., Dias, M., Postolache, O. & Girão, P. S. Wearable biopotential measurement using the TI ADS1198 analog front-end and textile electrodes. 2013 IEEE International Symposium on Medical Measurements and Applications (MeMeA), 2013. IEEE, 325-330.

Perez De Isla, L., Lennie, V., Quezada, M., Guinea, J., Arce, C., Abad, P., Saltijeral, A., Campos, N. C., Crespo, J., Gonzálvez, B., MacIa, A. & Zamorano, J. 2011. New generation dynamic, wireless and remote cardiac monitorization platform: A feasibility study. *International Journal of Cardiology,* 153**,** 83-85.

Perk, J., Mathes, P., Gohlke, H., Monpère, C., Hellemans, I., McGee, H., Sellier, P. & Saner, H. (eds.) 2007. *Cardiovascular Prevention and Rehabilitation*: Springer-Verlag London Limited.

Phukpattaranont, P. Improvement of signal to noise ratio (SNR) in ECG signals based on dual-band continuous wavelet transform. Signal and Information Processing Association Annual Summit and Conference (APSIPA), 2014 Asia-Pacific, 2014. IEEE, 1-4.

Pickering, T. G., Shimbo, D. & Haas, D. 2006. Ambulatory blood-pressure monitoring. *New England Journal of Medicine,* 354**,** 2368-2374.

Pincus, S. 1995. Approximate entropy (ApEn) as a complexity measure. *Chaos: An Interdisciplinary Journal of Nonlinear Science,* 5**,** 110-117.

Pincus, S. M. 1991. Approximate entropy as a measure of system complexity. *Proceedings of the National Academy of Sciences,* 88**,** 2297-2301.

Pincus, S. M. & Goldberger, A. L. 1994. Physiological time-series analysis: what does regularity quantify? *Am J Physiol Heart Circ Physiol,* 266**,** H1643-H1656.

Pirovano, M., Mainetti, R., Baud-Bovy, G., Lanzi, P. L. & Borghese, N. A. Self-adaptive games for rehabilitation at home. IEEE Conference on Computational Intelligence and Games, 2012. 179-186.

Piskorowski, J. 2009. Digital Q-Varying Notch IIR Filter With Transient Suppression transient suppression. *IEEE Transactions on Instrumentation and Measurement,* 59**,** 866-872.

Pitei, D., Ison, K., Edmonds, M. & Lord, M. 1996. Time-dependent behaviour of a force-sensitive resistor plantar pressure measurement insole. *Proceedings of the Institution of Mechanical Engineers, Part H: Journal of Engineering in Medicine,* 210**,** 121-125.

PJRC. n.d. *Teensy USB Development Board* [Online]. PJRC. Available: https://www.pjrc.com/store/teensy40.html [Accessed 2 March 2020].

Pola, T. & Vanhala, J. Textile electrodes in ECG measurement. 2007 3rd International Conference on Intelligent Sensors, Sensor Networks and Information, 2007. IEEE, 635-639.

Porr, B. 2019. *An efficient IIR filter library written in JAVA* [Online]. GitHub, Inc. Available: https://github.com/berndporr/iirj [Accessed 15 March 2019].

Preiss, D. & Fisher, J. 2008. A measure of confidence in Bland–Altman analysis for the interchangeability of two methods of measurement. *Journal of clinical monitoring and computing,* 22**,** 257-259.

Press, W. H. & Teukolsky, S. A. 1990. Savitzky-Golay smoothing filters. *Computers in Physics,* 4**,** 669-672.

Price, K. J., Gordon, B. A., Bird, S. R. & Benson, A. C. 2016. A review of guidelines for cardiac rehabilitation exercise programmes: Is there an international consensus? *Eur J Prev Cardiol,* 23**,** 1715-1733.

Puurtinen, M. M., Komulainen, S. M., Kauppinen, P. K., Malmivuo, J. A. & Hyttinen, J. A. Measurement of noise and impedance of dry and wet textile electrodes, and textile electrodes with hydrogel. 2006 International Conference of the IEEE Engineering in Medicine and Biology Society, 2006. IEEE, 6012-6015.

Raeiatibanadkooki, M., Quachani, S. R., Khalilzade, M. & Bahaadinbeigy, K. 2014. Real time processing and transferring ECG signal by a mobile phone. *Acta Informatica Medica,* 22**,** 389.

Rana, N. Application of force sensing resistor (FSR) in design of pressure scanning system for plantar pressure measurement. 2009 Second International Conference on Computer and Electrical Engineering, 2009. IEEE, 678-685.

Rattfält, L. 2013. *Smartware electrodes for ECG measurements: Design, evaluation and signal processing.* Linköping University Electronic Press.

Reinhard, J., Hayes-Gill, B. R., Schiermeier, S., Hatzmann, H., Heinrich, T. M. & Louwen, F. 2013. Intrapartum heart rate ambiguity: a comparison of cardiotocogram and abdominal fetal electrocardiogram with maternal electrocardiogram. *Gynecol Obstet Invest,* 75**,** 101-108.

Rijken, P. M. & Dekker, J. 1998. Clinical experience of rehabilitation therapists with chronic diseases: a quantitative approach. *Clinical Rehabilitation* [Online], 12. Available: http://nvl002.nivel.nl/postprint/PPpp828.pdf [Accessed 3 September 2015].

Rodríguez, A., Rodríguez, G., Almeida, R., Pina, N. & De Oca, G. M. 2010. Design and evaluation of an ECG Holter analysis system. *Comput Cardiol.* IEEE.

Rogers, K. (ed.) 2011. *The Cardiovascular System (The Human Body),* New York: Britannica Educational Publishing.

Rohrbach, G., Schopfer, D. W., Krishnamurthi, N., Pabst, M., Bettencourt, M., Loomis, J. & Whooley, M. A. 2017. The design and implementation of a home-based cardiac rehabilitation program. *Federal practitioner,* 34**,** 34.

Romagnoli, M., Alis, R., Guillen, J., Basterra, J., Villacastin, J. P. & Guillen, S. 2014. A novel device based on smart textile to control heart's activity during exercise. *Australas Phys Eng Sci Med,* 37**,** 377-84.

Rosero, S. Z., Kutyifa, V., Olshansky, B. & Zareba, W. 2013. Ambulatory ECG Monitoring in Atrial Fibrillation Management. *Prog Cardiovasc Dis,* 56**,** 143–152.

Roth, G. A., Abate, D., Abate, K. H., Abay, S. M., Abbafati, C., Abbasi, N., Abbastabar, H., Abd-Allah, F., Abdela, J. & Abdelalim, A. 2018. Global, regional, and national age-sex-specific mortality for 282 causes of death in 195 countries and territories, 1980–2017: a systematic analysis for the Global Burden of Disease Study 2017. *The Lancet,* 392**,** 1736-1788.

Roth, G. A., Johnson, C., Abajobir, A., Abd-Allah, F., Abera, S. F., Abyu, G., Ahmed, M., Aksut, B., Alam, T. & Alam, K. 2017a. Global, regional, and national burden of cardiovascular diseases for 10 causes, 1990 to 2015. *J Am Coll Cardiol,* 70**,** 1-25.

Roth, G. A., Johnson, C., Abajobir, A., Abd-Allah, F., Abera, S. F., Abyu, G., Ahmed, M., Aksut, B., Alam, T. & Alam, K. 2017b. Global, regional, and national burden of cardiovascular diseases for 10 causes, 1990 to 2015. *Journal of the American College of Cardiology,* 70**,** 1-25.

Sadanaga, T., Sadanaga, F., Yao, H. & Fujishima, M. 2006. An evaluation of ECG leads used to assess QT prolongation. *Cardiology,* 105**,** 149-154.

Salisbury, J. I. & Sun, Y. 2004. Assessment of chaotic parameters in nonstationary electrocardiograms by use of empirical mode decomposition. *Annals of biomedical engineering,* 32**,** 1348-1354.

Sameni, R., Shamsollahi, M. & Jutten, C. Filtering electrocardiogram signals using the extended Kalman filter. 2005 IEEE Engineering in Medicine and Biology 27th Annual Conference, 2006. IEEE, 5639-5642.

Sameni, R., Shamsollahi, M., Jutten, C. & Babaie-Zade, M. Filtering noisy ECG signals using the extended Kalman filter based on a modified dynamic ECG model. Computers in Cardiology, 2005, 2005. IEEE, 1017-1020.

Sameni, R., Shamsollahi, M. B., Jutten, C. & Clifford, G. D. 2007. A nonlinear Bayesian filtering framework for ECG denoising. *IEEE Transactions on Biomedical Engineering,* 54**,** 2172-2185.

Sandercock, G. R., Grocott-Mason, R. & Brodie, D. A. 2007. Changes in short-term measures of heart rate variability after eight weeks of cardiac rehabilitation. *Clinical Autonomic Research,* 17**,** 39-45.

Sankaran, S. 2012. Cardiovascular Disease. *In:* SANA LOUE & SAJATOVIC, M. (eds.) *Encyclopedia of Immigrant Health.* Springer Science and Business Media, LLC.

Sarela, A., Korhonen, I., Salminen, J., Koskinen, E., Kirkeb, O. & Walters, D. 2009. A home-based care model for outpatient cardiac rehabilitation based on mobile technologies. *Int Conf Pervasive Comput Technol Healthc.*: IEEE.

Särelä, A., Korhonen, I., Salminen, J., Koskinen, E., Kirkeby, O. & Walters, D. 2009. A home-based care model for outpatient cardiac rehabilitation based on mobile technologies. *Int Conf Pervasive Comput Technol Healthc.*: IEEE.

Sayadi, O. & Shamsollahi, M. B. 2008. ECG denoising and compression using a modified extended Kalman filter structure. *IEEE Transactions on Biomedical Engineering,* 55**,** 2240-2248.

Sazonov, E. & Neuman, M. R. (eds.) 2014. *Wearable Sensors: Fundamentals, implementation and applications*: Elsevier.

Schafer, R. W. 2011. What is a Savitzky-Golay filter. *IEEE Signal processing magazine,* 28**,** 111-117.

Scherer, J. A., Jenkins, J. M. & Nicklas, J. M. 1990. Synthesis of the 12-lead electrocardiogram from a 3-lead subset using patient-specific transformation vectors: an algorithmic approach to computerized signal synthesis. *Journal of electrocardiology,* 22**,** 128.

Schneegass, S. & Amft, O. 2017. *Smart textiles*, Springer.

Schofield, J. S., Evans, K. R., Hebert, J. S., Marasco, P. D. & Carey, J. P. 2016. The effect of biomechanical variables on force sensitive resistor error: Implications for calibration and improved accuracy. *Journal of biomechanics,* 49**,** 786-792.

Schuler, C. A. 2019. *Electronics : principles and applications,* New York, McGraw-Hill Education.

Schultheis, M. T. & Rizzo, A. A. 2001. The application of virtual reality technology in rehabilitation. *Rehabil Psychol,* 46**,** 296 - 311.

Schultz, C. P. 1993. Menu selection using adaptive force sensing resistor. Google Patents.

Schwaab, B. 2010. Cardiovascular rehabilitation. *The internist,* 51**,** 1231-1238.

Schwarz, A., Kazani, I., Cuny, L., Hertleer, C., Ghekiere, F., De Clercq, G., De Mey, G. & Van Langenhove, L. 2011. Electro-conductive and elastic hybrid yarns–The effects of stretching, cyclic straining and washing on their electro-conductive properties. *Materials & Design,* 32**,** 4247-4256.

Scilingo, E. P., Gemignani, A., Paradiso, R., Taccini, N., Ghelarducci, B. & De Rossi, D. 2005. Performance evaluation of sensing fabrics for monitoring physiological and biomechanical variables. *IEEE Transactions on information technology in biomedicine,* 9**,** 345-352.

Sedghamiz, H. 2013. An online algorithm for r, s and t wave detection. *Linkoping University, Dec*.

Sedghamiz, H. 2018. BioSigKit: A Matlab Toolbox and Interface for Analysis of BioSignals. *Journal of Open Source Software,* 3**,** 671.

Sedghamiz, H. & Santonocito, D. Unsupervised detection and classification of motor unit action potentials in intramuscular electromyography signals. 2015 e-health and bioengineering conference (ehb), 2015. IEEE, 1-6.

Shamim, W., Yousufuddin, M., Cicoria, M., Gibson, D., Coats, A. & Henein, M. 2002. Incremental changes in QRS duration in serial ECGs over time identify high risk elderly patients with heart failure. *Heart,* 88**,** 47-51.

Shanmugam, N. & Liew, R. 2012. The Implantable Loop Recorder—An Important Addition to the Armentarium in the Management of Unexplained Syncope. *Ann Acad Med Singapore* [Online], 41. Available: http://www.annals.edu.sg/pdf/41VolNo3Mar2012/V41N3p115.pdf [Accessed 14 March 2017].

Shenkman, H. J., Pampati, V., Khandelwal, A. K., McKinnon, J., Nori, D., Kaatz, S., Sandberg, K. R. & McCullough, P. A. 2002. Congestive heart failure and QRS duration: establishing prognosis study. *Chest,* 122**,** 528-534.

Shi, J., Liu, S., Zhang, L., Yang, B., Shu, L., Yang, Y., Ren, M., Wang, Y., Chen, J. & Chen, W. 2020. Smart Textile-Integrated Microelectronic Systems for Wearable Applications. *Advanced Materials,* 32**,** 1901958.

Shields Jr, R. W. 2009. Heart rate variability with deep breathing as a clinical test of cardiovagal function. *Cleve Clin J Med,* 76**,** S37-40.

Shyamal Patel, Hyung Park, Paolo Bonato, Leighton Chan & Rodgers, M. 2012. A review of wearable sensors and systems with application in Rehabilitation. *Journal of NeuroEngineering and Rehabilitation* [Online], 9. Available: https://jneuroengrehab.biomedcentral.com/articles/10.1186/1743-0003-9-21 [Accessed April 16, 2016].

Silberberg, J. L. Achieving medical device EMC: The role of regulations, standards, guidelines and publications. 2001 IEEE EMC International Symposium. Symposium Record. International Symposium on Electromagnetic Compatibility (Cat. No. 01CH37161), 2001. IEEE, 1298-1303.

Simon, D. 2001. Kalman filtering. *Embedded systems programming,* 14**,** 72-79.

Singh, Y., Tripathi, S. & Pandey, M. 2010. Analysis of digital IIR filter with Labview. *International Journal of Computer Applications,* 10**,** 23-30.

Soares, J. C., Vieira, Á., Postolache, O. & Gabriel, J. 2013. Development of a Kinect Rehabilitation System. *iJOE,* 9**,** 38-40.

Sørensen, J. S., Johannesen, L., Grove, U. S. L., Lundhus, K., Couderc, J.-P. & Graff, C. A comparison of IIR and wavelet filtering for noise reduction of the ECG. 2010 Computing in Cardiology, 2010. IEEE, 489-492.

Sotiriadis, S., Vakanas, L., Petrakis, E., Zampognaro, P. & Bessis, N. Automatic Migration and Deployment of Cloud Services for Healthcare Application Development in FIWARE. 30th International Conference on Advanced Information Networking and Applications Workshops, WAINA, 17 May, 2016. IEEE, 416-419.

SparkFun Electronics. n.d. *Lithium Ion Battery - 2Ah* [Online]. SparkFun Electronics. Available: https://www.sparkfun.com/products/13855 [Accessed 13 April 2019].

Spotlight Pty Ltd. 2020. *Birch Snap Fastener Pliers Red & Silver* [Online]. Available: https://www.spotlightstores.com/sewing-fabrics/haberdashery/fasteners/fastener-tools/birch-snap-fastener-pliers/BP80055977 [Accessed 25 April 2019].

Sroufe, L. A. 1971. Effects of depth and rate of breathing on heart rate and heart rate variability. *Psychophysiology,* 8**,** 648-655.

Standards Australia Limited/Standards New Zealand 2011. AS/NZS ISO 10535:2011 Hoists for the transfer of disabled persons - Requirements and test methods Standards Australia. SAI Global Limited.

Stanner, S. 2005. *Cardiovascular Disease: Diet, Nutrition and Emerging Risk Factors - The Report of a British Nutrition Foundation Task Force*, Blackwell Publishing for the British Nutrition Foundation.

Stephanou, P. J., Buchan, N. I., Burns, D. W., Lavery, K. A. & Ganapathi, S. K. 2015. Touchscreen with bridged force-sensitive resistors. Google Patents.

Stoica, P. & Moses, R. L. 2005. Spectral analysis of signals.

Stoppa, M. & Chiolerio, A. 2014. Wearable Electronics and Smart Textiles: A Critical Review. *Sensors* [Online]. Available: http://www.researchgate.net/profile/Alessandro_Chiolerio/publication/263741051_Wearable_Electronics_and_Smart_Textiles_A_Critical_Review/links/542ab8650cf277d58e88434e.pdf [Accessed 19 October 2016].

Subhasis Chaudhuri, Siddhartha Duttagupta & Pawar, T. D. 2009. Ambulation Analysis in Wearable ECG. New York: Springer Science+Business Media, LLC.

Suchetha, M., Kumaravel, N., Jagannath, M. & Jaganathan, S. K. 2017. A comparative analysis of EMD based filtering methods for 50 Hz noise cancellation in ECG signal. *Informatics in Medicine Unlocked,* 8**,** 54-59.

Sun, F., Yi, C., Li, W. & Li, Y. 2017. A wearable H-shirt for exercise ECG monitoring and individual lactate threshold computing. *Computers in Industry,* 92**,** 1-11

Sundar, A., Pahwa, V., Das, C., Deshmukh, M. & Robinson, N. 2016. A comprehensive assessment of the performance of modern algorithms for enhancement of digital volume pulse signals. *International Journal of Pharma Medicine and Biological Sciences,* 5**,** 91.

Swartz, M. A. 2001. The physiology of the lymphatic system. *Advanced drug delivery reviews,* 50**,** 3-20.

Takahashi, K., Suzuki, K. & Ieee 2015. An ECG Monitoring System Through Flexible Clothes with Elastic Material. *IEEE Healthcom* 305-310.

Takamatsu, S., Lonjaret, T., Crisp, D., Badier, J.-M., Malliaras, G. G. & Ismailova, E. 2015. Direct patterning of organic conductors on knitted textiles for long-term electrocardiography. *Scientific reports,* 5**,** 15003.

Tan, G., Dao, T. K., Farmer, L., Sutherland, R. J. & Gevirtz, R. 2011. Heart rate variability (HRV) and posttraumatic stress disorder (PTSD): a pilot study. *Applied psychophysiology and biofeedback,* 36**,** 27-35.

Tao, X. (ed.) 2001. *Smart Fibres, Fabrics and Clothing. Fundamentals and Applications* Woodhead Publishing Ltd.

Tao, X. 2005. *Wearable electronics and photonics*, Woodhead Publishing Ltd.

Teferra, M. N., Kourbelis, C., Newman, P., Ramos, J. S., Hobbs, D., Clark, R. A. & Reynolds, K. J. 2019a. Electronic textile electrocardiogram monitoring in cardiac patients: a scoping review protocol. *JBI Database System Rev Implement Rep,* 17**,** 147–156.

Teferra, M. N., Ramos, J. S., Fleury, A., Kourbelis, C., Newman, P., Hobbs, D., Clark , R. A. & Reynolds, K. J. 2019b. E-textile electrocardiogram (ECG) monitoring in cardiac patients: a scoping review. *JBI Database System Rev Implement Rep* 17**,** 1958–1998.

Tegehall, P.-E. 2006. Review of the impact of intermetallic layers on the brittleness of tin-lead and lead-free solder joints. *IVF project report,* 6**,** 1-63.

Texas Heart Institute. *Categories of Arrhythmias* [Online]. Texas Heart Institute. Available: https://www.texasheart.org/heart-health/heart-information-center/topics/categories-of-arrhythmias/ [Accessed].

Texas Instruments 2015. ADS1298: Low-Power, 8-Channel, 24-Bit Analog Front-End for Biopotential Measurements. Texas Instruments.

Texas Instruments Incorporated 2015. ADS129x Low-Power, 8-Channel, 24-Bit Analog Front-End for Biopotential Measurements. Texas Instruments Incorporated.

Texas Instruments Incorporated. n.d.-a. *ADS129x Low-Power, 8-Channel, 24-Bit Analog Front-End for Biopotential Measurements datasheet (Rev. K)* [Online]. Texas Instruments Incorporated. Available: http://www.ti.com/product/ADS1298 [Accessed 12 June 2018].

Texas Instruments Incorporated. n.d.-b. *TLV741P: 150mA Low-Dropout (LDO) Regulator With Foldback Current Limit for Portable Devices* [Online]. Available: http://www.ti.com/product/TLV741P [Accessed 22 October 2018].

The Department of Health. 2016. *Cardiovascular disease* [Online]. Available: http://www.health.gov.au/internet/main/publishing.nsf/Content/chronic-cardio#wha [Accessed 28 November 2017].

The MathWorks Inc. c2020a. *Nonparametric Methods* [Online]. The MathWorks, Inc. Available: https://au.mathworks.com/help/signal/ug/nonparametric-methods.html [Accessed 20 March 2020].

The MathWorks Inc. c2020b. *pwelch* [Online]. The MathWorks, Inc. Available: https://www.mathworks.com/help/signal/ref/pwelch.html?searchHighlight=pwelch&s_tid=srchtitle [Accessed 24 September 2020].

The MathWorks Inc. c2020c. *pyulear* [Online]. The MathWorks, Inc. Available: https://www.mathworks.com/help/signal/ref/pyulear.html?searchHighlight=pyulear&s_tid=srchtitle [Accessed 24 September 2020].

The MathWorks Inc. n.d. *sgolay* [Online]. Available: https://www.mathworks.com/help/signal/ref/sgolay.html [Accessed 21 May 2019].

Thomas, R. J., Beatty, A. L., Beckie, T. M., Brewer, L. C., Brown, T. M., Forman, D. E., Franklin, B. A., Keteyian, S. J., Kitzman, D. W. & Regensteiner, J. G. 2019. Home-based cardiac rehabilitation: a scientific statement from the American Association of Cardiovascular and Pulmonary Rehabilitation, the American Heart Association, and the American College of Cardiology. *Journal of the American College of Cardiology,* 74**,** 133-153.

Tong, R. 2018. *Wearable Technology in Medicine and Health Care*, Academic Press.

Trevethan, R. 2017. Sensitivity, specificity, and predictive values: foundations, pliabilities, and pitfalls in research and practice. *Frontiers in public health,* 5**,** 307.

Trindade, I. G., Machado da Silva, J., Miguel, R., Pereira, M., Lucas, J., Oliveira, L., Valentim, B., Barreto, J. & Santos Silva, M. 2016. Design and Evaluation of Novel Textile Wearable Systems for the Surveillance of Vital Signals. *Sensors,* 16**,** 24.

Trinkley, K. E., Lee Page, R., Lien, H., Yamanouye, K. & Tisdale, J. E. 2013. QT interval prolongation and the risk of torsades de pointes: essentials for clinicians. *Curr Med Res Opin,* 29**,** 1719-1726.

Tsukada, Y. T., Tokita, M., Murata, H., Hirasawa, Y., Yodogawa, K., Iwasaki, Y.-k., Asai, K., Shimizu, W., Kasai, N. & Nakashima, H. 2019. Validation of wearable textile electrodes for ECG monitoring. *Heart and vessels,* 34**,** 1203-1211.

Turakhia, M. P., Estes, N. A. M., Drew, B. J., Granger, C. B., Wang, P. J., Knight, B. P. & Page, R. L. 2012. Latency of ECG displays of hospital telemetry systems: a science advisory from the American Heart Association. *Circulation* [Online], 126. Available: http://circ.ahajournals.org/content/126/13/1665 [Accessed 16 March 2017].

Ueno, A., Akabane, Y., Kato, T., Hoshino, H., Kataoka, S. & Ishiyama, Y. 2007. Capacitive sensing of electrocardiographic potential through cloth from the dorsal surface of the body in a supine position: a preliminary study. *IEEE Trans Biomed Eng,* 54**,** 759-66.

Van Langenhove, L. (ed.) 2007. *Smart Textiles for Medicine and Healthcare: Materials, Systems and Applications* Cambridge: Woodhead Publishing Limited.

van Langenhove, L. 2015. *Advances in smart medical textiles: treatments and health monitoring*, Woodhead Publishing.

Varadan, V. K., Kumar, P. S., Oh, S., Mathur, G. N., Rai, P. & Kegley, L. E-bra with nanosensors, smart electronics and smart phone communication network for heart rate monitoring. Nanosensors, Biosensors, and Info-Tech Sensors and Systems 2011, 2011. International Society for Optics and Photonics, 79800S.

Vehkaoja, A., Verho, J., Cömert, A., Honkala, M. & Lekkala, J. Wearable System for EKG Monitoring-Evaluation of Night-Time Performance. International Conference on Wireless Mobile Communication and Healthcare, 2011. Springer, 119-126.

Vieira, A., Gabriel, J., Melo, C. & Machado, J. 2017. Kinect system in home-based cardiovascular rehabilitation. *Proc IMechE Part H: J Engineering in Medicine,* 231**,** 40-47.

Voss, A., Schroeder, R., Heitmann, A., Peters, A. & Perz, S. 2015. Short-term heart rate variability—influence of gender and age in healthy subjects. *PloS one,* 10**,** e0118308.

Wagner, S., Bonderover, E., Jordan, W. B. & Sturm, J. C. 2002. Electrotextiles: concepts and challenges. *Int J Hi Spe Ele Syst,* 12**,** 391-399.

Wang, J., Lin, C.-C., Yu, Y.-S. & Yu, T.-C. 2015. Wireless sensor-based smart-clothing platform for ECG monitoring. *Comput Math Methods Med*.

Wang, N. C., Maggioni, A. P., Konstam, M. A., Zannad, F., Krasa, H. B., Burnett, J. C., Grinfeld, L., Swedberg, K., Udelson, J. E. & Cook, T. 2008. Clinical implications of QRS duration in patients hospitalized with worsening heart failure and reduced left ventricular ejection fraction. *Jama,* 299**,** 2656-2666.

Watts, M. & Shoat, D. 1987. Trends in electrocardiograph design. *Journal of the Institution of Electronic and Radio Engineers,* 57**,** 140-150.

Weber, M. A. & Drayer, J. I. M. (eds.) 1984. *Ambulatory Blood Pressure Monitoring*: Springer-Verlag Berlin Heidelberg.

Webster, J. G. 2009. *Medical instrumentation: application and design*, John Wiley & Sons.

Wehr, G., Peters, R. J., Khalifé, K., Banning, A. P., Kuehlkamp, V., Rickards, A. F. & Sechtem, U. 2006. A vector-based, 5-electrode, 12-lead monitoring ECG (EASI) is equivalent to conventional 12-lead ECG for diagnosis of acute coronary syndromes. *Journal of electrocardiology,* 39**,** 22-28.

Wei, D., Kojima, T., Nakayama, T. & Sakai, Y. 2004. Method of deriving standard 12-lead electrocardiogram and electrocardiogram monitoring apparatus. Google Patents.

Weippert, M., Kumar, M., Kreuzfeld, S., Arndt, D., Rieger, A. & Stoll, R. 2010a. Comparison of three mobile devices for measuring R–R intervals and heart rate variability: Polar S810i, Suunto t6 and an ambulatory ECG system. *Eur J Appl Physiol,* 109**,** 779-786.

Weippert, M., Kumar, M., Kreuzfeld, S., Arndt, D., Rieger, A. & Stoll, R. 2010b. Comparison of three mobile devices for measuring R–R intervals and heart rate variability: Polar S810i, Suunto t6 and an ambulatory ECG system. *European journal of applied physiology,* 109**,** 779-786.

Welinder, A. 2009. *Alternative Lead Systems for Diagnostic Electrocardiography: Validation and Clinical Applicability*, Lund University.

Welinder, A., Feild, D. Q., Liebman, J., Maynard, C., Wagner, G. S., Wettrell, G. & Pahlm, O. 2006. Diagnostic conclusions from the EASI-derived 12-lead electrocardiogram as compared with the standard 12-lead electrocardiogram in children. *American heart journal,* 151**,** 1059-1064.

Weninger, M., Gander, E. & Mössenböck, H. Utilizing object reference graphs and garbage collection roots to detect memory leaks in offline memory monitoring. Proceedings of the 15th International Conference on Managed Languages & Runtimes, 2018. 1-13.

Widmaier, E. P., Raff, H. & Strang, K. T. 2014. *Vander's Human Physiology: The Mechanisms of Body Function,* New York, The McGraw-Hill Companies, Inc.

Willmott, C. J. & Matsuura, K. 2005. Advantages of the mean absolute error (MAE) over the root mean square error (RMSE) in assessing average model performance. *Climate research,* 30**,** 79-82.

Wojnarowski, T., Kotas, R., Marciniak, P., Tomala, R., Kulesza, Z. & Napieralski, A. ECG Signal Filtering for High Definition Holter Monitoring System. MEMSTECH, 2011. IEEE, 137-141

Woodruffe, S., Neubeck, L., Clark, R. A., Gray, K., Ferry, C., Finan, J., Sanderson, S. & Briffa, T. G. 2015. Australian Cardiovascular Health and Rehabilitation Association (ACRA) core components of cardiovascular disease secondary prevention and cardiac rehabilitation 2014. *Heart, Lung and Circulation,* 24**,** 430-441.

Woods, J. & Radewan, C. 1977. Kalman filtering in two dimensions. *IEEE transactions on Information theory,* 23**,** 473-482.

Wu, W., Pirbhulal, S., Sangaiah, A. K., Mukhopadhyay, S. C. & Li, G. 2018. Optimization of signal quality over comfortability of textile electrodes for ECG monitoring in fog computing based medical applications. *Future Gener Comput Syst,* 86**,** 515-526.

Xhyheri, B., Manfrini, O., Mazzolini, M., Pizzi, C. & Bugiardini, R. 2012. Heart rate variability today. *Progress in cardiovascular diseases,* 55**,** 321-331.

Xiang Chen, X., Lv, Y., Fang, R. R. Z., hong Xia, S., Li, H. & Tian, L. A wireless noncontact ECG detection system based on capacitive coupling. Healthcom, 2012. IEEE, 387-390.

Xu, P., Zhang, H. & Tao, X. 2008. Textile-structured electrodes for electrocardiogram. *Textile Progress,* 40**,** 183-213.

Yan, G.-X. & Kowey, P. R. (eds.) 2011. *Management of cardiac arrhythmias*: Springer.

Yapici, M. K., Alkhidir, T., Samad, Y. A. & Liao, K. 2015. Graphene-clad textile electrodes for electrocardiogram monitoring. *Sensors and Actuators B: Chemical,* 221**,** 1469-1474.

Young, B. 2019. New standards for ECG equipment. *Journal of electrocardiology,* 57**,** S1-S4.

Yu, X., Boehm, A., Neu, W., Venema, B., Marx, N., Leonhardt, S. & Teichmann, D. 2017. A wearable 12-lead ECG T-shirt with textile electrodes for unobtrusive long-term monitoring – Evaluation of an ongoing clinical trial. *EMBEC & NBC 2017.* Springer.

Zareba, W. 2013. Ambulatory ECG Monitoring: 50 Years Later. *Progress in Cardiovascular Diseases,* 56**,** 125 - 126.

Zhang, J. 2007. Effect of age and sex on heart rate variability in healthy subjects. *Journal of manipulative and physiological therapeutics,* 30**,** 374-379.

Zhang, Y., Sun, G. & Yang, Y. 2012. 12-lead ecg data acquisition system based on ads1298. *Procedia engineering,* 29**,** 2103-2108.

Zhang, Z.-B., Shen, Y.-H., Wang, W.-D., Wang, B.-Q. & Zheng, J.-W. 2011. Design and implementation of sensing shirt for ambulatory cardiopulmonary monitoring. *J. Med. Biol. Eng,* 31**,** 207-215.

Zheng, N., Wu, Z., Lin, M. & Yang, L. T. 2010. Enhancing battery efficiency for pervasive health-monitoring systems based on electronic textiles. *IEEE J Biomed Health Inform,* 14**,** 350-359.

Zhou, P., Li, Z., Wang, F. & Jiao, H. 2013. Portable wireless ECG monitor with fabric electrodes.

Zimmermann, K. A. 2016. *Lymphatic System: Facts, Functions & Diseases* [Online]. Available: http://www.livescience.com/26983-lymphatic-system.html [Accessed].

Zipes, D. P., Libby, P., Bonow, R. O., Mann, D. L. & Tomaselli, G. F. 2019. *Braunwald's Heart Disease: A Textbook of Cardiovascular Medicine*, Elsevier Health Sciences.